DESALINATION SUSTAINABILITY

DESALINATION SUSTAINABILITY

A Technical, Socioeconomic, and Environmental Approach

HASSAN A. ARAFAT
Masdar Institute of Science and Technology, Abu Dhabi, United Arab Emirates

Elsevier
Radarweg 29, PO Box 211, 1000 AE Amsterdam, Netherlands
The Boulevard, Langford Lane, Kidlington, Oxford OX5 1GB, United Kingdom
50 Hampshire Street, 5th Floor, Cambridge, MA 02139, United States

Notices
Knowledge and best practice in this field are constantly changing. As new research and experience broaden our understanding, changes in research methods, professional practices, or medical treatment may become necessary.

Practitioners and researchers must always rely on their own experience and knowledge in evaluating and using any information, methods, compounds, or experiments described herein. In using such information or methods they should be mindful of their own safety and the safety of others, including parties for whom they have a professional responsibility.

To the fullest extent of the law, neither the Publisher nor the authors, contributors, or editors, assume any liability for any injury and/or damage to persons or property as a matter of products liability, negligence or otherwise, or from any use or operation of any methods, products, instructions, or ideas contained in the material herein.

Library of Congress Cataloging-in-Publication Data
A catalog record for this book is available from the Library of Congress

British Library Cataloguing-in-Publication Data
A catalogue record for this book is available from the British Library

ISBN: 978-0-12-809791-5

Publisher: John Fedor
Acquisition Editor: Kostas Marinakis
Editorial Project Manager: Susan Ikeda
Production Project Manager: Maria Bernad
Cover Designer: Victoria Pearson

Typeset by SPi Global, India

CONTRIBUTORS

Maryam R. Al Shehhi
Masdar Institute of Science and Technology, Abu Dhabi, United Arab Emirates

Hassan A. Arafat
Khalifa University of Science and Technology, Abu Dhabi, United Arab Emirates

Nicole T. Carter
Congressional Research Service, US Library of Congress, United States

Sudip Chakraborty
Khalifa University of Science and Technology, Abu Dhabi, United Arab Emirates; Università della Calabria, Rende, Italy

Changkyoo Choi
Gwangju Institute of Science and Technology (GIST), Gwangju, Republic of Korea

Mike B. Dixon
MDD Consulting, Calgary, AB, Canada

Enrico Drioli
Institute on Membrane Technology (ITM-CNR), National Research Council, c/o The University of Calabria, Rende CS, Italy; University of Calabria, Rende, Italy; Hanyang University, Seoul, South Korea; King Abdulaziz University, Jeddah, Saudi Arabia

Mikel Duke
Victoria University, Melbourne, VIC, Australia

Hosni Ghedira
Masdar Institute of Science and Technology, Abu Dhabi, United Arab Emirates

Imen Gherboudj
Masdar Institute of Science and Technology, Abu Dhabi, United Arab Emirates

Nozipho N. Gumbi
University of South Africa, Florida, Johannesburg, South Africa; Karlsruhe Institute of Technology (KIT), Karlsruhe, Germany

Shadi W. Hasan
Khalifa University of Science and Technology, Abu Dhabi, United Arab Emirates

Moonhyun Hwang
Gwangju Institute of Science and Technology (GIST), Gwangju, Republic of Korea

Ikechukwu A. Ike
Victoria University, Melbourne, VIC, Australia

Jehad A. Kharraz
Karlsruhe Institute of Technology (KIT), Karlsruhe, Germany

In S. Kim
Gwangju Institute of Science and Technology (GIST), Gwangju, Republic of Korea

John H. Lienhard V
Massachusetts Institute of Technology, Cambridge, MA, United States

Savvina Loutatidou
Masdar Institute of Science and Technology, Abu Dhabi, United Arab Emirates

Francesca Macedonio
Institute on Membrane Technology (ITM-CNR), National Research Council, c/o The University of Calabria, Rende CS, Italy; University of Calabria, Rende, Italy

Bhekie B. Mamba
University of South Africa, Florida, Johannesburg, South Africa

Shefaa Mansour
Khalifa University of Science and Technology, Abu Dhabi, United Arab Emirates

Musthafa O. Mavukkandy
Khalifa University of Science and Technology, Abu Dhabi, United Arab Emirates

Sabelo D. Mhlanga
University of South Africa, Florida, Johannesburg, South Africa

Karan H. Mistry
Massachusetts Institute of Technology, Cambridge, MA, United States

Edward N. Nxumalo
University of South Africa, Florida, Johannesburg, South Africa

John D. Orbell
Victoria University, Melbourne, VIC, Australia

Bryce S. Richards
Karlsruhe Institute of Technology (KIT), Karlsruhe, Germany

Andrea I. Schäfer
Karlsruhe Institute of Technology (KIT), Karlsruhe, Germany

Mostafa H. Sharqawy
University of Guelph, Guelph, ON, Canada

Gregory P. Thiel
Massachusetts Institute of Technology, Cambridge, MA, United States

Tumelo G. Tshabalala
University of South Africa, Florida, Johannesburg, South Africa

PREFACE

Simply put, desalination (or desalinization) is the process of extracting fresh, potable water from saline water. The latter can be seawater or saline groundwater (referred to as brackish water). This separation of salt and water is typically achieved via two main technology streams: thermal and membrane-based desalination. The former involves boiling the saline water, then condensing and recovering the salt-free vapor, while the latter employs a membrane barrier that allows either the water or salt to pass through selectively. Reverse osmosis (RO) and electrodialysis are examples of the former and latter membrane types, respectively. Both thermal and membrane-based desalination technologies are energy intensive. A seawater RO plant, the most energy efficient desalination technology today, consumes an average of 4 kWh/m^3 of fresh water produced. That is approximately equivalent to the energy consumed while using a household iron continuously for 2 h. The cost of this energy, together with capital cost recovery, make up 60%–80% of the levelized cost of fresh water produced. Despite its energy intensity and cost, desalination was—and still is—an attractive solution for many regions suffering from water scarcity, especially those with abundant fossil fuel resources.

It is no surprise then that the birth place of utility-scale, large desalination plants is the Middle East, specifically, the oil producing Arabian Gulf countries (also known as Gulf Cooperation Council (GCC) countries). Reliance on desalination for potable water supply in some GCC countries has grown so much, it now constitutes more than 90% of total potable water supply in those countries. This by no means suggests that desalination is uniquely a Middle Eastern phenomenon. The United States, Spain, China, Australia, and Singapore are just examples of countries with a strongly growing desalination portfolio. In fact, over the last 20 years, the total global desalination capacity has increased by more than 15-fold. This tremendous growth was accompanied by a plethora of exciting innovations that helped improve the energy efficiency and cut the cost of desalination. New membranes, energy recovery devices, and effective pretreatment technologies are examples of those innovations. While these developments helped make desalination much more affordable than it used to be 30 years ago, it is still not a sustainable choice for all. Today's desalinated water cost of USD \$0.5–0.7/m^3, achievable by state of the art seawater RO plants, is still too high to bear for citizens of many developing countries, the same countries in a dire state of water scarcity. Truth is, fossil fuel-rich countries are also concerned about the sustainability of desalination as a long-term solution for water supply. With the oil age inevitably coming to an end one day, alternative energy sources will be needed to power the ever-increasing desalination plants. But, it is not only the depletion of energy that is worrisome as far as desalination is

concerned. The massive amounts of greenhouse gases emitted in the process of generating that energy are another major issue. Brine discharge from desalination plants, intake and outfall infrastructures, and their marine life disruption, topped with an array of intertwined sociopolitical impacts, are all detrimental to the sustainability of desalination. Today more than ever, a serious discussion on the sustainability of desalination and the promotion thereof is critical. This book is a humble start.

The last decade has witnessed a surge of emerging processes and concepts that were hoped to become sustainable alternatives for "traditional" desalination. These range from innovative, exploratory prototypes, such as moisture harvesting from ambient air, to the -closer-to-market solar-powered RO. There is no single metric against which the viability of all these emerging processes can be assessed. What we can have instead is an understanding of the issues of concern and how they apply vis-à-vis *any* desalination process. In this text, authors who are leaders in their respective fields were invited to write about various aspects of desalination sustainability. While the content of that text is by no means sufficient to cover the subject of desalination sustainability comprehensively, it sheds light on some of the technical, sociopolitical and environmental issues of concern. "Introduction: What is Sustainable Desalination?" chapter of this book elaborates on the concept of desalination sustainability and its underlying elements. "Membrane-Based Desalination Technology for Energy Efficiency and Cost Reduction" chapter looks into the hybridization of third-generation membrane-based desalination technologies with RO for improved energy efficiency and cost reduction. "Autonomous Solar-Powered Desalination Systems for Remote Communities" chapter focuses on assessing the sustainability of autonomous solar-powered desalination systems for remote communities. Such communities face infrastructure challenges in water provision, which provides unique opportunities for the implementation of autonomous, small-scale decentralized systems. "Thermodynamics, Exergy, and Energy Efficiency in Desalination Systems" chapter presents a simple, yet practical introduction of the tools necessary to analyze the thermodynamics and exergy of desalination systems. Such an approach is instrumental in assessing the energy efficiency of any desalination process. "Brine Management in Desalination Plants" chapter elaborates on brine management options in desalination plants. Brine discharge is one of the most cited environmental impacts of desalination and can be a show-stopper in permitting new desalination plants. And, on the subject of brine management, "Advanced Membrane -Based Desalination Systems for Water and Minerals Extracted From the Sea" chapter focuses on process intensification of membrane based desalination systems for both fresh water recovery and valuable minerals extraction from brine. Such an approach could lead to better process economics, less brine to handle, and enhanced overall process sustainability. "Nanoparticle Incorporation into Desalination and Water Treatment Membranes—Potential Advantages and Challenges" chapter dives into the world of nanomaterials and their growing use in desalination and water treatment membranes. Nanomaterials carry much promise in

terms of enhancing membrane flux and selectivity, as well as fouling reduction. The potential advantages and challenges of their use are discussed. One nanomaterial of particular interest is carbon nanotubes (CNTs). Hence, "Prospects and State-of-the-Art of Carbon Nanotube Membranes in Desalination Processes" chapter was dedicated to presenting the prospects and state-of-the-art of CNT membranes in desalination. "Harmful Algal Blooms: Threats to Sustainable Desalination and Early Warning Solutions" chapter is dedicated to harmful algal blooms (HABs) (also known as the red-tide phenomenon). HABs can seriously interrupt the operation of desalination plants, thus constituting a threat to the sustainability of desalination. So, this chapter discusses early warning solutions based on remote sensing. "Desalination as a Municipal Water Supply in the United States" chapter discusses desalination in the USA. Desalination in the USA is growing, with much of it applied to brackish water. The economic, legislative, environmental, and energy issues surrounding the application of desalination in the United States are discussed. Finally, "Commercialization of Desalination and Water Treatment Technology: Shining a Light on the Path From Research Project to Intellectual Property Acquisition" chapter attempts to answer the pressing question: "How does one move a new desalination concept from a research project to intellectual property acquisition, and then commercialization?"

Finally, I would like to express my sincere thanks and gratitude to the chapter authors of this book. This project would not have happened without their wonderful contributions. Their generosity in offering their valuable time and expertise, and in meeting all the deadlines despite their busy schedules, culminated in the successful publication of this book.

I now leave it in the hands of the reader to dive in!

Hassan A. Arafat

CHAPTER 1

Introduction: What is Sustainable Desalination?

Savvina Loutatidou*, Musthafa O. Mavukkandy*, Sudip Chakraborty*†, Hassan A. Arafat*
*Khalifa University of Science and Technology
†Università della Calabria, Rende, Italy

Contents

1. DESALINATION AND THE GROWING WATER SECURITY CONCERNS

Freshwater availability is critical for communities around the world, not only for covering their basic needs for potable water and irrigation but also for economic growth functions, such as energy production, tourism, and transportation. Prolonged failure to bring safe fresh water to a continuously thirsty world will inevitably lead to hardships, spread of diseases, and shorter life expectancy for the affected populations. This indisputable fact, in combination with dramatic changes brought about by climate change, rising water pollution, and recent population growth have cemented the importance of establishing water as a reliable and affordable commodity [1].

In light of a changing global economy, the surface and groundwater resources of many regions are no longer sufficient to meet the new demand levels [2]. For example, according to the NASA Earth Observatory, in 2013, excess withdrawal rates had already caused 21 of the world's 37 major freshwater aquifers to pass the tipping point where

Desalination Sustainability
http://dx.doi.org/10.1016/B978-0-12-809791-5.00001-8

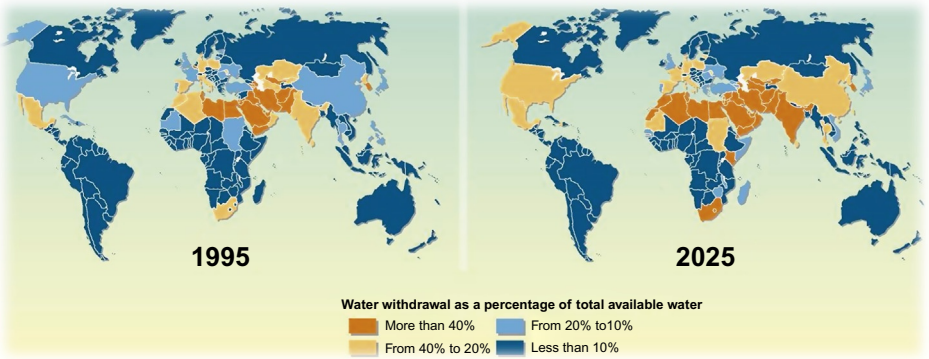

Fig. 1 Increased global water stress. *(UNEP/GRID-Arendal Maps and Graphics Library, 2009, Retrieved from: http://www.grida.no/graphicslib/detail/increased-global-water-stress_5694).*

extraction exceeded recharge [3]. As shown in Fig. 1, areas with considerable population density, particularly in the Mediterranean region, the Middle East, and South Asia, suffer from acute water scarcity. Initially, one could deduce that this scarcity is a predictable and thus controllable outcome of unsustainably using a finite natural resource. However, as millions of people in water-stressed areas are discovering, the regions suffering from depletion of existing freshwater sources keep widening, and the drive behind their water stress is not always easy to predict. For example, unprecedented prolonged droughts have affected myriads of communities residing in areas from Southern Africa to several Latin American counties and from large parts of rural China to urban centers of Australia. Another example of how water stress is posed by unforeseeable events is the massive displacement of people in the Middle East and North Africa that can spike the water demand in a region within a matter of months or less. Consequently, the detrimental effects of water scarcity have propelled the adoption of unconventional water supply strategies such as desalination, water imports, water reclamation, and so on [4].

Of the strategies mentioned previously, desalination—the conversion of saline water from oceans and brackish water sources into freshwater—is by far the most acknowledged as a credible and readily available source of water [5]. As seen in Fig. 2, 60% of all online desalination capacity provides municipalities with drinking water, and more than 30% covers industrial water demand. The accelerated awareness of water's strategic value for national security has placed desalination at the heart of the food-water-energy nexus. Water supply, energy generation, and food production are now recognized as integral elements, not externalities, of any sustainable future solution of the water crisis. Water is used for the extraction, processing, and refinement of fossil fuels and electricity generation. At the same time, energy sources are required for the pumping, moving, distribution, and treatment of water. In addition, water is a crucial input for food production, processing, and transport. Agriculture is the world's largest consumer of water resources (relevant activities account for 80%–90% of all freshwater use) [5]. The

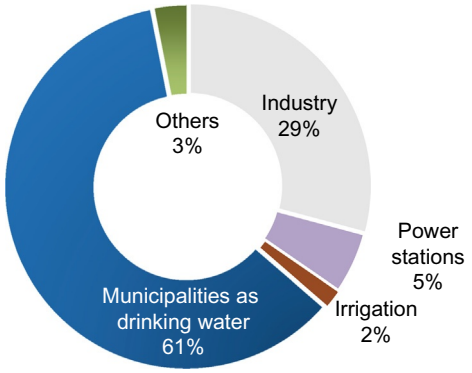

Fig. 2 Customer-type breakdown on the basis of global desalination capacity. Plants under "online," "presumed online," and "under construction" status were considered. The segment "others" includes plants for military purposes, units used in tourist facilities for drinking water production, discharge, demonstration, process, and water injection. *(Source of data: DesalData, 2016, Retrieved from: http://desaldata.com/).*

water-energy-food nexus intensity is a regional, national, or sub-national characteristic that depends on the local energy mix, demand characteristics, availability and accessibility of resource, and so on. Solving the issues of the nexus, apart from its humanitarian value, could be the one of the greatest business opportunities in the coming decades [6].

A major attraction of desalination is that it unlocks access to water sources that have previously been unsuitable for potable, agricultural, or industrial use. In most cases, this means that coastal cities can desalinate seawater for their municipal water supply (already many islands, e.g., in the Caribbean, also use desalination) and that landlocked cities can use brackish groundwater for the same purpose. These new sources of water may be more dependable and drought-proof than freshwater sources directly affected by annual or multiyear precipitation, runoff, and recharge rates [7,8]. According to the projections of the United Nations, the proportion of the world's population served by desalinated water will increase from 1% currently to 14% by 2025 [9]. Seeing that desalination will continue to be used to counterbalance impending water scarcity, its viability should be holistically assessed by policy makers, consumers, investors, and so on. In other words, a sustainability appraisal must take place to ensure that even in times of crisis, desalination is adopted as the optimal solution compared to other feasible alternatives. In a simplified manner, and drawing on the classical definition of sustainability, the main question to be asked is, "If we adopt desalination as our main source of fresh water today, can we guarantee that we don't compromise the ability of the next generations to similarly fulfill their water needs from an ecological, economic and social points of view?" The interplay of so many factors such as local, regional, and global politics, environmental constraints and regulations, future economy projections, cost of alternatives, and so on, all indicate that the realistic general answer to our question is, "It depends."

1.1 Evolution of Desalination Technology

Desalination technologies were developed over the past 50 years [1,7,10]. In the 1940s during WWII, development of desalination took a major step forward targeting mainly service to military establishments that operated in arid areas and needed a process to supply their troops with potable water. Since then, desalting—primarily of seawater—has flourished, particularly in water-scarce areas. Commercial desalination plants started making their appearance in the 1960s, mostly employing thermal processes. Among these, multistage flash (MSF) distillation technology became popular and many commercial plants were set up using this technique, especially in the Arabian Gulf. Membranes entered the desalination market in the late 1950s and electrodialysis (ED) was the first of these technologies to be developed commercially for brackish water treatment [10]. Almost at the same time, RO membranes were successfully developed and tested for desalination by researchers at the University of California, Los Angeles and the University of Florida. However, the initial RO modules were costly and were of limited capacity [11]. By the late 1960s, commercial desalination systems producing up to 8000 m^3/day—a very modest size in comparison to today's plants—had been installed in various parts of the world. Most of these installations used thermal processes [10]. However, the commercialization of polyamide thin film composite (PA-TFC) RO membranes in the 1970s, followed by the invention of energy-recovery devices, such as the pressure exchanger, in the 1990s, rapidly increased the adoption of RO desalination [12]. By the 1980s, desalination became a totally commercial enterprise and developments in both thermal and membrane technology leveraged an exponential growth in world desalination capacity. Today large scale commercial desalination plants exist in more than 150 countries, from Gulf States such as Saudi Arabia and United Arab Emirates (which are perceived as leaders of the industry's growth and maturity) to other European and Asian countries such as Spain, Portugal, Greece, China, and India [13].

Today desalination technologies are mainly classified in two main categories: thermal and membrane-based. The thermal processes utilize heat to distill the raw feed into water of very low salinity (in the form of vapor) mimicking the natural cycle of evaporation and condensation. External heat is utilized in subsequent low-pressure chambers where a fraction of the feed is vaporized and collected as distillate (final product). Membrane-based technologies, on the other hand, employ mechanical energy to create a pressure gradient across their membranes that retain most unwanted salt ions on the feed side and allow water molecules to permeate through [14].

The most mature technologies of thermal and membrane desalination are reverse osmosis (RO), multistage flash, multiple-effect distillation (MED), and ED [1]. There are also hybrid processes that combine both thermal and membrane separation mechanisms in a single unit or in sequential steps to produce potable water. An example of a hybrid technology widely used commercially is reverse osmosis combined with MSF or MED [1]. More recently developed are emerging technologies such as nanofiltration,

vapor compression, membrane distillation (MD), forward osmosis (FO), capacitance deionization, gas hydrates, adsorption desalination, pervaporation, freezing, humidification-dehumidification, solar stills, and so on [15]. Many of the emerging technologies can desalinate feeds of considerably higher salinity waters than the average seawater, making them suitable for zero-liquid-discharge (ZLD) schemes [1]. Some, for example, MD with over 50 years of relevant research, present a long history of technological advances driven by academic and commercial actors [4]. However, no aforementioned emerging technology has managed to compete on a commercial level with the mature technologies such as RO and MED, primarily in terms of cost. A breakdown on the basis of technology for all the installed desalination plants, noted as "Online" in April 2016 by the Global Water Intelligence, is shown in Fig. 3.

The current capacity breakdown of the desalination technology can be summarized as follows: RO (67%), MSF (21%), MED (7%), ED/EDR (3%), and emerging (2%) [13]. Spiral wound seawater reverse osmosis (SWRO) membrane is becoming the technology of choice for most large-scale industrial and municipal plants globally and is gaining momentum in the traditionally thermal market of the Gulf [16]. Nevertheless, unlike MED and MSF, RO lacks the ability to be coupled to power generation using by-product heat from power generation, a key advantage most pertinent to countries where low-grade heat is readily available or can be bought cheaply. Essentially, the selection of which technology to apply depends on many factors, such as the purposes of desalination, economics, the physical conditions of the plant site, raw water and product water qualities, and local technical knowhow and capacity. These factors are often changing as a result of technological developments and market drivers [17].

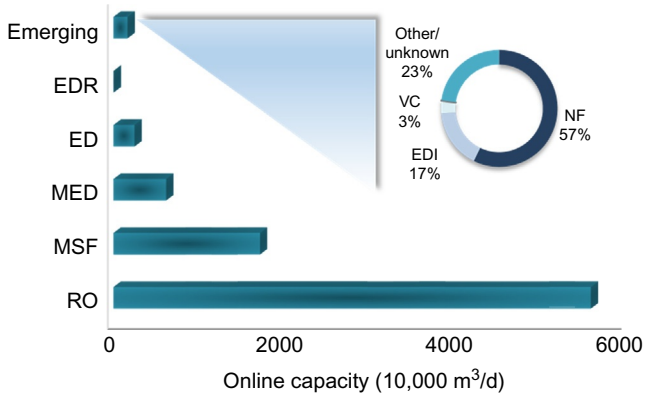

Fig. 3 Technology breakdown of the basis of installed global desalination capacity *(bar graph)*. The embedded pie chart showcases the technology breakdown of the emerging technologies plants. Plants classified as "online," "presumed online," and "under construction" status by April 2016 were considered in these statistics [13].

The following sections provide an overview of the current status of desalination vis-à-vis its relation to the three pillars of sustainability (environment, economics, and society). More in-depth discussions on some of these aspects are provided in subsequent chapters.

2. ENVIRONMENTAL IMPACT OF DESALINATION: CURRENT STATUS AND MITIGATION APPROACHES

2.1 Desalination and Global Energy Depletion

The environmental impact of desalination is indeed of concern for scientists and environmentalists across the globe [18,19]. SWRO desalination plants consume about 15,000 kWh per million gallons (kWh/MG) (4.0 kWh per cubic meter (kWh/m^3)) of water generated. The aforementioned estimates denote the energy demand of the desalination plants under standard operating conditions. The actual energy consumption may vary based on the actual process conditions, which are often not ideal and can be even higher than the reported energy consumption figures [20]. Furthermore, gross energy demand of a seawater desalination scheme depends largely on the objective that it seeks to accomplish, that is, replacement of the existent water supply with a pragmatic water source that endorses sustainable industrial and agricultural development. However, generation of a new water source more often than not leads to surplus energy consumption apropos of delivery, use, and disposal of the as-produced water [20]. Table 1 summarizes the comparison carried out between RO and other available desalination technologies such as MSF and MED, keeping energy consumption in perspective.

The energy requirements of a potential desalination scheme are governed by various factors pertaining to site selection and desalination plant design. Design aspects include the technology engineered or employed to carry out desalination, the energy recovery devices employed to bring about sizable energy recovery, and the rate of freshwater recovery (that is, the volume of treated water or fresh water generated per volume of brackish water or seawater drawn into the treatment plant). Site-specific considerations include the temperature of water at the inlet, salinity of source water, and the desired attributes of the treated product water [20]. In this regard, Fig. 4 provides an approximate estimate of the energy consumed by different elements of an RO-based desalination process.

The RO-based desalination process consumes nearly 70% of the total energy used, while pretreatment and posttreatment account for about 13% of the overall energy load. The remaining 7% of the energy consumed is ordinarily used to pump the saline feed water to the desalination plant through an intake system [20].

Given the escalating demand for fresh water, suitable technological modifications or advances in the existing desalination techniques are necessary in order to reduce the energy requirements for desalination and increase the efficiencies and cost-effectiveness of the desalination processes [21]. The past decade has witnessed considerable decline in

Table 1 Energy consumption by various desalination technologies

Technology	Type of energy	Energy requirement (kWh/m^3)[a]	Type of feed water
RO	Mechanical energy	Seawater (SW): 4–8 (el) Brackish water (BW): 2–3 (el)	SW or BW[b]
MSF	Electrical (stand-alone or cogeneration)	3.5–5.0 (el)	
	Thermal and mechanical energy (stand-alone)	69.44–83.33 (th)	SW
	Thermal and mechanical energy (with cogeneration)	44.44–47.22 (th)	
MED	Electrical energy (stand-alone)	1.5–0.5 (el)	SW or BW
	Electrical energy (with cogeneration)	1.5–2.5 (el)	
	Thermal energy (stand-alone)	41.67–61.11 (th)	
	Thermal energy (with cogeneration)	27.78 (th)	
ED	Electrical energy	1.7 (el)	BW

Data cataloged from T. Mezher, H. Fath, Z. Abbas, A. Khaled, Techno-economic assessment and environmental impacts of desalination technologies, Desalination 266 (2011) 263–273; T. Younos, K.E. Tulou, Energy needs, consumption and sources, J. Contemp. Water Res. Educ. 132 (2005) 27–38.

[a]"el" and "th" denote electric and thermal energy, respectively.

[b]*SW*, seawater; *BW*, brackish water.

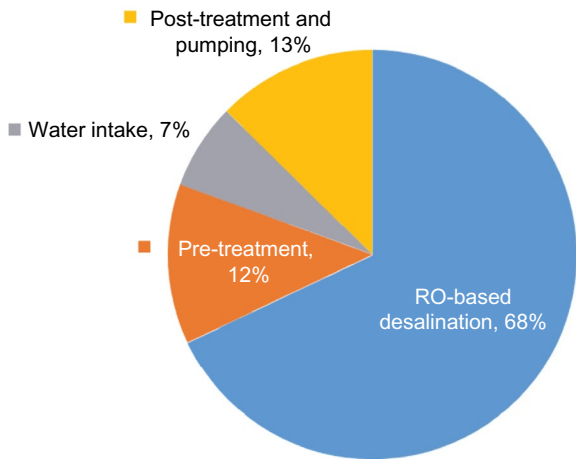

Fig. 4 Energy consumed in different stages of an RO-based desalination process. *(Source of data: H. Cooley, M. Heberger, Key Issues in Seawater Desalination in California: Energy and Greenhouse Gas Emissions, Pacific Institute, Preservation Park Oakland, California, 2013).*

the energy requirements of a desalination process, following the incorporation of pragmatic technological alterations. For instance, amalgamation of Pelton impulse turbines (PITs) with an RO-based desalination scheme brings about effective energy conservation, while integration of a conventional RO plant with hydraulic turbochargers leads to sizable energy recovery [22]. The PIT-RO combination is illustrated in Fig. 5. Pressure exchangers are now considered the state of the art in energy recovery devices in RO plants.

Nevertheless, the potential for a reduction in the consumption of energy in desalination plants is still widely possible. There is no possibility for reduction in energy consumption beyond a certain theoretically determined minimum energy requirement level. Still, the current desalination plants operate at three to four times their respective theoretical minimum energy requirement levels [20].

The production of electrical energy for RO plants is often achieved by conventional power plants, which rely on burning fossil fuels, thereby leading to the generation of polluting flue gases. The greenhouse gas emissions from these power plants, in turn, contribute to global warming [19]. The total quantum greenhouse gases that are emitted apropos of desalination is often termed the "the carbon footprint" of the desalination process and is expressed as the carbon dioxide equivalents (CO_2e) obtained either directly and indirectly from all activities, accumulated over the various life stages of the desalination project [23]. These greenhouse gas emissions can be eliminated or mitigated to a considerable extent once the desalination projects are suitably modified. In this regard, the desalination techniques can be powered using appropriate innocuous renewables, such as solar energy, tidal energy, geothermal energy, wind energy, and ocean thermal energy conversion methods [22,24]. Table 2 shows a comprehensive evaluation of the available renewable energy sources (RES) apropos of the possibilities for powering desalination plants.

These futuristic alterations may assuage certain energy-related bottlenecks pertaining to the operation of a desalination plant. RES can therefore be employed to minimize or reduce the existing greenhouse gas emissions. Nevertheless, if the larger context is kept in

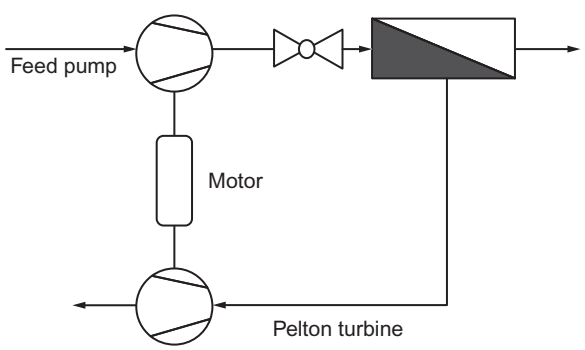

Fig. 5 Amalgamation of reverse osmosis (RO) with pelton impulse turbine (PIT) [22].

Table 2 Evaluation of various renewable energy inputs keeping the criteria for development and effective implementation of desalination processes

Criterion	Solar thermal energy	Photovoltaics (PV)	Wind energy	Geothermal energy
Competence for powering desalination technologies	Suitable for both desalination processes that require thermal power (for instance, multieffect distillation) and desalination techniques, such as RO, which mandate the use of electrical power. Solar thermal energy-powered RO is essentially more energy-efficient than Solar thermal energy-powered MED. (3)	Suitable for electrical power-driven desalination units, such as RO and electrodialysis (ED) desalination systems. (3)	Suitable for electrical power-driven desalination units, such as RO, ED, and mechanical vapor compression (MVC) thermal distillation-based desalination systems. (3)	Adequately suited for desalination plants that require thermal power. A high-pressure source of geothermal energy allows direct application of shaft power on desalination systems that are driven mechanically. Electrical power generated using high-temperature geothermal fluids is used to drive RO, ED, and MVC plants. (3)
Availability of suitable site and resources	Requirements conform satisfactorily to the criteria necessitated by desalination. (3)	Requirements conform satisfactorily to the criteria necessitated by desalination. (3)	Availability of resources depends considerably on location. (2)	Availability of resources delimited considerably by location. (1)

Continued

Table 2 Evaluation of various renewable energy inputs keeping the criteria for development and effective implementation of desalination processes—cont'd

Criterion	Solar thermal energy	Photovoltaics (PV)	Wind energy	Geothermal energy
Continuity of energy or power output	Power or energy output is ordinarily intermittent, thereby necessitating storage of energy. (1)	Power or energy output is ordinarily intermittent, thereby necessitating storage of energy. PV modules are, as such, equipped with suitable ancillary energy storage devices, such as batteries. (1)	Power or energy output is ordinarily intermittent, thereby necessitating storage of energy using equipment such as batteries. (1)	Geothermal power is continuous. (3)
Predictability of energy or power output	Relatively variable or unpredictable energy or power output. (2)	Relatively variable or unpredictable energy or power output. Power-conditioning devices, such as charge controllers and inverters, are hence required. PV modules, however, have a shelf life of about 20–30 years. (2)	Fluctuations in wind power considerably high and, as such, necessitate the use of a suitable control unit coupled with a battery system. (1)	Power output is adequately predictable. (3)

Note: 3: Substantial conformity to criterion; 2: Satisfactory conformity to criterion; 1: Poor or inadequate conformity to criterion.
Data compiled from A. Al-Karaghouli, L.L. Kazmerski, Energy consumption and water production cost of conventional and renewable-energy-powered desalination processes, Renew. Sustain. Energy Rev. 24 (2013) 343–356; M. Eltawil, Z. Zhengming, L. Yuan, Renewable energy powered desalination systems: technologies and economics-state of the art, in: 12th International Water Technology Conference, Alexandria, Egypt, 2008, pp. 1–38.

perspective, these RES are also marked by their own environmental, economic, and social costs [20].

Despite being environmentally benign and abundant, RES suffer from some serious handicaps, which inadvertently preclude their widespread commercial application in desalination systems [20,21]. The capital costs accompanying these renewable energy systems, for instance, are still quite exorbitant, and this in turn brings about sizable escalation in the cost of the water produced using desalination processes. Therefore scientific investigations of desalination processes are currently focused on potential avenues for future technological advances that might lead to a significant reduction in the capital costs of renewable energy systems, thereby significantly reducing water production costs [21]. Table 3 outlines energy demand or consumption and water production costs estimated for RES-desalination combinations.

Alternative desalination strategies, such as MD, FO, hybrid membrane-thermal desalination systems, and efficient waste heat or low-grade heat utilization, all have the potential to bring about an effective reduction in energy consumption. Fig. 6 delineates a schematic of a FO system. The FO process usually employs a suitable highly concentrated draw solution, wherein the activity of the draw solution is higher than that of the feed solution. This in turn induces the transport of water across the FO membrane via osmosis. Following the attainment of dynamic equilibrium, the components of the draw solution are separated from the fresh water [20].

The alternative desalination strategies offer a number of advantages over conventional desalination systems. For instance, the unpressurized FO systems are usually characterized by relatively lower operational and maintenance expenses than the RO-based desalination systems. Also, fouling of membranes, which severely impedes the treatment process in pressure-driven RO systems, is considerably mitigated in FO systems. Therefore FO treatment units demonstrate a relatively higher treatment efficiency than the conventional RO systems. However, these alternative desalination techniques are not entirely free of techno-economic drawbacks. The commercial-scale application of FO, for instance, is considerably constrained by the difficulties encountered while identifying and selecting a suitable draw solution and FO membrane. Thus implementation of these new-generation desalination techniques is currently restricted mostly to laboratories and pilot-scale facilities. Nevertheless, these techniques hold great promise in fields that cater to exploration and development of energy-efficient desalination [20]. Wherever possible, communities should also take into consideration other energy-efficient options, such as water reuse, storm water collection or capture, and rainwater harvesting [20].

2.2 Water Intake and Brine Discharge

Numerous studies have investigated the environmental impact of discharge from desalination plants on marine ecosystems [12,25]. These scientific appraisals have

Table 3 Energy requirement and water production costs pertaining to renewable energy sources (RES)-desalination combinations

RE-desalination process	Typical capacity of reported systems (m^3/day)	Energy demand (kWh/m^3)	Reported water production cost (US$/$m^3$)
Solar still	<100 Production rates: 4–6 L/(m^2 day)	Solar passive	1.3–23.80
Solar multieffect humidification (MEH)	1–100	Thermal: 29.6 Electrical: 1.5	2.6–6.5
Solar membrane distillation (MD)	0.15–10	45–59	10.5–19.5
Solar pond/MED	20,000–200,000	Thermal: 12.4–24.1 Electrical: 2–3	0.71–0.89
Solar pond/RO	20,000–200,000	Seawater: 4–6 Brackish water: 1.5–4	0.66–0.77
Solar concentrating solar power (CSP)/ MED	>5000	Thermal: 12.4–24.1 Electrical: 2–3	2.4–2.8
Solar PV/RO	<100	0.89–13 (based on reported energy statistics of installed plants) Seawater: 4–6 Brackish water: 1.5–4	11.7–15.6 6.5–9.1
Solar PV/ electrodialysis reversal (EDR)	<100	1.5–4	10.4–11.7
Wind/RO	50–2000	Seawater: 4–6 Brackish water:1.5–4	6.6–9.0 small capacity/1.95–5.2 for 1000 m^3/day
Wind/MVC	<100	7–12	5.2–7.8
Geothermal/MED	80	Thermal: 12.4–24.1 Electrical: 2–3	2–2.8

Data cataloged from A. Al-Karaghouli, L.L. Kazmerski, Energy consumption and water production cost of conventional and renewable-energy-powered desalination processes, Renew. Sustain. Energy Rev. 24 (2013) 343–356; A. Al-Karaghouli, D. Renne, L.L. Kazmerski, Solar and wind opportunities for water desalination in the Arab regions. Renew. Sustain. Energy Rev. 13 (2009) 2397–2407.

reported that major desalination plants directly extract water from the ocean by way of open water intakes. Consequently, marine fauna, such as fish, are inadvertently killed following impingement on intake screens. Smaller organisms such as larvae, fish eggs, and plankton, on the other hand, manage to pass through but are eventually killed following entrainment during saltwater processing [12,25]. The adverse effects

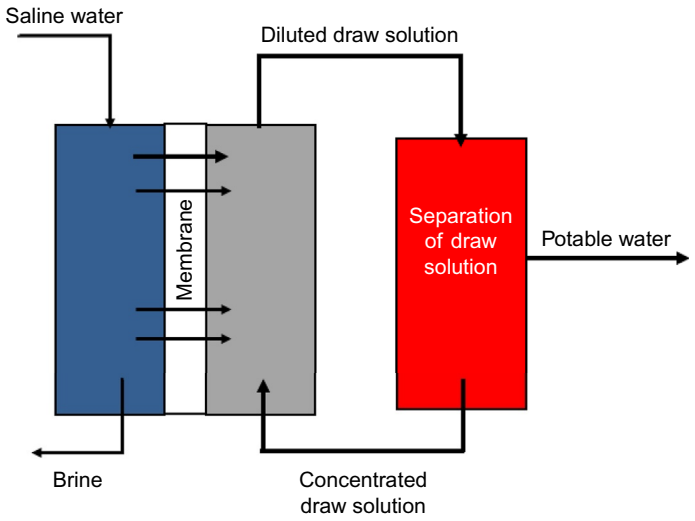

Fig. 6 Schematic of forward osmosis system [20].

or damage inflicted on the marine organisms and environment are usually influenced by diurnal, seasonal, or annual fluctuations in process conditions and are ordinarily site-specific and species-specific [25].

Therefore, several technological, operational, and design-based measures have been engineered and endorsed with an aim to mitigate the impact of the desalination plants' intake. For instance, the adoption of subsurface intake-based seawater extraction technology virtually eliminates entrainment and impingement, and consequentially reduces the impact on marine life that usually accompanies direct or open-water intake technology. The subsurface intakes are ordinarily marked by substantial seawater extraction from beneath the seafloor or beach, and may be positioned either onshore or offshore [25]. The sand functions as a natural prefiltration unit and facilitates sizable removal of silt, debris, algae, and other unwanted solid materials, besides reducing energy consumption and long-term operational costs. However, these subsurface intake systems are site-specific. Nevertheless, the employment of recently developed pragmatic drilling techniques, such as directional drilling, can enable the detection of potential extraction sites, even in locations where the surrounding conditions are unfavorable [25].

Another major environmental challenge pertains to the disposal of brine, or highly concentrated salt-laden process waste stream containing spent cleaning agents or solutions containing toxic chemicals [12,25]. In particular, major coastal desalination facilities usually release their respective concentrates into estuaries and oceans. The brine thus discharged is typically almost twice as saline as the receiving waters. Also, the density of the discharged brine is usually higher than that of the receiving waters. Therefore the brine manifests a propensity to sink and gradually spread along the floor of the ocean, to the

detriment of the benthic habitat [25]. Moreover, such discharge schemes lead to substantial increase in temperature and salinity and induce the accumulation of hydrocarbons, heavy metals, and other toxic antifouling chemicals in the receiving aquatic environment, thereby posing grave threat to marine ecosystems [12,26].

Studies attempting to monitor the ecological attributes of the marine environment have also revealed that the ecological impact of desalination plant discharges tends to vary considerably. For instance, the benthic community is usually not significantly affected, whereas the structures of marine soft-sediment communities, including coral reefs and seagrass ecosystems, undergo pronounced structural distortion following the release of ecotoxic desalination plant discharges into inadequately flushed marine milieus [12].

Effective measures therefore need to be implemented in order to ensure safe disposal of desalination concentrates and other toxic components present in the discharge from desalination plants. For instance, highly concentrated brine can be reasonably dispersed by means of multiport diffusers mounted on the discharge pipe. Such arrangements promote effective mixing. Brine dilution is also brought about by using treated effluents from a suitable wastewater treatment plant or by cooling water from power plants. Additionally, a sizable reduction in the quantity of chemicals used during desalination can mitigate the adverse environmental impact of desalination plant discharge. Pretreatment of the extracted source water, in particular, by means of environmentally benign membrane-based techniques, such as microfiltration and ultrafiltration, can considerably reduce the application of chemicals in the course of desalination. In this regard, development and use of membranes exhibiting reasonable fouling resistance can presumably lead to a decrease in the necessity for toxic antifouling chemicals. In addition, existing and newly developed coastal desalination plants can be suitably equipped with competent zero-liquid-discharge schemes that induce the evaporation of water from the desalination concentrates, thereby leaving only salt residues. Eventually, these residues can be safely disposed of or reused [25].

Effective monitoring and mitigation of the environmental impacts of desalination, moreover, entails comprehensive interpretation of discharge milieus apropos of desalination plants. A standard bottom-up environmental impact assessment (EIA) technique can be employed in such cases to evaluate and minimize the adverse impact of desalination on the receiving environment [27]. The effectiveness of EIA procedures is influenced primarily by the availability of adequate reference materials and the application of a pragmatic methodological strategy that subscribes adequately to the specifications and mandates of desalination projects. These attributes or measures facilitate the desalination-oriented application of EIAs on a much wider scale. The pertinent EIA procedures should therefore include the primary information on all principal impact of the desalination process. Also, a suitably tailored modular configuration can be incorporated to facilitate meticulous monitoring of the environmental impact engendered by each

desalination project. Additionally, the EIAs should be equipped with a scientific paradigm that can evaluate and assess the data obtained from before-after and control-impact monitoring activities and a decision-making strategy that balances the advantages and impacts or bottlenecks of desalination against those of other options available for water supply [27].

3. ECONOMIC SUSTAINABILITY OF DESALINATION

3.1 The Financial Aspects of Desalination

The desalination market has seen unprecedented growth in the past decade as coastal communities around the world are turning to seawater desalination (and to a lesser extent to brackish inland aquifers) to cover their water demand. Frost and Sullivan's analysis published in September 2015 predicted that the world's investment in desalination will double by 2020 [28]. As shown in Fig. 7, the top desalination markets between 2010 and 2015 were Saudi Arabia and China, followed by the United States, Israel, and India. Other countries investing heavily in desalination include Algeria, Spain, Australia, Kuwait, and the United Arab Emirates. Though building the capacity for desalination is a substantial cost for all these countries, many of the end users are in low-economic brackets. Lowering the cost of desalination is therefore essential to public authorities, operators, and end users.

The expenses incurred in desalination are spread over many stages: from R&D and design to construction and operation. The cost of a desalination plant comprises two main

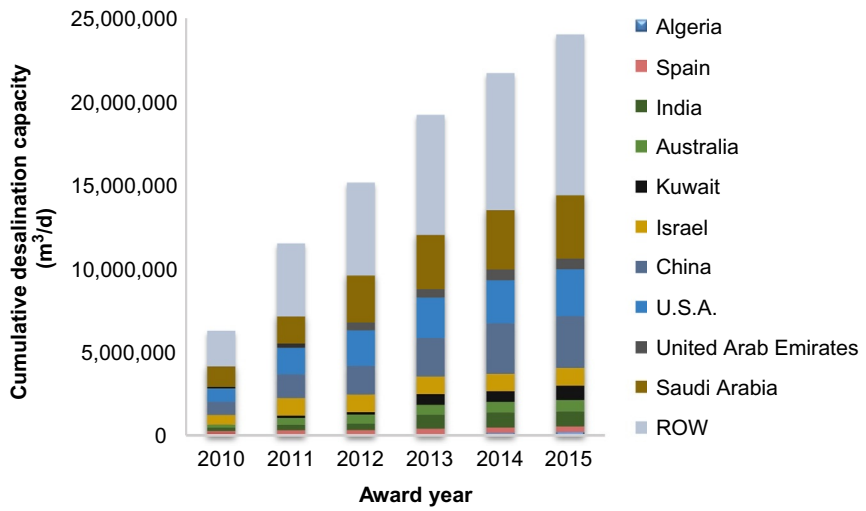

Fig. 7 Cumulative desalination capacity awarded between 2010 and 2015 for the 10 countries where the highest investment in desalination was observed in the same period [13]. "ROW" denotes "rest of world" with records of desalination plants awarded during the same period.

elements: the capital and the annual operating cost [11]. The operating cost, otherwise referred to as OPEX, is primarily determined by the cost of the energy utilized to power the plant and is naturally sensitive to fluctuations in energy prices. The capital cost (CAPEX), on the other hand, is incurred once, at the beginning of a plant's life. CAPEX consists of indirect and direct costs. Direct capital costs comprise the purchase cost of major equipment (e.g., high pressure pumps), the cost of auxiliary parts, land cost, engineering cost, and so on. The indirect capital costs include elements such as freight and insurance, construction, overhead, and so on [29]. The plant's amortized CAPEX and annual OPEX divided by the average annual production of desalinated water is referred to as the levelized cost of water (LWC), a common indicator used to compare the different desalination plants or options. It is very likely that other indirect costs (e.g., economic externalities, environmental externalities) are included in LWC values [30].

A number of different contract packages have been successfully implemented in the desalination industry. The recent trend of building large-capacity plants has directed governments to collaborate with the private sector, forming public-private transaction schemes referred to as independent water and power producers [31]. Other common project delivery schemes include Engineering, Procurement, Construction (EPC) and build-own-operate-transfer (BOOT). An EPC contract is formed by a direct agreement between the client and the EPC contractor. The EPC cost includes all the direct capital costs (apart from land cost) of the plant plus the EPC contractor's cost for services. The EPC services include detailed design, contractor permitting, and project-management costs. In return, the EPC contractor must deliver the project (the desalination plant) for a fixed contract cost and by a fixed date in such a way that the plant's final performance will be the same as the one guaranteed by the contractor in terms of output quantity, output quality, efficiency, and reliability [29]. In the EPC system, funds will be provided by the client based on the client's estimation. The contractor must execute the project per the expectations of the client.

BOOT contracts, on the other hand, are privately financed but with government guarantees [32]. Typically, in BOOT contracts, the water tariff is split between a CAPEX recovery component (meant to recover the CAPEX costs) and an O&M (operations and maintenance) component compensating for the variable O&M expenses, including those associated with energy demand. Increasing private sector's involvement helps transfer some of the project risk from the government to the private sector companies. In a BOOT contract, the contractor provides the funds, and based on the project's viability, the contractor can collect a fee from users for a specified period in order to recoup its funds. In a design, build, own, operate, and transfer (DBOOT) transaction, the contactor can do value engineering based on the scope of the project and can recoup its investment as in the case of BOOT [33]. As can be seen in Fig. 8, the involvement of the private sector in desalination grew steadily over the past 25 years. Today the majority of desalination plants are privately financed under different "BO" variations.

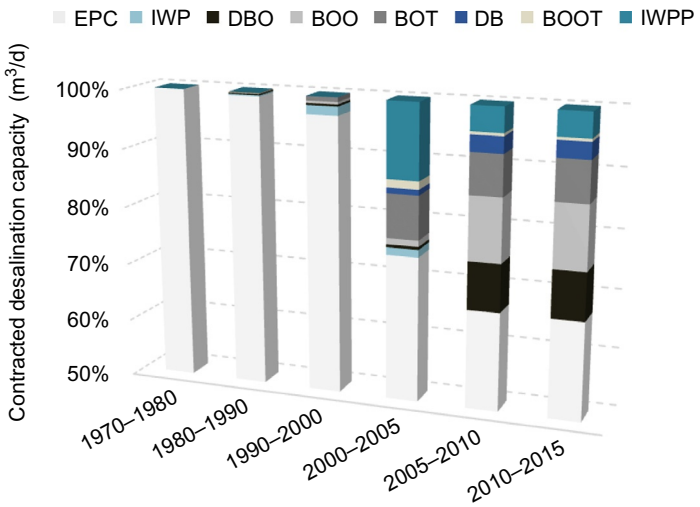

Fig. 8 Project delivery-type breakdown on the basis of global desalination capacity. The plants were allocated to the noted time periods based on their award year [13].

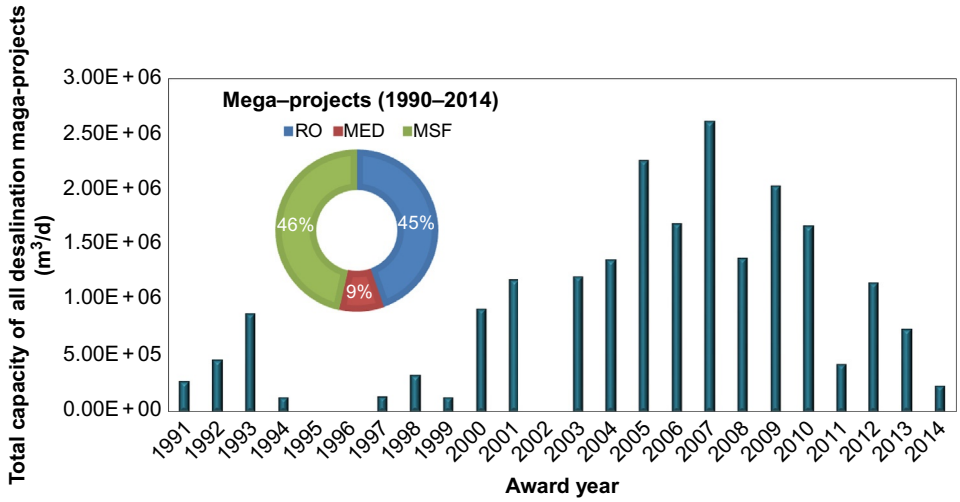

Fig. 9 Total capacity of mega-scale desalination projects that were awarded each year for the period 1991–2014. "Mega-scale" projects: installed desalination plants with a daily capacity equal to or above 100,000 m^3/day [13].

3.2 Mega-Scale Desalination

The rapid growth of the urban population increased the push for mega-scale desalination projects (which commonly refers to projects with a daily capacity of 100,000 m^3 or higher) [2,34], as illustrated in Fig. 9. Investment in mega-scale desalination started in

1991 and reached its peak in 2007. According to Global Water Intelligence, the largest online desalination plant today is a 12-unit MSF plant in Shoaiba, Saudi Arabia, that has a nominal capacity of 880,000 m^3/day [13].

Desalination's need for scalability (usually toward the mega-scale end) has greatly contributed to lower desalination costs by acting as a gateway for the private sector's involvement. Today the construction of large-scale desalination plants is possibly mainly due to commercialization of large-size off-the-shelf components such as high-pressure pumps and large energy recovery systems. The capacity of a desalination facility heavily impacts the capital cost: the larger the facility, the lower the CAPEX per unit of capacity (US$/$m^3$/day). Generally, the logic behind mega-scale projects is that one large capacity plant will be more cost-efficient—in terms of equipment, labor, maintenance, funds, and central distribution system—than multiple smaller capacity plants. This is particularly true with regard to mature desalination technologies with proven longevity. For example, once-through brine recirculation MSF plants can exceed a 30-year lifetime with carbon steel material. These are only competitive for 12-MGD (million gallons per day) projects and upward [17].

Privatization of desalination projects began in the Middle East at the end of the 1990s but has now become the main trend, particularly as a significant number of countries embark on mega-scale desalination for the first time [35]. Securing investments for development of large-scale water projects can be difficult, particularly in developing countries where access to governmental funds is limited. In addition, the recent financial crisis (beginning in 2008) spurred renewed interest in including the private sector in large-scale investments through public-private partnerships (PPP), in both developed and developing countries. In this way, many of the risks and delays are delegated to the private sector, and capital for public infrastructure can be raised without adding to the national debt. If the projects is state-owned, bidding can help governments utilize public funds transparently by granting the project to contractors on the basis of quality of service and cost-effectiveness. However, bidding is time- and money-consuming for both owners and candidate contractors. Alternatively, projects can be awarded without bids, and contractors are selected on the basis of previous activities, acquaintances, recommendations, and other criteria [36].

Given the return that such projects can yield, it is no wonder that the desalination industry has moved fast to cover the market niches where increased equipment unit sizes can leverage economy-of-scale advantages, for both thermal and membrane technologies [17]. Similarities in offered products and services along with new entrants are intensifying the competition and driving down prices, ultimately lowering the desalination's costs. For example, as shown in Fig. 10, the normalized EPC cost is very close for projects awarded to three leading BWRO contractors in the GCC region. Moreover, the average cost steadily declined from 1985 to 2013. This trend reflects how the accumulation of experience has mitigated many technological and managerial risks for new desalination

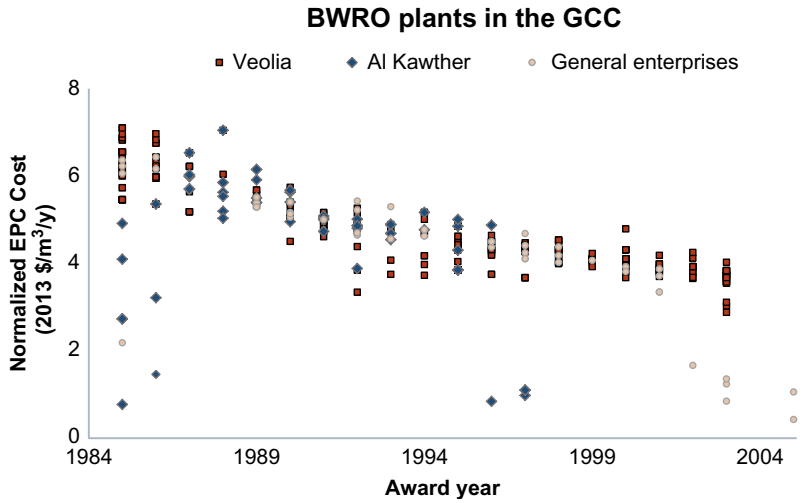

Fig. 10 Normalized EPC cost from 1985 to 2005 for three of the leading companies, in terms of number of contracts, in the GCC region for BWRO plants. *(Adapted from S. Loutatidou, B. Chalermthai, P.R. Marpu, H.A. Arafat, Capital cost estimation of RO plants: GCC countries versus southern Europe, Desalination 347 (2014) 103–111, doi:10.1016/j.desal.2014.05.033).*

projects and has lowered capital costs. In all new projects, the contractors' engineers and consultants had already established the information needed to avoid delays in the project development and had more experience in choosing equipment manufacturers, the companies' R&D departments introduced new and more cost-effective solutions, and so on [29]. It should be noted, however, that there are always practical limitations for capex and opex reduction because of a site's feed (raw water quality, fouling and scaling propensity, temperature), intake arrangements, product specifications, and so on [33].

3.3 Innovation as a Driver for Cost Reduction

During the International Desalination Association (IDA) World Congress in 2015, an extensive reference was made to the challenge posed to the desalination industry's sustainability by the high costs of pretreatment and desalting [4]. The viability of new desalination projects and service contracts is pivotal because they draw large amounts of funds from the national budget, either directly under public financing or indirectly through guarantees under private financing. Environmental and social considerations are without doubt important, but a difference of a few cents per m^3 of water produced might have a great impact on decision-makers. In the past 20 years, technological advances, capacity building, and fierce competition between contractors, consultants, and manufacturers have decreased the unit's costs, from an average of \$1.25–\$1.50 per m^3 in the early to mid-1990s [16] to around \$0.50 for large-scale SWRO [1]. Greater cost-effectiveness of water production has also alleviated the financial burden on end users. By observing

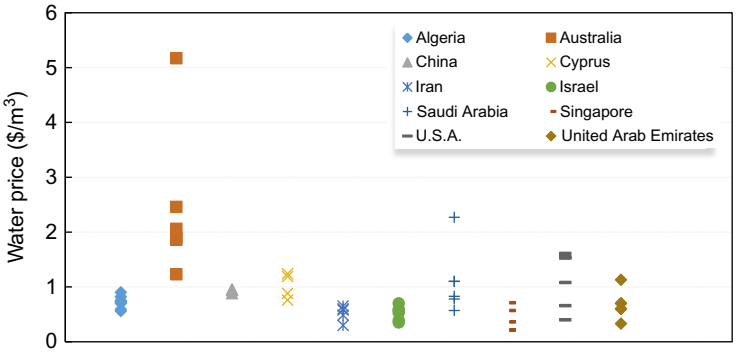

Fig. 11 Water price ranges for seawater desalination plants awarded from 1996 to 2015 in 10 different countries. The desalination plants were randomly chosen for each country. *(Source of data: DesalData, 2016, Retrieved from: http://desaldata.com/).*

the water prices for 60 randomly chosen seawater desalination plants awarded from 1996 to 2015, it can be deduced that end users rarely had to pay above $2 for desalinated water (Fig. 11). However, there are still many gateways through which desalination's financial sustainability can be improved. Following are some highlights on how innovation can lead to new opportunities for desalination investors.

Energy intensity and energy cost can have a profound effect on a desalination plant's economics [37]. Essentially, uncertainty in tomorrow's fossil fuel prices is also an uncertainty in the lifecycle cost of desalinated water. If the supplied energy becomes more costly, then desalination could become less attractive compared to other less energy-intensive options, such as water conservation, water purchases, and changes in water pricing. While energy efficiency has been commonly quoted in the past as the most effective way to reduce desalination's costly dependency on fossil fuel energy, the specific energy consumption of state-of-the-art RO (considered the most efficient technology) has already approached the thermodynamic minimum (as estimated for an RO stage, including high-pressure pumps, membranes, and energy recovery systems) [10].

Therefore, there is high market potential to support a shift from fossil-fuel-driven to renewable-energy-driven desalination systems, especially in energy-importing countries such as China or small island states [38]. The interest in renewables for desalination applications coincides with the recent expansion of the market share associated with small (10,000 m^3/day) desalination plants. Examples of where small-scale renewable-powered desalination make sense are installations at small island states, such as in the Pacific, and at isolated and remote industrial sites [39]. One should also take note of the growing establishment of hybrid electricity generation systems in developing countries that also encourages the synergy between desalting and renewables. Hybrid systems take advantage of the synergy of intermittent renewable energy production (commonly DC electricity from photovoltaic panels) and a base load fossil energy generation. Moreover,

small-scale desalination systems can take advantage of the significant advances made in positive displacement pump technology, which can typically result in efficiencies above 90% [16]. Further adding to the reliability of using renewables for off-grid operation is the high degree of automation in modern desalination plants with a number of built-in protection and safety systems for off-grid applications [33]. The global industrial market for advanced instrumentation equipment and specialized personnel is projected to grow and is an area for improvement (for example, quality permeate control with direct feed-back loop to pretreatment systems following programmed corrective measures) [10].

Regardless of the utilized energy source, the cost of desalinated water directly depends on the tariff imposed by the independent power (renewable or not) generation utility from which a desalination plant has to purchase electricity. Thus an attractive option for the plant is to take advantage of the off-peak power rate period(s), which is a common practice in many countries. Seeing that seasonal and daily water electricity demand patterns remain almost constant, a rational practice is to aim for excess water production during off-peak hours along with construction of additional storage. Sometimes the power suppliers provide additional power incentives for more aggressive power curtailment, for example 90% or more reduction of power use for a period of 6–12 h at least two times per month. In this case, the desalination plant designer and operators have to consider built-in flexibility and extra product water storage capacity to accommodate such curtailment schedules, which usually comes at increased upfront costs [33].

Consumables and equipment are other areas where the desalination market has a potential for improvement. The cost of consumables (e.g., chemicals) strongly depends on the facility's location with respect to manufacturing and distribution centers of the consumables. For equipment, such as pumps or evaporators, its function and material of construction play the most important role in their pricing [17]. Evidently, competition between desalination technology suppliers has driven the creation of innovative products that are meant to either cover market niches or improve the current performance and redefine the design standards. A report by the World Intellectual Property Organization [40] published in 2011 mentions that 25% of all desalination technology patent families established by 2011 all originated in the past 5 years. The breakthrough in SWRO by high-performance membranes is an indicative example. Previously, RO was considered to be a high-risk technology for seawater of high salinity, temperature, and fouling propensity, because severe membrane fouling or scaling can lead to prolonged out-of-service periods for a desalination plant during which no revenue will be generated by selling the desalinated water while, at the same time, fixed costs such as salaries and loan repayment will still be incurred [17]. Not only the OPEX but also the CAPEX of SWRO were greatly affected by the feed quality variations, as the design had to accommodate the worst-case scenario. However, advances in membrane element polymer chemistry and production processes have made RO membranes more durable and extended their average useful lifespan from 5 to 7 years. Similarly, seawater pretreatment using

ultrafiltration and microfiltration membrane systems is expected to further extend the membrane's useful life to over 7 years, thereby reducing replacement costs [36]. With the aging of the current pool of RO plants and with the doubling of installed capacity in the next 4 years, there is an opportunity for membrane replacement and retrofits.

Finally, the choice of materials for the main equipment units can also yield opportunities for cost reduction. For example, adoption of new materials such as super duplex or super austenitic alloys for high-pressure components of the SWRO can extend the equipment's useful life beyond its originally estimated operational period and subsequently reduce the overall lifecycle cost. In thermal technologies, material selection is critical because it governs the CAPEX of an installation. It is projected that application of materials with improved properties will also make a difference in the economics of the second-generation MSF plants (installed in the past 20 years) by making them last more than 40 years with maximum availability [17]. In addition, there is increased interest in replacing metallic heat exchangers with low-temperature polymeric evaporators (able to operate below 70°C) in desalination applications [41,42]. According to a recent review of Chen et al. [43], polymeric heat exchangers (configured as thin plastic sheets or plastic tubes) feature low-cost, lightweight and high-resistance to corrosiveness. In Christmann et al. [44], the heat transfer coefficients for a falling film plate evaporator made out of the high-performance polymer polyetheretherketone (PEEK) were comparable to typical values of metallic falling film heat exchangers at MED process conditions. However, there is need for further testing of such heat exchangers for desalination applications to ensure that no scaling occurs after wetting and adequate mechanical stability.

4. SOCIETY AND DESALINATION

4.1 Case Studies

Although desalination enables communities to produce fresh water from an almost unlimited supply of seawater or enormous amount of brackish water, only communities with affordable energy and water scarcity were able to afford it in the past because of its high cost and energy requirements. However, the cost of desalination is coming down, thanks to advancements in the technology, especially in the field of membranes. At the same time, the cost of alternative water supply options are still high, making desalination a promising solution. Nevertheless, it should be noted that substitution of a conventional water supply with desalination (of seawater/brackish water) involves changes in societal practices and therefore its social impact should be considered carefully. The high energy intensity and various environmental and societal impacts make desalination a highly debated issue. There are several cases where technically sound, environmentally benign, and economically viable desalination/water treatment options failed or faced challenges because of opposition from society. Those incidents reiterate the significance of public sentiment. Public sentiment is a product of complex synergies between many agents, for example, local public stakeholders, investors, media, and so on. Therefore, rather than

taking a fully theoretical approach in presuming potential issues and countermeasures, it might be more effective to learn from the industry's past experiences and most common faux pas cases. For this purpose, three widely publicized such cases were selected to serve as examples, as described next. Two of these examples are on wastewater reclamation for potable use. Although wastewater reuse is often cited as a viable alternative to desalination, as one can see, it can also face significant social resistance, even when advanced RO technology is used in the process.

4.1.1 The Wonthaggi Desalination Plant, Victoria, Australia

This is an example of the importance of public consultation and proactive communication between the decision-makers and the public. In 2007 an RO plant was introduced as a long-term solution to Melbourne's water security. However, people who opposed the project advocated for constructing additional dam capacity on various rivers (such as Macalister or Mitchell), using more recycled water or regulating the demand for water by various policy reforms or tariff changes. The period from 2007 to 2009 witnessed several protests and legal battles against the desalination plant with one of the major concerns being the privatization of the water. Although the local government won the legal battle in the end, the public's reactions delayed implementation of the project. The plant was finally commissioned in September 2012. But the water from the plant had to be flushed into the sea because it failed to meet the drinking water standards. After one month of trial operation and finalization of reliability testing, the plant achieved its full capacity in late 2012 [45].

4.1.2 The Singapore NEWater Project

Singapore's NEWater project is an interesting example of a country's determination to ensure its water security parallel with careful management of public opposition via various approaches, including intense public awareness programs. Although a small, rich island, Singapore heavily depended on its neighboring country, Malaysia, for drinking water [46]. This dependence became a sensitive issue in Singapore that eventually led to the exploration of alternative sources of water, resulting in the recycled water project, NEWater. The project aimed to use treated wastewater (or "used water," as referred to in Singapore) for potable applications following a thorough treatment scheme, including advanced membrane processes (including RO) and UV disinfection. However, Singapore's water authorities took people's opposition to the concept seriously, and as a result, the project started by indirectly mixing the recycled water with freshwater reservoirs, leading to indirect reuse. This was a wise decision by the project proponents, and public opposition decreased with time. Presently, four NEWater plants can meet up to 30% of Singapore's current water requirements. NEWater is expected to meet up to 55% of the country's water demands by 2060 [47]. Singapore's well-planned programs included its Public Utilities Board's (PUB) rigorous awareness campaigns, use of documentary feature film, wise utilization of all the available media, information sessions at

schools and other community centers, along with the dedicated NEWater Visitor Centre ("PUB NEWater"). PUB presented the public with examples of potable wastewater reuse in the United States (without negative health impacts), conducted and disseminated the results of over 150,000 scientific tests (including a study by an international expert panel for 2 years), and ensured that NEWater met all WHO and USEPA standards [48]. In order to reduce public anxiety, top government officials were photographed drinking the treated wastewater, and 1.5 million bottles of NEWater were circulated by the government for the public to try for themselves.

4.1.3 The Case of the City of San Diego, California

The city of San Diego depended heavily (almost 90% in 1990) on imported water supply. The water demand was expected to increase with time, and therefore a proposal was put forward (after a legal settlement in 1994) that involved building a 45 million gallon per day (MGD) water reclamation system. However, because there was not much demand for reclaimed water at that time for nonpotable uses, this proposal would have resulted in dumping excess reclaimed water into the ocean. Availability of excess reclaimed water along with the urge for water security prompted the authorities to propose a new project in which the reclaimed water would be infused into the potable water supply. Although the new proposal was approved by an expert panel and the California Department of Health Services, by 1999 the project stopped because of opposition from the public and political systems. There were several concerns about issues such as economic and racial favoritism along with the design and cost of the project and public health concerns [49]. Utilizing plants for using this reclaimed water for potable uses did not start to move forward until 2014.

4.2 Main Issues Affecting People's Attitudes Toward Desalination

Several potential issues can surface during the planning and construction phase. These include, for example, lack of trust in the developer, environmental concerns, change in land use, visual pollution, acoustic and aesthetic disturbances, disruption to recreational activities, local infrastructure such as housing and schools, risk to public safety, impact of construction on the use of roads, interruption to local business, and so on. Another set of issues can surface during the operational phase. These include impacts on the local fishing industry, as fish are killed on the intake screens by impingement while smaller microorganisms (e.g., plankton, fish eggs) are killed during later processing of water (entrainment). Moreover, the cost of water provision and public-private partnership arrangements in general are concerns. Following are some of the major issues affecting people's attitudes toward desalination:

Lack of trust in the technology: Even though there are many successful examples of RO plants with large capacity, people in certain communities will point to unsuccessful or

failed projects, such as the Tampa Bay, Florida, and the Yuma Desalter projects in Arizona, casting doubt on the viability of proposed desalination projects.

Concerns over environmental impacts: Society is more than ever concerned about the environmental impact of desalination, which were detailed earlier in this chapter. There are also instances where fisheries have declined after the introduction of large desalination projects. An example case is the decline in fisheries on the California coast since the 1970s. This decline in fisheries is due to either the shrinkage in estuaries and wetlands or poorly designed intake structures and brine discharge systems [50].

Desalinated water cost: When compared to the conventional water supply programs (e.g., groundwater or treated surface water), desalination is more costly.

Consideration of oceans as global commons: "Global Commons" denotes resources beyond the control of any single nation. There are four such global commons, namely the high seas, the atmosphere, Antarctica, and outer space [51]. Initiation of several desalination plants on/near seas makes the seas a local commodity rather than a global common. Although the benefits of the plant go to a local community, the accumulated burden of pollution and other detrimental impacts will be shared by the global community.

Concerns over privatization of water: Desalination produces expensive drinking water from a presumed free, public resource: seawater and brackish water. During the process of privatization of desalination plants, people's buying power and social equity are mostly ignored. Water is transformed from being an essential resource into an expensive commodity. This is especially true for privately owned or PPP desalination projects, as opposed to publically owned water supply projects. Most people do not welcome the idea of becoming dependent on private companies for the supply of water because it is a very sensitive and essential commodity. The problem is further complicated for communities that are accustomed to having access to free (or almost free) fresh water as a birthright.

Concerns over the quality of desalinated water: Reports show that desalinated water may contain constituents such as boron, endocrine disruptors, and algal toxins [52,53]. In some cases, the intake structures are placed next to the dumping area for sewage and storm water run-off (e.g., Huntington Beach, California). In other cases, the desalinated water may cause corrosion in pipes and other infrastructure if not alkalized properly [54].

Availability of alternative technologies/options: In general, people view water conservation and recycling/reuse of wastewater as more sustainable long-term practical solutions than seawater desalination [55]. Demand-side management is also advocated in many cases as an alternative to desalination. There are cases where desalination becomes an inevitable part of the water supply portfolio, despite public sentiment. In such cases, and in general, several measures can be considered in order to facilitate the implementation of such desalination projects smoothly.

Information management: Public perception is formed by a multitude of factors, such as information related to site-specific characteristics (socioeconomic, political, and environmental), awareness regarding various resources and technologies, and the local and global context [49]. Any uncertainty in the information may eventually have a huge influence on the overall public opinion. Therefore, authorities would be wise to ensure transparency in communicating information. In this regard, carefully designed surveys can collect details about public attitudes and concerns about desalination, which can significantly enhance the quality and effectiveness of information management.

Encouraging public participation: Public participation in decision-making and implementation of the project should be encouraged. This can eventually build the much required trust between people and the project proponents.

Better decision-making process: Sustainability evaluation of desalination, including an analytic hierarchy process (a multicriteria decision methodology) and a lifecycle assessment, can be used in order to aid the multicriteria-based decision-making. Moreover, a thorough analysis of flora and fauna around the desalination facility and a detailed plan on how to mitigate the impact on the species should be done. Various lessons learned from past experience should also be incorporated.

Social impact assessment (SIA) and social impact management plan (SIMP): SIA involves identification of various social and economic impacts that could occur during the construction and/or operation of the desalination plant. It also includes the evaluation of the predicted impacts and identification of various management measures for the predicted impacts. A social impact management plan (SIMP) can then be prepared enlisting all the possible solutions to the predicted impacts.

Adaptive management: This emphasizes the identification of critical uncertainties regarding natural resource dynamics and the design of diagnostic management experiments to reduce these uncertainties [56]. The broad social structure may be recognized, and management should be embedded within this structure. It involves a structured, iterative process of robust decision-making in the face of uncertainty, targeting to minimize the uncertainty over time via system monitoring. Therefore, it involves resource-management as well as collecting data for future improvement in the system's management. This process can be used to learn more about a system [57], and because the process involves a feedback loop and a learning algorithm, it can be used to improve future management.

5. CONCLUSION

Questioning the sustainability of desalination, one can indisputably claim that the facts of today may not be the facts of tomorrow. Innovation was greatly leveraged by the development of large-scale desalination projects, primarily in the Middle East. Indeed, desalination has evolved immensely over the past six decades, but there is still room for innovation to give mature technologies a cost-effective boost and to render the

emerging ones commercially competitive. Also emerging are concerns over the environmental impact of desalination. Few arguments exist to support desalination's environmental friendliness, with the issue of carbon emissions being constantly spotlighted and the impact of brine discharge still largely being overlooked by policymakers, owners, and contractors. Drastic solutions such as the adoption of renewable energy and ZLD brine treatment technologies have been extensively researched and cited in academia; however, they have only recently been implemented on a commercial scale. These initiatives could alleviate the public's mistrust of and hostility toward desalination as an industry, at least in the short-term. Keep in mind, however, that every desalination project is unique in terms of the context of its local community. Keys to addressing the concerns and relaxing the opposition of the public and local stakeholders are transparency of operations and effective communication of information to the public at all phases of the project. More important, of course, is a sincere effort to mitigate the negative impact of desalination, be it environmental, economic, or social in nature, by taking advantage of the wealth of progress and innovation achieved through six decades of research on this process. The rest of this book sheds some light on those aspects.

REFERENCES

[1] V.G. Gude, Desalination and sustainability – an appraisal and current perspective, Water Res. 89 (2016) 87–106, http://dx.doi.org/10.1016/j.watres.2015.11.012.
[2] M. Nair, D. Kumar, Water desalination and challenges: the Middle East perspective: a review, Desalin. Water Treat. 51 (10–12) (2013) 2030–2040, http://dx.doi.org/10.1080/19443994.2013.734483.
[3] NASA, Earth Observatory, (2013). Retrieved from: http://earthobservatory.nasa.gov/IOTD/view.php?id=86263.
[4] International Desalination Association, Challenges and opportunities for desalination and reuse: perspectives from leaders, IDA News (December) (2015).
[5] A. Siddiqi, L.D. Anadon, The water–energy nexus in Middle East and North Africa, Energy Policy 39 (8) (2011) 4529–4540, http://dx.doi.org/10.1016/j.enpol.2011.04.023.
[6] R. Ferroukhi, D. Nagpal, A. Lopez-Peña, T. Hodges, R.H. Mohtar, B. Daher, et al., Renewable Energy in the Water, Energy and Food Nexus, 2015, Retrieved December 10, 2016 from http://www.irena.org/DocumentDownloads/Publications/IRENA_Water_Energy_Food_Nexus_2015.pdf.
[7] A.M.H. El-Saie, Y.M.H. Ali EI-Saie, A. Deghedi Moneer, Perspectives and challenges for desalination in the 21st century, Desalination 135 (2001) 25–42.
[8] J. Gebel, S. Yüce, A new approach to meet the growing demand of professional training for the operating and management staff of desalination plants, Desalination 220 (1–3) (2008) 150–164, http://dx.doi.org/10.1016/j.desal.2007.01.029.
[9] Global Water Intelligence, Desalination Industry Enjoys Growth Spurt as Scarcity Starts to Bite, Retrieved from: https://www.globalwaterintel.com/desalination-industry-enjoys-growth-spurt-scarcity-starts-bite/, 2012.
[10] A. Bennett, 50th anniversary: desalination: 50 years of progress, Filtr. Sep. 50 (3) (2013) 32–39, http://dx.doi.org/10.1016/s0015-1882(13)70128-9.
[11] S. Corrado, Approaches to desalination project budgeting, Paper Presented at the International Conference on Desalination Costing, Limassol, Cyprus, 2004.
[12] D.A. Roberts, E.L. Johnston, N.A. Knott, Impacts of desalination plant discharges on the marine environment: a critical review of published studies, Water Res. 44 (18) (2010) 5117–5128, http://dx.doi.org/10.1016/j.watres.2010.04.036.

[13] DesalData, 2016, Retrieved from: http://desaldata.com/.
[14] S. Liyanaarachchi, L. Shu, S. Muthukumaran, V. Jegatheesan, K. Baskaran, Problems in seawater industrial desalination processes and potential sustainable solutions: a review, Rev. Environ. Sci. Biotechnol. 13 (2) (2013) 203–214, http://dx.doi.org/10.1007/s11157-013-9326-y.
[15] A. Subramani, J.G. Jacangelo, Emerging desalination technologies for water treatment: a critical review, Water Res. 75 (2015) 164–187, http://dx.doi.org/10.1016/j.watres.2015.02.032.
[16] A. Bennett, Cost effective desalination: innovation continues to lower desalination costs, Filtr. Sep. 48 (4) (2011) 24–27, http://dx.doi.org/10.1016/s0015-1882(11)70164-1.
[17] C. Sommariva, Desalination and Advance Water Treatment Economics and Financing, Balaban Publishers, Hopkinton, USA, 2007.
[18] D. Knights, I. MacGill, R. Passey, The sustainability of desalination plants in Australia: is renewable energy the answer? in: OzWater Conference, Sydney, 2007.
[19] J.J. Sadhwani, J.M. Veza, C. Santana, Case studies on environmental impact of seawater desalination, Desalination 185 (2005) 1–8.
[20] H. Cooley, M. Heberger, Key Issues in Seawater Desalination in California: Energy and Greenhouse Gas Emissions, Pacific Institute, Preservation Park Oakland, California, 2013.
[21] A. Al-Karaghouli, L.L. Kazmerski, Energy consumption and water production cost of conventional and renewable-energy-powered desalination processes, Renew. Sustain. Energy Rev. 24 (2013) 343–356.
[22] T. Younos, K.E. Tulou, Energy needs, consumption and sources, J. Contemp. Water Res. Educ. 132 (2005) 27–38.
[23] E. Shrestha, S. Ahmad, W. Johnson, P. Shrestha, J.R. Batista, Carbon footprint of water conveyance versus desalination as alternatives to expand water supply, Desalination 280 (2011) 33–43.
[24] V.G. Gude, N. Nirmalakhandan, S. Deng, Renewable and sustainable approaches for desalination, Renew. Sustain. Energy Rev. 14 (2010) 2641–2654.
[25] H. Cooley, N. Ajami, Key issues for seawater desalination in California, in: P.H. Gleick (Ed.), The World's Water: The Biennial Report on Freshwater Resources, Island Press/Center for Resource Economics, Washington, DC, 2014, , pp. 93–121.
[26] S. Miller, H. Shemer, R. Semiat, Energy and environmental issues in desalination, Desalination 366 (2015) 2–8, http://dx.doi.org/10.1016/j.desal.2014.11.034.
[27] S. Lattemann, T. Höpner, Environmental impact and impact assessment of seawater desalination, Desalination 220 (1) (2008) 1–15, http://dx.doi.org/10.1016/j.desal.2007.03.009.
[28] R. Water, Global Desalination Capacity Should Double by 2020 (2015). Retrieved from: https://www.rwlwater.com/global-desalination-capacity-should-double-by-2020/.
[29] S. Loutatidou, B. Chalermthai, P.R. Marpu, H.A. Arafat, Capital cost estimation of RO plants: GCC countries versus southern Europe, Desalination 347 (2014) 103–111, http://dx.doi.org/10.1016/j.desal.2014.05.033.
[30] K.P. Tsagarakis, New directions in water economics, finance and statistics, Water Sci. Technol. Water Supply 5 (6) (2005) 1.
[31] N. Ghaffour, T.M. Missimer, G.L. Amy, Technical review and evaluation of the economics of water desalination: current and future challenges for better water supply sustainability, Desalination 309 (2013) 197–207, http://dx.doi.org/10.1016/j.desal.2012.10.015.
[32] F. Lokiec, G. Kronenberg, Emerging role of BOOT desalination projects, Desalination 136 (1) (2001) 109–114, http://dx.doi.org/10.1016/S0011-9164(01)00172-2.
[33] N. Voutchkov, Desalination Engineering: Planning and Design, McGraw-Hill Professional, USA, 2012.
[34] J.R. Ziolkowska, R. Reyes, Impact of socio-economic growth on desalination in the US, J. Environ. Manage. 167 (2016) 15–22, http://dx.doi.org/10.1016/j.jenvman.2015.11.013.
[35] M. Schiffler, Perspectives and challenges for desalination in the 21st century, Desalination 165 (2004) 1–9, http://dx.doi.org/10.1016/j.desal.2004.06.001.
[36] A. Barak, Economic aspects of water desalination, Advances in Water Desalination, John Wiley & Sons, Inc., New York, USA, 2012. pp. 197–308.
[37] Water Reuse Association, White Paper: Seawater Desalination Costs, 2012, Retrieved December 5, 2016 from https://watereuse.org/wp-content/uploads/2015/10/WateReuse_Desal_Cost_White_Paper.pdf.

[38] M. Isaka, Water Desalination Using Renewable Energy: Technology Brief, Retrieved from: https://www.irena.org/DocumentDownloads/Publications/IRENA-ETSAP%20Tech%20Brief%20I12%20Water-Desalination.pdf, 2012.
[39] P.T. Review, Desalination: An Ocean of Hope, Retrieved from: http://www.paristechreview.com/2013/07/24/desalination-hope, 2013.
[40] H. Van der Vegt, I. Iliev, Q. Tannock, S. Helm, Desalination Technologies and the Use of Alternative Energies for Desalination, 2011, Retrieved November 5, 2016 from https://pdfs.semanticscholar.org/0989/de3cbaff4f50e0e16ece5020d5a51c3e262f.pdf.
[41] K. Bourouni, R. Martin, L. Tadrist, H. Tadrist, Experimental investigation of evaporation performances of a desalination prototype using the aero-evapo-condensation process, Desalination 114 (2) (1997) 111–128, http://dx.doi.org/10.1016/S0011-9164(98)00003-4.
[42] H.T. El-Dessouky, H.M. Ettouney, Plastic/compact heat exchangers for single-effect desalination systems. Desalination 122 (2) (1999) 271–289, http://dx.doi.org/10.1016/S0011-9164(99)00048-X.
[43] X. Chen, Y. Su, D. Reay, S. Riffat, Recent research developments in polymer heat exchangers – a review, Renew. Sustain. Energy Rev. 60 (2016) 1367–1386, http://dx.doi.org/10.1016/j.rser.2016.03.024.
[44] J.B.P. Christmann, L.J. Krätz, H.-J. Bart, Falling film evaporation with polymeric heat transfer surfaces, Desalination 308 (2013) 56–62, http://dx.doi.org/10.1016/j.desal.2011.05.027.
[45] Wonthaggi Desalination Plant, Victoria – Water Technology, n.d., Retrieved from: http://www.water-technology.net/projects/wonthaggidesalinatio/.
[46] Media blitz on the yuck factor, n.d., Retrieved from: http://www.singapore-window.org/sw02/020721st.htm.
[47] R. Collins, Hard sell for new water, Water Wastewater 14 (4) (2003) 39–40.
[48] Singapore Water Reclaimation Study Expert Panel Review and Study, Retrieved from: https://www.scribd.com/document/99865970/Singapore-Water-Reclaimation-Study-Expert-Panel-Review-and-Study.
[49] T.W. Hartley, Public perception and participation in water reuse, Desalination 187 (1) (2006) 115–126, http://dx.doi.org/10.1016/j.desal.2005.04.072.
[50] J.L. Dupavillon, B.M. Gillanders, Impacts of seawater desalination on the giant Australian cuttlefish Sepia apama in the upper Spencer Gulf, South Australia, Mar. Environ. Res. 67 (4–5) (2009) 207–218, http://dx.doi.org/10.1016/j.marenvres.2009.02.002.
[51] Global Commons, 2016, Retrieved from: http://www.unep.org/delc/GlobalCommons/tabid/54404/.
[52] N. Hilal, G.J. Kim, C. Somerfield, Boron removal from saline water: a comprehensive review, Desalination 273 (1) (2011) 23–35, http://dx.doi.org/10.1016/j.desal.2010.05.012.
[53] U. Yermiyahu, A. Tal, A. Ben-Gal, A. Bar-Tal, J. Tarchitzky, O. Lahav, Rethinking desalinated water quality and agriculture, Science 318 (5852) (2007) 920.
[54] A.M. Shams El Din, Three strategies for combating the corrosion of steel pipes carrying desalinated potable water, Desalination 238 (1) (2009) 166–173, http://dx.doi.org/10.1016/j.desal.2007.11.063.
[55] A.N. Angelakis, L. Bontoux, Wastewater reclamation and reuse in Eureau countries, Water Policy 3 (1) (2001) 47–59, http://dx.doi.org/10.1016/S1366-7017(00)00028-3.
[56] C.J. Walters, Is adaptive management helping to solve fisheries problems? Ambio 36 (4) (2007) 304–307, http://dx.doi.org/10.1579/0044-7447(2007)36[304:iamhts]2.0.co;2.
[57] C.S. Holling, P. United Nations Environment, P. Workshop on Adaptive Assessment of Ecological, Adaptive Environmental Assessment and Management, International Institute for Applied Systems Analysis, Laxenburg, Austria, 1978.

FURTHER READING

[1] A. Al-Karaghouli, D. Renne, L.L. Kazmerski, Solar and wind opportunities for water desalination in the Arab regions, Renew. Sustain. Energy Rev. 13 (2009) 2397–2407.
[2] M. Eltawil, Z. Zhengming, L. Yuan, Renewable energy powered desalination systems: technologies and economics-state of the art, in: 12th International Water Technology Conference, Alexandria, Egypt, 2008, pp. 1–38.

[3] J. Kucera (Ed.), Desalination: Water from Water, John Wiley & Sons, Inc., Hoboken, NJ, 2014.
[4] T. Mezher, H. Fath, Z. Abbas, A. Khaled, Techno-economic assessment and environmental impacts of desalination technologies, Desalination 266 (2011) 263–273.
[5] UNEP/GRID-Arendal Maps and Graphics Library, 2009, Retrieved from: http://www.grida.no/graphicslib/detail/increased-global-water-stress_5694.

CHAPTER 2

Membrane-Based Desalination Technology for Energy Efficiency and Cost Reduction

In S. Kim, Moonhyun Hwang, Changkyoo Choi
Gwangju Institute of Science and Technology (GIST), Gwangju, Republic of Korea

Contents

1. TRENDS AND LIMITATIONS OF LEADING DESALINATION TECHNOLOGIES

Desalination processes can be separated into many categories, but in general, the processes are thermal, membrane-based, and other technologies as shown in Fig. 1. Of these, thermal and membrane technologies are the leading processes in the desalination market. Prior to the 2000s, the most commonly used desalination technologies were based on thermal processes, including multistage flash (MSF), and multieffect distillation (MED). For this reason, thermal technologies have developed around the Middle East, where the energy cost is cheap, and where the reliability of this technology was proven by long-term operation. The gradual increase of energy costs prior to 2011 has seen membrane-based desalination technologies, and in particular reverse osmosis (RO), favored over thermal processes as the main technology in the market. In general, thermal

Desalination Sustainability
http://dx.doi.org/10.1016/B978-0-12-809791-5.00002-X

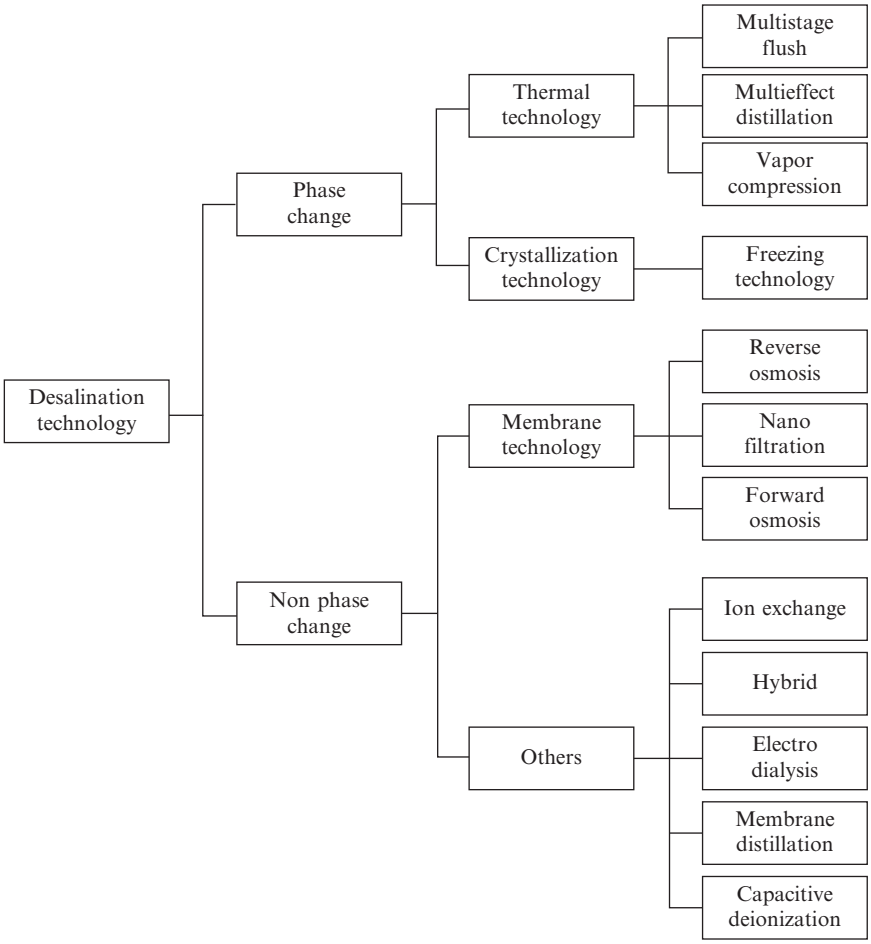

Fig. 1 Tech-tree of desalination processes.

processes are competitive in cost only under the conditions of cheap energy resources or high feed concentrations. In 2010, Global Water Intelligence [1] reported the water cost for MSF, MED, and seawater reverse osmosis (SWRO) to be 1.07, 0.83, and 0.76 US$/m^3, respectively. RO technology was deemed to be economical. In addition, Wittholz et al. [2] reported that in a plant capacity range from 10,000–500,000 m^3/d, the construction cost and water price for SWRO was 8.4%–60% and 23%–38% lower, respectively, compared to existing thermal technologies. Although these results show the economic superiority of SWRO, as shown in Fig. 2, thermal desalination plants account for 62.5% of the large desalination plants (capacities of over 50,000 m^3/d) built in the Middle East since 2010, thus showing that thermal technologies are primarily competitive in the Middle East, which is a world-leading market for desalination.

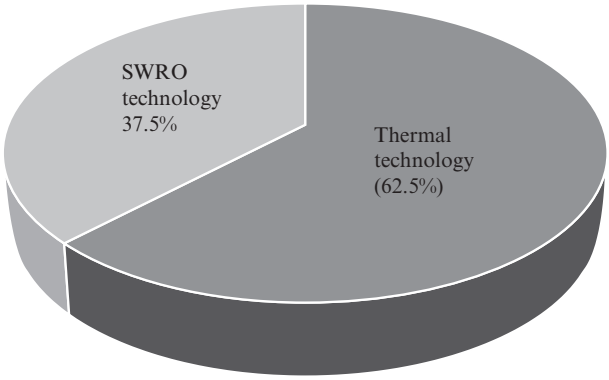

Fig. 2 Proportion of SWRO and thermal process plants constructed in a worldwide since 2010 (www.desaldata.com).

1.1 Trends of Thermal Desalination Processes

Thermal processes, particularly MSF and MED, are desalination technologies based on the principle of phase change, which converts seawater to vapor for fresh water and brine by heating. In thermal processes, the key operational factor is to change a highly salty feed to vapor at a relatively low temperature using the relationship between temperature and pressure (Fig. 3), based on the saturation water vapor pressure curve. The vapor, converted using the vapor pressure curve, condenses to fresh water after cooling. For this conversion process, a fixed energy, referred to as the latent heat, is always required; thus, thermal desalination technologies are not generally economical. Therefore, a cheaper heat source such as steam supplied from a power plant is needed in order to overcome this shortage.

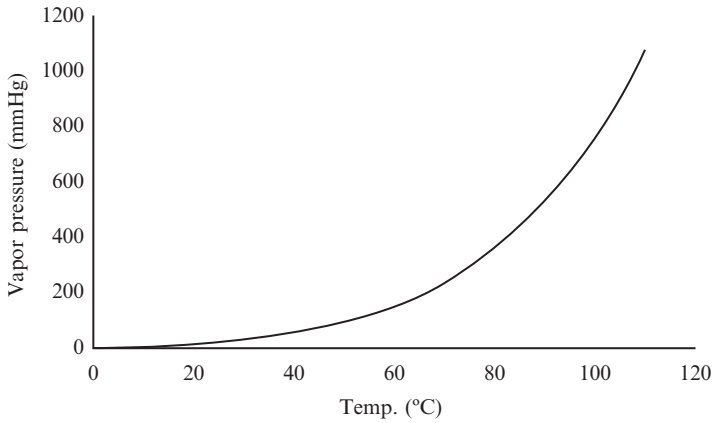

Fig. 3 Vapor pressure of water.

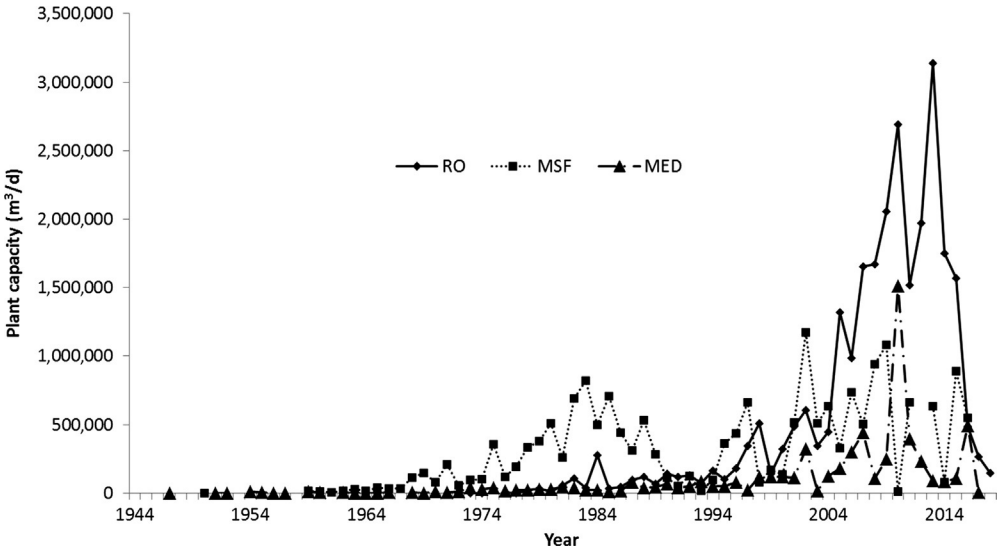

Fig. 4 Capacity of plants based on desalination technology [3].

Fig. 4 presents specific trends of processes used in the desalination market. In the 1980s, it was rare for MED plants to be constructed due to scaling problems in the O&M process, whereas MSF has become the leading desalination process since the 1960s, particularly in the Gulf region, due to its reliability and simplicity. However, at present, MED processes have returned as energy costs have increasingly factored in the construction of desalination plants, although energy costs are higher than in RO technologies. Indeed, projections in the Desalination Market 2016 indicate that RO will be the leading technology for the next 10 years, due to its low energy consumption, even though large thermal desalination plants are occasionally being constructed around the Gulf region.

1.2 Trends of SWRO Desalination Processes

The increase in the cost of oil to US$126.55 per barrel initiated a transition of major desalination technologies from thermal desalination to SWRO desalination, due to its lower energy demand. According to the Desalination Market 2016, SWRO desalination plants account for 90% of the desalination projects currently under bid and those to be constructed in the upcoming years [4]. This rapid transition from thermal technologies to SWRO desalination has mainly been driven by the cost competitiveness of membrane-based desalination technologies. This alteration significantly affected the global desalination market, especially with improvement in SWRO desalination technologies in terms of energy requirements.

1.2.1 The Development of Technology and Devices for Conventional RO Process

The design unit for the RO desalination process is defined as a "train." A train is composed of a high-pressure pump, an RO bank containing a number of vessels, and an energy recovery device (ERD), which can be operated as a standalone unit for desalination. Fig. 5 illustrates the conceptual arrangement of these key components of an RO train. In general, an SWRO desalination plant is comprised of several trains.

The total energy consumption required for SWRO desalination is strongly dependent on the energy consumed in the RO train. Voutchkov et al. [5] stated that, in general, under the feed water condition of total dissolved solids (TDS) of 35 g/L at 23°C, approximately 72% of the energy is consumed in the RO train during large SWRO processes, and intake, pretreatment, product water delivery, and others consume 5%, 10%, 8%, and 5% of total energy, respectively. The performance of SWRO membranes, efficiency of high pressure pumps, and the efficiency of ERDs will mainly determine the energy efficiency of RO trains. Fig. 6 shows the trend of energy consumption reduction as the development of these key components has proceeded [6]. Overall, the efficiency of high pressure pumps tends to increase as the total capacity of the SWRO plant expands [7]. There are currently two major categories of high pressure pumps: reciprocating pumps (e.g., positive displacement pumps and piston pumps) and centrifugal pumps. As the capacity of an SWRO plant decreases, it is likely that the reciprocating pumps are to be applied, due to their relatively high and consistent pump efficiencies. In contrast, centrifugal pumps are typically employed in large SWRO plant operations, with pump efficiencies in the range of 82%–88%. The Ashkelon SWRO desalination plant was renowned for its high pump capacity, in addition to having a pump efficiency of 88.5%—the highest value ever achieved at the time the plant was commissioned [8]. The design capacity of high pressure pumps is closely related to the unit train size and total plant capacity. Notably, the unit train size of large SWRO plants having total capacities above 50,000 m^3/d jumped from approximately 1.5–5 MGD in 2000 (Fig. 7).

Enlargement of the unit train size is directly connected to the energy consumption rate. Martinho et al. [9] reported that, for a recovery of RO below 45%, the

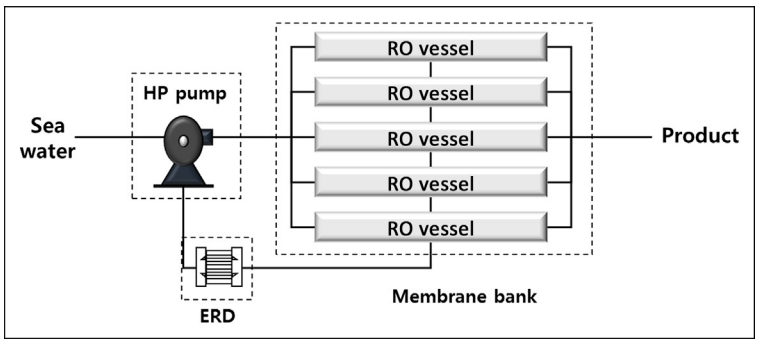

Fig. 5 Train definition.

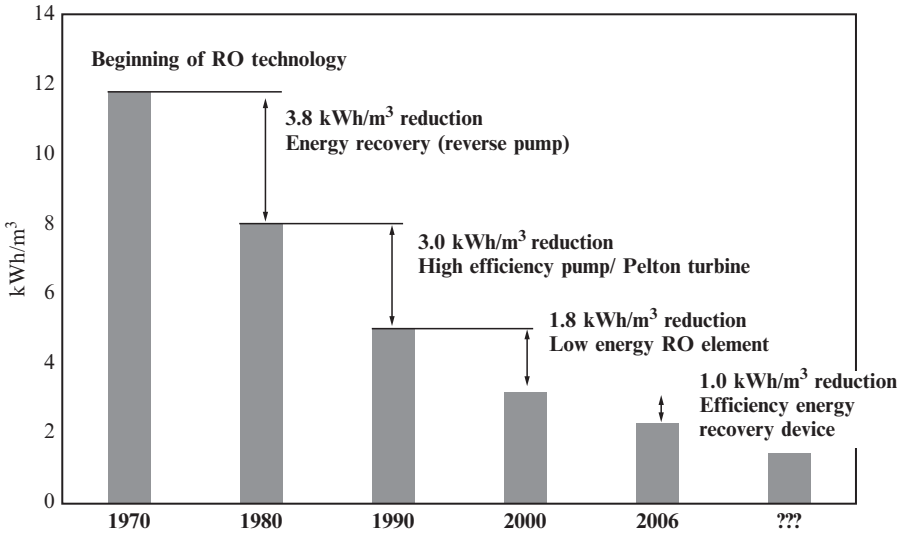

Fig. 6 Energy consumption as device development [6].

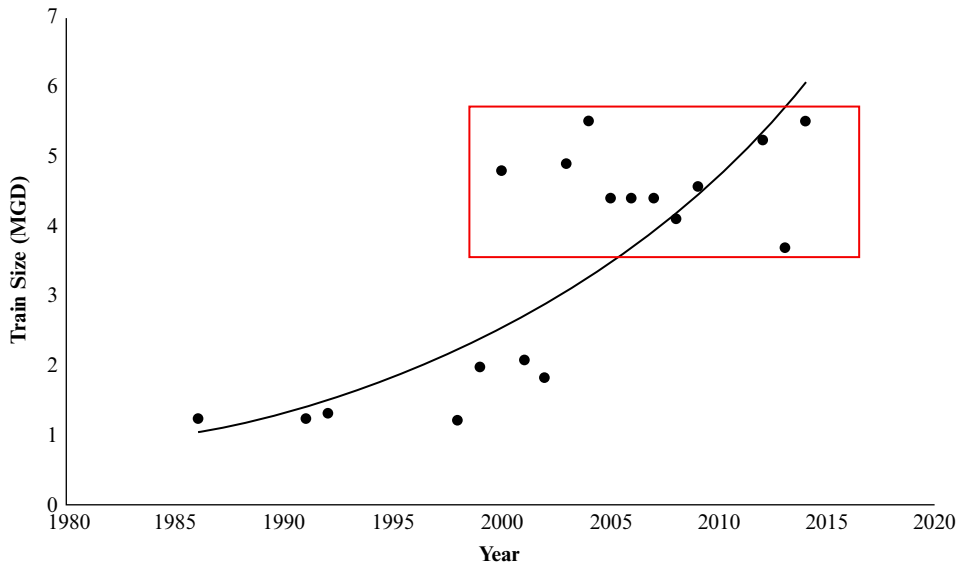

Fig. 7 Trends of train size (plants having larger than 10,000 m^3/d capacity, 1 MIGD = 4546 m^3/d) [3].

energy consumption rates for unit train sizes of 2500 m^3/d and 10,000 m^3/d were 3.56–3.37 kWh/m^3 and 3.17–3.02 kWh/m^3, respectively, leading to the conclusion that there exists a negative correlation between the unit train size and energy consumption. Nevertheless, as observed in Fig. 3, the unit train size ranges from 4 to 6 MGD

(i.e., approx. 15,000–23,000 m^3/d) for large SWRO plants having total capacities above 25 MGD (i.e., approx. 95,000 m^3/d). Of 5404 SWRO desalination plants in operation from 2000 to 2010, the capacities ranged from 0.0013 to 99.1 MGD (i.e., 5–375,000 m^3/d), with 99.2% (5363 plants) being below 26.4 MGD (100,000 m^3/d) in capacity. For unit train sizes beyond 6 MGD (23,000 m^3/d), it is unlikely that such a large unit train size would be employed due to its potential drawbacks in terms of pause (relative to O&M, in general), such as the need to replace RO membrane modules, unless the SWRO plant has total capacity of 500,000 m^3/d and above.

Another cornerstone that enabled the improved efficiency in energy consumption was the development and implementation of ERDs. There are three major types of ERDs: hydraulic to mechanical-assisted pumping, hydraulically driven pumping in series, and hydraulically driven pumping in parallel [10]. For example, for hydraulic to mechanical-assisted pumping, a Francis turbine was applied to desalination processes in the 1980s, replenishing the insufficient hydraulic energy of an HP pump by rotating the shaft by using the brine pressure. For hydraulically driven pumping in series, a turbo charger has been in use since the 1990s, boosting the pressure of the feed to the required operational pressure, which is partly pressurized by the HP pump. These types of ERDs have a low energy recovery efficiency due to energy loss in the shaft, impeller, nozzle, and turbine, whereas for hydraulically driven pumping in parallel, the isobaric type is 95% more efficient because it directly transfers pressure to the feed, as compared to the other types [10,11]. As the ERD efficiency improves to above 95%, it implies that there can only be minimal further developments in ERDs. In addition, the mass balance of these classes for train design is different because of differences in the respective systems for energy recovery. Fig. 8 illustrates the typical design for ERD types having 50,000 m^3/d of permeate and a 40% recovery.

RO membrane modules play a pivotal role in reducing energy. To summarize, there are two major pathways in RO membrane development. The first approach is to increase the membrane element dimension, and the second one is to improve the water flux (i.e., development of a high flux membrane). To date, a number of SWRO membrane elements with 16-in. diameters have been commercialized, and have been reported to improve the economic feasibility as they require fewer pipelines and metal frames and reduce membrane fouling [12]. Furthermore, Henthorne et al. [13] compared the use of different sizes of SWRO membrane elements (e.g., 8-, 16-, and 20-in. in diameter) and concluded that further economic benefits can be achieved (between 18.5% and 27%) by varying the plant capacities. The results of these studies imply that enlarging the SWRO membrane element is beneficial in reducing the capital expenditure (CAPEX). However, the use of larger membrane elements could also increase O&M issues such as membrane replacements, which needs to be further validated.

Improving the water flux correlates with alleviating the standard for boron concentration in the product water, as officially proclaimed by the World Health

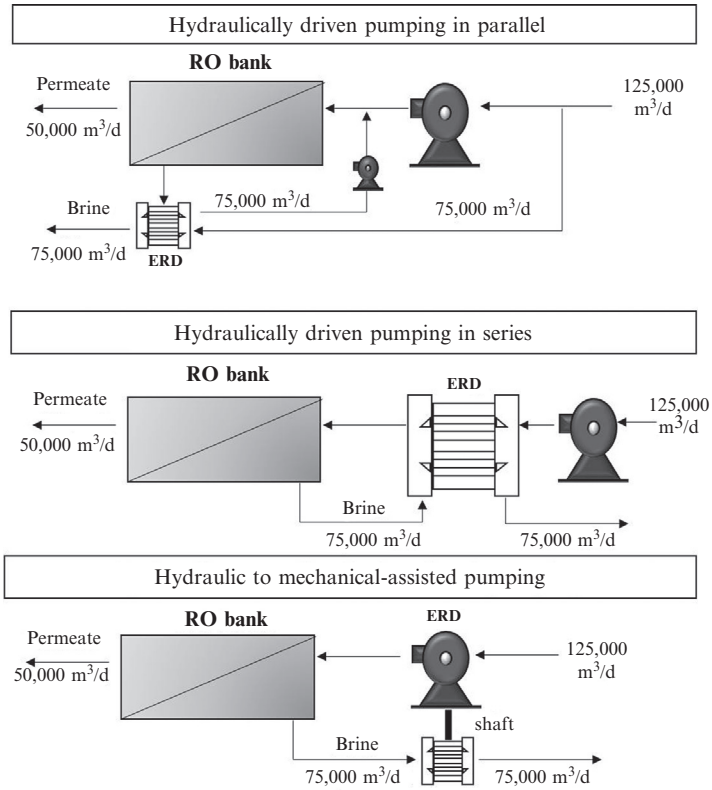

Fig. 8 Typical design of ERD types.

Organization (WHO). Based on health risk assessments conducted since 2009, the WHO relaxed the boron concentration standard for potable water from 0.5 to 2.4 mg/L in 2011 [14]. In this context, the eased regulation of boron concentration made boron selectivity less important for commercial SWRO membranes. In the wake of this change in standards, following the trends of RO membrane development, Hydranautics [15] has turned its focus to improving the water flux.

High flux membranes, such as the 17,000 GPD (salt rejection: 99.47%) membrane element from Dow Chemical and the 13,200 GPD (salt rejection: 99.8%), are actively being commercialized in the market. In the case of such high flux membranes, the rejection of salt and foulants tends to decrease, thus the implementation of high flux membrane elements should be critically assessed for regions requiring strict regulations on product water quality. Based on current studies, the development of ERDs and high flux membranes to date have enabled SWRO plant engineers to achieve a 2.5–4.0 kWh/m^3 specific energy consumption (SEC) [16].

1.2.2 Novel SWRO Configuration Design

Employing high flux membrane elements is advantageous due to the improved production rate, and lower energy consumption and capital cost. According to Wilf et al. [17], it is possible to achieve 3.0%, 3.2%, and 2.5% reductions in product water cost based on simulations employing high flux membranes with standard water qualities of the Atlantic/Pacific, Mediterranean, and Gulf regions, respectively. However, high flux membranes diminish the rejection of salts and foulants, which may then actually worsen the product water quality. In addition, the first membrane element in a pressure vessel is likely to be subject to high fouling propensity; according to Winters et al. [18], the fouling propensity may be escalated when high flux membranes are operated above the critical flux capacity of the element. By considering conventional pressure vessel designs and membrane element placements (typically 6–8 elements in a pressure vessel in series), the first and second elements are likely to be most significantly affected by membrane fouling. However, notable benefits of adopting high flux membranes include reductions in the required number of membrane elements and pressure vessels, a smaller pretreatment capacity, and reduction in energy costs. Furthering this effort, DOW Water Solutions developed an internal stage design (ISD) to accommodate high flux membranes within a pressure vessel, while arraying them along with different elements having varying product rates [19]. ISD employs low flux membrane elements at the head position and high flux membrane elements at the tail position. Fig. 9 presents the conceptual schematic of a typical ISD, with the El Coloso, Madinat Al-Jubail, and Yanbu Al-Sinaiyah plants being examples that adopted ISDs.

Based on desalination literature, ISD is positioned to be a plausible approach for improving SWRO plant performance. For example, Molina et al. [20] conducted an economic feasibility analysis, assuming a feed water temperature of 18°C and using salinity ranges from different regions (e.g., Australia, Saudi Arabia, and Israel), and reported that the water cost can be reduced from 0.67 to 0.64 US$/m^3. Under high fouling conditions,

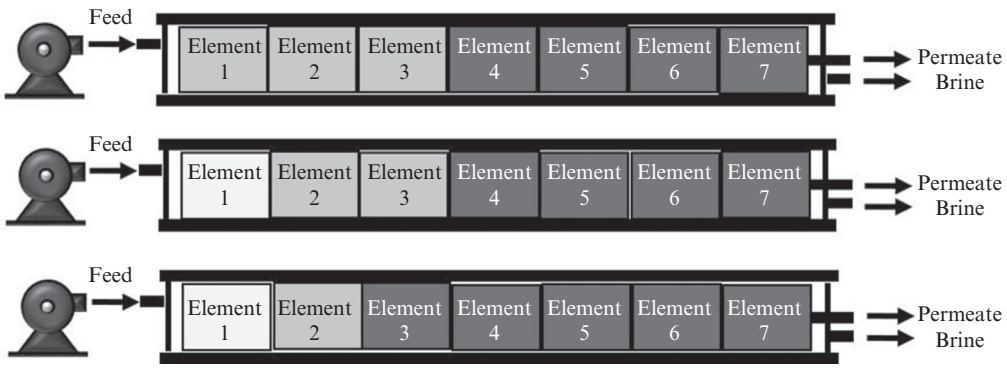

Fig. 9 Concept of internal staged design (the higher flux membrane, the more dark color).

however, ISD can be disadvantageous in terms of energy consumption, whereas factors such as chemical and replacement costs were active contributors in improving overall performance. In other studies, Penate and Garcia-Rodriguez [21] tested ISD configurations using SWRO membranes from Dow Chemical, Hydranautics, and Toray Chemical, and concluded that despite the slightly worsened product water quality as compared to conventional SWRO designs, the energy cost efficiency was improved by 8.3%, 5.4%, and 6.4%, respectively. Based on a series of simulations, the authors also suggested that adopting only high flux membranes was advantageous in the aspect of energy consumption, though the high flux membranes are likely to exhibit a high fouling propensity due to water flux that exceeds manufacturer design specifications. Nevertheless, the two studies indicate that ISD can be beneficial in terms of energy savings, but may suffer severe membrane fouling and potentially increased energy losses in the second pass.

SWRO plant designs can be categorized into two major design schemes: the conventional type given in Fig. 5, and the pressure center design depicted in Fig. 10. The latter design scheme was developed by IDE, and though it has been primarily adopted in SWRO plants in Israel it has also been recently implemented in the Carlsbad desalination plant in California, USA. One of the major advantages of the pressure center design is that it maximizes the unit pump capacity, thus maximizing the energy efficiency. The Ashkelon desalination plant employed this design and achieved an SEC of 3.9 kWh/m^3 and product water price of 0.53 US$/$m^3$ [8]. Table 1 summarizes the important design factors of SWRO plants constructed based on the pressure center design; except for the values for the Carlsbad desalination plant, it is clear that the design exhibits strong benefits in terms of product water cost.

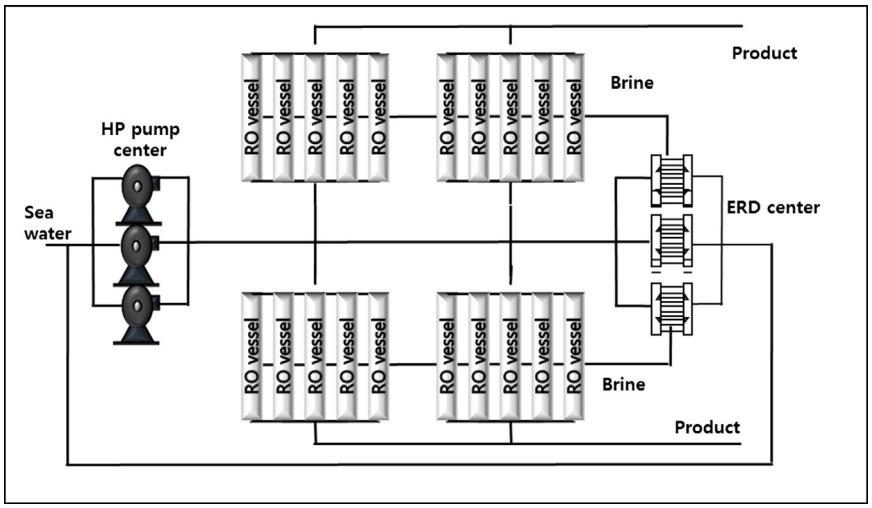

Fig. 10 New concept of RO train (pump and central ERD design).

Table 1 Desalination plant having pump and central ERD design [22,23]

Plant	Capacity (m^3/d)	Capital cost (million US$)	Energy consumption (kWh/m^3)	Water price (US$/$m^3$)
Ashkelon	330,000	212	3.85	0.68
Hadera	456,000	425	3.5	0.67
Sorek	540,000	400	3.5	0.52
Carlsbad[a]	200,000	530	3.56 (design)	1.61

[a]The SEC of the Carlsbad plant is the target SEC for the initial planning phase, not the actual SEC obtained during operation.

2. NOVEL MEMBRANE-BASED DESALINATION TECHNOLOGIES FOR REDUCING DESALINATION COST

2.1 Membrane Distillation Technology

2.1.1 MD Overview

Membrane distillation (MD) is a thermal process used to separate liquid and solid phases, allowing water to pass through the pores of an MD membrane via the vapor pressure difference resulting from temperature difference. MD was derived from a conventional distillation process, as both technologies require heat energy in the feed solution step for vaporization [24].

The advantages of MD include lower energy required for heating than conventional distillation processes, lower energy for pressure than RO-driven processes, a less expensive membrane, a high TDS removal rate and less fouling, and it can be combined with various energy sources [25,26]. However, the drawbacks of MD are that it has a lower flux than RO processes, high sensitivity flux due to the concentration and temperature polarization, high mass transfer resistance due to the air trapped in the membrane, and high heat loss under operating conditions [24].

MD processes are classified by heat and mass transfer phenomena within the membrane under different configurations: (1) direct contact membrane distillation (DCMD), (2) sweeping gas membrane distillation (SGMD), (3) vacuum membrane distillation (VMD), and (4) air-gap membrane distillation (AGMD).

2.1.2 Membrane Classification

2.1.2.1 Direct Contact Membrane Distillation

In DCMD, shown in Fig. 11, there is direct contact between the feed solution and membrane surface; hence, vapor is generated at the membrane surface on the feed side and passes to the permeate side via the pressure difference. Contaminants cannot pass through the membrane due to the hydrophobicity of the membrane. DCMD is currently popular because of its simple configuration [27–31].

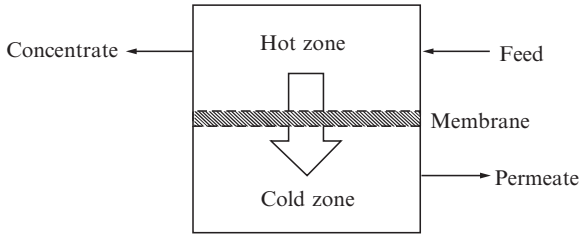

Fig. 11 Schematic diagram of DCMD.

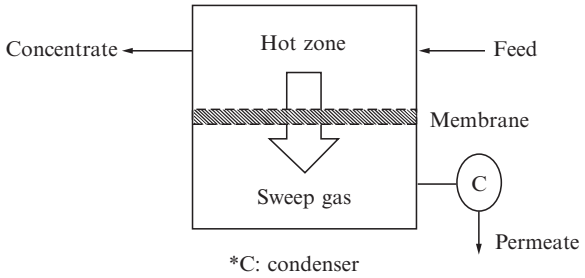

Fig. 12 Schematic diagram of SGMD.

2.1.2.2 Sweeping Gas Membrane Distillation

As presented in Fig. 12, SGMD uses condensed water to sweep the vapor away by using the gas at the permeate side. The gas layer prevents heat loss and thus improves the mass transfer efficiency. This process is more useful for the removal of volatile contaminants from an aqueous solution [32], though the major drawbacks of SGMD include the fact that it has a lower permeate rate due to the large sweep gas volume.

2.1.2.3 Vacuum Membrane Distillation

VMD uses a pump to create a vacuum on the permeate side, and because condensed water can get outside the module, the heat loss is minimal [27]. VMD can be used to separate volatile compounds from the aqueous solution [33–35]. Fig. 13 presents a schematic diagram of VMD.

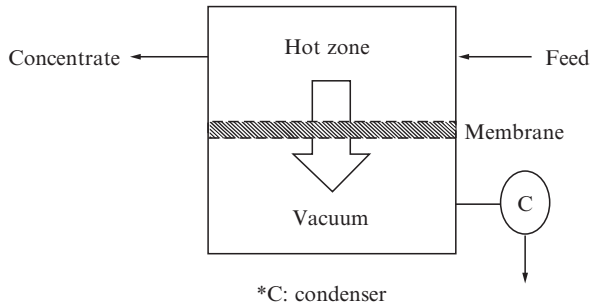

Fig. 13 Schematic diagram of VMD.

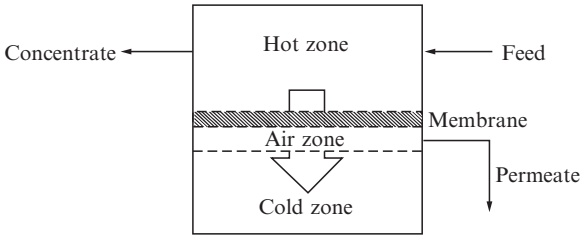

Fig. 14 Schematic diagram of AGMD.

2.1.2.4 Air-Gap Membrane Distillation

As shown in Fig. 14, AGMD is similar to DCMD in that the feed solution is in direct contact with the membrane surface. However, stagnant air is used to get the water to the membrane surface. The vapor phase condenses into water as it passes through the cold membrane in which the air gap exists.

The merit of this process is in reducing the heat loss, though it incurs a greater mass transfer resistance. Overall, AGMD is appropriate for desalination and aqueous volatile solutions [36–40].

2.1.2.5 Permeate-Gap Membrane Distillation

Permeate-gap membrane distillation (PGMD) is referred to as water gap and liquid gap MD, modified with AGMD. The permeate water, which is the liquid channel, is filled in the gap between the membrane and the condensing surface. The liquid channel reduces heat losses because of an additional heat transfer resistance. Therefore, the merits of PGMD shows more flux than AGMD. Fig. 15 shows the schematics of PGMD [41].

2.1.2.6 Conductive Gap Membrane Distillation

As shown in Fig. 16, conductive gap membrane distillation (CGMD) is located in the conductive gap between the membrane and the condensing surface to increase the thermal conductance of the gap. The conductive gap is filled with high or low conductivity materials such as metal mesh or sand [41].

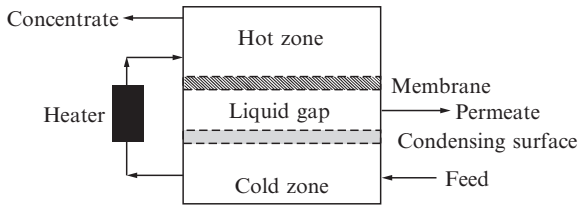

Fig. 15 Schematic diagram of PGMD.

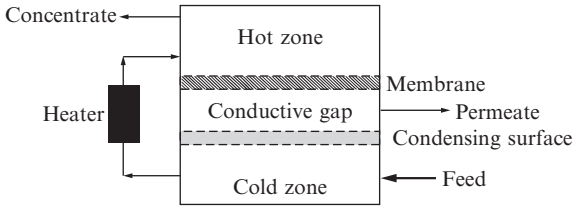

Fig. 16 Schematic diagram of CGMD.

2.1.3 MD Membranes

2.1.3.1 Membrane Fabrication

In MD, hydrophobic membranes are suitable and materials can be chosen by considering the cost, fabrication and assembly convenience, temperature, and conductivity. The membrane can be fabricated using phase inversion or thermally induced phase separation (TIPS), and phase inversion is preferred [42–45]. In addition, physical and chemical techniques, coatings, grafting, polymerization, etc., can be introduced for membrane modification [46].

Phase inversion is the point at which the liquid state of a polymer changes into a solid state. By solvent evaporation, extraction from vapor state, thermal and immersion extraction, and dry-wet phase inversion can affect membrane characteristics. These methods are useful for fabricating both asymmetric and symmetric membranes.

Poly(vinylidene fluoride-hexafluoropropylene) (PVDF-HEP) and polyvinylidene fluoride-tetrafluoroethylene (PVDF-TFE) are mainly used for making flat sheet and hollow fiber type membranes [47–50]. Membrane modification methods such as coating, grafting, and blending are then used to induce the hydrophilic material to have hydrophilic properties [51–58]. Recently, nanofiber membranes for AGMD and carbon nanotube membranes for DCMD were made for water desalination [59].

To date, various flat sheet membranes for MD have been fabricated, and the backbone material is mainly used with PVDF-TFE. The copolymer PVDF-HEP is more commonly used for asymmetric flat sheet membranes [60].

Hollow fiber membranes for MD are fabricated using other techniques. Of these membranes, asymmetric PVDF membranes fabricated using wet spinning techniques have various characteristics: a pore size range of 0.031–0.068 μm and effective porosity of 71–1516 m^{-1} under different morphology [61,62].

Most multilayer membranes have porous and hydrophobic properties. Various membranes have been developed in the last decade by research groups, including the Spanish and Canadian group, and tested in DCMD [61,63–71]. These groups commonly fabricate the membrane using different surface modifying macromolecules (SMMs), and different backbone materials of hydrophilic polymers; polyetherimide (PEI), polyethersulfone (PES) and polysulfone (PS). Also, solvents, additives, and fabrication methods are applied for the improvement of MD membrane performance.

2.1.4 Application and Commercialization of MD

MD has been used for a variety of feed solutions, including pure water production, heavy metal contained water, and in the food industry. However, applications have been limited to laboratory scale or pilot plants. Table 2 presents MD applications [24].

2.2 Forward Osmosis

2.2.1 FO Overview

Forward osmosis (FO) treatment systems have been primarily used for industrial wastewater (bench scale), landfill leachate (pilot and full scale), and liquid from the food industry (bench scale). FO processes can also be applied for potable reuse from wastewater, and the desalination of seawater [72]. The major merits of FO are that it does not require a large hydraulic pressure, it has a high rejection of a variety of contaminants, and has a lower fouling tendency than RO-based technologies. In addition, the pressure of FO incurs only a flow resistance in the membrane, simplifying the facility and reducing

Table 2 MD applications

MD process	Membrane type	Feed solution
DCMD	TF200	Pure water and humic acid
	PVDF	
DCMD	PVDF	Humic acid/NaCl
DCMD	PVDF	Pure water, NaCl, brackish, and seawater
DCMD	PVDF	Apple juice
DCMD	PTFE	Seawater and NaCl
AGMD		
DCMD	PTFE	Pure water
	PTFE	
	PVDE	
DCMD	PVDF	Pure water, NaCl, and sugar
DCMD	PTFE	Olive mill wastewater
DCMD	PVDF	Orange juice
DCMD	PVDF	Pure water, NaCl
DCMD	PVDF	Pure water and humic acid
DCMD	–	Heavy metal waste
DCMD	PTFE	Pure water, NaCl, bovine plasma, and bovine blood
AGMD	PTFE	LiBr and H_2SO_4
AGMD	PTFE	NaCl, H_2SO_4, NaOH, HCl and HNO_3
VMD	PTFE	Acetone, ethanol, isopropanol, and MTBE
VMD	PTFE	Pure water, ethanol, and degassing water
VMD	3MC	Pure water and ethanol
	3MB	
	3MA	
SGMD	PTFE	NaCl
	PTFE	

problems associated with membrane support. In food and pharmaceutical processes, FO has advantages because of its low pressure and temperature requirements; FO can also be applied in the medical sector because of its ability to slowly and accurately release drugs [73,74].

2.2.2 Classification of Osmotic Processes

Osmosis is the transport of water across a selectively permeable membrane from a compartment of higher water chemical potential to a compartment of lower water chemical potential. It is driven by the difference in solute concentration across a membrane that allows the passage of water, but rejects most solute molecules or ions. Osmotic pressure is the pressure which, if applied to the more concentrated solution, would prevent the transport of water across the membrane. FO uses the osmotic pressure differential across the membrane, rather than the hydraulic pressure differential (as in RO), as the driving force for transport of water through the membrane. The FO process results in the concentration of a feed stream and the dilution of a highly concentrated stream (referred to as the draw solution). The differences between FO, pressure-assisted osmosis (PAO), pressure-retarded osmosis (PRO), and RO in terms of the water direction due to pressure force are shown in Fig. 17 [72–75].

2.2.3 FO Membrane

In the 1960s, the membrane by Loeb-Sourirajan was developed with the high-performance RO membranes [72], and it was not until the 1990s that RO membranes were used in FO research. A list of recently developed FO membranes is shown in Table 3 [76]. The fabrication methods of these membranes are as follows: phase inversion-formed cellulosic membranes, thin film composite (TFC) membranes, and chemically modified membranes.

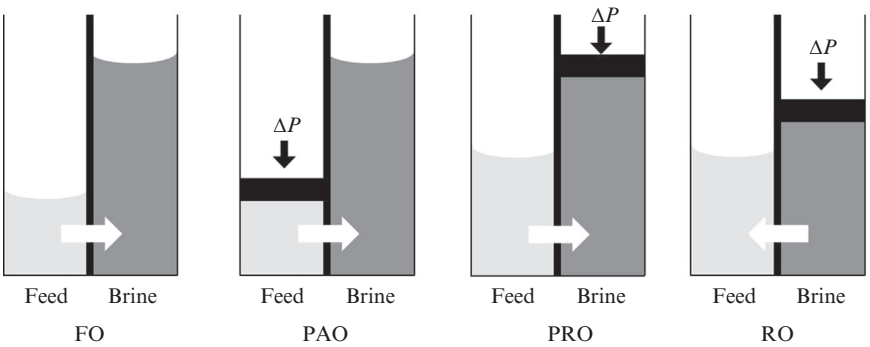

Fig. 17 Flow in FO, PAO, PRO, and RO.

Table 3 Developed FO membranes

Year	Membrane	Materials
2005	Capsule wall membrane	Cellulose acetate or ethyl cellulose
2007	Hollow fiber NF	Polybenzimidazole (PBI)
2008	Flat sheet cellulose acetate membrane	Cellulose acetate
2009	Dual-layer hollow fiber NF	PBI-PES/PVP
2010	Hollow fiber	PES substrates, polyamide active layer
2010	Hollow fiber NF	Cellulose acetate
2010	Flat sheet double-skinned	Cellulose acetate
2010	Flat sheet TFC membrane	Polysulfone (PSf) support, polyamide active layer
2010	Double dense-layer membrane	Cellulose acetate
2011	Modified RO	PSf support modified by polydopamine
2011	Flat sheet composite	Cellulose acetate cast on a nylon fabric
2011	Flat sheet composite	PAN substrate, multiple PAH/PSS polyelectrolyte layers
2011	Positively charged hollow fiber	PAI substrate treated by PEI
2011	Positively charged flat sheet	PAI substrate treated by PEI
2011	Flat sheet TFC polyamide	PES/SPSf substrate, polyamide active layer
2011	Flat sheet TFC polyamide	PES/sulfonated polymer substrate, Polyamide active layer
2011	Flat sheet TFC	PSf support, polyamide active layer
2011	Nanoporous PES	PES cast on PET fabric
2011	Cellulose ester membrane	Cellulose ester
2011	Flat sheet TFC polyamide	PES nanofiber support, polyamide active layer
2011	Flat sheet TFC polyamide	PES nanofiber support, polyamide active layer
2012	Polymeric nanofiber	Polyethylene terephthalate (PET) nanofiber, PSf microporous support, PA active layer
2012	Incorporated TFC PA	Super porous CNT nonwoven Bucky-paper (BP) support, PA active layer
2012	TFC PA	PES inner support layer and PAI active layer posttreated by PEI
2013	Dual layer hollow fiber NF	Stainless steel mesh substrate, micro-porous silica xerogel active layer
2014	Thin-film inorganic (TFI)	PSf-titanium dioxide nanocomposite substrate, PA active layer
2014	Thin-film nanocomposite (TFN) Tri-bore hollow fiber TFC	Matrimid 5218 polymer substrate, PA active layer

2.2.4 Application and Commercialization of FO

FO technology has potential in some applications for the water industry [77]. FO processes can be divided into two categories for water desalination: direct FO desalination, and indirect FO desalination. Fig. 18 illustrates the FO applications used in the water industry [78].

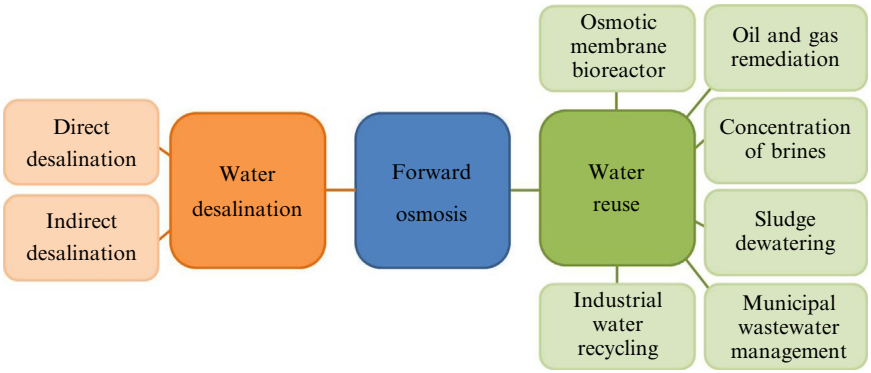

Fig. 18 Forward osmosis applications in the water industry.

Direct FO desalination is similar to other desalination processes, such as RO and nanofiltration (NF), in the way that fresh water is directly produced from seawater or brackish water. Direct FO uses a feed and draw solution; the feed solution is saline water and the draw solution is either a nonvolatile salt solution (NaCl) or volatile salt solution (ammonia–carbon dioxide) [79,80]. In the FO process, there is an additional need to separate the draw solution from the diluted draw solution in order to recover fresh water. The internal and external concentration polarization can take place in the osmosis-driven process. In the external concentration polarization, solutes accumulate at the active layer when the feed solution flows on the active layer of membrane. The draw solution is diluted within the porous structure of the membrane when water passes through the active layer of the membrane, and it is called as internal concentration polarization. Table 4 highlights the research and patents of direct FO desalination resulting from lab-scale, pilot-scale, and modeling [78].

Table 4 Research and patents of direct FO desalination technologies

Year	Feed solution	Posttreatment
2002	Seawater	Precipitation (cooling) and separation through thermal waste heat
2005–2011	NaCl (0.05–2 M)	Thermal decomposition
2006	N.D.	Magnetic field
2010	Contaminated water	Microfiltration
2011–2013	NaCl (0.034 M)	Dewatering hydrogels via external pressure
2011	Synthetic seawater	Ultrafiltration
2012	Brackish water	Nanofiltration
2012	Seawater, brackish water	Cloud point extraction (thermal process)
2012	Seawater, brackish water and contaminated water	Coalescer (thermal process) and nanofiltration
2013	NaCl (0.034 M)	Dewatering hydrogels via thermal process
2013	NaCl (0.086 M)	Metathesis precipitation
2013	Saline water, synthetic seawater	Magnetic field
2013	Synthetic brackish water	Solar-powered electrodialysis

2.3 Pressure-Retarded Osmosis Technology

2.3.1 PRO Overview

The principle of PRO can be explained using PRO osmosis phenomena (refer to Fig. 3). Fig. 19 presents a schematic of a typical PRO process [81]. In brief, contaminants in the feed should be removed in order to reduce membrane fouling in the PRO system. Treated saline water is supplied to the pressure exchanger under high hydraulic pressure by using a high-pressure pump. Treated fresh water is provided to the opposite side of the membrane under a low hydraulic pressure. The saline water faces the active layer and fresh water faces the support layer.

If the saline water passes through the membrane, then the pressure and saline water volume increase, which flows from the fresh water. Finally, salty water is converted into brackish water by dilution; this brackish water is supplied to two parts: one is a hydroturbine to generate electricity, and the other is a pressure exchanger to recover the energy. The pressure exchanger transfers the recovered energy to the salty water. Note that the efficiency of the pressure exchanger is important because of the minimization of energy loss. However, energy from the turbine is sufficient to replace the energy consumed by the PRO system [82–84].

To further improve the energy production of the PRO system, advanced membranes and modules, an increase in the salinity gradient, and system optimization methods are needed.

2.3.2 PRO Membrane and Performance

As mentioned above, improvement in PRO membrane performance is critical for advancing PRO processes. Recent studies have revealed that the performance of the PRO process depends on the membrane module design. Many researchers have reported that the membrane structure morphology is important for diminishing the salt accumulation in the support layer [85,86]. In addition, a high salt rejection rate and water flux, low concentration polarization effect, tolerance to pH and chlorination, and long-term

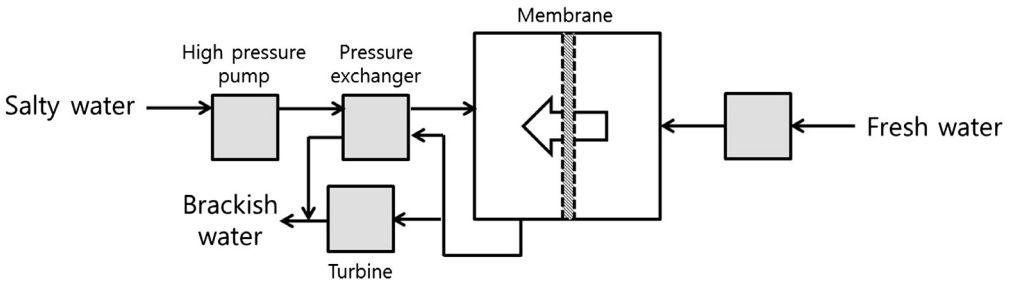

Fig. 19 Schematic diagram of a typical PRO process.

Table 5 Water flux effect on various types of PRO membranes

Feed solution	Draw solution	Water flux (L/(m^2 h))	Membrane orientation	Membrane type
50 mM NaCl	4 M NaCl	37.8	PRO	CTA membrane[a]
DI water	0.5 M NaCl	32.2	PRO	TFC membrane[b]
DI water	2 M NaCl	47.5	PRO	TFC membrane
3.5 M NaCl	2 M NaCl	22	PRO	TFC membrane
DI water	2 M NaCl	33	PRO	TFC membrane
3.5% NaCl	2 M NaCl	15	PRO	TFC membrane

[a]CTA HTI membrane: cellulose tri-acetate hydration technology innovations cellulose tri-acetate membrane.
[b]TFC membrane: thin film composition membrane.

mechanical strength and stable performance are essential [87]. The desired performance of PRO membranes is to sustain the mechanical strength at lower than osmotic pressure and low structure parameter, and maintain the high permeability and high salt rejection.

Two membrane types are now being used: cellulose tri-acetate (CTA), and TFC membranes. Cellulose acetate (CA) membranes are commonly used as PRO membranes. The merits of this material include high hydrophilicity (which enhances the water flux and reduces fouling), good mechanical strength, and high tolerance to chlorination. However, the main disadvantage is that it has limitations in its available pH range [86–89].

The water flux of PRO systems is higher than in FO processes; however, PRO is more sensitive to feed solution due to its higher fouling propensity. This sensitivity means using treated wastewater as a feed solution in PRO must be carefully considered. Table 5 shows the effect of water flux on various types of PRO membranes [90–92].

The advantages of TFC membranes are their high-power generation, high water flux, good mechanical strength, and tolerance for a broad pH range. However, TFC membranes are susceptible to oxidants and chlorination. The support layer of TFC membranes can be fabricated by phase inversion, and the active layer can be made by interfacial polymerization [93]. Table 6 presents the TFC membrane performance under PRO processes [92].

2.3.3 Application and Commercialization of PRO

The first generation of PRO membranes were prototypes introduced by Statkraft, fabricated using flat sheets of cellulose acetate that were spiral wound [93,94], with a performance of only around 0.5 W/m^2 [95]. The second generation was an RO element having a spiral wound TFC membrane. The power production rate per membrane area of a Statkraft plant having this membrane reached approximately 1 W/m^2 [94]. However, if the plant is to produce 2 MW of power, a membrane area of 2 km^2 is needed: unfortunately, the membrane area of the Statkraft power plant is only 2000 m^2. The main problem affecting PRO membranes is fouling. RO TFC membranes have a high

Table 6 Thin-film composite (TFC) membrane performance in PRO processes

Feed solution	Draw solution	Membrane type
0.06% NaCl	Seawater	Modified TFC membrane
0.2% NaCl	Seawater	Modified TFC membrane
0.5% NaCl	Seawater	Modified TFC membrane
0.06% NaCl	Seawater	GKSS TFC membrane
0.06% NaCl	6% NaCl	Modified TFC membrane
0.23% NaCl	6% NaCl	Modified TFC membrane
0.5% NaCl	6% NaCl	Modified TFC membrane
0.06% NaCl	Seawater	Modified TFC membrane
0.06% NaCl	7% NaCl	Modified TFC membrane
0.06% NaCl	4% NaCl	Modified TFC membrane
0.06% NaCl	24% NaCl	Modified TFC membrane
DI water	0.59 M NaCl	Modified TFC membrane
DI water	1 M NaCl	Modified TFC membrane
10 mMNaCl	1 M NaCl	Modified TFC membrane
80 mMNaCl	1 M NaCl	Modified TFC membrane
40 mMNaCl	1 M NaCl	Modified TFC membrane
80 mMNaCl	1 M NaCl	Modified TFC membrane
40 mMNaCl	1 M NaCl	Modified TFC membrane
80 mMNaCl	1 M NaCl	Modified TFC membrane
0.06 NaCl	Seawater	Modified TFC membrane

sensitivity to concentration polarization due to its dense support layer structure. Notably, the salt concentration in layers in the PRO system reduces the osmotic pressure. As such, one solution for improving the power performance and reducing membrane fouling is to pretreat the fresh water. Using river water as the fresh water source is not ideal as there is a lot of organic matter and silt, and its quality significantly varies with the seasons.

The pressure exchange is also an important factor for improving the efficiency. It can save around 60% of the energy input by reusing the wasted pressure. However, the energy production is only about 2 kW, which is not sufficient for use in a plant [96], and the Statkraft power plant was closed in 2013.

2.4 Novel Membrane-Based Technologies

2.4.1 Nanocomposite Membranes

A thin-film nanotechnology (TFN) membrane is used to synthesize Linde type A zeolite nanoparticles and a membrane thin film layer to improve the water flux when maintaining salt rejection [97]. This membrane can reduce the energy consumption rate to maintain a lower feed pressure at the same water flux. This membrane was fabricated using interfacial polymerization to spread one or more monomers in order to fabricate a

nanocomposite structure [98]. The characteristics of this membrane are that it has a smoother, more hydrophilic, and more negatively charged membrane surface than polyamide TFC membranes. Its hydrophilic property can improve the water permeability because water passes through the membrane in a hydrophilic channel, and its negatively charged surface enhances the ion exclusion, thus achieving a high salt rejection rate [99]. The hydrophilic nanoparticles lead to a greater hydrophilicity and less membrane fouling than found in polyamide membranes, which have hydrophobic properties. Table 7 presents a comparison of membrane-based technologies [100].

2.4.2 Aquaporin Membranes

Aquaporin originates from human tissues, and has a rapid and passive transport of water molecules [101]. The basic material of this membrane is protein, and water in aquaporin passes through the protein channel. The phenomena promoting water movement includes selective rapid diffusion and osmotic gradients. Aquaporin-1 (AQP1) has extracellular and intracellular channels that rapidly pass water in a single line, and protein channels prevent the unwanted ions using an electrostatic mechanism [102]. Ultimately, only water molecules can pass through the aquaporin, and the water flux of aquaporin membranes has been estimated to be more than 100 times that of a standard RO membrane. For example, the performance of Aquaporin Z with a novel triblock copolymer has a significantly high water flux and rejection rate [103].

2.4.3 Carbon Nanotube Membranes

The advantages of carbon nanotubes are their high-water flux, large surface area, and functionalization [104]. Because of these advantages, many researchers have evaluated their use for desalination. The water transport of carbon nanotubes is 2–5 times higher than that of RO when analyzed using the Hagen-Poiseuille equation, which leads to a significantly lower energy consumption [105]. The diameter of carbon nanotubes ranges from 6 to 11 Å, and their atomic smoothness and molecular ordering induces a high-water flux to pass water molecules through a 1-dimensional single line [106]. The greatest problem with using carbon nanotubes is based on the complexity of fabricating sub-nanometer tubes.

2.4.4 Graphene-Based Membranes

The advantages of graphene membranes are their fast water transport and high mechanical strength [107]. The principle of graphene membranes use is that there is less friction flow for water permeation in 2-dimensional graphene nanocapillaries, while achieving size exclusion by having a dominant sieving mechanism [108].

These properties of graphene are able to be mass produced, laminated, and flexible. If functionalized graphene can be used as an FO membrane, it will lead to a reduction in internal concentration polarization (ICP) and a higher water flux. However, graphene

Table 7 Comparison of membrane-based technologies

Technology	Advantages	Drawbacks	Treated water quality	Energy consumption	Cost impacts
Nanocomposite membranes	• High permeability • Low feed pressure	• More expensive membrane elements • Need to replace variable speed drive (VFD) on pumps in existing plants	• Similar to TFC RO membranes	• 1.7–2.5 kW-h/m^3	• Potential to reduce costs due to the increased flux and decrease of footprints
Aquaporin membranes	• High permeability • ~100% solute rejection • No need for applied pressure	• No synthetic technology for large-scale membrane • No verification of field tests • No guarantee for chemical resistance • No guarantee for mechanical strength	• 100% rejection of TDS	• Not known	• Cost cannot be estimated because this system is still bench-scale
Nanotube membranes	• High permeability around 10 times higher than RO • High salt rejection	• No guarantee for packing density of nanotubes • No verification of field tests • No guarantee for rejection of specific contaminants • No guarantee for functionalization of nanotubes • No guarantee for stability of nanomaterials • No guarantee of health risks incurred by the release ofnanomaterials in treated water	• More than 95% salt rejection	• Not known	• Cost cannot be estimated because this system is still bench-scale
Graphene-based membranes	• Good mechanical strength • Very high water flux • High rejection rate	• Need for applied pressure • No verification of field tests	• Not known	• Not known	• Cost cannot be estimated because this system is still bench-scale

membranes induce an osmotic pressure drop due to their thermodynamic restrictions. To commercialize graphene membranes, two solutions are needed: one is the possibility for the large-scale synthesis of graphene materials, and the other is the need for higher mechanical strength to endure the hydrostatic pressure in a plant [100].

2.4.5 Energy-Efficient RO Desalination Process

Countercurrent membrane cascades with recycling (CMCR) have been employed to increase energy recovery. Fig. 20 presents a typical CMCR process. CMCR is divided into permeation-enriching and retentate-enriching steps [109].

The Singapore Membrane Technology Center has studied an energy-efficient reverse osmosis (EERO) process to simply modify the CMCR [110]. Fig. 21 shows a schematic of EERO combined with single stage reverse osmosis (SSRO) and a 2-stage CMCR. EERO can reduce the specific energy consumption (SEC) to decrease

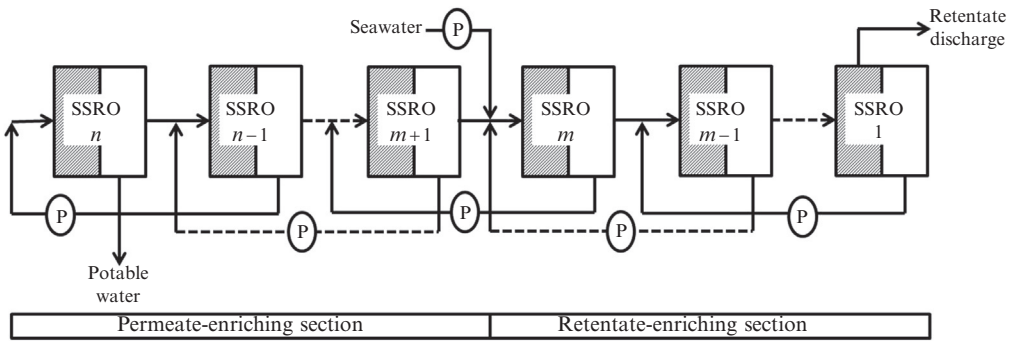

Fig. 20 Schematic of CMCR.

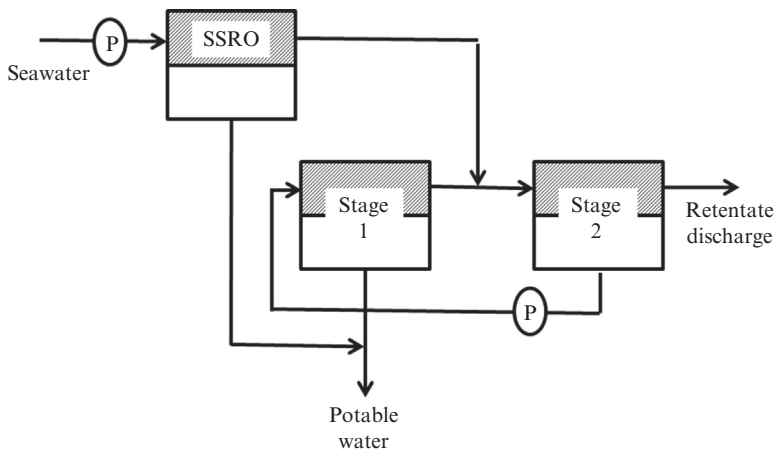

Fig. 21 Schematic of EERO combined with SSRO and 2-stage CMCR.

the osmotic pressure differential and increase the recovery rate. In Fig. 21, the retentate water from SSRO inflows as the feed water for CMCR between stage 1 (NF membrane) and stage 2 (RO membrane). The increase in the recovery rate by CMCR induces the SEC decrease, due to the reduction of the osmotic pressure difference and pumping costs.

An important property of the EERO process is that the interstage pump for high pressure in CMCR is not used at the same osmotic pressure difference as SSRO. Even though the retentate from SSRO has a higher concentration than the feed water, CMCR does not need the interstage pump to reduce the osmotic pressure difference. Permeate from stage 1 recycles to the retentate side of stage 2, and the retentate of stage 2 is supplied to stage 1, which includes the low salt removal by the NF membrane along with the SSRO retentate. This system can increase the energy recovery rate due to the reduction of the concentration difference in both stage 1 and 2 membranes.

3. HYBRID DESALINATION TECHNOLOGY FOR ENERGY EFFICIENCY AND COST REDUCTION

3.1 Limitation of FO Processes

FO, in theory, minimizes the external energy input, and treats the target water source based on the driving force induced by the osmotic pressure difference generated by a draw solution that has a higher osmotic pressure than the target feed. Modern Waters (UK) constructed and operated a standalone FO plant in Oman in 2011 to treat seawater, at a capacity of 100 m^3/d, resulting in a 4.9 kWh/m^3 SEC, an arguably lower value than an SWRO plant operating at 8.5 kWh/m^3 without considering ERDs: thus, the two SECs cannot be fairly compared, though it can be stated that the standalone FO plant revealed its potential to become a feasible option for alternative desalination processes [111]. Indeed, the direction of FO technology advances can be divided into membrane and module designs and draw solution developments. The first commercialized FO membranes were put on the market by HTI and Porifera, which now have successfully commercialized baffled membrane modules employing flat sheet membranes for FO applications. The commercialization of spiral-wound FO membrane modules by Toray Chemical Korea is right around the corner. The Porifera membrane exhibits, at a 1 M NaCl draw solution, approximately 30 LMH—which is comparable to the water flux of typical RO membranes [112]. As such, the low water flux of FO membranes, which was deemed one of its most critical limitations, has been comprehensively improved. The efficient draw solute recovery is still in need of development, however; thus, FO processes cannot yet be clearly deemed a plausible option in terms of energy consumption. Supporting this claim, Semiat et al. [113] reported that the FO process itself can only produce 0.3 kWh/m^3, whereas the 11 kWh/m^3 required for the draw solute recovery process makes the standalone FO process far from practical, as depicted in Fig. 22.

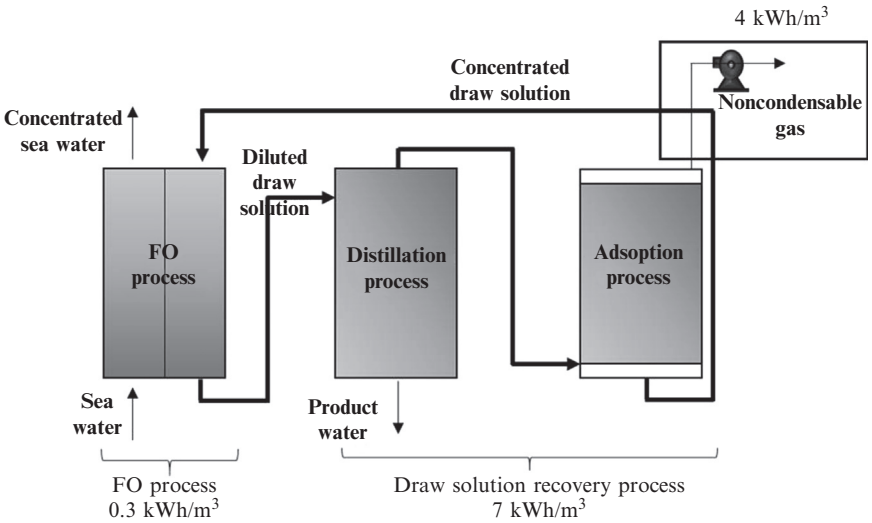

Fig. 22 Energy consumption in FO processes [113].

These results suggest that the draw solute recovery process plays a crucial role in the possible commercialization of a standalone FO process. To this end, numerous studies have been conducted in the attempt to develop energy efficient draw solutes. Table 8 summarizes the major draw solutes developed and the drawbacks of each. Other studies tested other types of draw solutes and worked to develop specific processes for the draw solutes, though no clear advantages were found. In 2015, Shaffer et al. [120] argued that, based on analyses of thermodynamic aspects, the minimum energy required to desalinate seawater cannot be further reduced, and that FO-RO hybrid desalination cannot reduce the energy consumption to below that of conventional SWRO desalination plants. Despite such drawbacks, the authors added that potential advantages can arise when FO is applied without the need for draw solute recovery, due to its low membrane fouling potential.

Table 8 Draw solution development and drawbacks

Reference	Draw solute	Drawbacks
Batchelder [114]	SO_2	Additional heat source
Frank [115]	Al_2SO_4	Sedimentation
Yaeli [116]	Glucose	High pressure
McGinnis and Elimelech [117]	NH_3-CO_2	Additional heat source
McCormick et al. [118]	Ethanol	Reverse diffusion of ethanol
Ling et al. [119]	Highly hydrophilic magnetic nanoparticles	Nanoparticle separation process needed

3.2 FO Hybrid Processes

3.2.1 FO-RO Hybrid Process

The FO-RO hybrid process is a multibarrier treatment system in which the FO system can initially remove dissolved contaminants with low energy consumption, and the RO system then fulfills the need for high salt rejection to produce potable water. In addition, this system promotes a reduction in energy consumption, increases the water recovery rate, and decreases the environmental impact of a desalination plant [117]. To commercialize this process, the FO process should be applied only as a pretreatment process before the RO process, with no draw solute recovery unit as reported in Shaffer et al. [118]. A schematic of an FO-RO hybrid system for water desalination is illustrated in Fig. 23.

The feed seawater of the RO system originating from FO is diluted, thereby significantly lowering the energy consumption, and the two systems can then reject a high concentration of contaminants in a tight, impaired stream, as shown in Fig. 23A. Cath et al. [119] reported that the potential of the advanced FO-RO concept, depicted in Fig. 23B, was assessed based on an economic evaluation using laboratory tests, and that this process was up to 38,000 US$/year more economical than standard RO processes under the condition of seawater 100 m^3/d (35 g/L), w/w 200 m^3/d (0.5 g/L), RO

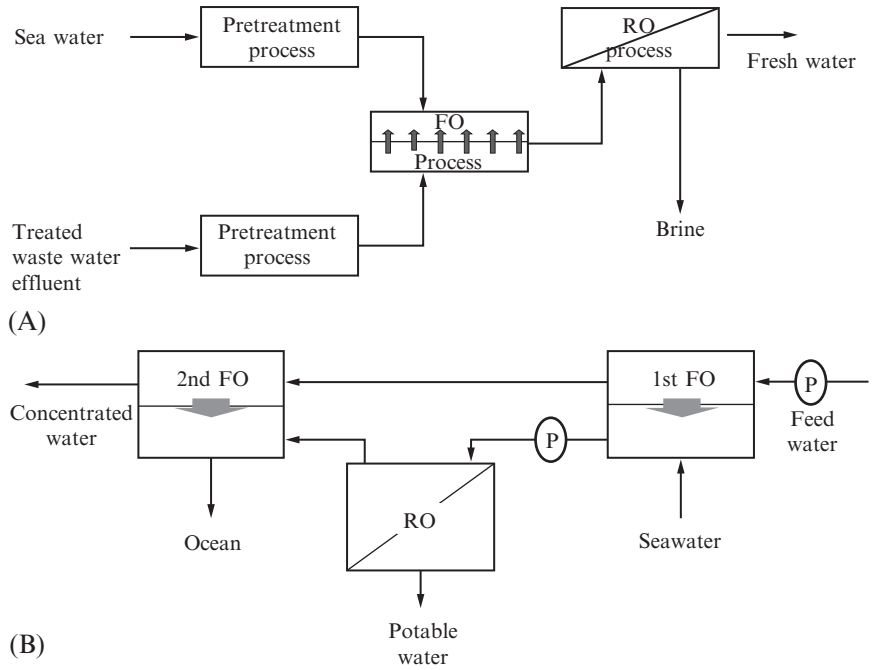

Fig. 23 Schematic of FO-RO hybrid process: (A) basic concept, and (B) refer to Cath et al. [119].

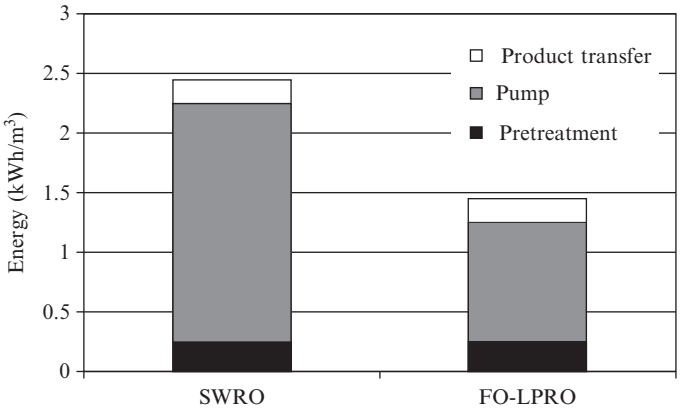

Fig. 24 Comparative estimation of energy cost for SWRO and hybrid FO-LPRO.

recovery rate 50%, and energy cost 0.3 US$/kWh. In this concept, the second FO system plays a role in reducing the environmental impact by diluting the RO brine before it can be stably released back into the ocean.

The FO-RO hybrid system was first referred to as low pressure reverse osmosis (LPRO) combined with FO by Yaeli [121], and was used to recover glucose. After that, Yangali-Quintanilla et al. [122] assessed the FO-LPRO for the desalination of Red Sea water. The estimated energy consumption of FO-LPRO was 1.3–1.5 kWh/m^3, or approximately 50% of the SWRO process. Fig. 24 shows a comparison of the energy consumption between RO and FO-LPRO hybrid systems. Energy consumption for pumps in FO-LPRO was around two times lower than that for the RO system.

The FO-RO hybrid was also simulated by Shaffer et al. [118]. In a comparison with a conventional 2-stage RO used to produce a final water product of 100,000 m^3/d, they showed that the FO-RO hybrid can achieve 2.93 kWh/m^3, which is a 0.86 kWh/m^3 lower energy consumption than the 2-stage RO. The SEC in Yangali-Quintanilla et al. [122] has a lower energy consumption than the simulation done by Shaffer et al. [118], and this result is attributed to the use of industrial wastewater as feed to dilute the seawater, such that no additional draw solute is required in the recovery process. However, by using a through cost analysis, it was found that the total capital cost of the hybrid process went above that of the 2-stage RO. Such a drawback is closely connected to the need for additional FO membrane costs and the low water flux of FO [123].

To date, it is possible to achieve a water flux of 30 LMH from a single module using 1 M NaCl as the draw solution, thus there still is potential to reduce capital costs by advancing and developing design factors. The use of impaired water sources as feed for FO in a hybrid scheme, however, may lead to limitations for end users of the product water (i.e., it may not be suitable for potable water and only applicable to industrial water supplies).

3.2.2 FO-MSF/MED Hybrid Process

Generally, feed water in the Middle East includes high salinity, high temperature, and high contaminants, and for this reason MSF and MED are commonly employed in similar regions. This highly contaminated seawater typically requires a pretreatment: however, current pretreatments cannot properly remove all dissolved solids, and thermal-driven technologies remain susceptible to scaling from organic matter and dissolved solids [124]. The dissolved solids are deposited on the surface of heat exchangers, thereby decreasing the heat transfer efficiency and reducing the operating temperature [125,126]. Nanofiltration (NF) membranes can remove dissolved solids as the pretreatment; however, the use of NF membranes increases the operational cost due to their susceptibly for fouling and need for frequent replacement [127,128]. Therefore, FO systems alone have been considered as an alternative technology to remove organic and inorganic matter [129,130].

3.2.3 FO-Electrodialysis Hybrid Process

Electrodialysis (ED) has been employed for brackish water desalination. ED can remove salt ions and charged organic matter using an ion exchange membrane [131]. The major advantage of ED is that it does not use pressure and thus can reduce the energy consumption. Also, ED has low instances of membrane fouling and scaling, and it is easy to clean the membrane through the chemical cleaning and a change of polarity [132]. Even though there are notable advantages of ED, the cost of electrodes and membranes remains high as ED membranes have a short lifespan when employed in a desalination plant. Notably, an FO-ED system using a photovoltaic (PV) cell as power, under small-scale conditions, could produce high quality water at a water production cost of 3.6–5.4 US$/$m^3$ [130].

3.3 Limitations of MD Technologies

MD applications have specific advantages due to their lower operating temperature and smaller required footprint compared to conventional thermal desalination techniques. But there are drawbacks, such as lower water recovery and lower removal rates of volatile substances such as ammonia. At one point, MD research seemed to stall due to such disadvantages, but it has once again resurfaced with the development of new MD module designs, and their potential applicability due to the rise of renewable and alternative energy sources (e.g.., solar energy, geothermal heat) as heat sources. In this context, several tests have been conducted in pilot scale. For example, Anderson et al. [133] operated cassette and stacking configurations for MD in field tests. Fane [134] obtained a flux of 2.1–5.1 kg/(m^2 h) at a temperature difference of 15.1–32°C, and Minier-Matar et al. [135] conducted vacuum multieffect MD and air-gap single MD tests, to obtain fluxes of 5 LMH and 6.1 LMH, respectively, under temperature conditions of 25.6–35°C.

Sirkar and Song [136] operated MD tests and achieved 15–33 kg/(m^2 h) of flux at a temperature difference of 36–70°C during three months of continuous operation.

These pilot test results reveal a clear trend in which the higher the temperature gradient, the higher the water flux. In the work done by Alkhudhiri et al. [27], the authors reviewed published research articles and summarized the flux variations under the feed temperature conditions of 5–81°C. Also, El-Bourawi et al. [137] showed that the feed temperature and the flux have an exponential relationship and summarized results obtained based on various operating conditions such as temperature, concentration, flow velocity, and stirring.

Other than the temperature gradient, it has been further suggested that vapor pressure, viscosity, density, thermal conductivity, heat capacity, and concentration polarization also affect the MD performance [138]. Nonetheless, it has been postulated that the major factors determining the membrane performance are temperature polarization (TP), membrane wetting, and conductive heat loss [131], in addition to the basic concepts described above. Of these major factors, TP and membrane wetting have been widely discussed. TP refers to the loss of driving force due to limited heat conductivity, and numerous attempts have been carried out to minimize the TP and enhance the water flux in various simulations and modeling approaches. Membrane wetting, another critical factor that governs the MD performance, diminishes the water vapor transport by blocking the porous structures with liquid phase, thereby enabling the feed water in liquid phase to be transported directly to the permeate side along with salts, resulting in a decrease in product water quality. Membrane wetting occurs when the vapor pressure reaches a critical pressure point, defined as the liquid entry pressure (LEP) [139]. LEP has a close connection to the surface tension, contact angles, and pore sizes and their shapes, and thus the temperature and species contained in the feed are crucial for determining the LEP [140,141].

As with membrane wetting, fouling and scaling induce a flux decline in a similar fashion. In theory, the feed and feed water cannot be in direct contact, meaning the nonoccurrence of fouling and scaling. However, with less fouling compared to pressure-driven membrane processes, there are studies that report the presence of fouling that diminished the flux; fouling inherently blocks the membrane pores and thus becomes one of the major causes of the flux decline. There is scientific evidence that fouling accelerates the TP across the membrane, resulting in a more rapid flux decline. It is also known that fouling in MD arises depending on temperature and feed water composition [139,141]. Table 9 summarizes the major causes of flux decline in MD operations and three key findings.

The most critical aspects affecting MD commercialization are flux improvement and the reduction of energy consumption. Compared to the water flux of a single SWRO module having a 17,000 GPD (approx. 65 LMH), water fluxes of 55–60 LMH obtained under feed temperature conditions of 81°C, and a 98.6 LMH derived at 79.8°C [138,159], excluding the robustness of the MD, are more likely to lead to uncompetitiveness in terms of economic factors.

Table 9 Research results for temperature polarization, membrane wetting, and fouling

Factor	Description	Reference
Temperature polarization (TP)	Effect of concentration	[142]
	Effect of stirring to improve water flux	[143–145]
	Effect of membrane spacer	[146]
	Heat and mass transfer modeling	[143,147,148]
	Use of a vacuum pump	[149]
Membrane Wetting	Effect of organic foulant concentration and modeling	[150]
	Effect of pore size and shape	[151]
	Flux recovery	[149,152]
Fouling	Biological fouling by biofilm	[138,153]
	Effect of salt on humic acid fouling	[154]
	Particulate fouling	[138]
	Scale formation	[155–158]

3.4 MD-Based Hybrid Technologies

3.4.1 RO-MD Hybrid Process

Although it has undeniable limitations as a standalone process, combining MD technology with another process for water desalination may reduce the brine discharge, and thus improve the water recovery rate, due to the features that are not affected by the salt concentration in the feed. In general, pressure-driven membrane processes are deemed applicable if hybridized with MD, because of these reasons.

MD hybridization has been categorized into RO-MD, UF-MD, and MF-MD by Suk and Matsuura [160], with RO-MD being considered the most promising application for seawater desalination. UF-MD was investigated for use in the purification of oily wastewater (Fig. 25), in which a UF unit was applied to the removal of oil and TOC, and an MD unit was used to remove TDS.

In one study by Karakulski et al. [161], MD was hybridized with UF-NF-RO to treat brackish water having salty concentrations of 415–430 mg/L (Fig. 26A). In this work, RO-MD was not used to improve the RO recovery but to treat the RO product once more with MD to further demineralize it. In contrast, Mericq et al. [162] investigated VMD in order to improve RO recovery by treating RO brine to improve water recovery (Fig. 26B), and subsequently achieved total recovery of 89%; the authors presented a minor effect of CP in which the scale formation induced by calcium-driven crystals partially affected the flux decline. Similarly, Ji et al. [163] combined MD with crystallization to achieve a 90% total recovery by treating the RO brine, and found that soluble organic substances may affect the water flux decline. In addition, Qu et al. [164] integrated DCMD into the treatment of RO brine, and achieved a high recovery rate.

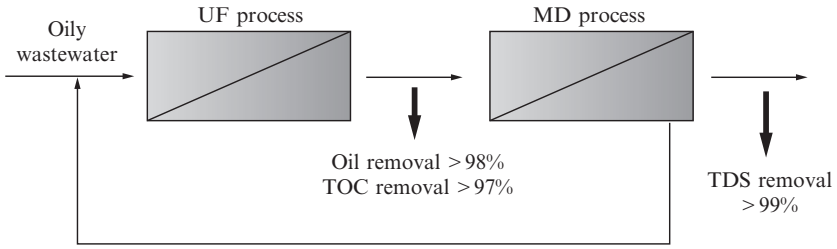

Fig. 25 Schematic of UF-MD hybrid for oily wastewater [160].

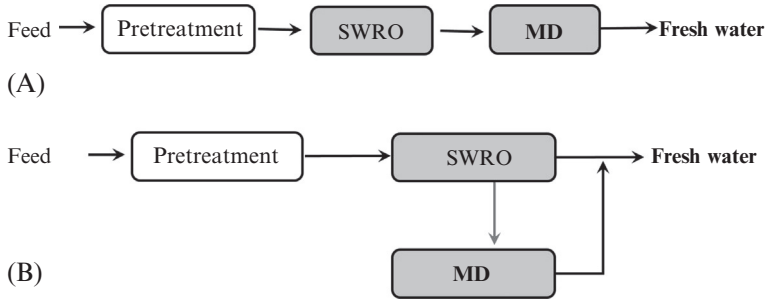

Fig. 26 Schematic of MD-RO hybrid processes: (A) MD-RO concept in Karakulski et al. [161], and (B) MD-RO concept in Mericq et al. [162].

3.4.2 FO-MD

The FO-MD hybrid process can be applied under robust feed solutions, because of the low fouling potential of FO. In this scheme, FO is first used to treat salinity and is then followed by MD, which targets recovering draw solutes; this concept was initiated by Cath et al. [165] in a patent publication in 2007. In this hybrid process, MD is used as a supportive process and the major focus is given to FO process operation and the draw solution utilized in FO.

The major challenge of FO-MD is the development of the draw solution, having a high FO flux, low reverse salt leakage, and low concentration polarization for MD. Recently, Ge et al. [166] synthesized novel draw solutes using polyelectrolyte. These solutions had good solubility, high water flux, and low salt leakage. The polyelectrolyte decreased the water flux by inducing high viscosity in a standalone FO; however, the high temperature decreased the viscosity in an FO-MD hybrid system, and the water flux significantly improved. Fig. 27 presents the schematic diagram of this FO-MD hybrid system.

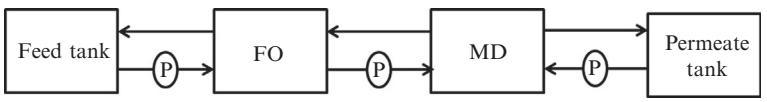

Fig. 27 Schematic diagram of FO-MD hybrid system.

An FO-MD hybrid has generally been studied to treat highly concentrated wastewater or valuable resource recovery, rather than for seawater desalination [167–169]. The work done by Zhang et al. [170] showed that it was possible to both treat oily wastewater and recover acetic acids, at a water recovery of up to 90%. Nevertheless, the authors reported that severe fouling occurred, resulting in a rapid water flux decline. In another study by Xie et al. [168,169], FO was implemented as a pretreatment to prevent MD from rapid fouling when treating digested sludge concentrate. It was found the FO-MD displayed better performance than MD only due to FO reversible fouling and the characteristic of FO, though there was some diffusion of trace organic contaminants toward the FO draw solution. Similarly, Wang et al. [171] tested FO-MD for use to treat bovine serum albumin (BSA) solutions by incorporating NaCl solution as the draw, and showed the same trends as in the previous work, ultimately concluding that the selection of a proper draw solute is key to the successful operation of FO-MD.

These results on membrane fouling are particularly important because MD requires feed streams having a high temperature and draw solutions that have a higher osmotic pressure than the MD feed stream, resulting in the back diffusion of draw solutes. It is a well-known fact that the back diffusion of draw solutes incurs a loss in the osmotic driving force, which consequently induces a flux decline. As such, maintaining a proper temperature balance and developing draw solutes that help improve it while incurring a minimal loss of the draw solute is crucial for the sustainable and continuous operation of the FO-MD hybrid process.

3.4.3 MD-Crystallizer

A membrane distillation-crystallizer (MD-C) can achieve a high recovery rate for water desalination [172]. The MD process concentrates the feed water so that the crystallizer can easily extract the salt. This system has been applied to separate inorganic salts, wastewater, protein solutions, etc. [173,174].

MD-Crystallization (MC) was, in fact, first employed in pharmaceutical industries, not in the field of desalination, to extract taurine from wastewater [175]. In seawater desalination, the MC process can achieve both higher water recovery and retrieval of valuable resources; Curcio et al. [60,176] first reported the results of such an application in 2001. The authors operated MD in the first phase of a treatment to concentrate NaCl solution for ease of crystallization, and then recovered NaCl from the concentrate. Using the same process scheme, Gryta [177] attained an NaCl production of 100 kg/(m^2 d). Tun et al. [178] targeted the retrieval of Na_2SO_4 by conducting batch experiments to analyze operating factors, and obtained Na_2SO_4 crystals having sizes between 60 and 80 μm. In addition, Edwie and Chung [179] operated MC at a feed temperature under 40°C for 3.5 days of continuous operation, and retrieved up to 34 kg/m^3 of NaCl. It was found that the retrieval rate is proportional to the operating temperature, but inversely proportional to the crystal size. The authors conducted the same set of experiments by synthesizing

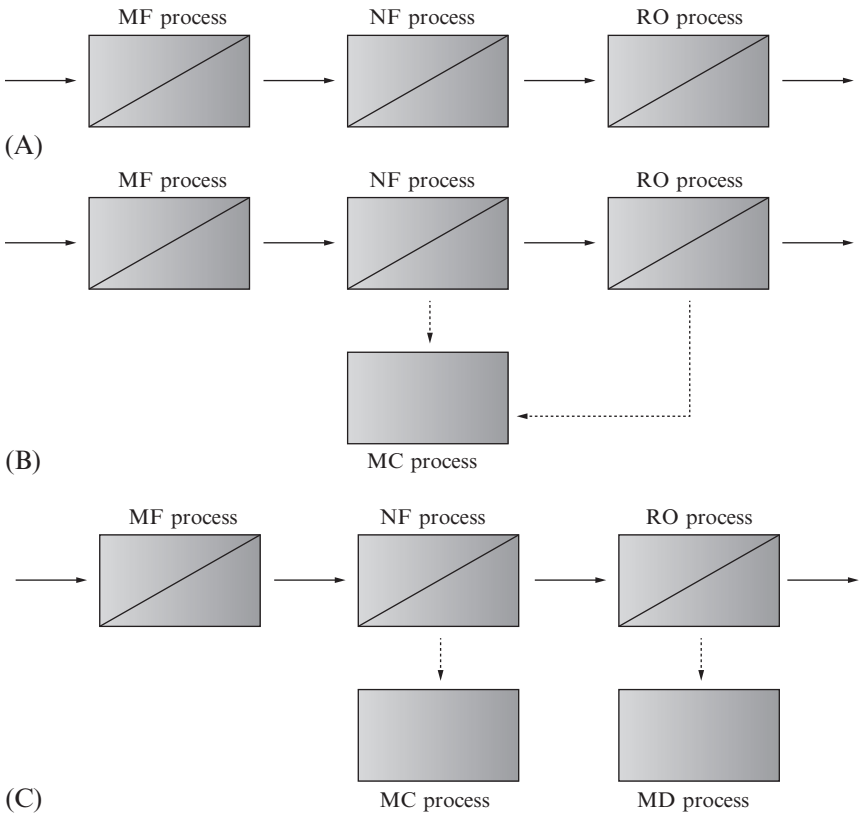

Fig. 28 Schematic diagram of MD-crystallizer hybrid systems. (A) modified RO process, (B) RO-MC process, (C) RO-MC-MD process.

three different types of MD membranes to investigate the effect on membrane wetting, and concluded that the dual-layer type performs better than the single-layer type.

Macedonio et al. [180] compared the economic aspects of RO and MD hybrids, as depicted in Fig. 28. In the case of using normal seawater as the feed stream, the authors compared three types of modified RO process (Fig. 28A), RO-MC process (Fig. 28B), and RO-MC-MD process (Fig. 28C) to confirm the economic benefits, and concluded that, in all cases, the MC/MD hybrid had no benefits. The major cause was the need for the additional energy required for MC and MD; such drawbacks can be alleviated when a geothermal heat source is available, resulting in energy consumptions of 1.54 kWh/m^3 for RO-MC and 1.61 kWh/m^3 for RO-MC-MD [180]. Despite such efforts, they reported that the water cost was always lower for the modified RO process (e.g., 0.39 US$/$m^3$ at the lowest) than for the hybrid processes (e.g., 0.43 US$/$m^3$). As such, there are currently no MD-based desalination technologies that can outperform conventional RO desalination, except for special cases in which waste heat is available, when considering both capital expenditure (CAPEX) and operating expenditure (OPEX).

3.4.4 Renewable Energy Driven MD

The primary disadvantage of the MD process is its high energy consumption. To reduce the energy input required for MD operations, employing renewable and alternative energy sources as the heat source has been spotlighted in recent years, and is likely the scheme that is closest to commercialization. Solar energy can also be combined with MD because there is no need to supply an exceedingly high temperature. Other heat sources, such as geothermal energy and wasted heat from cooling towers, can also be applied for MD processes [181,182].

In the solar-driven MD process, the flux varies due to the fluctuation of solar radiation [183,184]. In addition, membrane scaling and wetting is a serious problem in this system. To date, AGMD, DCMD, and VMD with internal heat recovery and external heat exchangers have been researched as solar-driven MD processes. The schematic of this solar-driven MD process is illustrated in Fig. 29.

Schwantes et al. [183] used solar energy and waste heat to operate MD desalination plants in three different countries (Namibia, Italy, and Spain), and Koschikowski et al. [184] reported the operational outcomes of a small-scale MD system that utilizes solar energy to establish an MD plant having a capacity of 0.2–20 m^3/d. In general, waste heat is typically available, whereas solar energy is only available in the presence of solar radiation; thus, the total production should be less [183]. Table 10 summarizes MD operations employing solar energy as the heat source.

When using MD, Kullab and Martin [185] gave a product water cost estimate of 8.9 US$/$m^3$ for an annual production of 24,000 m^3; Barnet and Jwaied [186] estimated costs to be 15–18 US$/$m^3$ without the use of solar energy as the heat source. These reports argue that the governing factors determining the economic feasibility include the lifetime of the MD membranes and the design period of the plant. In subsequent simulations, Hogan et al. [187] investigated the economic feasibility and suggested that due to the inverse proportional relationship between heat recovery and collection, the economic benefit initially increases but diminishes after reaching a critical heat recovery point. Such a trend is mainly attributed to the large proportion of the heat exchanger in terms of

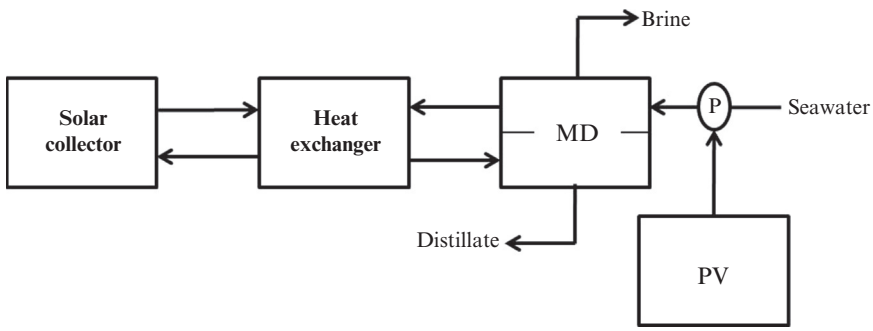

Fig. 29 Schematic of solar-driven MD process.

Table 10 Operational results in various solar energy MD system [183]

Heat source	Feed condition	Production (m^3/d)
Namibia (solar energy)	Saline groundwater (28,000 ppm)	208
Italy (waste heat from diesel engines)	Seawater (35,000 ppm)	3.69
Spain (solar energy)	Seawater (35,000 ppm)	1.4
Solar energy	Seawater	0.13
Solar energy	1 g/L NaCl	6.5 LMH
	35 g/L	5.6 LMH
Solar energy	55,000 μS/cm	0.083–0.46 LMH
Solar energy	Groundwater	0.11–0.28 (~32.19 LMH)
Solar energy (solar pond)	0 M	5.8 LMH
	0.6 M	4.2 LMH
	2.0 M	3.3 LMH
	4.0 M	2.9 LMH

capital expenditure, and the authors concluded having an appropriate design for the heat recovery system is the most pivotal factor that governs the economic feasibility of MD desalination. To date, the need for additional heat sources makes MD an uncompetitive process compared to RO, but based on the operational reports from MEMSTILL in Singapore, MD can indeed be a plausible option when using waste heat as the heat source [188].

4. SUMMARY

The aim of this chapter is to understand the principle, trend, and limitations of membrane-based desalination technologies. The first part explains the trend of water desalination technologies, the second part describes the basic principle of membrane-based processes and novel technologies, and the last part introduces the hybrid processes with water desalination technologies focusing on energy efficiency and cost reduction.

Prior to the 2000s, thermal technologies were the leading processes in the desalination market. The most commonly used desalination technologies were based on thermal processes, including MSF and MED. However, the RO process has been a dominant technology worldwide since the 2000s, due to the lower energy consumption and water production cost.

Other types of membrane-based technologies are MD, FO and PRO. However, these processes have some specific drawbacks when independently applied as the main

technology in the plant in terms of energy consumption, water flux, membrane fouling, etc. The novel membranes have been vigorously developed through the R&D project; however, there seems to be a necessity to refine further for practice.

REFERENCES

[1] Desalination Markets 2010, Global Water Intelligence, 2010.
[2] M.K. Wittholz, B.K. O'Neill, C.B. Colby, D. Lewis, Estimating the cost of desalination plants using a cost database, Desalination 229 (2008) 10–20.
[3] www.desaldata.com.
[4] Desalination Markets 2016, Global Water Intelligence, 2015.
[5] N. Voutchkov, World Class Desalination Energy & the Environment, (2011). www.adelaide.edu.au.
[6] C. Campos, The Economics of Desalination for Various Uses, www.rac.es/ficheros/doc/00731.pdf.
[7] B. Liberman, I. Liberman, Starting procedure of high-pressure pump with de-rated motor for large-scale SWRO trains, Desalination 132 (2000) 293–298.
[8] B. Sauvet-Goichon, Ashkelon desalination plant-a successful challenge, Desalination 203 (2007) 75–81.
[9] A. Martinho, The high pressure pump train on reverse osmosis plants. Experience and current trends, Desalination 138 (2001) 219–222.
[10] M.J. Guirguis, Energy Recovery Devices in Seawater Reverse Osmosis Desalination Plants with Emphasis on Efficiency and Economical Analysis of Isobaric versus Centrifugal Devices (Thesis of Master in University of South Florida), 2011.
[11] A.M. Farooque, A.T.M. Jamaluddin, A.R. Al-Rewell, P.A.M. Jalaluddin, S.M. Marwani, S.S.A. Al-Mobayed, A.H. Qasim, Comparative Study of Various Energy Recovery Devices Used in SWRO Process, Issued as Technical Report No. TR.3807/EVP02005, 2004.
[12] T.I. Yun, C.J. Gabelich, M.R. Cox, A.A. Mofidi, R. Lesan, Reducing costs for large-scale desalting plants using large-diameter, reverse osmosis membranes, Desalination 189 (2006) 141–154.
[13] P.E. Lisa Henthorne, C. Bartels, R. Bergman, M. Hallan, P. Kanppe, J. Losier, P. Metcalfe, M. Peery, I. Shelby, Large Diameter RO Technology, www.grahamtek.com.
[14] Guidelines for Drinking-Water Quality, fourth ed., WHO, 2011.
[15] C.R. Bartels, R. Franks, W. Bates, Design advantages for SWRO using advanced membrane technology, IDA J. Desalin. Water Reuse 2 (2010) 21–25.
[16] C. Fritzmann, J. Lowenberg, T. Wintgens, T. Melin, State-of-the-art reverse osmosis desalination, Desalination 216 (2007) 1–76.
[17] M. Wilf, S. Tedesco, H. Arnold, J. Hudkins, Effective design of seawater RO systems with new generation of high permeability membrane elements, in: IDA World Congress, San Diego, USA, 2015.
[18] H. Winter, Twenty years experience in seawater reverse osmosis and how chemicals in pretreatment affect fouling of membrane, Desalination 110 (1997) 93–96.
[19] World Intellectual Property Organization, Apparatus for Treating Solutions of High Osmotic Strength, Patent Application Number PCT/US2005/006224, 2005.
[20] V. Garcia Molina, M. Busch, P. Sehn, Cost savings by novel seawater reverse osmosis elements and design concepts, Desalin. Water Treat. 7 (2009) 160–177.
[21] B. Penate, L. Garcia-Rodriguez, Reverse osmosis hybrid membrane inter stage design: a comparative performance assessment, Desalination 281 (2011) 354–363.
[22] E. Spiritos, C. Lipchin, Desalination in Israel, Water Policy in Israel: Context, Issues and Options, Global Issues in Water Policy 4, Springer, Netherlands, 2013. pp. 101–123 (Chapter 7).
[23] Carlsbad Seawater Desalination Project, Energy Minimization and Greenhouse Gas Reduction Plan, http://carlsbaddesal.com/, 2008.
[24] A. Alkhudhiri, N. Darwish, N. Hilal, The membrane distillation: a comprehensive review, Desalination 287 (2012) 2–18.
[25] H. Kurokawa, T. Sawa, Heat recovery characteristics of membrane distillation, Heat Transfer Jpn. Res. 25 (1996) 135–150.

[26] J.B. Gálvez, L.G. Rodríguez, I.M. Mateos, Seawater desalination by an innovative solar-powered membrane distillation system: the MEDESOL project, Desalination 246 (2009) 567–576.
[27] P. Wang, T.S. Chung, Design and fabrication of lotus-root-like multi-bore hollow fiber membrane for direct contact membrane distillation, J. Membr. Sci. 421–422 (2012) 361–374.
[28] L. Francis, H. Maab, A. AlSaadi, S. Nunes, N. Ghaffour, G.L. Amy, Fabrication of electro spun nanofibrous membranes for membrane distillation application, Desalin. Water Treat. 51 (2013) 1337–1343.
[29] H. Yu, X. Yang, R. Wang, A.G. Fane, Numerical simulation of heat and mass transfer indirect membrane distillation in a hollow fiber module with laminar flow, J. Membr. Sci. 384 (2011) 107–116.
[30] M. Gryta, M. Barancewicz, Influence of morphology of PVDF capillary membranes on the performance of direct contact membrane distillation, J. Membr. Sci. 358 (2010) 158–167.
[31] G. Zuo, R. Wang, R. Field, A.G. Fane, Energy efficiency evaluation and economic analyses of direct contact membrane distillation system using Aspen Plus, Desalination 283 (2011) 237–244.
[32] E. Curcio, E. Drioli, Membrane distillation and related operations – a review, Sep. Purif. Rev. 34 (1) (2005) 35–86.
[33] S. Bandini, G.C. Sarti, Heat and mass transport resistances in vacuum membrane distillation per drop, AIChE J. 45 (1999) 1422–1433.
[34] S. Bandini, C. Gostoli, G.C. Sarti, Separation efficiency in vacuum membrane distillation, J. Membr. Sci. 73 (2–3) (1992) 217–229.
[35] K.W. Lawson, D.R. Lloyd, Membrane distillation. I. Module design and performance evaluation using vacuum membrane distillation, J. Membr. Sci. 120 (1) (1996) 111–121.
[36] F.A. Banat, J. Simandl, Desalination by membrane distillation: a parametric study, Sep. Sci. Technol. 33 (2) (1998) 201–226.
[37] M.C. García-Payo, M.A. Izquierdo-Gil, C. Fernández-Pineda, Air gap membrane distillation of aqueous alcohol solutions, J. Membr. Sci. 169 (1) (2000) 61–80.
[38] J. Walton, H. Lu, C. Turner, S. Solis, H. Hein, Solar and Waste Heat Desalination by Membrane Distillation, College of Engineering University of Texas, El Paso, 2004.
[39] S. Kimura, S.I. Nakao, S.I. Shimatani, Transport phenomena in membrane distillation, J. Membr. Sci. 33 (3) (1987) 285–298.
[40] F.A. Banat, J. Simandl, Membrane distillation for dilute ethanol: separation from aqueous streams, J. Membr. Sci. 163 (2) (1999) 333–348.
[41] J. Swaminathan, H.W. Chung, D.M. Warsinger, F.A. AlMarzooqi, H.A. Arafat, J.H. Leinhard, Energy efficiency of permeate gap and novel conductive gap membrane distillation. J. Membr. Sci. (2016) 171–178, http://dx.doi.org/10.1016/j.memsci.2015.12.017.
[42] M. Mulder, Basic Principles of Membrane Technology, Kluwer Academic Publishers, Dordrecht, Netherlands, 1992.
[43] T. Matsuura, Synthetic Membranes and Membrane Separation Processes, CRC Press, Boca Raton, FL, 1994.
[44] I. Pinnau, B.D. Freeman, Membrane formation and modification, in: ACS Symposium Series, vol. 744, American Chemical Society, Washington, DC, 2000.
[45] D.R. Lloyd, K.E. Kinzer, H.S. Tseng, Microporous membrane formation via thermally induced phase separation: I. Solid–liquid phase separation, J. Membr. Sci. 52 (1990) 239–261.
[46] M. Khayet, Membranes and theoretical modeling of membrane distillation: a review, Adv. Colloid Interface Sci. 164 (2011) 56–88.
[47] C. Feng, B. Shi, G. Li, Y. Wu, Preliminary research on microporous membrane from F2.4 for membrane distillation, Sep. Purif. Technol. 39 (2004) 221–228.
[48] C. Feng, B. Shi, G. Li, Y. Wu, Preparation and properties of microporous membrane from poly(vinylidenefluoride-co-tetrafluoroethylene) (F2.4) for membrane distillation, J. Membr. Sci. 237 (2004) 15–24.
[49] M.C. García-Payo, M. Essalhi, M. Khayet, Preparation and characterization of PVDF-HFP copolymer hollow fiber membranes for membrane distillation, Desalination 245 (2009) 469–473.
[50] M.C. García-Payo, M. Essalhi, M. Khayet, Effects of PVDF-HFP concentration on membrane distillation performance and structural morphology of hollow fiber membranes, J. Membr. Sci. 347 (2010) 209–219.

[51] M. Khayet, J.I. Mengual, T. Matsuura, Porous hydrophobic/hydrophilic composite membranes: application in desalination using direct contact membrane distillation, J. Membr. Sci. 252 (2005) 101–113.
[52] Z. Jin, D.L. Yang, S.H. Zhang, X.G. Jian, Hydrophobic modification of poly(phtalazinoneether sulfone ketone) hollow fiber membrane for vacuum membrane distillation, J. Membr. Sci. 310 (2008) 20–27.
[53] K.Y. Wang, S.W. Foo, T.S. Chung, Mixed matrix PVDF hollow fiber membranes with nanoscale pores for desalination through direct contact membrane distillation, Ind. Eng. Chem. Res. 48 (2009) 4474–4483.
[54] S. Cerneaux, I. Stuzynska, W.M. Kujawski, M. Persin, A. Larbot, Comparison of various membrane distillation methods for desalination using hydrophobic ceramic membranes, J. Membr. Sci. 337 (2009) 55–60.
[55] B. Li, K.K. Sirkar, Novel membrane and device for direct contact membrane distillation-based desalination process, Ind. Eng. Chem. Res. 43 (2004) 5300–5309.
[56] B. Li, K.K. Sirkar, Novel membrane and device for vacuum membrane distillation based desalination process, J. Membr. Sci. 257 (2005) 60–75.
[57] Z.D. Hendren, J. Brant, M.R. Wiesner, Surface modification of nanostructured ceramic membranes for direct contact membrane distillation, J. Membr. Sci. 331 (2009) 1–10.
[58] Z. Ma, Y. Hong, L. Ma, M. Su, Superhydrophobic membranes with ordered arrays of nano spiked micro channels for water desalination, Langmuir Lett. 25 (2009) 5446–5450.
[59] C. Feng, K.C. Khulbe, T. Matsuura, R. Gopal, S. Kaur, S. Ramakrishna, M. Khayet, Production of drinking water from saline water by air-gap membrane distillation using polyvinylidenefluoride nanofiber membrane, J. Membr. Sci. 311 (2008) 1–6.
[60] M. Khayet, C. Cojocaru, M.C. García-Payo, Experimental design and optimization of asymmetric flat-sheet membranes prepared for direct contact membrane distillation, J. Membr. Sci. 351 (2010) 234–245.
[61] B. Wu, X. Tan, K. Li, W.K. Teo, Removal of 1,1,1-trichloroethane from water using apoly(vinylidenefluoride) hollow fiber membrane module: vacuum membrane distillation operation, Sep. Purif. Technol. 52 (2006) 301–309.
[62] B. Wu, K. Li, W.K. Teo, Preparation and characterization of poly(vinylidenefluoride) hollow fiber membranes for vacuum membrane distillation, J. Appl. Polym. Sci. 106 (2007) 1482–1495.
[63] M. Qtaishat, D. Rana, M. Khayet, T. Matsuura, Preparation and characterization of novel hydrophobic/hydrophilic polyetherimide composite membranes for desalination by direct contact membrane distillation, J. Membr. Sci. 327 (2009) 264–273.
[64] M. Qtaishat, D. Rana, T. Matsuura, M. Khayet, Effect of surface modifying macromolecules stoichiometric ratio on composite hydrophobic/hydrophilic membranes characteristics and performance in direct contact membrane distillation, AIChE J. 55 (2009) 3145–3151.
[65] M. Qtaishat, T. Matsuura, M. Khayet, K.C. Khulbe, Comparing the desalination performance of SMM blended polyethersulfone to SMM blended polyetherimide membranes by direct contact membrane distillation, Desalin. Water Treat. 5 (2009) 91–98.
[66] M. Qtaishat, M. Khayet, T. Matsuura, Novel porous composite hydrophobic/hydrophilic polysulfone membranes for desalination by direct contact membrane distillation, J. Membr. Sci. 341 (2009) 139–148.
[67] M. Khayet, T. Matsuura, Application of surface modifying macromolecules for the preparation of membranes for membrane distillation, Desalination 158 (2003) 51–56.
[68] M. Khayet, D.E. Suk, R.M. Narbaitz, J.P. Santerre, T. Matsuura, Study on surface modification by surface-modifying macromolecules and its applications in membrane-separation processes, J. Appl. Polym. Sci. 89 (2003) 2902–2916.
[69] M. Khayet, T. Matsuura, J.I. Mengual, Porous hydrophobic/hydrophilic composite membranes: estimation of the hydrophobic-layer thickness, J. Membr. Sci. 266 (2005) 68–79.
[70] M. Qtaishat, M. Khayet, T. Matsuura, Guidelines for preparation of higher flux hydrophobic/hydrophilic composite membranes for membrane distillation, J. Membr. Sci. 329 (2009) 193–200.
[71] D.E. Suk, T. Matsuura, H.B. Park, Y.M. Lee, Synthesis of a new type of surface modifying macromolecules (nSMM) and characterization and testing of nSMM blended membranes for membrane distillation, J. Membr. Sci. 277 (2006) 177–185.

[72] T.Y. Cath, A.E. Chilress, M. Elimelech, Forward osmosis: principles, applications, and recent developments, J. Membr. Sci. 281 (2006) 70–87.
[73] P.P. Bhatt, Osmotic Drug Delivery Systems for Poorly Soluble Drugs, Pharma Ventures Ltd., Oxford, UK, 2004.
[74] Y.P. Chun, S.J. Kim, G.J. Millar, D. Mulcahy, I.S. Kim, L. Zou, Forward osmosis as a pre-treatment for treating coal seam gas associated water: flux and fouling behaviours, Desalination (2015). http://dx.doi.org/10.1016/j.desal.2015.09.012.
[75] M. Qasim, N.A. Darwish, S. Sarp, N. Hilal, Water desalination by forward (direct) osmosis phenomenon: a comprehensive review, Desalination 374 (2015) 47–69.
[76] N. Akther, A. Sodiq, A. Giwa, S. Daer, H.A. Arafat, S.W. Hasan, Recent advancements in forward osmosis desalination: a review, Chem. Eng. J. 281 (2015) 502–522.
[77] R. Valladares Linares, Z. Li, S. Sarp, S.S. Bucs, G. Amy, J.S. Vrouwenvelder, Forward osmosis niches in seawater desalination and wastewater reuse, Water Res. 66 (2014) 122–139.
[78] L. Chekli, S. Phuntsho, H.K. Shon, S. Vigneswaran, J. Kandasamy, A. Chanan, A review of draw solutes inforward osmosis process and their use in modern applications, Desalin. Water Treat. 43 (1–3) (2012) 167–184.
[79] Q. Ge, M. Ling, T.S. Chung, Draw solutions for forward osmosis processes: developments, challenges, and prospects for the future, J. Membr. Sci. 442 (2013) 225–237.
[80] G. Han, S. Zhang, X. Li, T.S. Chung, Progress in pressure retarded osmosis (PRO) membranes for osmotic power generation, Prog. Polym. Sci. 51 (2015) 1–27.
[81] K. Gerstandt, K.V. Peinemann, S.E. Skilhagen, T. Thorsen, T. Holt, Membrane processes in energy supply for an osmotic power plant, Desalination 224 (2008) 64–70.
[82] T. Thorsen, T. Holt, The potential for power production from salinity gradients by pressure retarded osmosis, J. Membr. Sci. 335 (2009) 103–110.
[83] F. Dinger, T. Trondle, U. Platt, Optimization of the energy output of osmotic power plants, J. Renewable Energy 7 (2013) 1–7.
[84] J.R. McCutcheon, M. Elimelech, Influence of concentrative and dilutive internal concentration polarization on flux behavior in forward osmosis, J. Membr. Sci. 284 (2006) 237–247.
[85] T. Nguyen, E.T. Yun, I.C. Kim, Y.N. Kwon, Preparation of cellulose triacetate/cellulose acetate (CTA/CA)-based membranes for forward osmosis, J. Membr. Sci. 433 (2013) 49–59.
[86] X. Wang, Z. Huang, L. Li, S. Huang, E.H. Yu, K. Scott, Energy generation from osmotic pressure difference between the low and high salinity water by pressure retarded osmosis, J. Technol. Innov. Renewable Energy 1 (2012) 122–130.
[87] T.S. Chung, S. Zhang, K.Y. Wang, J. Su, M.M. Ling, Forward osmosis processes: yesterday, today and tomorrow, Desalination 287 (2012) 78–81.
[88] J.L. McCutcheon, R.L. McGinnis, M. Elimelech, The Ammonia Carbon Dioxide Forward Osmosis Desalination Process, Water Conditioning & Purification, 2006.
[89] F. Helfer, C. Lemckert, Y.G. Anissimov, Osmotic power with pressure retarded osmosis: theory, performance and trends – a review, J. Membr. Sci. 453 (2014) 337–358.
[90] C.Y. Tang, Q. She, W.C.L. Lay, R. Wang, A.G. Fane, Coupled effects of internal concentration polarization and fouling on flux behavior of forward osmosis membranes during humic acid filtration, J. Membr. Sci. 354 (2010) 123–133.
[91] A. Altae, A. Sharif, Pressure retarded osmosis: advancement in the process applications for power generation and desalination, Desalination 356 (2015) 31–46.
[92] S. Chou, R. Wang, L. Shi, Q. She, C. Tang, A.G. Fane, Thin-film composite hollow fiber membranes for pressure retarded osmosis (PRO) process with high power density, J. Membr. Sci. 389 (2012) 25–33.
[93] S.E. Skilhagen, Osmotic power – a new, renewable energy source, Desalin. Water Treat. 15 (2010) 271–278.
[94] Statkraft, Result of Operation 2010–2012, Statkraft Energy Sources, Available from: http://www.statkraft.com/energy-sources/osmotic-power/prototype/result-of-operation-2010-2012.aspx, 2012.
[95] S.E. Skilhagen, Osmotic power: a new, renewable source of energy, in: Proceedings of the 3rd Annual European Renewable Energy Markets, Platts, Berlin, 2012.

[96] D. Melanson, Norway's Statkraft Kick-Starts World's First Osmotic Power Plant, Engadget, Available from: http://www.engadget.com/2009/11/25/norways-Statkraft-kick-starts-worlds-first-osmotic-power-plant/ (25 November, 2009).
[97] B.H. Jeong, E.M.V. Hoek, Y. Yan, A. Subramani, X. Huang, G. Hurwitz, A.K. Ghosh, A. Jawor, Interfacial polymerization of thing film nanocomposites: a new concept for reverse osmosis membranes, J. Membr. Sci. 294 (2007) 1–7.
[98] C.J. Kurth, J.A. Koehler, M. Zhou, B.A. Holmberg, R.L. Burk, Hybrid Nanoparticle TFC Membranes, Patent US 8603340B2, 2014.
[99] M.M. Pendergast, A.K. Ghosh, E.M.V. Hoek, Separation performance and interfacial properties of nanocomposite reverse osmosis membranes, Desalination 308 (2013) 180–185.
[100] A. Subramani, J.G. Jacangelo, Emerging desalination technologies for water treatment: a critical review, Water Res. 75 (2015) 164–187.
[101] M.M. Pendergast, E.M.V. Hoek, A review of water treatment membrane nanotechnologies, Energy Environ. Sci. 4 (2011) 1946–1971.
[102] P. Agre, Aquaporin Water Channels, Nobel Lecture, Stockholm, Sweden, 2003.
[103] M. Kumar, M. Grzelakowski, J. Zilles, M. Clark, W. Meier, Highly permeable polymeric membranes based on the incorporation of the functional water channel protein Aquaporin Z, Proc. Natl. Acad. Sci. U.S.A. 104 (2007) 20719–20724.
[104] T. Humplik, J. Lee, S.C. O'Hern, B.A. Fellman, M.A. Baig, S.F. Hassan, M.A. Atieh, F. Rahman, T. Laoui, R. Karnik, E.N. Wang, Nanostructured materials for water desalination, Nanotechnology 22 (2011) 292001.
[105] S. Ahadian, Y. Kawazoe, An artificial intelligence approach for modeling and prediction of water diffusion inside a carbon nanotube, Nanoscale Res. Lett. 4 (2009) 1054–1058.
[106] A. Kalra, S. Garde, G. Hummer, Osmotic water transport through carbon nanotube membranes, Proc. Natl. Acad. Sci. U.S.A. 100 (2003) 10175–10180.
[107] B. Mi, Graphene oxide membranes for ionic and molecular sieving, Science 343 (2014) 740–742.
[108] R.R. Nair, H.A. Wu, P.N. Jayaram, I.V. Grigorieva, A.K. Geim, Unimpeded permeate of water through helium-leak-tight graphene-based membranes, Science 335 (2012) 442–443.
[109] T.H. Chong, S.L. Loo, W.B. Krantz, Energy-efficient reverse osmosis desalination process, J. Membr. Sci. 473 (2015) 177–188.
[110] T.H. Chong, S.L. Loo, W.B. Krantz, Energy-Efficient Reverse Osmosis (EERO) Process, United State Patent Application, No. 61/972,718, 2014.
[111] N.A. Thompson, P.G. Nicoll, Forward Osmosis Desalination: A Commercial Reality, IDA World Congress, Perth, Australia, 2011.
[112] I. Roh, C. Li, S. Kaur, R. Revanur, J. Klare, C. Benton, E. Desormeaux, O. Bakajin, Development of high performance of membrane and element for high recovery at minimal energy cost, in: The 8th International Desalination Workshop, 2015, , pp. 10–12.
[113] R. Semiat, J. Sapoznik, D. Hasson, Energy aspects in osmosis processes, Desalin. Water Treat. 15 (2012) 228–235.
[114] R.L. McGinnis, M. Elimelech, Energy requirements of ammonia-carbon dioxide, forward osmosis: influence of draw and feed solution concentrations on process performance, J. Membr. Sci. 278 (2006) 114–123.
[115] P. McCormick, J. Pellegrino, F. Mantovani, G. Sarti, Water, salt and ethanol diffusion through membranes for water recovery by forward (direct) osmosis processes, J. Membr. Sci. 325 (2008) 467–478.
[116] M.M. Ling, K.Y. Wang, T.S. Chung, Highly water soluble magnetic nanoparticles as novel draw solutes in forward osmosis for water reuse, Ind. Eng. Chem. Res. 49 (2010) 5869–5876.
[117] E.T. Yang, K.Y. Kim, K.J. Chae, M.Y. Lee, I.S. Kim, Evaluation of energy and water recovery in forward osmosis-bioelectrochemical hybrid system with cellulose triacetate and polyamide asymmetric membrane in different orientations, Desalin. Water Treat. 57 (16) (2016) 4706–7413.
[118] D.L. Shaffer, N.Y. Yip, J. Gilron, M. Elimelech, Seawater desalination for agriculture by integrated forward and reverse osmosis: improved product water quality for potentially less energy, J. Membr. Sci. 415–416 (2012) 1–8.

[119] T.Y. Cath, J.E. Drewes, C.D. Lundin, A novel hybrid forward osmosis process for drinking water augmentation using impaired water and saline water sources, WERC, Water Research Foundation, New Mexico and Denver, USA, 2009.
[120] D.L. Shaffer, J.R. Werber, H. Jaramillo, S. Lin, M. Elimelech, Forward osmosis: where are we now? Desalination 356 (2015) 271–284.
[121] J. Yaeli, Method and Apparatus for Processing Liquid Solutions of Suspensions Particularly Useful in the Desalination of Saline Water, US Patent 5,098,575, 1992.
[122] V. Yangali-Quintanilla, Z. Li, R. Valladares, Q. Li, G. Amy, Indirect desalination of Red Seawater with forward osmosis and low pressure reverse osmosis for water reuse, Desalination 280 (2011) 160–166.
[123] N.T. Hancock, N.D. Black, T.Y. Cath, A comparative life cycle assessment of hybrid osmotic dilution desalination and established seawater desalination and wastewater reclamation processes, Water Res. 46 (2012) 1145–1154.
[124] B.V. Bruggen, C. Vandecasteele, Distillation vs. membrane filtration: overview of process evolutions in seawater desalination, Desalination 143 (2002) 207–218.
[125] A.N.A. Mabrouk, H.E.B.S. Fath, Techno-economic analysis of hybrid high performance MSF desalination plant with NF membrane, Desalin. Water Treat. 51 (2013) 844–856.
[126] A. Altaee, G. Zaragoza, A conceptual design of low fouling and high recovery FO-MSF desalination plant, Desalination 343 (2014) 2–7.
[127] T. Mezher, H. Fath, Z. Abbas, A. Khaled, Techno-economic assessment and environmental impacts of desalination technologies, Desalination 266 (2011) 263–273.
[128] A. Altaee, A. Mabrouk, K. Bourouni, A novel forward osmosis membrane pretreatment of seawater for thermal desalination processes, Desalination 326 (2013) 19–29.
[129] A. Altaee, A. Mabrouk, K. Bourouni, P. Palenzuela, Forward osmosis pretreatment of seawater to thermal desalination: high temperature FO-MSF/MED hybrid system, Desalination 339 (2014) 18–25.
[130] C. Charcosset, A review of membrane processes and renewable energies for desalination, Desalination 245 (2009) 214–231.
[131] T. Xu, C. Huang, Electrodialysis-based separation technologies: a critical review, AIChE J. 54 (2008) 3147–3159.
[132] A.H. Galama, M. Saakes, H. Bruning, H.H.M. Rijnaarts, J.W. Post, Seawater predesalination with electrodialysis, Desalination 342 (2014) 61–69.
[133] S.T. Anderson, N. Kjellander, B. Rodesjo, Design and field tests of a new membrane distillation desalination process, Desalination 56 (1985) 345–354.
[134] A.G. Fane, R.W. Schofield, C.J.D. Fell, The effect use of energy in membrane distillation, Desalination 64 (1987) 231–243.
[135] J. Minier-Matar, A. Hussain, A. Janson, F. Benyahia, S. Adham, Field evaluation of membrane distillation technology for desalination of highly saline brines, Desalination 351 (2014) 101–108.
[136] K.K. Sirkar, L. Song, Pilot-Scale Studies for Direct Contact Membrane Distillation-Based Desalination Process, Desalination and Water Purification Research and Development Program Report No. 134, 2009.
[137] M.S. El-Bourawi, Z. Ding, M. Ma, M. Khayet, A framework for better understanding membrane distillation separation process, J. Membr. Sci. 285 (2006) 4–29.
[138] R.W. Schofield, A.G. Fane, C.J.D. Fell, R. Macoun, Factors affecting flux in membrane distillation, Desalination 77 (1990) 279–294.
[139] C.A. Smolders, A.C.M. Franken, Terminology for membrane distillation, Desalination 72 (1989) 249–262.
[140] R. Saffarini, H. Arafat, R. Thomas, Influence of pore structure on membrane wettability in membrane distillation, in: The 6th Jordan International Chemical Engineering Conference, Amman, Jordan, 2012.
[141] K.W. Lawson, D.R. Lloyd, Membrane distillation, J. Membr. Sci. 124 (1997) 1–25.
[142] L. Martinez-Diez, M.I. Vazquez-Gonzalez, Temperature and concentration polarization in membrane distillation of aqueous salt solutions, J. Membr. Sci. 156 (1999) 265–273.

[143] R.W. Schofield, A.G. Fane, C.J.D. Fell, Heat and mass transfer in membrane distillation, J. Membr. Sci. 33 (1987) 299–313.
[144] J.M. Ortiz de Zarate, F. Garcia-Lopez, J.I. Mengual, Temperature polarization in non-isothermal mass transport through membranes, J. Chem. Soc. Faraday Trans. 86 (16) (1990) 2891–2896.
[145] A. Velazquez, J.I. Mengual, Temperature polarization coefficients in membrane distillation, Ind. Eng. Chem. Res. 34 (1995) 585–590.
[146] N.N. Chernyshov, G.W. Meindersma, A.B. de Haan, Comparison of spacers for temperature polarization reduction in air gap membrane distillation, Desalination 183 (2005) 363–374.
[147] M. Qtaishat, T. Matsuura, B. Kruczek, M. Khayet, Heat and mass transfer analysis in direct contact membrane distillation, Desalination 219 (2008) 272–292.
[148] M. Gryta, M. Tomaszewska, Heat transport in the membrane distillation process, J. Membr. Sci. 144 (1998) 211–222.
[149] L. Pena, J.M. Ortiz de Zarate, J.I. Mengual, Steady state in membrane distillation: influence of membrane wetting, J. Chem. Soc. Faraday Trans. 89 (1993) 4333–4338.
[150] A.C.M. Franken, J.A.M. Nolten, M.H.V. Mulder, D. Bargeman, C.A. Smolders, Wetting criteria for the applicability of membrane distillation, J. Membr. Sci. 33 (1987) 315–328.
[151] K. Schneider, W. Holzand, R. Wollbeck, Membrane and modules for transmembrane distillation, J. Membr. Sci. 39 (1988) 25–42.
[152] E. Drioli, Y. Wu, Membrane distillation: an experimental study, Desalination 53 (1985) 339–346.
[153] M. Gryta, The assessment of microorganism growth in the membrane distillation system, Desalination 142 (2002) 79–88.
[154] M. Khayet, J.I. Mengual, Effect of salt concentration during the treatment of humic acid solutions by membrane distillation, Desalination 168 (2004) 373–381.
[155] M. Gryta, M. Tomaszewska, K. Karakulski, Wastewater treatment by membrane distillation, Desalination 198 (2006) 67–73.
[156] M. Gryta, K. Karakulski, Water demineralisation by NF/MD integrated processes, Desalination 177 (2005) 109–119.
[157] F. He, J. Gilron, H. Lee, L. Songand, K.K. Sirkar, Potential for scaling by sparingly soluble salts in crossflow DCMD, J. Membr. Sci. 311 (2008) 68–80.
[158] F. He, K.K. Sirkar, J. Gilron, Studies on scaling of membranes in desalination by direct contact membrane distillation: $CaCO_3$ and mixed $CaCO_3/CaSO_4$ systems, Chem. Eng. Sci. 64 (2009) 1844–1859.
[159] P. Wang, M.M. Teoh, T.S. Chung, Morphological architecture of dual-layer hollow fiber for membrane distillation with higher desalination performance, Water Res. 45 (2011) 5489–5500.
[160] D.E. Suk, T. Matsuura, Membrane-based hybrid processes: a review, Sep. Sci. Technol. 41 (2006) 595–626.
[161] K. Karakulski, M. Gryta, A. Morawski, Membrane processes used for potable water quality improvement, Desalination 145 (2002) 315–319.
[162] J.P. Mericq, S. Laborie, C. Cabassud, Vacuum membrane distillation of seawater reverse osmosis brines, Water Res. 44 (2010) 5260–5273.
[163] X. Ji, E. Curcio, S.A. Obaidani, G.D. Profio, E. Fontananova, E. Drioli, Membrane distillation crystallization of seawater reverse osmosis brines, Sep. Sci. Technol. 71 (2010) 76–82.
[164] D. Qu, J. Wang, L. Wang, D. Hou, Z. Luan, B. Wang, Integration of accelerated precipitation softening with membrane distillation for high recovery desalination of primary reverse osmosis concentrate, Sep. Sci. Technol. 67 (2009) 21–25.
[165] T.Y. Cath, A.E. Childress, C.R. Martinetti, Combined Membrane Distillation Forward Osmosis Systems and Methods of Use, United States Patent Application 12/303318, 2007.
[166] Q. Ge, J. Su, G.L. Amy, T.S. Chung, Exploration of polyelectrolytes as draw solutes in forward osmosis processes, Water Res. 46 (2012) 1318–1326.
[167] J. Su, R.C. Ong, P. Wang, T.S. Chung, B.J. Helmer, J.S. de Wit, Advanced FO membranes from newly synthesized cap polymer for wastewater reclamation through an integrated FO-MD hybrid system, AIChE J. 59 (2012) 1245–1254.

[168] M. Xie, L.D. Nghiem, W.E. Price, M. Elimelech, Toward resource recovery from wastewater: extraction of phosphorus from digested sludge using a hybrid forward osmosis membrane distillation process, Environ. Sci. Technol. Lett. 1 (2014) 191–195.
[169] M. Xie, L.D. Nghiem, W.E. Price, M. Elimelech, A forward osmosis–membrane distillation hybrid process for direct sewer mining: system performance and limitations, Environ. Sci. Technol. 47 (2014) 13486–13493.
[170] S. Zhang, P. Wang, X.Z. Fu, T.S. Chung, Sustainable water recovery from oily wastewater via forward osmosis-membrane distillation (FO-MD), Water Res. 52 (2014) 112–121.
[171] K.Y. Wang, M.M. Teoh, A. Nugroho, T.S. Chung, Integrated forward osmosis-membrane distillation (FO-MD) hybrid system for the concentration of protein solutions, Chem. Eng. Sci. 66 (2011) 2421–2430.
[172] E. Drioli, G. DiProfio, E. Curcio, Progress in membrane crystallization, Curr. Opin. Chem. Eng. 1 (2012) 178–182.
[173] X. Ji, E. Curcio, S. AlObaidani, G. DiProfio, E. Fontananova, E. Drioli, Membrane distillation-crystallization of seawater reverse osmosis brines, Sep. Purif. Technol. 71 (2010) 76–82.
[174] F. Edwie, T.S. Chung, Development of simultaneous membrane distillation crystallization (SMDC) technology for treatment of saturated brine, Chem. Eng. Sci. 98 (2013) 160–172.
[175] Y. Wu, Y. Kong, J. Liu, J. Zhang, J. Xu, An experimental study on membrane–distillation crystallization for treating waste water in taurine production, Desalination 80 (1991) 235–242.
[176] E. Curcio, A. Criscuoli, E. Drioli, Membrane crystallizers, Ind. Eng. Chem. Res. 40 (2001) 2679–2684.
[177] M. Gryta, Concentration of NaCl solution by membrane distillation integrated with crystallization, Sep. Purif. Technol. 37 (2002) 3535–3558.
[178] C.M. Tun, A.G. Fane, J.T. Matheickal, R. Sheikholeslami, Membrane distillation-crystallization of concentrated salts-flux and crystal formation, J. Membr. Sci. 257 (2005) 144–155.
[179] F. Edwie, T.S. Chung, Development of hollow fiber membranes for water and salt recovery from highly concentrated brine via direct contact membrane distillation and crystallization, J. Membr. Sci. 421–422 (2012) 111–123.
[180] F. Macedonio, E. Curcio, E. Drioli, Integrated membrane systems for seawater desalination: energetic and exergetic analysis, economic evaluation, experimental study, Desalination 203 (2007) 260–276.
[181] A.E. Jansen, J.W. Assink, J.H. Hanemaaijer, J. Medevoort, E. Sonsbeek, Development and pilot testing of full-scale membrane distillation modules for deployment of waste heat, Desalination 323 (2013) 55–65.
[182] D. Singh, K.K. Sirkar, Desalination of brine and produced water by direct contact membrane distillation at high temperatures and pressures, J. Membr. Sci. 389 (2012) 380–388.
[183] R. Schwantes, A. Cipollina, F. Gross, J. Koschikowski, D. Pfeifle, M. Rolletschek, V. Subiela, Membrane distillation: solar and waste heat driven demonstration plants for desalination, Desalination 323 (2013) 93–106.
[184] J. Koschikowski, M. Wieghaus, M. Rommel, Solar thermal-driven desalination plants based on membrane distillation, Desalination 156 (2003) 295–304.
[185] A. Kullab, C. Liu, A. Martin, Solar desalination using membrane distillation-technical evaluation case study, in: International Solar Energy Society Conference, Orlando, FL, August 2005.
[186] F. Banat, N. Jwaied, Economic evaluation of desalination by small-scale autonomous solar-powered membrane distillation units, Desalination 220 (2008) 566–573.
[187] P.A. Hogan, A.G. Sudjito, G.L. Fane, Morrison, desalination by solar heated membrane distillation, Desalination 81 (1991) 81–90.
[188] A. Jansen, M. Bikel, Water treatment, how do membrane position today? in: Developing Future Water Technologies – Membranes, Dipoli, Espoo, Finland, 2011.

FURTHER READING

[1] G.W. Batchelder, Process for the Demineralization of Water, US Patent 3,171,799, 1965.
[2] B.S. Frank, Desalination of Sea Water, US Patent 3,670,897, 1972.
[3] T.Y. Cath, V.D. Adams, A.E. Childress, Experimental study of desalination using direct contact membrane distillation: a new approach to flux enhancement, J. Membr. Sci. 228 (2004) 5–16.

CHAPTER 3

Autonomous Solar-Powered Desalination Systems for Remote Communities

Jehad A. Kharraz, Bryce S. Richards, Andrea I. Schäfer
Karlsruhe Institute of Technology (KIT), Karlsruhe, Germany

Contents

Desalination Sustainability
http://dx.doi.org/10.1016/B978-0-12-809791-5.00003-1

1. INTRODUCTION

Remote areas face particular infrastructure challenges relating to the provision of clean drinking water and electricity [1]. The installation of classical centralized water and electricity systems in such areas is economically unfavorable because of the typically low population densities and the distance from highly populated or developed settlements. If one views this situation through the lens of "the cup being half empty," then it could be construed as a disadvantage; however, "the cup being half full" approach indicates that this situation could provide unique opportunities for small-scale, decentralized autonomous systems to be implemented to overcome the challenges. Although water is often available, it is often not potable because of the presence of dissolved contaminants such as salts, arsenic, fluoride, uranium, and nitrate, as well as many other organic and inorganic contaminants [2]. Desalination and treatment of such waters can be achieved using membrane technology. Membrane technology offers an ideal solution in many aspects, such as better removal of contaminants, high efficiency in terms of high water production and water fed ratios, smaller footprint than conventional filtration technologies, and variable filtration ratings because they employ different classes of membranes ranging from microfiltration to reverse osmosis allowing for precise contaminant removal at the lowest cost. Decentralized and autonomous systems that are appropriate for remote areas can be realized by coupling membrane processes with renewable energy sources such as solar and wind energy.

Despite the fact that renewable energy-powered membrane (RE-membrane) desalination systems are technically capable of addressing the problem of poor water quality that causes severe health problems within societies, the implementation and uptake of such technology is still not as rapid as expected [3]. RE-membrane systems can also effectively operate without the need for energy storage components as water can be stored as the final product [4]. Although in this way batteries could be eliminated from the system, doing so could also result in higher efficiencies because the generated electricity is immediately consumed. However, based on power fluctuations because of solar irradiance fluctuations, the overall productivity might not be higher. It is anticipated that the elimination of batteries could enable such RE-membrane systems to be more robust and reliable. Such systems provide a sustainable solution for the provision of safe drinking water in remote communities that is technically possible, economically feasible, and environmentally friendly.

In this chapter, an assessment of system availability and sustainability of autonomous solar-powered desalination systems (particularly reverse osmosis, membrane distillation, and electrodialysis) for remote communities is presented. In particular, the chapter covers currently limited cost data and technical viewpoints, as well as state-of-the-art options for such systems. Water and energy efficiency as well as social, economic, and environmental aspects are also discussed. A number of water qualities spanning from surface water and brackish groundwater to seawater sources are reviewed with a focus on dissolved contaminants.

2. WATER NEEDS FOR REMOTE COMMUNITIES

2.1 Remote Community Water Supplies and the Need for Autonomous Systems

The lack of infrastructure for both clean drinking water and electricity poses a challenge in remote areas, particularly in developing countries [5]. The typically low population densities mean that it is economically unfavorable to install classical centralized systems for the provision of water and electricity. However, there is a need to provide an alternative supply of water and energy to remote communities to ensure that their right to basic necessities of life is provided. This state of affairs provides a unique opportunity for RE-membrane systems to meet this challenge in the form of small-scale, autonomous, decentralized systems [6].

2.2 Water Quality and Quantity Requirements in Remote Communities

Safe drinking water is defined as being safe enough for drinking and food preparation. While urban areas can more easily be served by large centralized treatment systems, remote and rural areas are much more difficult and expensive to serve. Remote communities worldwide often lack access to safe drinking water, and the water can be either of poor quality, of limited quantity, or both. It is currently estimated that over 780 million people in the world lack access to safe drinking water, especially in rural and remote communities [7]. This is significantly affecting their economy [8] and causes death and illness from water-related diseases that can easily be prevented.

An improved water source is defined by the World Health Organization (WHO) as one that, by nature of its construction or through active intervention, is likely to be protected from outside contamination, in particular from contamination with fecal matter [9]. Fig. 1 illustrates the global drinking water coverage based on drinking water sources in 2015: (i) by region, (ii) by developmental status, and (iii) by urban and rural areas [9]. Fig. 2 shows the global physical and economic water scarcity [10]. Almost one-fifth and one-fourth of the world's population live in areas of physical scarcity and economic water scarcity, respectively [11]. Economic water scarcity means scarcity of water in areas where the infrastructure necessary to take the water from its sources such as rivers and aquifers is lacking. By 2050, 1800 million people will be living in regions with absolute water scarcity [12]. Lack of centralized water systems in rural and remote areas of developing countries forces the use of unimproved water sources and untreated natural water sources such as lakes, rivers, rainwater, and groundwater. Those sources usually are not well protected and are exposed to microbial and chemical pollutants [2].

The upper part of Fig. 3 shows the different water sources and their percent of freshwater and total water, while the lower part shows the classification of water sources based on their salinity [13]. It has been estimated that drinking contaminated water is responsible for the death of 1.5 million people annually, with more than 90% of those being children [7].

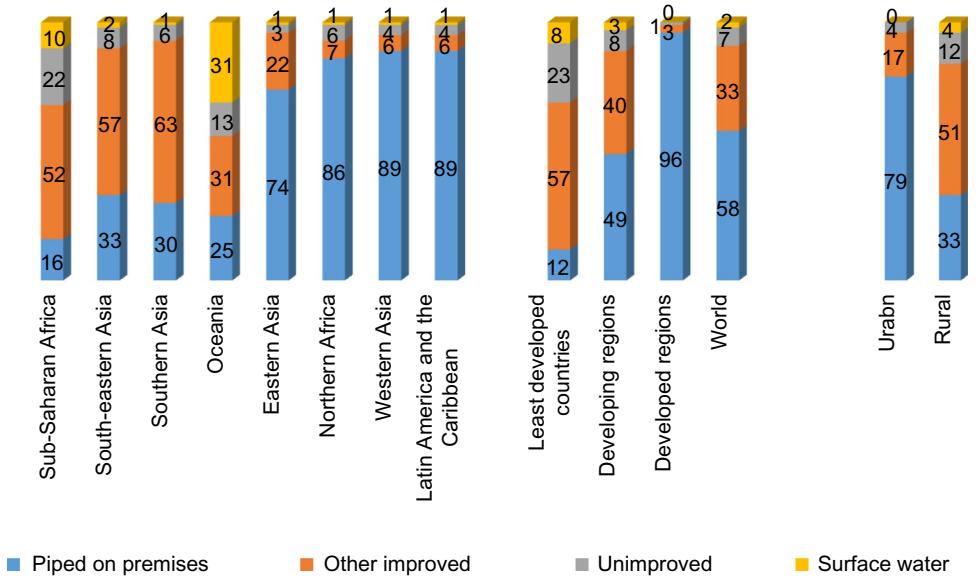

Fig. 1 Drinking water coverage (%) in 2015 by region and developmental status and by urban and rural areas [9].

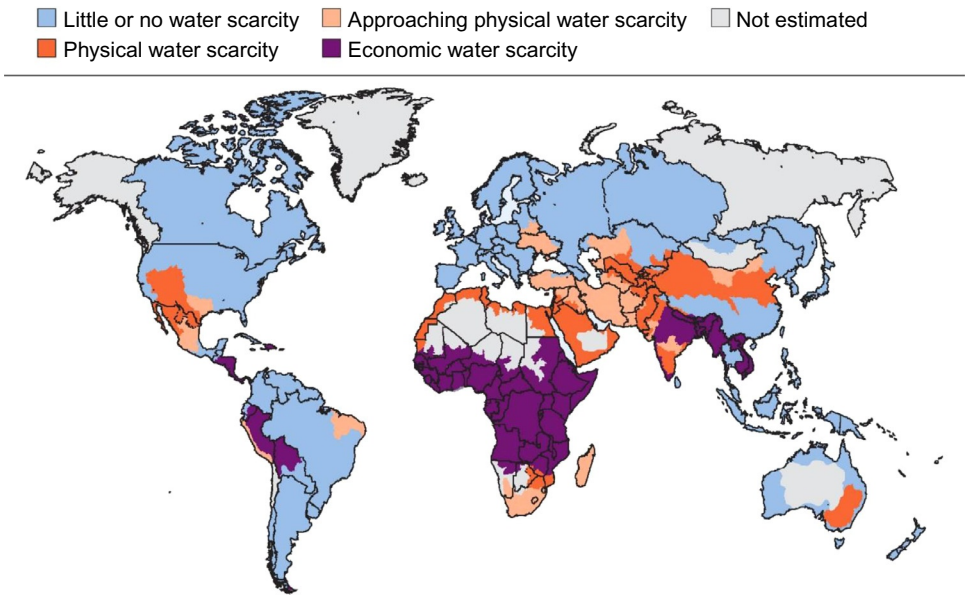

Fig. 2 Global physical and economic water scarcity (© 2007 IWMI [10]).

Water source	Percent of freshwater	Percent of total water
Oceans, seas, and bays	–	96.5
Ice caps, glaciers, and permanent snow	68.7	1.74
Groundwater	–	1.69
Fresh	30.1	0.76
Saline	–	0.93
Soil moisture	0.05	0.001
Ground ice and permafrost	0.86	0.022
Lakes	–	0.013
Fresh	0.26	0.007
Saline	–	0.006
Atmosphere	0.04	0.001
Swamp water	0.03	0.0008
Rivers	0.006	0.0002
Biological water	0.003	0.0001

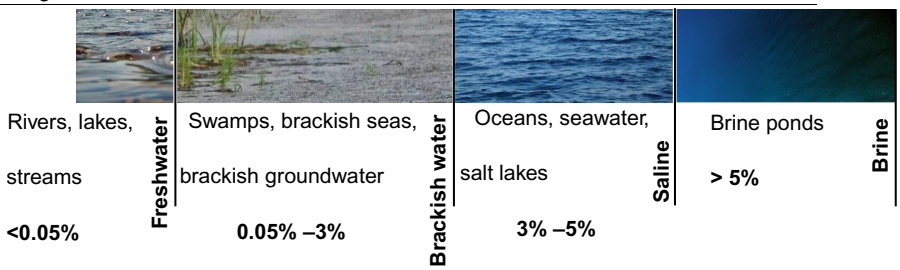

Fig. 3 Upper part showing a table of the different water sources and their percent of fresh water and total water, and lower part showing a schematic representing the classification of water sources based on their salinity. *(Adapted from I. Shiklomanov, World fresh water resources, in: P.H. Gleick (Ed.), Water in Crisis: A Guide to the World's Fresh Water Resources, Oxford University Press, New York, 1993).*

Moreover, there is a continuous increase in risk of contamination for existing water sources as well as an increase in demand for clean water because of population growth.

2.3 Availability and Quality of Renewable Energy Resources

Renewable energy (RE) is energy that is collected from naturally replenished resources such as sunlight, wind, waves, tides, and geothermal heat. In contrast to other traditional energy sources, which are area-specific and are concentrated in specific countries that possess a particular fossil fuel source, RE resources exist over all geographical areas. In 2013 RE contributed to 19% of the global primary energy consumption and 22% of electricity generation. [14]. While these numbers remain in the minority, the globally installed capacity for many RE technologies grew at annual rates of 10%–60% over the past decade. Fig. 4 shows the global growth of RE, excluding all hydro through 2014 [15].

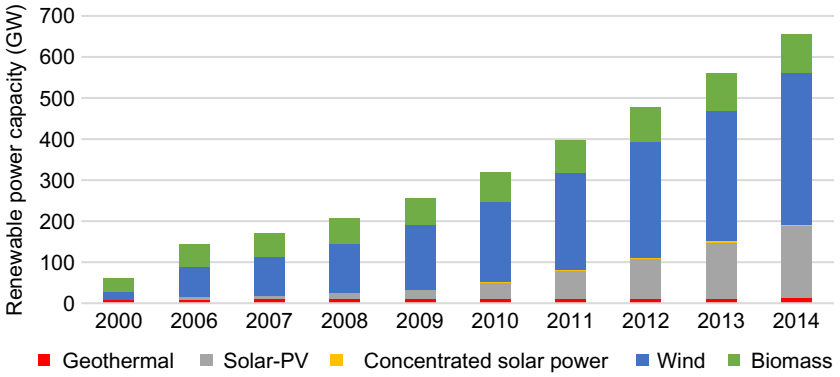

Fig. 4 Global renewable power capacities, excluding all hydro. *(Data adapted from The International Renewable Energy Agency (IRENA), Renewable Energy Capacity Statistics, IRENA, 2015).*

RE generators can range from a small 10 W photovoltaic (PV) panel up to several hundred MW solar and wind farms. RE technologies are well suited for remote areas and developing countries, typically being designed to operate more than 20 years in fairly harsh environments.

Among the RE resources, solar energy is considered an important source. Depending on the way they capture and distribute or convert solar energy into solar power, its technologies are usually categorized as either passive solar or active solar. In passive solar, heat is generated directly from the sun's rays to heat spaces, whereas active solar uses mechanical and electrical equipment to enhance the conversion of solar energy to heat and electric power. Solar energy is available in a large magnitude, which makes it a highly attractive source of electricity. In addition, there is a significant synergy between the areas that receive high solar irradiance and the areas that have water scarcity problems and therefore often low-population densities [16].

Solar irradiance is defined as the amount of solar radiant energy that hits a surface per unit area per unit time. The world map [16a] (Fig. 5) illustrates the long-term annual and daily averages of solar irradiance [17]. Solar radiation can vary in intensity depending on the geographic location and is unevenly distributed throughout the world. It is predominantly higher near the equator, but it is also governed by other local geographic and meteorological effects, as well as anthropogenic phenomena. This variance is mainly due to the variation in solar altitude, cloud coverage, and degree of pollution [11]. PV modules convert the sunlight into direct current (DC) electricity producing solar power via a system that has no moving parts. By 2050 solar power, including both PV and solar thermal, is expected to become the world's largest source of electricity, with solar PV contributing to 16% of global consumption [18]. For wind energy, the previously described synergy does not follow; however, wind-powered desalination systems would be more relevant in coastal regions at high latitudes and also for seawater desalination on islands [19].

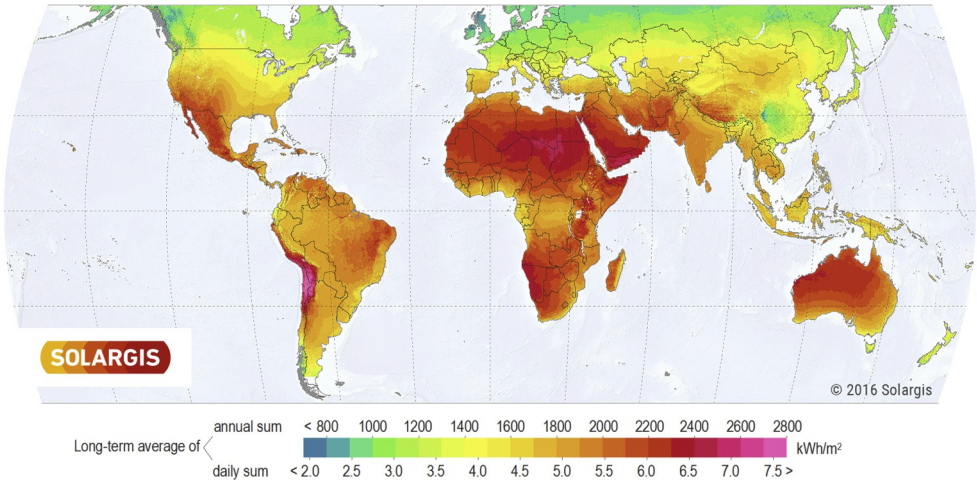

Fig. 5 Global solar irradiation. *(Adapted from GHI Solar Map © 2016 Solargis).*

Coupling desalination systems with RE sources represents an attractive solution for providing drinking water in remote areas where no electricity grid is available. However, solar-powered desalination systems are currently not a common technology, with RE-powered desalination systems currently contributing only 0.02% of the total installed desalination capacity [20]. This situation is not surprising for emerging technologies, and typical reasons are availability, cost, and sustainability, [21] and possibly the perception that such technologies are too expensive or inappropriate, especially for developing countries. Although RE-membrane systems could be installed in remote areas that suffer from freshwater shortage, the capital cost, which remains relatively high for both desalination and RE technologies, could present a barrier [22], while operating costs are comparatively low for "fuel" such as sunlight and wind. The main obstacles to the deployment of such technologies in remote areas include technical support, infrastructure, lack of skilled workers for operation and maintenance (O&M), adaptive capacity of communities to transfer and develop a technology that is specifically suited to local conditions, service networks, availability of spare parts, and robustness of the technology [23]. These issues affect the sustainability of a RE-membrane system and need to be addressed for long-term success.

2.4 Small-Scale and Autonomous Water Supply Systems

In remote areas, it is more cost-effective to build small-scale water supply systems than to transport water, sometimes over long distances [3,24]. Small-scale systems would typically treat and supply around 1000 to 10,000 L/day of potable water. Using the WHO guidelines for water consumption of 5 L/person/day for drinking and cooking [25], such a

supply would be enough for a village or small town (population 200–2000). It should be noted that for larger populations, upscaling is easier, and the cost per L typically reduces with scale. Small-scale water supply systems are the backbone of the water supply systems for rural and remote areas in many parts of the world. For instance, in the pan-European region, approximately 30% of the total population live in rural areas, in which small-scale water supplies predominantly prevail [26]. Such supplies could include wells, boreholes, springs, rainwater tanks, and storm water harvesting [27]. Those untreated water sources may contain potentially pathogenic agents, chemical pollutants, and other components affecting taste and odor [28]. Different techniques are used to treat and purify such water sources so they can be safely used, including heating and boiling, filtration, activated charcoal absorption (use of activated carbon filters to address organic contamination, taste, or objectionable odors), chemical disinfection (e.g., chlorine, ozone), distillation and solar distillation, and flocculation. Such techniques are often used in combination [29].

RE water supply systems offer an attractive solution for remote areas. Those systems are autonomous and independent of the electricity grid and are produced from sources that are freely available in nature, with a degree of dependency on weather, location, and season.

3. ENERGY ISSUES

3.1 Assessment of Energy Efficiency

Desalination is an energy-intensive process. All desalination processes require a certain amount of electrical and/or thermal energy to drive the separation of saline water into pure water and concentrate brine, depending on the particular desalination process. For instance, membrane desalination processes such as reverse osmosis (RO) and electrodialysis (ED) require electricity as their primary source of energy, whereas thermal energy is the primary source for distillation desalination processes such as multistage flashing (MSF) and multieffect distillation (MED), in addition to electricity as a secondary source to drive associated pumps. Solar energy is one of the most promising RE sources for coupling with desalination because it can be converted to thermal energy (using solar stills or solar thermal collectors systems) or electrical energy (using PV or solar thermal power plants coupled with steam-driven electric generators).

The free energy change is used to estimate the theoretical specific energy consumption (SEC) of seawater desalination and is reported to be 0.7 kWh/m^3 of product water [30]. This theoretical minimum value is estimated at zero recovery (the volume of fresh water produced per unit volume of seawater); however, for a given recovery, this value could be higher, for instance, 0.97 kWh/m^3 for 50% recovery and 1.29 kWh/m^3 for 75% recovery [31,32]. Nevertheless, the actual SEC for desalination is higher than those theoretical values and increases as a function of salt concentration. Fig. 6 shows the dependence of the SEC on the salt concentration in the feed solution for different desalination

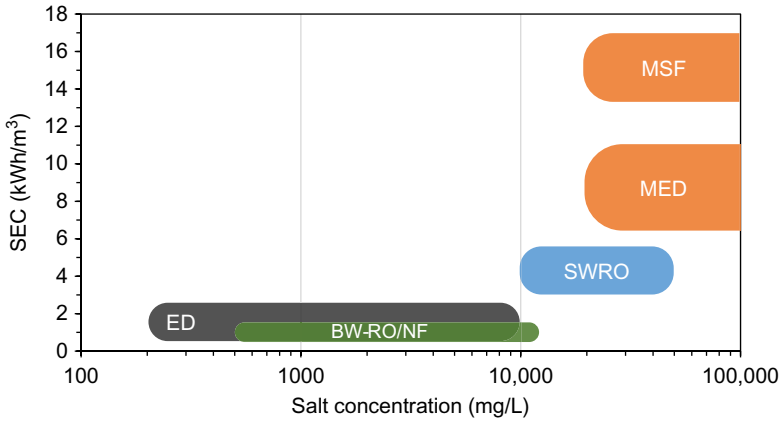

Fig. 6 Feed salt concentration and specific energy consumption for different desalination technologies. *(Data adapted from DOW, FILMTEC Membranes, Basics of RO and NF: Desalination Technologies and Filtration Processes, Technical Report; N. Hilal, H. Al-Zoubi, A.W. Mohammad, N.A. Darwish, Nanofiltration of highly concentrated salt solutions up to seawater salinity, Desalination 184 (1–3) (2005) 315–326; A.C. Twort, D.D. Rathnayaka, M.J. Brandt, Water Supply, fifth ed., IWA Publishing; C. Fritzmann, J. Loewenberg, T. Wintgens, T. Melin, State-of-the-art of reverse osmosis desalination, Desalination 216(1–3) (2007) 1–76; S. Loupasis, Technical Analysis of Existing RES Desalination Schemes – RE Driven Desalination Systems REDDES, Report, 2002; H. Fath, V.J. Subiela Ortin, Planning, implementation, operation and monitoring of ADS units, in: Adira Handbook, "A Guide to Autonomous Desalination Concepts", 2008; D. Reza, S.N. Al-zubaidy, Energy efficient reverse osmosis desalination process, Int. J. Environ. Sci. Dev. 3(4) (2012) 339–345).*

technologies. In remote areas, either surface water or brackish groundwater is usually available but requires treatment in order to be deemed safe drinking water. Fig. 7 shows the energy requirements to produce safe drinking water from different water sources [33]. The two most common technologies for desalination of brackish groundwater, which also happen to be the two most common for solar-powered desalination, are RO and ED, which have an average SEC of 1–2 kWh/m^3 [30] and 1.7 kWh/m^3 [34], respectively.

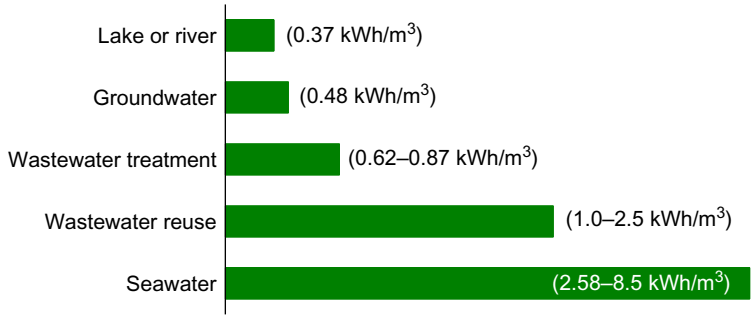

Fig. 7 Energy required by existing plants to produce safe drinking water from various sources (where lake or river is surface water) [33].

Small-scale photovoltaic powered reverse osmosis (PV-RO) systems for brackish water desalination have shown a great potential for providing low-cost drinking water in remote areas. De Munari et al. reported an average SEC of 3.2 kWh/m^3 for a small-scale PV-RO system with a capacity of 764 L/day treating feed water with a salinity of 3700 mg/L [35]. Qiblawey et al. [36] investigated two lab-scale PV-RO plants (with and without batteries) for brackish water desalination with two different total dissolved solid (TDS) concentrations (350 mg/L and 720 mg/L). SEC values of 1.1–4.3 kWh/m^3 for the system operated with batteries and 1.1–1.5 kWh/m^3 for the batteryless system were reported, respectively. Photovoltaic powered electrodialysis (PV-ED) systems are largely used in small-scale units in remote areas. Kuroda et al. [37] investigated a small-scale PV-ED system with a slightly brackish water feed salinity of 1000 mg/L. The system was able to provide 2.8 m^3/day of fresh water with a SEC of 0.82 kWh/m^3. Another PV-ED system with a capacity of 18 m^3/day was investigated by Lichtwardt and Remmers [38] with a brackish water feed salinity of 900 mg/L reported a SEC of 0.8 kWh/m^3.

Karimi et al. [39] conducted pilot-scale experimental work and software modeling to investigate the SEC of the two most common solar-powered brackish water desalination technologies, PV-RO and PV-ED, when operated with different feed salinities, flow rates, and temperature. The motivation was to explore the techno-economic feasibility of such systems for drinking water provision in remote communities and to determine the effects of temperature, salinity, and flow rate on the energy requirements of the two systems. Both PV-RO and PV-ED experiments were conducted in parallel to eliminate any source of error in the energy consumption because of fluctuations in temperature and feed water composition. The experimental results showed that permeate flow rate and feed water salinity significantly affected the SEC of both ED and RO systems. Compared with RO, the SEC of ED was found to be more sensitive to the variation in feed water salinity. Increasing the feed water temperature had a positive effect by reducing the energy consumption for both systems, although the energy reduction was more significant for the RO than for the ED system (increasing the feed water temperature from 25°C to 35°C resulted in 21% and 13% decrease in SEC for RO and ED, respectively). For RO, decreasing the temperature and increasing the permeate flow rate resulted in an increasing SEC (30% increase in permeate flow rate resulted in 48% increase in SEC). It was also concluded that the SEC of RO is significantly lower than that of ED for desalinating higher salinity water (ED had 34% SEC more than RO when desalinating higher-salinity brackish water with a conductivity of 3530 μS/cm). Moreover, the increase of permeate flow rate increased the SEC of ED more significantly than it affected the RO system, which was due to the negative effect of dilute flow rate on ion removal in the ED process, which is attributed to the shorter residence time [39].

When replacing the RO modules with nanofiltration (NF) modules, further energy savings have been found. For example, Richards et al. tested a PV-powered membrane

system containing a single 4-inch diameter membrane module for treating water with a total dissolved solids (TDS) content of 5300 mg/L in Central Australia [40]. Here it was demonstrated that the SEC could be decreased from 2.4 to 1.5 kWh/m^3 when replacing the BW30 membrane module with either a NF90 or an ESPA4 module, while the permeate quality remained (in this case) within the target value. The reduced SEC is largely driven by the improved flux through the NF modules. However, by using an even looser membrane (TFC-S), the SEC reduced slightly to 1.4 kWh/m^3, while the permeate quality decreased by a factor of four compared to either NF90 or ESPA4. Thus, for brackish water applications, it is apparent that NF membranes have the potential for improved energy efficiency and increased productivity, as long as they are carefully matched to feed water and permeate quality requirements.

Although energy analysis has been well studied for many membrane desalination processes, including RO, ED, and MSF, the SEC of the somewhat newer membrane distillation (MD) processes has been less studied [41]. Moreover, for the different solar-powered laboratory systems and pilot-scale MD systems (both experimentally and theoretically), different and conflicting results and conclusions have been reported. The reported SEC varied widely depending on the operation parameters and the configuration used and ranged between 1 and 9000 kWh/m^3 [42–49]. MD processes require both thermal energy, as a primary source to heat up the feed solution and cool down the permeate, and electrical energy, as a secondary source, to power the pumps and compressors. The effect of different MD parameters operating on the SEC has not been studied in depth to date and is most commonly reported for fixed operating conditions [30]. In addition, in some MD studies, the authors reported only the thermal component of the system efficiency [41,50], although the electrical energy consumption cannot be ignored [51]. Indeed, to estimate the energy efficiency of MD systems, the concept of gained output ratio (GOR) has been applied in recent studies [52,53]. GOR is defined as the ratio of heat associated with mass transfer to the energy input and reflects how well the energy input in a system is utilized for water production, with higher GOR values indicating better system performance [30]. However, the energy input required to produce 1 m^3 of permeate water—the SEC—provides a much better way of determining the overall energy efficiency in MD systems.

Koschikowski et al. [48] tested a compact solar-powered desalination plant based on a spiral wound air gap MD module. The plant operated at a flow rate of 350 L/h with an evaporator inlet temperature of 75°C, and the reported SEC was ~117 kWh/m^3. In the same study, SEC values ranging from 140 to 200 kWh/m^3 at different operating conditions (flow rates and inlet evaporator temperatures) were reported. Banat et al. [45] studied an autonomous solar-powered MD unit for brackish water desalination with a capacity of 120 L/day and reported a thermal energy usage of 200–300 kWh/m^3. The same authors studied a larger solar-powered MD unit with untreated seawater feed and reported the SEC to be between 200 and 300 kWh/m^3 [44].

The effect of the membrane area on SEC was studied by Winter et al. [54]. Distilled water was used as feed. They considered a spiral-wound liquid gap MD (LGMD) module with membrane areas of 5, 10, and 14 m^2. The hot feed and cold permeate temperatures were 80°C and 25°C, respectively. Increasing the membrane area from 5 to 14 m^2 decreased the SEC by 57.1% without having a big influence on the total distillate output rates, and a further reduction in SEC was achieved through higher feed flow rates. The overall reported SEC values were in the range 130–207 kWh/m^3. Raluy et al. [55] tested a solar-powered LGMD desalination unit with different membrane areas and a capacity range of 1–117 L/day and reported SEC values of 68.8–499.1 kWh/m^3.

Overall, it is concluded that increasing the membrane surface area significantly lowers the SEC of the MD module and has no significant effect on the distillate output rates.

3.2 Energy Fluctuations and Storage

The solar resource varies during a day as well as throughout the year, resulting in fluctuations in solar irradiance. On a clear day, solar irradiance values can typically reach 1000–1100 W/m^2, and for different geographic locations, the path of the sun can be easily predicted; however, clouds and shadows cast by trees and buildings and wind and ambient temperatures will all lead to fluctuations in the power of a PV system [56]. Fig. 8 shows an example of the fluctuations encountered during a solar day, where the morning was free of clouds, and during the afternoon large clouds occasionally shaded the system. In addition, an example of the variation in wind energy, which in this case

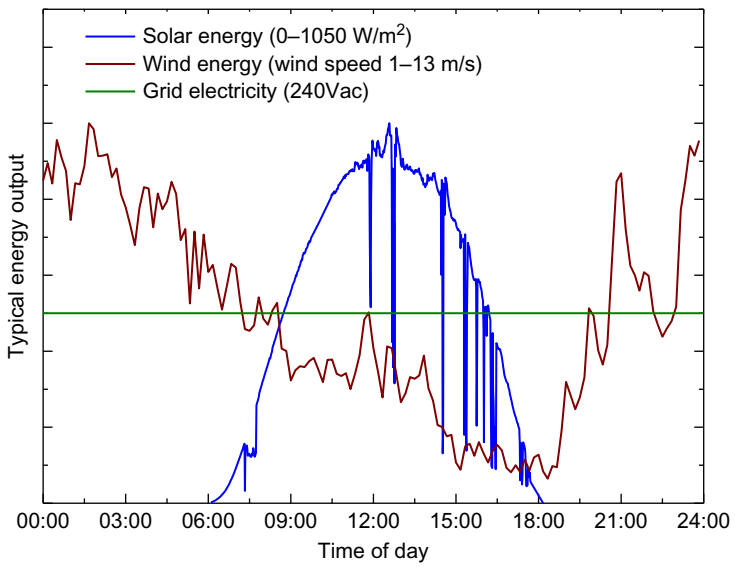

Fig. 8 Typical solar and wind energy fluctuations compared to grid electricity.

was blowing more during the night, is shown. This is an example of how solar and wind energy resources can be synergistic if both technologies are combined in one system. Finally, Fig. 8 plots the output from standard grid electricity, which in the majority of developed countries exhibits almost no variation throughout the day, although in developing countries this can be interrupted at irregular intervals because of electricity management strategies from the utilities as well as blackouts.

In order to determine the effect of both RE resource fluctuations and intermittency on the output of a PV-RO system, the "worst case" variations in solar irradiance were evaluated in terms of frequency, magnitude, and duration of on- and off-periods as illustrated in Fig. 9. The key outcomes from this study were (i) shorter off-periods resulting in good performance being achieved quickly and (ii) short-term availability of power resulting in dramatic improvement of the system's performance [56].

In order to counter the effect of fluctuations, many PV-powered desalination systems use batteries in order to store energy during the daytime when solar energy is available and then to reuse it at night. While the use of batteries to store electrical energy in a well-designed RE-membrane system allows continuous operation and enables the production of a specific amount of water at a defined quality, it can result in many problems. For instance, lead acid batteries have a relatively short lifespan when supplying a daily load, typically between 3 and 5 years, though sometimes as little as 2 years under extreme circumstances [57]. These batteries have a typical charge-in/charge-out efficiency of 75%–80% [58], thus reducing the overall system efficiency by 20%–25% as well as increasing the system cost. In addition, high ambient temperatures can significantly affect the batteries' performance and accelerate their degradation. High temperatures also

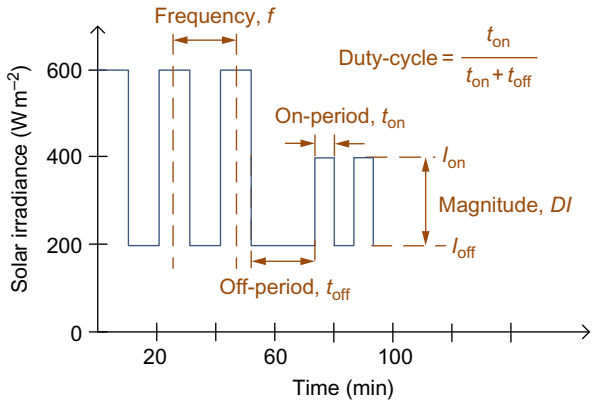

Fig. 9 Worst-case fluctuations, with different magnitudes, frequencies, on- and off-periods, as well as duty cycles, that were used for step-testing a PV-RO system. *(Adapted from B.S. Richards, D.P.S. Capao, W.G. Frueh, A.I. Schaefer, Renewable energy powered membrane technology: impact of solar irradiance fluctuations on performance of a brackish water reverse osmosis system, Sep. Purif. Technol. 156 (2015) 379–390).*

increase the self-discharge rate of the batteries, which leads to a decrease in the charge efficiency and a reduction of the battery's capacity, which as a result increases the need for battery replacement and consequently the O&M cost. Moreover, for PV-powered systems, the PV modules' arrays are designed for a typical lifetime of *at least* 20 years. Thus, if a 20-year RE-membrane system life is assumed to minimize the life-cycle cost of such systems, then the batteries will need to be replaced four to seven times during this period at significant cost. Moreover, in remote regions, there are limited facilities for battery recycling, and thus a risk of environmental hazards caused by improper disposal.

One alternative to batteries that is relevant to small-scale RE-membrane systems and that can be used for buffering energy fluctuations and intermittency is the use of supercapacitors. Unlike batteries, which rely on a chemical reaction, supercapacitors are energy storage devices that are based on the build-up of positive and negative charges within an electrolytic solution, and they have been implemented in RE power supply systems [59,60]. Park et al. showed the advantages of supercapacitors in buffering short-term wind fluctuations and intermittency for a wind-based RO system [61]. Compared to batteries, supercapacitors are considered more suitable in cases where charge/discharge occurs over periods of 3–5 min, that can endure >500,000 charge/discharge cycles, and that require zero maintenance [62]. Their main disadvantage is their high self-discharge rate—depending on the state of charge this has been reported to range from 0.5% to 40% after 24 h [63]—which means that storage efficiency is now time-dependent. However, Park et al. demonstrated that the most frequently occurring wind gusts had a duration of about 1 min, and therefore supercapacitors are well suited to the task of such energy buffering [61].

3.3 Direct Coupling: The Issue of Fluctuations

If a RE-membrane system does not possess any electrical energy storage, then it is a "directly coupled" desalination system, where the majority of available electricity is utilized to produce clean drinking water and then the product (water) is stored in a tank. The main motivation for realizing a directly coupled RE-membrane system is to remove the batteries, which are regarded as the weakest link in such a system. However, membrane systems are typically designed to work under constant flow and constant pressure to reduce the possibility of causing any damage to the membranes [64]. Thus intermittency and fluctuations of solar radiation over short periods represent a challenge for a directly connected system [65]. The operation of a directly connected system from a fluctuating and intermittent RE resource results in a power supply that mimics these variations and translates them into variations in flow and pressure. While this paradigm challenges the classical design rules of membrane systems, it is worth mentioning that enhanced system performance has been demonstrated [66,67]. Park et al. [67] tested a wind-powered RO system with synthetic brackish water without energy storage and over a range of wind

speeds under fluctuating conditions. When operating at average wind speeds of 7.0 m/s or more, the permeate flux and salinity (quantity and quality) were unaffected by fluctuations up to a turbulence intensity of 0.4 and within this operating range, and was independent of the fluctuation period. They concluded that their wind-membrane system can operate within a safe operating window (SOW) with large power fluctuations.

It has been reported that energy fluctuations may negatively affect system performance, mainly because of the immediate impact on pressure/flow and the subsequent effect on both permeate quality and quantity, as well as causing fouling to the membranes [40]. Liu et al. [19] state that fouling is a major problem with an intermittent RO system and special care is required for feed water pretreatment. Mathew et al. [68] described a small-scale membrane system with an intermittent operation due to energy fluctuations and showed the importance of feed water pretreatment in such systems to minimize biological fouling during periods when the systems are not in operation. Pretreatment in such systems maximize the systems' efficiency and increase the membranes' lifetime [19] and can be achieved with ultrafiltration (UF) pretreatment. Thomson et al. [66] found that during periods when the systems are not in operation, the feed flow stops but that salt continues to penetrate the membrane, affecting the permeate quality as well as increasing the potential for membrane fouling. To address this problem, these authors suggested that an automated valve could be used to reject product water exceeding a threshold concentration, thus improving the overall permeate quality of the system. Membrane module manufacturers recommend maintaining a constant permeate flow rate in order to minimize damage to the membranes and consequently increase lifetime [64]. Interestingly, other studies have also shown that variable unsteady flows can help decrease concentration polarization (CP) as well as membrane fouling [69]. Power fluctuations might also have advantages by reducing CP and membrane fouling, leading to an increase in the overall system performance. When there are fluctuations in energy and the pressure falls below the osmotic pressure, the permeate flows in reverse through the system and can potentially act as a "natural backwash," reducing the need for membrane cleaning in the long-term [65]. Overall, the potential for operating a directly coupled RE-membrane in the long-term remains to be fully evaluated.

4. RENEWABLE ENERGY-POWERED WATER TECHNOLOGIES/SYSTEMS

4.1 Overall Desalination Technologies

Desalination is a process of removing salt and minerals from salt water to produce fresh water suitable for human consumption, such as for drinking and food preparation. Desalination is an energy-intensive process, which makes the desalinated water more expensive than other freshwater sources such as surface and groundwater that do not usually require desalination. However, in remote areas, which often have natural water sources that are not well protected and that are exposed to contamination by chemicals and

microbial pollutants and that are often brackish, desalination technology can be the best solution to providing safe drinking water.

Solar-powered desalination systems are considered the most promising and most used RE-desalination technology. In fact, around 70% of RE-desalination systems worldwide are solar-driven [70], as both thermal and/or electrical loads can be met. Solar-powered desalination systems can be classified as direct and indirect, as shown in Fig. 10. Direct desalination systems are those that use solar energy directly without needing energy conversion, such as solar stills and solar humidification dehumidification systems. Indirect desalination systems can be further classified as membrane-based and nonmembrane-based systems. Table 1 details the advantages and disadvantages of different direct and indirect solar desalination systems [72].

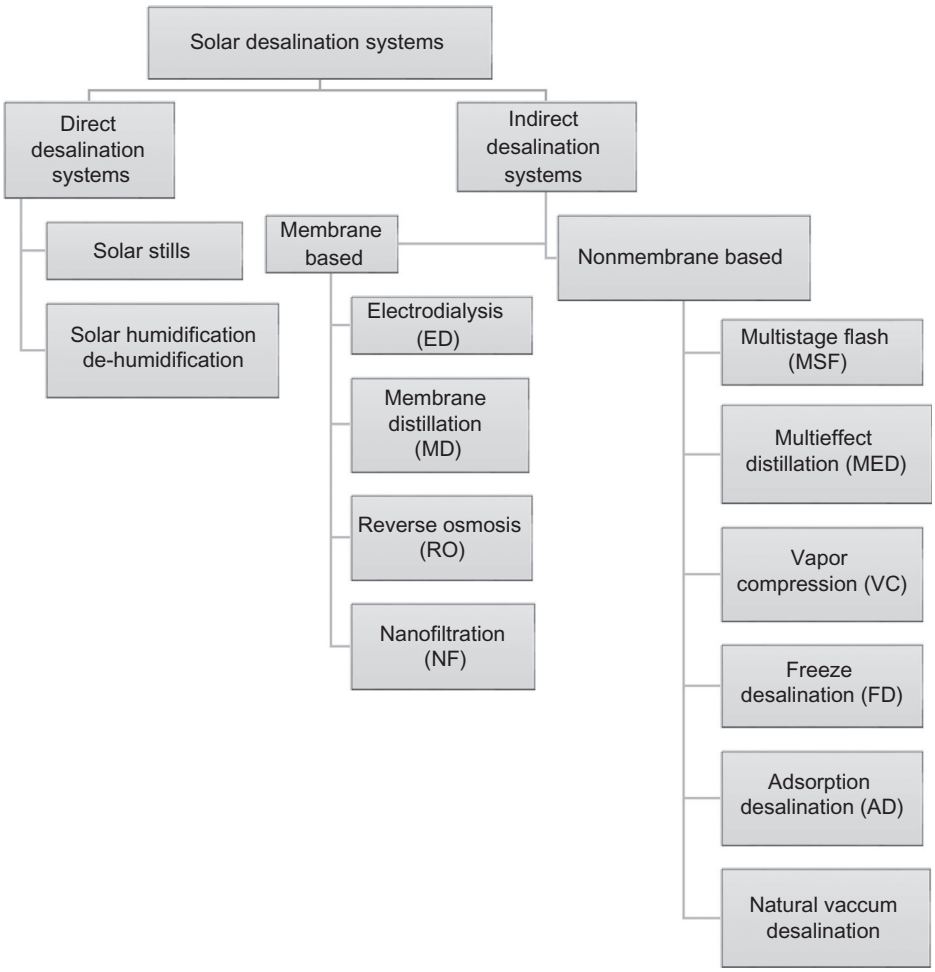

Fig. 10 Classification of direct and indirect solar desalination systems [71].

Table 1 Advantages and disadvantages of different direct and indirect solar desalination systems

	Advantages	Disadvantages
Direct desalination systems		
Solar stills	+ High-quality product water + Ease of construction	– Large area is required – Low distillate yield per m^2 – Low efficiency – Low overall performance
Solar humidification-dehumidification	+ Low O&M costs + Fit for decentralized systems + Can use low-grade energy	– High capital cost – Efficient operation requires large number of stages – High water production cost
Indirect solar desalination systems		
Nonmembrane processes		
Multistage flash (MSF)	+ Best fit for large scale + Tolerates feed water of any quality + Produce water with high quality + No pretreatment required	– High energy requirements – High capital cost – Corrosion likely to happen
Multieffect distillation (MED)	+ Low thermal energy consumption + Operation at low temperatures + High-quality water produced + No pretreatment required	– Electrical power also needed (vacuum pump) – High capital cost – Corrosion likely to happen
Vapor compression (VC)	+ High efficiency + Low energy consumption + Suitable for small systems + Pretreatment partially required + High-quality water produced	– Initial high cost – High water production cost – Corrosion of compressor
Adsorption	+ Low fouling (no biofouling) and corrosion due to operation at low temperature + Low maintenance requirements + Energy-efficient technology	– Limitations in charge efficiency

Continued

Table 1 Advantages and disadvantages of different direct and indirect solar desalination systems—cont'd

	Advantages	Disadvantages
Membrane processes		
PV-NF/RO	+ Suitable for brackish and groundwater treatment + Low power consumption + Can build portable or compact units	– Pretreatment required – Biological fouling possible – Short lifetime for membrane
ED	+ High water recovery + Low membrane fouling and scaling + Pretreatment partially required + Low pressures operation	– Permeate containing microorganisms – Unable to remove nonionic substances
MD	+ Reduction of noncondensable species vapor phase + High concentration at low pressures and temperatures + Reduction of osmotic limits + Integration with other membrane operations	– Energy consumption – Fluxes lower than in other membrane processes – Some membrane materials still too expensive

Adapted from H. Sharon, K.S. Reddy, A review of solar energy driven desalination technologies, Renew. Sustain. Energy Rev. 41 (2015) 1080–1118; E. Drioli, A. Criscuoli, L.P. Molero, Membrane distillation, in: S. Vigneswaran (Ed.), Water and Wastewater Treatment Technologies, Eolss Publishers Co. Ltd., Oxford, United Kingdom, 2009.

Membrane-based desalination systems are capable of removing different contaminants simultaneously and reliably [73]. Moreover, the technology is scalable from very small to very large systems, which makes it a favorable choice for small-scale treatment systems for supplying safe drinking water to remote communities. Therefore the next section focuses on such systems. Table 2 shows the possible combinations of solar energy with a range of desalination technologies. The technologies that are most compatible with small-scale systems are shaded.

4.2 Solar-Powered Membrane Based Desalination Systems

When considering solar-powered desalination systems for remote areas, membrane-based technologies including PV-RO, PV-ED, and solar-MD systems are the most common choices because of their economic and technical advantages; thus they are described here in more detail. Fig. 11 shows pictures of several RE-powered desalination technologies: (A) PV-NF/RO for fluoride removal from brackish groundwater and surface water in Northern Tanzania; (B) solar-MD used for desalinating seawater in Pantelleria Island, Italy; and (C) PV-ED for treatment of wells/spring brackish water in St. Paul Monastery, Red Sea, Egypt. Table 3 details the daily drinking water production capacity and SEC of a dozen such solar-membrane systems that have been implemented worldwide. It can be seen that for small-scale systems, PV-EDs have the lowest energy requirements followed by PV-NF/ROs. Replacing the RO modules with NF modules reduces the energy requirements without exceeding the permeate quality target value [40]. Compared with PV-EDs and PV-NF/ROs, solar-MDs have the highest energy requirements, and the reported SEC for solar-MD systems varied widely depending on the operation parameters and the configuration used.

4.3 Photovoltaic-Powered Reverse Osmosis (PV-RO)

RO is the second most dominant desalination technology. In RO, high pressure is applied to a saline feed water to pass through dense membranes, which because of their

Table 2 Possible combinations of solar energy with desalination technologies

		Solar stills	NF/RO	ED	MD	MVC	TVC	MSF	MED
Solar-passive		**×**							
PV			**×**	**×**		×			
Thermal collectors					**×**				×
Concentrated solar power (CSP)	Thermal				**×**		×	×	×
	Electrical		**×**	**×**		×			

Bolded "×" represents technologies that are most compatible with small-scale systems.
Adapted from M. Papapetrou, M. Wieghausand, C. Biercamp, Roadmap for the Development of Desalination Powered by Renewable Energy, Frauhnofer Verlag, 2010.

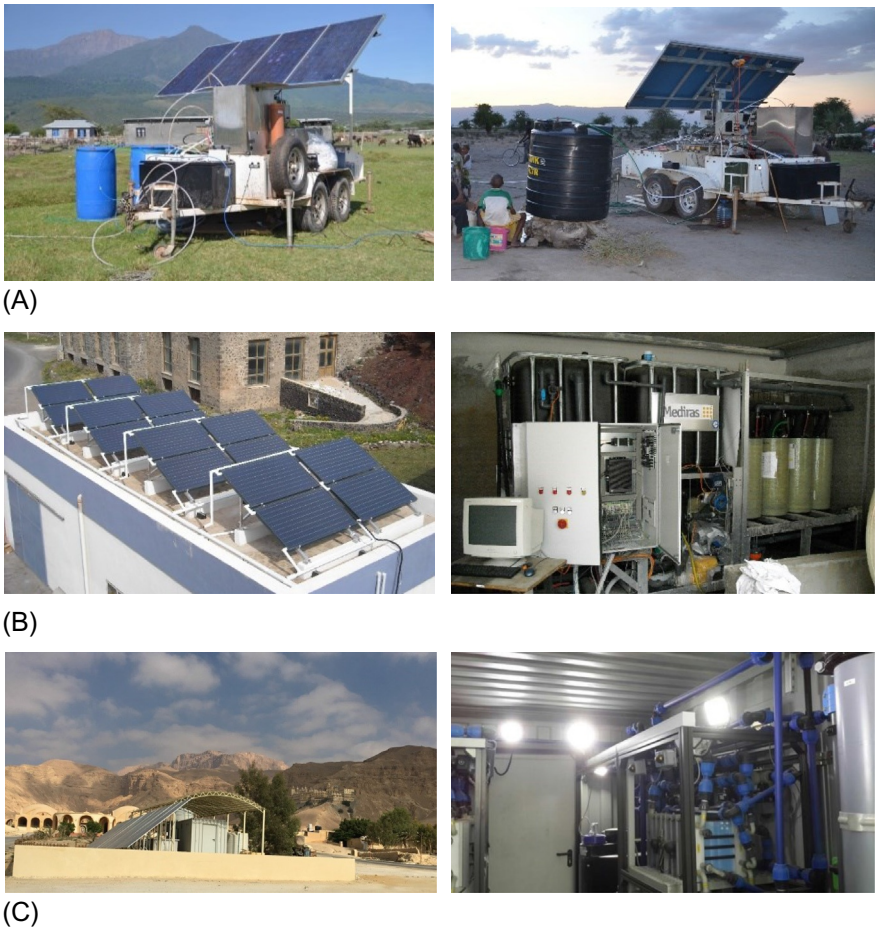

Fig. 11 Pictures of renewable energy-powered desalination technologies: (A) PV-NF/RO in Northern Tanzania, © Schäfer, (B) solar-MD in Pantelleria Island, Italy, © Cipollina, and (C) PV-ED in St. Paul Monastery, Red Sea, Egypt, © Rapp.

hydrophilic nature, allow water to pass through. RO membranes have high salt rejection (SR, >90%) and typically high recovery ratios (RR) of more than 50% with low SEC. RO membranes are prone to fouling and scaling necessitating pretreatment, which results in higher maintenance cost and environmental impact [71].

A simplified general design scheme of a PV-RO desalination plant system is presented in Fig. 12. PV-RO desalination systems are a combination of PV modules and RO membranes. The PV solar panels generate a direct current (DC) electrical energy, which is used to power the pumps to generate the pressure required for the feed water to permeate through the RO membranes [78]. As discussed previously, the pump in such systems can be directly connected to the PV panels without the need for batteries, and storage is achieved via permeate in tanks. PV-RO systems can be used for the desalination of both

Table 3 Energy demand and daily water production capacity of different solar-powered membrane systems

RE-membrane technology	Capacity (m^3/day)	SEC (kWh/m^3)	Details	Ref.
PV-NF/RO	0.764	3.2	Brackish water, feed salinity 7400 mg/L, salt rejection (SR) 96%	[35]
	50	8	Brackish water, feed salinity 3500 mg/L, performance ratio (PR) 70%	[74]
	0.192	1.3 (w/o battery)–2.7 (w/ battery)	Brackish water, feed salinity 720 mg/L, SR 98%, recovery ratio (RR) 15%	[36]
	2	15	RR 15%	[74]
	0.9	4.3–4.6	Seawater, feed salinity 35,000 mg/L, SR 99.2%, RR 8%	[75]
PV-ED	2.8	0.82	Brackish water, feed salinity 1000 mg/L	[37]
	200	0.6–1	Brackish water, feed salinity 700 mg/L	[76]
	18	0.8	Brackish water, feed salinity 900 mg/L	[38]
Solar-MD	0.064	647	Brackish water, feed salinity 670 mg/L, SR 99.5%	[43]
	0.1	200–300	Brackish water, RR 1%–4%	[45]
	0.08	144	Seawater, feed salinity 35,000 mg/L	[77]
	0.44	200–300	Seawater, feed salinity 55,000 mg/L, RR 3%–4.5%	[44]

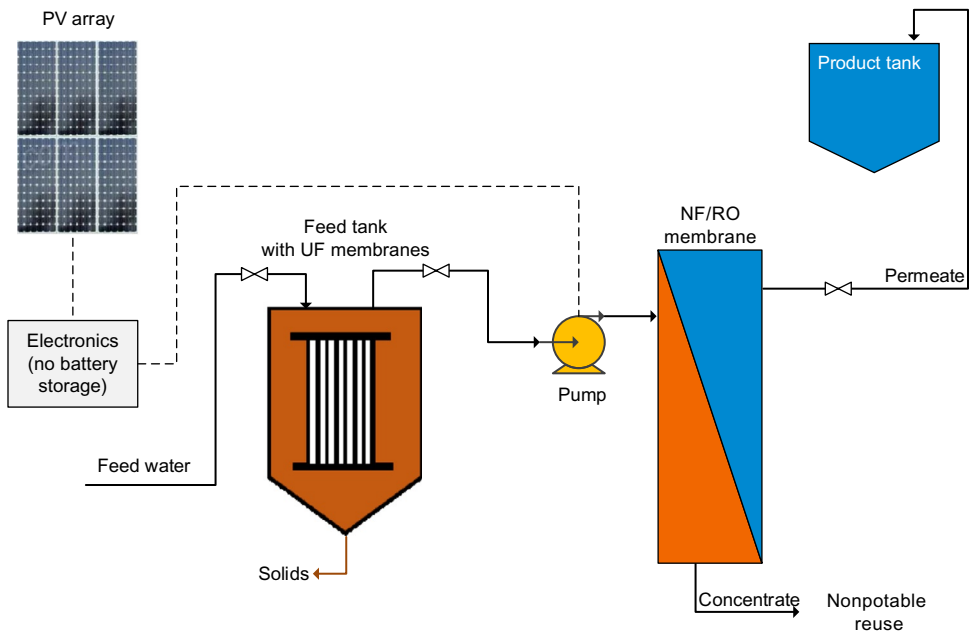

Fig. 12 Schematic diagram of the components of a directly coupled PV-RO system.

brackish water and seawater [79]. Present conversion efficiencies of silicon PV modules are typically in the range of 16%–18% [80], while modules are selling for about $0.50/W, the cheapest in the entire history of PV technology so far. In addition, the socioeconomic and environmental benefits were found to be better in PV-RO systems when compared with RO systems that are powered by diesel generators [81].

The combination of PV and RO modules is considered one of the most promising RE-membrane technologies. First, both PV and membranes are mature technologies that have reached a competitive cost, and costs continue to decrease as the technology advances and the market share increases. In addition, since both membrane modules and solar panels are modular in nature, PV-RO systems can be resized to meet increased future demand.

The world's first stand-alone PV-RO desalination plant was installed in Jeddah, Saudi Arabia, in 1980 with a capacity of 6.5 m^3/day and was able to meet the drinking water demands of 250 people [82]. The performance of a PV-RO system with a capacity of 1.5 m^3/day in the northern part of Mexico was evaluated by Petersen et al. [83]. The increase in the operating pressure of PV-RO systems can improve the permeate quantity, the recovery of the system as well as the product salinity. Al-Suleimani and Nair [84] evaluated the performance of a PV-RO unit with a 5 m^3/day capacity and a 20-year projected lifetime for a remote area in Oman. They concluded that the PV-RO unit was more economically attractive than the same capacity RO unit operated by a diesel generator over the project's full lifetime but that it would not be competitive for a more limited period. They found that the cost of water produced by diesel-powered RO and PV-RO systems was $8.68/$m^3$ and $6.52/$m^3$, respectively. Soric et al. [85] developed a directly coupled PV-RO system that was capable of producing 1 m^3/day of clean permeate. The system consisted of five PV modules providing a power of around 500 W in optimal conditions, an RO unit, pumps, and an electric regulator. They used an electric regulator in order to provide stable voltage to the pumps while protecting energy peaks. The regulator was built around a 250 Farad supercapacitor used as a buffer between the PV modules and the pump. It had the advantage of loading and discharging with very strong power without damaging the components, which represented a major advantage for starting the pump. It had an automated control that measured the voltage across the terminals of the device and controlled "cut relays" that allowed the inlet power from PV modules or the output power to the pump to be cut. The relays could cut the power without a slow decrease in voltage [85]. The batteryless PV-RO system was able to continuously operate from 10 a.m. to 5 p.m. during the summer months when solar energy was available. The entire PV array was covered by the shade of trees by 5:30 p.m., thus electrical production and production of water was not achieved until the next day. The yearly water production was estimated, taking into account that no production was achieved during the winter months, and was found to be 275–373 m^3 with productions superior to the daily m^3 for summer months.

In RO the system efficiency, power consumption, feed water salinity, and membrane configurations all affect the cost of produced water [86]. In PV-RO units, the system efficiency is dependent on the efficiencies of all the individual components. Thus the implementation of high-efficiency components—PV modules pump, electronics—as well as choosing robust components (such as durable membranes) will help realize a robust system design and reduce the cost of water production in the long term.

4.4 Photovoltaic-Powered Electrodialysis (PV-ED)

Electrodialysis (ED) is a desalination technology that uses selective membranes that transport ions under the influence of an electrical field. An ED unit contains a number of cation and anion exchange membranes that are stacked in an alternating fashion between the cathode and the anode and that are separated by the saline water. The cation exchange membranes have negative fixed groups, whereas the anion exchange membranes have positive fixed groups. When DC voltage is applied, a potential difference between the two electrodes results. The positive ions pass through the cation exchange membranes and are retained by the anion exchange membranes. The negative ions, however, pass through the anion exchange membranes and are retained by the cation exchange membranes. The transported ions are accumulated in specific compartments and are discharged as a brine, while the adjacent compartments contain the water with the decreased salt concentration. To prevent salt deposition in the membranes, the polarity is usually reversed every 20 min [87].

PV-ED systems are mostly used for brackish water desalination. The DC electricity is used to power the ED stack directly, though an inverter can be used if desired to provide AC electrical energy for the pumping system. However, directly connected PV-ED systems without battery usage have also been implemented [88,89]. In such systems, the water is produced during the day when sunlight is available and stored (rather than saved as electrical energy) to be used during the night. As with PV-RO, PV-ED systems have the environmental advantage of avoiding improper disposal of batteries, which occurs in remote areas where proper disposal facilities are not available [90].

Fig. 13 shows a schematic diagram of a PV-ED system. Kuroda et al. [37] proposed a PV-ED system whereby the PV power output was used to partially desalinate the feed seawater during the daytime when solar radiation was high. During times of low solar irradiance, the produced water was desalinated again to produce fresh water. As a result, they achieved a reduction in the battery capacity, although it should be pointed out that the SEC for a PV-ED system treating seawater will be extremely high. Mahabala et al. [89] implemented a batteryless PV-ED system in Thar Desert, India, which proved to be a good option for remote areas. The system was tested for 1 year and produced drinking water at a 1000 L/day rate with a SEC of 5 kWh/m^3. The PV arrays of the system were manually tracked daily and monthly in order to enhance system efficiencies. Ishimaru [76]

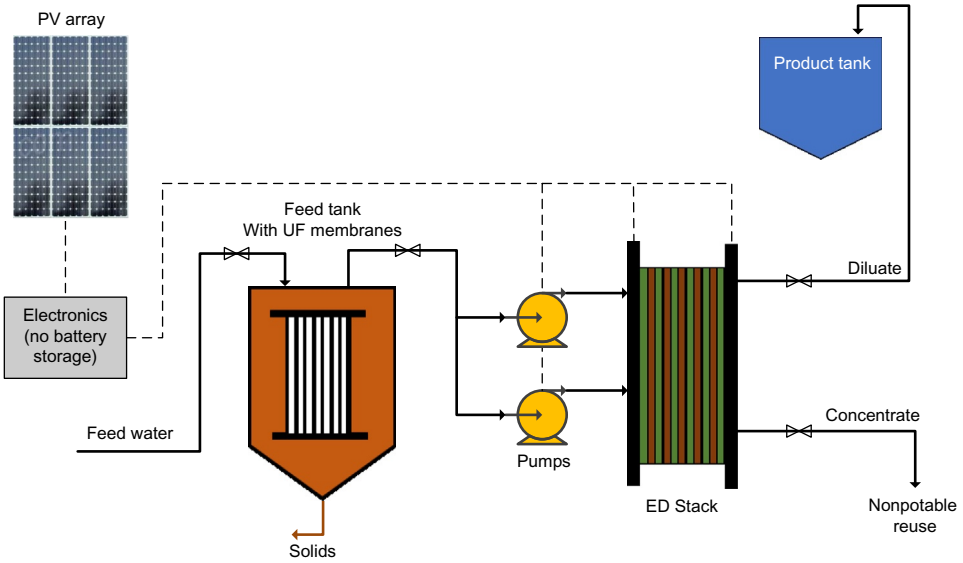

Fig. 13 Schematic diagram of the components of a directly coupled PV-ED system.

experimented with a PV-ED unit for brackish water desalination at Fukue city, Nagasaki, Japan, and was able to produce drinking water in the range of 200–375 m^3/day. The system achieved a lower actual SEC than the expected design value of 1.92 kWh/m^3 because of a lower concentration of brackish water.

Ortiz et al. [88] installed a directly coupled PV-ED system for brackish water desalination in Spain. An overall effective membrane surface area of 4.4 m^2 was used, and two experiment configurations with eight (experiment 1) and four (experiment 2) PV panels each with an area of 0.5 m^2 and a peak power of 38.5 W were used. All the experiments were carried out at ambient temperature using test solutions containing 2000 mg/L NaCl as initial concentrate and dilute solutions with an electrolyte of 0.05 M Na_2SO_4. Experiment 1 ran for 3.5 h and had a drinking water production rate of 0.29 m^3/h while experiment 2 ran for 0.45 h and had a drinking water production rate of 0.22 m^3/h. It was concluded that the type of arrangement of the solar panels needs to be optimized and has a strong influence on water production.

When compared with PV-RO, PV-ED systems have advantages in terms of both the desalination process and the PV panels [91]. For instance, ED membranes have a longer lifespan because of their higher mechanical and chemical stability [92]. Additionally, because of the process reversal, they experience less membrane fouling and scaling [92]. Moreover, the process can be easily started and shut down for intermittent operation. In terms of PV usage as a power supply, PV-ED systems can be powered directly with DC current eliminating the need for a DC-AC inverter, although doing so is also possible in directly connected PV-RO systems that use DC pumps [93]. The lack of additional electronics eliminates the energy loss associated with the transformation and thus saves energy.

4.5 Solar-Powered Membrane Distillation (Solar-MD)

Membrane distillation (MD) is a mostly thermally driven desalination process. MD is based on the use of a hydrophobic membrane as an interface between the hot liquid feed and vapor phases that cause water to evaporate [94]. The hydrophobic membrane allows only the vapor to pass through its pores, thereby preventing the liquid feed from passing. MD is usually categorized in four main configurations: direct contact (DC), vacuum (V), air gap (AG), and sweeping gas membrane distillation. Regardless of the configuration, the hot feed is always in direct contact with the membrane surface, and the driving force is always applied in the permeate side. In DCMD, an aqueous solution colder than the feed solution is maintained in direct contact with the permeate side of the membrane. In VMD, vacuum is applied on the downstream side of the membrane using a vacuum pump. In AGMD, a stagnant air gap is interposed between the membrane and a condensation surface at the permeate side. The evaporated volatile molecules flow across the membrane pores and the air gap to a colder surface inside the membrane module. In sweeping gas MD, a cold inert gas sweeps the permeate side of the membrane carrying the vapor molecules, and condensation takes place outside the membrane module [95]. Fig. 14 shows the system configuration of a typical solar-AGMD system. The thermal

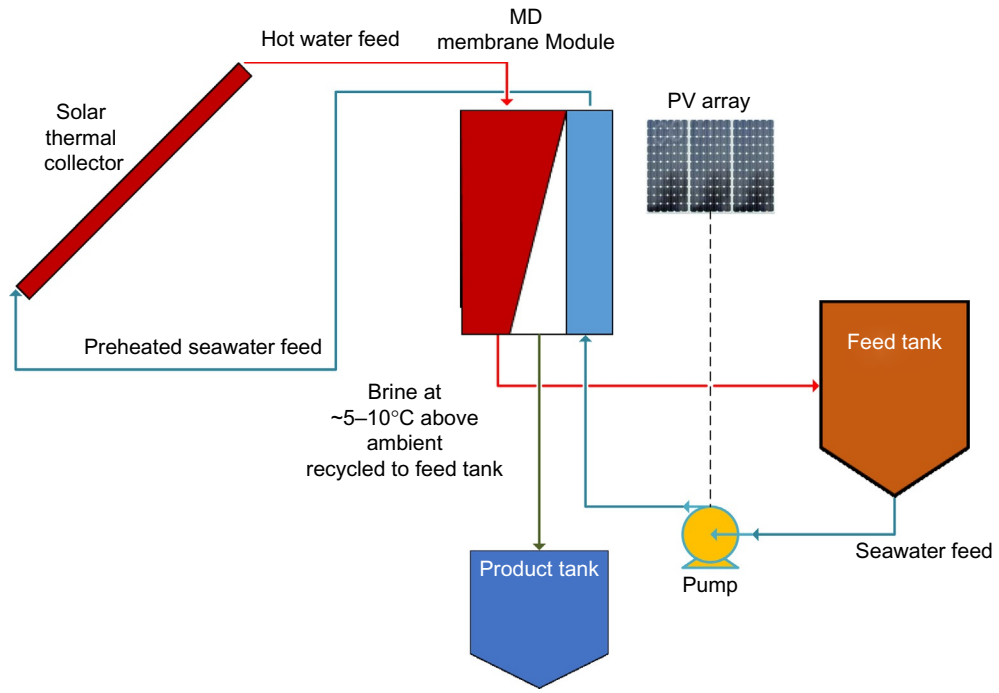

Fig. 14 Schematic diagram of the components of a solar-powered air gap membrane distillation unit. The MD process gets the required energy from solar thermal collectors, while a small PV panel provides the electrical energy needed for the pumps.

energy required for the MD process is obtained by solar thermal collectors, and a small PV array is also used to provide the required electrical energy needed for the pumps. The internal energy recovery of latent heat of vaporization results in a temperature lift and preheating of the feed. The preheated feed then enters the solar collectors, achieving a further temperature lift before it enters the module evaporator. This way, the internal energy recovery significantly reduces the required solar collector area [96].

A solar-MD system for drinking water production in arid rural areas of Australia was carried out by Hogan et al. [49]. Simulations and experimental studies were carried out, and under a constant flow rate and feed temperature, increasing the effective membrane area increased the permeate production rate. Saffarini et al. [96] carried out water production cost comparisons between different solar-powered MD systems. The water production cost for direct contact MD, air gap MD, and vacuum MD were $\$12.7/m^3$, $\$18.26/m^3$, and $\$16.02/m^3$, respectively, for a recovery ratio of 4.4%. It should be noted that it is possible to achieve higher recovery ratios in MD processes [97]. The water production cost of air gap MD was reduced when the effective membrane length was increased and the air gap width and feed channel depth decreased. Banat et al. [45] evaluated the performance of a small-scale solar-MD system in Irbid, Jordan. A 5.73 m^2 solar collector to heat the feed water and a PV module of 860 W (total area of 1310×654 mm^2) was used to supply electricity for the feed pump and magnetic valves. A spiral wound module with effective membrane area of 10 m^2 was employed. The distillate flow rate was varying because of the variable solar irradiance that reached its peak value of 2.5 L/h.m^2 at midday. Water production cost was largely dependent on the lifetime of both the membrane and the plant; a water production cost of $\$15/m^3$ was reported.

Gemma et al. [55] presented an operational experience of 5 years performance of a solar-MD demonstration plant in Pozo Izquierdo, Gran Canaria Island (Spain). The overall performance was found to be satisfactory. They used an enhanced version of a DCMD unit, and the membrane units were replaced three times during the plant's 5-year operation. They also reported a high-quality distillate with a production rate ranging from 5 L/day for the lowest daily production over the 5 years and 120 L/day for the highest daily production over the 5 years, depending on the weather conditions. A thermal-only SEC in the range of 140–350 kWh/m^3 was determined.

5. OPERATION AND MAINTENANCE

5.1 Safe Operating Window

A directly coupled RE-membrane system has constraints that enable it to achieve good system performance and to adopt the best operation strategy. Constraints that determine the optimum operating strategy for variable power operation of an RE-membrane system result in a safe operating window (SOW).

The SOW gives a range within which it is technically desirable to operate the system such that it will result in maximizing the permeate water production while minimizing the energy requirements, as well as decrease the possibility of performance degradation that can result from a high-recovery operation. Feron [98] was the first to propose the concept of SOW for the transient operation of a wind-powered seawater RO system. The conclusion was that operating from a fluctuating and intermittent power source is not expected to cause any major problems as long as the on/off cycling of the plant was controlled in such a way that the rate of pressure change and the cycling frequency would not damage the membrane. Feron used the constraints of the membrane characteristics (maximum feed water pressure, maximum concentrate flow rate, minimum concentrate flow rate, and maximum permeate concentration) to derive a curved-sided quadrilateral SOW. He proposed two recommendations to allow wind-membrane seawater plants to deal with a variable wind resource: (1) modifying the membrane area, and (2) allowing a transient operation within the SOW constraints. However, he concluded that both recommendations were economically unfeasible at that time (1995) because they involved underutilization of an expensive membrane area and only a relatively minor increase in productivity in contrast to the increased complexity of the plant.

The first experimental investigation of an operating strategy for transient operation of RE-membrane plants within a SOW was performed by Richards et al. [99] for treating brackish water (2750–10,000 mg/L TDS). The SOW was constrained by several factors: (i) the pressure and flow rate limits of the pump motor, (ii) the maximum recommended recovery, and (iii) the feed water osmotic pressure. At lower salinities (2750–5500 mg/L), the 30% maximum recovery was the main constraint, while osmotic pressure was the main constraint when treating 10,000 mg/L feed water. Different operating strategies were evaluated, and the optimum operating strategy that resulted in the lowest SEC while at the same time maintaining good retention was constant recovery. However, the implementation of this approach can be difficult in practice; thus, in order to provide a more robust and effective solution in remote areas, a constant set-point mode was recommended as the operating strategy for such systems with a minor reduction in performance. Richards et al. used additional experimental constraints than Feron [98] originally used, which resulted in a curve-sided pentagon SOW, as shown in Fig. 15 [99]. In Fig. 15 SOW is constrained by (i) min. recovery illustrating the min. TMP required to produce flux, which depends on feed concentration and no flux obtained below this line, (ii) the max. set-point pressure of the regulating valve on the concentrate stream at standard conditions of pump power and feed flow rate, (iii) the max. rated pump power restricting the operating limits of TMP and feed flow rate, (iv) max. recommended recovery to prevent scaling and fouling and lower the power consumption, and (v) min. set-point pressure of the regulating valve on the concentrate stream at standard conditions. The developed method demonstrates the possibility of operating without energy storage and can be used in performance evaluation of a wide range of membrane filtration systems.

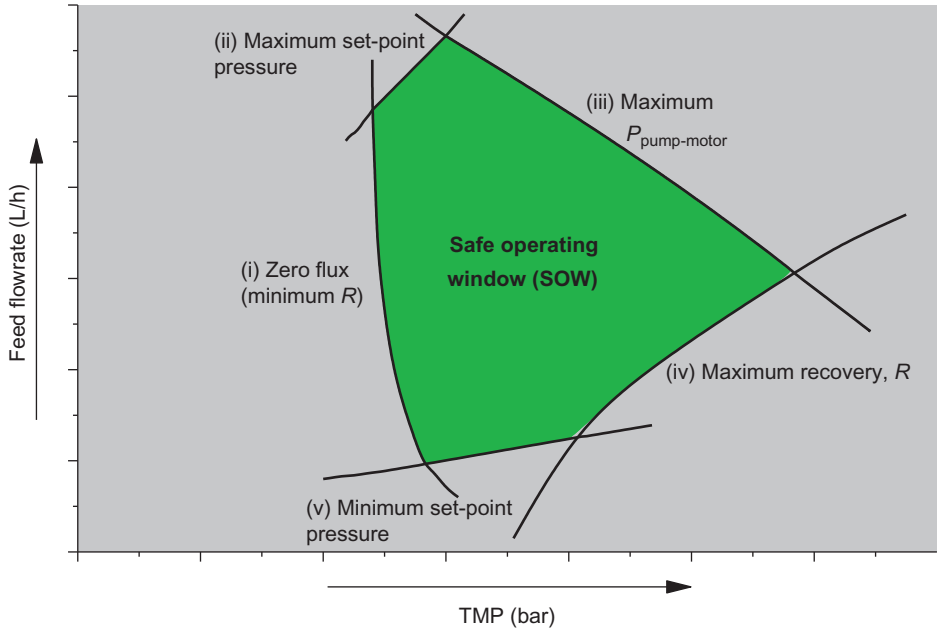

Fig. 15 Principle of the experimentally determined SOW. *(Adapted from B.S. Richards, G.L. Park, T. Pietzsch, A.I. Schäfer, Renewable energy powered membrane technology: safe operating window of a brackish water desalination system, J. Membr. Sci. 468 (2014) 400–409).*

5.2 Fouling, Cleaning, and Maintenance

Small-scale RE-membrane systems for water provision in remote communities are usually operated and maintained by personnel from the community who may receive only minimal training. The performance of the membranes in such systems degrades as a function of their operation and the chemistry of feed water [100], typically within 2–5 years for RO membranes [101]. Membranes are prone to different types of fouling, such as inorganic/scaling, organic fouling, colloidal fouling, and biofouling. Table 4 lists definitions of the different membrane fouling types [102]. Degradation and fouling of membranes result in the reduced production of clean water, in addition to decreasing their lifespan [103]. It is therefore necessary to clean the membranes periodically to maintain performance, which is usually achieved by procedures such as chemical cleaning and flushing. In flushing, part of the clean water product is allowed to flow back from the feed water inlet along the surface of the membrane, which removes loosely deposited particles. This flushing is not able to remove hard scale; however, it can remove early-stage scaling minerals [104]. For chemical cleaning, the chemicals used depend on the fouling type. This method starts with slowly circulating the chemical solution (usually acid solutions for inorganic precipitates and alkaline solutions for organic fouling including biological matter) followed by soaking it between 30 min to a full day, then

Table 4 Types of membrane fouling

Fouling type	Definition
Inorganic fouling (scaling)	The accumulation of inorganic precipitates and soluble minerals, such as calcium carbonate, on the membrane surface or within the membrane pores. This happens when the concentration of chemical species at the membrane surface reaches supersaturated concentrations.
Colloidal/particulate fouling	Suspended particles in the water, called colloids, carried to the membrane surface by the permeate flow, fall into the size range of particles, coalesce, and form a soft cake layer.
Biofouling	Attachment of microorganisms on the membrane surface and its support forming a biofilm. When bacteria attach to the membrane surface, colonies start to grow and produce an extracellular polymeric substance layer, the biofilm.
Organic fouling	Fouling caused by source water containing, for example, macromolecules like natural organic matters (NOM) common in surface water (lakes, rivers). Organic fouling is considered the most significant factor contributing to flux decline.

Adapted from R.W. Baker, Membrane Technology and Applications, second ed., John Wiley & Sons Ltd., England, 2004.

recirculating it at a high rate for 30–60 min, and finally flushing it with clean water for approximately 60 min [105]. Chemical cleaning cannot always fully remove foulants. The membranes are likely to wear out after several years of operation (typically 2–5 years for RO, based on operating conditions [100,106]) and a combination of several other reasons, including general deterioration, irreversible fouling, and high-pressure feed water.

General maintenance guidelines for membrane cleaning are usually provided by membrane manufacturers and depend on the type of membrane and operating conditions that are usually steady and often set to start cleaning at a certain pressure or flux [107]. However, such guidelines are usually general and may not be suitable for a specific system or site conditions. On one hand, more frequent cleaning results in too much use of product water and chemicals. On the other hand, less frequent cleaning results in the build up of more foulants on the surface of the membrane, which results in a decrease in the rate of water production, increased costs, and possibly permanent membrane damage. It is thus important to have optimal cleaning protocol for such small systems, which is likely beyond the expertise of local operators [100]. Condition-based maintenance (CBM) for conventional RO systems has been proposed [108]. In CBM, operational parameters are monitored, and when the measurements reach a predetermined threshold, maintenance actions are performed. CBM is effective for conventional large-scale systems, but optimizing a CBM protocol for a small-scale system requires detailed search methods and extensive trial and error practices [100], which are not possible for operators who aren't experts in this kind of work.

Kelly et al. [100] used a simple physics-based model of RO membrane fouling and remediation to find maintenance schedules that maximize water production and minimize water costs in small-scale PV-RO systems for remote communities under deterministic conditions. Those models can help inexperienced operators know when and what type of cleaning should be done for the optimization of small-scale systems. For small PV-RO systems operating in remote locations, the large uncertainties impact on the range of cleaning schedules required such that a prescheduled maintenance program will not be able to maximize water production under changing conditions. However, the same authors are carrying out further research to develop an algorithm that also uses sensor information in real time to estimate the state of the system as a function of time and then applying optimal planning methods to predict when the next remediation treatment should occur [100]. There is potential for using model-based methods to permit nonexperts to operate a PV-RO system under uncertain, changing conditions, while still meeting the community's water demand.

6. SOCIOECONOMIC INTEGRATION, COSTS, PUBLIC PERCEPTION, AND MARKET POTENTIAL

6.1 Socioeconomic Integration

The effective application of RE technologies requires a comprehensive understanding of sustainable development [109]. This means it is essential to find a balance between the three main goals of sustainability: the social, the economic, and the environmental goals. However, the main barrier to doing so is the compatibility between those goals, which make trade-offs inevitable. For instance, one dilemma might be to decide what comes first, protection of the environment and human well-being or economic growth. Grubert et al. [110] explained how complicated the relationship between these three goals is, which in turn affects the quality and sustainability of society. Goosen et al. [109] suggested that achieving a balance between the three could be achieved by educating people—such as industrial workers, decision-makers, and students—as this is primarily the cultural change stimulator. Table 5 list some factors affecting sustainability in RE-desalination systems.

Desalination using RE in areas that possess abundant natural gas and oil reserves, such as the Arabian Gulf, might not be widespread. However, such fossil fuels are not renewable and in the long term represent a unsustainable solution. Moreover, the demand for fossil fuel for desalination in those areas is expected to increase even more with the constant increase in population. For instance, in 2008 Saudi Arabia had a total oil and gas production of 10.8 million barrels per day (bbl/day) of which 25% was consumed within the country [111,112]. Water desalination and electricity generation accounted for a big share of the internal energy demands. Moreover, the population is expected to more than

Table 5 Sustainability factors for renewable energy-powered desalination systems

Social	Economic	Environmental
• Health and hygiene • Safe water • Accessibility/distance • Maintenance requirements (staff) • Reliability/system downtime • Employment opportunities • Time saved water fetching • Increased access to education • Gender equality • Reduced child mortality	• Cost of water • System capital cost • Operation and maintenance cost • Cost and supply of spare parts • Development opportunity due to water availability • Reduced cost of health care (illness and disability) • Energy demand and availability • Local business and job opportunities	• Membrane concentrate disposal • CO_2 emission (energy requirements) • Cleaning chemicals • Land use • Transport requirements • Water use for cleaning • Membrane, photovoltaics, other parts disposal • Increased water utilization through availability

triple to 100 million by 2050 [113]. In order to provide fresh water for the population, 50% of the fossil fuel production is projected to be used by then inside the country's income (because of export losses) and increase pollution, making the solution even less sustainable. These environmental challenges provide a key motivation even in these regions toward RE-desalination.

RE-desalination, solar distillation in particular, faces a key challenge in terms of system efficiency. In solar desalination and during the evaporation and condensation processes, the system efficiency is covered by high heat and mass transfers; thus the surfaces should be designed carefully, aiming for heat transfer efficiency, reliability, and good economics [114]. For example, solar stills can achieve high efficiency by ensuring a high feed water temperature, high temperature difference between feed and condensing surface, and low vapor leakage [115]. Moreover, solar-powered desalination at the moment does not appear as a viable economic option for very large-scale applications [109]. However, solar desalination systems for remote areas are usually small- and medium-scale, which makes solar-powered desalination more appealing in such locations. In addition, although conventional desalination processes require constant and continuous energy requirements, solar energy is available only during the day time with variations in intensity from morning to evening and reaching a peak at midday [116].

International efforts to decrease the cost of RE for desalination applications could be increased to make them more competitive with the large-scale conventional technologies. In rural and remote areas where electricity infrastructure is not even available, small systems powered by RE are already offering favorable and often economically sustainable solutions.

6.2 Costs of Small-Scale RE-Membrane Systems

Many parameters affect the cost of small-scale RE-membrane systems, including location, system capacity, feed water quality, membrane type, battery usage, and choice of RE type. However, because of the limited number of studies published on the novel nature of the technology and usually the unique setup of each system, it is difficult to find reliable cost data for small-scale RE-membrane systems in the literature. In addition, there is an absence of long-term data on operating experience and, consequently, reliable operation and maintenance or even life-cycle cost.

Table 6 shows the reported water generation cost for possible combinations of solar energy and desalination technologies [4]. Part of the variability of data is due to the comparison between mature large-scale conventional technologies and immature (for many) small-scale technologies. RE-powered technologies and water production costs in solar-powered MD, for instance, are expected to continue to be expensive until market penetration is more mature. For example, Ali et al. [71] and Paparetrou et al. [121] reported PV-RO water cost at \$3–\$27/m^3 and \$5–\$15.6/m^3, respectively. In other reports, MD water costs ranged between \$10.4/m^3 and \$19.5/m^3 [71,116]. When coupled with solar PV energy, MD and ED, as compared to the pressure-driven membrane processes, are predicted to cost significantly more, primarily because these technologies are at an earlier stage of development. Also, Table 6 shows that using batteries can significantly affect the final water production costs.

In RE-membrane systems, the installed membrane, RE source, and system auxiliaries each cost roughly one-third of the capital cost [4]. It is important, however, to note that the capital cost for those systems (e.g., \$15,840–\$98,040 for PV-RO as shown in Table 6) lies within the infrastructure cost range for remote locations. For example, the cost for

Table 6 Water production cost of some possible combinations of solar energy with desalination technologies

	Typical capacity (m^3/day)	Water cost (\$/m^3)	Notes	Ref.
PV-RO (seawater)	3	2.9	Batteryless system tested at lab scale. Capital cost \$33,200.	[117]
PV-RO (brackish water)	5–7.5	6.5	Pilot study system in Oman with batteries. Capital cost \$98,040.	[118]
	1	5.9	Batteryless system tested in field in Australia. Capital cost \$15,840.	[93]
PV-ED	2.8	16	Capital cost approximately \$10,150.	[119]
PV-MD	0.1	15	In Jordan. Feed water is brackish. Capital cost \$7695.	[120]

Adapted from A.I. Schäfer, G. Hughes, B.S. Richards, Renewable energy powered membrane technology: a leapfrog approach to rural water treatment in developing countries? Renew. Sustain. Energy Rev. 40 (2014) 542–556.

10 km of water mains ranges between $19,900 and $123,230 in Kenya and Sri Lanka [122], respectively. Thus, depending on the number of people served by such mains, installing community-scale RE-membrane systems might offer a better solution when compared to the capital cost of increasing the coverage of water mains. The best solution will vary in scale and according to local conditions and, consequently, must be determined on a case-by-case basis.

The operating costs of RE-membrane systems or, in other words, the cost of water produced from RE-membrane systems (which are energy-dependent and are affected by operating conditions such as operating pressure and recovery) is lower than some of the reported water costs in Africa, as shown by an extensive study on RE-membrane rural water treatment by Schäfer et al. [4]. They analyzed how operating costs of RE-membrane systems in some African areas appear to be very favorable in comparison to the open water market. However, it was argued that it cannot be assumed that all people will choose or be able to pay for water. Many villagers instead use free water sources or occasionally buy small amounts of water for consumption purposes only. It was concluded that the cost of implementing a RE-membrane system in a remote area is not as big a barrier as traditionally thought. The effectiveness of membrane treatment was addressed before demonstrating the efficiency in the removal of specific contaminants, and in this way, yielded a high-quality product. As a result, the cost of small-scale RE-membrane systems seems promising in remote locations, and they represent an effective alternative where centralized water and electricity infrastructures are not available.

6.3 Public Perception/Acceptance

Public acceptance of RE-powered desalination technologies is of particular importance in order for the technology to be successful and sustainable, especially in remote areas. Although the literature has focused on the social, economic, technical, and environmental aspects of RE-powered desalination technologies, this section focuses more on the public's perception of such systems.

In order for solar desalination technologies to be socially sustainable, they must be accepted by the people in the community where they are implemented, and they need to meet the community's water needs via a suitable maintenance and operation plan [123]. Greece is an example in which public acceptance played a vital role in the success or failure of such technologies. Solar stills that were donated at no cost to users were destroyed by the community [124]. This example may reveal part of the problem; that is, people need to pay for their services, even if only partially, so that they bear some responsibility in the services. To ensure the success and public acceptance of the implementation of a new RE-powered desalination technology, it is better to consider the social aspects prior to implementation. This acceptance might be achieved by examining

the community's needs and willingness (and ability) to pay for the implementation, the availability of human resources or external service providers for management, the O&M of the system, and how a prototype of the system is accepted by the community. Werner and Schäfer [123] studied the social sustainability of a PV-RO system at different sites in Central Australia. Social factors, such as the units' capacity to meet the communities' water needs in terms of quality and quantity, the communities' response to the units, and the human resources available to operate and maintain the units, were determined. Managerial and operational actions were recommended to ensure the social sustainability of the units; these recommendations related mostly to the recovery rate, the choice of membrane, and the maintenance provisions. The (research) prototype used particular membranes and operating parameters and suggested that social needs could be better met if the units adapted different parameters. The overall sustainability of the units was dependent on this adaptability.

Public acceptance cannot be better demonstrated than in the case of Ngare Nanyuki in Northern Tanzania. People there expect to drink pure water coming from the nearby volcanoes of Mount Meru and Mount Kilimanjaro, which are symbolic of pure water (many bottled waters carry their names), even though many sources of the mountains' natural water have extremely high levels of fluoride, which is toxic to the human body. To make this point, the water unit (using UV) in the public secondary school was disguised as a replica of Mount Meru to educate the students (Fig. 16). A nearly black stream treated with membrane desalination to produce high-quality drinking water (Fig. 17) was not accepted because people thought the black water (natural swamp water with a high

Fig. 16 Water treatment system being demonstrated in Mount Meru for public acceptance purposes *(Ngare Nanyuki, Tanzania, © Schäfer).*

Fig. 17 Water produced with brackish water RO had low acceptability by some villagers because of their belief that it was "bewitched" black feed water *(Ngare Nanyuki, Tanzania, © Schäfer).*

organic and fluoride content) was bewitched and did not believe the technology could change the water. Similar reports of the public's lack of acceptance exist in campaigns to reuse "toilet to tap" water, and these reports highlight a significant hindrance to the implementation of such technology [125,126]. Dolnicar and Schäfer [127] studied the public's perception and acceptance of recycled and desalinated water through a questionnaire. Among many other questions was an open-ended question in which respondents were asked to state their main concerns about recycled desalinated water. The respondents raised health concerns as a main issue, with 55% saying that recycled water is more risky from a health perspective.

6.4 Market Potential

RE-desalination is currently attracting the interest of governments, politicians, and stakeholders. This acceptance is attributed to the additional energy requirements associated with the quickly growing desalination market and the associated environmental and socioeconomic issues. In assessing the market potential, the first step is usually to look at low-capacity systems. Because of their suitability for remote areas where the alternatives are few, several low-capacity RE-desalination systems have already been built and tested in different parts of the world. Moreover, in countries where desalination contributes to a large share of their water supply, such as Saudi Arabia and the United Arab Emirates, the first large-scale RE-desalination systems are being installed [128,129].

Depending on its typical capacity range and developmental stage, solar desalination can be used in different market segments. Systems can be classified in four main categories: (i) very small-scale systems with a capacity of a few liters of water per day, (ii) small-scale systems producing several cubic meters per day, (iii) medium-scale systems producing hundreds of cubic meters per day, and (iv) large-scale systems producing thousands of cubic meters per day [130]. The potential market for each category is large and also depends on the development stage. Fig. 18 shows different common solar desalination technologies according to their capacity range and development stage.

The main target of the very small-scale category is typically a single user or household, and this category is suitable for remote areas where both electricity and water supply are unreliable. Maintenance of single-household systems is, however, incredibly challenging. The market for such systems is large, such as families living in remote areas and small health centers. There is also real potential for such systems worldwide, including in areas such as North Africa and small islands in the Mediterranean (in addition to the already established household market in developed countries).

The market potential for small-scale systems of less than 10 m^3/day is also large and is similar to that of very small-scale systems, but instead of covering the water needs for single end users, such systems are targeting more than 100 people, and their highest market potential is for small groups and systems for all inhabitants of a small community in remote areas. PV-RO represents the highest potential and main technology in this category. In this size range, maintenance is clearly more manageable.

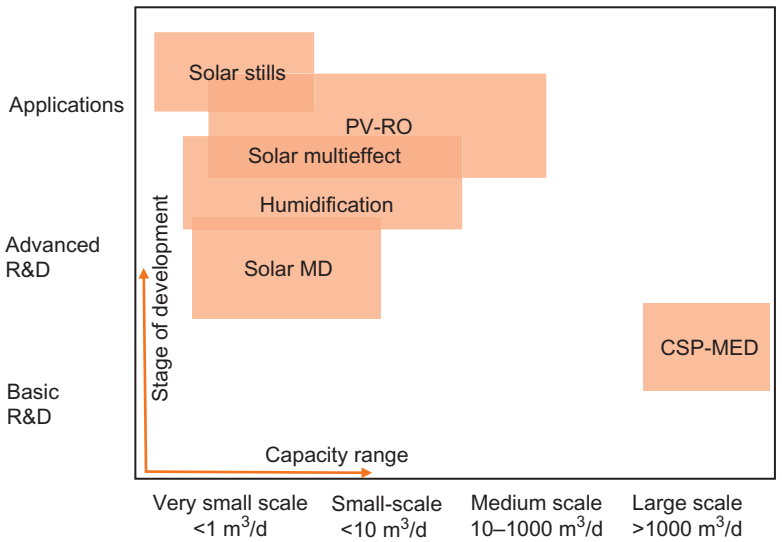

Fig. 18 Solar desalination technologies based on their typical capacity and developmental stages. *(Adapted from M. Papapetrou, M. Wieghausand, C. Biercamp, Roadmap for the Development of Desalination Powered by Renewable Energy, Frauhnofer Verlag, 2010).*

The medium-scale category is suitable for small villages that do not have access to electricity and water or where the cost for electricity is high and the local grid can be unstable. The market for such systems includes towns with 500–50,000 inhabitants, including islands and many towns in the Middle East. Larger systems are usually well served by the industry, even though coupling with RE is still emerging.

The large-scale category (more than 1000 m^3/day) is not intended for small communities in remote areas but is more suitable for communities with centralized municipal water supplies. Such systems are expected to be used more widely, especially in countries where the implementation of RE energy, including desalination, is becoming a high priority in many areas. For instance, in some states in Australia, desalination developers are obliged to generate electricity from RE sources that is equivalent to the consumption of the desalination plant [130].

Hetal et al. [131] showed that RO is the main user of RE in desalination with a market share of 62%, where 32% of RE provided was PV for RO. Table 7 shows the market share of different RE-desalination systems in 2015.

Ghermandi and Messalem [78] addressed market concerns by carrying out an extensive assessment of the experience gathered from solar-powered RO desalination and concluded that, for large-scale solar desalination, CSP-RO desalination is the most promising field for development. They suggested that large-scale CSP-RO systems may compete with conventional RO desalination systems in the medium term and thus gain large market shares. The combination of desalination and CSP, however, is still in the research and development stage, and some aspects are not yet properly determined in terms of achieving effective integration of the technologies [132]. However, the same authors suggested that for small-scale systems in remote areas where grid electricity and water infrastructure are not available, PV-RO presents a cost-competitive option, and the market share of PV-RO desalination plants will likely increase [78]. The fast progress of both CSP and PV solar technologies offers the best future for the broad installation of these sustainable water supply technologies [115].

Table 7 Distribution of renewable energy-powered desalination technology [131]

Renewable energy desalination system combination	Installed capacity (%)
Photovoltaic-reverse osmosis (PV-RO)	32
Photovoltaic-electrodialysis (PV-ED)	6
Solar-multiple-effect distillation (solar-MED)	13
Solar-multistage flash (solar-MSF)	6
Wind-reverse osmosis (wind-RO)	19
Wind-vapor compression (wind-VC)	5
Others	19
Total	100

Grubert et al. [110] developed a modifiable tool that helps policymakers decide on appropriate locations for desalination facilities, based on selected criteria. For this purpose, Grubert et al. applied geographic information system (GIS)-based multicriteria decision analysis (MCDA) in order to select desalination sites. Their work showed a way to help decision makers combine economically, environmentally, and socially defined criteria simultaneously to decide on the best location for a desalination plant.

7. ENVIRONMENTAL ISSUES

As indicated in Table 4, a number of environmental concerns are related to desalination technologies. Naturally, RE-desalination overcomes the major factors of desalination, which are energy demand and consequently CO_2 emissions. Other factors such as concentrate treatment or membrane disposal are factors that may hinder implementation, especially in remote areas. Therefore substantial development is still needed in those areas.

7.1 CO_2 Emissions

Worldwide, it is estimated that around 18,000 desalination plants were operating in 2015, yielding a maximum production capacity of over 88 million m^3/year of potable water [133]. As a result, water desalination is associated with considerable CO_2 emissions, and it is reported that the currently operating desalination plants worldwide emit around 76 million tons/year of CO_2 [134]. Moreover, with the increasing issue of access to potable water, desalination is expected to further increase in order to meet water demands; thus if no actions are undertaken, CO_2 emissions are expected to grow to at least around 218 million tons/year in 2040 [135].

A life-cycle assessment (LCA) of desalination processes [136] showed that RO processes produce CO_2 emissions of 1.78 kg/m^3 of produced water and are one order of magnitude less than that of thermal processes, with MSF found to be the technology that most pollutes the atmosphere. Thus, although such absolute figures must always be treated with great caution, RE-powered desalination can certainly lead to a significant reduction in CO_2 emissions because the energy is clean and does not result in pollution of the atmosphere and emissions. Operating water treatment technologies that depend entirely on RE sources can significantly reduce CO_2 emissions and promote the deployment of low-carbon desalination technologies [135].

Davis [137] suggested a technology that could help to mitigate the environmental concerns associated with brine disposal as well as offsetting CO_2 emissions. The technology uses solar energy to decompose the brine converting magnesium chloride into magnesium oxide that, when discharged into the oceans, would gradually absorb ambient CO_2 through conversion to magnesium carbonate or bicarbonate. This was claimed to result in a theoretical net absorption capacity per freshwater output of 8 kg CO_2/m^3.

7.2 Concentrate Management

In solar-powered desalination as well as other RE- and non-RE-powered desalination technologies, concentrate is an environmental concern that needs to be managed properly, and lack of appropriate solutions as well as the cost of concentrate treatment regularly inhibit technology uptake. The first priority therefore must be either to avoid concentrate generation (e.g., through low recovery operations that allow the nonpotable use of such marginally concentrated concentrates) or to produce low volumes of highly concentrated concentrates that facilitate resource recovery. Before being discharged into waterbodies or other locations, concentrate needs to be treated. Zero-liquid-discharge (ZLD), which requires a combination of treatment technologies, is becoming a common target [138,139]. The direct disposal of concentrates into waterbodies has several effects, including affecting the water ecosystems such as by eutrophication, variation in pH values, discharge of heavy metals, as well as other problems such as the accumulation of highly concentrated salt on the seafloor [23]. One way to reduce the effect of direct concentrate disposal is through dilution with other waters, such as municipal wastewaters, natural seawater, or power plant cooling waters before discharging the concentrates into receiving waterbodies [140,141]. Other options for brine disposal or treatment include surface water discharge, deep well injection, and solar evaporation [142–144]. A PV-RO plant was installed in the village of Amarika in Northern Namibia as part of the German-Namibian project, "CuveWaters." [145] The 10.8 m^3 of concentrate was disposed of via reinjection wells and an evaporation pond [146].

Brine concentration technologies that are thermal-based are well established; however, they require high capital cost, are energy-intensive, and usually are not economically viable for large-scale applications. In comparison to thermal-based technology, membrane-based technologies for brine concentration require less energy. However, using membranes makes it essential to use concentrate pretreatments in order to decrease the intensity of scale-forming ions and ultimately decrease scale formation on the membranes' surfaces. Complete ZLD can be achieved by combining both thermal- and membrane-based technologies for concentrate treatment. However, treatment costs would be expected to increase considerably for ZLDs because of their higher capital costs and energy consumption [147]. After RO desalination, recovery of nutrients and valuable compounds from the concentrate [148–150] can be achieved using other efficient technologies, such as electrodialysis [151], forward osmosis, [152–154] and membrane distillation [153], which in addition to resource recovery, result in a significant reduction of brine volume. The volume of brine, level of treatment, characteristics of the brine, and disposal method all affect the cost of concentrate management and disposal [142,143].

7.3 Cleaning Chemicals

Almost all desalination units, whether membrane- or thermal-based, rely on chemicals for cleaning. In RO plants, for instance, chemical cleaning intervals depend on feed water quality and the efficiency of the pretreatment system, with intervals typically ranging from 3 to 6 months [155]. The chemicals used in RO cleaning can be acidic solutions to remove scaling and dissolve metal oxides or alkaline solutions to remove organic fouling, biofouling, and silt deposits on the membranes. Cleaning solutions include additional additive chemicals to enhance the cleaning process. In alkaline solutions, the commonly used additive chemicals are detergents such as dodecylbenzene sulfonate and dodecylsulfate or oxidants such as sodium hypochlorite and sodium perborate [155]. Complexing agents and biocides such as ethylenediamine tetraacetic acid (EDTA) are used for membrane disinfection and to improve the removal of scale and biofilms. Most of these cleaning, antiscaling, and disinfection chemicals appear in the reject stream and may be hazardous to aquatic life [156]. As a result, their disposal into receiving waterbodies must be strictly regulated. To remove any potential toxicity, it is recommended to neutralize the extremely alkaline and acidic solutions and to treat the additional cleaning additives before discharging them into receiving waterbodies [157]. In solar-MD, the solar thermal collectors may contain potentially hazardous fluid to transfer heat. The disposal of such fluids may present an environmental concern, so they should be disposed of properly [158].

7.4 Public Health and Water Quality Concerns

Desalination and RE-membrane treatment systems provide fresh water that typically lacks minerals essential to human health. This presents a public health concern, as some minerals that are removed are considered necessary for human health. Two examples are fluoride and magnesium. According to the WHO, there is a relationship between magnesium intake deficits and sudden cardiac death rates [159]. A study undertaken to provide recommendations for meeting optimal water quality requirements for water distribution quality control showed the importance of remineralization through blending desalinated water with natural water to achieve the desired quality [160]. In order to meet the standards for potable water set by the WHO, posttreatment of desalinated water is necessary [161].

Ovadia et al. [162] reported a possible link between iodine deficiency and seawater desalination. A small convenience sample of Israeli adults in the Ashkelon district where SWRO-desalinated, iodine-poor water has been the main source of drinking water since 2011 was studied. An apparent iodine deficiency among the euthyroid adults surveyed was detected. The estimated mean daily dietary intake of iodine was 25% lower than the recommended dietary allowance (150 μg/day). Unfiltered tap water was estimated to provide only 16% of the mean daily iodine intake. Sixty-six percent of the participants showed elevated values of serum thyroglobulin (Tg), indicating a high prevalence of apparent iodine deficiency in this sample. The researchers concluded that there is a need for reliable

data on iodine intake and status to clarify the effects of SWRO desalination on health, especially for populations in regions that are increasingly dependent on desalinated water [162].

7.5 Life-Cycle Analysis (LCA)

Life-cycle analysis (LCA) is considered one of the most used and reliable environmental assessment methods. In LCA, a cradle-to-grave approach is followed to analyze the environmental impact associated with a system. It gives a complete picture because it analyzes all the stages in the life of the system, including raw material extraction, production, usage, and disposal [163]. Consequently, LCA can be considered a versatile tool for the environmental analysis of RE-membrane systems as compared to other water supply systems that do not rely on RE sources.

Jijakli et al. [164] studied and compared the environmental impact of three desalination systems through comprehensive environmental modeling. The three systems were a decentralized PV-RO system for brackish water treatment, a passive solar still, and truck delivery from a conventional centralized RO plant powered by conventional fossil fuels. It was concluded that the PV-RO system had the least environmental impact compared to the other two systems. Energy source and material selection are important parameters to be considered in the selection of the most environmentally friendly system. In the solar still system, the solar still tank is a significant component of the system, so its materials play a role in its environmental impact. The study gave policymakers insight into RE-desalination and thus promoted the deployment of environmentally friendly desalination technologies. Raluy et al. [165] studied the global environmental analysis of the integration of RE with desalination technologies and evaluated the life cycle of airborne emissions associated with desalination technologies using four different electricity production models in France, Spain, Norway, and Portugal. They found that the RE-based Norwegian grid produced the lowest emissions among the four and presented the most environmentally friendly option. Stokes and Horvath [166] compared six different electricity mixes for desalination, importation, and recycling-based water supply sources. The electricity mixes include the US national mix, California's average electricity mix, the European Union 2020 mix, solar PV, solar thermal, and a hypothetical low emissions mix. The electricity production models with higher shares of RE resulted in the least environmental impact of all three water source categories. Raluy et al. [165] as well as Stokes and Horvath [166] concluded that the environmental impact of desalination plants is strongly affected significantly by the "greenness" of the electricity supply and that fuel mixes with a large share of RE resulted in a lower impact on the environment.

To conclude the sustainability aspects of small-scale, solar-powered membrane desalination systems, Table 8 shows a comparison of the three dominant technologies—PV-RO, PV-ED, and solar-MD—to four issues—social, economic, technological, and environmental. Table 8 shows that economic issues related to water

Table 8 Comparison of the three dominant small-scale solar-membrane desalination technologies against four categories: social issues, economic issues, technological issues, and environmental issues

	PV-RO	PV-ED	Solar-MD
Social issues—the people			
Good community acceptance [167]	●	◒	◒
Minimal cultural gap between end-users and project developers [123]	◒	◒	◒
Proven RE-membrane system reliability /independent decentralized operation [168]	●	●	◒
Minimal labour needs for O&M [169, 170]	◒	◒	◒
Meeting water needs of community (quantity and quality) [47]	●	◒	◒
Small-scale systems represent control issue (Authorities prefer centralized control and familiar technologies) [121]	◒	◒	◒
Economic issues—the profit			
Cost of water [171]	◒	◒	○
Low capital and O&M costs [120]	○	○	○
Low energy requirements [116]	●	●	◒
Investment remains unprofitable (eroded by competing water supply subsidies) [172]	◒	◒	◒
Small and medium-sized enterprises lack the financial resources and local expertise to enter remote markets [121]	◒	◒	◒
Lack of thorough market analysis (size, location, market potential) [110]	◒	◒	◒
Technological issues—Performance and reliability			
Good system efficiency [114]	●	●	◒
Suitability for large scale systems [121]	●	●	○
Copes with energy fluctuations [65–67]	◒	●	◒
Risk of poor integration of system components (system performs as a sum of the whole) [173]	◒	◒	●
Good local availability of components and spare parts [121]	◒	◒	◒
Membrane lifetime [174]	◒	◒	◒

Table 8 Comparison of the three dominant small-scale solar-membrane desalination technologies against four categories: social issues, economic issues, technological issues, and environmental issues—cont'd

	PV-RO	PV-ED	Solar-MD
Environmental issues—the planet			
Concentrate management	◒	◒	◒
CO_2 emissions [135, 164]	●	●	●
Batteries disposal (for systems that use batteries)	○	○	○
Cleaning chemicals (including hazardous fluids used to transfer heat in solar thermal systems)	◒	◒	○
Public health concerns (iodine deficiency, heavy metals, antiscalants)	◒	◒	◒
Membranes disposal	◒	◒	◒
Land use	●	◒	◒
Water use for cleaning (backwash, PV cleaning)	◒	●	●

The three symbols indicate:

○ = issue not well addressed with this technology;

◒ = partially meets requirement;

● = fully addresses the issue at hand.

production costs and energy requirements are still not well addressed with solar-MD and are still high in comparison with the other two. PV-RO and PV-ED seem to fully and partially address most of the issues at hand, with capital and O&M costs still an issue that is not well addressed in all three technologies.

ACKNOWLEDGMENTS

Research funding through the Helmholtz Rekrutierungsinitiative for AIS and BSR is gratefully acknowledged. *Asante sana* to James Lilian (Ngare Nanyuki Secondary School) for the guidance of water treatment in Tanzania and a memorable dinner with his wife Lilian. Dr. Andrea Cipollina, Università degli Studi di Palermo, for providing pictures of the solar-MD system. Dr. Hans-Jürgen Rapp from DEUKUM GmbH for providing pictures of the PV-ED system. Prof. Hassan Arafat for helpful discussions on the Triple P concept.

REFERENCES

[1] World Health Organisation (WHO), UN-Water Global Annual Assessment of Sanitation and Drinking Water (GLAAS) 2012 Report: The Challenge of Extending and Sustaining Services, WHO, Geneva, 2012.

[2] M.A. Shannon, P.W. Bohn, M. Elimelech, J.G. Georgiadis, B.J. Marinas, A.M. Mayes, Science and technology for water purification in the coming decades, Nature 452 (7185) (2008) 301–310.
[3] M. Peter-Varbanets, C. Zurbrugg, C. Swartz, W. Pronk, Decentralized systems for potable water and the potential of membrane technology, Water Res. 43 (2) (2009) 245–265.
[4] A.I. Schäfer, G. Hughes, B.S. Richards, Renewable energy powered membrane technology: a leapfrog approach to rural water treatment in developing countries? Renew. Sustain. Energy Rev. 40 (2014) 542–556.
[5] WHO, UN-Water Global Annual Assessment of Sanitation and Drinking Water (GLAAS) 2012 Report: The Challenge of Extending and Sustaining Services, WHO, Geneva, 2012.
[6] V.G. Gude, N. Nirmalakhandan, S. Deng, Renewable and sustainable approaches for desalination, Renew. Sustain. Energy Rev. 14 (9) (2010) 2641–2654.
[7] AusAID, Civil Society Water, Sanitation and Hygiene (WASH) Funds, Technical Report, 2012.
[8] G. Hutton, L. Haller, J. Bartram, Global cost-benefit analysis of water supply and sanitation interventions, J. Water Health 5 (4) (2007) 481–502.
[9] WHO, UNICEF, Progress on Sanitation and Drinking-Water: 2015 Update, WHO Press, 2015.
[10] D. Molden, K. Frenken, R. Barker, C. de Fraiture, B. Mati, M. Svendsen, C. Sadoff, C. M. Finlayson, Trends in water and agricultural development, in: D. Molden (Ed.), Water for Food, Water for Life: A Comprehensive Assessment of Water Management in Agriculture, Earthscan and International Water Management Institute (IWMI), London, 2007, p. 63.
[11] United Nation's Water (UN-Water), Food and Agriculture Organization (FAO), Coping with Water Scarcity: Challenge of the Twenty-First Century, UN-Water, FAO, 2007.
[12] UN-Water Factsheet on Water Scarcity, UN-Water, 2013.
[13] I. Shiklomanov, World fresh water resources, in: P.H. Gleick (Ed.), Water in Crisis: A Guide to the World's Fresh Water Resources, Oxford University Press, New York, 1993.
[14] REN21, Renewables 2014: Global Status Report, REN21, Paris, 2014.
[15] The International Renewable Energy Agency (IRENA), Renewable Energy Capacity Statistics, IRENA, 2015.
[16] B.S. Richards, A.I. Schafer, Design considerations for a solar-powered desalination system for remote communities in Australia, Desalination 144 (1–3) (2002) 193–199.
[16a] SolarGIS, Global horizontal irradiation (GHI) solar map, http://solargis.com/products/maps-and-gis-data/free/download/world (access date 23 March 2017).
[17] GHI Solar Map © 2016 Solargis.
[18] International Energy Agency (IEA), Technology Roadmap: Solar Photovoltaic Energy, IEA, 2014.
[19] C.C.K. Liu, J.W. Park, R. Migita, G. Qin, Experiments of a prototype wind-driven reverse osmosis desalination system with feedback control, Desalination 150 (3) (2002) 277–287.
[20] E. Delyannis, V. Belessiotis, A historical overview of renewable energies, in: Proc. Mediterranean Conference on Renewable Energy Sources for Water Production, Santorini, Greece, 10–12 June 1996, EURORED Network, CRES, EDS, 1996, pp. 13–17.
[21] M.A. Eltawil, Z. Zhengming, L. Yuan, A review of renewable energy technologies integrated with desalination systems, Renew. Sustain. Energy Rev. 13 (9) (2009) 2245–2262.
[22] A. De Munari, A.I. Schäfer, Membrane plants for drinking water provision in remote Scottish communities: performance, costs and lessons learnt, Presented at the Membranes in the Production of Drinking and Industrial Water Conference, NTNU Trondheim, Norway, 2010.
[23] A. Perez-Gonzalez, A.M. Urtiaga, R. Ibanez, I. Ortiz, State of the art and review on the treatment technologies of water reverse osmosis concentrates, Water Res. 46 (2) (2012) 267–283.
[24] P. Glueckstern, Design and operation of medium- and small-size desalination plants in remote areas: new perspective for improved reliability, durability and lower costs, Desalination 122 (1999) 123–140.
[25] World Health Organization (WHO), Domestic Water Quantity, Service, Level and Health, WHO, Geneva, Switzerland, 2003.
[26] World Health Organization (WHO), United Nations Economic Commission for Europe, Small-Scale Water Supplies in the Pan-European Region: Background, Challenges and Improvements, WHO, 2010.
[27] B. Skinner, Small-scale water supply: a review of technologies. ITDG Publishing; 2003.
[28] AWWA, Problem Organisms in Water: Identification and Treatment, third ed., American Waterworks Association, 2004.

[29] C.D. Ericsson, R. Steffen, H. Backer, Water disinfection for international and wilderness travelers, Clin. Infect. Dis. 34 (3) (2002) 355–364.
[30] M. Khayet, Solar desalination by membrane distillation: dispersion in energy consumption analysis and water production costs, Desalination 308 (2013) 89–101 (a review).
[31] A. Piacentino, E. Cardona, Advanced energetics of a multiple-effects-evaporation (MEE) desalination plant. Part II: potential of the cost formation process and prospects for energy saving by process integration, Desalination 259 (1–3) (2010) 44–52.
[32] K.S. Spiegler, Y.M. El-Sayed, The energetics of desalination processes, Desalination 134 (1–3) (2001) 109–128.
[33] D. Talbot, Desalination out of desperation, MIT Technol. Rev. (2014).
[34] T. Younos, K.E. Tulou, Energy needs, consumption and sources, J. Contemp. Water Res. Educ. 132 (2009) 27–38.
[35] A. De Munari, D.P.S. Capao, B.S. Richards, A.I. Schaefer, Application of solar-powered desalination in a remote town in South Australia, Desalination 248 (1–3) (2009) 72–82.
[36] H. Qiblawey, F. Banat, Q. Al-Nasser, Laboratory setup for water purification using household PV-driven reverse osmosis unit, Desalin. Water Treat. 7 (1–3) (2009) 53–59.
[37] O. Kuroda, S. Takahashi, S. Kubota, K. Kikuchi, Y. Eguchi, Y. Ikenaga, N. Sohma, K. Nishinoiri, S. Wakamatsu, S. Itoh, An electrodialysis sea-water desalination system powered by photovoltaic cells, Desalination 67 (1987) 33–41.
[38] M.A. Lichtwadt, H.E. Remmers, Water treatment using solar-powered electrodialysis reversal, in: Mediterranean Conference on Renewable Energy Sources for Water Production, 1996.
[39] L. Karimi, L. Abkar, M. Aghajani, A. Ghassemi, Technical feasibility comparison of off-grid PV-EDR and PV-RO desalination systems via their energy consumption, Sep. Purif. Technol. 151 (2015) 82–94.
[40] B.S. Richards, D.P.S. Capão, A.I. Schäfer, Renewable energy powered membrane technology. 2. The effect of energy fluctuations on performance of a photovoltaic hybrid membrane system, Environ. Sci. Technol. 42 (12) (2008) 4563–4569.
[41] M. Khayet, Membranes and theoretical modeling of membrane distillation: a review, Adv. Colloid Interface Sci. 164 (1–2) (2011) 56–88.
[42] J. Koschikowski, M. Wieghaus, M. Rommel, V. Subiela Ortin, B. Penate Suarez, J.R. Betancort Rodriguez, Experimental investigations on solar driven stand-alone membrane distillation systems for remote areas, Desalination 248 (1–3) (2009) 125–131.
[43] H.E.S. Fath, S.M. Elsherbiny, A.A. Hassan, M. Rommel, M. Wieghaus, J. Koschikowski, M. Vatansever, PV and thermally driven small-scale, stand-alone solar desalination systems with very low maintenance needs, Desalination 225 (1–3) (2008) 58–69.
[44] F. Banat, N. Jwaied, M. Rommel, J. Koschikowski, M. Wieghaus, Performance evaluation of the "large SMADES" autonomous desalination solar-driven membrane distillation plant in Aqaba, Jordan, Desalination 217 (1–3) (2007) 17–28.
[45] F. Banat, N. Jwaied, M. Rommel, J. Koschikowski, M. Wieghaus, Desalination by a "compact SMADES" autonomous solar-powered membrane distillation unit, Desalination 217 (1–3) (2007) 29–37.
[46] G.W. Meindersma, C.M. Guijt, A.B. de Haan, Water recycling and desalination by air gap membrane distillation, Environ. Prog. 24 (4) (2005) 434–441.
[47] S. Bouguecha, B. Hamrouni, M. Dhahbi, Small scale desalination pilots powered by renewable energy sources: case studies, Desalination 183 (1–3) (2005) 151–165.
[48] J. Koschikowski, M. Wieghaus, M. Rommel, Solar thermal-driven desalination plants based on membrane distillation, Desalination 156 (1–3) (2003) 295–304.
[49] P.A. Hogan, A.G. Sudjito, G.L. Fane, Desalination by solar heated membrane distillation, Desalination 81 (1–3) (1991) 81–90.
[50] S. Al-Obaidani, E. Curcio, F. Macedonio, G. Di Profio, H. Ai-Hinai, E. Drioli, Potential of membrane distillation in seawater desalination: thermal efficiency, sensitivity study and cost estimation, J. Membr. Sci. 323 (1) (2008) 85–98.
[51] V.A. Bui, L.T.T. Vu, M.H. Nguyen, Simulation and optimisation of direct contact membrane distillation for energy efficiency, Desalination 259 (1–3) (2010) 29–37.
[52] G. Zuo, R. Wang, R. Field, A.G. Fane, Energy efficiency evaluation and economic analyses of direct contact membrane distillation system using Aspen Plus, Desalination 283 (2011) 237–244.

[53] H. Lee, F. He, L. Song, J. Gilron, K.K. Sirkar, Desalination with a cascade of cross-flow hollow fiber membrane distillation devices integrated with a heat exchanger, AICHE J. 57 (7) (2011) 1780–1795.
[54] D. Winter, J. Koschikowski, M. Wieghaus, Desalination using membrane distillation: experimental studies on full scale spiral wound modules, J. Membr. Sci. 375 (1–2) (2011) 104–112.
[55] R. Gemma Raluy, R. Schwantes, V.J. Subiela, B. Penate, G. Melian, J. Rosa Betancort, Operational experience of a solar membrane distillation demonstration plant in Pozo Izquierdo-Gran Canaria Island (Spain), Desalination 290 (2012) 1–13.
[56] B.S. Richards, D.P.S. Capao, W.G. Frueh, A.I. Schaefer, Renewable energy powered membrane technology: impact of solar irradiance fluctuations on performance of a brackish water reverse osmosis system, Sep. Purif. Technol. 156 (2015) 379–390.
[57] M. Thomson, M.S. Miranda, D. Infield, A small-scale seawater reverse-osmosis system with excellent energy efficiency over a wide operating range, Desalination 153 (1–3) (2003) 229–236.
[58] D. Linden, T.B. Reddy, Handbook of Batteries, third ed., McGraw-Hill, New York, 2002.
[59] C. Abbey, G. Joos, Supercapacitor energy storage for wind energy applications, IEEE Trans. Ind. Appl. 43 (3) (2007) 769–776.
[60] M. Perrin, Y.M. Saint-Drenan, F. Mattera, P. Malbranche, Lead-acid batteries in stationary applications: competitors and new markets for large penetration of renewable energies, J. Power Sources 144 (2) (2005) 402–410.
[61] G.L. Park, A.I. Schäfer, B.S. Richards, Renewable energy-powered membrane technology: supercapacitors for buffering resource fluctuations in a wind-powered membrane system for brackish water desalination, Renew. Energy 50 (2013) 126–135.
[62] A. Burke, R&D considerations for the performance and application of electrochemical capacitors, Electrochim. Acta 53 (3) (2007) 1083–1091.
[63] M. Beaudin, H. Zareipour, A. Schellenberglabe, W. Rosehart, Energy storage for mitigating the variability of renewable electricity sources: an updated review, Energy Sustain. Dev. 14 (4) (2010) 302–314.
[64] DOW Water Solutions, DOW FILMTEC™ Membranes, Product Data Sheet BW30-4040. http://www.dow.com/en-us/markets-and-solutions/products/DOWFILMTECBrackishWaterReverseOsmosis4Elements/DOWFILMTECBW304040 (access date 22 May 2017).
[65] G.L. Park, A.I. Schaefer, B.S. Richards, The effect of intermittent operation on a wind-powered membrane system for brackish water desalination, Water Sci. Technol. 65 (5) (2012) 867–874.
[66] M. Thomson, D. Infield, Laboratory demonstration of a photovoltaic-powered seawater reverse-osmosis system without batteries, Desalination 183 (1–3) (2005) 105–111.
[67] G.L. Park, A.I. Schaefer, B.S. Richards, Renewable energy powered membrane technology: the effect of wind speed fluctuations on the performance of a wind-powered membrane system for brackish water desalination, J. Membr. Sci. 370 (1–2) (2011) 34–44.
[68] K. Mathew, S. Dallas, G.E. Ho, M. Anda, A solar-powered village water supply system from brackish water, in: A.A.M. Sayigh (Ed.), World Renewable Energy Congress VI, Brighton, Pergamon, Brighton, 2000, pp. 2061–2064.
[69] A. Abbas, N. Al-Bastaki, Flux enhancement of RO desalination processes, Desalination 132 (1–3) (2000) 21–27.
[70] K. Quteishat, A. Abu-Arabi, Promotion of Solar Desalination in the MENA Region, Middle East Desalination Research Center, Muscat, Oman, 2006.
[71] M.T. Ali, H.E.S. Fath, P.R. Armstrong, A comprehensive techno-economical review of indirect solar desalination, Renew. Sustain. Energy Rev. 15 (8) (2011) 4187–4199.
[72] H. Sharon, K.S. Reddy, A review of solar energy driven desalination technologies, Renew. Sustain. Energy Rev. 41 (2015) 1080–1118.
[73] M. Mulder, Basic principles of membrane technology, second ed., Kluwer Academic Publishers, The Netherlands, 1996.
[74] M. Papapetrou, E.S. Mohamed, D. Manolakos, G. Papadakis, V.J. Subiela, B. Penate, Operating RE/desalination units, in: Seawater Desalination, Springer, Berlin, Heidelberg, 2009, pp. 247–272.

[75] D. Manolakos, E.S. Mohamed, I. Karagiannis, G. Papadakis, Technical and economic comparison between PV-RO system and RO-Solar Rankine system. Case study: Thirasia island, Desalination 221 (1–3) (2008) 37–46.
[76] N. Ishimaru, Solar photovoltaic desalination of brackish-water in remote areas by electrodialysis, Desalination 98 (1–3) (1994) 485–493.
[77] V.J. Subiela, J.A. de la Fuente, G. Piernavieja, B. Penate, Canary Islands Institute of Technology (ITC) experiences in desalination with renewable energies (1996–2008), Desalin. Water Treat. 7 (2009) 220–235.
[78] A. Ghermandi, R. Messalem, Solar-driven desalination with reverse osmosis: the state of the art, Desalin. Water Treat. 7 (1–3) (2012) 285–296.
[79] E.S. Mohamed, G. Papadakis, E. Mathioulakis, V. Belessiotis, A direct coupled photovoltaic seawater reverse osmosis desalination system toward battery based systems – a technical and economical experimental comparative study, Desalination 221 (1–3) (2008) 17–22.
[80] Fraunhofer Institute for Solar Energy Systems (ISE), Photovoltaics Report, 2014.
[81] W. Gocht, A. Sommerfeld, R. Rautenbach, T.H. Melin, L. Eilers, A. Neskakis, D. Herold, V. Horstmann, M. Kabariti, A. Muhaidat, Decentralized desalination of brackish water by a directly coupled reverse osmosis photovoltaic system – a pilot plant study in Jordan, Renew. Energy 14 (1–4) (1998) 287–292.
[82] W.W. Boesch, World's first solar powered reverse osmosis desalination plant, Desalination 41 (1982) 233–237.
[83] G. Petersen, S. Fries, J. Mohn, A. Muller, Wind and solar powered reverse osmosis desalination units – description of two demonstration projects, Desalination 31 (1979) 501–509.
[84] Z. Al-Suleimani, V.R. Nair, Desalination by solar-powered reverse osmosis in a remote area of the Sultanate of Oman, Appl. Energy 65 (2000) 367–380.
[85] A. Soric, R. Cesaro, P. Perez, E. Guiol, P. Moulin, Eausmose project desalination by reverse osmosis and batteryless solar energy: design for a 1 m^3 per day delivery, Desalination 301 (2012) 67–74.
[86] H.M. Laborde, K.B. Franca, H. Neff, A.M.N. Lima, Optimization strategy for a small-scale reverse osmosis water desalination system based on solar energy, Desalination 133 (2001) 1–12.
[87] H.M.N. AlMadani, Water desalination by solar powered electrodialysis process, Renew. Energy 28 (12) (2003) 1915–1924.
[88] J.M. Ortiz, E. Expósito, F. Gallud, V. García-García, V. Montiel, A. Aldaz, Electrodialysis of brackish water powered by photovoltaic energy without batteries: direct connection behaviour, Desalination 208 (1–3) (2007) 89–100.
[89] M.R. Adiga, S.K. Adhikary, P.K. Narayanan, W.P. Harkare, S.D. Gomkale, K. P. Govindan, Performance analysis of photovoltaic electrodialysis desalination plant at Tanote in Thar desert, Desalination 67 (1987) 59–66.
[90] H. Lund, The McGraw-Hill Recycling Handbook, second ed., McGraw-Hill, New York, 2001.
[91] M.S. Mohsen, J.O. Jaber, A photovoltaic-powered system for water desalination, Desalination 138 (1–3) (2001) 129–136.
[92] H. Strathmann, Assessment of Electrodialysis Water Desalination Process Costs, in: Proceedings of the International Conference on Desalination Costing, Limassol, Cyprus, 2004 Dec. 6, pp. 32–54.
[93] A.I. Schaefer, A. Broeckmann, B.S. Richards, Renewable energy powered membrane technology. 1. Development and characterization of a photovoltaic hybrid membrane system, Environ. Sci. Technol. 41 (3) (2007) 998–1003.
[94] J.A. Kharraz, M.R. Bilad, H.A. Arafat, Flux stabilization in membrane distillation desalination of seawater and brine using corrugated PVDF membranes, J. Membr. Sci. 495 (2015) 404–414.
[95] P. Phungsai, Development of Thermophilic Anaerobic Membrane Distillation Bioreactor (Master of Engineering Thesis), Asian Institute of Technology, 2013.
[96] R.B. Saffarini, E.K. Summers, H.A. Arafat, J.H. Lienhard, Economic evaluation of stand-alone solar powered membrane distillation systems, Desalination 299 (2012) 55–62.
[97] L.M. Camacho, L. Dumee, J. Zhang, J.-D. Li, M. Duke, J. Gomez, S. Gray, Advances in membrane distillation for water desalination and purification applications, Water 5 (1) (2013) 94–196.

[98] P. Feron, The use of wind power in autonomous reverse osmosis seawater desalination, Wind Eng. 9 (1985) 180–199.
[99] B.S. Richards, G.L. Park, T. Pietzsch, A.I. Schäfer, Renewable energy powered membrane technology: safe operating window of a brackish water desalination system, J. Membr. Sci. 468 (2014) 400–409.
[100] L. Kelley, H. Elasaad, S. Dubowsky, Autonomous operation and maintenance of small-scale PVRO systems for remote communities, Desalin. Water Treat. 55 (10) (2014) 2843–2855.
[101] S.A. Avlonitis, K. Kouroumbas, N. Vlachakis, Energy consumption and membrane replacement cost for seawater RO desalination plants, Desalination 157 (1–3) (2003) 151–158.
[102] R.W. Baker, Membrane Technology and Applications, second ed., John Wiley & Sons Ltd., England, 2004.
[103] J.A. Kharraz, M.R. Bilad, H.A. Arafat, Simple and effective corrugation of PVDF membranes for enhanced MBR performance, J. Membr. Sci. 475 (2015) 91–100.
[104] A. Sagiv, R. Semiat, Backwash of RO spiral wound membranes, Desalination 179 (1–3) (2005) 1–9.
[105] DOW Chemical Company, Cleaning Procedures for DOW FILMTEC FT30 Elements, Form No. 609-23010-021, DOW Chemical Company, Midland, MI, 2011.
[106] DOW Chemical Company, FILMTEC™ Membranes, System Design: Membrane System Design Guideline for Commercial Elements, Tech Manual Excerpt, Form No. 609-02054-0812.
[107] A.M. Bilton, L.C. Kelley, S. Dubowsky, Photovoltaic reverse osmosis – feasibility and a pathway to develop technology, Desalin. Water Treat. 31 (1–3) (2011) 24–34.
[108] J. Kucera, Reverse Osmosis, Scrivener Publishing, LLC, Salem, MA, 2010.
[109] M.F.A. Goosen, H. Mahmoudi, N. Ghaffour, Today's and future challenges in applications of renewable energy technologies for desalination, Crit. Rev. Environ. Sci. Technol. 44 (9) (2014) 929–999.
[110] E.A. Grubert, A.S. Stillwell, M.E. Webber, Where does solar-aided seawater desalination make sense? A method for identifying sustainable sites, Desalination 339 (2014) 10–17.
[111] U.S. Energy Information Administration, Saudi Arabia's Key Energy Statistics, https://www.eia.gov/beta/international/country.cfm?iso=SAU (Accessed 23 March 2017).
[112] U.S. Energy Information Administration (EIA), Annual Energy Outlook 2010, Washington DC, 2010.
[113] U.S. Census Bureau, Table A-4 Population by Region and Country 1950–2050, 2004.
[114] N. Ghaffour, V.K. Reddy, M. Abu-Arabi, Technology development and application of solar energy in desalination: MEDRC contribution, Renew. Sustain. Energy Rev. 15 (9) (2011) 4410–4415.
[115] N. Ghaffour, J. Bundschuh, H. Mahmoudi, M.F.A. Goosen, Renewable energy-driven desalination technologies: a comprehensive review on challenges and potential applications of integrated systems, Desalination 356 (2015) 94–114.
[116] Y.-D. Kim, K. Thu, N. Ghaffour, K.C. Ng, Performance investigation of a solar-assisted direct contact membrane distillation system, J. Membr. Sci. 427 (2013) 345–364.
[117] Z. Al Suleimani, V.R. Nair, Desalination by solar-powered reverse osmosis in a remote area of the Sultanate of Oman, Appl. Energy 65 (1–4) (2000) 367–380.
[118] M. Thompson, M. Miranda, J. Gwilliam, A. Rowbottom, I. Draisey, Batteryless Photovoltaic Reverse-Osmosis Desalination System, Energy Technology Support Unit (ETSU), Harwell, UK, 2001.
[119] M. Lichtwardt, H. Remmers, Water treatment using solar powered electro-dialysis reversal, in: Proceedings of the Mediterranean Conference on Renewable Energy Sources for Water Production, Santorini, Greece, 1996, pp. 88–92.
[120] F. Banat, N. Jwaied, Economic evaluation of desalination by small-scale autonomous solar-powered membrane distillation units, Desalination 220 (1–3) (2008) 566–573.
[121] M. Paparetrou, M. Wieghaus, C. Biercamp, Roadmap for the development of desalination powered by renewable energy, Promotion for Renewable Energy for Water Production Through Desalination. Fraunhofer Verlag; 2010.
[122] Africa Infrastructure Country Diagnostic (AICD), WSS Utility Database, 2009.
[123] M. Werner, A.I. Schäfer, Social aspects of a solar-powered desalination unit for remote Australian communities, Desalination 203 (1–3) (2007) 375–393.
[124] E.E. Delyannis, V. Belessiotis, Solar application in desalination: the Greek islands experiment, Desalination 100 (1–3) (1995) 27–34.
[125] J.G. Milliken, L.C. Lohman, Analysis of baseline survey: public attitudes about Denver water and wastewater reuse, J. Am. Waterworks Assoc. 77 (1985) 72.

[126] M. Po, J.D. Kaercher, B.E. Nancarrow, Literature review of factors influencing public perceptions of water reuse. In: CSIRO Land and Water, Technical Report 54/03, December 2003, CSIRO Land and Water; Australia.
[127] S. Dolničar, A.I. Schäfer, Public perception of desalinated versus recycled water in Australia, in: 2006 AWWA Desalination Symposium, Invited Presentation, 7–9 May, Honolulu, Hawaii, 2006.
[128] The Water Network, UAE to Set Up World's Largest Solar Desalination Plant, Online Report, https://thewaternetwork.com/article-FfV/uae-to-set-up-world-s-largest-solar-desalination-plant-461P8TxgZwCKfhcn-uk_Kg.
[129] Water Technology, Al Khafji Solar Saline Water Reverse Osmosis (Solar SWRO) Desalination Plant, Saudi Arabia, Online Report, Available from: http://www.water-technology.net/projects/al-khafji-solar-saline-water-reverse-osmosis-solar-swro-desalination-plant/ (Accessed 7 March 2016).
[130] M. Papapetrou, M. Wieghausand, C. Biercamp, Roadmap for the Development of Desalination Powered by Renewable Energy, Frauhnofer Verlag, Stuttgart, Germany, 2010.
[131] K.T. Hetal, D.B. Upadhyay, A.H. Rana, Seawater desalination processes, IJESRT 3 (2014) 638–646.
[132] P. Palenzuela, D.-C. Alarcon-Padilla, G. Zaragoza, Large-scale solar desalination by combination with CSP: techno-economic analysis of different options for the Mediterranean Sea and the Arabian Gulf, Desalination 366 (2015) 130–138.
[133] International Desalination Association (IDA), IDA Desalination Yearbook 2015–2016, IDA, 2015.
[134] Masdar, Global CO_2 Emissions of Water Desalination Plants, Internal Report, 2015.
[135] Global Clean Water Desalination Alliance, An International Initiative to Reduce CO_2 Emissions in the Desalination Sector "H_2O minus CO_2" – Concept Paper, 2015.
[136] G. Raluy, L. Serra, J. Uche, Life cycle assessment of MSF, MED and RO desalination technologies, Energy 31 (13) (2006) 2361–2372.
[137] P.A. Davies, Solar thermal decomposition of desalination reject brine for carbon dioxide removal and neutralisation of ocean acidity, Environ. Sci.: Water Res. Technol. 1 (2015) 131–137.
[138] P. Chelme-Ayala, D.W. Smith, M.G. El-Din, Membrane concentrate management options: a comprehensive critical review, Can. J. Civ. Eng. 36 (6) (2009) 1107–1119.
[139] A. Subramani, J.G. Jacangelo, Treatment technologies for reverse osmosis concentrate volume minimization: a review, Sep. Purif. Technol. 122 (2014) 472–489.
[140] M. Meneses, J.C. Pasqualino, R. Cespedes-Sanchez, F. Castells, Alternatives for reducing the environmental impact of the main residue from a desalination plant, J. Ind. Ecol. 14 (3) (2010) 512–527.
[141] D.A. Roberts, E.L. Johnston, N.A. Knott, Impacts of desalination plant discharges on the marine environment: a critical review of published studies, Water Res. 44 (18) (2010) 5117–5128.
[142] M. Ahmed, W.H. Shayya, D. Hoey, J. Al-Handaly, Brine disposal from reverse osmosis desalination plants in Oman and the United Arab Emirates, Desalination 133 (2) (2001) 135–147.
[143] J.M. Arnal, M. Sancho, I. Iborra, J.M. Gozálvez, A. Santafé, J. Lora, Concentration of brines from RO desalination plants by natural evaporation, Desalination 182 (1–3) (2005) 435–439.
[144] L. Malaeb, G.M. Ayoub, Reverse osmosis technology for water treatment: state of the art review, Desalination 267 (1) (2011) 1–8.
[145] CuveWaters Project Overview Website, Available from: http://www.cuvewaters.net/Project-overview.6.0.html (Accessed 27 January 2016).
[146] M. Brenda, C. Treskatis, K. Skrypka, W. Urban, Desalination Pilot Plants in the Osumati Region – Final Technical Report, Unpublished 2013.
[147] J. Morillo, J. Usero, D. Rosado, H. El Bakouri, A. Riaza, F.-J. Bernaola, Comparative study of brine management technologies for desalination plants, Desalination 336 (2014) 32–49.
[148] M. Gryta, Concentration of NaCl solution by membrane distillation integrated with crystallization, Sep. Sci. Technol. 37 (15) (2002) 3535–3558.
[149] R. Ibáñez, A. Pérez-González, P. Gómez, A.M. Urtiaga, I. Ortiz, Acid and base recovery from softened reverse osmosis (RO) brines. Experimental assessment using model concentrates, Desalination 309 (2013) 165–170.
[150] M. Reig, S. Casas, C. Aladjem, C. Valderrama, O. Gibert, F. Valero, C.M. Centeno, E. Larrotcha, J.L. Cortina, Concentration of NaCl from seawater reverse osmosis brines for the chlor-alkali industry by electrodialysis, Desalination 342 (2014) 107–117.
[151] C. Jiang, Y. Wang, Z. Zhang, T. Xu, Electrodialysis of concentrated brine from RO plant to produce coarse salt and freshwater, J. Membr. Sci. 450 (2014) 323–330.

[152] W. Tang, H.Y. Ng, Concentration of brine by forward osmosis: performance and influence of membrane structure, Desalination 224 (1–3) (2008) 143–153.
[153] C.R. Martinetti, A.E. Childress, T.Y. Cath, High recovery of concentrated RO brines using forward osmosis and membrane distillation, J. Membr. Sci. 331 (1–2) (2009) 31–39.
[154] K. Lutchmiah, A.R. Verliefde, K. Roest, L.C. Rietveld, E.R. Cornelissen, Forward osmosis for application in wastewater treatment: a review, Water Res. 58 (2014) 179–197.
[155] Water Consultants International, An Environmental Literature Review and Position Paper for Reverse Osmosis Desalination Plant Discharges, Final Report, 2006.
[156] M.A.E. Wahab, A.Z. Hamoda, Effect of desalination plants on the marine environment along the red sea, Egypt, Int. J. Mar. Sci. 28 (2) (2012) 27–36 (Case Study).
[157] Potential Impacts of Seawater Desalination, Available from: http://www.paua.de/Impacts.htm#cleaning (Accessed 15 March 2016).
[158] Solar Energy and the Environment, Available from: http://www.eia.gov/Energyexplained/?page=solar_environment (Accessed 15 March 2016).
[159] World Health Organization (WHO), Nutrients in Drinking Water: Water, Sanitation and Health Protection and the Human Environment, WHO, Geneva, 2005.
[160] N. Avni, M. Eben-Chaime, G. Oron, Optimizing desalinated sea water blending with other sources to meet magnesium requirements for potable and irrigation waters, Water Res. 47 (7) (2013) 2164–2176.
[161] Potable Water: Emerging Global Problems and Solutions, Springer, Switzerland, 2014.
[162] Y.S. Ovadia, D. Gefel, S. Turkot, D. Aharoni, S. Fytlovich, A.M. Troen, Estimated iodine intake and status in euthyroid adults exposed to iodine-poor water, in: Israeli Association Public Health Physicians Conference, 2014.
[163] H. Baumann, A. Tillman, The Hitch Hiker's Guide to LCA: An Orientation in Life Cycle Assessment Methology and Application, Studentlitteratur, Sweden, 2004.
[164] K. Jijakli, H. Arafat, S. Kennedy, P. Mande, V.V. Theeyattuparampil, How green solar desalination really is? Environmental assessment using life-cycle analysis (LCA) approach, Desalination 287 (2012) 123–131.
[165] R.G. Raluy, L. Serra, J. Uche, Life cycle assessment of desalination technologies integrated with renewable energies, Desalination 183 (1–3) (2005) 81–93.
[166] J.R. Stokes, A. Horvath, Energy and air emission effects of water supply, Environ. Sci. Technol. 43 (2009) 2680–2687.
[167] R. Robinson, G. Ho, K. Mathew, Development of a reliable low-cost reverse-osmosis desalination unit for remote communities, Desalination 86 (1) (1992) 9–26.
[168] J. Ayoub, R. Alward, Water requirements and remote arid areas: the need for small-scale desalination, Desalination 107 (2) (1996) 131–147.
[169] B. Bouchekima, A solar desalination plant for domestic water needs in arid areas of South Algeria, Desalination 153 (1–3) (2003) 65–69.
[170] H.E.S. Fath, F.M. El-Shall, G. Vogt, U. Seibert, A stand alone complex for the production of water, food, electrical power and salts for the sustainable development of small communities in remote areas, Desalination 183 (1–3) (2005) 13–22.
[171] G. Fiorenza, V.K. Sharma, G. Braccio, Techno-economic evaluation of a solar powered water desalination plant, Energ. Convers. Manage. 44 (14) (2003) 2217–2240.
[172] International Bank for Reconstruction and Development/The World Bank, Renewable Energy Desalination: An Emerging Solution to Close MENA's Water Gap, MENA Development Report, Washington DC, 2012.
[173] N. Ghaffour, T.M. Missimer, G.L. Amy, Technical review and evaluation of the economics of water desalination: current and future challenges for better water supply sustainability, Desalination 309 (2013) 197–207.
[174] A.W. Mohammad, N.L. Yong, Nanotechnology approach in nanofiltration membrane fabrications for environmental applications, Recent Advances in Energy, Environment and Development, 137–143. http://www.wseas.org/main/books/2013/CambridgeUSA/ENVMECH.pdf.

FURTHER READING

[1] DOW, FILMTEC Membranes, Basics of RO and NF: Desalination Technologies and Filtration Processes, Technical Report; 2011.
[2] N. Hilal, H. Al-Zoubi, A.W. Mohammad, N.A. Darwish, Nanofiltration of highly concentrated salt solutions up to seawater salinity, Desalination 184 (1–3) (2005) 315–326.
[3] M.J. Brandt, K.M. Johnson, A.J. Elphinston, D.D. Ratnayaka, Twort's Water Supply, fifth ed., Butterworth-Heinemann, Oxford, UK, 2016.
[4] C. Fritzmann, J. Loewenberg, T. Wintgens, T. Melin, State-of-the-art of reverse osmosis desalination, Desalination 216 (1–3) (2007) 1–76.
[5] S. Loupasis, Technical Analysis of Existing RES Desalination Schemes – RE Driven Desalination Systems REDDES, Report, 2002.
[6] H. Fath, V.J. Subiela Ortin, Planning, implementation, operation and monitoring of ADS units, Adira Handbook, "A Guide to Autonomous Desalination Concepts", Istanbul Technical University, Istanbul, Turkey, 2008.
[7] D. Reza, S.N. Al-zubaidy, Energy efficient reverse osmosis desalination process, Int. J. Environ. Sci. Dev. 3 (4) (2012) 339–345.
[8] E. Drioli, A. Criscuoli, L.P. Molero, Membrane distillation, in: S. Vigneswaran (Ed.), Water and Wastewater Treatment Technologies, Eolss Publishers Co. Ltd., Oxford, United Kingdom, 2009

CHAPTER 4

Thermodynamics, Exergy, and Energy Efficiency in Desalination Systems

John H. Lienhard V*, Karan H. Mistry*, Mostafa H. Sharqawy†, Gregory P. Thiel*
*Massachusetts Institute of Technology, Cambridge, MA, United States
†University of Guelph, Guelph, ON, Canada

Chapter Outline

Desalination Sustainability
http://dx.doi.org/10.1016/B978-0-12-809791-5.00004-3

Nomenclature

Symbols

A^{ϕ}	Modified Debye-Hückel parameter ($kg^{1/2}/mol^{1/2}$)
a	Activity
B_{ij}, B_{ij}^{ϕ}	Pitzer parameter, second virial coefficient (kg/mol)
B'_{ij}	Pitzer binary interaction parameter (kg^2/mol^2)
B	Membrane distillation coefficient (kg/m^2 Pa s)
b	Molality (mol/kg)
C	Modified van 't Hoff coefficient (kPa kg/g)
C_{ij}, C_{ij}^{ϕ}	Pitzer parameter, unlike-charged interactions (kg^2/mol^2)
C_p	Heat capacity at constant pressure (J/K)
CV	Control volume
c	Concentration (mol/L); specific heat capacity (J/kg K)
c_p	Specific heat capacity at constant pressure (J/kg K)
c_v	Specific heat capacity at constant volume (J/kg K)
D_i	Distillate from effect i (kg/s)
$D_{f,\,i}$	Distillate from flashing in effect i (kg/s)
$D_{fb,\,i}$	Distillate from flashing in flash box i (kg/s)
d_{ch}	Flow channel depth (m)
e	Elementary charge (C); specific exergy (J/kg)
e_d	Specific exergy destroyed (J/kg)
e_f	Specific flow exergy (J/kg)
F	Extended Debye-Hückel function, Eq. (B.1)
G	Gibbs free energy (J)
g	Specific Gibbs free energy (J/kg)
H	Enthalpy (J)
h	Specific enthalpy (J/kg)
h_{fg}	Latent heat of vaporization (J/kg)
h_{sf}	Latent heat of freezing (J/kg)
I	Ionic strength (mol/kg)
i	van 't Hoff factor (−)
K_b	Ebullioscopic constant (K mol/kg)
K_f	Cryoscopic constant (K mol/kg)
k_B	Boltzmann's constant (J/K)
L	Length (m)
M_i	Molar mass of species i (g/mol)
M	Mixture average molar mass (g/mol)
m	Mass (kg)
$\dot{m}$	Mass flow rate (kg/s)
N_A	Avogadro's number (6.022140×10^{23} per mol)
N_i	Amount of species i (mol)
n	Number of effects or stages (−)
p	Pressure (kPa)
$\dot{Q}$	Heat transfer rate (W)
$\dot{Q}_{least}$	Least heat of separation (W)
$\dot{Q}_{least}^{min}$	Minimum least heat of separation (W)
$\dot{Q}_{sep}$	Heat of separation (W)
R	Ideal gas constant (J/kg K)
$\bar{R}$	Molar gas constant, 8.31446 (J/mol K)

r	Recovery ratio ([kg/s product]/[kg/s feed])
S	Entropy (J/K)
$\dot{S}_{\text{gen}}$	Entropy generation rate (W/K)
s	Specific entropy (J/kg K)
s_{gen}	Specific entropy generation per unit fluid (J/kg K)
$\mathcal{S}_{\text{gen}}$	Specific entropy generation per unit water produced (J/kg K)
T	Temperature (K)
T_0	Ambient (dead state) temperature (K)
T_{H}	Temperature of hot side reservoir (K)
U	Internal energy (J)
u	Specific internal energy (J/kg)
V	Volume (m^3)
$\bar{v}$	Molar volume (m^3/mol)
v	Specific volume (m^3/kg)
$\dot{W}$	Work transfer rate (W)
$\dot{W}_{\text{least}}$	Least work of separation (W)
$\dot{W}_{\text{least}}^{\text{min}}$	Minimum least work of separation (W)
$\dot{W}_{\text{rev}}$	Reversible work (W)
$\dot{W}_{\text{sep}}$	Work of separation (W)
w	Specific work (J/kg); mass fraction (kg/kg or g/kg); width (m)
w_{s}	mass fraction of salts (salinity)
x	Quality (kg/kg); mole fraction
Z	Pitzer function, $\sum_i b_i \lvert z_i \rvert$ (mol/kg); generalized compressibility (−)
z	Charge number

Greek

α	Pitzer parameter ($kg^{1/2}/mol^{1/2}$)
β	Pitzer parameter (kg/mol)
γ_x, γ_b, γ_c	Rational, molal, and molar activity coefficient
δ_{b}	Boiling point elevation (K)
δ_{f}	Freezing point depression (K)
Δ	Change in a variable
Δp_{sat}	Vapor pressure lowering (Pa)
ε_0	Vacuum permittivity
ε_{r}	Relative permittivity
η	Mole ratio of salt in seawater (−), efficiency
η_{e}	Isentropic efficiency of expander (−)
η_{p}	Isentropic efficiency of pump/compressor (−)
η_{II}	Second Law/exergetic efficiency (−)
θ	Pitzer parameter (kg/mol)
κ	Constant in Eq. (A.13)
λ	Constant in Eq. (A.13)
λ_{ij}	Pitzer parameter, uncharged interactions (kg/mol)
μ	Chemical potential (J/mol)
ν	Stoichiometric coefficient
$\dot{\Xi}_{\text{destroyed}}$	Exergy destruction rate (W)
$\dot{\Xi}$	Exergy flow rate (W)
π	Osmotic pressure (Pa)
ρ	Density (kg/m^3)
Φ_{ij}, Φ_{ij}^{ϕ}	Pitzer parameter, like-charged interactions (kg/mol)

Φ'_{ij}	Pitzer parameter, like-charged interactions (kg^2/mol^2)
ϕ	Osmotic coefficient
Ψ_{ijk}	Pitzer parameter, ternary interactions (kg^2/mol^2)

Subscripts

0	Environment, or global dead state
a*, *X	Anion
atm	Atmospheric
b	Brine, molal basis
c*, *M	Cation
d	Desalination, diluent
f	Flashing
F	Feed
i	*i*th species, inlet state
n*, *N	Neutral species
o	Outlet state
p	Product
pp	Power plant
s	Steam; salt
sat	Saturated state
sw	Seawater
w	Water

Superscripts

id	Ideal solution
ex	Excess property
s	Isentropic
′	Stream before exiting CV
∘	Standard (reference) state
*	Restricted dead state

Acronyms

BH	Brine heater
CAOW	Closed air open water
CD	Chemical disequilibrium
ERI	Energy Recovery Inc.
FF	Forward feed
GOR	Gained output ratio
HP	High pressure
HX	Heat exchanger
IF	Incompressible fluid
IG	Ideal gas
MED	Multiple effect distillation
MVC	Mechanical vapor compression
OT	Once through
PR	Performance ratio

PX	Pressure exchanger
RDS	Restricted dead state
RO	Reverse osmosis
TD	Temperature disequilibrium
TDS	Total dead state
WH	Water heated

1. INTRODUCTION

Desalination is an energy-intensive process, and reduction of energy consumption is central to the development and design of all desalination processes. At the heart of the process is the chemical energy of separating water and dissolved salts. This minimum amount of energy will always be required, no matter how desalination is to be accomplished. The entire desalination system, however, brings additional energy consumption to the process of desalinating water, as a result of a variety of inefficiencies that are present in any real system. The total energy consumed is normally several times greater than the minimum chemical energy of separation. Identifying and reducing this additional energy consumption requires thermodynamic analysis of the desalination system.

The minimum separation energy can be characterized as work, in the thermodynamic sense of the word. Examples of thermodynamic work include the work done by high pressure pumps in moving water, the work done by the rotating shaft of an electric motor, and the work done by current flowing in an electric field. So, we commonly speak of the minimum or least work of separation as defining the thermodynamic limit of performance for a desalination process. The least work is usually higher when the salinity of the source water is higher.

A real desalination system will require greater amounts of work, owing to factors such as losses in pumps, hydraulic pressure behind membranes that greatly exceeds osmotic pressure, or incomplete energy recovery from high pressure brines. From a thermodynamic viewpoint, the losses or irreversibilities of components in a desalination system can be measured in terms of the entropy they generate. Entropy production directly increases the energy requirements of a system that produces a given amount of desalinated water. Entropy is produced whenever friction occurs and when heat is transferred through a difference in temperature.

Work is a form of energy transfer, but it is distinct from energy in the form of heat. Most often, work is generated by heat transferred from a high-temperature source (perhaps a burning fuel in a combustor), through some process (expansion of steam through a turbine perhaps), to a low-temperature sink (the cooling water in a plant condenser). The number of joules of work generated (by the steam turbine) is substantially less than the number of joules of heat transferred from the high-temperature source, with the

difference between them ending up as heat transfer to the low-temperature sink. This difference is greater when the high-temperature source is cooler. Any inefficiencies in the system, perhaps from friction or from large temperature differences in heat exchangers, will reduce the amount of work that can be produced.

The difference between heat and work is essential to characterizing and evaluating thermal desalination processes, and more so because many desalination systems that are driven by heat also consume significant electrical energy, which is a form of work. Heat and work cannot be added or compared directly. Heat gains its potential to do work from the presence of a significant temperature difference between the high-temperature source and the low-temperature sink. Consequently, thermodynamic methods, in the form of exergy analysis, are essential in assessing the efficiency of a thermal desalination process, especially when comparing such a process to a work-driven desalination process. Heat transfer between two temperatures represents a source of exergy, as does any work transfer, but a given amount of heat transfer provides less exergy when taken from a lower-temperature source. Thus exergetic methods are all the more important when thermal processes are to be driven by low-temperature heat sources, such as common solar collectors. Exergy is destroyed by friction or when heat is transferred to a lower temperature. In fact, any process that generates entropy destroys exergy in the process.

In this chapter, we introduce the concepts and methods required for assessing the thermodynamic efficiency of desalination systems. In Section 2, thermodynamic laws for open systems (those through which fluids flow) are given and key results on the chemical thermodynamics of electrolyte mixtures (salts dissolved in water) are summarized, including the Pitzer model. Osmotic pressure and boiling point elevation are discussed. Section 3 introduces exergy analysis of desalination. With these tools in hand, Section 4 proceeds to the thermodynamic analysis of desalination processes. The work and heat of separation are derived, and the role of entropy generation and exergy destruction are identified. Important sources of entropy production are described and equations for their evaluation are given. Finally, Section 5 applies these methods to give brief assessments of the causes of inefficiency in several representative desalination systems. The appendices to this chapter give some useful correlations for the thermodynamic properties of seawater and further details of one of the electrolyte models.

2. THERMODYNAMIC ESSENTIALS

This chapter deals with the energy consumption of desalination systems: how it is evaluated, what its limits are, and how to push real systems closer to those limits. The key to answering these questions is a ground-up understanding of efficiency, η—strictly, the *Second Law Efficiency*. Conceptually, η is the fraction of energy consumed that *must* be consumed according to the laws of physics, or

$$\eta = \frac{\text{Minimum energy input}}{\text{Actual energy input}} \tag{1}$$

Conceptually, the actual energy input is

$$\begin{aligned}\text{Actual energy input} = {} & \text{Minimum energy input} \\ & + \text{Energy to overcome losses}\end{aligned} \tag{2}$$

A more rigorous definition of η and the interplay between the three preceding terms are described in the sections that follow; but first, in order to understand the details of each of these terms, we require some thermodynamic basics. In this section, using the Gibbs free energy as the fundamental thermodynamic function, we will provide a brief overview of the essential thermodynamic concepts and terms used throughout the remainder of the chapter.

2.1 Thermodynamic Analysis of Open Systems

An open system, or control volume (CV), is shown in Fig. 1: streams flow into the system at some inlet state(s) *i*, undergo a change of state within the CV, and exit at state(s) *o*. A work or heat transfer may occur across the boundary of the system to effect the streams' change of state or as a consequence of their change of state. We fix the system boundary temperature at T_0.

The First Law of Thermodynamics for this system reads

$$\frac{dU}{dt} = \dot{Q} + \dot{W} + \sum_i \dot{H}_\mathrm{i} - \sum_o \dot{H}_\mathrm{o} \tag{3}$$

where U is the internal energy of the system, $\dot{Q}$ is the net heat transfer rate into the system, $\dot{W}$ is the net rate at which work is done on the system, and $\dot{H}_\mathrm{i}$ and $\dot{H}_\mathrm{o}$ are the enthalpy inflows and outflows, respectively. The Second Law of Thermodynamics for this system is

$$\frac{dS}{dt} = \frac{\dot{Q}}{T_0} + \sum_i \dot{S}_\mathrm{i} - \sum_o \dot{S}_\mathrm{o} + \dot{S}_\mathrm{gen} \tag{4}$$

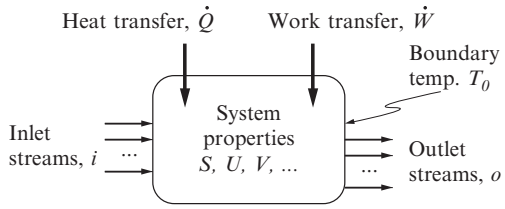

Fig. 1 In an open system, streams *i* enter the system at some state, undergo a change of state and exit as outlet streams *o*. A work transfer $\dot{W}$ and/or a heat transfer $\dot{Q}$ may accompany the change in state. The system has instantaneous properties, such as internal energy *U*, entropy *S*, and volume *V*.

where S is the entropy of the system, $\dot{Q}/T_0$ is the rate of entropy transfer into the system; $\dot{S}_i$ and $\dot{S}_o$ are the entropy inflows and outflows, respectively; and $\dot{S}_{gen}$ is the entropy generation rate within the CV.

Multiplying Eq. (4) by the boundary temperature T_0 and subtracting it from Eq. (3), we find that the heat transfer terms cancel; and at steady state we are left with

$$0 = \dot{W} + \sum_i (\dot{H}_i - T_0 \dot{S}_i) - \sum_o (\dot{H}_o - T_0 \dot{S}_o) - T_0 \dot{S}_{gen} \tag{5}$$

If we define the CV such that the streams enter and exit at T_0, then H and S are also evaluated at T_0, and the preceding reduces to

$$\dot{W} = \sum_o \dot{G}_o - \sum_i \dot{G}_i + T_0 \dot{S}_{gen} \tag{6}$$

where the grouping $H - TS$ is the Gibbs free energy, G.

Eq. (6) illustrates the fundamental variables involved in desalination system energetic analysis. When $\dot{S}_{gen} = 0$, the system is *reversible*, and $\dot{W}$ becomes $\dot{W}_{rev}$, the reversible work associated with the streams changing from their inlet to their outlet states:

$$\dot{W}_{rev} = \sum_o \dot{G}_o - \sum_i \dot{G}_i \tag{7}$$

Thus we see that differences in Gibbs free energy determine a system's reversible limits; consequently, $T_0 \dot{S}_{gen}$ is identically equal to the energy required to overcome the losses that produce $\dot{S}_{gen}$.

In cases where the outlet streams have different temperatures than the inlet stream, a CV analysis will not isolate Gibbs energy in the same way, and the reversible work would differ because it would be possible to extract additional work from the differences in temperature relative to T_0. In those situations, exergy is discarded with the leaving streams (see discussion in Section 4.1.1). Some cases of this type are analyzed in Section 5. A formulation using flow exergy (Section 3) would also account for these differences in outlet state.

The two groupings in Eq. (6), ΔG and $T_0 \dot{S}_{gen}$, are the building blocks for thermodynamic analysis of desalination systems: G determines the limits, and precise identification of $\dot{S}_{gen}$ guides avenues for improvement. In addition, as we will see shortly, when G is known for a substance as a function of temperature and pressure, it contains all of the necessary information to compute efficiency, including $T_0 \dot{S}_{gen}$.

2.2 Thermodynamic Properties of Mixtures

As discussed in Section 2.1, G serves two useful purposes in our analyses. First, the property itself defines the reversible work associated with any change in state. Second, because its conjugate variables are temperature and pressure, which are measurable

and controllable thermodynamic variables, it provides a convenient basis with which to correlate substance behavior. A model describing G for aqueous solutions (e.g., seawater) is thus essential.

2.2.1 Gibbs Energy as a Fundamental Thermodynamic Function

Once a thermodynamic state is fixed, any thermodynamic property *at that state* can be computed as a function of any other complete set of independent properties *at that state*. However, there are specific independent variables, called conjugate variables, that when used to formulate a property, yield all thermodynamic properties of the substance at *any state*.

The conjugate variables for G are temperature T, pressure p, and number of moles of species i, N_i (equivalently mole fraction, molality, or other measures of concentration). This can be shown as follows. With the definition of $G = H - TS = U + pV - TS$,

$$dG = dU + p\,dV + V\,dp - T\,dS - S\,dT \tag{8}$$

By the fundamental relationship of thermodynamics, $dU = T\,dS - p\,dV + \sum_i \mu_i\,dN_i$, and so

$$dG = -S\,dT + V\,dp + \sum_i \mu_i\,dN_i \tag{9}$$

Thus knowledge of $G = f(T, p, N_i)$ allows one to compute all thermodynamic properties of the substance, as shown for several properties by the relationships in Table 1. With these properties, the actual energy consumption, the losses, and the energy required to overcome the losses, $T_0\dot{S}_{\text{gen}}$, can be computed (see Eqs. 3, 4).

Table 1 Relationships between $G = f(T, p, N_i)$ and several thermodynamic variables

Property	Expression
Entropy	$S = -\left(\frac{\partial G}{\partial T}\right)_{p,N_i}$
Molar volume	$\bar{v} = \frac{1}{N}\left(\frac{\partial G}{\partial p}\right)_{T,N_i}$
Enthalpy	$H = G - T\left(\frac{\partial G}{\partial T}\right)_{p,N_i} = -T^2\left(\frac{\partial (G/T)}{\partial T}\right)_{p,N_i}$
Heat capacity	$C_{\text{p}} = -T\left(\frac{\partial^2 G}{\partial T^2}\right)_{p,N_i}$
Chemical potential	$\mu_i = \left(\frac{\partial G}{\partial N_i}\right)_{T,p}$

2.2.2 Standard Formulations for Gibbs Energy and the Chemical Potential

By definition, any extensive mixture property X can be written as the weighted sum of partial molar properties over each species i

$$X = \sum_i \left(\frac{\partial X}{\partial N_i}\right)_{T,p,N_{j\neq i}} N_i \tag{10}$$

where the partial molar property, $\partial X/\partial N_i$, physically represents the change in mixture X with an incremental addition of species i. Thus the Gibbs free energy of the solution can be written as

$$G = \sum_i \left(\frac{\partial G}{\partial N_i}\right)_{T,p,N_{j\neq i}} N_i \tag{11}$$

But since T and p are the conjugate variables of G (see Eq. 9), the chemical potential μ_i *is* the partial molar Gibbs free energy, $\left(\frac{\partial G}{\partial N_i}\right)_{T,p,N_{j\neq i}}$.

The chemical potential may be written as

$$\mu_i \equiv \left(\frac{\partial G}{\partial N_i}\right)_{T,p,N_{j\neq i}} = \mu_i^\circ + \bar{R}\,T\,\ln a_i \tag{12}$$

where the superscript ∘ denotes the standard (or reference) state, $\bar{R}$ is the molar (universal) gas constant, T is the absolute temperature in kelvin, and a_i is the activity of species i in the solution. For solutes, the reference state is usually a hypothetical solution of infinite dilution and unit concentration (i.e., 1 mol/L or 1 mol/kg, etc.) at the same temperature. For solvents (water), the reference state is typically the pure liquid at the same temperature. Depending on the convention, the reference pressure may or may not be fixed at 1 atm [1, 2].

Chemical activity is often termed a "thermodynamic concentration," and is related to the change in energy of a component as it is added to a mixture, that is, as its concentration changes. For solutes, it is modeled as the product of the activity coefficient γ and a measure of concentration, giving several possible formulations:

$$a_{x,i} = \gamma_{x,i} x_i, \quad a_{b,i} = \gamma_{b,i} b_i / b^\circ, \quad a_{c,i} = \gamma_{c,i} c_i / c^\circ \tag{13}$$

where x_i is mole fraction, b_i is molality, and c_i is molar concentration (moles per unit volume) of species i. The reference quantities c° and b° usually have a magnitude of unity and thus often not written explicitly.

In the ideal solution model, the first building block in mixture thermodynamics, the rational activity coefficient $\gamma_x = 1$. Physically, in an ideal solution, the introduction of a solute causes little change in the average interaction potential between all species.

This can approximate real solution behavior when, for example, the solution is very dilute[1] and solvent-solvent interactions are negligibly small. The model can also be suitable for mixtures of two chemically similar components. For a mixture of toluene and benzene, for example, benzene-benzene interactions are like those of benzene-toluene and toluene-toluene [4]. The activity coefficient γ thus represents departures from ideal solution behavior, and is the lynchpin in computing G for electrolyte solutions.

For water, the solvent, deviations from ideality are often expressed as an osmotic coefficient, the form of which is also dependent on the concentration scale:

$$\phi_x = -\frac{\mu_w^\circ - \mu_w}{\bar{R}\,T\,\ln x_w} \tag{14a}$$

$$\phi_b = \frac{\mu_w^\circ - \mu_w}{\bar{R}\,T M_w \sum_i b_i} \tag{14b}$$

The water activity is related to the osmotic coefficient by the relation $\mu_w - \mu_w^\circ = \bar{R}\,T\,\ln a_w$. For an ideal solution, $\phi_x = \phi_b = 1$.

The water activity a_w is not independent of the solute activities, and it is usually calculated from solute activity using the Gibbs-Duhem relationship. The latter is found by equating Eq. (9) and the differential form of Eq. (11), $dG = \sum_i d(\mu_i N_i)$:

$$\sum_i N_i\, d\mu_i = -S\, dT + V\, dP \tag{15}$$

All models for activity must satisfy this relationship. At constant temperature and pressure, Eq. (15) can be restated on a mole fraction basis by dividing through by N:

$$\sum_i x_i d\mu_i = 0 \tag{16}$$

This equation can be manipulated to find the solvent activity, a_w as

$$d\,\ln a_w = -\frac{1}{x_w}\sum_{i\neq w}\frac{d(\gamma_i x_i)}{\gamma_i} \tag{17}$$

Analogous expressions can be found for the other concentration scales.

2.2.3 Ideal Solutions and Deviations From Ideality as Functions of Activity

A common modeling approach for the activity coefficient is to model the energetic contributions that lead to deviations from ideality—the excess Gibbs free energy—and

[1] In dilute systems, the difference between γ_x, γ_b, and γ_c is generally quite small, so in the ideal solution model, all activity coefficients are commonly taken as unity. Formulas for converting from one activity coefficient scale to another are straightforward to use and can be found in Ref. [3].

then differentiate to compute an activity coefficient. Because of the relationships between $G = f(T, p, N_i)$ and the suite of thermodynamic properties, such models are also related to deviations from ideality for all other thermodynamic properties: the excess enthalpy, excess entropy, excess volume, and so on. These relationships are discussed briefly later.

The Gibbs free energy can be written as the sum of ideal and excess components

$$G = G^{\mathrm{id}} + G^{\mathrm{ex}} \tag{18}$$

Based on the definitions of chemical potential (Eq. 12) and osmotic coefficient (Eq. 14), and the condition for ideality, G^{id} can be written on a mole fraction or molal scale, respectively, as

$$\frac{G^{\mathrm{id}}}{N} = \sum_i \left(\mu^{\circ}_{x,i} + \bar{R}\,T\,\ln x_i\right) x_i \tag{19a}$$

$$\frac{G^{\mathrm{id}}}{m_{\mathrm{w}}} = \left(\mu^{\circ}_{w} - \bar{R}\,T M_w \sum_{j\,\in\,\mathrm{solutes}} b_j\right) b_w + \sum_{j\,\in\,\mathrm{solutes}} \left(\mu^{\circ}_{b,j} + \bar{R}\,T\,\ln b_j\right) b_j \tag{19b}$$

The excess component is similarly written on any of the concentration scales, and yields the following expressions for the activity coefficient:

$$\ln\gamma_{x,i} = \frac{\partial G^{\mathrm{ex}}/\bar{R}\,T}{\partial N_i}, \qquad \ln\gamma_{b,i} = \frac{\partial G^{\mathrm{ex}}/m_{\mathrm{w}}\bar{R}\,T}{\partial b_i} \tag{20}$$

Combining this ideal-excess breakdown with the relationships shown in Table 1, we can find the properties of ideal solutions and formulate deviations as a function of the activities and their pressure and temperature derivatives. We will show the procedure explicitly for entropy and enthalpy; several other properties are shown in Table 2.

Table 2 Relationships between partial molar excess thermodynamic properties and the activity coefficient

Property	Expression
Partial molar excess entropy	$-\bar{R}\left(T\left.\dfrac{\partial \ln\gamma_i}{\partial T}\right\|_P + \ln\gamma_i\right)$
Partial molar excess volume	$\bar{R}\,T\left.\dfrac{\partial \ln\gamma_i}{\partial P}\right\|_T$
Partial molar excess enthalpy	$-\bar{R}\,T^2\left.\dfrac{\partial \ln\gamma_i}{\partial T}\right\|_P$
Partial molar excess heat capacity	$-\bar{R}\,T^2\left(\left.\dfrac{\partial^2 \ln\gamma_i}{\partial T^2}\right\|_P + \dfrac{2}{T}\left.\dfrac{\partial \ln\gamma_i}{\partial T}\right\|_P\right)$

For an ideal solution, the entropy and enthalpy are

$$S^{\mathrm{id}} = -\left(\frac{\partial G^{\mathrm{id}}}{\partial T}\right)_{P,x_i} = -\sum_i N_i \left(\left.\frac{\partial \mu_i^\circ}{\partial T}\right|_P + \bar{R}\,\ln x_i\right) \tag{21}$$

$$H^{\mathrm{id}} = \sum_i N_i \left(\mu_i^\circ - T\left.\frac{\partial \mu_i^\circ}{\partial T}\right|_P\right) \tag{22}$$

When a solution undergoes an isothermal, isobaric change of state by the addition (or removal) of some species, the corresponding change in entropy and enthalpy are known as the *entropy of mixing* and the *enthalpy of mixing*, respectively. For an ideal solution, we are left with

$$\Delta S_{\mathrm{mix}}^{\mathrm{id}} = -\bar{R}\Delta\left(\sum_i N_i\,\ln x_i\right) \tag{23}$$

$$\Delta H_{\mathrm{mix}}^{\mathrm{id}} = 0 \tag{24}$$

Because ideal solutions have zero enthalpy of mixing, the isothermal, isobaric change in Gibbs free energy—the reversible work associated with salt dissolution or desalination (cf. Eq. 7)—is identically equal to $T\Delta S_{\mathrm{mix}}^{\mathrm{id}}$:

$$\Delta G_{\mathrm{mix}}^{\mathrm{id}} = \bar{R}\,T\Delta\left(\sum_i N_i\,\ln x_i\right) \tag{25}$$

All desalination processes must overcome the entropy of mixing.

Deviations from these ideal approximations are entirely contained within the temperature and pressure dependence of the activity coefficient. The excess entropy is

$$S^{\mathrm{ex}} = -\left(\frac{\partial G^{\mathrm{ex}}}{\partial T}\right)_{P,N_i} = -\sum_i N_i \underbrace{\bar{R}\left(T\left.\frac{\partial\,\ln\gamma_i}{\partial T}\right|_{P,x_i} + \ln\gamma_i\right)}_{\text{partial molar excess entropy}} \tag{26}$$

and the excess enthalpy is

$$H^{\mathrm{ex}} = G^{\mathrm{ex}} - T\left(\frac{\partial G^{\mathrm{ex}}}{\partial T}\right)_{P,N_i} = -\sum_i N_i \underbrace{\left(\bar{R}\,T^2\left.\frac{\partial\,\ln\gamma_i}{\partial T}\right|_{P,x_i}\right)}_{\text{partial molar excess enthalpy}} \tag{27}$$

Relationships for the other properties are shown in Table 2, and mimic those shown in Table 1, with G^{ex} replaced by $\mu^{\mathrm{ex}} = \bar{R}\,T\,\ln\gamma_i$.

2.3 Activity Coefficient Models for Electrolytes

Thus far we have seen that knowledge of G allows us to predict the limits of desalination system performance, that knowledge of $G = f(T, P, N_i)$ allows us to predict all properties of a solution, and that γ and ϕ reflect departures from ideal solution behavior. In this section, we will review some common models for activity coefficients in aqueous electrolyte solutions: the Debye-Hückel Limiting Law, the Davies equation, and the Pitzer model. For a salt MX that dissociates as

$$M_{\nu_M}\,\mathrm{X}_{\nu_X} \leftrightarrow \nu_M\, M^{z_M} + \nu_X\, X^{z_X} \tag{28}$$

it is typical to report values of a mean activity coefficient, $\gamma_\pm$, which is defined as

$$\gamma_\pm^{\nu} = \gamma_M^{\nu_M} \gamma_X^{\nu_X} \tag{29}$$

where $\nu = \nu_M + \nu_X$. Values of the mean molal activity coefficient $\gamma_{b,\pm}$ for NaCl are shown in Fig. 2: as model complexity increases from the Debye-Hückel Limiting Law, the models are more accurate over larger concentration domains.

Debye-Hückel Theory

For very dilute ionic solutions, the most important addition to mixture energy is that which is derived from ionizing the salt as it dissolves, which is reflected in electrostatic interactions between ions. Through a combination of electrostatics and statistical mechanics, the Debye-Hückel theory [6] provides an expression for the activity coefficient that is accurate for solutions of ionic strength up to about 0.01 molal. Full derivations can be found in a variety of texts, for example, [3], and the resulting expression for activity coefficient is

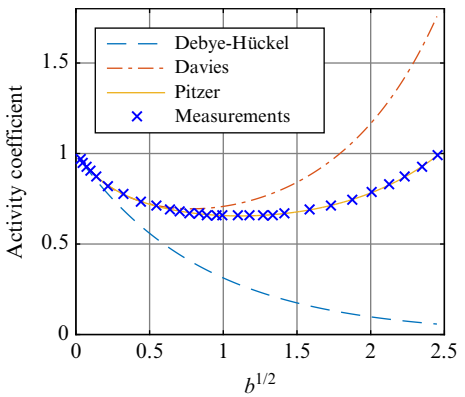

Fig. 2 A comparison of three models for the activity coefficient of NaCl shows that the simpler Debye-Hückel and Davies models are limited to concentrations below about 0.01 and 0.5 mol/kg, respectively. Measured data is an average over several values in literature provided in Ref. [5].

$$\ln\gamma_{x,\pm} = -A|z_M z_X|\sqrt{I} = -|z_M z_X|\left[\frac{e^3(2N_A\rho_w)^{1/2}}{8\pi(\varepsilon_r\varepsilon_0 k_B T)^{3/2}}\right]\sqrt{I} \tag{30}$$

where z_M and z_X are the cation and anion charge numbers, e is the elementary charge, N_A is Avogadro's number, ε_r is the dielectric constant (relative permittivity) of the solvent, ε_0 is the vacuum permittivity, k_B is the Boltzmann constant, ρ_w is the density of pure water, and I is the molal ionic strength. The molal ionic strength is defined as

$$I = \frac{1}{2}\sum_i b_i z_i^2 \tag{31}$$

Eq. (30) is known as the Debye-Hückel Limiting Law, which has a square-root dependence on ionic strength. To first order, most expressions for activity coefficient are characterized by a square-root dependence on ionic strength, reflecting the long-range electrostatic contributions to the excess Gibbs free energy that are the first to appear as solute concentration increases from zero. The temperature dependence of the Debye-Hückel activity coefficient is not quite $T^{-3/2}$ because the dielectric constant is also a function of temperature.

Davies Equation

Several other equations exist that extend the Debye-Hückel Limiting Law using mostly empirical or semiempirical methods, and these can be found in, for example, [3, 7]. The general approach is to add concentration and/or ionic strength-dependent terms to the Debye-Hückel expression to capture the curvature of γ versus concentration (Fig. 2) that arises from the increasing importance of short-range interactions as solute concentration increases further. One particularly useful equation that requires no adjustable parameters for a particular electrolyte is given by Davies [8]

$$-\log\gamma_{x,\pm} = 0.50|z_M z_X|\left(\frac{\sqrt{I}}{1+\sqrt{I}} - 0.20I\right) \tag{32}$$

which is approximate for ionic strengths up to about 0.1 and a temperature of 25°C.

Pitzer Model

The Pitzer model [9–12] is based on a virial expansion of the excess Gibbs free energy, and extends the Debye-Hückel model to account for short-range interactions between solute pairs and triplets. Detailed derivations are given in Refs. [9, 10, 13]. For calculations beyond the dilute limit, the Pitzer model is among those most widely used for single and mixed electrolytes. The model has been validated and used for calculations in several

mixed electrolytes, for example, [7, 14]. Of the three models discussed in this section, the Pitzer model is the most accurate one for seawater and its concentrates.

Expressions are available for the mean molal activity coefficient, but for added flexibility, we will give the single ion expressions here.[2] We also provide an expression for uncharged solutes, which may also exist in mixed electrolytes or arise as a result of ion-pairing in concentrated mixtures.

The activity coefficient of an individual cation, M, is given by

$$\begin{aligned}\ln\gamma_M = {} & z_M^2 F + \sum_a b_a (2B_{Ma} + ZC_{Ma}) \\ & + \sum_c b_c \left(2\Phi_{Mc} + \sum_a b_a \Psi_{Mca} \right) \\ & + \sum_{a<a'} \sum b_a b_{a'} \Psi_{aa'M} \\ & + |z_M| \sum_c \sum_a b_c b_a C_{ca} + \sum_n b_n (2\lambda_{nM})\end{aligned} \tag{33}$$

For an individual anion, X, the expression is analogous:

$$\begin{aligned}\ln\gamma_X = {} & z_X^2 F + \sum_c b_c (2B_{cX} + ZC_{cX}) \\ & + \sum_a b_a \left(2\Phi_{Xa} + \sum_c b_c \Psi_{Xac} \right) \\ & + \sum_{c<c'} \sum b_c b_{c'} \Psi_{cc'X} \\ & + |z_X| \sum_c \sum_a b_c b_a C_{ca} + \sum_n b_n (2\lambda_{nX})\end{aligned} \tag{34}$$

The activity coefficient of uncharged species N (e.g., aqueous CO_2) is

$$\ln\gamma_N = \sum_c b_c (2\lambda_{Nc}) + \sum_a b_a (2\lambda_{Na}) \tag{35}$$

The molal osmotic coefficient ϕ_b is calculated from the expression

[2] Of course, as the activity of an individual ion cannot be measured explicitly, the physical meaning of such expressions is unclear. However, as noted by Harvie and Weare [11], the combination of Eqs. (33), (34) in the form of a measurable mean activity coefficient produces the same equation as Pitzer [10], and is far more convenient for calculations in mixed electrolytes.

$$
\begin{aligned}
(\phi-1)\sum_i m_i = 2\Bigg[&\frac{-A^{\phi}I^{3/2}}{1+1.2\sqrt{I}} \\
&+\sum_c\sum_a b_c b_a\left(B_{ca}^{\phi}+ZC_{ca}\right) \\
&+\sum_{c<c'}\sum b_c b_{c'}\left(\Phi_{cc'}^{\phi}+\sum_a b_a\Psi_{cc'a}\right) \\
&+\sum_{a<a'}\sum b_a b_{a'}\left(\Phi_{aa'}^{\phi}+\sum_c b_c\Psi_{aa'c}\right) \\
&+\sum_n\sum_a b_n b_a\lambda_{na}+\sum_n\sum_c b_n b_c\lambda_{nc}\Bigg]
\end{aligned}
\tag{36}
$$

in which $Z=\sum_i|z_i|m_i$, M_w is the molar mass of water, and the remainder are functions quantifying particular solute interactions, as defined below. Subscript c denotes cations other than M, a denotes anions other than X, and n denotes uncharged (neutral) solutes. Summation over all i indicates a sum over all solutes; likewise summation over all c, a, and n denotes a sum over all cations, anions, and neutral solutes, respectively. The summation notations $c<c'$ and $a<a'$ indicate that the sum should be performed over all distinguishable cation pairs and anion pairs, respectively. Equations for A^{ϕ}, B_{ij}, B_{ij}^{ϕ}, F, Φ_{ij}, and Φ_{ij}^{ϕ} are given in Appendix B.

2.4 Colligative Properties: Boiling Point Elevation, Freezing Point Depression, Vapor Pressure Lowering, and Osmotic Pressure

Mixture properties that depend on the total mole numbers of dissolved substances, but not the specific chemical species dissolved in a solvent, are called colligative properties. Colligative properties are truly independent of the chemical species dissolved only when the solution is very dilute, so that the solution behaves as an ideal mixture. They must be corrected to some degree at higher concentrations, typically through the osmotic coefficient.

Four colligative properties of great importance in desalination system analysis relate to chemical equilibrium between two phases or two different mixture concentrations: the boiling point elevation, δ_b; the freezing point depression, δ_f; the osmotic pressure, π; and the vapor pressure lowering, Δp_{sat}. In osmotically driven processes, such as reverse osmosis (RO) and forward osmosis (FO), the flux of pure water across the membrane is a function of π. Likewise, in thermal systems, such as multistage flash (MSF), multieffect distillation (MED), and mechanical vapor compression (MVC), the evaporative flux is a function of δ_b; and in freeze desalination, the ice formation rate is a function of δ_f. In membrane distillation (MD), the flux of water vapor across the membrane is a function

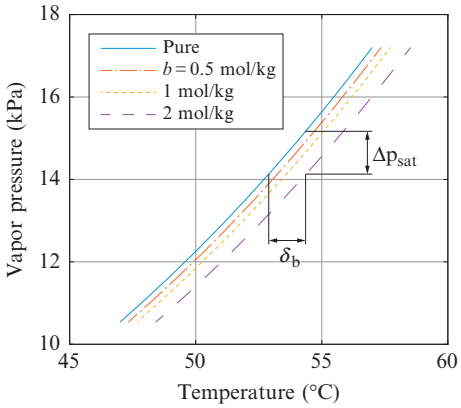

Fig. 3 The vapor pressure curve for sodium chloride solutions: the boiling point elevation (δ_b) and the vapor pressure lowering (Δp_{sat}) increase with increasing salt concentration (b). The curves are computed from Eq. (43) using the equations of Pitzer [2] and Saul and Wagner [15].

of Δp_{sat}. Accurate values of δ_b, δ_f, π, and Δp_{sat} are thus needed for a wide range of salinities and temperatures.

2.4.1 Boiling Point Elevation

Adding salt to water increases its boiling temperature at a given pressure. The boiling point elevation, δ_b, is the difference between the saturation temperatures of a solution, T_{sat}, and of its pure solvent, T°_{sat} at a fixed pressure (Fig. 3). It tends to be an increasing function of salt concentration and vapor pressure (equivalently, solvent saturation temperature). As with all of the colligative properties, it is related to the activity of the solvent (water), and can thus be written as a function of ϕ_b

$$\delta_b = T_{sat} - T^\circ_{sat} = \frac{\bar{R}\, T^{\circ 2}_{sat}}{h^\circ_{fg}} \phi_b \sum_i b_i \tag{37}$$

where $\bar{R}$ is the molar gas constant, and h°_{fg} is enthalpy of vaporization of pure water.[3] For low salinities, ϕ_b is close to one (Fig. 4), and so δ_b has a nearly linear dependence on salinity. A good approximation for the boiling point elevation is therefore given by the linear equation

$$\delta_b = K_b b \tag{38}$$

where b is the total molality of the solute ions in moles/kg-solvent, the ebullioscopic constant K_b is defined as

[3] Eq. (37) is valid when $\delta_b \ll T^\circ_{sat}$ and h°_{fg} does not change significantly between T_{sat} and T°_{sat}, which is true for seawater at typical thermal desalination operating conditions. Likewise, Eq. (40) is valid when $\delta_f \ll T^\circ_f$ and h°_{sf} does not change significantly between T_f and T°_f.

$$K_b = \frac{\bar{R}\, T_{sat}^{\circ 2}}{h_{fg}^{\circ}} \tag{39}$$

and T_{sat}° is in kelvin. For water at 1 atm, $K_b = 0.513$ K kg/mol.

2.4.2 Freezing Point Depression

The boiling point elevation's analog at the solid-liquid phase boundary is the freezing point depression, δ_f. The freezing point depression is the difference between the freezing temperatures of a solution, T_f, and of its pure solvent, T_f°. A mirror of δ_b, δ_f increases with increasing salt concentration, and can be written similarly[3]

$$\delta_f = T_f^{\circ} - T_f = \frac{\bar{R}\, T_f^{\circ 2}}{h_{sf}^{\circ}} \phi_b \sum_i b_i \tag{40}$$

where h_{sf}° is enthalpy of fusion of pure water. Like the boiling point elevation, we can define a linear relationship for the freezing depression at low salinities, where ϕ_b is near unity:

$$\delta_f = K_f b \tag{41}$$

The prefactor K_f is known as the cryoscopic constant:

$$K_f = \frac{\bar{R}\, T_f^{\circ 2}}{h_{sf}^{\circ}} \tag{42}$$

Like the ebullioscopic constant, T_f° is an absolute temperature (i.e., in K). For water at 1 atm, $K_f = 1.86$ K kg/mol.

2.4.3 Vapor Pressure Lowering

The boiling point elevation is considered at a fixed pressure. The equivalent effect at a fixed temperature is the vapor pressure lowering, Δp_{sat} (Fig. 3). A solution maintained at fixed temperature will require a greater vacuum for solvent to evaporate. The vapor pressure of water in solution is related to the activity of water[4] by

$$\ln\left(\frac{p_{sat}}{p_{sat}^{\circ}}\right) = \ln a_w \tag{43}$$

[4] Eq. (43) is valid when the fugacity coefficients and the Poynting correction factor are near unity, that is, when the vapor behaves ideally and the pressure is not too high. For a 2 mol/kg NaCl solution at 80°C, Eq. (43) overpredicts the vapor pressure by less than 0.001% relative to the general expression for vapor-liquid equilibrium that includes fugacity coefficients and the Poynting correction factor; see Glasstone [1] for details.

The vapor pressure lowering is the difference between the vapor pressures of the solution, p_{sat}, and of the pure solvent, p°_{sat}, at fixed temperature. In terms of the osmotic coefficient, the vapor pressure lowering is thus

$$\ln\left(\frac{\Delta p_{sat}}{p^{\circ}_{sat}}+1\right)=-\phi_b M_w\sum_i b_i \tag{44}$$

where M_w is the molar mass of the solvent. For sufficiently dilute solutions, where ϕ_b is near one, Eq. (44) reduces to Raoult's Law for the vapor pressure of the solvent:

$$p_{sat}=p^{\circ}_{sat}x_w=\frac{p^{\circ}_{sat}}{1+M_w\sum_i b_i} \tag{45}$$

2.4.4 Osmotic Pressure

The osmotic pressure represents the pressure that must be applied to a solution to maintain equilibrium with the pure solvent at a fixed temperature. Osmotic pressure rises as the solute concentration increases, and it is proportional to the absolute temperature. For a nonideal electrolyte solution such as seawater, the osmotic coefficient characterizes the deviation from ideal solution behavior. The osmotic pressure for a solution composed of multiple solutes may be expressed in terms of the molality of solutes as [3]

$$\pi=-\frac{\rho_w}{M_w}\bar{R}\,T\,\ln a_w=\phi_b\bar{R}\,T\rho_w b \tag{46}$$

where π is the osmotic pressure; ϕ_b is the molal osmotic coefficient (Eq. 14b); $\bar{R}$ is the molar gas constant; T is the absolute temperature in kelvin; ρ_w is the density of the solvent, in this case pure water; M_w is the molar mass of the solvent; and b is the total molality of the solute ions in moles/kg-solvent.[5] The total molality of the ions in seawater can be written as a function of the salinity as

$$b=31.843\frac{w_s}{1-w_s} \tag{47}$$

where w_s is the salt mass fraction of the solution in kg-salt/kg-solution, and 31.843 is a constant that takes into account the weighted average of the molecular weight of each dissolved solute of the seawater constituents that have the same relative composition at any salt concentration.

[5] Eq. (46) is valid when water can be modeled as an incompressible fluid and when μ°_w is pressure-dependent (Section 2.2.2). Strictly, therefore, a_w should be evaluated at the reference pressure plus π, but evaluating it at 1 bar only leads to small errors up to moderately high pressures (e.g., for a 4 mol/kg NaCl solution at 25°C, $\ln a_w$ at 200 bar is 0.8% higher than at 1 bar). Glasstone [1] provides an alternative formulation of osmotic pressure for a pressure-independent reference state.

The osmotic coefficient is a function of salinity and temperature (Section A.5). Using a piecewise fit for the osmotic coefficient function (i.e., Eqs. A.11, A.13), the osmotic pressure of seawater can be calculated from Eq. (46) for a range of salinity of 0–120 g/kg and a range of temperature of 0–200°C.

In the literature, a linearized expression for the osmotic pressure modeled on the van 't Hoff equation is widely used for quick calculation of the seawater osmotic pressure. The van 't Hoff equation itself applies to very dilute (or ideal) solutions ($\phi_b = 1$)

$$\pi = i\bar{R}Tc \tag{48}$$

where i is the van 't Hoff factor (accounting for dissociation of the solute), and c is the molarity of the solution (mol/L). We can define a modified van 't Hoff coefficient to make a linear approximation to the osmotic pressure function, Eqs. (46), (47), as follows:

$$\pi = Cw_s \tag{49}$$

The modified van 't Hoff coefficient, C, is determined to be 73.45 kPa kg/g for seawater at 25°C. The linear model represented by Eq. (49) can be used for a salinity range of 0–70 g/kg, which is a typical range for many desalination applications. For this range, the maximum deviation from the nonlinear osmotic pressure function, Eq. (46), is 6.8%. The osmotic pressure, Eq. (46), the osmotic coefficient, Eqs. (A.11), (A.12), and the linear osmotic pressure, Eq. (49), are shown as a function of salinity in Fig. 4.

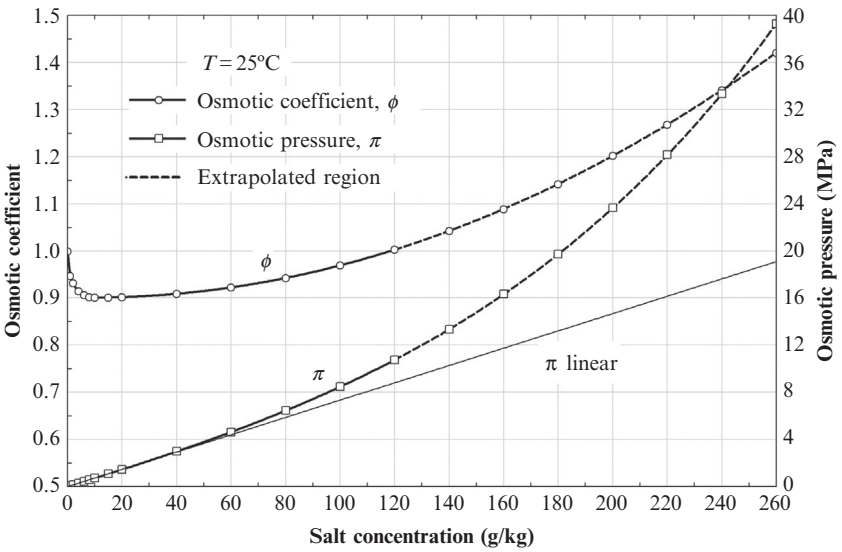

Fig. 4 Seawater molal osmotic coefficient and osmotic pressures versus salinity for a fixed temperature shown on the *left- and right-hand axes*. The osmotic coefficient curve and nonlinear osmotic pressure curves are extrapolated for salinities greater than 120 g/kg and these sections are shown as *bold-dashed lines*. The linear osmotic pressure curve is *solid*.

3. EXERGY ANALYSIS

Exergy is the maximum amount of work obtainable when a thermodynamic system is brought into equilibrium from its initial state to the environmental (dead) state. In this regard, the state of the environment must be specified. The system is considered to be at zero exergy when it reaches the environment state, which is called the dead state. The equilibrium can be divided into thermal, mechanical, and chemical equilibrium. These equilibria are achieved when the temperature (T), pressure (p), and concentration (w) of the system reach the values found in the surrounding environment (T_0, p_0, and w_0, respectively). Therefore exergy consists of a thermomechanical exergy and a chemical exergy. The thermomechanical exergy is the maximum work obtained when the temperature and pressure of the system changes to the environment temperature and pressure (T_0, p_0) with no change in the concentration. In this case, we say that thermomechanical equilibrium with the environment occurs. The chemical exergy is the maximum work obtained when the concentration of each substance in the system changes to its concentration in the environment at the environment pressure and temperature (T_0, p_0). In that case, chemical equilibrium occurs.

For a control mass (closed system), the exergy, e, can be mathematically expressed as [16, 17]

$$e = (u - u^*) + p_0(v - v^*) - T_0(s - s^*) + \sum_{i=1}^{n} w_i\left(\mu_i^* - \mu_{i,0}\right)/M_i. \tag{50}$$

where u, s, v, μ_i, w_i, and M_i are the specific internal energy, specific volume, specific entropy, chemical potential of species i, mass fraction of species i, and molar mass of species i, respectively. Properties with superscript $*$ in the preceding equation are determined at the temperature and pressure of the environment (T_0, p_0) but at the same composition or concentration of the initial state. This is referred to as the restricted dead state, in which only the temperature and pressure are changed to the environmental values. However, the properties with subscript 0 in the preceding equation (i.e., $\mu_{i,0}$) are determined at the temperature, pressure, and concentration of the environment (T_0, P_0, w_0), which is called the global dead state.

For a CV (open system), the flow exergy, e_f, can be calculated by adding the flow work to the exergy in Eq. (50), which mathematically can be expressed as [16, 17]:

$$e_f = e + v(p - p_0) \tag{51}$$

Knowing that $h = u + pv$, and eliminating e in Eq. (51) using Eq. (50), the flow exergy can be rewritten as

$$e_f = (h - h^*) - T_0(s - s^*) + \sum_{i=1}^{n} w_i\left(\mu_i^* - \mu_{i,0}\right)/M_i \tag{52}$$

If the system and the environment are both the same pure substance (e.g., pure water), the chemical exergy, which is the last term in Eqs. (50), (52), will vanish. However, for a multicomponent system (e.g., seawater, exhaust gases) the chemical exergy must be considered. Ignoring it may lead to unrealistic and illogical results for the exergy variation with the concentration.

The following section discusses the variation of exergy and flow exergy with temperature, pressure, and composition. In particular, we show that the (control mass) exergy is never negative, whereas the (CV) flow exergy can be negative if the system pressure is less than the dead state pressure. Changes in temperature or composition relative to the dead state values create the potential to do work by transferring heat or mass between the system and the environment, leading to positive exergy values in all cases.

3.1 Exergy Variation

The exergy of a control mass system, given by Eq. (50), and the exergy of a CV system, which is the flow exergy given by Eq. (52), are intensive thermodynamic properties that represent the maximum obtainable work per unit mass of the system. They are functions of the initial state as well as the environment state. However, if the environmental state is specified (T_0, p_0, w_0), the exergy is a function only of the system initial state (T, p, w).

In this section we examine how the exergy (for a control mass system) and the flow exergy (for a CV system) change with the temperature, pressure, and mass concentration of the initial state with respect to the environmental dead state, assuming the environmental dead state is at $T = T_0$, $p = p_0$, and $w = w_0$, and assuming an ideal gas mixture that satisfies the ideal gas relation ($pv = RT$) and that has equivalent mixture properties R, c_p, and c_v (ideal gas constant $R = \bar{R}/M$, where M is the mixture average molar mass; specific heat at constant pressure; and specific heat at constant volume, respectively).

3.1.1 *Case 1:* $\mathbf{p = p_0}$, $\mathbf{w = w_0}$ *but* $\mathbf{T \neq T_0}$

In this case, the chemical exergy, which is the last term in Eq. (50), vanishes, and the exergy can be written for an ideal gas mixture as

$$e = c_v(T - T_0) + p_0\left(\frac{RT}{p} - \frac{RT_0}{p_0}\right) - T_0\left[c_p \ln\left(\frac{T}{T_0}\right) - R \ln\left(\frac{p}{p_0}\right)\right] \tag{53}$$

For $p = p_0$

$$e = c_v(T - T_0) + R(T - T_0) - T_0 c_p \ln\left(\frac{T}{T_0}\right) \tag{54}$$

Using $c_p = c_v + R$, the exergy will be

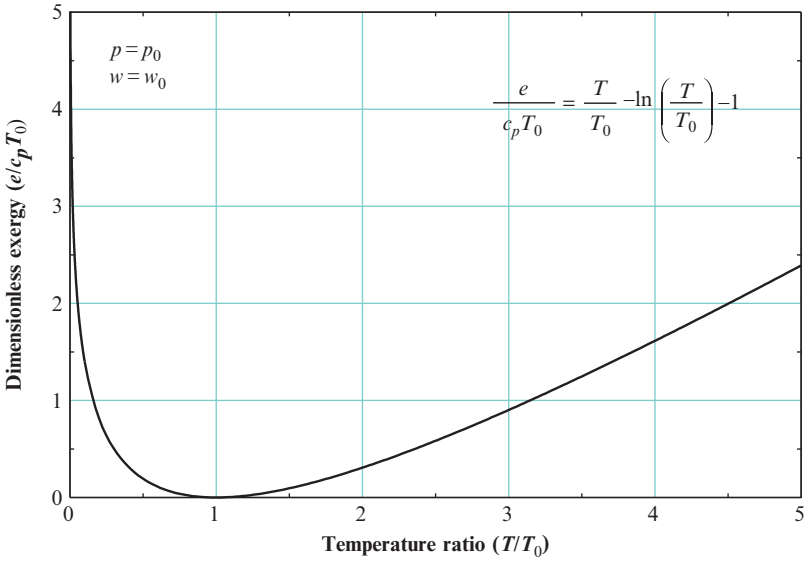

Fig. 5 Dimensionless exergy as a function of temperature ratio.

$$e = c_p T_0 \left[\frac{T}{T_0} - \ln\left(\frac{T}{T_0}\right) - 1\right] \tag{55}$$

Eq. (55), considered for the case when the pressure and concentration are equal to the dead state, shows that the exergy is always positive at any temperature other than the dead state temperature (Fig. 5). If the system has a temperature equal to the dead state ($T/T_0 = 1$), the exergy is zero. The positive exergy is due to the heat that can be transferred between the system temperature and the dead state temperature, in one direction or the other as appropriate, to operate a heat engine cycle that can produce work. The same result, Eq. (55), can be obtained for a CV system using the flow exergy equation, Eq. (52). Therefore, as long as $p = p_0$, $w = w_0$, any temperature difference between the system state and the dead state will result in positive exergy and positive flow exergy.

3.1.2 Case 2: T = T_0, w = w_0 *but* p≠p_0

In this case, the chemical exergy again vanishes, and the exergy of a control mass is again given by Eq. (53). For $T = T_0$, the exergy will be

$$e = RT_0 \left[\frac{p_0}{p} + \ln\left(\frac{p}{p_0}\right) - 1\right] \tag{56}$$

Eq. (56), for the case when the temperature and concentration are equal to the dead state, shows that the exergy of the control mass system is always positive at any pressure other

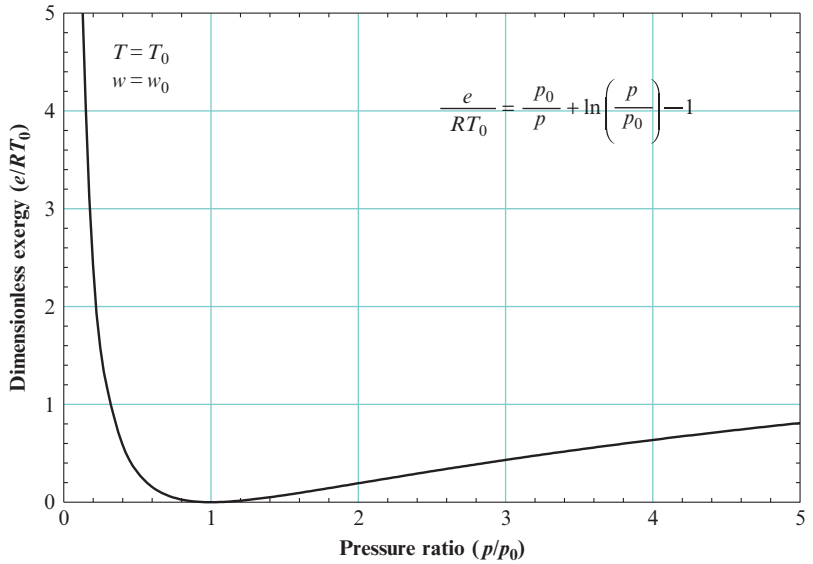

Fig. 6 Dimensionless exergy of a control mass system as a function of pressure ratio.

than the dead state pressure (Fig. 6). If the system has a pressure equal to the dead state pressure ($p/p_0 = 1$), the exergy is zero. The positive exergy is due to the mechanical work that can be obtained by expansion (if $p > p_0$) or compression (if $p < p_0$) of the system to reach the environment pressure.

For temperatures different from the dead state ($T \neq T_0$), one may show that the minimum of Eq. (53) with respect to pressure occurs for $p/p_0 = T/T_0$ and that the value at the minimum is positive. Thus the control mass system has positive or zero exergy for any temperature and pressure when $w = w_0$.

For a CV (open system), however, the signs on exergy can behave differently. The flow exergy, given by Eq. (52), can be written for an ideal gas mixture (with $w = w_0$) as

$$e_f = c_p(T - T_0) - T_0\left[c_p \ln\left(\frac{T}{T_0}\right) - R \ln\left(\frac{p}{p_0}\right)\right] \tag{57}$$

For $T = T_0$ the flow exergy will be

$$e_f = RT_0 \ln\left(\frac{p}{p_0}\right) \tag{58}$$

It is clear from Eq. (58) that the flow exergy of a CV system may be positive or negative depending on the pressure of the system. If the pressure of the CV system is higher than the dead state pressure (i.e., $p > p_0$), a flow stream can be expanded reversibly (e.g., using a turbine) to the environment pressure and produce work resulting in a positive flow

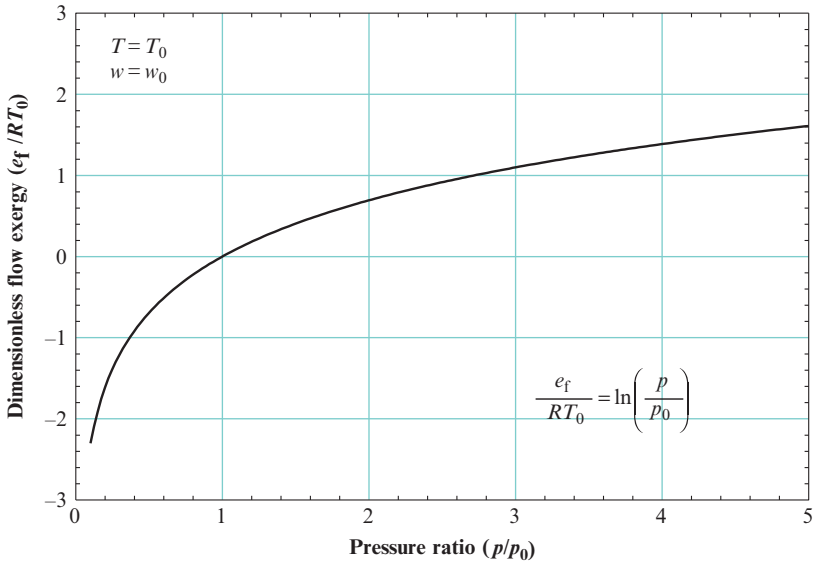

Fig. 7 Dimensionless flow exergy as a function of pressure ratio.

exergy. However, if the pressure is lower than the dead state pressure (i.e., $p < p_0$), an external work should be applied to compress the flow stream (e.g., using a compressor) to the environment pressure resulting in a negative flow exergy (Fig. 7). Therefore the exergy of the control mass is positive at any pressure other than the dead state pressure; however, the exergy of the CV (flow exergy) can be negative at pressures lower than the dead state pressure.

3.1.3 Case 3: T = T_0, p = p_0 *but* w≠w_0

In this case, when $T = T_0$ and $p = p_0$, the first two terms in the exergy equation, Eq. (50), and flow exergy equation, Eq. (52), vanish. The only remaining term is the last term, which is the chemical exergy. The exergy or flow exergy in this case can be written as follows:

$$e = e_f = \sum_{i=1}^{n} w_i \left(\mu_i^* - \mu_{i,0}\right)/M_i \tag{59}$$

For an ideal mixture model, the chemical potential differences are given, using Eqs. (12), (13) with $\gamma_{x,\,i} = 1$, as

$$\mu_i - \mu_i^\circ = \bar{R}\,T\,\ln\left(x_i\right) \tag{60}$$

where x_i is the mole fraction, μ_i° is evaluated at a hypothetical standard state for the component i, and it is not equal to $\mu_{i,0}$. Therefore the chemical potential differences in Eq. (59) can be written as

$$\mu_i^* - \mu_{i,0} = \left(\mu_i^* - \mu_i^\circ\right) - \left(\mu_{i,0} - \mu_i^\circ\right) = \bar{R}\,T\,\ln\left(\frac{x_i}{x_{i,0}}\right) \tag{61}$$

Substituting Eq. (61) into Eq. (59) yields, with $R_i = \bar{R}/M_i$,

$$e = e_f = \sum_{i=1}^{n} w_i R_i T\,\ln\left(\frac{x_i}{x_{i,0}}\right) \tag{62}$$

Assuming for simplicity that the mixture consists of two substances (1 and 2) and using $T = T_0$ yields

$$e = e_f = w_1 R_1 T_0\,\ln\left(\frac{x_1}{x_{1,0}}\right) + w_2 R_2 T_0\,\ln\left(\frac{x_2}{x_{2,0}}\right) \tag{63}$$

We may eliminate w_i in favor of x_i using the following two relationships

$$w_1 R_1 = x_1 R \tag{64a}$$

$$w_2 R_2 = x_2 R \tag{64b}$$

where R is the gas constant for the mixture. We also know that

$$x_1 = 1 - x_2 \tag{65a}$$

$$x_{1,0} = 1 - x_{2,0} \tag{65b}$$

Substituting Eqs. (64a)–(65b) into Eq. (63) and dropping the subscript 2 yields

$$e = e_f = RT_0\left[(1-x)\,\ln\left(\frac{1-x}{1-x_0}\right) + x\,\ln\left(\frac{x}{x_0}\right)\right] \tag{66}$$

Now, we can prove mathematically that Eq. (66) is always positive at any mole fraction other than x_0 by taking the first derivative with respect to x:

$$\frac{\partial e}{\partial x} = RT_0\left[\,\ln\left(\frac{x}{x_0}\right) - \,\ln\left(\frac{1-x}{1-x_0}\right)\right] \tag{67}$$

From Eq. (66), at $x = x_0$, the exergy (and flow exergy) is zero. From Eq. (67) at $x < x_0$, the first derivative (slope) is negative, meaning that the exergy is decreasing. And at $x > x_0$, the first derivative (slope) is positive, meaning that the exergy is increasing. Thus the point $x = x_0$ is a minimum.

The variation of exergy (or flow exergy) with mole fraction is shown in Fig. 8, in which exergy is always positive, except for a value of zero at the dead state concentration. The positive value of exergy arises from the potential for a mass transfer process, which can be used to produce work by transferring a solute between the high or low concentration of the system and the concentration of the environmental dead state. Because the chemical exergy is additive in both Eqs. (50), (52), the same behavior will clearly occur for any selected dead state.

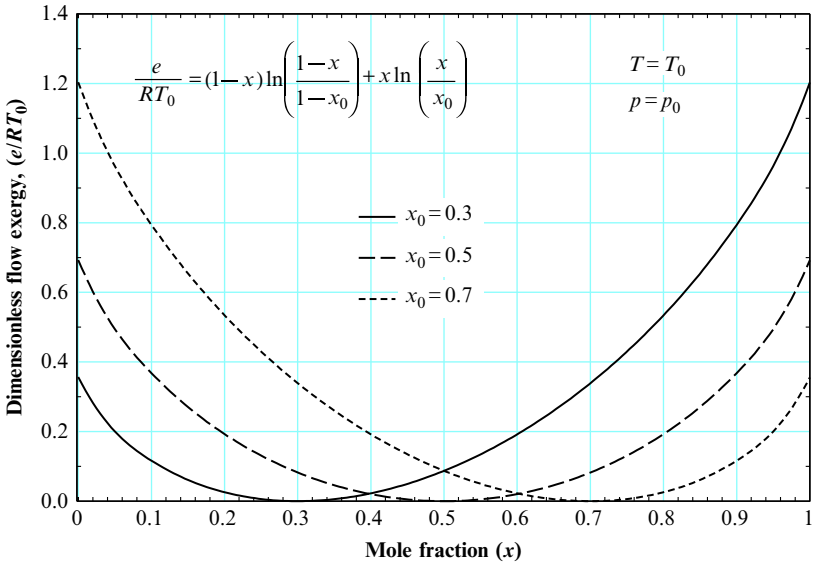

Fig. 8 Dimensionless flow exergy as a function of concentration.

We have shown mathematically that, for an ideal mixture gas, the exergy of the control mass system is always positive at any temperature, pressure, and mass concentration other than the dead state, while the exergy of a CV system (the flow exergy) may have negative values if the pressure of the system is lower than the dead state pressure. The same conclusion can be obtained for real systems using actual thermodynamic data. In the following section, the exergy and flow exergy of seawater are calculated to demonstrate the various trends.

3.2 Seawater Exergy

The correlations given in Appendix A for the thermodynamic properties of seawater are used to calculate the flow exergy of seawater. In this regard, the (environment) dead state should be specified.[6] In seawater desalination systems, the intake seawater condition of the desalination plant is usually taken as the environment dead state condition. This condition varies from place to place depending on the geographical location of the desalination plant (ambient temperature, altitude, salinity of the seawater source). In addition, the pressure of the intake seawater depends on the depth of the intake system, which varies from 5 to 50 m. Therefore the dead state pressure may change from 1 to 5 atmospheres.

[6] However, it is important to mention that the selection of the dead state does not affect the exergy difference between any two states.

The effect of changing the environmental dead state as well as the initial state on seawater flow exergy is shown in Figs. 9–11. Fig. 9 shows the specific flow exergy of seawater as it changes with the initial state temperature when the pressure and salt concentration are equal to the dead state values. As shown in this figure, the flow exergy is zero at the dead state temperature. It is always positive at any temperature other than the dead state temperature. This is true for any selected dead state temperature; therefore whenever there is a difference in temperature between the system and environment, there will be a thermal potential difference that makes the flow exergy positive.

Fig. 10 shows the specific flow exergy of seawater as it changes with the salt concentration of the initial state temperature when the pressure and temperature are equal to the dead state values. As shown in this figure, the flow exergy is always positive at any concentration other than the dead state concentration. This fact is true for any selected dead state salt concentration: whenever a concentration difference exists between the system and environment, the flow exergy is positive. For instance, if the salt concentration of the flow stream is higher than the salt concentration at the dead state, pure water can flow from the environment to the flow stream through a semipermeable membrane. This will increase the static head of the flow stream and can produce work (exergy) though a hydropower turbine [18]. The same thing will happen if the salt concentration of the flow stream is lower than that of the environmental dead state, but the flow of water in this case will be from the flow stream to the environment. This is clearly illustrated in Fig. 10, which is applicable for any selected dead state.

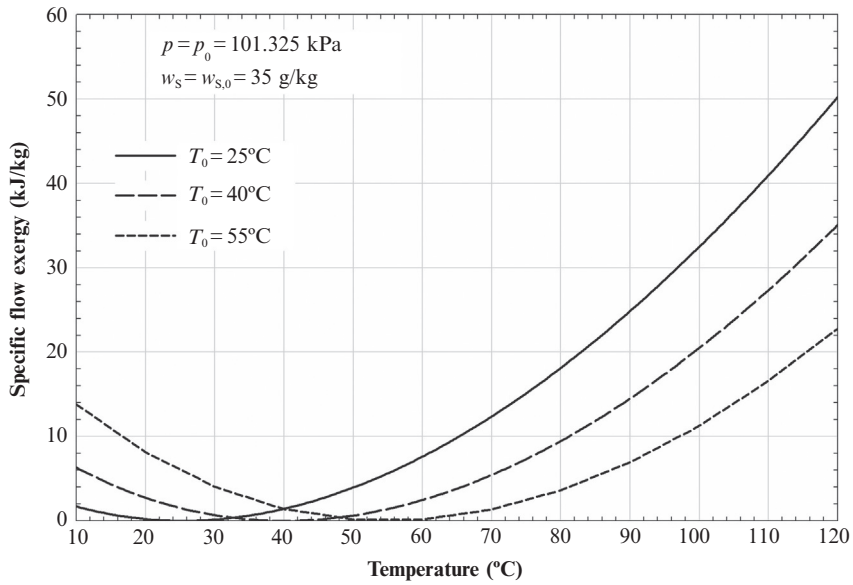

Fig. 9 Specific flow exergy of seawater as a function of temperature.

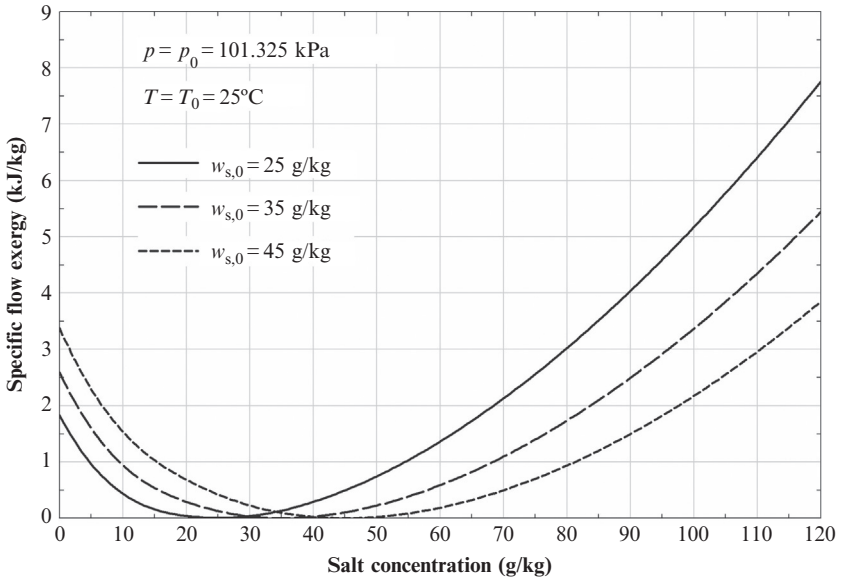

Fig. 10 Specific flow exergy of seawater as a function of salt concentration.

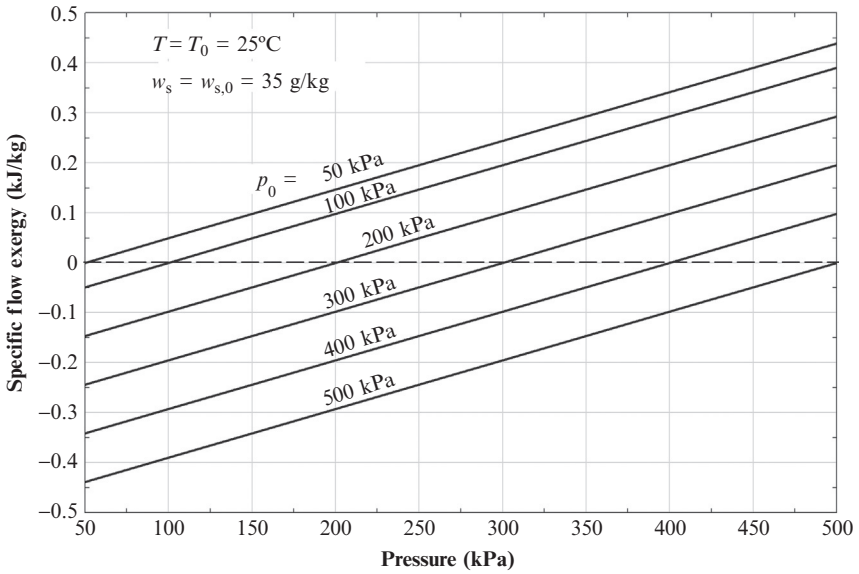

Fig. 11 Specific flow exergy of seawater as a function of pressure.

The effect of changing the dead state pressure is shown in Fig. 11. As shown in this figure, the flow exergy is zero at the dead state pressure. Flow exergy is positive at pressures higher than the dead state pressure and negative at pressures lower than the dead state pressure. In contrast, the exergy of a control mass system (closed system) is always positive, irrespective of whether the pressure is higher or lower than the dead state pressure, as shown in Fig. 12.

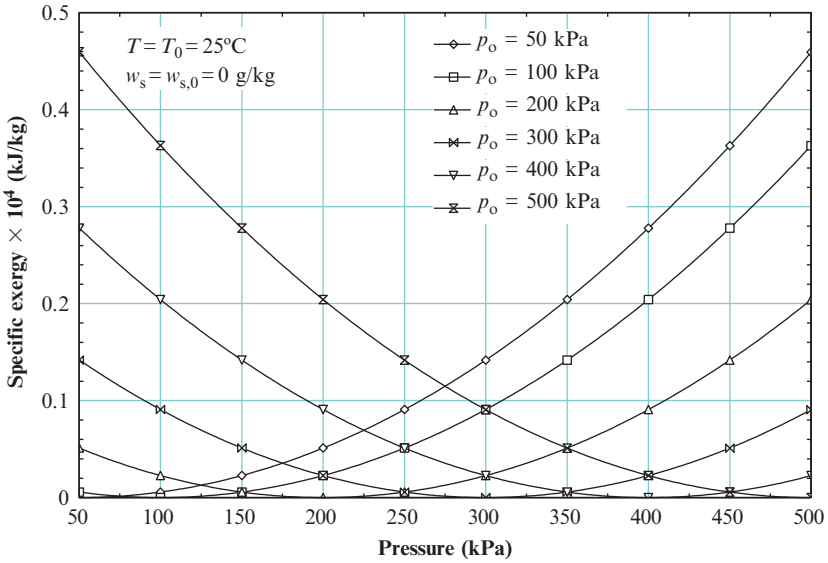

Fig. 12 Specific exergy of water as a function of pressure (closed system).

4. THERMODYNAMIC ANALYSIS OF DESALINATION PROCESSES

In this section, a consistent definition of Second Law efficiency for desalination systems based on the least work of separation is presented [19]. Additionally, the required work of separation is decomposed into the least work of separation plus the contribution from all significant sources of irreversibility within the system, and methods of evaluating the entropy generation due to specific physical processes are derived. In Section 5, these methods are applied to four common desalination systems.

4.1 Derivation of Performance Parameters for Desalination

4.1.1 Work and Heat of Separation

Consider a simple black-box separator model for a desalination system, with a separate CV surrounding it at some distance, as shown in Fig. 13. The work of separation entering the system is denoted by $\dot{W}_{sep}$ and the heat transfer into the system is $\dot{Q}$. Stream "sw" is the incoming seawater, stream "p" is pure water (product), and stream "b" is the concentrated brine. By selecting the CV sufficiently far from the physical plant, all the inlet and outlet streams enter and leave the CV at ambient temperature, T_0, and pressure, p_0. Additionally, the heat transfer, $\dot{Q}$, occurs at ambient temperature.

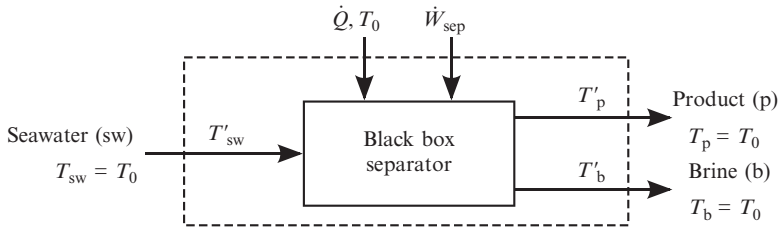

Fig. 13 When the control volume is selected suitably far away from the physical system, all inlet and outlet streams are at ambient temperature and pressure. The temperature of the streams inside the control volume, denoted by T'_i, might not be at T_0.

The logic underlying this latter formulation is that the exergy of the outlet streams attributable to thermal disequilibrium with the environment is not deemed useful. In other words, the purpose of a desalination plant is to produce pure water, not pure *hot* water. Consider separately the thermal conditions at the desalination system boundary (solid box) and the distant CV boundary (dashed box). Product and reject streams may exit the desalination system at temperatures T'_p and T'_b, different than ambient temperature, T_0. The exergy associated with these streams could be used to produce work that would offset the required work of separation. However, if the exergy associated with thermal disequilibrium is not harnessed in this way, but simply discarded, entropy is generated as the streams are brought to thermal equilibrium with the environment. This entropy generation is analyzed in Section 4.2.5. Similarly, pressure disequilibrium would result in additional entropy generation [18]. In general, differences in concentration between the various streams represent a chemical disequilibrium which could also be used to produce additional work; however, since the purpose of the desalination plant is to split a single stream into two streams of different concentrations, the outlet streams are not brought to chemical equilibrium with the environment.

The least work and least heat of separation are calculated by evaluating the First and Second Laws of Thermodynamics for the distant CV. The convention that work and heat input to the system are positive is used.

$$\dot{W}_{sep} + \dot{Q} + (\dot{m}h)_{sw} = (\dot{m}h)_p + (\dot{m}h)_b \tag{68a}$$

$$\frac{\dot{Q}}{T_0} + (\dot{m}s)_{sw} + \dot{S}_{gen} = (\dot{m}s)_p + (\dot{m}s)_b \tag{68b}$$

In Eqs. (68a), (68b), $\dot{m}_i$, h_i, and s_i are the mass flow rate, specific enthalpy, and specific entropies of the seawater (sw), product (p), and brine (b) streams. The First and Second Laws are combined by multiplying Eq. (68b) by ambient temperature, T_0, and

subtracting from Eq. (68a) while noting that the specific Gibbs free energy is, $g = h - Ts$ (all evaluated at $T = T_0$):

$$\dot{W}_{\text{sep}} = \dot{m}_{\text{p}} g_{\text{p}} + \dot{m}_{\text{b}} g_{\text{b}} - \dot{m}_{\text{sw}} g_{\text{sw}} + T_0 \dot{S}_{\text{gen}} \tag{69}$$

4.1.2 Least Work and Heat of Separation

In the limit of reversible operation, entropy generation is zero and the work of separation becomes the reversible work of separation, which is also known as the least work of separation:

$$\dot{W}_{\text{least}} \equiv \dot{W}_{\text{sep}}^{\text{rev}} = \dot{m}_{\text{p}} g_{\text{p}} + \dot{m}_{\text{b}} g_{\text{b}} - \dot{m}_{\text{sw}} g_{\text{sw}} \tag{70}$$

Eqs. (69), (70) should be evaluated using seawater properties [20].[7]

In order to gain better physical insight into the separation process, it is instructive to consider how the least work varies with recovery ratio. The recovery ratio is defined as the ratio of the mass flow rate of product water to the mass flow rate of feed seawater:

$$r \equiv \frac{\text{Product water}}{\text{Inlet seawater}} = \frac{\dot{m}_{\text{p}}}{\dot{m}_{\text{sw}}} \tag{71}$$

Using a simple mass balance ($\dot{m}_{\text{sw}} = \dot{m}_{\text{p}} + \dot{m}_{\text{b}}$) and normalizing Eq. (70) by the amount of water produced gives:

$$\frac{\dot{W}_{\text{least}}}{\dot{m}_{\text{p}}} = g_{\text{p}} + \frac{\dot{m}_{\text{sw}} - \dot{m}_{\text{p}}}{\dot{m}_{\text{p}}} g_{\text{b}} - \frac{\dot{m}_{\text{sw}}}{\dot{m}_{\text{p}}} g_{\text{sw}} = g_{\text{p}} + \left(\frac{1}{r} - 1\right) g_{\text{b}} - \frac{1}{r} g_{\text{sw}} \tag{72}$$

The Gibbs free energy of each of the streams in Eq. (72) is evaluated using seawater properties [20], as a function of temperature and salinity. Provided the inlet salinity and the product salinity is known, then the brine salinity is found using a mass balance:

$$w_{\text{s, b}} = \frac{\dot{m}_{\text{sw}} w_{\text{s, sw}} - \dot{m}_{\text{p}} w_{\text{s, p}}}{\dot{m}_{\text{b}}} = \frac{w_{\text{s, sw}}}{1 - r} - \frac{r w_{\text{s, p}}}{1 - r} \tag{73}$$

Since the least work is evaluated assuming all streams leave the CV at ambient temperature, Eq. (72) is a function of temperature, inlet salinity, product salinity, and recovery ratio.

[7] The least work should not depend on the thermodynamic frame of reference chosen for analysis. Indeed, using the Gibbs-Duhem relationship, we can show that the result we derive using a CV analysis, Eq. (70), is identical to the result obtained from a control mass (CM) approach. As $\dot{m}g = \dot{G}$, expanding Eq. (70) in terms of salt (s) and water (w) using Eq. (11) yields: $\dot{W}_{\text{least}} = \dot{G}_{\text{p}} + \dot{G}_{\text{b}} - \dot{G}_{\text{sw}} = \dot{N}_{\text{w,p}} \mu_{\text{w,p}} + \dot{N}_{\text{s,p}} \mu_{\text{s,p}} + \dot{N}_{\text{w,b}} \mu_{\text{w,b}} + \dot{N}_{\text{s,b}} \mu_{\text{s,b}} - \dot{N}_{\text{w,sw}} \mu_{\text{w,sw}} - \dot{N}_{\text{s,sw}} \mu_{\text{s,sw}}$. Rewriting the differences as integrals, $\Delta \dot{N} \mu = \int d(\dot{N} \mu)$, and considering a pure product ($d\dot{N}_{\text{s}} = 0$ and $\mu_{\text{w,p}} = \mu_{\text{w}}^{\circ}$), all remaining terms like $\dot{N} d\mu$ sum to zero by Gibbs-Duhem, Eq. (15). The result, $W_{\text{least}} = \int_{\text{sw}}^{b} RT \ln a_{\text{w}} dN_{\text{w}}$, is identical to Eq. (12) in Ref. [21], which is obtained using a CM approach.

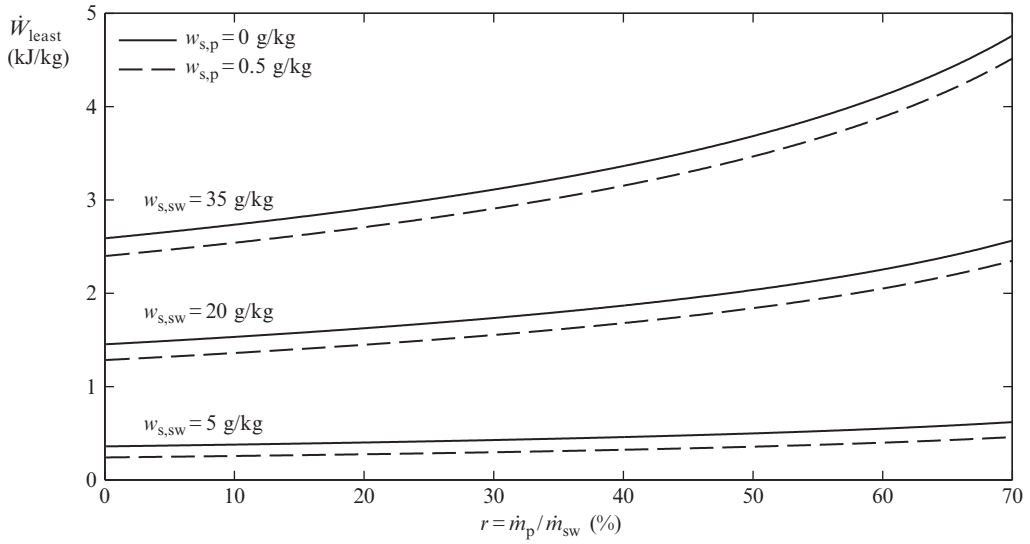

Fig. 14 The least work of separation is minimized when the recovery ratio approaches zero.

Holding temperature constant at 25°C, the least work of separation is plotted as a function of these variables in Fig. 14.[8] It is seen that regardless of inlet salinity and product salinity, the least work is minimized as the recovery ratio approaches zero. This is true in general because, in the limit of zero recovery, the only stream that experiences an energy change is the product stream. At finite recovery, work must also be provided to supply the chemical potential energy change of the brine stream due to a change in salinity. Since the least work is defined per unit mass of product, the least work represents the amount of energy necessary to create 1 kg of pure water plus the amount of energy necessary to change the chemical potential of the brine stream.

From Fig. 14, it can be seen that the least work of separation is minimized as the recovery ratio approaches zero (i.e., infinitesimal extraction).

$$\dot{W}_{least}^{min} \equiv \lim_{r \to 0} \dot{W}_{least} \tag{74}$$

Using seawater properties [20] and assuming an inlet salinity of 35 g/kg, zero salinity water product, and $T = 25°C$, the least work of separation at infinitesimal recovery is 2.59 kJ/kg.

Eq. (69) represents the amount of work required to produce a kilogram of pure water. If heat is used to power a desalination system instead of work, the heat of separation is a

[8] These curves have been updated relative to those in Ref. [19], using the newer Gibbs energy correlation in Ref. [20] rather than the older one from Ref. [22]. This has changed the values of least work at the lowest salinities.

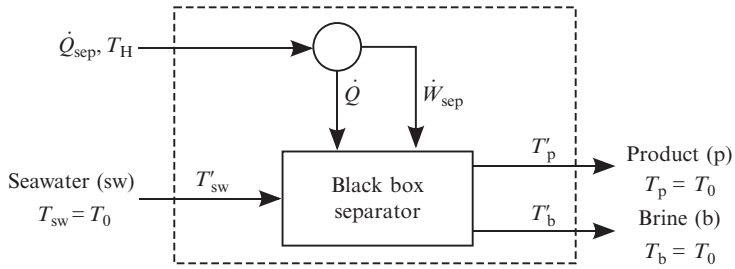

Fig. 15 Addition of a high-temperature reservoir and a Carnot engine to the control volume model shown in Fig. 13.

more relevant parameter. Recalling that heat engines produce work and reject heat, the calculation of the heat of separation is straightforward. Fig. 15 shows the CV from Fig. 13 but with a reversible heat engine providing work of separation.

If the heat is provided from a high-temperature reservoir, then the First Law for the heat engine is

$$\dot{Q}_{sep} = \dot{W}_{sep} + \dot{Q} \tag{75}$$

Assuming a reversible heat engine operating between the high-temperature reservoir at T_H and ambient temperature T_0 and considering work per unit mass produced,

$$\frac{\dot{W}_{sep}}{\dot{m}_p} = \frac{\dot{Q}_{sep}}{\dot{m}_p} - \frac{\dot{Q}}{\dot{m}_p} = \frac{\dot{Q}_{sep}}{\dot{m}_p}\left(1 - \frac{T_0}{T_H}\right) \tag{76}$$

where the second equality holds as a result of the entropy transfer that occurs in a reversible heat engine operating between two heat reservoirs. Therefore the heat of separation is

$$\frac{\dot{Q}_{sep}}{\dot{m}_p} = \frac{\dot{W}_{sep}}{\left(1 - \frac{T_0}{T_H}\right)\dot{m}_p} = \frac{\dot{W}^{rev}_{sep} + T_0\dot{S}_{gen}}{\left(1 - \frac{T_0}{T_H}\right)\dot{m}_p} \tag{77}$$

where the second equality holds by combining Eqs. (69), (70). Note that Eq. (77) can also be derived from Eqs. (68a), (68b) if $\dot{W}_{sep}$ is set to zero and the temperature in the Second Law is set to T_H [23]. Equations for the least heat of separation, $\dot{Q}_{least}$, and the minimum least heat of separation, $\dot{Q}^{min}_{least}$, can be obtained from Eq. (77) in the same manner as the corresponding work equations.

In practice, the entropy generation term in Eqs. (69), (77) often dominates over the least work or least heat. Therefore the parameter, $\dot{S}_{gen}/\dot{m}_p$, is of critical importance to the

performance of desalination systems [23]. This term is referred to as the specific entropy generation, $\mathcal{S}_{gen}$, and is a measure of entropy generated per unit of water produced:

$$\mathcal{S}_{gen} = \frac{\dot{S}_{gen}}{\dot{m}_p} \tag{78}$$

In the preceding formulation, all streams enter and exit the system at ambient temperature. Therefore the specific exergy destroyed, e_d, in the system is equal to the product of $\mathcal{S}_{gen}$ and the ambient temperature. This term is physically reflective of the same phenomenon that produces Eq. (78):

$$e_d = \frac{T_0 \dot{S}_{gen}}{\dot{m}_p} \tag{79}$$

4.1.3 Least Work of Separation for Salt Removal

Thus far we have considered the removal of water from a saline feed. But suppose we wished instead to remove salt from the feed, resulting in pure salt and pure water. The results are given for an NaCl solution, but the methodology can be applied to other mixtures.

Employing the same CV formulation we have used up to this point (see Section 2.1, Eq. 7 and Section 4.1.1, Eq. 70), the inlet stream is the feed F, and the outlet streams are the salt (product) p and the pure water stream d. When all three streams are at the same temperature and pressure, Eq. (7) applies, and

$$\dot{W}_{rev} = \dot{G}_F - \dot{G}_d - \dot{G}_p \tag{80}$$

Each $\dot{G}$ can be expanded in terms of water and salt, $\dot{G} = (\dot{N}\mu)_w + (\dot{N}\mu)_s$, but because the d and p streams are pure, $\dot{N}_{w,d} = \dot{N}_{w,F}$ and $\dot{N}_{s,p} = \dot{N}_{s,F}$, so

$$\dot{W}_{rev} = \dot{N}_{w,F}(\mu_{w,F} - \mu_{w,d}) + \dot{N}_{s,F}(\mu_{s,F} - \mu_{s,p}) \tag{81}$$

When solid and aqueous salt are in equilibrium, that is, at the solubility equilibrium, the chemical potentials of salt in the solid and aqueous phases are equal. Thus $\mu_{s,p} = \mu_s^\circ + RT \ln a_{s,p}$, where $a_{s,p}$ is the activity of the salt in a saturated solution. The d stream is pure, so $a_{w,d} = 1$, and $\mu_{w,d} = \mu_{w,d}^\circ$. Dividing the LHS side of Eq. (81) by $RT\dot{N}_{s,p}$ and the RHS by the numerically equal term $RT\dot{N}_{s,F}$, Eq. (81) reduces to

$$\frac{\dot{W}_{rev}}{RT\dot{N}_{s,p}} = \frac{1}{b_{s,F}M_w} \ln(a_{w,F}) + \ln\left(\frac{a_{s,F}}{a_{s,p}}\right) \tag{82}$$

At 25°C and atmospheric pressure, the solubility of NaCl is 6.147 mol/kg, $\gamma_{b,\pm} = 1.006$, and so $a_{s,p} = (\gamma_{b,\pm} b)^2 = 38.24$ (see Fig. 2 and [2]). For a 0.62 mol/kg NaCl solution, a rough approximation of seawater, $a_{w,F} = 0.9796$ and $a_{s,F} = 0.1734$. The least work for salt removal is thus 307 kJ/kg salt produced, or equivalently 11.1 kJ/kg water

removed—over four times the least work required to separate saltwater into brine and water! This figure is also a good approximation to the minimum energy required for zero-liquid-discharge (ZLD) seawater desalination. (In ZLD, all of the water in the seawater is converted to fresh water, so the recovery ratio is the mass fraction of water in the seawater, or about 96.5%.)

4.1.4 Second Law Efficiency

The Second Law (or exergetic) efficiency is employed as a measure of the thermodynamic reversibility of a desalination system. Unlike First Law efficiency, which measures the amount of an energy source that is put to use, Second Law efficiency, η_{II}, measures the extent of irreversible losses within a system. A completely reversible system will have a Second Law efficiency of 1 even though the First Law efficiency is likely to be lower. Bejan et al. [24] define the exergetic efficiency as the ratio of the exergy of the process products to the process fuel. In other words, the exergetic efficiency is the ratio of the useful exergy of the outputs of the process ($\dot{\Xi}_{\text{out,useful}}$) to the exergy of the process inputs ($\dot{\Xi}_{\text{in}}$):

$$\eta_{II} \equiv \frac{\dot{\Xi}_{\text{out,useful}}}{\dot{\Xi}_{\text{in}}} = 1 - \frac{\dot{\Xi}_{\text{destroyed}} + \dot{\Xi}_{\text{lost}}}{\dot{\Xi}_{\text{in}}} \tag{83}$$

The second equality in Eq. (83) is valid since the useful exergy out is equal to the exergy minus the sum of the exergy destroyed ($\dot{\Xi}_{\text{destroyed}}$) and the exergy lost ($\dot{\Xi}_{\text{lost}}$). Exergy destroyed represents lost available work due to irreversibilities within the system. Exergy lost represents lost available work due to discarding streams to the environment that carry exergy. Note that when the material inputs to the system are taken to be at equilibrium with the environment, Ξ_{in} equals Ξ_{fuel}, $\Xi_{\dot{W}_{\text{sep}}}$, or $\Xi_{\dot{Q}_{\text{sep}}}$, depending on the energy input. Additionally, Eq. (83) is equivalent to the definition used by Kahraman and Cengel [25].

Prior to applying Eq. (83) to desalination systems, it is important to understand the differences between the three definitions of work that are presented. The work of separation, $\dot{W}_{\text{sep}}$, is the actual amount of work necessary to produce a given amount of water from a fixed feed stream using a real separation process. The least work of separation, $\dot{W}_{\text{least}}$, represents the amount of work necessary to produce the same amount of product water from the feed stream while operating under reversible conditions. Finally, the minimum least work, $\dot{W}^{\text{min}}_{\text{least}}$, is the minimum required work of separation in the limit of reversible operation and infinitesimal extraction. As a result, the following relation will always hold:

$$\dot{W}_{\text{sep}} > \dot{W}_{\text{least}}(r > 0) > \dot{W}^{\text{min}}_{\text{least}}(r = 0) \tag{84}$$

In a desalination process, purified water is considered to be the useful product. The useful exergy associated with pure water is the minimum least work (or heat) of separation that is required to obtain purified water from feed water of a given salinity (i.e., infinitesimal extraction of pure water with inlet and outlet streams at ambient temperature).

The minimum least work (at zero recovery), rather than the least work (at finite recovery), is used since it represents the actual exergetic value of pure water. To further illustrate, when analyzing a unit of pure water, it is impossible to know the process that was used to produce it. Therefore the minimum energy required to produce it must be the exergetic value and $\dot{\Xi}_{\text{out,useful}} = \dot{W}^{\text{min}}_{\text{least}}(r=0)$.

Since the CV is defined so that the inlet stream is at the dead state, the only exergy input to the system comes in the form of either a work ($\dot{W}_{\text{sep}}$) or heat ($\dot{Q}_{\text{sep}}$) input (exergy of the feed stream is zero). The work of separation is equivalent to the useful work done within the system plus the exergy destroyed within that system.

In order to calculate the work of separation, two equivalent processes may be considered. The first involves a separation process where the products are brought to thermal and mechanical equilibrium with the environment, whereas the brine is also brought into chemical equilibrium (total dead state, TDS). The reversible work required to achieve this process corresponds to the least work at zero recovery. The total work of separation is given by the sum of the reversible work required plus the exergy destruction associated with entropy generated in the separation and run-down to equilibrium processes:

$$\dot{W}_{\text{sep}} = \dot{W}^{\text{min}}_{\text{least}}(r=0) + T_0 \dot{S}^{\text{TDS}}_{\text{gen}} \tag{85}$$

The second process involves a separation process where the products are only brought to thermal and mechanical equilibrium with the environment (restricted dead state, RDS). The reversible work required to achieve this process corresponds to the least work at finite recovery. The total work of separation again is given by the sum of the reversible work required plus the exergy destruction associated with entropy generated in this process:

$$\dot{W}_{\text{sep}} = \dot{W}_{\text{least}}(r>0) + T_0 \dot{S}^{\text{RDS}}_{\text{gen}} \tag{86}$$

It can be shown that Eqs. (85), (86) are equivalent.[9] Note that the work of separation for a system can also be directly evaluated using a First Law analysis.

As result, when Eq. (83) is applied to a desalination system that receives both work and heat input, it should be written as

$$\eta_{\text{II}} = \frac{\text{Least exergy of separation}}{\text{Exergy input}} = \frac{\dot{W}^{\text{min}}_{\text{least}}}{\dot{W}_{\text{sep}} + \dot{Q}_{\text{sep}}\left(1 - \dfrac{T_0}{T_{\text{H}}}\right)} \tag{87}$$

For the case of a purely work-driven system, such as reverse osmosis desalination, this becomes

[9] Substitution of $\dot{W}^{\text{min}}_{\text{least}}$ from Eq. (124) into Eq. (86) while noting that $\dot{S}^{\text{TDS}}_{\text{gen}} = \dot{S}^{\text{RDS}}_{\text{gen}} + \dot{S}^{\text{brine RDS}\rightarrow\text{TDS}}_{\text{gen}}$ exactly gives Eq. (85).

$$\eta_{\mathrm{II}} = \frac{\dot{W}_{\mathrm{least}}^{\mathrm{min}}}{\dot{W}_{\mathrm{sep}}} = \frac{\dot{W}_{\mathrm{least}}^{\mathrm{min}}}{\dot{W}_{\mathrm{least}}^{\mathrm{min}} + T_0 \dot{S}_{\mathrm{gen}}^{\mathrm{TDS}}} = \frac{\dot{W}_{\mathrm{least}}^{\mathrm{min}}}{\dot{W}_{\mathrm{least}} + T_0 \dot{S}_{\mathrm{gen}}^{\mathrm{RDS}}} \tag{88}$$

For a heat-driven system, Eq. (83) can be written in terms of the least heat of separation:

$$\eta_{\mathrm{II}} = \frac{\dot{Q}_{\mathrm{least}}^{\mathrm{min}}}{\dot{Q}_{\mathrm{sep}}} = \frac{\dot{Q}_{\mathrm{least}}^{\mathrm{min}}}{\dot{Q}_{\mathrm{least}}^{\mathrm{min}} + \left(1 - \frac{T_0}{T_{\mathrm{H}}}\right)^{-1} T_0 \dot{S}_{\mathrm{gen}}^{\mathrm{TDS}}} = \frac{\dot{Q}_{\mathrm{least}}^{\mathrm{min}}}{\dot{Q}_{\mathrm{least}} + \left(1 - \frac{T_0}{T_{\mathrm{H}}}\right)^{-1} T_0 \dot{S}_{\mathrm{gen}}^{\mathrm{RDS}}} \tag{89}$$

Clearly, the two definitions of Second Law efficiency presented in Eqs. (88), (89) are bounded by 0 and 1 because $\dot{W}_{\mathrm{sep}} > \dot{W}_{\mathrm{least}}$ and $\dot{Q}_{\mathrm{sep}} > \dot{Q}_{\mathrm{least}}$. Observe that $\dot{W}_{\mathrm{least}}$ and $\dot{Q}_{\mathrm{least}}$ are functions of feed salinity, product salinity, recovery ratio, and T_0. Additionally, η_{II} will only equal 1 in the limit of completely reversible operation, as expected. Note that the selection of the CV suitably far away such that all streams are at thermal and mechanical equilibrium allows for this bounding.

Three relevant Second Law-based performance parameters for desalination systems have been discussed thus far: specific entropy generation, Eq. (78); specific exergy destruction, Eq. (79); and Second Law efficiency, Eqs. (88), (89). This section will focus on specific entropy generation and Second Law efficiency.

4.1.5 Energetic Performance Parameters

Three often-used parameters are key to describing the energetic performance of desalination systems. The first, called gained output ratio (GOR), is the ratio of the enthalpy required to evaporate the distillate (or equivalently, the energy release in condensation) and the heat input to the system, or

$$\mathrm{GOR} \equiv \frac{\dot{m}_{\mathrm{p}} h_{\mathrm{fg}}(T_0)}{\dot{Q}_{\mathrm{sep}}} \tag{90}$$

In essence, GOR is a measure of how many times the latent heat of vaporization is captured in the condensation of pure water vapor and reused in a subsequent evaporation process to create additional pure water vapor from a saline source. By the First Law of Thermodynamics, a thermal desalination system that has no such heat recovery requires at least the latent heat of vaporization multiplied by the mass of pure water produced as its energy input: its GOR is approximately one (or less when feed heating and heat losses are taken into account). It is important to note that Eq. (90) is valid as written only for a desalination system driven by heat; that is, a thermal desalination system. A work-driven desalination system, in contrast, uses electricity or shaft work to drive the separation process. Normally, this work is produced by a thermal process, such as a heat engine. Thus to evaluate the heat input required for a work-driven desalination system, a First Law efficiency of the process that produces the work of separation must be known.

The second parameter, known as the performance ratio (PR), is defined as the ratio of the mass flow rate of product water to that of the heating steam:

$$\mathrm{PR} \equiv \frac{\dot{m}_\mathrm{p}}{\dot{m}_\mathrm{s}} \tag{91}$$

For a thermal desalination system in which the heat input is provided by condensing steam, as is typical of large-scale thermal processes such as MED and MSF, the values of PR and GOR are quite similar. In that case, the two parameters differ only by the ratio of the latent heat of vaporization at the distillate and heating steam temperatures. That is, $\mathrm{GOR} = \mathrm{PR} \times \dfrac{h_\mathrm{fg}(T_0)}{h_\mathrm{fg}(T_\mathrm{steam})}$. (Some authors interchange these definitions of GOR and PR.)

The third parameter, specific electricity consumption (SEC), is best suited to work-driven desalination systems. It is defined as the ratio of the work of separation (or work input) to the mass flow rate of product water, or

$$\mathrm{SEC} \equiv \frac{\dot{W}_\mathrm{sep}}{\dot{m}_\mathrm{p}} \tag{92}$$

As was the case with GOR, because thermal and electrical energy are not directly comparable, numerical values of SEC cannot be compared between thermal- and work-driven systems. SEC as defined by Eq. (92) should only be used for desalination systems driven by work.

4.2 Analysis of Entropy Generation Mechanisms in Desalination

Several common processes in desalination systems result in entropy generation, including heat transfer, pressure differentials, and nonequilibrium conditions. By utilizing the ideal gas and incompressible fluid models, simple expressions are derived to show the important factors in entropy generation for various physical processes. Physical properties, evaluated at a representative reference state of 50°C, are provided in Table 3 for pure

Table 3 Representative values of reference state constants for Eqs. (94a), (94b), (96a), (96b)

Pure water and vapor constants, T_sat = 50°C, p_sat = 12.3 kPa				
c	4.18 kJ/kg K		h°_IG	2590 J/kg
c_p	1.95 kJ/kg K		h°_IF	209 J/kg
R	0.462 kJ/kg K		s°_IG	8.07 J/kg K
v	1.01×10^{-3} m^3/kg		s°_IF	0.704 kJ/kg K
Seawater constants, 50°C, 35,000 mg/kg				
c	4.01 kJ/kg K		h°_IF	200 J/kg
v	0.986×10^{-3} m^3/kg		s°_IF	0.672 kJ/kg K

water [26] and seawater [22]. Proper selection of the reference state is discussed below. In all equations in this section, states 1 and 2 are the inlet and outlet states, respectively, for each process.

Before analyzing the entropy generation mechanisms, the ideal gas and incompressible fluid models are discussed. By definition, the density of an incompressible fluid does not vary, and the specific heat capacities at constant pressure and constant volume are the same ($c_p = c_v = c$). As a result, an incompressible fluid is one which satisfies the following equations:

$$dh_{IF} = c\,dT + v\,dp \tag{93a}$$

$$ds_{IF} = c\frac{dT}{T} \tag{93b}$$

Integrating Eqs. (93a), (93b) from an arbitrary reference state to the state of interest while assuming constant specific heat (c) yields the following expressions:

$$h_{IF} = c(T - T^{\circ}) + v(p - p^{\circ}) + h^{\circ}_{IF} \tag{94a}$$

$$s_{IF} = c\,\ln\frac{T}{T^{\circ}} + s^{\circ}_{IF} \tag{94b}$$

Similarly, an ideal gas follows the equation of state, $pv = RT$, and is governed by the following equations:

$$dh_{IG} = c_p dT \tag{95a}$$

$$ds_{IG} = c_p\frac{dT}{T} - R\frac{dp}{p} \tag{95b}$$

Integrating Eqs. (95a), (95b) from an arbitrary reference state to the state of interest while assuming constant specific heat at constant pressure, c_p, yields the following expressions:

$$h_{IG} = c_p(T - T^{\circ}) + h^{\circ}_{IG} \tag{96a}$$

$$s_{IG} = c_p\,\ln\frac{T}{T^{\circ}} - R\,\ln\frac{p}{p^{\circ}} + s^{\circ}_{IG} \tag{96b}$$

For increased accuracy, the generalized compressibility model, $pv = ZRT$ can be used instead if R is replaced with ZR in Eqs. (95a), (95b), (96a), (96b) and all future equations.

When evaluating Eqs. (94a), (94b), (96a), (96b), the physical properties (specific heat, volume, compressibility factor, etc.) and reference values of enthalpy and entropy should be evaluated at a suitable reference state. The reference state should be selected as the saturated state corresponding to the average temperature between the inlet and outlet streams. Representative values of these constants, evaluated for pure water [26] at 50°C, are provided in Table 3. For seawater, the average salinity should be used. Representative values of these constants, evaluated for seawater [22] at 50°C and 35 g/kg, are

also provided in Table 3. It should be noted that the specific heat of seawater is significantly lowered with increasing salinity. Therefore these approximations should not be used for processes in which composition substantially changes. Instead, Gibbs free energy should be used (Section 4.2.6).

4.2.1 Flashing

When liquid water near saturation conditions passes through a throttle, a portion will vaporize as a result of the pressure drop through the device. The exiting fluid is thus a mixture of liquid and low pressure vapor and can be modeled as an incompressible fluid and ideal gas, respectively. Application of the First and Second Laws to the flash box (throttle) CV reduces to

$$h_{1,\mathrm{IF}} = h_2 = (1-x)h_{2,\mathrm{IF}} + xh_{2,\mathrm{IG}} \tag{97a}$$

$$s_{\mathrm{gen}}^{\mathrm{flashing}} = s_2 - s_1 = \left[(1-x)s_{2,\mathrm{IF}} + xs_{2,\mathrm{IG}}\right] - s_{1,\mathrm{IF}} \tag{97b}$$

Substitution of Eqs. (94a), (94b), (96a), (96b) into Eqs. (97a), (97b) with simplification gives the quality and entropy generation due to flashing.

The entropy generated in this process is

$$\begin{aligned} s_{\mathrm{gen}}^{\mathrm{flashing}} = c\,\ln\frac{T_2}{T_1} + x\Big\{&(c_{\mathrm{p}}-c)\,\ln T_2 - R\,\ln p_2 \\ &+\left[s_{\mathrm{IG}}^{\circ} - s_{\mathrm{IF}}^{\circ} - (c_{\mathrm{p}}-c)\,\ln T^{\circ} + R\,\ln p^{\circ}\right]\Big\} \end{aligned} \tag{98}$$

where the quality, x, is given by

$$x = \frac{c(T_1 - T_2) + v(p_1 - p_2)}{(c_{\mathrm{p}}-c)\,T_2 - vp_2 + \left[h_{\mathrm{IG}}^{\circ} - h_{\mathrm{IF}}^{\circ} - (c_{\mathrm{p}}-c)\,T^{\circ} + vp^{\circ}\right]} \tag{99}$$

and c_{p} is the specific heat at constant pressure, c is the specific heat of an incompressible fluid, R is the ideal gas constant for steam, v is the specific volume of the liquid, h_{IG}° and s_{IG}° are the enthalpy and entropy for steam at the reference state, and h_{IF}° and s_{IF}° are the enthalpy and entropy for liquid water at the reference state.

4.2.2 Flow Through an Expansion Device Without Phase Change

Although the physical causes for pressure drops differ when considering flow through expanders, pipes, throttles, membranes, and other flow constrictions, the CV equations that govern the entropy generated remains constant. As with the analysis of the flashing case, the First and Second Laws for an isenthalpic process simplify to

$$w = \frac{\dot{W}}{\dot{m}} = h_2 - h_1 \tag{100a}$$

$$s_{\mathrm{gen}} = s_2 - s_1 \tag{100b}$$

For an expansion device, the isentropic efficiency, η_e, is defined as

$$\eta_e \equiv \frac{w}{w^s} = \frac{h_2 - h_1}{h_2^s - h_1} \tag{101}$$

where w is the work produced per unit mass through the device, and w^s is the work produced assuming isentropic expansion.

For entropy generation in the expansion of an incompressible fluid, Eq. (94b) shows that for an isentropic expansion from p_1 to p_2, $T_2^s = T_1$. Combining this result with Eqs. (94a), (100a), (101) and solving for T_2 gives

$$T_2 = T_1 + \frac{v}{c}(p_1 - p_2)(1 - \eta_e) \tag{102}$$

Substitution of Eqs. (94b), (102) into Eq. (100b) yields the entropy generated due to irreversible expansion of an incompressible fluid:

$$s_{gen}^{expansion,IF} = c \ln\left[1 + \frac{v}{cT_1}(p_1 - p_2)(1 - \eta_e)\right] \approx \frac{v}{T_1}(p_1 - p_2)(1 - \eta_e) \tag{103}$$

In the limit of a completely irreversible pressure drop (such as through a throttle) in which no work is generated, $\eta_e = 0$ and Eq. (103) reduces to

$$s_{gen}^{\Delta p,IF} = c \ln\left[1 + \frac{v}{cT_1}(p_1 - p_2)\right] \approx \frac{v}{T_1}(p_1 - p_2) \tag{104}$$

For entropy generation in the expansion of an ideal gas, Eq. (96b) shows that for an isentropic expansion from p_1 to p_2,

$$T_2^s = T_1\left(\frac{p_2}{p_1}\right)^{R/c_p}$$

Combining this result with Eqs. (96a), (100a), (101) and solving for T_2 gives

$$T_2 = T_1\left\{1 + \eta_e\left[\left(\frac{p_2}{p_1}\right)^{R/c_p} - 1\right]\right\} \tag{105}$$

Substitution of Eqs. (96b), (105) into Eq. (100b) yields the entropy generated due to irreversible expansion of an ideal gas:

$$s_{gen}^{expansion,IG} = c_p \ln\left\{1 + \eta_e\left[\left(\frac{p_2}{p_1}\right)^{R/c_p} - 1\right]\right\} - R \ln\frac{p_2}{p_1} \tag{106}$$

In the limit of a completely irreversible pressure drop (such as through a throttle) in which no work is generated, $\eta_e = 0$ and Eq. (106) reduces to

$$s_{gen}^{\Delta p,IG} = -R \ln\frac{p_2}{p_1} \tag{107}$$

Based on Eqs. (104), (107), for an incompressible fluid, entropy generation is determined by the pressure difference, whereas for an ideal gas, it is determined by the pressure ratio.

4.2.3 Pumping and Compressing

Application of the First and Second Laws to a pump (or compressor) CV yields Eqs. (100a), (100b). For pumping and compressing, the isentropic efficiency, η_p, is defined as

$$\eta_p \equiv \frac{w^s}{w} = \frac{h_2^s - h_1}{h_2 - h_1} \tag{108}$$

For entropy generation in pumping, assume that the liquid can be modeled as an incompressible fluid. Eq. (94b) shows that for an isentropic expansion from p_1 to p_2, $T_2^s = T_1$. Combining this result with Eqs. (94a), (100a), (108) and solving for T_2 gives

$$T_2 = T_1 + \frac{v}{c}(p_2 - p_1)\left(\frac{1}{\eta_p} - 1\right) \tag{109}$$

Substitution of Eqs. (94b), (109) into Eq. (100b) yields the entropy generated due to irreversible pumping:

$$s_{gen}^{pumping} = c \ln\left[1 + \frac{v}{cT_1}(p_2 - p_1)\left(\frac{1}{\eta_p} - 1\right)\right] \approx \frac{v}{T_1}(p_2 - p_1)\left(\frac{1}{\eta_p} - 1\right) \tag{110}$$

The entropy generated due to irreversible pumping can also be derived by noticing that the difference between the actual work and the reversible work is simply the exergy destruction. Since irreversibilities during the compression process of an incompressible fluid will result in only minor changes in temperature (i.e., $T_2 \approx T_1$), the entropy generation can be determined by dividing the exergy destruction by the inlet temperature in accordance with Gouy-Stodola theorem [16]:

$$\begin{aligned} s_{gen}^{pumping} &= \frac{\Xi_d}{T_1} = \frac{w - w^s}{T_1} = \frac{h_2 - h_2^s}{T_1} = \frac{h(T_2, p_2) - h(T_1, p_2)}{T_1} \\ &= \frac{v}{T_1}(p_2 - p_1)\left(\frac{1}{\eta_p} - 1\right) \end{aligned} \tag{111}$$

Note that Eq. (111) is simply the Taylor series expansion of the second term of Eq. (110). This alternate derivation is only appropriate because the pumping process is nearly isothermal.

For entropy generation in vapor compression, assume that both the inlet and outlet vapor can be modeled as an ideal gas that follows the generalized compressibility form. Eq. (96b) shows that for an isentropic expansion from p_1 to p_2,

$$T_2^s = T_1 \left(\frac{p_2}{p_1}\right)^{R/c_p}$$

Combining this result with Eqs. (96a), (100a), (108) and solving for T_2 gives

$$T_2 = T_1 \left\{ 1 - \frac{1}{\eta_p} \left[1 - \left(\frac{p_2}{p_1}\right)^{R/c_p} \right] \right\} \tag{112}$$

Substitution of Eqs. (96b), (112) into Eq. (100b) yields the entropy generated due to irreversible compression:

$$s_{gen}^{compression} = c_p \ln \left\{ 1 - \frac{1}{\eta_p} \left[1 - \left(\frac{p_2}{p_1}\right)^{R/c_p} \right] \right\} - R \ln \frac{p_2}{p_1} \tag{113}$$

Note that unlike in the incompressible fluid case, Eq. (113) cannot be derived through the use of the Gouy-Stodola theorem since the compression of a gas is not an isothermal process.

4.2.4 Approximately Isobaric Heat Transfer Process

Actual heat exchangers always have a pressure drop associated with viscous forces. However, without knowledge of specific flow geometry or the local temperature and pressure fields, it is impossible to partition entropy generation according to particular transport phenomena. For example, Bejan [27] has shown that for a simple, single-fluid heat exchanger, comparing the trade-off between entropy generation due to heat transfer across a finite temperature difference and pressure drop across a finite flow volume yields a thermodynamically optimal heat exchanger geometry.

In heat exchangers within typical desalination processes, however, the effect of pressure drop on physical properties is insignificant. Thus entropy generation may be calculated as a function of terminal temperatures alone. For the range of temperatures and flow configurations encountered in the present analysis, this approximation holds for fluids that may be modeled as both ideal gases and incompressible fluids.

The entropy generation equation for a heat exchanger is

$$\dot{S}_{gen}^{HX} = [\dot{m}(s_2 - s_1)]_{stream\,1} + [\dot{m}(s_2 - s_1)]_{stream\,2} \tag{114}$$

In the case of a device that transfers heat at a relatively constant pressure, an approximate expression may be developed for entropy generation as a function of inlet and outlet temperatures alone. Entropy may be written as

$$ds = \frac{1}{T} dh - \frac{v}{T} dp \tag{115}$$

Integrating Eq. (115) at constant pressure gives

$$s_2 - s_1 = \int_1^2 \frac{1}{T} dh \tag{116}$$

For an ideal gas, Eq. (115) is written as Eq. (95b), which can be integrated at constant pressure to give

$$s_2 - s_1 = c_p \ln \frac{T_2}{T_1} \tag{117}$$

For an incompressible fluid, entropy is not a function of pressure as seen in Eq. (93b). Therefore the entropy difference is given by

$$s_2 - s_1 = c \ln \frac{T_2}{T_1} \tag{118}$$

If it is now assumed that the heat exchanger is adiabatic with respect to the environment and that there is no work, then the preceding equations can be substituted into Eq. (114).

For an isobaric phase change from a saturation state (either liquid or vapor), the entropy change is

$$s_2 - s_1 = x s_{fg} = x(s_{IG} - s_{IF}) \quad \text{for evaporation} \tag{119a}$$

$$= (x-1)s_{fg} = (x-1)(s_{IG} - s_{IF}) \quad \text{for condensation} \tag{119b}$$

where x is the quality at the exit of the process.

4.2.5 Thermal Disequilibrium of Discharge Streams

Referring again to Fig. 13, the entropy generated in bringing outlet streams from the system CV to the ambient temperature reached at the exit of the distant CV may be calculated. Consider a stream that is in mechanical, but not thermal equilibrium, with the environment (Fig. 16). The environment acts as a heat reservoir, and through an irreversible heat transfer process, the stream is brought to thermal equilibrium.

The First and Second Laws for this CV give

$$\dot{Q} = \dot{m}_i(h_i - h_i') \tag{120a}$$

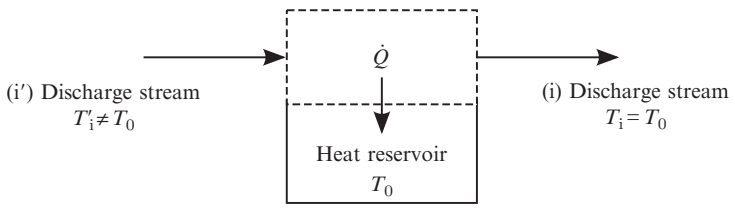

Fig. 16 Entropy is generated in the process of a stream reaching thermal equilibrium with the environment.

$$\dot{S}_{\text{gen}} = \dot{m}_i \left[(s_i - s_i') - \frac{\dot{Q}}{T_0} \right] = \dot{m}_i \left[(s_i - s_i') - \frac{h_i - h_i'}{T_0} \right] \tag{120b}$$

For incompressible fluids at mechanical equilibrium with the environment, $s_i - s_i' = c_i \ln \frac{T_0}{T_i}$ and $h_i - h_i' = c_i(T_0 - T_i)$. Substituting into Eq. (120b) gives the entropy generated in bringing a stream of incompressible fluid to thermal equilibrium with the environment:

$$\dot{S}_{\text{gen}}^{T \text{ disequilibrium}} = \dot{m}_i c_i \left[\ln\left(\frac{T_0}{T_i}\right) + \frac{T_i}{T_0} - 1 \right] \tag{121}$$

4.2.6 Chemical Disequilibrium of Concentrate Stream

When considering a desalination system, the concentrate is typically considered to be waste and is discharged back to the ocean. Since the concentrate is at higher salinity than the ocean, entropy is generated in the process of restoring the concentrate to chemical equilibrium (also called distributive equilibrium) with the seawater. This entropy generation can be calculated in one of two ways.

First, consider the addition of the concentrate stream at the RDS to a large reservoir of seawater at the TDS. An exergy balance governing the mixing of the concentrate stream with the seawater reservoir is written as:

$$\dot{\Xi}_{\text{destroyed}}^{\text{mixing}} = -[(\dot{m}_c + \dot{m}_{\text{sw}}^{\text{reservoir}})g_{\text{out}} - \dot{m}_c g_c - \dot{m}_{\text{sw}}^{\text{reservoir}} g_{\text{sw}}] \tag{122}$$

where $\dot{\Xi}_{\text{destroyed}}^{\text{mixing}}$ is the exergy destroyed as a result of irreversible mixing. In the limit that $\dot{m}_c / \dot{m}_{\text{sw}}^{\text{reservoir}} \to 0$, the mixed state g_{out} approaches g_{sw} and the concentrate stream is brought to chemical equilibrium with the environment. Using the Gouy-Stodola theorem [16], the exergy destroyed due to irreversible mixing can be used to evaluate the entropy generated as the concentrate stream runs down to chemical equilibrium:

$$\dot{S}_{\text{gen}}^{\text{concentrate RDS}\to\text{TDS}} = \frac{\dot{\Xi}_{\text{destroyed}}^{\text{mixing}}}{T_0} \tag{123}$$

The mixing process described by Eq. (122) is analogous to the separation process shown in Fig. 13 performed in reverse.

A second method to evaluate the entropy generation due to chemical disequilibrium of the concentrate stream is based on the least work of separation. When considering the CV given by Fig. 13 and the minimum least work of separation, there is an infinitesimally small product stream of pure water along with a stream of concentrate of salinity that is infinitesimally above that of seawater. Therefore the concentrate stream is in thermal, mechanical, and nearly chemical equilibrium with the environment. If, however, there is a finite recovery ratio, the concentrate stream salinity is greater than that of seawater.

Additionally, as the recovery ratio increases, the flow rate of the concentrate stream decreases and flow rate of the product water increases (assuming fixed input feed rate). Since the concentrate stream is not at equilibrium with the environment, there is a chemical potential difference that can be used to produce additional work. This additional work is exactly equal to the difference between the least work of separation, Eq. (70), and the minimum least work of separation, Eq. (74). When the concentrated concentrate is discarded to the ocean, this work potential is lost. Therefore, entropy generation due to chemical disequilibrium of the concentrate stream can also be evaluated through the use of the Gouy-Stodola theorem, as follows:

$$T_0 \dot{S}_{\text{gen}}^{\text{concentrate RDS}\rightarrow\text{ TDS}} = \dot{W}_{\text{least}}(r>0) - \dot{W}_{\text{least}}^{\min}(r=0) \tag{124}$$

Evaluation of entropy generation using Eqs. (123), (124) gives equivalent results.

5. ENTROPY GENERATION MECHANISMS IN SEAWATER DESALINATION TECHNOLOGIES

Using the methods developed in preceding section, the component and system level entropy production and Second Law efficiency of several common seawater desalination technologies are now evaluated. Four simple examples of common systems are considered: forward feed, multiple effect distillation (MED); direct contact membrane distillation (DCMD); single effect mechanical vapor compression (MVC); and single-stage reverse osmosis (RO). These examples serve to illustrate the application of the models and methods to both thermally driven and work-driven desalination processes. These analyses may alternatively be done using the flow exergy function described in Section 3.

5.1 Multiple Effect Distillation

A very simple model based on approximations from Mistry et al. [28], El-Sayed and Silver [29], Darwish et al. [30], and El-Dessouky and Ettouney [31] is used to generate all the temperature profiles and mass flow rates within a forward feed (FF) multiple effect distillation (MED) cycle (Fig. 17).

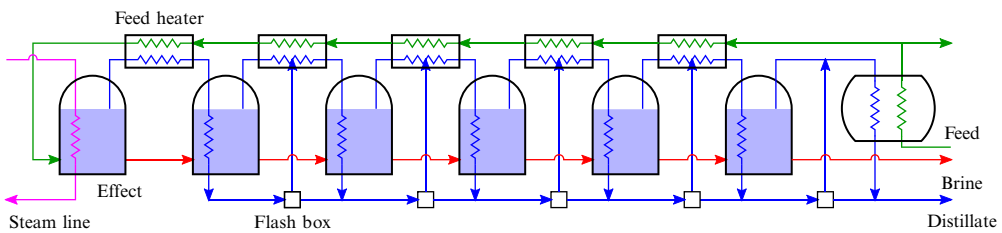

Fig. 17 A typical flow path for a forward feed multiple effect distillation system.

Several common approximations are made: The temperature drop between effects is assumed to be constant, $\Delta T = (T_{\text{steam}} - T_{\text{last effect}})/n$. Additionally, the driving temperature difference between condensing vapor and evaporating brine and the temperature rise across feed heaters are both taken to be ΔT. The temperature rise in the condenser is set to 10°C.

The distillate is approximated as pure water, and it is assumed that distillate is produced in each effect (D_i) at a rate of 99% of that produced in the previous effect (i.e., $D_{i+1} = 0.99D_i$) to approximate the effect of increasing latent heat with decreasing effect temperature. Distillate produced from flashing in each effect is given by $D_{\text{f},i} = \dot{m}_{\text{b},i-1} c_{\text{p},i} \Delta T / h_{\text{fg},i}$, where $m_{\text{b},\ i-1}$ is the brine from the previous effect, which becomes the feed to the current effect. The remainder of the distillate is produced from boiling in the effect. There is no flashing in the first effect. Distillate produced from flashing in the flash boxes is given by $D_{\text{fb},i} = \sum_{j=1}^{i-1} D_j c_{\text{p},i} \Delta T / h_{\text{fg},i}$, for $i \geq 2$. The quality of the distillate leaving the feed heater is calculated using an energy balance on the heater, $\dot{m}_{\text{F}} c_{\text{p},i} \Delta T = (D_i + D_{\text{fb},i})(1 - x_i) h_{\text{fg}}$, where $\dot{m}_{\text{F}}$ is the mass flow rate of the feed seawater.

Water and salinity mass balances for the effects are

$$\dot{m}_{\text{b},i-1} = D_i + \dot{m}_{\text{b},i} \tag{125}$$

$$\dot{m}_{\text{b},i-1} w_{\text{s,b},i-1} = \dot{m}_{\text{b},i} w_{\text{s,b},i} \tag{126}$$

where $w_{\text{s,b},i}$ is the salinity of the ith brine stream.

An energy balance on the first effect gives the required amount of heating steam: $\dot{m}_s h_{\text{fg},s} = D_1 h_{D,1} + \dot{m}_{\text{b},1} h_{\text{b},1} - \dot{m}_{\text{F}} h_{\text{F}}$. Accurate properties for seawater [22] and steam [26], including enthalpies, entropies, specific heats, and so on, are used and evaluated at each state.

The inputs to the simplified MED FF model with six effects include: 1 kg/s of distillate, seawater salinity of 42 g/kg, maximum salinity of 70 g/kg, steam temperature of 70°C, last effect temperature of 40°C, and seawater (and environment) temperature of 25°C.

Using the preceding approximations and inputs, all thermodynamic states for the MED FF system are found. Entropy generation in each component is computed by using a CV for each component. Pumping work and entropy generated due to flashing in effects are evaluated using Eqs. (98), (110), respectively.

Fig. 18 shows the entropy generated in each component, whereas Fig. 19 shows the percentage of entropy generated in each type of component. Entropy generated during pumping is not included in the figure since it is much less than 1% of the overall amount. Looking at Fig. 19, it is clear that heat transfer is the dominant source of entropy generation in MED systems since most of the generation occurs in the heat exchange devices (effects, feed heaters, and condenser). It was found that entropy generated due to flashing in the effects was very small.

Although the effects result in the greatest portion of the entropy generated, it is important to note that the condenser is the single greatest source of irreversibility, as seen

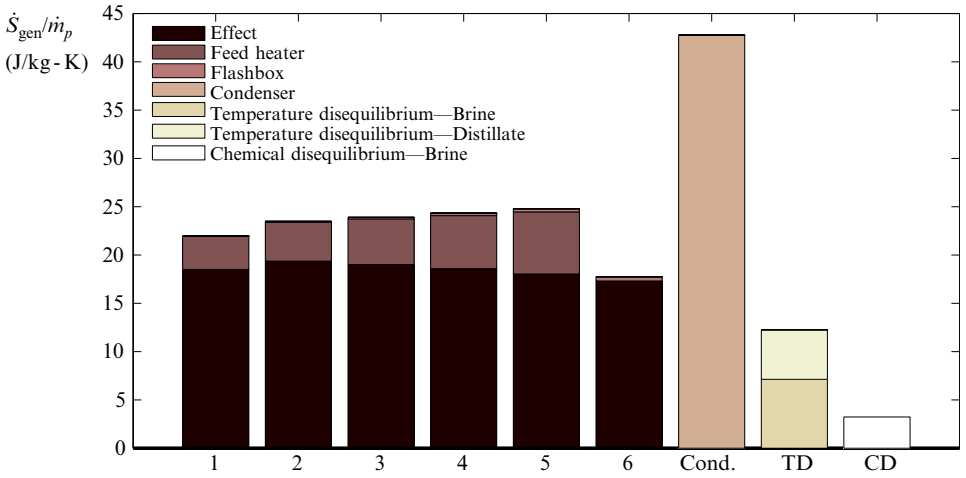

Fig. 18 Entropy production in the various components of a six-effect forward feed multiple effect distillation system.

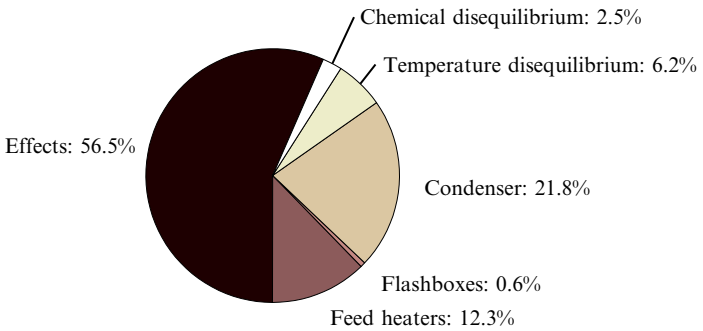

Fig. 19 Relative contribution of sources of entropy generation in a forward feed multiple effect distillation system. Irreversibilities in the effects dominate. Total specific entropy generation is 196 J/kg-K.

in Fig. 18. The condenser is such a large source of entropy generation as a result of the large temperature difference between the condensed vapor and the cooling water or feed stream.

Many modern MED plants operate using a thermal vapor compressor (TVC). The TVC is used to entrain the vapor from the final effect and reinject it into the first effect. MED-TVC plants have much higher performance ratios than non-TVC plants, and they reduce the size of the final condenser, thus reducing this large source of irreversibilities. It is important to note, however, that the TVC is also a highly irreversible device so that total entropy production may not be reduced as much.

Finally, it is seen that for this MED plant, entropy generated as a result of the nonequilibrium discharge of the brine and distillate corresponds to approximately 8.7% of the plant's overall losses. The Second Law efficiency, accounting for disequilibrium of the discharge, is $\eta_{II} = 5.9\%$. Additionally, PR = 5.2 and GOR = 5.4.

5.2 Direct Contact Membrane Distillation

DCMD is a membrane-based thermal distillation process in which heated feed passes over a hydrophobic microporous membrane [32]. The membrane holds back a meniscus of water near the pores. On the opposing side, cooled fresh water passes over the membrane. The temperature difference between the water streams induces a vapor pressure difference that drives evaporation through the pores. This can be described in terms of a vapor pressure difference multiplied by a membrane distillation coefficient B, which represents the diffusion resistance through the pores. It is based on material properties and pore geometry, and depends weakly on temperature and is assumed to be constant for this calculation. On the feed side, boundary layers in concentration, temperature, and momentum are present, with corresponding diffusional transport of heat and mass. On the cooler fresh water side, there is condensation of vapor and warming of the fresh water, with boundary layer processes similar to those on the feed side. DCMD has been successfully used to produce fresh water at small scale (0.1 m^3/day) [33–36].

A transport process model for DCMD based on validated models by Bui et al. [37] and Lee et al. [36] was implemented to obtain the permeate flux and outlet temperatures of a DCMD module. The calculation of system performance used heat transfer coefficients calculated from correlations based on module geometry [38]. While the Bui et al. [37] model used a hollow-fiber membrane configuration, the present calculations are done for a flat-sheet configuration. Membrane geometry and operating conditions are taken from some pilot-sized plants the literature [39, 40]. Seawater enters the system at 27°C and 35,000 mg/kg total dissolved solids at a mass flow rate of 1 kg/s. The inlet feed is preheated to a constant temperature of 85°C, and the required heat is provided by a 90°C source. The permeate side contains fresh water with an inlet flow rate of 1 kg/s. The resulting recovery ratio for this system is 4.4%. The regenerator is a liquid-liquid heat exchanger with a terminal temperature difference of 3 K. The pressure drop through the thin channel in the membrane module was found to be the dominant pressure drop in the system and was the basis for calculating the entropy generation due to pumping power. Properties for seawater [22] were used in the calculation. A schematic diagram of the system is shown in Fig. 20, with module geometry and constants shown.

Entropy generation was calculated for each component in the system by using a CV analysis. Fig. 21 shows the breakdown of entropy generation in each component.

The greatest source of entropy generation is the module. This is owed mostly to diffusion through the pores and to a lesser extent heat conduction losses, as only a thin

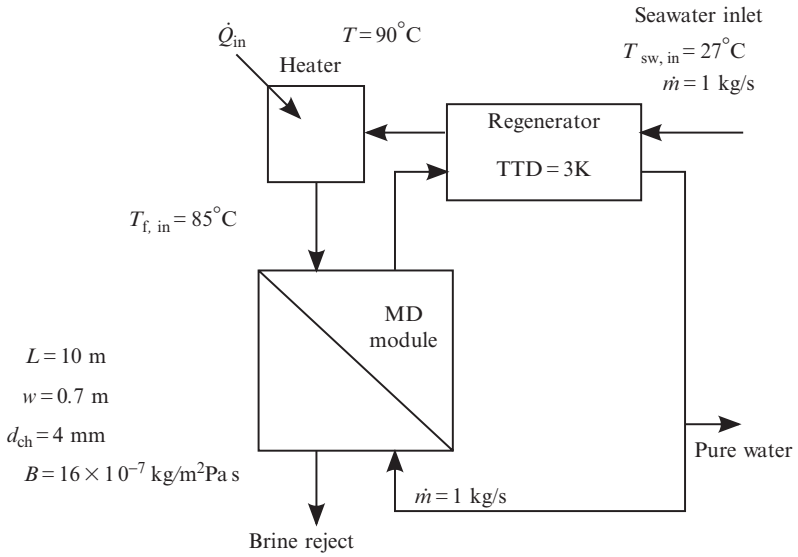

Fig. 20 Flow path for a basic direct contact membrane distillation system.

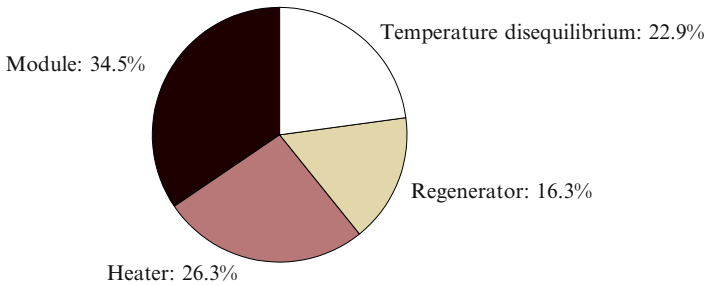

Fig. 21 Relative contribution of sources of entropy generation in a direct contact membrane distillation system. Total specific entropy generation is 925.4 J/kg-K.

membrane separates the cold and hot streams in the module. The small pore size contributes substantially to the diffusion resistance; the pore diameter is usually on the order of 1000 times less than the membrane thickness. Recent work [41] has also shown that equating the inlet flowrate of one stream with the outlet flow rate of the other stream instead of equating the module streams' inlet flow rates, as done here, achieves better thermal balancing in DCMD. Such thermal balancing reduces the entropy generation [42] in the module and can result in a 10%–20% improvement in efficiency [41]. The heater contributes substantially due to the large amount of heat transferred, and the large temperature difference between the source temperature (usually a steam saturation temperature) and the heater inlet. The regenerator has lower entropy generation as it transfers energy through a lower-temperature difference, which remains constant

throughout its length. The discharge temperature disequilibrium entropy generation is low compared to other thermal systems, as the brine reject temperature is lower. Additionally, since the recovery ratio is low, the chemical disequilibrium of the brine is also negligible (entropy generation due to brine disequilibrium is approximately three orders of magnitude smaller than from other sources). Like most other systems discussed here, the entropy generation contributed by low pressure-rise circulation pumping is negligible.

Reducing the top temperature, $T_{f,in}$, results in a net increase in specific entropy generation. This is primarily due to the heater, as a lower top temperature gives rise to a higher temperature difference in the heater. Specific entropy generation in the module goes down slightly, as evaporation happens at a lower temperature; however, this is negated by an increase in specific entropy generation in the regenerator, as water production decreases faster than the temperature gradient in the regenerator. Entropy generation to temperature disequilibrium goes up primarily owing to the lower recovery ratio and additional brine reject.

Given the MD's low recovery ratio and high discharge temperature, entropy generation is high when compared to other desalination systems, and as a result $\eta_{II} = 1.0\%$, as calculated with Eq. (88) and taking into account all sources of entropy generation. Other configurations of MD, such as conductive-gap MD (CGMD), can cut overall energy consumption in half relative to DCMD [43].

5.3 Mechanical Vapor Compression

A simple single-effect mechanical vapor compression (MVC) model is considered. A schematic diagram of the process is shown in Fig. 22. The design values chosen for the process are guided by those reported for single-stage MVC plants analyzed by Veza [44] and Aly [45], and are listed in Table 4.

The inlet pressure to the compressor is taken to be the average of the saturation pressure of seawater at a salinity corresponding to the average of the feed and reject salinity. The regenerating heat exchanger is thermally balanced, and thus the temperature

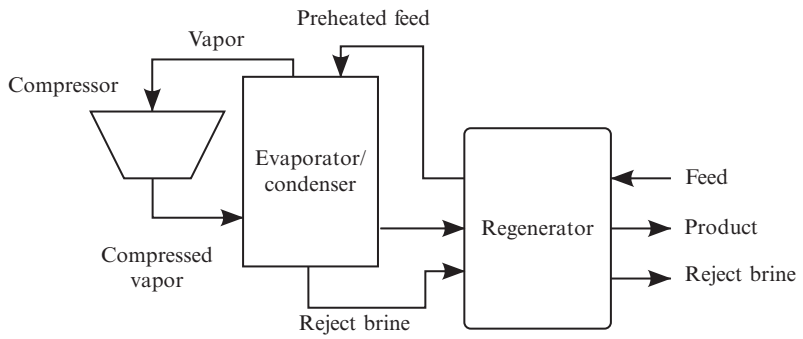

Fig. 22 Single-effect mechanical vapor compression process.

Table 4 MVC design inputs

Input	Value
Seawater inlet temperature	25°C
Seawater inlet salinity	35 g/kg
Product water salinity	0 g/kg
Discharged brine salinity	58.33 g/kg
Top brine temperature	60°C
Pinch: evaporator-condenser	2.5 K
Recovery ratio	40%
Isentropic compressor efficiency	70%
Compressor inlet pressure	19.4 kPa

Table 5 MVC model outputs

Output	Value
Specific electricity consumption	8.84 kWh/m^3
Discharged brine temperature	27.2°C
Product water temperature	29.7°C
Compression ratio	1.15
Second Law efficiency, η_{II}	8.5%

difference is taken to be constant between the rejected brine and the feed stream and also between the product water and the feed stream. By employing energy conservation equations for each component, the unknown thermodynamic states can be computed (an explicit model for energy consumption is given in Ref. [46]). Knowing the thermodynamic states at each point, the entropy generated within each component can be calculated along with the entropy generated when the discharged brine is returned to a body of water with the same composition and temperature as the feed. The key outputs from the model are reported in Table 5. The breakdown of entropy generation among components is indicated in Fig. 23.

The majority of entropy generation may be attributed to heat transfer across a finite temperature difference from the condensation process to the evaporation process. Entropy generation within the regenerator is less significant, primarily because the sensible heat transferred in the regenerator is substantially smaller than the large amount of latent heat recovered in the evaporator-condenser. Entropy generation due to irreversibility within the compressor is important and depends on the compression ratio and its isentropic efficiency. Entropy generated in returning concentrated brine to a body of seawater is considerable as the recovery ratio is high (40%). Entropy generated in returning product streams to the temperature of inlet seawater is small as the regenerator is effective in bringing these streams to a temperature close to that of the inlet seawater.

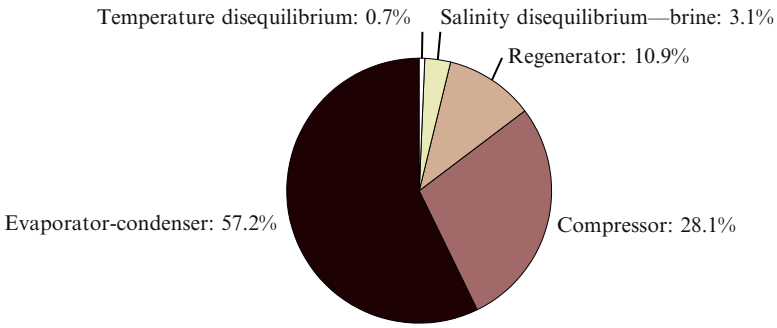

Fig. 23 Relative contribution of sources of entropy generation in a mechanical vapor compression system. Total specific entropy generation is 98.0 J/kg-K. Contributions of the temperature disequilibrium of the distillate and brine streams are 0.5% and 0.2%, respectively.

The preceding MVC system is a simple single-effect system, satisfactory for demonstrating the distribution of entropy generation throughout MVC plants. Detailed thermoeconomic models with multiple effects have been analyzed in literature [47]. Research has also been undertaken on improving the heat transfer coefficients within the evaporation and condensation processes of phase change. Lara et al. [48] investigated high temperature and pressure MVC, where dropwise condensation can allow greatly enhanced heat transfer coefficients. Lukic et al. [49] also investigated the impact of dropwise condensation upon the cost of water produced. Such improvements in heat transfer coefficients reduced the driving temperature difference in the evaporator-condenser leading to a lower compression ratio and thus reduced compressor work requirements per unit of water produced. As the present analysis shows, reduction of entropy generation within the evaporator-condenser and the compressor are crucial if exergetic efficiency is to be improved.

5.4 Reverse Osmosis

A typical flow path for a single-stage reverse osmosis (RO) plant with energy recovery is shown in Fig. 24 [50]. Since RO is a mechanically driven system and thermal effects are of second order to pressure effects, reasonably accurate calculations can be performed while only considering pressure work. The following approximations are made.

Feed seawater is assumed to enter at ambient temperature and pressure (25°C, 1 bar) and at standard seawater salinity (35 g/kg). Pure water (0 g/kg salinity) is assumed to be produced at a recovery ratio of 40%. Further, it is assumed that 40% of the feed is pumped to 69 bar using a high pressure pump, while the remaining 60% is pumped to the same pressure using a combination of a pressure exchanger driven by the rejected brine as well as a booster pump. The high pressure, booster, and feed pump efficiencies are assumed to be 85%. The concentrated brine loses 2 bar of pressure through the RO module, while the product leaves the module at 1 bar. Energy Recovery Inc. [50] makes a direct contact

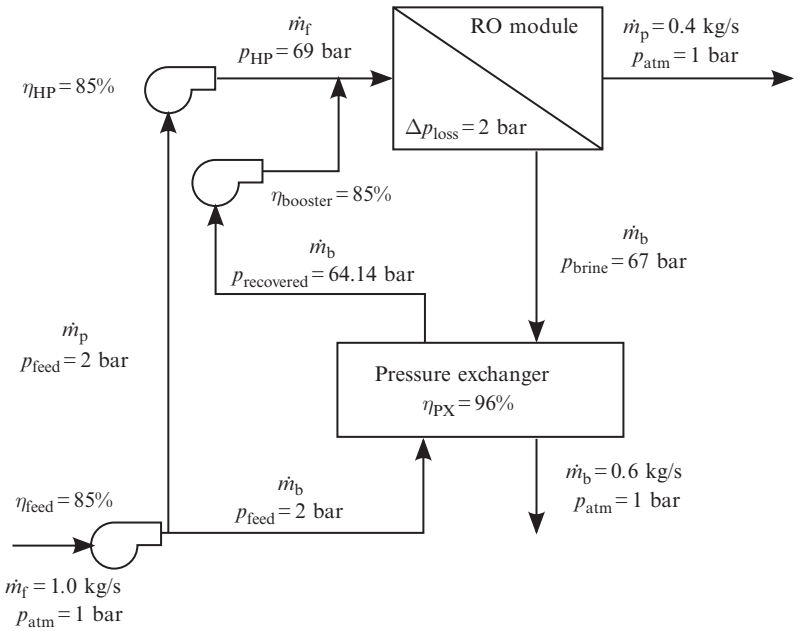

Fig. 24 A typical flow path for a single-stage reverse osmosis system.

pressure exchanger that features a single rotating part. The pressure exchanger pressurizes part of the feed using work produced through the depressurization of the brine in the rotor. Eqs. (94a), (101), (108) are used to match the work produced in expansion to the work required for compression. Assuming the expansion and compression processes are 98% efficient [50], the recovered pressure is calculated as

$$p_{\text{recovered}} = p_{\text{feed}} - \eta_{\text{expansion}}\eta_{\text{compression}}\left(\frac{\rho_{\text{feed}}}{\rho_{\text{brine}}}\right)(p_{\text{brine}} - p_{\text{atm}}) \tag{127}$$

and the pressure exchanger efficiency is evaluated using ERI's definition [50]:

$$\eta_{\text{PX}} = \frac{\sum_{\text{out}} \text{Pressure} \times \text{Flow}}{\sum_{\text{in}} \text{Pressure} \times \text{Flow}} \tag{128}$$

Density of seawater is evaluated using seawater properties [22].

Using the preceding assumptions, approximations, and inputs, the entropy generated in the various components can be directly calculated using equations derived in Section 4.2. The entropy generated in the high pressure pump, booster pump, and the feed in the pressure exchanger is evaluated using Eq. (110). The entropy generated through the expansion of the pressurized brine in the pressure exchanger is evaluated using Eq. (103).

Additional consideration is necessary for the entropy generation in the RO module because both the mechanical and chemical state of the seawater is changing. The pure product stream's pressure is 68 bar less than the feed, and the brine is 2 bar less with an outlet salinity of 58.3 g/kg. To capture these effects, the Second Law of Thermodynamics may be applied to a control volume surrounding the module, accounting for entropy flow in and out, entropy generation, and heat transfer, $\dot{Q}_{\text{mod}}$, into the control volume boundary. Heat transfer is necessary if we evaluate the outlet streams at the inlet temperature, and to find the heat transfer we must also use the First Law on the same volume:

$$(\dot{m}h)_{\text{p}} + (\dot{m}h)_{\text{b}} - (\dot{m}h)_{\text{sw}} = \dot{Q}_{\text{mod}} \tag{129a}$$

$$(\dot{m}s)_{\text{p}} + (\dot{m}s)_{\text{b}} - (\dot{m}s)_{\text{sw}} = \dot{S}_{\text{gen, mod}} + \frac{\dot{Q}_{\text{mod}}}{T_0} \tag{129b}$$

To evaluate the enthalpy and entropy changes, the physical properties of seawater are needed as function of temperature, pressure, and salinity. Since seawater is nearly incompressible, its entropy is essentially independent of p and can be evaluated without accounting for pressure change (e.g., using the package of Sharqawy et al. [22]). The effect of pressure on enthalpy cannot be ignored, although it can also be approximated using an incompressible substance model. Instead, the pressure-dependent property package of Nayar et al. can be used [20]. The property changes

$$\Delta\dot{H} = \dot{m}_{\text{p}} h\left(T_0, p_{\text{atm}}, w_{\text{s,p}}\right) + \dot{m}_{\text{b}} h(T_0, p_{\text{brine}}, w_{\text{s,b}}) - \dot{m}_{\text{f}} h(T_0, p_{\text{HP}}, w_{\text{s,f}})$$
$$\Delta\dot{S} = \dot{m}_{\text{p}} s\left(T_0, p_{\text{atm}}, w_{\text{s,p}}\right) + \dot{m}_{\text{b}} s(T_0, p_{\text{brine}}, w_{\text{s,b}}) - \dot{m}_{\text{f}} s(T_0, p_{\text{HP}}, w_{\text{s,f}})$$

are found to have the values $\Delta\dot{H} = -2.70\,\text{kW}$ and $\Delta\dot{S} = -4.42\,\text{W/K}$. From these, the First and Second Laws give $\dot{Q}_{\text{mod}} = -2.70\,\text{kW}$ (out of the control volume) and $\dot{S}_{\text{gen, mod}} = 4.65\,\text{W/K}$.

Regarding the heat transfer, if the system were adiabatic, the outlet streams would be warmer (by roughly 0.7 K if they had the same temperature) but the value of $\dot{S}_{\text{gen, mod}}$ would be essentially the same. The energy dissipated by pump inefficiency results in small increases in the high pressure feed temperature (around 0.4 K), which is also assumed to be removed by heat transfer to the environment. Only negligible entropy generation results from these heat transfers out of the system because the temperature differences above T_0 are so small (see Eq. 121).

Mistry et al. [19] used the incompressible fluid model to find the module entropy generation as the sum of the entropy change of composition (at fixed T and p), the entropy generation from depressurizing the product ($\Delta p = 68$ bar), and the entropy generation from depressurizing the brine ($\Delta p = 2$ bar). Algebra shows that that approach is also consistent with the First and Second Laws.

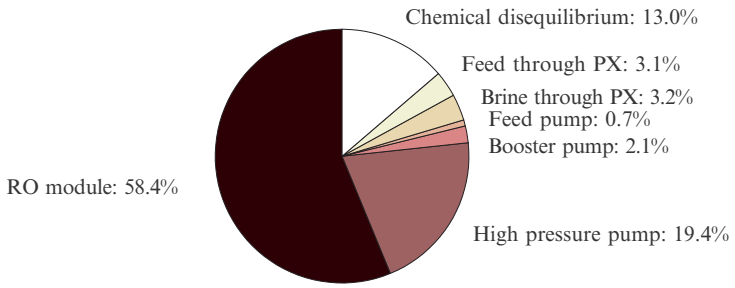

Fig. 25 Relative contribution of sources to entropy generation in the reverse osmosis system. Irreversibilities associated with product flow through the membrane dominates. Total specific entropy generation is $S_{gen}^{TDS} = 19.9\,J/kg\,K$.

Fig. 25 is a pie chart showing the relative amounts of entropy generation within the single-stage RO system. The greatest irreversibility occurs within the RO module, and the diffusion of water through the very high pressure drop of the RO membrane is the principal source of this irreversibility. Note that the high pressure pump moves this same mass of water through the same pressure difference, but does so at 85% efficiency and therefore generates substantially less entropy than the zero efficiency flow through the membrane.

For these conditions, the minimum least work is found to be 2.59 kJ/kg, and the total entropy generation is $S_{gen}^{TDS} = 19.9\,J/kg\,K$. Therefore, from Eq. (85), the required work of separation is 8.53 kJ/kg (2.37 kWh/m^3), and the Second Law efficiency, per Eq. (88), is 30.4%.

Since RO systems tend to operate at higher Second Law efficiency than thermal plants, the irreversibility due to discharge disequilibrium of the brine stream has a larger contribution to the total entropy generation. As seen in Fig. 25, the high salinity of the brine accounts for 13% of the plant's total irreversibility. The only way to reduce this effect is to lower the recovery ratio or to implement an osmotic power recovery device (such as a pressure-retarded osmosis system) on the reject brine stream.

When trying to improve RO systems, designers target the irreversibilities in the module. The simplest way to improve the performance of the system is to use a two (or more)-stage RO system (e.g., as described in [51]). In a two-stage system, water is extracted at a lower recovery ratio from the first stage, resulting in a lower brine concentration. Since the required pressure of the feed is dependent on the osmotic pressure, which itself is a function of the feed concentration, a lower recovery ratio means that lower pressures are needed in the first stage. Next, the brine from the first stage is then further pressurized to the top pressure and additional water is extracted in a second stage. Even though the same top pressure is reached, since the first stage operates with a lower pressure drop across the membranes, less total entropy is generated in the two-stage system.

Batch processing of seawater, in which a charge of seawater is slowly pressurized as permeate is removed through membranes, can maintain a relatively smaller difference between hydraulic and osmotic pressure throughout the process [42]. This reduces the entropy generation and lowers the energy consumption per unit permeate. Semi-batch processes have been commercialized, for example, by Desalitech Ltd. [52], and report significant reductions in energy. True batch processes, such as those recently invented at MIT, could cut the energy requirements even further [53].

6. SECOND LAW EFFICIENCY FOR A DESALINATION SYSTEM OPERATING AS PART OF A COGENERATION PLANT

Many large-scale desalination processes use a cogeneration scheme, in which low temperature steam and electricity from a power plant are used to drive a desalination plant. Additional primary energy (fuel), beyond that needed for electricity production, must be provided to drive the desalination system. Thus, it is useful to consider the amount of additional heat energy that must be provided to the power plant in order to generate the heat and work needed to power the desalination plant. In order to do so, consider a cogeneration system in which a power plant is connected to a desalination plant, as shown in Fig. 26. In this system, a heat input ($\dot{Q}_H$) is provided to a power plant. This heat input is equal to the amount of heat necessary to drive the power plant ($\dot{Q}_{pp}$) plus the additional amount necessary to generate steam and electricity for the desalination plant ($\dot{Q}_d$ to produce $\dot{Q}_{sep}$ and $\dot{W}_{sep}$). The power plant produces a net amount of work equal to the desired plant work production ($\dot{W}_{pp}$) plus the amount of work necessary to drive the desalination plant ($\dot{W}_{sep}$). Note that typically fuel, rather than heat, is the primary energy input to cogeneration systems, and therefore the analysis should be done in

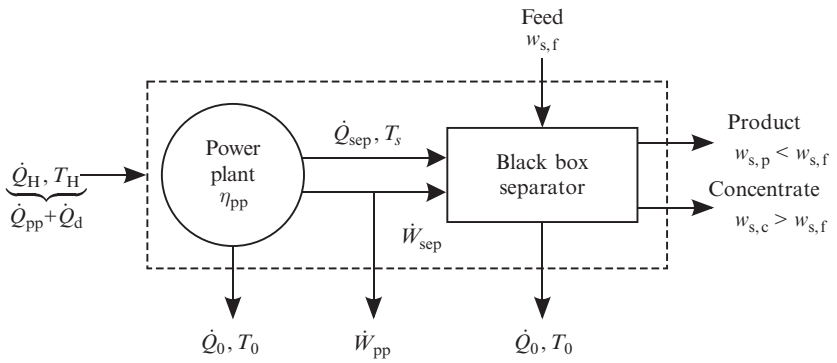

Fig. 26 The power plant converts heat input into work output, work for the desalination plant (represented as an unspecified black box separator), and heat for the desalination plant. It is assumed that the power plant operates at a Second Law efficiency of η_{pp}.

terms of the amount of fuel required to drive the power plant plus the additional amount of fuel required to produce the heat and work necessary to drive the desalination plant ($\dot{m}_{\text{fuel}} = \dot{m}_{\text{pp}} + \dot{m}_{\text{d}}$). However, for simplicity and with the goal of highlighting the difference between work- and heat-driven systems, the CV for this analysis is drawn under the assumption that heat, and not fuel, is transferred into the system. The effect of including the combustor in the analysis is now discussed briefly.

The following derivation is based on the work of Mistry and Lienhard [54] and El-Sayed and Silver [29]. The First and Second Laws of Thermodynamics are written about the power plant CV:

$$\dot{Q}_{\text{pp}} + \dot{Q}_{\text{d}} = \dot{Q}_{\text{sep}} + \dot{Q}_0 + \dot{W}_{\text{pp}} + \dot{W}_{\text{sep}} \tag{130a}$$

$$\dot{S}_{\text{gen}} + \frac{\dot{Q}_{\text{pp}}}{T_{\text{H}}} + \frac{\dot{Q}_{\text{d}}}{T_{\text{H}}} = \frac{\dot{Q}_{\text{sep}}}{T_{\text{s}}} + \frac{\dot{Q}_0}{T_0} \tag{130b}$$

Multiplying the Second Law by T_0 and substituting into the First Law to eliminate heat transfer to the ambient environment ($\dot{Q}_0$) gives

$$\dot{W}_{\text{pp}} + \dot{W}_{\text{sep}} = \left(\dot{Q}_{\text{pp}} + \dot{Q}_{\text{d}}\right)\left(1 - \frac{T_0}{T_{\text{H}}}\right) - \dot{Q}_{\text{sep}}\left(1 - \frac{T_0}{T_{\text{s}}}\right) - T_0\dot{S}_{\text{gen}} \tag{131}$$

In order to deal with the irreversibilities within the system, the rate of entropy generation is assumed to be proportional to the amount of work produced by a reversible power plant operating within the same heat transfer loads. That is,

$$T_0\dot{S}_{\text{gen}} \propto \left(\dot{W}_{\text{pp,rev}} + \dot{W}_{\text{sep,rev}}\right) = \left(\dot{Q}_{\text{pp}} + \dot{Q}_{\text{d}}\right)\left(1 - \frac{T_0}{T_{\text{H}}}\right) - \dot{Q}_{\text{sep}}\left(1 - \frac{T_0}{T_{\text{s}}}\right) \tag{132}$$

Letting the constant of proportionality be $(1 - \eta_{\text{pp}})$, where $\eta_{\text{pp}} = \eta/\eta_{\text{Carnot}}$ is the Second Law efficiency of the power plant, η is the First Law (energy) efficiency of the power plant, and η_{Carnot} is the Carnot efficiency of a power plant operated between T_{H} and T_0,

$$T_0\dot{S}_{\text{gen}} = \left[\left(\dot{Q}_{\text{pp}} + \dot{Q}_{\text{d}}\right)\left(1 - \frac{T_0}{T_{\text{H}}}\right) - \dot{Q}_{\text{sep}}\left(1 - \frac{T_0}{T_{\text{s}}}\right)\right]\left(1 - \eta_{\text{pp}}\right) \tag{133}$$

Substituting $T_0\dot{S}_{\text{gen}}$ into Eq. (131) gives

$$\dot{W}_{\text{pp}} + \dot{W}_{\text{sep}} = \left(\dot{Q}_{\text{pp}} + \dot{Q}_{\text{d}}\right)\left(1 - \frac{T_0}{T_{\text{H}}}\right)\eta_{\text{pp}} - \dot{Q}_{\text{sep}}\left(1 - \frac{T_0}{T_{\text{s}}}\right)\eta_{\text{pp}} \tag{134}$$

Since the goal is to determine how much additional heat is necessary to drive the desalination system, $\dot{Q}_{\text{d}}$ must be independent of the amount of work produced by the power plant. Consider the same power plant in which the desalination system is not operating and the power plant is producing a net output of $\dot{W}_{\text{pp}}$. Then setting $\dot{Q}_{\text{d}}$, $\dot{Q}_{\text{sep}}$, and $\dot{W}_{\text{sep}}$ to zero, $\dot{Q}_{\text{pp}}$ is found to be

$$\dot{Q}_{pp} = \frac{\dot{W}_{pp}}{\left(1 - \frac{T_0}{T_H}\right)\eta_{pp}} \tag{135}$$

which is consistent with the definition of the First Law efficiency, η. Substituting this back into the preceding equation results in $\dot{Q}_{pp}$ and $\dot{W}_{pp}$ canceling out. Solving for $\dot{Q}_d$,

$$\dot{Q}_d = \frac{\dot{W}_{sep}}{\left(1 - \frac{T_0}{T_H}\right)\eta_{pp}} + \dot{Q}_{sep}\frac{\left(1 - \frac{T_0}{T_s}\right)}{\left(1 - \frac{T_0}{T_H}\right)} \tag{136}$$

In order to evaluate the Second Law efficiency of the desalination plant, one might think to use the exergetic value of the work and heat inputs to the plant,

$$\dot{\Xi}_{sep} = \dot{W}_{sep} + \left(1 - \frac{T_0}{T_s}\right)\dot{Q}_{sep} \tag{137}$$

for the denominator in Eq. (83) since it represents the total exergy input to the desalination system. While this would be correct for a stand-alone system, $\dot{W}_{sep}$ and $\dot{Q}_{sep}$ do not represent the true exergy inputs for the entire separation system which is contained within the dashed border in Fig. 26. Instead, the exergy input to drive the desalination system is that due to the extra heat transfer provided to the power plant, $\dot{Q}_d$. Therefore the Second Law efficiency should be evaluated based on this quantity. Substituting Eq. (136) into Eq. (83) gives

$$\eta_{II} = \frac{\dot{\Xi}^{min}_{least}}{\dot{\Xi}_{in}} = \frac{\dot{W}^{min}_{least}}{\dot{Q}_d\left(1 - \frac{T_0}{T_H}\right)} = \frac{\dot{W}^{min}_{least}}{\frac{\dot{W}_{sep}}{\eta_{pp}} + \dot{Q}_{sep}\left(1 - \frac{T_0}{T_s}\right)} \tag{138}$$

The important difference between using Eqs. (137) and (136) is the fact that the work input ($\dot{W}_{sep}$) is divided by the Second Law efficiency of the power plant. This effectively accounts for the fact that the work is not produced reversibly from the heat source and therefore cannot be directly compared with the thermal exergy input. If there is no work input, then $\dot{W}_{sep} = 0$ and Eq. (138) correctly reduces the ratio of the least heat of separation (based on T_s) to the actual heat input to the desalination system itself. Similarly, if there is no heat input, then $\dot{Q}_{sep} = 0$ and Eq. (138) reduces to

$$\eta_{II} = \eta_{pp}\frac{\dot{W}^{min}_{least}}{\dot{W}_{sep}} \tag{139}$$

In the limit of reversible operation for the power plant (i.e., $\eta_{pp} = 1$), Eq. (139) reduces to Eq. (88). The Second Law efficiency of the power plant is present in Eq. (139) since the

work used to power the desalination plant is produced irreversibly. Had the losses in the combustor been included in this analysis, both $\dot{W}_{sep}$ and $\dot{Q}_{sep}$ in Eq. (138) would be divided by the Second Law efficiency of the combustor, $\eta_{II,combustor}$. This would have the effect of reducing the Second Law efficiency of the desalination process in proportion to the Second Law efficiency of the combustor. Both the heat and work terms would be affected equally since the losses occur prior to the power generation process.

In order to better understand the energetic behavior of both membrane and thermal systems, a parametric study of Eq. (138) is conducted in the following two sections for systems using standard seawater as the feed source (35 g/kg, 25°C). Under these conditions, the minimum least work of separation of seawater per kilogram of product is 2.71 kJ/kg [19].[10] The Second Law efficiency is evaluated under two different conditions: (1) work is the only input to the desalination system; and (2) heat at 100°C is the primary input and the amount of pumping work is varied.

6.1 Desalination Powered by Work

For desalination systems that are powered entirely using work, $\dot{Q}_{sep} = 0$ and Eq. (138) reduces to Eq. (139). As a result, it is clear that unless the power plant operates reversibly, a work-powered desalination system can never achieve 100% Second Law efficiency, even if the desalination process is conducted reversibly. This result is unavoidable because the primary energy source in the cogeneration scheme is heat to the power plant, not electricity to the desalination plant. For the following study, the power plant is assumed to be a representative combined cycle plant operating between 1400 and 298.15 K with a First Law efficiency of $\eta = 52.8\%$ and a Second Law efficiency of $\eta_{pp} = 67.2\%$ [55]. The Second Law efficiency of a work-driven desalination plant is shown in Fig. 27 as a function of $\dot{W}_{sep}$ starting at a minimum value of $\dot{W}_{sep} = \dot{W}_{least}$.

All work-driven systems in this cogeneration scheme pay an energetic penalty on efficiency since the initial energy source (heat) must go through a conversion process (power plant) that operates irreversibly, and therefore the limiting Second Law efficiency as $\dot{W}_{sep} \to \dot{W}_{least}$ is η_{pp}, not 1. If the primary source of energy was considered to be mass of fuel, then the limiting Second Law efficiency would be equal to the product of the Second Law efficiencies of the combustor and the power plant, that is, $\eta_{II,\ combustor}\eta_{pp}$. The typical range of operation for current RO technologies is in 2.5–5 kWh/m^3 and is highlighted in Fig. 27. RO systems with energy recovery tend to be on the lower end of this range, while systems without energy recovery tend to be on the higher end of this range. Exact values are a function of system design and feed water characteristics [56–61]. This corresponds to Second Law efficiency values ranging from approximately 10% to 20%.

[10] More recent values of seawater thermodynamic properties reduce this value by 4.4%, to 2.59 kJ/kg. For consistency with [19], we retain the older value for the calculations that follow.

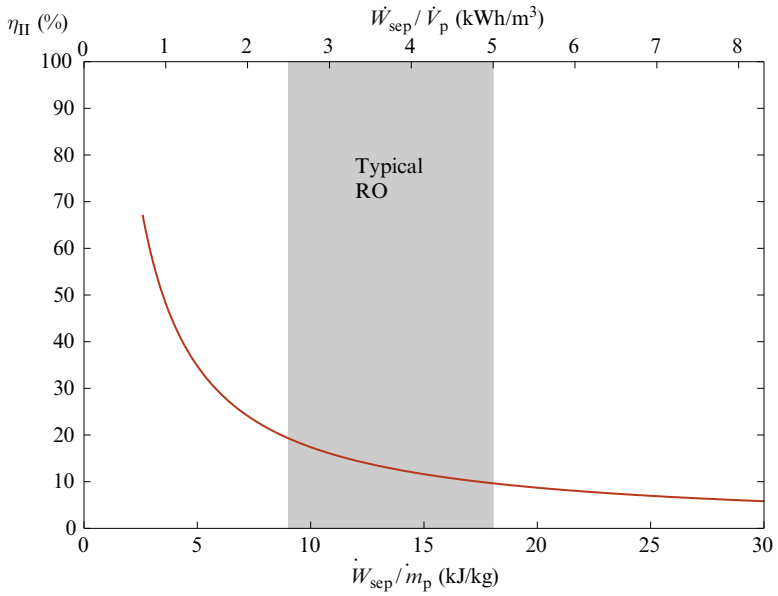

Fig. 27 The Second Law efficiency of a work-driven desalination system operating in a cogeneration scheme can never reach 100% unless the power plant operates reversibly. Typical values for current reverse osmosis systems are *highlighted*. Feed water is at $T_0 = 25°C$ and $w_{s,f} = 35$ g/kg.

6.2 Desalination Powered by Cogenerated Heat and Work

Nearly all large-scale thermal desalination systems are connected to a power plant since large quantities of steam are required to provide heating to the feed. The Second Law efficiency of a thermal desalination plant operating using steam at 100°C with pump work requirements ranging from 0 to 4 kWh/m^3 is shown in Fig. 28. In the case of zero pump work, 100% Second Law efficiency is theoretically possible. However, once pump work is required, the possible Second Law efficiency drops substantially (e.g., approximately 50% for 0.5 kWh/m^3 of electrical work to drive pumps). Clearly, regardless of what the required heat of separation is the additional requirement of pump work results in a decrease in the Second Law efficiency.

The results shown in Fig. 28 are generated based on the assumption that all energy provided to the desalination system originally comes from a common energy source, $\dot{Q}_d$. This value of heat input is then substituted into Eqs. (83), (137) to get Eq. (138). Should a desalination plant have energy inputs from multiple primary energy sources, then the analysis to derive the correct form of η_{II} will change slightly. All energy inputs should be traced to their primary sources (as was done for $\dot{W}_{sep}$ and $\dot{Q}_{sep}$ from $\dot{Q}_d$), and then each primary input should be combined based on the exergetic value as done in Eq. (137).

Based on Figs. 27 and 28, when a desalination plant operates as part of a cogeneration scheme, the work-driven systems (based on currently available technology) always behave in an exergetically more favorably manner than the thermal-driven

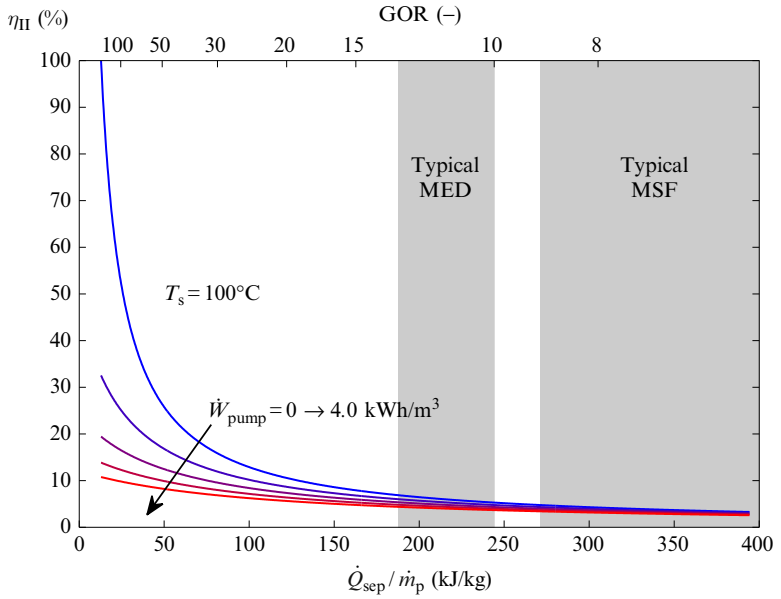

Fig. 28 Second Law efficiency for a thermal desalination plant requiring work for pumping. Lines for pump work are in increments of 0.5 kWh/m^3. As the pump work increases, the Second Law efficiency decreases. Feed water is at $T_0 = 25°C$ and $w_{s,f} = 35$ g/kg.

systems (i.e., higher η_{II}). This is true even when accounting for the energy penalty that comes from converting the source heat to work, and it is even further exemplified when considering that thermal systems typically require large amounts of electrical work for pumping (these are sometimes as high as the work requirements for an RO system by itself).

The present results are based on a Second Law efficiency of $\eta_{pp} = 67\%$, representative of a combined cycle plant. If a less efficient Rankine cycle plant were considered, having a First Law efficiency of 30%–35%, a representative η_{pp} might be 45%–55%, depending on the top steam temperature. The difference between the work-driven and heat systems would decrease somewhat, but work driven (membrane) systems would remain much more efficient than thermal systems.

Although current membrane systems are more efficient from a Second Law viewpoint, it should not be concluded that there is no role for thermal systems. Ultimately, several factors are considered when selecting a desalination technology, including capital and operating costs, quality of feed water, and existing expertise and infrastructure. Although the work systems are favored energetically, these other factors can lead to thermal systems being more desirable for a given location or application.

7. SUMMARY

Reducing energy consumption is a key tool for minimizing the environmental footprint and increasing the sustainability of desalination. Using thermodynamic analysis,

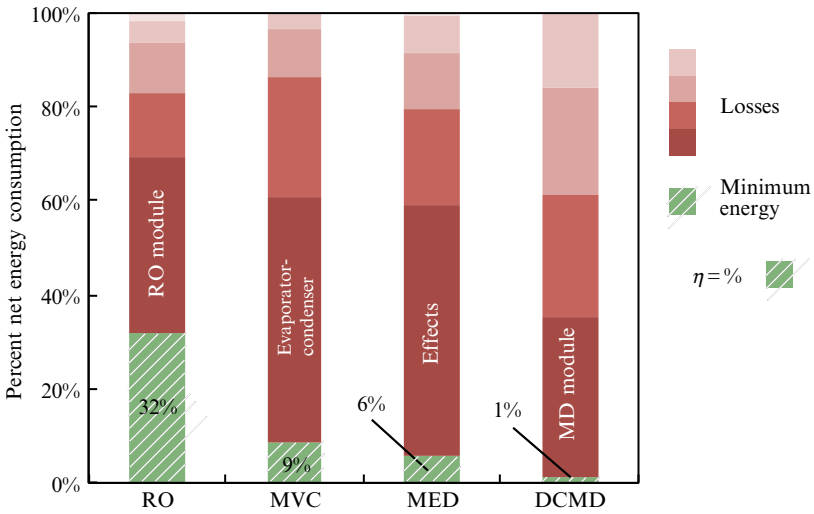

Fig. 29 The net energy consumption for each technology assessed in Section 5 is divided into minimum energy (or efficiency) and losses on a percentage basis. Only the primary loss mechanism is labeled. The two work-driven technologies, MVC and RO, have the highest exergetic efficiency. In each system, the core component doing the separation is the greatest source of inefficiency, but auxiliary components also contribute significantly to overall irreversibility.

we have shown how to benchmark systems and process designs against physical limits, how to model the thermodynamic properties of saline waters, and how feed water properties and environmental conditions can affect actual and minimum energy consumption. Entropy generation has been shown to characterize the energetic deficit relative to reversible operation, and equations were developed to quantify the degree of irreversibility, or inefficiency, in individual processes and desalination system components. Identifying components with relatively large entropy production focuses efficiency-driven (re)design onto those components that will have the greatest impact on overall system performance.

In Section 5, we applied these tools to analyze a suite of desalination systems, including both established and emerging technologies. The results of this analysis are shown in Fig. 29, where we see that work-driven technologies operate closest to the reversible limit, and that one or two components in each technology stand out as the largest sources of irreversibility in each system. Tow et al. [62] reported the Second Law efficiency of a range of real systems operating at various salinities, as shown in Fig. 30. The highest efficiencies are found for seawater reverse osmosis plants.[11]

[11] These results are based on the exergy entering the desalination system itself, in contrast with the results of Section 6, which refer exergy inputs to the power plant of a coproduction system.

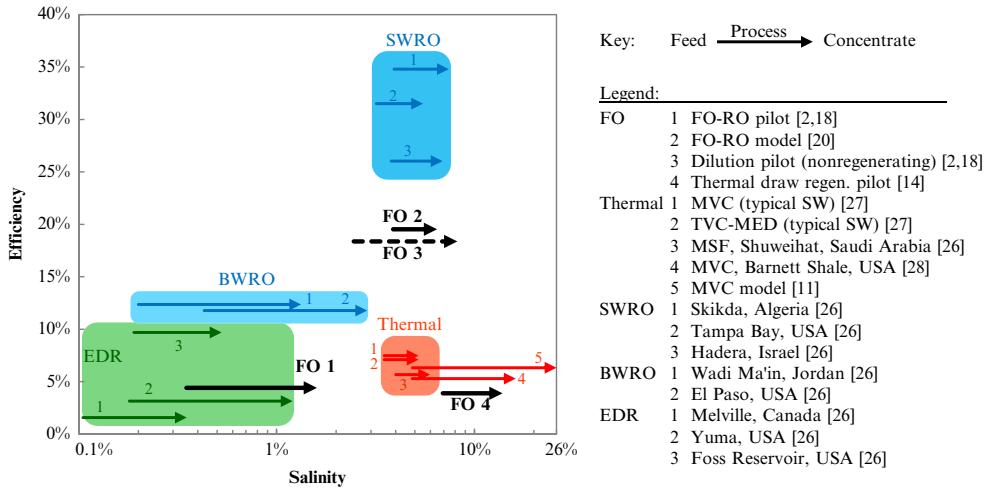

Fig. 30 Efficiency-salinity map of desalination processes, with salinity in percent by weight. Processes are represented with *arrows* that begin and end at the feed and concentrate salinities, respectively. Citation numbers in chart refer to those in Ref. [62].

Other studies that capitalize on thermodynamic methods of this chapter have been considered: high salinity brine desalination [46]; balancing of forward osmosis (FO) mass exchangers [62]; energy efficiency of FO relative to RO for seawater desalination [63]; performance optimization of humidification-dehumidification desalination [23, 64–67]; efficiency of desalination driven by waste heat [68]; energy requirements of a variety of hybrid desalination systems, for example, [69, 70]; and even Second Law efficiencies that incorporate the costs of electricity and heat [71].

Population growth is increasingly straining our limited supply of renewable fresh water, and associated fossil energy emissions threaten our atmosphere. Projections of rising climate variability necessitate greater resilience in our water systems. For all these reasons, the need for more efficient and sustainable desalination is urgent. The concepts and methods developed here provide a framework for assessing and improving the efficiency of both established and emerging desalination technologies.

APPENDIX A. SEAWATER PROPERTIES CORRELATIONS

Seawater is a complex electrolyte solution of water and salts. The salt concentration, w_s, is the total amount of dissolved solids present in a unit mass of seawater. It is usually expressed by the salinity (on reference-composition salinity scale) as defined by Millero et al. [72], which is currently the best estimate for the absolute salinity of seawater. In this appendix, correlations of seawater thermodynamic properties, namely specific volume, specific enthalpy, specific entropy, specific heat, chemical potential, and osmotic coefficient to be used in thermodynamic analysis calculations of this chapter, are given. In this

regard, the thermodynamic properties of seawater are calculated using the correlations provided by Sharqawy et al. [22]. These correlations fit the data extracted from the seawater Gibbs energy function of IAPWS 2008 [73]. They are polynomial equations given as functions of temperature and salinity at atmospheric pressure (or saturation pressure for temperatures over normal boiling temperature). In these correlations, the reference state for the enthalpy and entropy values is taken to be the triple point of pure water (0.01°C) and at zero absolute salinity.

For other correlations of seawater thermophysical properties, including pressure dependence, the equations provided by Nayar et al. [20] are recommended. A full set of codes for calculating seawater thermophysical properties are available without charge at http://web.mit.edu/seawater.

A.1 Specific Volume

The specific volume is the inverse of the density as given by Eq. (A.1). Both are intensive properties; however, in thermodynamics literature, it is preferred to use the specific volume instead of the density because it is directly related to the flow work. The density of seawater is higher than that of pure water due to the salts; consequently, the specific volume is lower. The seawater density can be calculated by using Eq. (A.2) given by Sharqawy et al. [22], which fits the data of Isdale and Morris [74] and Millero and Poisson [75], for a temperature range of 0–180°C and salt concentration of 0–0.16 kg/kg and has an accuracy of ± 0.1%. The pure water density is given by Eq. (A.3), which fits the data extracted from the IAPWS [76] with an accuracy of ± 0.01%.

$$v_{sw} = 1/\rho_{sw} \tag{A.1}$$

$$\rho_{sw} = \rho_w + w_s\left(a_1 + a_2\, T + a_3\, T^2 + a_4\, T^3 + a_5 w_s\, T^2\right) \tag{A.2}$$

$$\begin{aligned}\rho_w = {} & 9.999 \times 10^2 + 2.034 \times 10^{-2} T - 6.162 \times 10^{-3} T^2 \\ & + 2.261 \times 10^{-5} T^3 - 4.657 \times 10^{-8} T^4\end{aligned} \tag{A.3}$$

Here v_{sw} is the specific volume of seawater in m^3/kg, ρ_{sw} and ρ_w are the density of seawater and pure water, respectively, in kg/m^3, T is the temperature in °C, w_s is the salt concentration in kg_s/kg_{sw}, and

$$\begin{aligned}a_1 = 8.020 \times 10^2, \quad a_2 = -2.001, \quad a_3 = 1.677 \times 10^{-2} \\ a_4 = -3.060 \times 10^{-5}, \quad a_5 = -1.613 \times 10^{-5}\end{aligned} \tag{A.4}$$

Fig. A.1 shows the specific volume of seawater calculated from Eq. (A.1) as it changes with temperature and salt concentration. It is shown that the specific volume of seawater is less than that of pure water by about 8.6% at 0.12 kg/kg salt concentration and 120°C. It is important to mention that for incompressible fluids (e.g., seawater) the variation of the specific volume with pressure is very small and can be neglected in most desalination practical problems. The error in calculating the specific volume is less than 1% when the

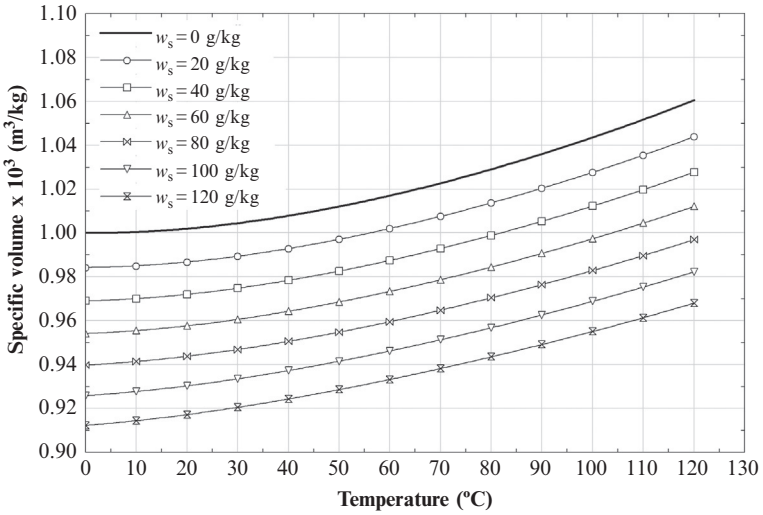

Fig. A.1 Seawater specific volume variations with temperature and salt concentration.

pressure is varying from the saturation pressure to the critical pressure in the compressed liquid region. Therefore, Eq. (A.1) can be used at pressures higher than the atmospheric pressure (up to the critical pressure) and at pressure lower than the atmospheric pressure (up to the saturation pressure) with a negligible error (less than 1%).

A.2 Specific Enthalpy

The specific enthalpy of seawater is lower than that of pure water since the heat capacity of seawater is less than that of pure water. It can be calculated using Eq. (A.5) given by Sharqawy et al. [22], which fits the data extracted from the seawater Gibbs energy function of IAPWS [73], for a temperature range of 10–120°C and salt concentration range of 0–0.12 kg/kg and has an accuracy of ±0.5%. The pure water specific enthalpy is given by Eq. (A.6), which fits the data extracted from the IAPWS [76], with an accuracy of ±0.02%. It is valid for a temperature range of 5–200°C.

$$h_{sw} = h_w - w_s\left(b_1 + b_2 w_s + b_3 w_s^2 + b_4 w_s^3 + b_5 T + b_6 T^2 + b_7 T^3 + b_8 w_s T + b_9 w_s^2\, T + b_{10} w_s T^2\right) \tag{A.5}$$

$$h_w = 141.355 + 4202.070 \times T - 0.535 \times T^2 + 0.004 \times T^3 \tag{A.6}$$

Here h_{sw} and h_w are the specific enthalpy of seawater and pure water, respectively, in J/kg, $10 \le T \le 120$°C, $0 \le w_s \le 0.12$ kg/kg, and

$$\begin{aligned} &b_1 = -2.348 \times 10^4, b_2 = 3.152 \times 10^5, b_3 = 2.803 \times 10^6, b_4 = -1.446 \times 10^7, \\ &b_5 = 7.826 \times 10^3, b_6 = -4.417 \times 10^1, b_7 = 2.139 \times 10^{-1}, b_8 = -1.991 \times 10^4, \\ &b_9 = 2.778 \times 10^4, b_{10} = 9.728 \times 10^1 \end{aligned} \tag{A.7}$$

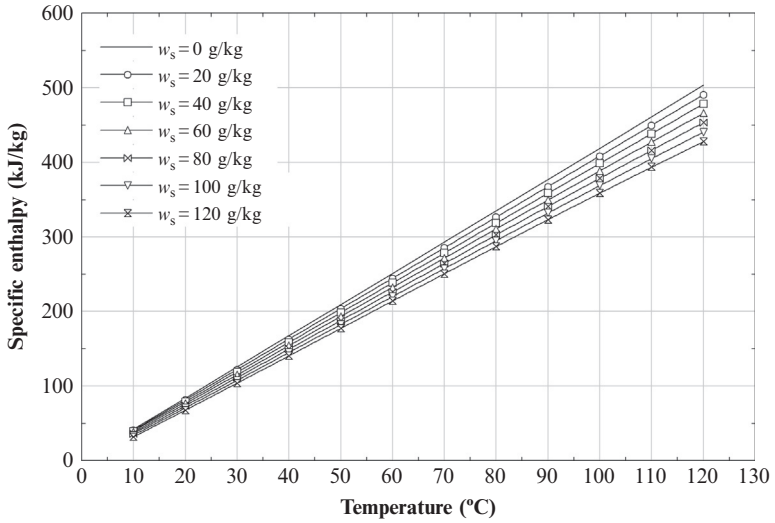

Fig. A.2 Seawater specific enthalpy variations with temperature and salt concentration.

Fig. A.2 shows the specific enthalpy of seawater calculated from Eq. (A.5) as it changes with temperature and salt concentration. The specific enthalpy of seawater is less than that of pure water by about 14% at 0.12 kg/kg salt concentration and 120°C.

The influence of pressure on the specific enthalpy has been analyzed and correlated by Nayar et al. [20].

A.3 Specific Entropy

The specific entropy of seawater is lower than that of pure water. It can be calculated using Eq. (A.8) given by Sharqawy et al. [22], which fits the data extracted from the seawater Gibbs energy function of IAPWS [73], for a temperature range of 10–120°C and salt concentration range of 0–0.12 kg/kg and has an accuracy of ±0.5%. The pure water specific entropy is given by Eq. (A.9), which fits the data extracted from the IAPWS [76], with an accuracy of ±0.1%. It is valid for $T = 5$–200°C.

$$s_{sw} = s_w - w_s\left(c_1 + c_2 w_s + c_3 w_s^2 + c_4 w_s^3 + c_5 T + c_6 T^2 + c_7 T^3 + c_8 w_s T + c_9 w_s^2 T + c_{10} w_s T^2\right) \tag{A.8}$$

$$s_w = 0.1543 + 15.383 \times T - 2.996 \times 10^{-2} \times T^2 + 8.193 \times 10^{-5} \times T^3 - 1.370 \times 10^{-7} \times T^4 \tag{A.9}$$

Here s_{sw} and s_w are the specific entropy of seawater and pure water, respectively, in J/kg K, $10 \le T \le 120$°C, $0 \le w_s \le 0.12$ kg/kg, and

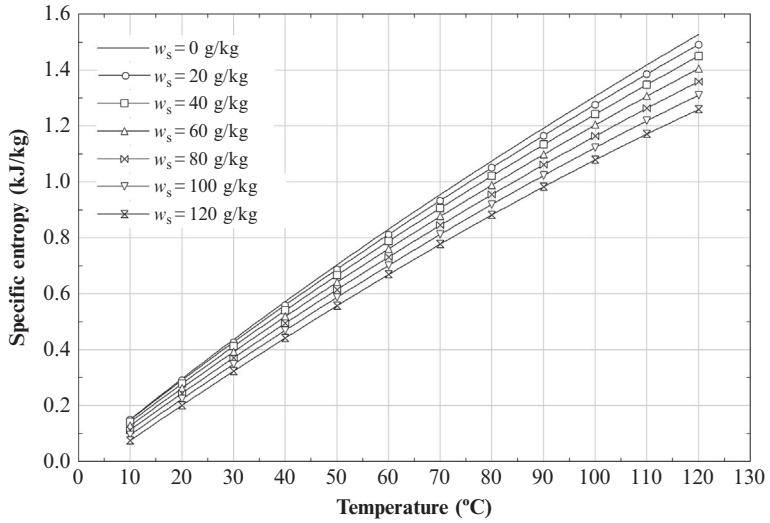

Fig. A.3 Seawater specific entropy variations with temperature and salt concentration.

$$c_1 = -4.231 \times 10^2, c_2 = 1.463 \times 10^4, c_3 = -9.880 \times 10^4, c_4 = 3.095 \times 10^5,$$
$$c_5 = 2.562 \times 10^1, c_6 = -1.443 \times 10^{-1}, c_7 = 5.879 \times 10^{-4}, c_8 = -6.111 \times 10^1, \quad \text{(A.10)}$$
$$c_9 = 8.041 \times 10^1, c_{10} = 3.035 \times 10^{-1}$$

Fig. A.3 shows the specific entropy of seawater calculated from Eq. (A.8) as it changes with temperature and salt concentration. It is shown that the specific entropy of seawater is less than that of fresh water by about 18% at 0.12 kg/kg salt concentration and 120°C. It is important to mention that for incompressible fluids (e.g., seawater) the variation of specific entropy with pressure is very small and can be neglected in most practical cases [17]. Therefore, Eq. (A.8) can be used at pressures different than the atmospheric pressure.

A.4 Chemical Potential

The chemical potentials of water in seawater and salts in seawater may be calculated using the equations given by Nayar et al. [20]. Fig. A.4 shows the chemical potential of water in seawater calculated as it changes with temperature and salt concentration. Fig. A.5 shows the chemical potential of salts in seawater as it changes with temperature and salt concentration. It is seen in Fig. A.4 that the chemical potential of water in seawater decreases with both temperature and salt concentration, while the chemical potential of salts in seawater increases with both temperature and salt concentration, as seen in Fig. A.5.

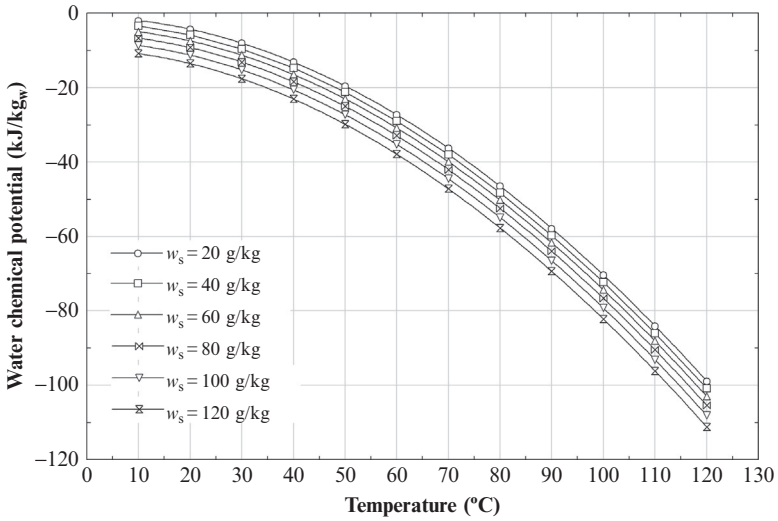

Fig. A.4 Chemical potential of water in seawater.

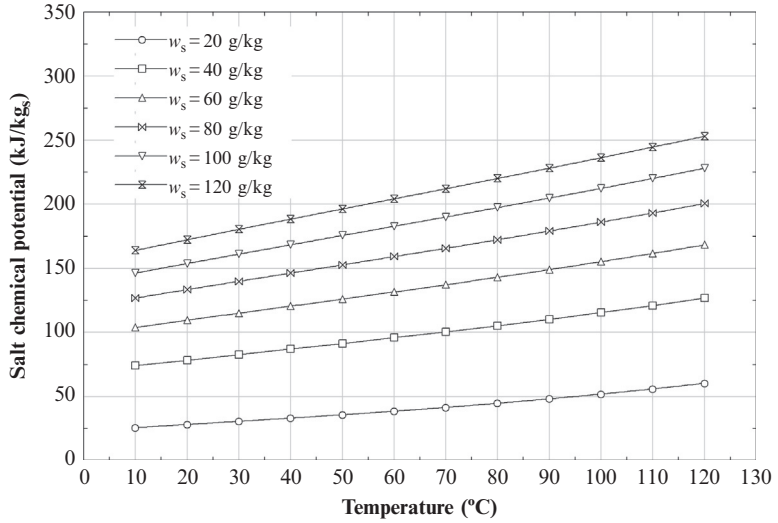

Fig. A.5 Chemical potential of salts in seawater.

A.5 Osmotic Coefficient

The molal osmotic coefficient of a solution, Eq. (14b), can be determined from vapor pressure, boiling point elevation, and freezing point measurements. Sharqawy et al. [22] reviewed the literature for osmotic coefficient data and provided a correlation that is based on the data of Bromley et al. [77] due its wide parameter range of 0–200°C in

temperature and 10–120 g/kg in salinity with a maximum deviation of ±1.4% and a correlation coefficient of 0.991. This correlation is

$$\begin{aligned}\phi_b = {} & a_1 + a_2 T + a_3 T^2 + a_4 T^4 + a_5 w_s \\ & + a_6 w_s T + a_7 w_s T^3 + a_8 {w_s}^2 + a_9 {w_s}^2 T + a_{10} {w_s}^2 T^2\end{aligned} \tag{A.11}$$

where

$$\begin{aligned}&a_1 = 8.9453 \times 10^{-1}, a_2 = 4.1561 \times 10^{-4}, a_3 = -4.6262 \times 10^{-6}, \\ &a_4 = 2.2211 \times 10^{-11}, a_5 = -1.1445 \times 10^{2}, a_6 = -1.4783 \times 10^{0}, \\ &a_7 = -1.3526 \times 10^{-5}, a_8 = 7.0132 \times 10^{6}, a_9 = 5.696 \times 10^{4}, \\ &a_{10} = -2.8624 \times 10^{2}\end{aligned} \tag{A.12}$$

Eq. (A.11) has a validity of $0 \leq T \leq 200°C$ and $0.010 \leq w_s \leq 0.120$ kg/kg, with an accuracy of ±1.4%. However, this correlation is limited to a salinity of 10 g/kg and cannot be extended to lower salinities (i.e., for dilute solutions). It is possible for a seawater stream to become diluted to a salinity below 10 g/kg in certain osmotically driven processes. Literature values and correlations of the osmotic coefficient for diluted seawater with a salinity of 10 g/kg and below that adhere to this proper physical limit are difficult to find. As described by the Debye-Hückel theory, the osmotic coefficient for a mixture approaches a value of 1 with decreasing salinity and does so independently of temperature. Therefore, an extension of the correlation provided by Sharqawy et al. [22] was developed by Sharqawy et al. [78] in 2013. By using the theoretical expression for the osmotic coefficient of dilute solutions given by Brønsted [79], the correct behavior as $b \to 0$ can be obtained

$$\phi_b = 1 - \kappa\sqrt{b} + \lambda b \tag{A.13}$$

where b is the molality of the solution given by Eq. (47), and κ and λ are two fitting parameter constants. To find the value of these constants, Eq. (A.13) and its first derivative with respect to salt concentration are set to equal the value of ϕ_b given by Eq. (A.11) its first derivative with respect to salt concentration at 0.010 kg/kg, forming two equations with the two constants as unknowns. At 25°C, the two constants are found to be $\kappa = 0.3484$ and $\lambda = 0.3076$. (For the complete correlation of κ and λ as function of temperature, please see Ref. [20].) The final osmotic coefficient function is now set to be a piecewise function with Eq. (A.13) forming the function for $0 \leq w_s < 0.010$ kg/kg and Eq. (A.11) forming the $0.010 \leq w_s \leq 0.120$ kg/kg section.

A.6 Specific Heat Capacity at Constant Pressure

The specific heat capacity at constant pressure for seawater is less than that of freshwater, which reduces the amount of sensible heat that can be transferred at the same temperature

difference. The specific heat capacity can be calculated by using Eq. (A.14) given by Jamieson et al. [80], which fits the experimental measurements with an accuracy of ±0.3%. Eq. (A.14) is valid for temperatures of 0–180°C and salt concentration range of 0–0.18 kg/kg.

$$c_{p,sw} = A + B(T + 273.15) + C(T + 273.15)^2 + D(T + 273.15)^3 \tag{A.14}$$

Here $c_{p,sw}$ is in kJ/kg K, T in °C, w_s in g/kg (*not* kg/kg for this property correlation), and

$$A = 5.328 - 9.76 \times 10^{-2} w_s + 4.04 \times 10^{-4} w_s^2 \tag{A.15}$$

$$B = -6.913 \times 10^{-3} + 7.351 \times 10^{-4} w_s - 3.15 \times 10^{-6} w_s^2 \tag{A.16}$$

$$C = 9.6 \times 10^{-6} - 1.927 \times 10^{-6} w_s + 8.23 \times 10^{-9} w_s^2 \tag{A.17}$$

$$D = 2.5 \times 10^{-9} + 1.666 \times 10^{-9} w_s - 7.125 \times 10^{-12} w_s^2 \tag{A.18}$$

Fig. A.6 shows the specific heat of seawater calculated from Eq. (A.14) as a function of temperature and salt concentration. It is shown that the specific heat of seawater is less than that of fresh water by about 16% at a salt concentration of 0.16kg/kg.

It is important to mention here that the last coefficient in Eq. (A.16) was printed with a positive sign in the original paper [80]. However, the correlation matches the experimental data given in the original paper only if a negative sign is used. We believe that there is a typographical error in the original paper, and we have adopted a negative sign here.

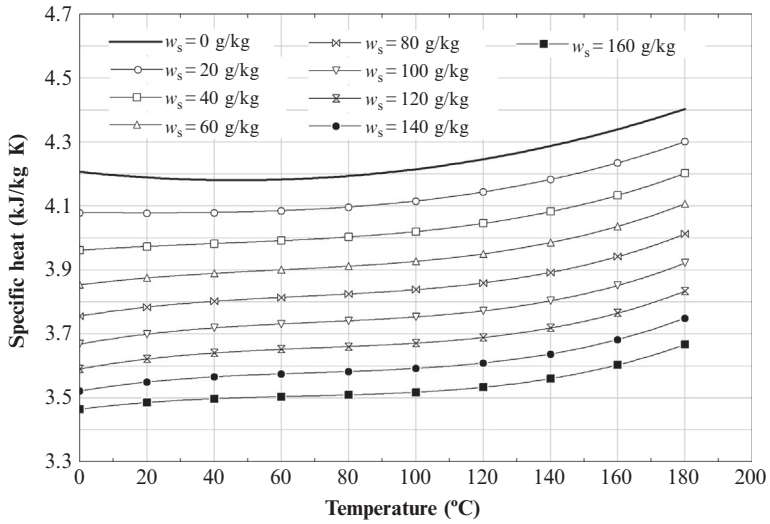

Fig. A.6 Specific heat of seawater.

Table A.1 Seawater thermodynamic properties: $T_0 = 25$ °C, $p = p_0 = 101.325$ kPa, $w_s = w_{s,0} = 0.035$ kg/kg

T (°C)	v (m^3/kg)	u (kJ/kg)	h (kJ/kg)	s (kJ/kg K)	μ_w (kJ/kg)	μ_s (kJ/kg)	e_f (kJ/kg)
10	0.000974	40.0	40.1	0.144	−3.12	64.57	1.71
15	0.000975	59.8	59.9	0.214	−4.10	66.54	0.77
20	0.000976	79.7	79.8	0.282	−5.45	68.50	0.20
25	0.000977	99.7	99.8	0.350	−7.15	70.46	0.00
30	0.000978	119.6	119.7	0.416	−9.20	72.41	0.14
35	0.000980	139.6	139.7	0.482	−11.60	74.38	0.62
40	0.000982	159.6	159.7	0.546	−14.33	76.35	1.42
45	0.000984	179.7	179.8	0.610	−17.40	78.35	2.53
50	0.000986	199.7	199.8	0.672	−20.80	80.36	3.94
55	0.000989	219.8	219.9	0.734	−24.52	82.41	5.64
60	0.000991	239.9	240.0	0.795	−28.56	84.49	7.62
65	0.000994	260.0	260.1	0.855	−32.92	86.61	9.87
70	0.000997	280.1	280.2	0.914	−37.58	88.77	12.37
75	0.000999	300.3	300.4	0.972	−42.55	90.98	15.13
80	0.001003	320.4	320.5	1.029	−47.82	93.25	18.14
85	0.001006	340.5	340.6	1.086	−53.38	95.57	21.39
90	0.001009	360.7	360.8	1.142	−59.23	97.95	24.86

A.7 Tabulated Data

Tabulated data for seawater thermodynamic properties are given in Table A.1 using the equations presented in this appendix, and the equations for chemical potential given by Nayar et al. [20]. The properties include specific volume, specific internal energy, specific enthalpy, specific entropy, chemical potentials, and specific flow exergy. These are given at temperature of 10–90°C, salt concentration of 0.035 kg/kg (absolute salinity 35 g/kg), and pressure of 101.325 kPa. However, the equations presented in the appendix can be used up to temperature of 120°C. In this case for temperatures higher than the normal boiling temperature, the pressure is the saturated pressure, and the state of the seawater is the saturated liquid state. For the flow exergy values given in Table A.1, the environment dead state is selected at $T_0 = 25$°C, $p_0 = 101.325$ kPa and $w_{s,0} = 0.035$ kg/kg.

As previously noted, a full set of codes for calculating seawater thermophysical properties are available without charge at http://web.mit.edu/seawater.

APPENDIX B. PITZER PARAMETERS

This appendix discusses the terms in the Pitzer equations for the activity and osmotic coefficients (Eqs. 33–36) in aqueous solutions. The term F is based on an extended Debye-Hückel function [6], reflecting the characteristic first-order-square-root dependence on ionic strength caused by long-range electrostatic interactions:

$$F = -A^{\phi}\left(\frac{\sqrt{I}}{1+1.2\sqrt{I}} + \frac{2}{1.2}\ln(1+1.2\sqrt{I})\right) + \sum_{c}\sum_{a} b_c b_a B'_{ca} + \sum_{c<c'}\sum b_c b_{c'} \Phi'_{cc'} + \sum_{a<a'}\sum b_a b_{a'} \Phi'_{aa'} \tag{B.1}$$

The parameter A^{ϕ} is related to the Debye-Hückel limiting law, and is given by

$$A^{\phi} = \frac{1}{3}\left[\frac{e^3(2N_0\rho_w)^{1/2}}{8\pi(\epsilon_r\epsilon_0 k_b T)^{3/2}}\right] \tag{B.2}$$

where ρ_w is the density of pure water. Data for the relative permittivity of pure water as a function of temperature can be obtained from Uematsu and Franck [81].

Interactions between cations and anions are represented by the functions B_{ij}, B'_{ij}, B^{ϕ}_{ij}, and C_{ij}:

$$B_{MX} = \beta^{(0)}_{MX} + \beta^{(1)}_{MX} g\left(\alpha_{MX}\sqrt{I}\right) + \beta^{(2)}_{MX} g(12\sqrt{I}) \tag{B.3a}$$

$$B'_{MX} = \beta^{(1)}_{MX} g'\left(\alpha_{MX}\sqrt{I}\right)/I + \beta^{(2)}_{MX} g'\left(12\sqrt{I}\right)/I \tag{B.3b}$$

$$B^{\phi}_{MX} = \beta^{(0)}_{MX} + \beta^{(1)}_{MX}\exp\left(-\alpha_{MX}\sqrt{I}\right) + \beta^{(2)}_{MX}\exp\left(-12\sqrt{I}\right) \tag{B.3c}$$

$$C_{MX} = \frac{C^{\phi}_{MX}}{2|z_M z_X|^{1/2}} \tag{B.3d}$$

where $\alpha_{MX} = 2.0$ for $j-1$ electrolytes and $\alpha_{MX} = 1.4$ for $2-2$ and higher electrolytes. The parameters $\beta^{(i)}_{MX}$ are tabulated for a given ion pair, and $\beta^{(2)}_{MX}$ is associated with complex formation and generally only nonzero for $2-2$ electrolytes. The functions $g(x)$ and $g'(x)$ are

$$g(x) = 2(1-(1+x)e^{-x})/x^2 \tag{B.4a}$$

$$g'(x) = -\frac{2}{x^2}\left[1-\left(1+x+\frac{x^2}{2}\right)e^{-x}\right] \tag{B.4b}$$

Interactions between like-charged pairs are represented by Φ_{ij} and Φ'_{ij}:

$$\Phi_{ij} = \theta_{ij} + {}^{E}\theta_{ij}(I) \tag{B.5a}$$

$$\Phi'_{ij} = {}^{E}\theta'_{ij}(I) \tag{B.5b}$$

$$\Phi^{\phi}_{ij} = \theta_{ij} + {}^{E}\theta_{ij}(I) + I\,{}^{E}\theta'_{ij}(I) \tag{B.5c}$$

Here the only adjustable parameter for a given ion pair is θ_{ij}. The terms ${}^{E}\theta_{ij}(I)$ and ${}^{E}\theta'_{ij}(I)$ represent excess free energy arising from electrostatic interactions between asymmetric electrolytes (i.e., ions with charge of like sign and unlike magnitude), and are functions of ionic strength only, as

$$ {}^{E}\theta_{ij} = \frac{z_i z_j}{4I}\left(J_0(x_{ij}) - \frac{1}{2}J_0(x_{ii}) - \frac{1}{2}J_0(x_{jj})\right) \tag{B.6a} $$

$$ {}^{E}\theta'_{ij} = \frac{z_i z_j}{8I^2}\left(J_1(x_{ij}) - \frac{1}{2}J_1(x_{ii}) - \frac{1}{2}J_1(x_{jj})\right) - \frac{{}^{E}\theta_{ij}}{I} \tag{B.6b} $$

where

$$ J_0(x) = \frac{1}{4}x - 1 + \frac{1}{x}\int_0^\infty \left[1 - \exp\left(-\frac{x}{y}e^{-y}\right)\right] y^2\, dy \tag{B.6c} $$

$$ J_1(x) = \frac{1}{4}x - \frac{1}{x}\int_0^\infty \left[1 - \left(1 + \frac{x}{y}e^{-y}\right) \times \exp\left(-\frac{x}{y}e^{-y}\right)\right] y^2\, dy \tag{B.6d} $$

and

$$ x_{ij} = 6 z_i z_j A^{\phi}\sqrt{I} \tag{B.6e} $$

The integrals in Eqs. (B.6c), (B.6d) can be calculated numerically.

In summary, the adjustable parameters are as follows. There are three to four per unlike-charged pair, $\beta^{(0)}_{MX}$, $\beta^{(1)}_{MX}$, $\beta^{(2)}_{MX}$, and C^{ϕ}_{MX}; one per like-charged pair, θ_{ij}; and one per cation-cation-anion and anion-anion-cation triplet, Ψ_{ijk}. The values of these parameters can be found in a variety of sources, some of which contain slightly different values. Tables of values can be found in, for example, Refs. [7, 10, 12, 82–84].

In principle, each of the adjustable binary and ternary parameters ($\beta^{(i)}_{MX}$, C^{ϕ}_{MX}, θ_{ij}, and Ψ_{ijk}) are functions of temperature. Unfortunately, a complete set of these data as a function of temperature over the range of interest are generally unavailable in open literature (although some significant collections are available, e.g., [10, 83, 84]). However, Silvester and Pitzer have noted that the temperature derivatives of these parameters are often small [85], and much of the temperature variation in activity coefficient is confined to A^{ϕ} (Eq. B.2) both in the parameter's explicit temperature dependence, as well as implicitly through variations in the dielectric constant [86]. In addition, solubility computations by DeLima and Pitzer [87] were not impaired by using room temperature values for the mixing parameters (θ_{ij} and Ψ_{ijk}) up to 473 K—well outside the temperature range of typical desalination systems.

REFERENCES

[1] S. Glasstone, Thermodynamics for Chemists, D. Van Nostrand Company, Inc., New York, NY, 1947.
[2] K.S. Pitzer, J.C. Peiper, R.H. Busey, Thermodynamic properties of aqueous sodium chloride solutions, J. Phys. Chem. Ref. Data 13 (1) (1984) 1–102.

[3] R.A. Robinson, R.H. Stokes, Electrolyte Solutions, second ed., Dover, Mineola, NY, 2002.
[4] P. Atkins, J. de Paula, Atkins' Physical Chemistry, eighth ed., W.H. Freeman and Company, New York, NY, 2006.
[5] W. Hamer, Y. Wu, Osmotic coefficients and mean activity coefficients of uni-univalent electrolytes in water at 25°C, J. Phys. Chem. Ref. Data 1 (4) (1972) 1047–1099.
[6] P. Debye, E. Hückel, Zur Theorie der Elektrolyte, Phys. Z. 24 (9) (1923) 185–206.
[7] J.F. Zemaitis, D.M. Clark, M. Rafal, N.C. Scrivner, Handbook of Aqueous Electrolyte Thermodynamics, Wiley-AIChE, Hoboken, NJ, USA, 1986.
[8] C.W. Davies, The extent of dissociation of salts in water. Part VIII. An equation for the mean ionic activity coefficient of an electrolyte in water, and a revision of the dissociation constants of some sulphates, J. Chem. Soc. (1938) 2093–2098.
[9] K.S. Pitzer, J.J. Kim, Thermodynamics of electrolytes. IV. Activity and osmotic coefficients for mixed electrolytes, J. Am. Chem. Soc. 96 (18) (1974) 5701–5707.
[10] K.S. Pitzer, A thermodynamic model for aqueous solutions of liquid-like density, Rev. Mineral. Geochem. 17 (1987) 97–142.
[11] C.E. Harvie, J.H. Weare, The prediction of mineral solubilities in natural waters: the Na-K-Mg-Ca-Cl-SO_4-H_2O system from zero to high concentration at 25°C, Geochim. Cosmochim. Acta 44 (1980) 981–997.
[12] C.E. Harvie, N. Møller, J.H. Weare, The prediction of mineral solubilities in natural waters: the Na-K-Mg-Ca-H-Cl-SO_4-OH-HCO_3-CO_3-CO_2-H_2O system to high ionic strengths at 25°C, Geochim. Cosmochim. Acta 48 (1984) 723–751.
[13] K.S. Pitzer, Thermodynamics of electrolytes. I. Theoretical basis and general equations, J. Phys. Chem. 77 (2) (1973) 268–277.
[14] K.H. Mistry, H.A. Hunter, J.H. Lienhard V, Effect of composition and nonideal solution behavior on desalination calculations for mixed electrolyte solutions with comparison to seawater, Desalination 318 (2013) 34–47.
[15] A. Saul, W. Wagner, International equations for the saturation properties of ordinary water substance, J. Phys. Chem. Ref. Data 16 (1987) 893–901.
[16] A. Bejan, Advanced Engineering Thermodynamics, third ed., John Wiley & Sons, Inc., Hoboken, NJ, 2006.
[17] M.J. Moran, Availability Analysis: A Guide to Efficient Energy Use, ASME Press, New York, NY, 1989.
[18] M.H. Sharqawy, J.H. Lienhard V, S.M. Zubair, On exergy calculations of seawater with applications in desalination systems, Int. J. Therm. Sci. 50 (2) (2011) 187–196.
[19] K.H. Mistry, R.K. McGovern, G.P. Thiel, E.K. Summers, S.M. Zubair, J.H. Lienhard V, Entropy generation analysis of desalination technologies, Entropy 13 (10) (2011) 1829–1864.
[20] K.G. Nayar, M.H. Sharqawy, L.D. Banchik, J.H. Lienhard V, Thermophysical properties of seawater: a review and new correlations that include pressure dependence, Desalination 387 (2016) 1–24.
[21] R.W. Stoughton, M.H. Lietzke, Calculation of some thermodynamic properties of sea salt solutions at elevated temperature from data on NaCl solutions, J. Chem. Eng. Data 10 (3) (1965) 254–260.
[22] M.H. Sharqawy, J.H. Lienhard V, S.M. Zubair, Thermophysical properties of seawater: a review of existing correlations and data, Desalin. Water Treat. 16 (2010) 354–380.
[23] K.H. Mistry, J.H. Lienhard V, S.M. Zubair, Effect of entropy generation on the performance of humidification-dehumidification desalination cycles, Int. J. Therm. Sci. 49 (9) (2010) 1837–1847.
[24] A. Bejan, G. Tsatsaronis, M. Moran, Thermal Design & Optimization, John Wiley & Sons, Inc., New York, NY, 1996.
[25] N. Kahraman, Y.A. Çengel, Exergy analysis of a MSF distillation plant, Energy Convers. Manag. 46 (15–16) (2005) 2625–2636.
[26] W. Wagner, A. Pruss, The IAPWS formulation 1995 for the thermodynamic properties of ordinary water substance for general and scientific use, J. Phys. Chem. Ref. Data 31 (2) (2002) 387–535.
[27] A. Bejan, General criterion for rating heat-exchanger performance, Int. J. Heat Mass Transf. 21 (5) (1978) 655–658.
[28] K.H. Mistry, M.A. Antar, J.H. Lienhard V, An improved model for multiple effect distillation, Desalin. Water Treat. 51 (4–6) (2013) 807–821.

[29] Y.M. El-Sayed, R.S. Silver, Principles of Desalination, vol. A, chap. 2: Fundamentals of Distillation, second ed., Academic Press, New York, NY, 1980, pp. 55–109.
[30] M.A. Darwish, F. Al-Juwayhel, H.K. Abdulraheim, Multi-effect boiling systems from an energy viewpoint, Desalination 194 (1–3) (2006) 22–39.
[31] H.T. El-Dessouky, H.M. Ettouney, Fundamentals of Salt Water Desalination, Elsevier, Amsterdam, 2002.
[32] K.W. Lawson, D.R. Lloyd, Membrane distillation, J. Membr. Sci. 124 (1) (1997) 1–25.
[33] J.M. Rodriguez-Maroto, L. Martinez, Bulk and measured temperatures in direct contact membrane distillation, J. Membr. Sci. 250 (1–2) (2005) 141–149.
[34] L. Martinez-Diez, F.J. Florido-Diaz, Desalination of brines by membrane distillation, Desalination 137 (1–3) (2001) 267–273.
[35] L. Song, B. Li, K.K. Sirkar, J.L. Gilron, Direct contact membrane distillation-based desalination: novel membranes, devices, larger-scale studies, and a model, Ind. Eng. Chem. Res. 46 (8) (2007) 2307–2323.
[36] H. Lee, F. He, L. Song, J. Gilron, K.K. Sirkar, Desalination with a cascade of cross-flow hollow fiber membrane distillation devices integrated with a heat exchanger, AIChE J. 57 (7) (2011) 1780–1795.
[37] V.A. Bui, L.T.T. Vu, M.H. Nguyen, Modelling the simultaneous heat and mass transfer of direct contact membrane distillation in hollow fibre modules, J. Membr. Sci. 353 (1–2) (2010) 85–93.
[38] J.H. Lienhard IV, J.H. Lienhard V, A Heat Transfer Textbook, fourth ed., Dover Publications, Mineola, NY, 2011. http://ahtt.mit.edu.
[39] H.E.S. Fath, S.M. Elsherbiny, A.A. Hassan, M. Rommel, M. Wieghaus, J. Koschikowski, M. Vatansever, PV and thermally driven small-scale, stand-alone solar desalination systems with very low maintenance needs, Desalination 225 (1–3) (2008) 58–69.
[40] F. Banat, N. Jwaied, M. Rommel, J. Koschikowski, M. Wieghaus, Desalination by a "compact SMADES" autonomous solar-powered membrane distillation unit, Desalination 217 (1–3) (2007) 29–37.
[41] J. Swaminathan, H.W. Chung, D.M. Warsinger, J.H. Lienhard V, Simple method for balancing direct contact membrane distillation, Desalination 383 (2016) 53–59.
[42] G.P. Thiel, R.K. McGovern, S.M. Zubair, J.H. Lienhard V, Thermodynamic equipartition for increased second law efficiency, Appl. Energy 118 (2014) 292–299.
[43] J. Swaminathan, H.W. Chung, D.M. Warsinger, F.A. Al-Marzooqi, H.A. Arafat, J.H. Lienhard V, Energy efficiency of permeate gap and novel conductive gap membrane distillation, J. Membr. Sci. 502 (2016) 171–178.
[44] J.M. Veza, Mechanical vapour compression desalination plants—a case study, Desalination 101 (1) (1995) 1–10.
[45] S.E. Aly, Gas turbine total energy vapour compression desalination system, Energy Convers. Manag. 40 (7) (1999) 729–741.
[46] G.P. Thiel, E.W. Tow, L.D. Banchik, H.W. Chung, J.H. Lienhard V, Energy consumption in desalinating produced water from shale oil and gas extraction, Desalination 366 (2015) 94–112.
[47] A.S. Nafey, H.E.S. Fath, A.A. Mabrouk, Thermoeconomic design of a multi-effect evaporation mechanical vapor compression (MEE-MVC) desalination process, Desalination 230 (1–3) (2008) 1–15.
[48] J.R. Lara, G. Noyes, M.T. Holtzapple, An investigation of high operating temperatures in mechanical vapor-compression desalination, Desalination 227 (1–3) (2008) 217–232.
[49] N. Lukic, L.L. Diezel, A.P. Fröba, A. Leipertz, Economical aspects of the improvement of a mechanical vapour compression desalination plant by dropwise condensation, Desalination 264 (1–2) (2010) 173–178.
[50] Energy Recovery Inc, ERI power model, (2010). http://www.energyrecovery.com/resource/power-model/.
[51] M. Elimelech, W.A. Phillip, The future of seawater desalination: energy, technology, and the environment, Science 333 (6043) (2011) 712–717.
[52] Desalitech Ltd, Doing away with RO energy-recovery devices, Desalin. Water Reuse 20 (2) (2010) 26–28.
[53] D.M. Warsinger, E.W. Tow, K.G. Nayar, L.A. Maswadeh, J.H. Lienhard V, Energy efficiency of batch and semi-batch reverse osmosis desalination, Water Res. 103 (2016) 272–282.

[54] K.H. Mistry, J.H. Lienhard V, Generalized least energy of separation for desalination and other chemical separation processes, Entropy 15 (6) (2013) 2046–2080.
[55] M.J. Moran, H.N. Shapiro, Fundamentals of Engineering Thermodynamics, sixth ed., John Wiley & Sons, Inc., Hoboken, NJ, 2007.
[56] Global Water Intelligence, DesalData.com, (2013). http://desaldata.com.
[57] J.E. Miller, Review of water resources and desalination technologies, Sandia National Laboratories, Livermore, CA, 2003. SAND 2003-0800.
[58] G.J. Crisp, Actual energy consumption and water cost for the SWRO systems at Perth, in: Desalination: An Energy Solution, International Desalination Association, Huntington Beach, CA, November 2–3, 2010. IDA_HB2010-Crisp.
[59] R.L. Stover, Isobaric energy recovery technology—history and future opportunities, in: Desalination: An Energy Solution, International Desalination Association, Huntington Beach, CA, November 2–3, 2010 IDA_HB2010-Stover.
[60] R.L. Stover, Seawater reverse osmosis with isobaric energy recovery devices, Desalination 203 (1–3) (2007) 168–175.
[61] C. Fritzmann, J. Löwenberg, T. Wintgens, T. Melin, State-of-the-art of reverse osmosis desalination, Desalination 216 (1–3) (2007) 1–76.
[62] E.W. Tow, R.K. McGovern, J.H. Lienhard V, Raising forward osmosis brine concentration efficiency through flow rate optimization, Desalination 366 (2015) 71–79.
[63] R.K. McGovern, J.H. Lienhard V, On the potential of forward osmosis to energetically outperform reverse osmosis desalination, J. Membr. Sci. 469 (2014) 245–250.
[64] R.K. McGovern, G.P. Thiel, G.P. Narayan, S.M. Zubair, J.H. Lienhard V, Performance limits of single and dual stage humidification dehumidification desalination systems, Appl. Energy 102 (2013) 1081–1090.
[65] G.P. Narayan, K.M. Chehayeb, R.K. McGovern, G.P. Thiel, S.M. Zubair, J.H. Lienhard V, Thermodynamic balancing of the humidification dehumidification desalination system by mass extraction and injection, Int. J. Heat Mass Transf. 57 (2) (2013) 756–770.
[66] F. Al-Sulaiman, G.P. Narayan, J.H. Lienhard V, Exergy analysis of a high-temperature-steam-driven, varied-pressure, humidification-dehumidification system coupled with reverse osmosis, Appl. Energy 103 (2013) 552–561.
[67] K.M. Chehayeb, G.P. Narayan, S.M. Zubair, J.H. Lienhard V, Thermodynamic balancing of a fixed-size two-stage humidification dehumidification desalination system, Desalination 369 (2015) 125–139.
[68] D.M. Warsinger, K.H. Mistry, K.G. Nayar, H.W. Chung, J.H. Lienhard V, Entropy generation of desalination powered by variable temperature waste heat, Entropy 17 (2015) 7530–7566.
[69] R.K. McGovern, S.M. Zubair, J.H. Lienhard V, The benefits of hybridizing electrodialysis with reverse osmosis, J. Membr. Sci. 469 (2014) 326–335.
[70] J. Swaminathan, K.G. Nayar, J.H. Lienhard V, Mechanical vapor compression-membrane distillation hybrids for reduced specific energy consumption, Desalin, Water Treat. 57 (55) (2016) 26507–26517.
[71] K.H. Mistry, J.H. Lienhard V, An economics-based second law efficiency, Entropy 15 (2013) 2736–2765.
[72] F.J. Millero, R. Feistel, D.G. Wright, T.J. McDougall, The composition of standard seawater and the definition of the reference-composition salinity scale, Deep Sea Res. I Oceanogr. Res. Pap. 55 (2008) 50–72.
[73] International Association for the Properties of Water and Steam, Release on the IAPWS formulation for the thermodynamic properties of seawater, (2008).
[74] J.D. Isdale, R. Morris, Physical properties of sea water solutions: density, Desalination 10 (1972) 329–339.
[75] F.J. Millero, A. Poisson, International one-atmosphere equation of state of seawater, Deep Sea Res. Part A Oceanogr. Res. Pap. 28 (1981) 625–629.
[76] Release on the IAPWS formulation 1995 for the thermodynamic properties of ordinary water substance for general and scientific use, International Association for the Properties of Water and Steam, 1996.
[77] L.A. Bromley, D. Singh, P. Ray, S. Sridhar, S.M. Read, Thermodynamic properties of sea salt solutions, AIChE J. 20 (1974) 326–335.

[78] M.H. Sharqawy, L.D. Banchik, J.H. Lienhard V, Effectiveness-mass transfer units (ε-MTU) model of an ideal pressure retarded osmosis membrane mass exchanger, J. Membr. Sci. 445 (2013) 211–219.
[79] K.S. Pitzer, Thermodynamics, third ed., McGraw-Hill, Inc., New York, NY, 1995.
[80] D.T. Jamieson, J.S. Tudhope, R. Morris, G. Cartwright, Physical properties of sea water solutions: heat capacity, Desalination 7 (1969) 23–30.
[81] M. Uematsu, E.U. Franck, Static dielectric constant of water and steam, J. Phys. Chem. Ref. Data 9 (4) (1980) 1291–1306.
[82] H.-T. Kim, W.J. Frederick, Evaluation of Pitzer ion interaction parameters of aqueous electrolyte solutions at 25°C. 2. Ternary mixing parameters, J. Chem. Eng. Data 33 (1988) 278–283.
[83] R.T. Pabalan, K.S. Pitzer, Thermodynamics of concentrated electrolyte mixtures and the prediction of mineral solubilities to high temperatures for mixtures in the system Na-K-Mg-Cl-SO_4-OH-H_2O, Geochim. Cosmochim. Acta 51 (1987) 2429–2443.
[84] F.J. Millero, D. Pierrot, A chemical equilibrium model for natural waters, Aquat. Geochem. 4 (1998) 153–199.
[85] L.F. Silvester, K.S. Pitzer, Thermodynamics of electrolytes. X. Enthalpy and the effect of temperature on the activity coefficients, J. Solut. Chem. 7 (5) (1978) 327–337.
[86] L.F. Silvester, K.S. Pitzer, Thermodynamics of electrolytes. 8. High-temperature properties, including enthalpy and heat capacity, with application to sodium chloride, J. Phys. Chem. 81 (19) (1977) 1822–1828.
[87] M.P. de Lima, K.S. Pitzer, Thermodynamics of saturated electrolyte mixtures of NaCl with Na_2SO_4 and with $MgCl_2$, J. Solut. Chem. 12 (3) (1983) 187–199.

CHAPTER 5

Brine Management in Desalination Plants

Shefaa Mansour, Hassan A. Arafat, Shadi W. Hasan
Khalifa University of Science and Technology, Abu Dhabi, United Arab Emirates

Contents

1. INTRODUCTION

One main concern related to desalination technologies is the discharge of brine and its environmental impact. After the extraction of large volumes of fresh water using desalination processes, such as reverse osmosis (RO), water with huge amounts of concentrated salt (called brine) is discharged into the sea or inland waterbodies. This in turn threatens marine ecosystems and aquatic species. The high level of concentrated salt associated with pretreatment chemicals results in a high risk of endangering the flora and fauna living in the sea [1,2]. Einav et al. (2002) noted that the concentration of salt in RO brine is 1.3–1.7 times the concentration of the original seawater used as feed [2]. In addition to salinity, other harmful effects of brine include temperature and dissolved chemicals. High brine temperatures are encountered in thermal technologies such as multistage flashing (MSF) and multieffect distillation (MED) and pose a threat to marine life that can lead to the death of species if they are exposed to such waters for a long period of time. Also, dumping brine into the sea has a negative effect because of the pretreatment chemical residues present in brine, such as sodium hypochlorite (NaOCl) and sodium hexametaphosphate $(NaPO_3)_6$ [3].

Desalination Sustainability
http://dx.doi.org/10.1016/B978-0-12-809791-5.00005-5

Because of the world's exponential increase in brine generated by seawater desalination, improving its disposal methods and exploring the use of different technologies as treatment options are becoming increasingly essential. The choice of the most appropriate brine disposal method depends on a number of factors, including the brine's volume, its components, and the geographic location at its point of discharge. Further factors include the accessibility of a discharge spot, both capital and operation costs, and the approval of the public [4]. This chapter discusses different brine disposal methods and their environmental impact, brine discharge modeling, and the potential uses for brine salts after extraction.

Figs. 1 and 2 indicate the growing interest in brine discharge and management as well as the diversity of issues being studied in relation to brine. The two figures were generated based on the references used within this chapter, ranging from 2000 to 2015.

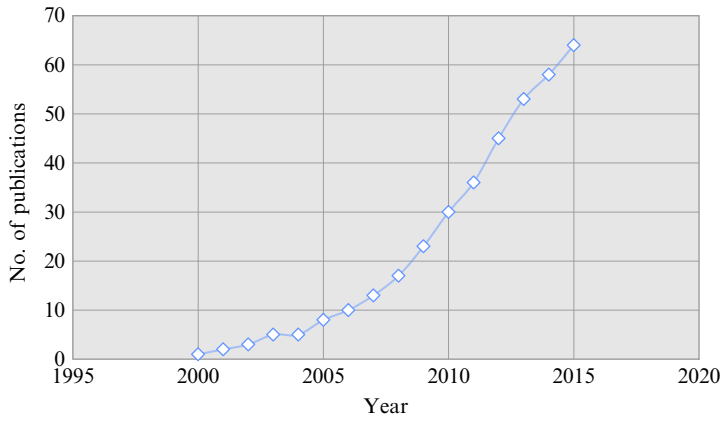

Fig. 1 Cumulative publications on desalination brine used in this chapter (2000–15).

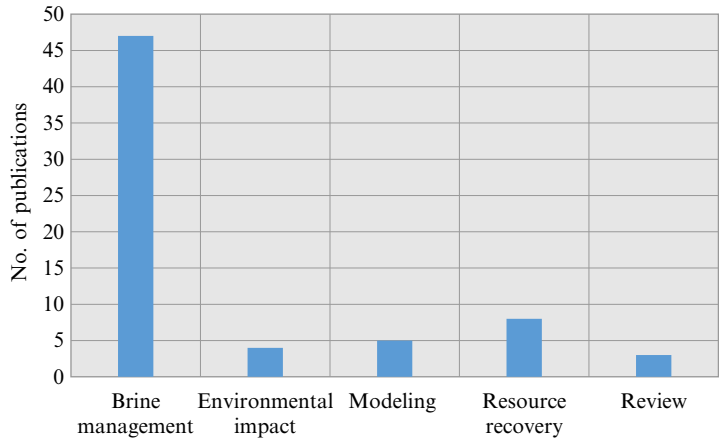

Fig. 2 Subjects of publications on desalination brine used in this chapter (2000–15).

1.1 Brine Disposal Methods

Brine disposal can be broadly divided into sea and inland disposal. Seawater discharge is the common practice whenever a desalination plant is within close proximity to the sea. Brine sea surface discharge was primarily implemented over the years because of the absence of environmental regulations. This caused a buildup of salinity on the shores near desalination plants and led to pollution in marine environments. The three main factors impacting marine species as a result of brine discharge are salinity, temperature, and total alkalinity. Species react differently to changes in concentration; that is, some improve in productivity while others can die. Species that are young, invertebrates in particular, are more susceptible to salinity changes than older species. An added impact of this discharge is the migration of fish species, which reduces their ability to survive [5].

Thermal pollution resulting from brine temperatures greater than ocean temperatures increases the temperature of the sea, thus negatively impacting marine life and their natural balance through behavioral changes. A temperature increase up to 15°C was observed [6]. Temperature variations impact marine species in terms of their growth and reproduction, with plankton and fish being most susceptible to this change [6]. Generally speaking, temperature variations in seawater are found to have both positive and negative impacts on the marine flora and fauna, with results differing based on the species and the degree of variation in temperature.

The effect of the total alkalinity of the seawater is defined in terms of the number of equivalents of calcium carbonate ($CaCO_3$) in water. The tolerance of marine species toward a change in the alkalinity rate as a result of brine discharge has not been well documented because of experimental data limitations. However, such measurements need to be done to fully identify the impact this condition has on marine species [7].

Table 1 shows the impact of the three previously mentioned brine parameters on marine species. Table 2 shows examples of the salinity tolerance limits of different species.

Table 1 Brine impact on marine species

Factor	Impact	Species
Salinity	Rate of growth, development, species breeding activity	*Brown trout, salmon, rainbow trout*
Temperature	Growth rate, reproduction behavior	*Moina Mangolica*
Total alkalinity	Species mortality	Macroalgae, mussels, seagrasses, epifauna, plankton, echinoids, and cuttlefish

Adapted from D. Roberts, E. Johnston, N. Knott, Impacts of desalination plant discharges on the marine environment: a critical review of published studies, Water Resour. 44 (2010) 5117–5128. http://dx.doi.org/10.1016/j.watres.2010.04.036; R. Danoun, Desalination Plants: Potential Impacts of Brine Discharge on Marine Life, The University of Sydney, Australia, 2007, p. 59.

Table 2 Salinity tolerance limits of various marine species

Species	Salinity tolerance limit (ppm)
Cymodocea nodosa seagrasses	40,000
Posidonia oceanica seagrasses	39,000
Zostera noltii seagrasses	41,000
Caulerpa prolifera algae	55,000
Mussels	60,000

Adapted from P. Palomar, I. Losada, Impacts of Brine Discharge on the Marine Environment: Modelling as a Predictive Tool, Desalination, Trends and Technologies, 2011.

1.1.1 Seawater Brine Disposal Method

For quite some time, disposal of brine in seawater was considered the cheapest and safest method because of its rapid mixing and dilution rates [4]. Today most large desalination plants with high water production dispose of brine through the submerged seawater method. This process is intended for brine dilution within the mixing zone, resulting in fewer adverse effects on aquatic life. The mixing zone is positioned around the point of discharge, which enhances seawater dilution (Fig. 3). Improvements in disposal methods can be made through a number of adjustments according to Malcangio et al. (2010), including the use of long discharge pipes and by diluting brine in water that will be discharged from the system [8].

The volume of rejected brine from seawater desalination plants can be reduced through an enhanced permeate recovery. This approach unfortunately produces a more

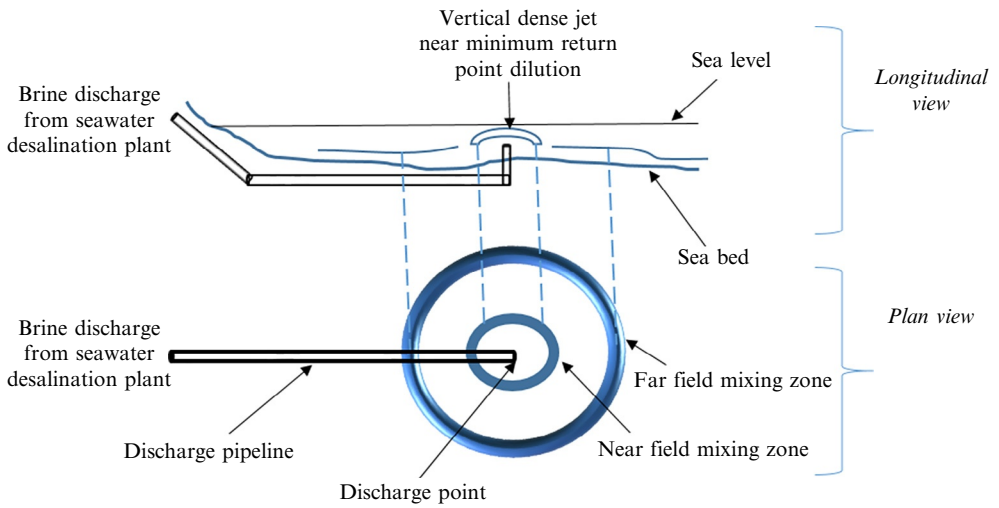

Fig. 3 Mixing zone approach. *(Adapted from N. Ahmad, R. Baddour, Minimum return dilution method to regulate discharge of brine from desalination plants, Can. J. Civ. Eng. 41 (2014) 389–395, http://dx.doi.org/10.1139/cjce-2012-0528).*

concentrated brine that needs to be diluted prior to its discharge. Surprisingly, this mitigation method is not as environmentally effective as it may appear. Although this method leads to a reduction in the brine volume, it increases the concentration of chemicals and minerals. This problem can be solved through dilution before disposal [4]. Dilution can be done through an increase in the disposal area through which the brine is spread in the sea [9].

Another proposed brine discharge improvement is the optimization of the discharge angle above the horizontal. Brine discharge at an angle within the range of 30–45 degrees above the horizontal rather than at an angle of 60 degrees to the horizontal was discussed by Malcangio et al. (2010). Discharging the brine at an angle within the 30- to 45-degree range above the horizontal results in enhanced levels of dilution, more efficient brine transport through weak water currents, and a greater ability to discharge concentrate within close proximity to the shore. These factors allow for a reduction in the cost for dumping. Fig. 4 shows images of brine discharge at an angle. Another improvement, which was suggested by Malcangio et al. (2010), involves the use of shorter discharge pipes [8].

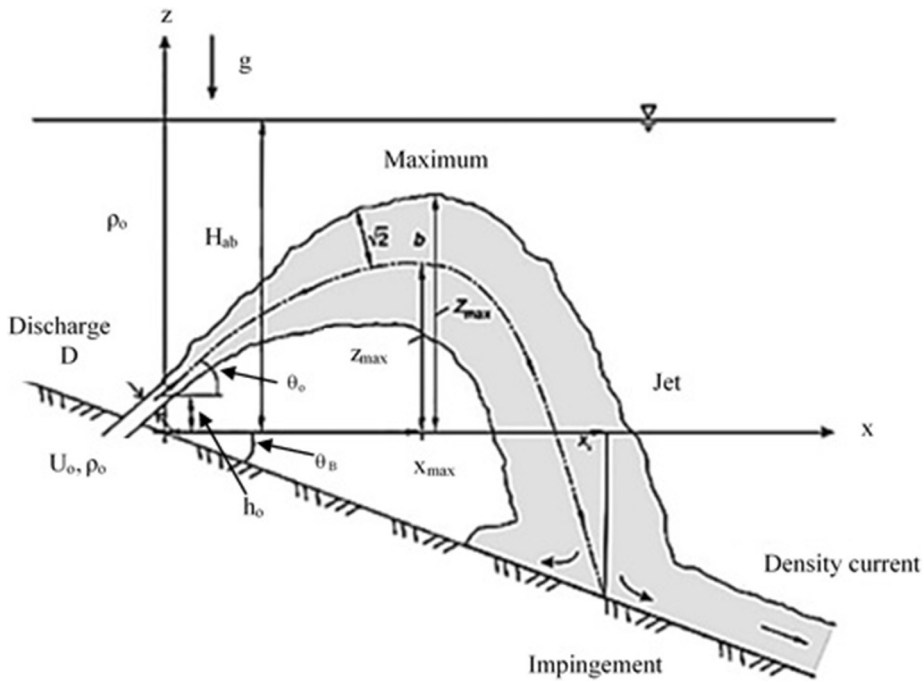

Fig. 4 Seawater brine discharge at an angle. *(Obtained from T. Bleninger, G. Jirka, Modelling and environmentally sound management of brine discharges from desalination plants, Desalination 221 (2008) 585–597, http://dx.doi.org/10.1016/j.desal.2007.02.059).*

Furthermore, adverse environmental effects can be lessened by improving the mixing dilution by using multiple discharge ports. The latter are used for flow distribution over a large area for the enhanced dilution of large discharge volumes. Another improvement is the mixing of brine with treated wastewater effluent prior to sea discharge in order to reduce the brine's salinity. The constituents of the wastewater determine whether the water is suitable for brine mixing prior to discharge [7].

1.1.2 Inland Discharge Methods

Similar to seawater desalination brine discharge, several inland brine discharge methods exist, including sewer discharge, deep well injections, evaporative ponds, and land application. Zero-liquid-discharge (ZLD) schemes for inland desalination have also been implemented and are discussed in subsequent sections in detail.

Brine disposal through sewage systems has been found to reduce the biological oxygen demand of domestic sewage water that goes through sewage systems, thus improving the quality of wastewater. Nonetheless, brine can result in a rise in the salinity of the wastewater and thereby affect its treatment by overwhelming the capacity of the system. A further disadvantage of this disposal method is the use of high-salinity-treated wastewater in agriculture because some plant species cannot tolerate those salinities. Brine discharge into evaporation ponds is the most widely implemented inland brine discharge method. It is commonly used in arid environments allowing for natural evaporation of brine. Of all the methods, evaporation ponds are thought to be the most appropriate for brine concentration because of the ease of obtaining manageable solid waste and a pure liquid flow that is well suited for direct discharge or reuse applications [10]. This method is usually implemented in arid areas with abundant sunlight. Furthermore, these ponds are used in storing drained saline water tables that result in soil salinity issues. This approach is also considered to be economical and eco-friendly if certain guidelines relating to its design, construction, maintenance, and operation are taken into consideration. Furthermore, this method of disposal has been noted to be the least expensive in terms of its high evaporation rates and its low cost of land [4]. This process is considered to be more economic in comparison with natural evaporation because of the reduction of the environmental costs associated with thermal energy consumption for evaporation [10]. Some disadvantages of inland brine discharge include its requirement for a larger area of land when evaporation rates are low. Furthermore, drinkable water aquifers can become polluted as a result of leakage from poorly built evaporation ponds. By sealing these ponds with liners, the risk of contaminating groundwater is reduced [4].

The work performed by Arnal et al. (2005) determined the feasibility of applying natural evaporation, while comparing it to conventional evaporation used for the concentration of brackish desalination plants brine. The aim of the study was to decrease the consumption of energy through a natural evaporation application of brine. Wet surfaces such as capillaries were subjected to wind action, which allowed a high surface density

resulting in good evaporation flow for enhanced efficiency while consuming low energy. Henceforth, these capillaries allow water evaporation and brine surface crystallization. As a result, the final solid deposits were suitable for industrial applications, and the evaporated liquid was suitable for condensing and reuse. This concept was tested through laboratory experiments on brackish water desalination plants' brines. Different adsorbents were studied for an increase in vaporization through an increase in the evaporation surface. The study concluded that the use of natural evaporation is a feasible method for desalination plants' brine concentration [10].

The use of brine in land applications such as irrigation has helped protect natural environments, specifically waterbodies, by spraying this concentrate on high-salinity-tolerant species [11]. A study in India was carried out to determine the effect of brine disposal on groundwater and soil. There was a detected seepage of this brine that resulted in an elevated groundwater hardness as a result of an increased level of sodium and chloride, which in turn increased the salinity of the soil, thus reducing its productivity. The accumulation of inorganic compounds and heavy metals in groundwater supply and soil from brine results in chronic health effects [12].

In the deep well injection method of disposal, liquid waste is injected into porous subsurface rock formations. An important factor in this method is the selection of an appropriate location because of the geological and hydrogeological settings. For instance, these wells must not be situated in areas that are susceptible to earthquakes. Concentrate is contained with the help of the porous rocks where waterproof rocks such as shale and clay protect aquifers against contamination. As such, there are certain conditions for the deep well injection brine disposal method. There needs to be proper understanding of the hydrogeological settings in order to select an injection site that does not result in contaminating freshwater supplies. This method is not considered economically viable except for larger desalination plants because of the high cost of drilling and instillation. The design of the well, surveying, and testing are used for determining how well suited this process is from an economic and environmental perspective. The tested parameters studied are the confinement conditions, receptor zone, and subsurface hydrodynamics. The deep well injection method is an environmentally safe method used in brine disposal since the wells have the ability to store this waste for a long period of time and because of the appropriate design, construction, and operation of this method [13]. This method can also make use of already existing oil and gas wells that have been depleted. On the downside, a lot of factors need to be considered before the implementation of this method. Some applications have been presented in the literature, such as the El Paso, Texas, study in which deep well injection of brine from brackish water desalination was performed [14]. In a study in Naples, Florida, the brine from nanofiltration (NF) and RO treatment plants used for producing drinking water was managed through deep well injection. Through monitoring of this well, no impact on the groundwater and aquifers was observed [15].

ZLD is a technology that aims at providing alternatives to all the disposal methods. This method has the dual purpose of treating concentrate for the production of both fresh water and dry salts, thus preventing the discharge of waste into the environment. ZLD has the ability to reach 100% water recovery, in comparison with 70%–85% for inland desalination. Furthermore, it helps protect natural resources such as groundwater and land. The recovery of dry salts for industrial purposes further enhances the popularity of this technology. However, the process involved in the use of mechanical evaporators in ZLD is expensive in terms of energy needs. Also, further research needs to be conducted for the evaluation of the technical and economic feasibility of ZLD [13].

The different disposal methods discussed are summarized in Table 3.

1.2 Economics of Brine Disposal

To assess their sustainability, brine discharge methods must be evaluated not only in terms of their environmental impact but also from an economic perspective. For instance, the construction of an evaporation pond over an acre of land will have an associated cost ranging from $100,000 to $200,000. So a brine flow of 100 gpm needs about 50 acres of land, and the associated cost of construction will range from $10 to $20 million, which does not

Table 3 Summary of brine discharge methods

Discharge method	Description	Environmental concern	Reference
Seawater	Most common discharge method for offshore discharge; known as submerged discharge; also implemented using multiple diffusers	Pollutes marine environment	[3]
Sewer	Sewage system discharge	Large amounts of brine can impact the performance of biological treatment	[3]
Evaporation ponds	Brine discharged into a pond where upon evaporation the salts accumulate	In the case of pond seepage, groundwater aquifers can be contaminated	[3,10]
Land application	The use of brine in irrigating halophytes	Large-scale production can result in very saline soil	[3]
Deep well injection	Nondrinkable aquifers injected with brine	Causes groundwater contamination and soil salinization in the case of large-scale operations	[3]
Zero-liquid-discharge	Method used to evaporate water content of brine and crystallize salt	Uses expensive mechanical evaporators for the treatment of concentrate	[3,13]

Table 4 Cost of brine discharge methods in the case of a concentrate flow rate of 0.5 mgd

Brine discharge method	Cost factors	Cost
Evaporation ponds	Dike height, liner thickness, and land	At 8-ft/year for 12-ft dike height and 120 mil thickness = $6,578,000
Land application (spray irrigation)	Brine flow and loading	At 20-ft/year loading = $163,000
Deep well injection	Brine flow and well depth	At a well depth of 5000 ft = $4,212,000
Zero-liquid-discharge	Brine flow, cost of electricity, and brine concentrator rejection level	At 5 $/kW/h at 2% rejection = $800,000

make the construction of evaporation ponds for brine discharge cost-effective, nor is it resource-effective because water is lost through evaporation. ZLD systems, on the other hand, are very economical in comparison with other brine discharge methods. However, the cost of their water production is higher than that of inland desalination plants. The higher cost results from use of units such as secondary brine concentration units used for enhanced recovery [11]. Comparing brine discharge options in terms of their cost, we can say that evaporation ponds and brine use in agriculture are costly because of the land requirement, making ZLD a better alternative. However, ZLD systems are costly in terms of their construction. Mickley (2006) compared the costs of the different brine disposal methods and the main factors affecting those costs. Table 4 shows the cost of brine disposal methods in the case of a concentrate flow rate of 0.5 mgd [16].

The one factor significantly impacting the cost of brine disposal is the brine flow rate because an increase in the flow results in a major increase in the cost of disposal. In the case of evaporation ponds, an increased area of land leads to an increase in the cost. A further increase results from the combined effect of a greater liner thickness as well as dike height. For the land application, an increase in the loading value can significantly reduce the cost. For deep well injection, an increase in the well depth results in a major cost rise. In the case of ZLD systems, an increase in the cost of electricity along with brine disposal results in a major increase in the cost of discharge [16].

1.3 Social Aspects of Brine Discharge

On a social level, there is much concern regarding the public's acceptance of brine discharge. Establishing brine discharge regulations by setting discharge limits can help minimize this concern [17]. Based on the region and the authority in charge, different

Table 5 Brine discharge limits

Region	Brine discharge salinity limit
California, United States	Absolute $\leq$ 40 ppt
Sydney, Australia	Increment $\leq$ 1 ppt
Okinawa, Japan	Increment $\leq$ 1 ppt
Abu Dhabi, UAE	Increment $\leq$ 5%

standards around the world have been set for brine discharge into coastal waters. Examples are presented in Table 5 [18].

When it comes to public acceptance of desalination and the problems associated with it, people around the world react differently where different factors play a role. Opinions are influenced by the severity of water scarcity in a region as well as the significance of desalination in the development of the country. In regions such as the Middle East and North Africa (MENA), where people are highly dependent on desalinated water for their way of life, there does not seem to be much public objection, though a lack of education in the region regarding the technology and its impact also plays a role. In areas like Oman, the desalination capacity is low, which prevents the public from acknowledging the severity of the environmental impact associated with the technology. The public's acceptance of desalination could change if its capacity increases. In North America, there is a clear public understanding of the negative environmental impact of desalination plants, which limits the growth of this technology in that region. In European countries, most people have had few concerns about desalination. However, as awareness regarding the environmental costs increases, this attitude is being altered [19].

2. MODELING OF BRINE DISCHARGE

Brine discharge configurations can be modeled through the use of software tools that enable the analysis of brine's impact on the environment. Three main software tools are used, CORMIX (Cornell Mixing Zone Expert), VISUAL PLUMES, and VISJET, to analyze discharge in both stagnant and dynamic settings. A schematic of a general brine discharge model is presented in Fig. 5 [20]. These numerical models are used for accurate design estimations and for the prediction of the effect of brine on water quality. CORMIX software is the most well-known one for modeling brine discharge in part because it was approved by the Environmental Protection Agency (EPA). This model is used as a Hydrodynamic Mixing Zone Model and a decision support system for analyzing, predicting, and designing pollutants dumped into aquatic environments. This steady-state model mimics effluent disposal under different circumstances of discharge. It is used for the assessment of the environmental impact of mixing zone point source discharges. Therefore it can be used for analyzing submerged single and multiport brine discharge as well as for floating surface discharge [5].

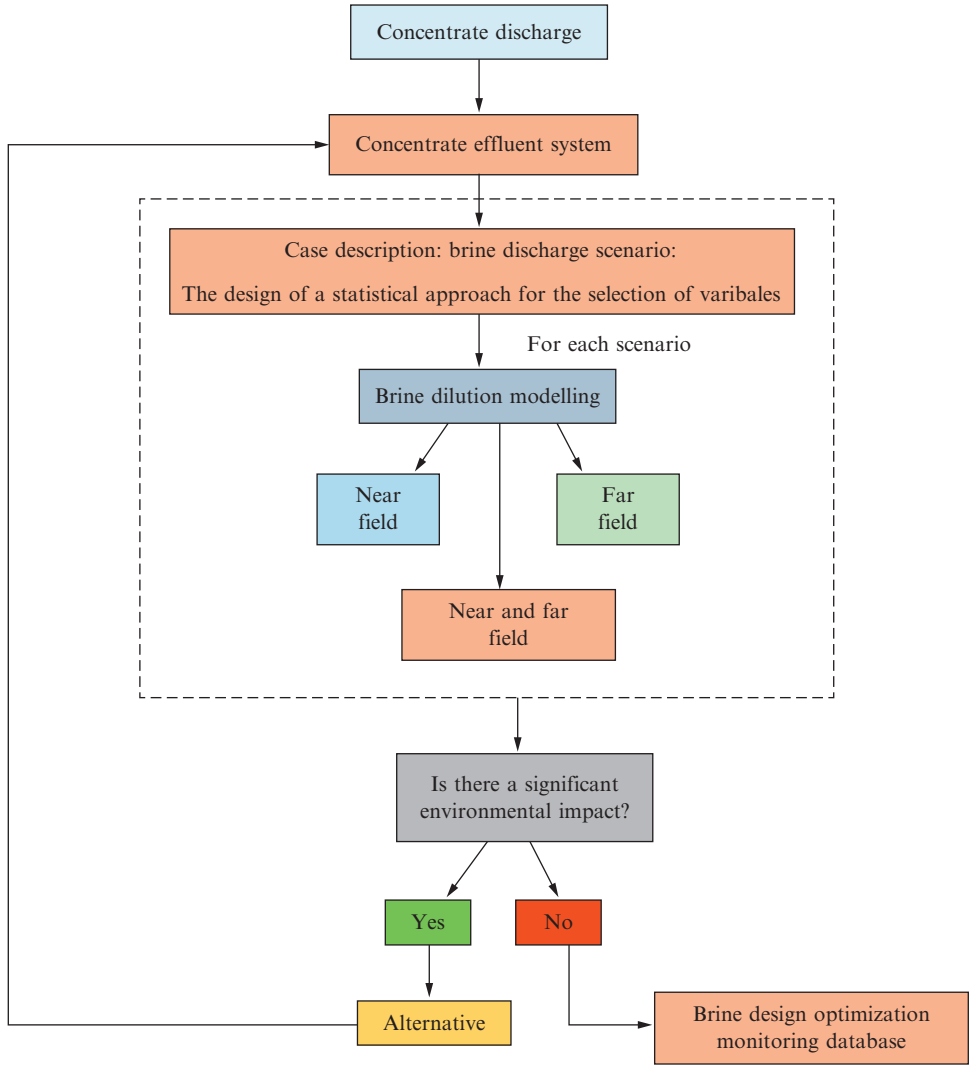

Fig. 5 Modeling brine discharge schematic. *(Adapted from P. Palomar, I. Losada, Impacts of Brine Discharge on the Marine Environment: Modelling as a Predictive Tool, Desalination, Trends and Technologies, 2011).*

The CorJet model existing within the CORMIX software helps in determining suitable design parameters such as the discharge angle. The discharge angle needs to be chosen appropriately for maximum dilution leading to the least environmental affect to the marine life. Applied design practices work at the discharge angle of 60 degrees above horizontal, which is believed to result in the highest dilution. However, CorJet angles of about 30–45 degrees above horizontal are suggested to be more advantageous

in terms of dilution. Furthermore, CorJet can be used for the development of a density current resulting from initial effluent mixing. This density current is affected by topographical structures, such as channels and depressions, affecting spatial factors leading to weak mixing, thereby impacting the benthic community [21].

VISUAL PLUMES was developed by the EPA for mimicking positively, negatively, and neutrally buoyant effluents that are discharged into the sea as in the case of CORMIX. This model takes into account discharge configurations, properties of the effluent, and brine characteristics such as temperature and salinity. This modeling software applies only to near field areas. It is characterized by its ability to imitate the discharge over time [20].

VISJET (Innovative Modeling and Visualization Technology for Environmental Impact Assessment), on the other hand, simulates positively and negatively buoyant releases. This model considers the same characteristics as VISUAL PLUMES where near-field modeling is also a limitation. Multiport jet discharges within this model can be performed because the interactions among jets is not taken into account, thus treating them as single-port jets. For this reason, in the case of multiport discharge, more experiments with more exact optical techniques need to be done to gather experimental data. Therefore numerical tools for discharge configuration models need to be established and compared to commercial modeling tools for near field brine discharge [22]. Through the validation of commercial tools used in the modeling of discharges into near field regions in both stagnant and dynamic environments, one can interpret the shortcomings of these models. Through this enhancement, uncertainties in brine discharge simulations using these commercial models can be minimized. The main features of the three software tools are summarized in Table 6.

Table 6 Summary of the brine modeling tools

Software	Tools	Applications	Capabilities
CORMIX	CORMIX 1 CORMIX 2 D-CORMIX CORJET	Single port jets: Submerged and emerged Submerged multiport jets Direct surface discharge Submerged jets: single and multiport	Detailed description of path, velocity, and dilution
VISUAL PLUMES	UM3	Submerged jets: single and multiport	Detailed description of path, velocity, and dilution
VISJET	JetLag	Submerged jets: single and multiport	Simulation of various design parameters such as port diameter, port height, and velocity for each diffuser jet

Adapted from P. Palomar, I. Losada, Impacts of Brine Discharge on the Marine Environment: Modelling as a Predictive Tool, Desalination, Trends and Technologies, 2011; P. Palomar, J. Lara, I. Losada, M. Rodrigo, A. Alvárez, Near field brine discharge modelling part 1: analysis of commercial tools, Desalination 290 (2012) 14–27, http://dx.doi.org/10.1016/j.desal.2011.11.037.

Some literature studies have relied on these software tools to model brine discharge. For example, Alameddine et al. (2007) modeled the effect of the thermal desalination plant effluent on the disposal of reject brine into the Arabian Gulf Sea [5]. Through the simulation of different scenarios using the CORMIX model, different factors were studied using temperature change as an indicator. During the course of this study, Alameddine et al. (2007) simulated the brine plume expansion starting from the ongoing discharge of the blowdown brine from an MSF desalination plant [5]. Three expected scenarios for the Arabian Gulf were studied for comparison. The first study examined the suitability of surface discharge outfalls; the second study evaluated the development of the brine plume using a single-port submerged outfall where the brine was dumped at a depth of four km away from the coast; and the third study assessed the dilution rates obtained through the use of multiport diffusers. The brine blowdown temperature was chosen as an indicator since it is a conservative pollutant, meaning that it does not interact with other contaminants. This allowed for exact explanations of dilution and mixing processes. The final conclusions from this simulation indicated that this brine dispersion method of surface discharge outfalls in the Gulf was unsuitable. The use of multiports in dilution was found to be effective where a 300 m mixing zone yielded a 10-fold dilution rate, thus reducing the associated environmental impacts. This study concluded that single and multiport outfalls are more efficient in reducing the temperature compared with surface discharge. This model was limited in terms of its discharge simulation of large volumes in shallow regions as well as its lack of verification with field measurements [5]. In a study performed by Malcangio et al. (2010), a brine disposal location with minimal environmental impact on marine species was determined. In this study, a three-dimensional model for brine discharge was used to study brine outfall in the coastal region along the south of Italy. The modeling results indicated that shortening the brine wastepipe reduced the impact on vegetation [8]. A study in Western Australia revealed that the modeling results displayed an increase in the temperature of the sea by 0.1–0.5°C through a seven km^2 area as a result of the discharge [6].

3. TECHNOLOGIES USED IN BRINE TREATMENT

Different classes of technologies can be used in brine discharge coupling allowing for enhanced recovery of resources. Such resources include water, salt, and energy. The technologies used in water recovery can be classified in two categories, thermal- and membrane-based systems, which are discussed in detail in the following section.

3.1 Thermal-Based Technologies

A commonly used thermal method for the management of brine is natural evaporation through the use of evaporation ponds. This method is deemed appropriate for large areas of available land and sun exposure [1]. However, this method is not being used for brines

containing a high total dissolved solids (TDS) content resulting from high saturation of low-solubility scaling salts. Another evaporation method used for this treatment is the wind aided intensified evaporation (WAIV) method [23–26]. This method is based on the use of vertical wetted packing towers that use wind power for the evaporation of densely packed wetted surfaces. This technique minimizes the need for land and can achieve an evaporation rate up to 90% compared to evaporations ponds [1,25]. The WAIV method was tested on brines from RO and RO-electrodialysis (ED), displaying an evaporation rate 10-fold greater than that achieved through natural evaporation where the concentrate salinity was found to increase by 23%. This method displays potential in the recovery of salts from brine for raw material use [23]. In a study by Oren et al. (2010), the treatment of ED brine using WAIV displayed a 70% TDS removal allowing for the recovery of magnesium salts. The use of an alternating current for brine evaporation known as ohmic evaporator can be used for the management of brines of concentrations exceeding 80,000 ppm. An alternating electric current at a frequency of 60 Hz with an electric field strength of 24–87 V/cm passes through a conductive material of high resistance resulting in ohmic heating, thus raising the temperature [27]. At an electric field strength of 56 V/cm, the ohmic evaporator results in a recovery rate of 81%–93.5% where the rate of ohmic heating is dependent on the square of the strength of electric field and electrical conductivity (Fig. 6).

Another thermal process used in brine minimization is the brine evaporative cooler/concentrator (BECC). The operating principle behind this is cooling via evaporation where the dual purpose of this process is to cool the brine being circulated as well as concentrate the brine that is to be disposed [28]. Through the recovery of latent heat of evaporation, the system is cooled where an air humidity within the range of 40%–70% results in a cooling range of 5–10°C [29]. This method results in the production of high purity permeate with an overall system recovery of 95%–99% (Fig. 7).

Brine freezing through crystallization can also be implemented where a eutectic temperature needs to be arrived at through brine heat loss. A brine crystallizer known as the forced circulation method uses the compressor vapor for heating RO concentrate and recirculating brine allowing for evaporation and thus salt crystallization [30]. This method evaporates the brine without boiling it through the use of a heat exchanger under pressure. The solidified crystals can be used for industrial applications [17]. The use of the eutectic freeze crystallization (EFC) process to treat hypersaline brines was found to be less energy-consuming than evaporative crystallization. A study performed by Randall et al. (2011) on RO brine using this method resulted in a 97% recovery while allowing for the recovery of 96.4% purity sodium sulfate and 98% purity calcium sulfate [31] (Fig. 8).

The treatment of brine through desalination technologies such as MED and mechanical vapor compression (MVC) has also been studied [32]. In MED, the steam of one stage heats the concentrate of the next allowing for an increase in recovery depending on the number of effects that can amount up to 93%. As for MVC, it recompresses the vapor

Fig. 6 An illustration of the WAIV technology. *(Obtained from J. Gilron, Y. Folkman, R. Savliev, M. Waisman, O. Kedem, WAIV – wind aided intensified evaporation for reduction of desalination brine volume, Desalination 158 (2003) 205–214, http://dx.doi.org/10.1016/S0011-9164(03)00453-3).*

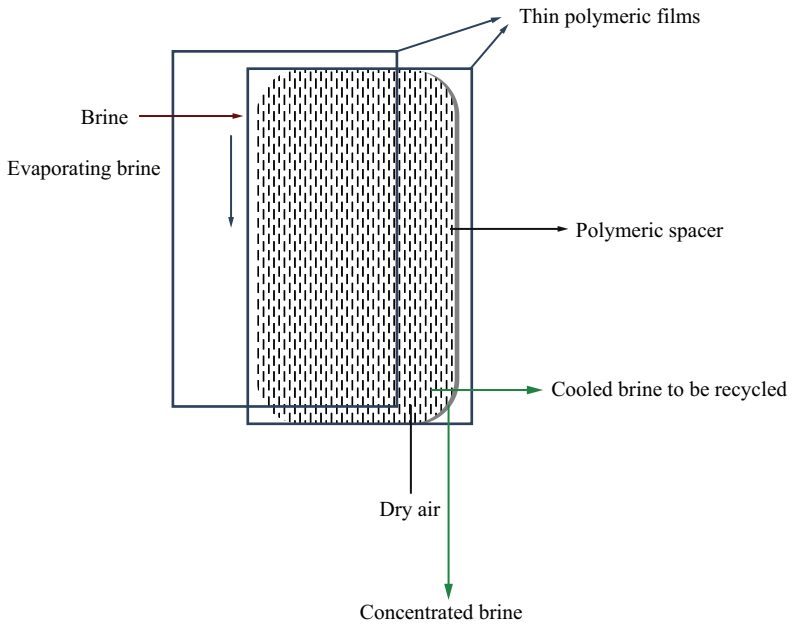

Fig. 7 An illustration of the BECC technology. *(Adapted from A. Cipollina, G. Micale, L. Rizzuti, A brine evaporative cooler/concentrator for autonomous thermal desalination units, Desalin. Water Treat. 31 (2011) 269–278, http://dx.doi.org/10.5004/dwt.2011.2345).*

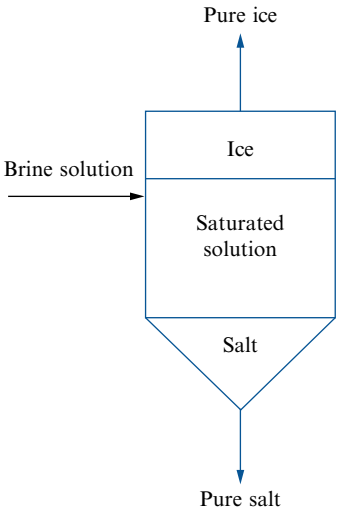

Fig. 8 An illustration of the EFC technology. *(Adapted from M.J. Fernández-Torres, F. Ruiz-Beviá, M. Rodríguez-Pascual, H. Von Blottnitz, Teaching a new technology, eutectic freeze crystallization, by means of a solved problem, Educ. Chem. Eng. 7 (2012) e163–e168, http://dx.doi.org/10.1016/j.ece.2012.07.002).*

produced through evaporation where it can be used to minimize the brine volume up to 92% [32]. In a study by Lara et al. (2008), the effect of the operating temperature on the system was found significant. For example, operating at a temperature of 172°C instead of 80°C increased the brine salinity by 15% [33].

3.2 Membrane-Based Technologies

Several membrane-based methods are used in the treatment of brine, specifically from RO. Three such methods are the plate and frame configuration, vibratory shear enhanced processing (VSEP), and disc tube (DT) filtrations [34,35]. These processes minimize the overall volume of brine through enhanced water recovery. Oscillations of 50 Hz created by torsion result in vibratory shear at the surface of the membrane that is used in brine treatment. Through this constant cross-flow process, the overall recovery of the feed water amounts to 93% from the original 75% while minimizing the occurrence of scaling (Figs. 9 and 10).

Other membrane processes used electrical potential as a driving force for treatment such as ED, electrodialysis reversal (EDR), and electrodialysis metathesis (EDM) [26,36–40]. Through the use of ion exchange membranes, the water is separated from the ions where cations are passed toward the negatively charged cathode and the anions toward the anode. The use of those techniques in treatment not only reduces the volume of the concentrate and enhances the water recovery but also protects the environment

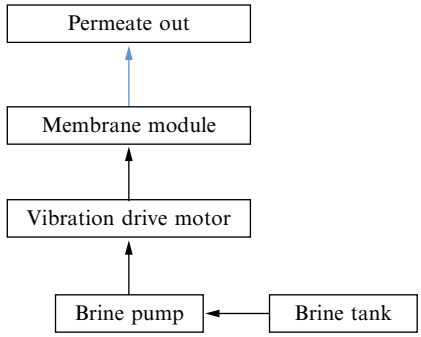

Fig. 9 An illustration of the VSEP technology. *(Obtained from M. Petala, A. Zouboulis, Vibratory shear enhanced processing membrane filtration applied for the removal of natural organic matter from surface waters, J. Membr. Sci. 269 (2006) 1–14, http://dx.doi.org/10.1016/j.memsci.2005.06.013).*

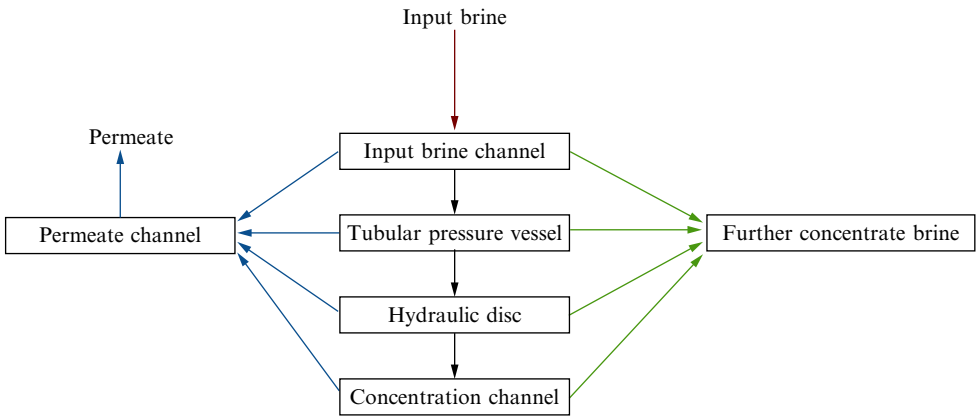

Fig. 10 An illustration of the DT technology. *(Adapted from T. Peters, High advanced open channel membrane desalination (disc tube module), Desalination 134 (2001) 213–219, http://dx.doi.org/10.1016/S0011-9164(01)00128-X).*

against environmental discharge. EDR operates in the same way as ED except for the fact that the voltage is applied in reverse about three to four times an hour with an overall water recovery of 97% [41], which can be increased to about 98.9% through the use of a pretreatment system [40]. EDM is considered to be a zero discharge desalination process, maximizing water recovery and allowing for the collection of the solid brine salts. A study reported the use of EDM for the treatment of RO/NF brine where four ion exchange membranes were used for the removal of salts through the process of metathesizing, also known as switching-partners. EDM is advantageous in terms of fouling where it is not influenced by organic and inorganic substances. The cost of this treatment method ranges between \$0.64 and \$11.21/m^3 of permeate where a crystallizer is used for maximum water recovery and solid salts assemblage [40].

Forward osmosis (FO) is another membrane-based process that is largely studied for its brine treatment application. In FO, the less concentrated water of the feed moves toward the more concentrated solution passing through a membrane that is selectively permeable to water. The driving force of the process results from a difference in the osmotic pressures of the solutions where the feed solutions need to be reconcentrated for the maintenance of the driving force [1,32,42–44]. This method is more advantageous than RO because of its reduced energy consumption due to the use of natural osmotic flow rather than reversing the flow. However, the membranes designed for this application are not very reliable, and the draw solution is not regularly available, both of which limit this application. In different cases in the United States, FO was used in the treatment of brine from RO desalination plants where brines with concentrations of 7500 and 17,500 ppm TDS were treated using a cellulose triacetate membrane. FO recoveries of up to 90% were obtained resulting in an overall process recovery exceeding 96% and 98%, respectively, whereas the solution with a higher TDS had a lower recovery because of reduction in the driving force [43].

Membrane distillation (MD) is considered to be both a membrane and thermal technology that operates based on a vapor pressure gradient resulting from the temperature difference across the membrane [42,45]. This process has four configurations that are all based on the principle of a vapor pressure gradient across the membrane in which volatile substances pass through a microporous, hydrophobic membrane. The four types are direct contact (DCMD), air gap (AGMD), vacuum (VMD), and sweeping gas MD (SGMD), with DCMD being the most commonly applied in studies because of its ease of application. Through evaporation on the feed side of the membrane and condensation of water vapor on the permeate side, fresh water is collected in the DCMD. MD has the advantage of low cost, minimal organic and biofouling, and the ability to be coupled with renewable energy sources such as solar and geothermal. On the downside, low permeate fluxes are a common result [46–49]. A schematic for the representation of RO brine concentration using the DCMD is illustrated in Fig. 11.

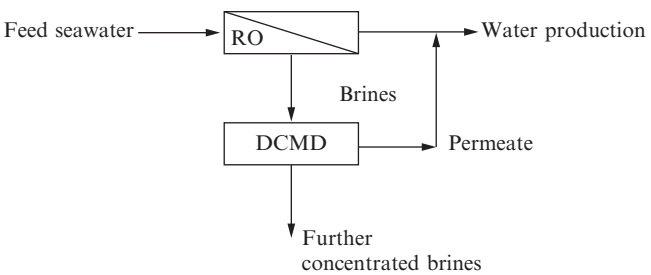

Fig. 11 Schematic of RO reject brine water recovery using DCMD process. *(Adapted from J. Morillo, J. Usero, D. Rosado, H. El, A. Riaza, F. Bernaola, Comparative study of brine management technologies for desalination plants, Desalination 336 (2014) 32–49, http://dx.doi.org/10.1016/j.desal.2013.12.038).*

DCMD has been noted in the literature as a suitable process for the treatment of brine for enhanced water recovery from both thermal and membrane desalination plants. In a study performed on a thermal desalination plant's brine, the feasibility of enhanced recovery from concentrate was performed on a bench scale unit [48]. Synthetic brine with a concentration of 70,000 ppm prepared with sodium chloride (NaCl) was treated during the course of this study. The study concluded that the use of DCMD in the treatment of brine released from thermal desalination plants was a feasible solution in which high purity distillate was obtained. Vacuum-enhanced direct contact MD (VEDCMD) is an MD method where the DCMD system is improved through vacuum installation. Brine treatment resulted in water recovery of 81% with an accumulative from RO and VEDCMD of 96% [43]. In another study, Li et al. (2015) used the DCMD in the treatment of high salinity brine in which it was found to be a promising technology for brine management [50]. The fouling of the DCMD in the treatment of RO brine was investigated by Zhang et al. (2015), and organic fouling was found to develop over long-term operations [51].

In a study on the use of AGMD in brine treatment, multistage AGMD was performed where high water recovery was obtained. The effect of the number of stages on the performance of the system was studied where a one-stage AGMD process allowed for a maximum water recovery of 5%–8%. In a 4-stage AGMD process, higher water recoveries of 24.7% and 22.2% were obtained. In a multistage AGMD process of 14 stages, a theoretical analysis of the case showed that a water recovery of 88.2% can be obtained, deeming this method suitable [52]. Duong et al. (2015) investigated the use of a pilot-scale AGMD in the treatment of RO brine coming from coal seam gas (CSG). The treatment was performed through the combination of UF/RO and spiral-wound AGMD where an overall water recovery of 95% was obtained [53]. In a study where the VMD was used for this treatment, synthetic solutions of a salinity of 300,000 mg/L were studied. A water recovery of 89% was obtained in which high salinities resulted in membrane surface scaling as a result of low solubility calcium compounds such as $CaSO_4$ and $CaCO_3$ [54]. Table 7 summarizes the results from the MD brine treatment studies.

Although MD displays a lot of potential in terms of brine treatment applications, it is limited by its disadvantages, including wetting of the membrane that affects the performance of the operation. In a study where DCMD was used to treat high salinity RO brine using hollow-fiber polyvinylidene fluoride, the effect of certain operating conditions on membrane wetting and fouling was investigated. These factors were feed temperature, flow rate, and concentration. For high temperature feed solutions, salts resulted in an enhanced membrane wetting impacting the flux and salt rejection by reducing their performance. Through theoretical model development and simulation, the flux and distillate conductivity were found to be mostly influenced by the concentration factor (CF). CF values of less than 3.5 did not allow crystallization of $CaSO_4$ because of its higher solubility as well as its higher ionic strength. As for values greater than 3.5, $CaSO_4$ crystallization increased the

Table 7 Summary of MD brine treatment studies

MD type	Desalination plant discharge	Study type	Feed type	Feed salinity (ppm)	Application	Reference
DCMD	Thermal	Bench scale	Synthetic saline solutions	70,000	Treatment of brine from a thermal desalination plant in Qatar used in treating water from the Arabian Gulf	[48]
VEDCMD	Membrane	Bench scale	Real RO brine	17,500	Treatment of brine resulting from the treatment of brackish water from a membrane desalination plant	[43]
AGMD	Membrane	Pilot study	Real CSG RO brine	8000	Treatment of CSG RO brine from a pilot gas well in Australia	[55]
VMD	Membrane	Bench scale	Real and synthetic RO brines	64,000–300,000	Treatment of synthetic RO brine and real brine from a seawater desalination plant used in the treatment of water coming from the Mediterranean Sea	[54]

fouling effect, whereas higher temperatures resulted in more fouling. For long DCMD operations, square $CaSO_4$ crystals formed at 77°C, and snowflake crystals formed at 55°C [55].

3.3 Resource Recovery

3.3.1 Energy Recovery

In addition to water recovery, energy can be recovered from brine through several methods maximizing efficiency from technical and economic perspectives. Energy can be generated as a result of a salinity gradient. The main principle is that high pressure RO pressure exchangers can be used to recover excess pressure from the brine disposal stream where it can be reused in the desalination process. This in turn minimizes the amount of overall energy required for the process. Therefore the mixing of different salt concentration water streams can be used in energy generation. This gradient results from the mixing of the high salinity brines with seawater, river water, or municipal wastewater. An example of this energy generation is the mixing of 1 m^3 of a 100,000 ppm brine with 1 m^3 river water, resulting in an energy production of 1.6 kWh. For a brine concentration of 250,000 ppm, the same mixing resulted in an energy generation of 4.03 kWh. This energy utilization makes this method highly competitive with the other brine disposal methods. This form of energy is consistent with the sustainable energy goals for the production of clean, renewable energy with no environmental impact in terms of CO_2 production [56].

Brine energy recovery systems have been placed in two categories. The first system requires the use of pressure exchangers for the direct transfer of the brine pressure to the feed. In the second system, the brine pressure is transferred to turbines and pumps for the production of mechanical power. The two systems differ in the high pressure pump flow. In the first system, the high pressure pump pumps only part of the feed flow, whereas the second system pumps the whole feed flow. As a result, the first system will have an energy recovery efficiency of about 96%, whereas the second one will have an efficiency of around 87%. However, the pressure exchanger system is more expensive in terms of equipment and maintenance than the turbine system [57]. Currently studied methods in literature on the generation of energy from disposed brine include pressure retarded osmosis (PRO) and reverse electrodialysis (RED). In the PRO process, a semipermeable membrane is used in which two solutions are being pumped to opposite sides of the membrane. These solutions are the low salinity feed and the high salinity draw solutions. As a result of an osmotic pressure gradient, permeate is collected through the flow of water from the feed to the draw solution through the membrane. The use of a hydro turbine in depressurizing the draw stream allows for the recovery of energy. Through improved membrane characteristics such as water permeability, the energy produced from this method can be increased [58]. In the RED process, a salinity gradient between a high concentration brine solution and a low salinity effluent is used in the production of

electricity. This is done in the presence of cation- and anion-exchange membranes (CEM and AEM) that separate the solutions. Through this process, the cations pass through the CEM, while the anions pass through the AEM allowing for the removal of salts from the water. Through the use of electrodes, this chemical potential is converted into an electrical one. The use of highly concentrated brine within the unit provides higher energy recovery than the use of seawater does. This in turn not only reduces the environmental impact of brine but also enhances the water recovery of the system. Modeling experimental results obtained by Li et al. (2013) indicated that the RED-RO hybrid unit can result in a significant reduction in process-specific energy consumption by 76.7% [39].

3.3.2 Salt Recovery

Another valuable resource that can be recovered from brine is the salt present in the brine, which has various constituents with numerous commercial purposes [59]. Methods of salt recovery varying from evaporation to separation to freezing have been investigated largely in the research industry because of the economic benefits of brine salt [4]. The extraction of salts through evaporation and cooling has been used worldwide, as opposed to the rapidly growing membrane separation processes. The uses for membrane-based methods have grown because of the development of cost-effective membranes of high performance, such as ED. Other salt recovery techniques such as ion-exchange, eutectic freezing, and chemical processing can also be used to recover salts. These techniques differ in cost, with MSF distillation and ED tending to be more expensive than NF and membrane crystallization, evaporation, and ion exchange methods. Enhanced methods of salt extraction are hybrid systems combining multiple methods for improved recovery while reducing brine volume. Some examples include MSF, multiple-effect evaporation (MEE), and vapor compression (VC). These distillation methods allow water to boil in the absence of the addition of heat as a result of a reduction in water vapor pressure [60]. The use of a semipermeable membrane for the separation of water from solutes through a pressure difference such as RO can also be used. Furthermore, NF, which is another membrane separation process, can be used for the removal of heavy metals [60]. Examples of the different brine salts and their industrial applications are shown in Table 8.

RO membranes have displayed salt recovery applications ranging from aqueous solutions, dyeing effluent, chemical industries wastewater, and agricultural drainage water treatment. Another method of salt recovery is ED where membranes undergo anion and cation exchange in the presence of an anode and a cathode in an applied electric field. This method has commonly been used in the separation of salts from seawater as well as groundwater. Furthermore, it has been used in the concentration of calcium and sulfate ions allowing for the minimum occurrence of fouling. This method requires the use of a solid cation exchanger, known as a resin, through which feed water is passed making this method a costly one. Therefore it is deemed suitable only for the treatment of low salinity solutions. As for the EFC method, the concurrent crystallization of salt and ice occurs

Table 8 Salt products extracted from brine and their potential industrial applications

Salt product	Industrial uses
Calcium carbonate	Dye used in paper coating
Calcium chloride	Road-base preservative and prevention of dust accumulation
Gypsum-magnesium hydroxide	Engine lubrication and fertilizer stabilizer
Magnesium hydroxide	Agricultural use for pH adjustments of soils and lakes and biological treatment of wastewater
Sodium chloride	Food processing application and agricultural fertilizer
Sodium sulfate	Manufacturing of paper

Adapted from M. Ahrned, D. Hoey, M. Thumarukudyd, M. Goosen, M. Al-haddabi, A. Al-belushi, Feasibility of salt production Corn inland RO desalination plant reject brine : a case study, Desalination 158 (2003) 109–117.

through freezing in which the eutectic temperature is reached. This method has been used for the recovery of $MgSO_4 \cdot 7H_2O$ from an industrial stream and copper sulfate ($CuSO_4$) crystals from a $CuSO_4$ solution. This method is advantageous over evaporative crystallization because of its low energy requirement, where energy can be reduced by up to 70% while achieving 100% conversion into water and salt. The use of chemical additives in the precipitation of salts is another method used in the recovery of brine salts. One such example is the addition of $NaHCO_3/Na_2CO_3$ for enhanced gypsum precipitation, where Na_2SO_4 and $MgSO_4$ can be recovered. Salts such as $CaCO_3$ have also been recovered from NF brine by the chemical addition of $NaHCO_3/Na_2CO_3$. Furthermore, $MgSO_4 \cdot 7H_2O$ can be recovered from NF retentate using $NaHCO_3/Na_2CO_3$ for $CaSO_4$ precipitation [60]. The different salt recovery methods and their applications are presented in Table 9.

3.3.2.1 Brine Salt Applications

Several brine applications have been implemented in the literature, such as the fermentation of cucumbers in calcium chloride ($CaCl_2$) brine. This study was performed by Wilson et al. (2015) [61]. In a study performed by Abdul-Wahab and Al-weshahi (2009), the onsite production of sodium hypochlorite as a commodity product extracted from brine was studied. This valuable product is commonly used as an active disinfecting compound as an alternative to chlorine (Cl_2) since it is more environmentally friendly and economically viable. Through the electrolysis of the brine solution in the presence of a low voltage DC current of about 10 V, NaOCl is instantly produced. Through the process of onsite electro-chlorination, any threats associated with transport, storage, and handling of chemicals is eliminated thus protecting the atmosphere from the possibility of gas releases. For reduced cost, the plant for this production can be located near a desalination plant [44].

The use of the SAL-PROC technology for the analysis of the technical viability of brine treatment was investigated for Petroleum Development Oman (PDO) with operating plants in Bahja, Rima, Nimr, and Marmul. SAL-PROC is an integrated process used in the extraction of dissolved elements from inorganic saline waters. This process is performed through multiple evaporation and cooling, accompanied by mineral and

Table 9 Summary of brine salt extraction

Salt recovery methods	Method description	Examples	Applications
Evaporation and cooling	Water is vaporized then condensed through distillation allowing for salt extraction (MSF, MEE, and VC)	Sodium chloride, sodium sulfate, potassium salt, and magnesium salt	Used in recovering sodium sulfate decahydrate and sodium chloride from brine
Membrane separation	A semipermeable membrane is used where water diffuses through the membrane separating from salt (RO and NF)	Sodium chloride and magnesium sulfate	Sodium chloride recovery from waste brine
Electrodialysis (ED)	Salt separation through the use of anion- and cation-exchange membranes that are placed between an anode and a cathode in the presence of an applied electric field where ions migrate toward the electrodes	Chlorine and magnesium chloride	Used in the reduction of sulfate ions to prevent gypsum crystallization as a result of evaporation
Ion exchange	Salt recovery by passing the feed water through a column containing the active form of a solid cation exchanger (an organic resin) that exchanges positive ions present in the feed water	–	Salt removal from tap water
Eutectic freezing crystallization (EFC)	Continuous feed freezing is performed until the eutectic temperature is reached. Upon heat removal salts are crystallized	Copper sulfate	Recovery of copper sulfate from solution
Chemical processes	Limiting gypsum precipitation for minimized loss of salts such as Na_2SO_4 and $MgSO_4$ (limiting loss of SO_4^{2-} through gypsum precipitation and by adding $NaHCO_3$/Na_2CO_3)	Calcium carbonate	Recovery of calcium carbonate from NF brine through the addition of sodium bicarbonate and sodium carbonate

Adapted from D. Kim, A review of desalting process techniques and economic analysis of the recovery of salts from retentates, Desalination 270 (2011) 1–8, http://dx.doi.org/10.1016/j.desal.2010.12.041.

chemical processing. The results of the analysis displayed that salts such as gypsum, NaCl, $Mg(OH)_2$, $CaCl_2$, $CaCO_3$, and Na_2SO_4 can be obtained from this treatment. In the end, the products were found to be worth $895,000/year [59]. In a study by Macedonio et al. (2013), valuable salts that can be collected from brine and crystallized have been estimated using a software known as the PHREEQC. The performance of this software was tested using a membrane crystallizer bench-scale plant where the experimental results were found to be in good agreement with the simulated ones [62].

Moreover, a study carried out by Sánchez et al. (2015) in Brazil's semiarid areas investigated the joint use of reject brine for the growth of *Spirulina cyanobacteria* as well as the irrigation of halophyte fodder plants [63]. Those two were chosen because of their good performance in saline waters. The initial stage of the process was the *Spirulina* cultivation stage, which was followed by brine coming into a mixture pond for enrichment with the organic matter waste from agriculture. This brine was then used for irrigation. The use of brine in irrigation was critical to the quality of the brine because it must be well suited to the needs of the soil and crops. This method was developed further through the use of brine in the growth of crops through local livestock manure mixing. In using reject brine in irrigation, the forage yielded a much greater production of 5.5–8.5 ton/ha year compared to that attained in other arid regions of South America where those crops are cultivated as wild crops. The species involved in the experiments were found to be intolerant toward the high salinity of the brine. One exception was one sunflower plant known as the Red Sun that displayed promise under such hydroponic conditions. This joint production scheme thrived in converting this environmental issue into a useful activity with economic benefit. However, one disadvantage of this method was land salinization. All in all, this brine salt application was found to be most suitable for salt tolerant plants such as halophytes [63]. A schematic summarizing the proposed application of reject brine in this paper is presented in Fig. 12.

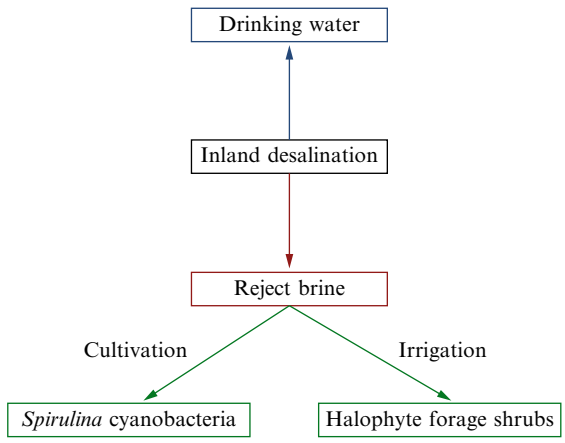

Fig. 12 Proposed inland applications of reject brine. *Obtained from A. Sánchez, I. Nogueira, R. Kalid, Uses of the reject brine from inland desalination for fish farming, Spirulina cultivation, and irrigation of forage shrub and crops, Desalination 364 (2015) 96–107, http://dx.doi.org/10.1016/j.desal.2015.01.034.*

4. CONCLUSIONS

Although desalination plants are providing water resources for many water-stressed countries across the world, the process of brine discharge is leading to many environmental problems, mostly impacting marine species in the sea. This chapter focused on different brine disposal methods, their impact on different species, and the reuse of concentrate in different applications. The chapter also covered brine management focusing on the treatment of brine using thermal and membrane technologies. Furthermore, different technologies used in salt recovery and some brine salt applications were discussed. Brine characterized as a hypersaline effluent sinking to the bottom of the sea affects water quality and harms benthic species where the behavior of brine disposal is modeled. Some recommendations for enhanced brine discharge system design allowing for a reduced environmental impact include enhancements in the brine discharge system design that can minimize the environmental impacts of this disposal on the marine ecosystems. Recommendations for this improvement include placing discharge systems in areas that are not protected as well as those with high turbulence for enhanced dilution. The features of the discharge area as well as the dilution effect need to be taken into account in the discharge design such that the concentrations of the seawater remain within standards set by environmental protection agencies. Enhanced dilution and mixing can be achieved through an increase in the discharge velocity where an optimum discharge velocity is about 4–5 m/s. Currently, some existing models are used in the assessment of brine discharge. The expansion of these models can result in an enhanced assessment of brine discharge in the future [21]. As for inland desalination practices, they all have their own set of advantages and disadvantages; in the latter case, they tend to contaminate natural groundwater supplies as well as the quality of soil that is to be used for agricultural practices. As for ZLD technologies, they aim at providing cost-effective methods of brine management for the efficient use of water and salts [11]. These technologies are a highly recommended options that not only enhance water recovery but also make use of salts through appropriate methods of brine concentration and salt recovery. The commonly used commercial brine discharge modeling software tools are CORMIX, VISUAL PLUMES, and VISJET, whereas new online modeling methods such as MEDVSA are developing. Because of the growth in the number of desalination plants worldwide, more studies need to be carried out for an improved understanding of field mixing and impingement zone [21]. When selecting an appropriate method for brine treatment, the method must be one that is cost-effective, energy-efficient, environmentally friendly, and implementable within the region [64]. A greater effort needs to be put into public awareness and increasing policymakers' knowledge about the environmental issues related to brine discharge [3].

REFERENCES

[1] J. Morillo, J. Usero, D. Rosado, H. El, A. Riaza, F. Bernaola, Comparative study of brine management technologies for desalination plants. Desalination 336 (2014) 32–49, http://dx.doi.org/10.1016/j.desal.2013.12.038.

[2] R. Einav, K. Hamssib, D. Periyb, The footprint of the desalination processes on the environment. Desalination 152 (2002) 141–154, http://dx.doi.org/10.1016/S0011-9164(02)01057-3.

[3] N. Ahmad, R. Baddour, A review of sources, effects, disposal methods, and regulations of brine into marine environments. Ocean Coast. Manag. 87 (2014) 1–7, http://dx.doi.org/10.1016/j.ocecoaman.2013.10.020.

[4] M. Ahmed, W. Shayya, D. Hoey, A. Mahendran, R. Morris, J. Al-Handaly, Use of evaporation ponds for brine disposal in desalination plants. Desalination 130 (2000) 155–168, http://dx.doi.org/10.1016/S0011-9164(00)00083-7.

[5] I. Alameddine, M. El-Fadel, Brine discharge from desalination plants: a modeling approach to an optimized outfall design. Desalination 214 (2007) 241–260, http://dx.doi.org/10.1016/j.desal.2006.02.103.

[6] D. Roberts, E. Johnston, N. Knott, Impacts of desalination plant discharges on the marine environment: a critical review of published studies, Water Resour. 44 (2010) 5117–5128, http://dx.doi.org/10.1016/j.watres.2010.04.036.

[7] R. Danoun, Desalination Plants: Potential Impacts of Brine Discharge on Marine Life, The University of Sydney, Australia, 2007. p. 59.

[8] D. Malcangio, A. Petrillo, Modeling of brine outfall at the planning stage of desalination plants. Desalination 254 (2010) 114–125, http://dx.doi.org/10.1016/j.desal.2009.12.005.

[9] G. Mauguin, P. Corsin, Concentrate and other waste disposals from SWRO plants: characterization and reduction of their environmental impact, Desalination 182 (2005) 355–364, http://dx.doi.org/10.1016/j.desal.2005.02.033.

[10] J. Arnal, M. Sancho, I. Iborra, J. Goza´lvez, A. Santafe, J. Lora, Concentration of brines from RO desalination plants by natural evaporation, Desalination 182 (2005) 435–439, http://dx.doi.org/10.1016/j.desal.2005.02.036.

[11] K. Elsaid, N. Bensalah, A. Abdel-wahab, Inland desalination: potentials and challenges, Adv. Chem. Eng. (2012) 1–33, http://dx.doi.org/10.5772/33134.

[12] A. Mohamed, M. Maraqa, J. Al Handhaly, Impact of land disposal of reject brine from desalination plants on soil and groundwater, Desalination 182 (2005) 411–433, http://dx.doi.org/10.1016/j.desal.2005.02.035.

[13] B. Ladewig, B. Asquith, Deep Well Injection, Desalination Concentrate Management, Springer, Berlin, Heidelberg, 2012. pp. 49–57. http://dx.doi.org/10.1007/978-3-642-24852-8.

[14] B. Hutchison, Desalination of brackish groundwater and deep well injection of concentrate in El Paso, Texas, Water Resour. (2009) 5428–5436, http://dx.doi.org/10.1061/41036(342)551.

[15] M. Lee, W. Li, B. Tansel, H. Brogdon, P. Mattausch, Concentrate management by deep well injection at North County Regional Water Treatment Plant in Naples, Collier County, FL. Am. Soc. Civil Eng. (2010) 3519–3528, http://dx.doi.org/10.1061/41114(371)359.

[16] M. Mickley, Membrane Concentrate Disposal: Practices and Regulation, Desalination and Water Purification Research and Development Program 123, The National Technical Information Service (NTIS), Springfield, VA, 2006 p. 312.

[17] S. Culligan, Report on the Evaluation of Existing Methods on Brine Treatment and Disposal Practices, SOL-BRINE, 2012, p. 94.

[18] S. Jenkins, J. Paduan, P. Roberts, J. Weis, Management of Brine Discharges to Coastal Waters Recommendations of a Science Advisory Panel, Southern California Coastal Water Research Project, 2012, p. 100.

[19] W. Münk, Ecological and Economic Analysis of Seawater Desalination Plants, University of Karlsruhe, Karlsruhe, Germany, 2008. 119.

[20] P. Palomar, I. Losada, Impacts of Brine Discharge on the Marine Environment: Modelling as a Predictive Tool, Desalination, Trends and Technologies, 2011.

[21] T. Bleninger, G. Jirka, Modelling and environmentally sound management of brine discharges from desalination plants, Desalination 221 (2008) 585–597, http://dx.doi.org/10.1016/j.desal.2007.02.059.
[22] P. Palomar, J. Lara, I. Losada, M. Rodrigo, A. Alvárez, Near field brine discharge modelling part 1: analysis of commercial tools, Desalination 290 (2012) 14–27, http://dx.doi.org/10.1016/j.desal.2011.11.037.
[23] L. Katzir, Y. Volkmann, N. Daltrophe, E. Korngold, R. Mesalem, Y. Oren, WAIV – wind aided intensified evaporation for brine volume reduction and generating mineral byproducts, Desalin. Water Treat. 13 (2010) 63–73, http://dx.doi.org/10.5004/dwt.2010.772.
[24] F. Macedonio, L. Katzir, N. Geisma, S. Simone, E. Drioli, J. Gilron, Wind-aided intensified evaporation (WAIV) and membrane crystallizer (MCr) integrated brackish water desalination process: advantages and drawbacks, Desalination 273 (2011) 127–135, http://dx.doi.org/10.1016/j.desal.2010.12.002.
[25] J. Gilron, Y. Folkman, R. Savliev, M. Waisman, O. Kedem, WAIV – wind aided intensified evaporation for reduction of desalination brine volume, Desalination 158 (2003) 205–214, http://dx.doi.org/10.1016/S0011-9164(03)00453-3.
[26] Y. Oren, E. Korngold, N. Daltrophe, R. Messalem, Y. Volkman, L. Aronov, et al., Pilot studies on high recovery BWRO-EDR for near zero liquid discharge approach, Desalination 261 (2010) 321–330, http://dx.doi.org/10.1016/j.desal.2010.06.010.
[27] A.M. Assiry, Application of ohmic heating technique to approach near-ZLD during the evaporation process of seawater, Desalination 280 (2011) 217–223, http://dx.doi.org/10.1016/j.desal.2011.07.010.
[28] A. Cipollina, G. Micale, L. Rizzuti, A brine evaporative cooler/concentrator for autonomous thermal desalination units, Desalin. Water Treat. 31 (2011) 269–278, http://dx.doi.org/10.5004/dwt.2011.2345.
[29] M. Pereira, J. Mendes, P. Horta, N. Korovessis, Final design of an advanced solar dryer for salt recovery from brine effluent of an MED desalination plant, Desalination 211 (2007) 222–231, http://dx.doi.org/10.1016/j.desal.2006.03.596.
[30] F. Farahbod, D. Mowla, M. Jafari Nasr, M. Soltanieh, Experimental study of forced circulation evaporator in zero discharge desalination process, Desalination 285 (2012) 352–358, http://dx.doi.org/10.1016/j.desal.2011.10.026.
[31] D. Randall, J. Nathoo, A. Lewis, A case study for treating a reverse osmosis brine using eutectic freeze crystallization — approaching a zero waste process, Desalination 266 (2011) 256–262, http://dx.doi.org/10.1016/j.desal.2010.08.034.
[32] A. Subramani, J. Jacangelo, Treatment technologies for reverse osmosis concentrate volume minimization: a review, Sep. Purif. Technol. 122 (2014) 472–489, http://dx.doi.org/10.1016/j.seppur.2013.12.004.
[33] J. Lara, G. Noyes, M. Holtzapple, An investigation of high operating temperatures in mechanical vapor-compression desalination, Desalination 227 (2008) 217–232, http://dx.doi.org/10.1016/j.desal.2007.06.027.
[34] W. Shi, M. Benjamin, Effect of shear rate on fouling in a vibratory shear enhanced processing (VSEP) RO system, J. Membr. Sci. 366 (2011) 148–157, http://dx.doi.org/10.1016/j.memsci.2010.09.051.
[35] T. Peters, High advanced open channel membrane desalination (disc tube module), Desalination 134 (2001) 213–219, http://dx.doi.org/10.1016/S0011-9164(01)00128-X.
[36] K. Ghyselbrecht, E. Van Houtte, L. Pinoy, J. Verbauwhede, B. Van Der Bruggen, B. Meesschaert, Treatment of RO concentrate by means of a combination of a willow field and electrodialysis, Resour. Conserv. Recycl. 65 (2012) 116–123, http://dx.doi.org/10.1016/j.resconrec.2012.06.003.
[37] A. Tran, Y. Zhang, N. Jullok, B. Meesschaert, L. Pinoy, B. Van der Bruggen, RO concentrate treatment by a hybrid system consisting of a pellet reactor and electrodialysis, Chem. Eng. Sci. 79 (2012) 228–238, http://dx.doi.org/10.1016/j.ces.2012.06.001.
[38] E. Korngold, L. Aronov, N. Daltrophe, Electrodialysis of brine solutions discharged from an RO plant, Desalination 242 (2009) 215–227, http://dx.doi.org/10.1016/j.desal.2008.04.008.

[39] W. Li, W. Krantz, E. Cornelissen, J. Post, A. Verliefde, C. Tang, A novel hybrid process of reverse electrodialysis and reverse osmosis for low energy seawater desalination and brine management, Appl. Energy 104 (2013) 592–602, http://dx.doi.org/10.1016/j.apenergy.2012.11.064.
[40] C. He, G. Carpenter, P. Westerhoff, Demonstrating an innovative combination of ion exchange pretreatment and electrodialysis reversal for reclaimed water reverse osmosis concentrate minimization, Water Reuse Research Foundation, 2013.
[41] P. Xu, T. Cath, A. Robertson, M. Reinhard, J. Leckie, J. Drewes, Critical review of desalination concentrate management, treatment and beneficial use, Environ. Eng. Sci. 30 (2013) 502–514, http://dx.doi.org/10.1089/ees.2012.0348.
[42] C. Kazner, S. Jamil, S. Phuntsho, H.K. Shon, T. Wintgens, S. Vigneswaran, Forward osmosis for the treatment of reverse osmosis concentrate from water reclamation: process performance and fouling control, Water Sci. Technol. 69 (2014) 2431–2437, http://dx.doi.org/10.2166/wst.2014.138.
[43] C. Martinetti, A. Childress, T. Cath, High recovery of concentrated RO brines using forward osmosis and membrane distillation, J. Membr. Sci. 331 (2009) 31–39, http://dx.doi.org/10.1016/j.memsci.2009.01.003.
[44] S. Abdul-Wahab, M. Al-weshahi, Brine management: substituting chlorine with on-site produced sodium hypochlorite for environmentally improved desalination processes, Water Resour. Manage. (2009) 2437–2454, http://dx.doi.org/10.1007/s11269-008-9389-7.
[45] L. Camacho, L. Dumée, J. Zhang, J. De Li, M. Duke, J. Gomez, et al., Advances in membrane distillation for water desalination and purification applications, Water 5 (2013) 94–196, http://dx.doi.org/10.3390/w5010094.
[46] K. Sirkar, L. Song, Pilot-Scale Studies for Direct Contact Membrane Distillation-Based Desalination Process, Desalination and Water Purification Research and Development Program, 2009.
[47] N. Dow, J. Zhang, M. Duke, J. Li, S. Gray, E. Ostarcevic, Membrane Distillation of Brine Wastes, Water Quality Research Australia, 2008.
[48] S. Adham, A. Hussain, J. Matar, R. Dores, A. Janson, Application of membrane distillation for desalting brines from thermal desalination plants, Desalination 314 (2013) 101–108, http://dx.doi.org/10.1016/j.desal.2013.01.003.
[49] A. Childress, Existing and Emerging Technology Innovations: Membrane Technologies and Energy Use for Desalination, Department of Civil and Environmental Engineering, University of Southern California, 2013, p. 36.
[50] J. Li, Y. Guan, F. Cheng, Y. Liu, Treatment of high salinity brines by direct contact membrane distillation: effect of membrane characteristics and salinity, Chemosphere 140 (2015) 143–149, http://dx.doi.org/10.1016/j.chemosphere.2014.12.006.
[51] P. Zhang, P. Knötig, S. Gray, M. Duke, Scale reduction and cleaning techniques during direct contact membrane distillation of seawater reverse osmosis brine, Desalination 374 (2015) 20–30, http://dx.doi.org/10.1016/j.desal.2015.07.005.
[52] H. Geng, J. Wang, C. Zhang, P. Li, H. Chang, High water recovery of RO brine using multi-stage air gap membrane distillation, Desalination 355 (2015) 178–185, http://dx.doi.org/10.1016/j.desal.2014.10.038.
[53] H. Duong, A. Chivas, B. Nelemans, M. Duke, S. Gray, T. Cath, Treatment of RO brine from CSG produced water by spiral-wound air gap membrane distillation – a pilot study, Desalination 366 (2015) 121–129, http://dx.doi.org/10.1016/j.desal.2014.10.026.
[54] J. Mericq, S. Laborie, C. Cabassud, Vacuum membrane distillation of seawater reverse osmosis brines, Water Resour. 44 (2010) 5260–5273, http://dx.doi.org/10.1016/j.watres.2010.06.052.
[55] J. Ge, Y. Peng, Z. Li, P. Chen, S. Wang, Membrane fouling and wetting in a DCMD process for RO brine concentration, Desalination 344 (2014) 97–107, http://dx.doi.org/10.1016/j.desal.2014.03.017.
[56] M. Ahmad, P. Williams, Application of salinity gradient power for brines disposal and energy utilisation, Desalin. Water Treat. 10 (2009) 220–228, http://dx.doi.org/10.5004/dwt.2009.924.
[57] Energy Considerations in Membrane Treatment and Brine Disposal, Membrane Treatment, 5.
[58] W. Akram, M.H. Sharqawy, J.H. Lienhard, Energy Utilization of Brine from an MSF Desalination Plant, 2013, p. 12.

[59] M. Ahrned, D. Hoey, M. Thumarukudyd, M. Goosen, M. Al-haddabi, A. Al-belushi, Feasibility of salt production Corn inland RO desalination plant reject brine: a case study, Desalination 158 (2003) 109–117.
[60] D. Kim, A review of desalting process techniques and economic analysis of the recovery of salts from retentates, Desalination 270 (2011) 1–8, http://dx.doi.org/10.1016/j.desal.2010.12.041.
[61] E. Wilson, S. Johanningsmeier, J. Osborne, Consumer acceptability of cucumber pickles produced by fermentation in calcium chloride brine for reduced environmental impact, J. Food Sci. 80 (2015) 1360–1367, http://dx.doi.org/10.1111/1750-3841.12882.
[62] F. Macedonio, C. Quist-Jensen, O. Al-Harbi, H. Alromaih, S. Al-Jlil, F. Al Shabouna, Thermodynamic modeling of brine and its use in membrane crystallizer, Desalination 323 (2013) 83–92, http://dx.doi.org/10.1016/j.desal.2013.02.009.
[63] A. Sánchez, I. Nogueira, R. Kalid, Uses of the reject brine from inland desalination for fish farming, Spirulina cultivation, and irrigation of forage shrub and crops, Desalination 364 (2015) 96–107, http://dx.doi.org/10.1016/j.desal.2015.01.034.
[64] T. Poulson, C. Sub-committee, Central Arizona Salinity Study Strategic Alternatives for Brine Management in the Valley of the Sun, 2010.

FURTHER READING

[1] N. Ahmad, R. Baddour, Minimum return dilution method to regulate discharge of brine from desalination plants, Can. J. Civ. Eng. 41 (2014) 389–395, http://dx.doi.org/10.1139/cjce-2012-0528.
[2] M.J. Fernández-Torres, F. Ruiz-Beviá, M. Rodríguez-Pascual, H. Von Blottnitz, Teaching a new technology, eutectic freeze crystallization, by means of a solved problem, Educ. Chem. Eng. 7 (2012) e163–e168, http://dx.doi.org/10.1016/j.ece.2012.07.002.
[3] M. Petala, A. Zouboulis, Vibratory shear enhanced processing membrane filtration applied for the removal of natural organic matter from surface waters, J. Membr. Sci. 269 (2006) 1–14, http://dx.doi.org/10.1016/j.memsci.2005.06.013.

CHAPTER 6

Advanced Membrane-Based Desalination Systems for Water and Minerals Extracted From the Sea

Francesca Macedonio[*,†], **Enrico Drioli**[*,†,‡,§]
[*]Institute on Membrane Technology (ITM-CNR), National Research Council, c/o The University of Calabria, Rende CS, Italy
[†]University of Calabria, Rende, Italy
[‡]Hanyang University, Seoul, South Korea
[§]King Abdulaziz University, Jeddah, Saudi Arabia

Contents

1. INTRODUCTION

In the last decades, potable water production from sea and brackish water is no longer considered a minor or secondary water resource in many water-stressed countries. For example, Ghaffour [1] reports that Qatar and Kuwait rely on 100% desalinated water for domestic and industrial supplies. In the past decade, large-scale seawater reverse osmosis (SWRO) desalination plants were constructed in Spain [2] and Israel [3]. Greenlee et al. [4] report that in 2009 over 16,000 desalination plants were in operation worldwide. Among these (i) six of the eleven countries with the greatest desalination production capacity are located in the Middle East; (ii) Saudi Arabia is the world leader with approximately 26% of global production capacity; (iii) the United States ranks second, with 17% of the world's desalination production; (iv) Spain and Italy hold the majority of the European desalination capacity, with each country having 2.6% of the world's production capacity [5]; and (v) Algeria plans to increase its number of plants from 10 to 43 by the year 2019, with a production goal of 2 million m^3/day.

Ghaffour et al. [6] state that in 2013 the total global desalination capacity was around 66.4 million m^3/day, and it was expected to reach about 100 million m^3/day by 2015.

Desalination Sustainability
http://dx.doi.org/10.1016/B978-0-12-809791-5.00006-7

Schiermeier [7] reports that in 2016 desalination was projected to exceed 116 billion m^3/day, twice the rate of global water production by desalination in 2008.

More than 50% of the total desalination investments are for SWRO projects mainly because of their lower investment and total water cost (TWC) as compared with conventional source developments, their smaller footprint, and the continuing technological advances enabling RO desalination to treat higher raw-water salinities such as the Arabian Gulf seawater. Thermal processes will also continue to be utilized, especially where energy is available at a low cost. For example, multistage flash distillation, MSF, is the most frequently applied thermal desalination technology in the Middle Eastern market due to the low cost of fossil fuel-based energy in this region and to its ability to combine with electric energy generation (cogeneration of steam and electricity). Currently, RO is the leader in future desalination installations because it can produce fresh water (from seawater) at one-half to one-third the cost of distillation [7]. Many developments over the past three decades have contributed to a reduction in the unit water cost of RO desalination, particularly the following:

- Membrane performance (with respect to increased salt rejection, increased surface area per unit volume, increased flux, improved membrane life, recovery ratio, and capacity to work at higher pressure)
- Membrane cost
- Reduction in energy consumption (Fig. 1) caused by more efficient energy recovery systems (i.e., systems able to recover energy from brine through Pelton turbines, or turbochargers, hydraulic pressure boosters, pressure exchangers, etc.)
- Improvement of pumping systems
- Improvements in pretreatment processes (including microfiltration, (MF)/ultrafiltration, and (UF) membranes)
- Development of high boron rejection membranes
- Reduction in use of chemicals with improved membrane performance
- Increase in plant capacity (which increased by a factor of 10 between 1995 and 2010)
- Use of the build, own, operate, transfer (BOOT) contracts

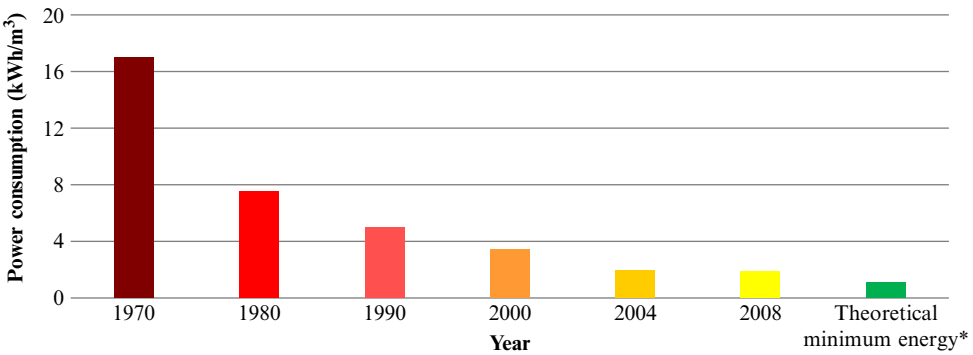

Fig. 1 History of power consumption required for seawater reverse osmosis (SWRO) desalination processes. *(From M. Elimelech, W.A. Phillip, The future of seawater desalination: energy, technology, and the environment. Science 333(6043) (2011) 712–717).*

Despite the great success of desalination, there are several concerns because of its potential adverse environmental impacts, the main ones being energy consumption, brine disposal, air pollutants, and greenhouse gas emissions.

Although current SWRO desalination plants consume only 3–4 kWh/m^3 of fresh water produced [1,8] (very low compared with thermal desalination plants), that's still three to four times higher than the practical minimum energy demand. Because of the need for extensive pretreatment and posttreatment, electric power is 19%–40% of the TWC, and the emissions are between 1.4 and 1.8 kg CO_2 per cubic meter of produced water [9]. Moreover, the disposal of SWRO brines raises serious environmental risks because of their high salinity (about twice that of seawater) and the presence of chemicals (such as antiscalants, coagulants, surfactants, alkaline and acid solutions, metal-chelating agents) used in pretreatment or as cleaning chemicals.

Until now, the measures adopted to reduce energy consumption and gas emissions have been recourses to renewable energy sources, whereas dilution of high salinity brines with other waste streams (such as power plant cooling water) or utilization of efficient diffuser systems or an accurate choice of the discharge zone with favorable hydrodynamics for the rapid dissipation of the salinity load are generally used to minimize the impact of high salinity brines.

Energy consumption and the environmental impact of discharged brines can be further reduced through the implementation of membrane-based pretreatment and posttreatment technologies. As a matter of fact, the adoption of pressure-driven membrane operations (such as microfiltration, MF, and ultrafiltration, UF) in the pretreatment stages of a desalination can handle a large variation in raw water quality and still produce water for the RO unit that is of better quality than water produced by conventional pretreatment technology. Membrane pretreatment systems are also more compact, use fewer chemicals, reduce the fouling rate and thus the frequency and use of chemical cleanings, and have lower operating costs than conventional seawater pretreatment processes.

Development of innovative technologies, such as membrane crystallization (MCr), provides unprecedented opportunities for the treatment and reuse of brine streams of desalination plants, reducing the brine disposal problem, thus approaching the concept of "zero-liquid-discharge" (ZLD) and "total raw materials utilization" [9–12]. The latter are strategies aimed at processing the concentrates to produce dry salts and water.

The present chapter highlights the use of MCr for extracting materials from seawater and desalination concentrate. In this sense, the brine disposal problem might be completely reversed. If we consider desalination a process for the recovery of salts necessary for the development of our industrial society, then water production becomes a process well integrated with the recovery of raw materials for reuse. The overall cost of the final water must be well recalculated if combined with the production of valuable salt. Water and raw material production might be part of a single integrated production system. New membrane operations well integrated with the traditional ones might offer this opportunity.

2. MINING FROM SEAWATER

The oceans contain vast quantities of dissolved ions that could be extracted, most of which are fundamental for the development of our society. Currently, four components are extracted from seawater, principally table salt (sodium chloride) and the by-products (potassium chloride, magnesium salts, and bromide salts). Extraction of other components may be feasible, provided the elements are sufficiently valuable or rare on land, such as lithium, uranium, radium, gold, barium, molybdenum, and strontium. An example can be found in uranium and in its increasing demand in past decades (as an energy source); in fact, the annual uranium requirements are projected to increase from 61,500 tons in 1997 to 75,000 tons in 2020 (Fig. 2).

The uranium concentration of sea water is low, around 0.0033 ppm. However, taking into account the large amount of seawater, the quantity of contained uranium is vast—some 4 billion tons (about 1000 times more than known terrestrial resources recoverable at a price of up to $130 per kg). Therefore extraction of uranium from seawater could serve as insurance in case supplies of uranium for nuclear reactors ever become scarce [13]. The most advanced system today employs plastic fibers with uranium-binding chemical groups grafted onto their surface.

Another example can be found in lithium, whose demand has already doubled over the past decade, and it is expected to more than double over the next 10 years. Lithium consumption is estimated to exceed 400,000 tons by 2025. Historically, growth was driven largely by the demand for lithium used in the small format lithium-ion battery (i.e., rechargeable batteries used in consumer devices such as cell phones, laptops, digital cameras, and handheld power tools). Future growth in the demand for lithium is

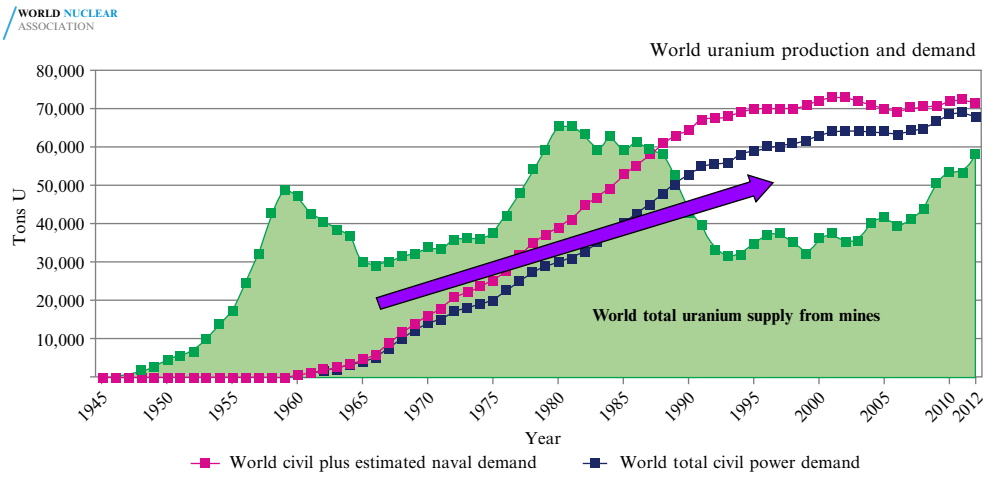

Fig. 2 World uranium production and demand (http://www.world-nuclear.org/info/Nuclear-Fuel-Cycle/Uranium-Resources/Uranium-Markets (last access on July 24, 2015).

expected to come from both continued growth in the small format lithium-ion battery and from new demand for the large format lithium-ion battery used in applications such as hybrid, plug-in-hybrid, and full electric vehicles, as well as for battery applications in the utility grid storage industry.

The total lithium content of seawater is immense and is estimated as being 230 billion - tons. In seawater lithium exists at a relatively constant concentration of 0.14–0.25 parts per million (ppm); higher concentrations approaching 7 ppm are found near hydrothermal vents. Lithium can be separated from other elements in igneous minerals, or lithium salts can be extracted from the water of mineral springs, brine pools, and brine deposits. The metal is produced electrolytically from a mixture of fused lithium chloride and potassium chloride.

The interest in mining the oceans makes sense when the amount of dissolved metal ions is compared to the estimated reserves on land and to the total mass of minerals being currently extracted worldwide (Table 1).

Table 1 lists seawater concentrations of metal ions contained in higher concentration and their total amounts, assuming a total ocean volume of 1.3×10^9 km^3 [17]. The comparison of the total oceanic abundance of the various considered ions with their land reserves shows the presence of huge amounts of minerals in the sea, in most cases considerably greater than the estimated reserves on land. Moreover, the amount of minerals being extracted worldwide is, in some cases, comparable to their estimated reserves on land (e.g., as is happening to Al and to a lesser extent to Sr, Ni, Zn, Fe, Cu, and Mn) [17]. Moreover, when the amount of water desalinated worldwide today (65.2 million m^3/day) is considered, and it is supposed to be produced through reverse osmosis (RO) technology (recovery factor 45%, salt rejection 99.6%), the produced brine will contain, for some components, minerals in amounts comparable to or higher than those extracted today (see Table 1).

Traditionally, the most concentrated ions in seawater (such as sodium chloride) are extracted by evaporation [17,18]. Ions such as Mg and K can subsequently be recovered by electrolytical processes [17,18]. These methods are not practical for low concentration ions, and their main problem lies in the huge amount of water that needs to be processed. Several researchers [18,20] have proposed extraction schemes for a range of elements. Le Dirach et al. [21] identified eight elements as being potentially economically and technically viable, as shown in Table 2. The protocol retained comprises four steps: (i) first, phosphorus is extracted through purification by alum, (ii) caesium is recovered through a liquid-liquid extraction approach, (iii) indium is then recovered by another liquid-liquid extraction with the help of organic acids, (iv) in the final phase, germanium and magnesium are extracted, and (iv) the remaining solution is principally composed of sodium and potassium chlorides, which are separated by hot lixiviation techniques, using the different solubilities of NaCl and KCl. However, the protocol of extraction, elaborated on and proposed by Le Dirach et al., needs experimental verification in order to be feasible.

Table 1 Concentrations and estimated amounts of dissolved metal ions in the sea compared with the estimated land resources and with the total mass extracted today

Element	Concentration in seawater (g/L)[a]	Total oceanic abundance (tons)[b]	Mineral reserves on land (tons)[c]	Production in 2014 (tons)[d]	Concentration in brine (ton/y)[e]
Cl	19.40	2.522×10^{16}	n.a.	n.a.	9.22×10^{8}
Na	10.80	1.404×10^{16}	n.a.	n.a.	5.13×10^{8}
Mg	1.29	1.677×10^{15}	2.20×10^{9} (from [14])	9.07×10^{5}	6.13×10^{7}
Ca	0.41	5.343×10^{14}	n.a.	n.a.	1.95×10^{7}
K	0.39	5.096×10^{14}	8.30×10^{9} (from [15])	n.a.	1.86×10^{7}
Br	0.070	8.749×10^{13}	Large	4.11×10^{5} (in the form of bromine)	3.20×10^{6}
Sr	0.00810	1.053×10^{13}	6.8×10^{6}	3.18×10^{5}	3.85×10^{5}
Li	0.00017	2.210×10^{11}	1.35×10^{7}	3.60×10^{4}	8.08×10^{3}
Ba	0.0000210	2.730×10^{10}	3.50×10^{8} (in the form of barite)	9.26×10^{6} (in the form of barite)	9.98×10^{2}
Mo	0.0000100	1.300×10^{10}	1.10×10^{7}	2.66×10^{5}	4.75×10^{2}
Ni	0.0000066	8.580×10^{9}	8.10×10^{7}	2.40×10^{6}	3.14×10^{2}
Zn	0.0000050	6.500×10^{9}	2.30×10^{8}	1.33×10^{7}	2.38×10^{2}
Fe	0.0000034	4.420×10^{9}	8.70×10^{10}	3.22×10^{9}	1.62×10^{2}
U	0.0000033	4.290×10^{9}	2.60×10^{6}–5.47×10^{6} (from [15])	6.65×10^{4} (from [15])	8.64×10^{1}
As	0.0000026	3.380×10^{9}	n.a.	4.60×10^{4} (in the form of arsenic trioxide)	1.24×10^{2}
V	0.0000019	2.470×10^{9}	1.50×10^{7}	7.80×10^{4}	9.03×10^{1}
Al	0.0000010	1.300×10^{9}	6.37×10^{7}	4.93×10^{7}	4.75×10^{1}
Cu	0.0000009	1.170×10^{9}	7.00×10^{8}	1.87×10^{7}	4.28×10^{1}
Se	0.0000009	1.170×10^{9}	1.20×10^{5}	n.a.	4.28×10^{1}
Mn	0.0000004	5.200×10^{9}	5.70×10^{8}	1.80×10^{7}	1.90×10^{1}
Cr	0.0000002	2.600×10^{9}	$>4.80 \times 10^{8}$	2.90×10^{7}	9.50
Cd	0.0000001	1.430×10^{9}	n.a.	2.20×10^{4}	5.23

n.a.: not available.

[a]Seawater element concentrations are taken from [16].

[b]Total oceanic abundance is calculated assuming a total ocean volume of 1.3×10^{9} km^3.

[c]Mineral reserves are from USGS data [17] except for uranium reserves for which the values are given from [18]. The USGS [19] does not provide data for the world reserves of sodium and calcium. All land reserves are in terms of pure elements, except for aluminum, which is given in terms of smelter production and capacity. Detailed world arsenic reserves data are unavailable but thought to be at least twenty times world production [19].

[d]Mineral production data are from [19] except for uranium data, which is from [18]. In this case, the value reported is the total uranium consumption rather than the mineral production, which is about two-thirds of the total.

[e]Brine element concentrations calculated assuming a total amount of desalinated water of 65.2×10^{6} m^3/day produced through reverse osmosis technology with recovery factor 45% and salt rejection 99.6%.

From A. Brunetti, F. Macedonio, G. Barbieri, E. Drioli, Membrane engineering for environmental protection and sustainable industrial growth: options for water and gas treatment, Environ. Eng. Res. 20(4) (2015) 307–328.

Table 2 List of potentially economic extracts from seawater

Element	Concentration (mg L^{-1})	Major use	Selling price ($ kg^{-1})
Na	10,500	Fertilizers	0.13
Mg	1350	Alloys	2.80
K	380	Fertilizers	0.15
Rb	0.12	Lasers	79,700
P	0.07	Fertilizers	0.02
In	0.02	Metallic protection	300
Cs	0.0005	Aeronautics	63,000
Ge	0.00007	Electronics	1700

From J. Le Dirach, S. Nisan, C. Poletiko, Extraction of strategic materials from the concentrated brine rejected by integrated nuclear desalination systems, Desalination 82(1–3) (2005) 449–460 with permission of Elsevier.

If oceans contain huge amounts of organic and inorganic elements to be extracted, then desalination residues are highly saline and could also be used for the extraction of minerals. Moreover, the brine of desalination plants is currently regarded as waste that can have a high negative environmental impact when disposed of. Therefore the exploitation of ocean for minerals and water could minimize the brine disposal problem and raw material deficiency. Various studies can be found in the literature for the recovery of the compounds present in the retentate steams of the desalination plants. For example, Turek [19] suggested dual-purpose desalination-salt production systems. Specifically, he proposed UF-NF-MSF-crystallization and UF-NF-RO-MSF-crystallization processes for the recovery of salts and water by the desalination plants. By assuming a cost of NaCl equal to $30/ton, Turek calculated a water cost equal to $0.71/$m^3$ in UF-NF-MSF-crystallization systems and $0.43/$m^3$ in UF-NF-RO-MSF-crystallization systems, respectively, which was competitive with those of potable water produced in thermal or RO seawater plants. Jeppesen et al. [11] showed that recovery of sodium chloride from RO concentrate could significantly lower the cost of potable water production if employed in conjunction with thermal processing systems. Moreover, Jeppesen et al. [22] indicated that the recovery of rubidium from seawater might be a potential source of revenue (even though they had little available information on the extraction costs for rubidium and claimed that further work was needed to characterize the economics of the rubidium extraction process). Finally, they asserted that the removal of phosphorus from RO concentrate was not economically viable, but had substantial environmental benefits because it can minimize the environmental impact associated with phosphorus in the marine environment, including algal blooms, eutrophication, and damage to coral organisms.

Drioli and coworkers [21] utilized MCr for the exploitation of seawaters and brine streams of the desalination plants. They claimed that MCr offers the possibility to process the concentrate streams until water and dry salts of high quality and controlled properties are obtained, transforming the traditional brine disposal cost into a potentially new and

profitable market. These systems have multiple benefits: avoiding discharge to surface or ground waters, flexibility in site selection, and efficient reuse of water. Moreover, MCr represents a very interesting opportunity for a real decrease of desalination costs. In the following sections, the strategy of desalination processes with MCr units are described.

3. ZERO LIQUID DISCHARGE STRATEGY THROUGH INTEGRATED MEMBRANE-BASED DESALINATION SYSTEMS: DESCRIPTION OF THE PROCESS

Membrane engineering with its various operations can address the objective of ZLD and the growing problems of water stress and mineral depletion. All these issues can be addressed in an integrated way in which different membrane operations can be used in RO pretreatment and posttreatment. As previously mentioned, some other pressure-driven membrane processes can be utilized in RO pretreatment as interesting alternatives to conventional processes (i.e., chemicals and mechanical filtration units). In particular, MF (a low-pressure membrane process for the removal of colloidal and suspended micrometer-size particles), UF (another low-pressure membrane process typically used to retain macromolecules, colloids, and solutes with molecular weights greater than few thousand), and NF (a high-pressure membrane process for the removal of turbidity, microorganisms, hardness, and most parts of multivalent ions) are becoming standard and efficient pretreatment options for seawater and brackish water desalination. Other benefits arising from the utilization of pressure-driven membrane processes in the pretreatment steps are the possibility to handle a large variation in raw water quality, the smaller footprint, and the opportunity to increase RO flux and water recovery.

For minimizing the brine disposal problem, the ultimate achievement is to operate the system with ZLD, or near ZLD, where the recovery would approach 100%. In ZLD, most of the water in the concentrate is recovered as product by completely separating the salt from the water. A ZLD system has therefore the advantages of maximizing water production, of producing minerals, of minimizing brine disposal, of being used in any geographical location, and of being easily accepted by the local community because of its positive environmental effects and minimal waste production. Conventional ZLD systems can include thermal evaporators, crystallizers, brine concentrators, and spray dryers [4]. While these systems are technologically available, the energy required to achieve near 100% recovery in such a system is high and often not financially possible, except for very small RO systems [18]. Lower energy consumption with respect to conventional thermal processes can be achieved by combining RO systems with MD and/or MCr units [22,23]. The latter are systems utilizing a hydrophobic membrane with an appropriate pore structure as a fixed interface between two different phases without dispersing one phase into another. In these processes the membrane does not act as a

selective barrier but rather sustains the interfaces. The separation process is based on the principles of phase equilibrium.

Conventional systems have some important advantages, such as high interfacial area per volume unit, low operating temperatures and pressure, high rejection, modular design, easy scale-up, less membrane fouling, and low sensitivity to concentration polarization phenomenon. Drawbacks are related to the presence of an additional mass transport resistance (the membrane itself) and to the rather limited range of the operating pressures below the breakthrough threshold. Their performance strongly depends on the properties of the membranes used. In general, a high hydrophobicity (for aqueous applications) is required to prevent wetting and mixing between the different phases in contact; elevated permeability leads to high fluxes; high chemical and thermal stability are necessary to improve the membrane resistance to chemical attack; and it is resistance to degradation and decomposition.

MD and MCr can be used for mitigating the impact of concentrates on the environment and for the recovery of the valuable contained components. In particular:

1. *Membrane distillation (MD)* is a membrane process that combines both membrane technology and evaporation processing in one unit. It involves the transport of water vapor through the pores of hydrophobic membranes via a partial pressure difference across the membrane (Fig. 3).

   With respect to conventional desalination technologies such as multistage flash distillation and RO (techniques involving high thermal energy and high operating pressure, respectively, finally resulting in excessive operating costs), MD offers the attractiveness of operation at atmospheric pressure and low temperatures (30–90°C), with the theoretical ability to achieve 100% salt rejection. Moreover, MD is not limited by concentration polarization phenomena as is the case in RO. A previous work [24] showed that no concentrated polarization occurs with MD at concentrations up to 300 g/L. A relatively small flux decline is observed when concentration

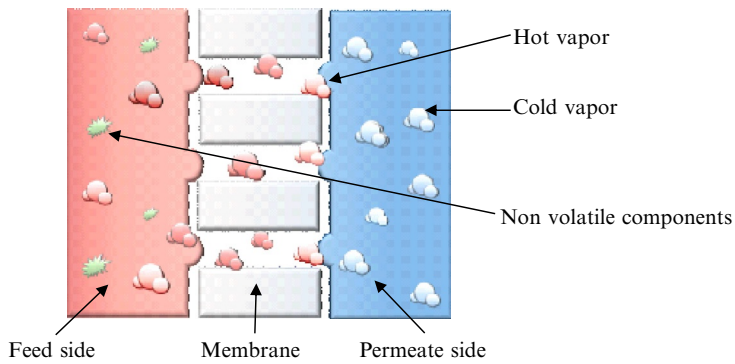

Fig. 3 Membrane distillation process.

and viscosity increase, but this is due to thermodynamic effects: when the salt concentration increases, the activity coefficient is modified, which can explain the water flux decrease. However, this flux decline is low in comparison with the one observed (of about 70% of the initial flux) with RO, which is due to both osmotic pressure and concentration polarization.

2. *Membrane crystallization (MCr)* is perceived as an alternative technology for producing crystals and pure water from supersaturated solutions; the use of the MD technique in the concentration of a solution by solvent removal in the vapor phase is utilized in this application.

   MCr is able to promote crystals' nucleation and growth in a well-controlled pathway, starting from undersaturated solutions. In a membrane crystallizer, the membrane matrix acts as a selective gate for solvent evaporation, modulating the final degree and the rate for the generation of the supersaturation. Therefore the possibility to act on the trans-membrane flow rate, by changing the driving force of the process, allows modulation of the final properties of the crystals produced both in terms of structure (polymorphism) and morphology (habit, shape, size, and size distribution). The experimental evidence that can be found in several published articles [25–27], validate the effectiveness of MCr as an advanced method for performing well-behaved crystallization processes.

MD and MCr are both efficient tools for improving seawater desalination processes:

1. Integration of a MD unit to process RO retentate could (a) increase the amount of recovered water and (b) reduce the amount of discharged brine.
2. Integration of a MCr unit to process RO retentate could (a) enhance the water recovery factor, (b) minimize the discharged brine, and (c) produce valuable crystalline products.

The studies carried out by Drioli and coworkers [14,28–31] showed that the introduction of a MCr unit on NF and RO retentate streams of an integrated membrane-based desalination system constituted by MF/NF/RO increases plant recovery factor to as much as 92.8%, higher than that of an RO unit (about 45%) and much higher than that of a typical MSF (about 10%–20%). Moreover, it has been experimentally shown that the presence of an organic compound (i.e., humic acid) in the retentate inhibits crystals' growth rate [32]. This proved the necessity to optimize the NF/RO pretreatment steps, in order not only to reduce the NF/RO membrane fouling but also to control the crystallization kinetics that are linked with the nature and the amount of the foreign species existing in the highly concentrated brines emerging from the NF and RO stages. In some studies on MCr [32], a rapid decrease in trans-membrane flux has been observed because of the deposition of crystals on the membrane, which reduced the membrane's permeability. This problem can be minimized through proper design of the process and proper control of the operative conditions. With respect to the best control of operative conditions, temperature polarization is an important factor depressing the driving force

and hereby the process performance [33]. Finally, the additional advantage of MD and MCr of a low working temperature provides the possibility of utilizing waste heat and other sustainable energy resources (such as geothermal or solar energy).

The proposed strategy is therefore to adopt integrated membrane-based desalination systems with MCr units for the simultaneous recovery of water and minerals from seawater, for the reduction of brine disposal problems, and for the improvement of the environmental sustainability of desalination plants. In order to be attractive, a technology must not only be technically viable but also profitable. In the following section, a preliminary cost analysis of the integrated desalination system is described, too.

4. ECONOMICS AND ENERGY CONSUMPTION OF THE PROCESS

Economics is one of the most important factors determining industrial decisions. Water is the cheapest product on earth, yet sometimes the cost of water is too high for certain consumers. In general, it is difficult to analyze and compare the costs of the current desalination plants and technologies because the cost of desalted water depends on many factors, such as the location of the plant, its capacity, the salinity and quality of the feed water available at the selected site, and the energy cost at the site under consideration. Moreover, thermal desalination is generally more cost-intensive than RO desalination, although the cost of desalination has been declining over time.

When desalination started in the late 1950s, the cost was not deemed as important as it is today because the main challenge was to produce fresh water from seawater for boilers and drinking purposes on ships. Later in the 1960s and early 1970s, desalination technologies (thermal processes) were widely available for commercial production, but the cost was too high. Membrane processes began to be competitive in the 1970s and started the trend toward cost reduction. In 1975 seawater desalination costs were quoted as being about \$2.10/m^3 (Southwest Florida Regional Planning Council, 1980) [34]. Since that time, the cost for desalination has continued to decrease causing the water price to drop to \$0.50/m^3 [35] for large-scale SWRO plants and for specific local conditions to \$1.00/m^3 for MSF. RO desalination costs comprise all the treatment steps, including pretreatment and posttreatment processes but excluding water distribution costs. The reduction of the cost of desalted water through thermal processes was due to material improvements, process innovation, equipment costs, and increasing competition, whereas prices of SWRO processes fell because of the significant technological development of membrane materials, the improvement of pumping systems, the application of energy recovery systems, and the use of the build, own, operate, transfer (BOOT) contracts. By 2003 these factors had lowered SWRO desalination costs to as little as 0.53 \$/m^3 for the Ashkelon desalination plant [36] and to 0.48 \$/m^3 for the desalination plant at Tuas, Singapore [37]. For brackish water reverse osmosis desalination (BWRO), Wilf [38] estimates costs in the range of \$0.2–\$0.3 /m^3. Wilf's estimations are not far from the real

values. An example can be found in the El Paso Desalination Plant (Texas), which produces drinking water by treating previously unusable brackish groundwater (recovery factor ≈ 83%) with a production cost of less than 0.41 $/m^3. For the Ashkelon SWRO plant, Maurel [39] reported that the cost of desalted had adjusted many times and increased to $0.655/m^3 in 2006 and to $0.778/m^3 in 2008.

Recent water price bids for SWRO plant BOOT contracts exceeded these very low water prices because of ever-increasing construction and energy costs, whereas the cost for SWRO energy consumption and RO membranes continued to drop.

The TWC of various desalination plants using different technologies and contract types are summarized in Table 3. The main differences in the total price for similar plants are due to specific conditions such as the necessity to install complex pretreatment systems or to severe environmental regulations.

Fig. 4 shows the TWC of various SWRO plants; the reduction from 1991 to 2003 was mainly due to the described technological developments; the recent increase was due to the restrictive environmental regulations, to the necessity to utilize sophisticated pretreatment systems, and so on.

Potential areas for cost savings are related to further improvements in RO operations, such as [14]:

Table 3 Water cost of different recent large-scale projects [34,40]

Site	Start-up	Capacity (m^3/d)	Contract type	Cost ($/$m^3$)
Fujairah 2 MED/SWRO	2011	460,000/136,000	IWPP	
Adelaide SWRO 2-pass	2011	273,000	DBOM[a]	
Sydney SWRO 2-pass	2010	250,000	DBO[b]	
Hadera SWRO	2010	347,900	BOOT	0.63
Shuaiba MSF	2010	880,000 900 MW	BOO	0.95
Marafiq MED-TVC	2009	800,000	IWPP	0.83
Skikda SWRO	2008	100,000	BOT[c]	0.73
Oxnard BWRO (salinity = 1.38 g/L)	2008	28,400		0.31
Alicante 2 SWRO	2008	65,000	DBO	
Hamma SWRO	2008	200,000	BOO	0.82
El Paso BWRO (2.55 g/L)	2007	55,670	DBB[d]	0.41
Perth SWRO 2-pass	2007	143,700	BOT	1.20
Palmachim SWRO	2007	110,000	BOO	0.78
Rabigh MED-TVC	2005	25,000	BOOT	1.15

[a]DBOM: design build operate and maintain.
[b]DBO: design build operate.
[c]BOT: build own transfer.
[d]DBB: design bid build.

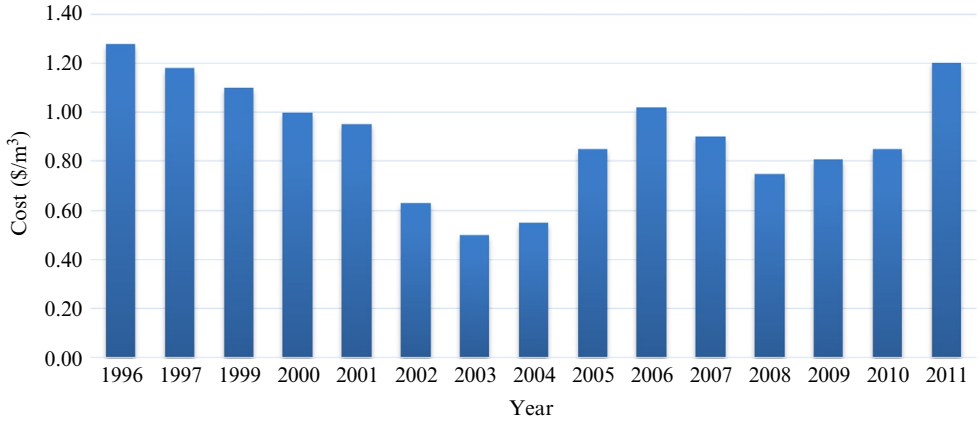

Fig. 4 TWC of different SWRO plants in operation and contracted. *(From N. Ghaffour, T.M. Missimer, G.L. Amy. Technical review and evaluation of the economics of water desalination: current and future challenges for better water supply sustainability, Desalination 309 (2013) 197–207).*

1. Research in novel membrane materials and polymer chemistry for the development of membranes that are highly resistant to chlorine attack, thus eliminating the need for dechlorination of the RO feed and rechlorination after the membrane system, reducing the overall cost of RO and the recourse to chemical additions.
2. Development of water treatment systems coupled with renewable energy sources in order to allow significant reduction in energy consumption.
3. Recourse to membrane pretreatment in order to (i) decrease costs associated with plant footprint, RO membrane replacement costs, and chemical costs, and (ii) increase recovery and permeate flux related to lower fouling rates.
4. Enhancement of transport mechanisms and improvement of module design (e.g., further research in the transport properties of polymer, carbon- and carbon-nanotube-based, zeolite, and mixed-matrix membranes).
5. Integration of MCr on NF and/or RO brine for mineral extraction from the sea and desalted water production. With this strategy, the cost of the desalination plant and of the water produced will have to be calculated with particular attention on the raw materials produced.

Economic evaluations of integrated membrane-based desalination processes with MCr units on NF and/or RO brine streams can be found in [30,33,41]. In these works various process designs were analyzed. In particular, Drioli and coworkers in [41] modeled different combinations of membrane units. All the studied flow sheets were based on the presence of MF, followed by NF and finally by RO (FS3). The differences among them related to the type of concentration units involved (membrane crystallizers and/or MD) and the streams they treated (NF and/or RO brines). In particular, MCr operated on NF brine in FS4, on RO brine in FS5 (Fig. 5), and on both RO and NF brine in FS6. In the

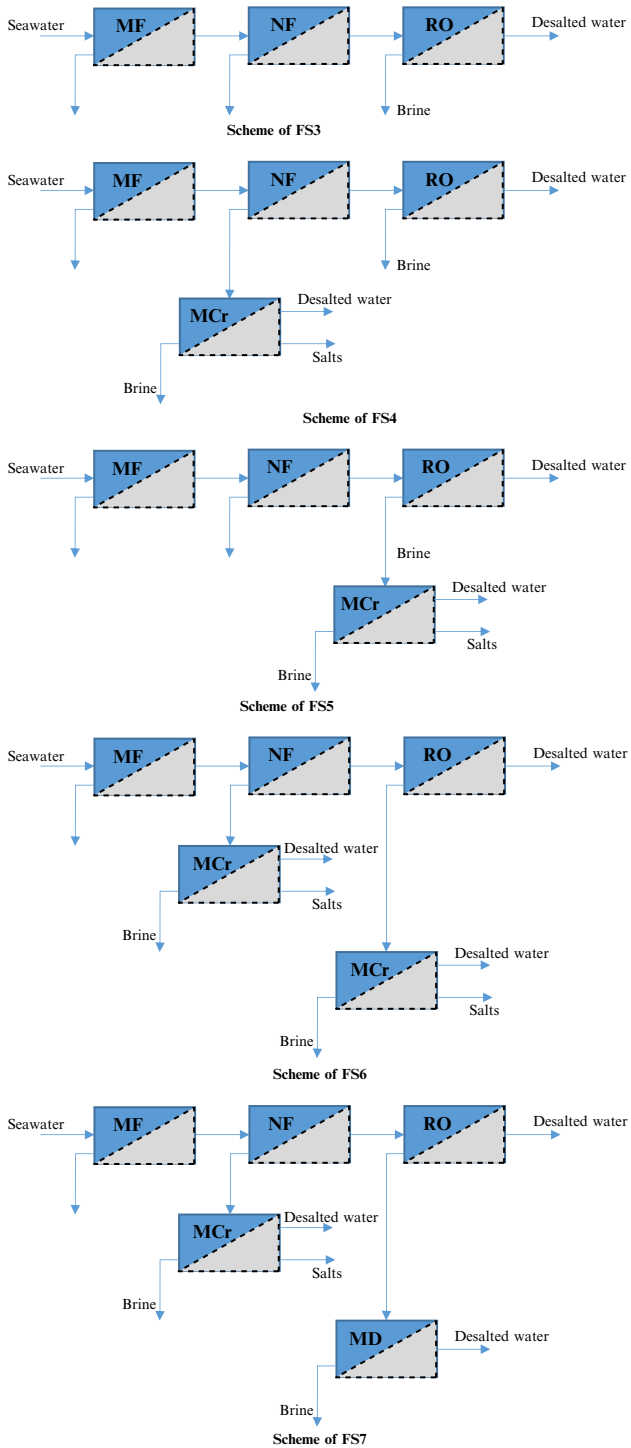

Fig. 5 Scheme of flow sheets from FS3 to FS7.

last flow sheet (FS7), MCr was introduced on NF brine, while MD operated on RO brine. In each MD/MCr process, the fresh water coming from the RO was used as cold water stream.

The proposed desalination systems have been compared on the basis of their energetic requirement, water cost, amount of discharged brine, and the fresh water and salts (NaCl and/or $MgSO_4*7H_2O$) produced.

The results achieved for some of the studied membrane-based desalination systems are reported in Tables 4 and 5.

Considering the same feed flow rate for all the proposed flow sheets (1051 m^3/h), by introducing a MCr unit on NF brine (FS4), the quantity of fresh water produced is higher than it is on RO brine (FS5) because MCr works at the same degree of efficiency, but in FS5 on a lower brine flow rate. Taking into account that MCr is not limited by concentration polarization phenomena, the higher its feed flow rate, the more fresh water it can produce.

The introduction of a membrane crystallizer unit on both retentate streams increases the plant recovery factor so much that it can reach values higher than 90% in FS6, a value higher than that of a conventional membrane desalination process (such as a typical

Table 4 Product characteristics for some of the analyzed flow sheets

Flow sheet[a]	FS3 or MF + NF + RO	FS4 or MF + (NF + MCr) + RO	FS5 or MF + NF + (RO + MCr)	FS6 or MF + (NF + MCr) + (RO + MCr)	FS7 or MF + (NF + MCr) + (RO + MD)
Water recovery factor (%)	49.0	71.5	69.9	92.4	88.4
Produced salts ($CaCO_3$, NaCl, and/or $MgSO_4*7H_2O$)[b]	//	5648	14875	20523	5648
Energy consumption (kWh/m^3)	3.64	19.37	18.30	26.91	28.11
Energy consumption with EERD[c] (kWh/m^3)	3.03	18.95	17.87	26.59	27.77
Energy consumption with EERD and TERD[d] [KWh/m3]	3.03	2.08	2.13	1.61	1.68

//, no salts production.

[a]The same feed flow rate for all the analyzed flow sheets (1051 m^3/h).

[b]$CaCO_3$ is achieved from NF/RO brine, before MCr treatment, through reactive precipitation with anhydrous sodium carbonate Na_2CO_3, in order to limit calcium sulfate precipitation during MCr operation. NaCl and $MgSO_4*7H_2O$ are produced through MCr from NF/RO brine.

[c]EERD: electrical energy recovery device.

[d]TERD: thermal energy recovery device.

From E. Drioli, A. Criscuoli, F. Macedonio (Eds.), Membrane-Based Desalination: An Integrated Approach (MEDINA), Iwa Publishing, 2011.

Table 5 Desalted water unit cost comparison

	Fresh water cost[a] ($/m^3)	Freshwater cost with EERD[a] ($/m^3)	Freshwater cost with EERD and TERD[a] ($/m^3)	Freshwater cost considering the gain for the salt sale ($/m^3)
FS3	0.459	0.407	//	//
FS4	0.675	0.639	0.513	0.256
FS5	0.596	0.560	0.441	−0.017
FS6	0.730	0.703	0.515	−0.058
FS7	0.739	0.710	0.514	0.400

EERD, electrical energy recovery device; *TERD*, thermal energy recovery device; //, not reported because there is neither TERD nor salt production in FS3.
[a]Potable water cost calculated not considering the gain for the salts sale.
With permission from IWA Publishing E. Drioli, A. Criscuoli, F. Macedonio (Eds.), Membrane-Based Desalination: An Integrated Approach (MEDINA), Iwa Publishing, 2011.

RO unit, which is about 45%) and higher than that of a typical MSF (which is about 10%–20%). Compared to FS6, in FS7 the quantity of produced fresh water decreases because MD has a lower recovery factor (77%) with respect to MCr.

The highest production of salts occurs when the membrane crystallizer unit operates on both retentate streams (FS6).

From an energetic point of view, the introduction of MCr and/or MD (in FS4, FS5, FS6, and FS7) creates a thermal energy requirement because of the retentate flow rate, which must be heated and which increases the global energy demand. In FS5, where the RO brine must be further concentrated in a MCr unit, the thermal energy necessary is reduced below that of the other systems because a lower flow rate has to be heated. In FS6, where both retentate streams must be heated, the total energy consumption is the highest. The same thing occurs in FS7. However, if thermal energy is available in the plant, then the energy requirements of the integrated systems with MCr/MD decrease, reaching values competitive with those of the other desalination processes.

In all the examined flow sheets, the fresh water cost is lower than that of thermal desalination processes (about \$0.9–\$1.4/m^3 for MSF [6,37] and \$0.7–\$1.0 for MED/TVC [37]) and ranges from \$0.41/m^3 for FS3 with Pelton turbine like Electrical Energy Recovery system, to \$0.74/m^3 for FS7 if the gain for the salts sale is not considered. The higher water cost in the integrated system with the MCr is due to the thermal demand of the MCr unit needed for heating the brine. If thermal energy is available in the plant, the water cost is reduced to about \$0.44–0.52/m^3. However, it should be pointed out that in an integrated system with a MCr unit, the quantity of produced salts is high enough that the gain for the salts' sale covers more than the entire cost of the desalination process, particularly in systems with a MCr operation on both NF and RO retentate streams (FS6). Therefore the FS6-integrated desalination process becomes

attractive from an economical point of view, not to mention the environmental benefits because of the minimized waste disposal.

In order to correctly evaluate the real benefits of the proposed strategy, much effort is being made to define different indicators that take into account the effects of industrial processes on the environment, the economy, and society. It is generally agreed that the metrics must include parameters that are clearly defined, simple, measurable, and objective rather than subjective and that they must drive businesses, governments, and communities toward more sustainable practices. Over the past 10–15 years, a number of metrics have been proposed, some of which are reported in Table 6.

Mass intensity takes into account the yield, stochiometry, solvent, and reagents used in the reaction mixture and expresses this on a weight/weight basis rather than as a percentage. In the ideal situation, MI would approach 1. Total mass includes everything that is used in a process or process step.

Waste intensity (or E Factor) draws attention to the quantity of waste that is produced for a given mass of product. Waste intensity also exposes the relative wastefulness of different sectors of the chemical processing industry, including industries as diverse as petrochemicals, specialities, and pharmaceuticals. This metric may certainly be used by industry and can, if used properly, spur innovation that results in a reduction of waste.

The mass indicators define both environmental impacts and raw material utilization (e.g., emissions and mass intensity), while the energy indicators evaluate the energy consumption of the alternatives.

Clearly, wasted resources and energy consumption may have significant cost implications.

Table 6 Metrics

Category	Metric	Unit
Mass	$\text{Mass intensity} = \dfrac{\text{Total mass}}{\text{Mass of product}}$	kg/kg
Energy	$\text{Energy efficiency or intensity} = \dfrac{\text{Total process energy}}{\text{Mass of product}}$	MJ/kg
Ecotoxicity	$\text{Ecotoxicity} = \dfrac{\text{Total (mass persistent + bioaccumulative)}}{EC_{50}\text{material} / EC_{50}\text{DDTcontrol}}$	kg
	$\text{Waste Intensity} = \dfrac{\text{Total waste}}{\text{Mass of product (fresh water + salts)}}$	kg/kg
Safety	Thermal hazard Reagent hazard Pressure (high/low) Hazardous by-product formation	
Economic	Cost	$ or €

EC_{50}: Concentration at which 50% of the organisms in an acute toxicity test die during the fixed time period of the study.

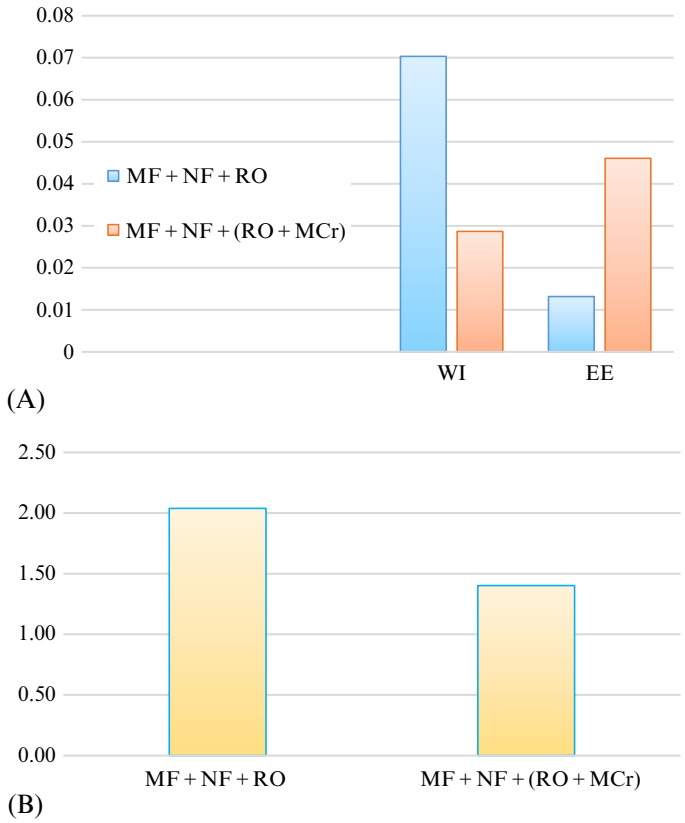

Fig. 6 (A) Waste (WI [kg/kg]), energy (EE [MJ/kg]) and (B) mass (MI [kg/kg]) intensity for various membranes' desalination systems.

MI, EE, and WI also provide a useful evaluation and comparison of the various membrane-based desalination systems.

An example can be found in Fig. 6 where the previously cited indexes estimated for an SWRO plant utilizing MF and NF as RO pretreatment (indicated with FS3 or MF + NF + RO) are compared with those of an SWRO plant utilizing membrane pretreatment and MCr as posttreatment of RO brine (indicated with FS5 or MF + NF + (RO + MCr)). The results achieved confirm that the recourse to MCr significantly reduces the brine disposal problem.

Brunetti et al. [17] indicate that the utilization of these indicators can also help during the design phase for individuating the most convenient process design. An example can be found in Fig. 7 where MI, EE, and WI are utilized for the comparison of three different situations, with MCr used for the exploitation of NF brine, or RO brine, or both. The lowest (i.e., best) value of MI for the desalination process with MCr on

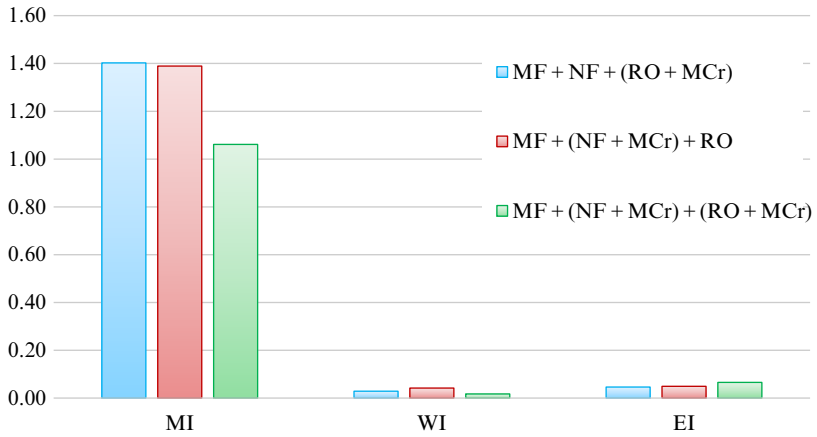

Fig. 7 Mass (MI [kg/kg]), waste (WI [kg/kg]), and energy (EI [MJ/kg]) intensity for various membrane-based desalination systems with MCr for the concentration of brine.

NF brine (indicated with FS4 or MF + (NF + MCr) + RO) with respect to that with MCr on RO brine (indicated with FS5 or MF + NF + (RO + MCr)) is due to the higher brine flow rate of NF than that of RO. However, the energy consumption (and the energy efficiency) of the system will also be higher because of the higher flow rate, which has to be heated. These trends will be, of course, accentuated in a desalination system with MCr units concentrating both NF and RO brine streams (indicated with FS6 or MF + (NF + MCr) + (RO + MCr)). The latter will have, on the other hand, the great advantage of minimizing the environmental impact of the whole desalination plant, which is proved by a WI approaching 0.

Therefore the utilized metrics give information about the water recovery factor, the energy consumption, and the amount of discharged brine but in a clearer way and allow easy and prompt comparison of different process designs. Other metrics can be defined and utilized for the evaluation of the impact of the membrane operations on the production lines. Examples can be found in the work carried out by Criscuoli et al. [42] and Brunetti et al. [16], where indicators that take into account some other parameters of the industrial processes, such as size, weight, volume, flexibility, and modularity of the plants can be found. These metrics can be coupled with the existing tools for comparing new and traditional processes with respect to other aspects of the production plants, always in the logic of Process Intensification (PI).

5. CONCLUSIONS AND FUTURE PERSPECTIVES

Water stress, increasing energy consumption, mineral depletion, and sustainability are already critical issues. Process engineering is one of the disciplines that is more involved in the technological innovations necessary to face these strongly interconnected

problems. As a matter of fact, water is also needed for energy generation and energy is also needed in desalination and for the production of raw materials (especially in mining where large amounts of energy and water are necessary), and all the industrial processes have an environmental impact.

Recently, process engineering has suggested the logic of PI to resolve these problems. Membrane technology, whose basic aspects satisfy the requirements of the PI strategy, can represent a problem-solver with inter-correlated solutions. In the past years, membrane operations have been assigned a key role in water reclamation schemes that are aimed at higher water quality reuse applications (i.e., RO is considered one of the most promising technologies for desalting salty waters). Moreover, the traditional membrane separation operations (e.g., MF, UF, NF, RO), widely used in many different applications, are today combined with new membrane systems such as MD and MCr. At present, the redesign of important industrial production cycles by combining various membrane operations suitable for separation and conversion units, and thus realizing highly integrated membrane processes, is an attractive opportunity because of the synergistic effects that can be attained. The overall concept introduced can be summarized as follows: Desalination operations must be combined with the recovery of various chemicals present in the brine of NF and/or RO desalination plants. To achieve this objective, membrane engineering can help bring to fruition new desalination systems based on integrated membrane operations. Specifically, rather than use conventional pretreatment, membrane pretreatment must be adopted in order to minimize membrane fouling, thereby reducing operating costs. In the posttreatment stage, the presence of MCr, thanks to its intrinsic characteristic of temperature-driven membrane processes, allows production of fresh water and minerals from highly concentrated feeds (such as brine streams).

Therefore the introduction of a MCr unit downstream from a NF and/or RO retentate increases the overall recovery factor, thus reducing the volume of concentrated streams that are usually discharged by the desalination plants and recovering the dissolved salts in the form of high-quality crystals. A new mining strategy is thus suggested for the recovery of valuable salts in well-controlled polymorph forms directly from the brine streams of the desalination plants.

A considerable amount of research has been conducted in attempts to improve MCr technology. An example can be found in the FP6 EU project MEDINA [43], where a program aimed at improving design and operation practices of the current membrane-based desalination plants was already developed. The project's team tried to solve or at least decrease some critical issues of sea and brackish water desalination systems, such as improvement of water quality, enhancement of the recovery factor, reduction of water cost, and minimizing the brine disposal problem. For solving and/or alleviating these problems, an approach based on the integration of different operations in RO pretreatment and posttreatment stages was proposed and studied. In particular, MCr was studied as a technology for improving the productivity of desalination systems, recovering some

of the valuable ions present in the highly concentrated streams of desalination plants, and reducing their environmental impact.

Other examples can be found in the Megaton project in Japan and in the SEAHERO project in South Korea. The projects' first emphasis was mainly on increasing the desalination capacity. However, in the second part of the projects, brine disposal issues were also addressed. Hybrid systems with MD and pressure retarded osmosis units were proposed for the extraction of valuable resources from the brine, the minimization of the environmental impact of the brine, and the recovery of energy. Moreover, the SEAHERO project suggested a hybrid forward osmosis/RO system for increasing the recovery factor by 30%, and thereby reducing the brine volume at the same time. This hybrid desalination process can reduce the energy consumption to less than 2.5 kWh/m^3 and the water price to $0.6 /ton.

One of the latest projects to launch is the Global MVP project (set to run from 2013 to 2018 in South Korea) [43]. This project aims to further develop "third generation" desalination plants by introducing an additional step to achieve a valuable resource recovery stage. This project focuses on lithium and strontium recovery from the discharged RO brine, but in fact several other compounds might be recovered from RO brine.

Despite its great potential, MCr is still far from fulfilling all expectations. To overcome the existing barriers and find further use for this technology in industry, new and better membranes, improved design of the membranes and modules, and overall better engineering are necessary. Moreover, accurate modeling to scale it up or down easily is needed, and significant multidisciplinary research efforts that can contribute to the development of this technology are needed.

REFERENCES

[1] N. Ghaffour, The challenge of capacity-building strategies and perspectives for desalination for sustainable water use in MENA, Desalin. Water Treat. 5 (2009) 48–53.
[2] G.L.M. von Medeazza, "Direct" and socially-induced environmental impacts of desalination, Desalination 185 (2005) 57.
[3] Y. Dreizin, A. Tenne, D. Hoffman, Integrating large scale seawater desalination plants within Israel's water supply system, Desalination 220 (2008) 132.
[4] L.F. Greenlee, D.F. Lawler, B.D. Freeman, B. Marrot, P. Moulin, Reverse osmosis desalination: water sources, technology, and today's challenges, Water Res. 43 (9) (2009) 2317–2348.
[5] J.E. Miller, Review of Water Resources and Desalination Technologies, Available from: Sandia National Laboratories, http://www.prod.sandia.gov/cgi-bin/techlib/access-control.pl/2003/030800.pdf, 2003.
[6] K. Qteishat, Desalination and water affordability, in: SITeau International Conference, Casablanca, Morocco, January 2009.
[7] Q. Schiermeier, Purification with a pinch of salt: climate change, growing populations and political concerns are prompting governments and investors from California to China to take a fresh look at desalination, Quirin Schiermeier wades in, Nature 452 (2008) 260.
[8] M. Elimelech, W.A. Phillip, The future of seawater desalination: energy, technology, and the environment, Science 333 (6043) (2011) 712–717.

[9] S. Lattemann, T. Höpner, Environmental impact and impact assessment of seawater desalination, Desalination 220 (2008) 1–15.
[10] B. Van der Bruggen, L. Braeken, The challenge of zero discharge: from water balance to regeneration, Desalination 188 (1–3) (2006) 177–183.
[11] T. Jeppesen, L. Shu, G. Keir, V. Jegatheesan, Metal recovery from reverse osmosis concentrate, J. Clean. Prod. 17 (2009) 703–707.
[12] F. Macedonio, E. Drioli, A.A. Gusev, A. Bardow, R. Semiat, M. Kurihara, Efficient technologies for worldwide clean water supply, Chem. Eng. Process. Process Intesif. 51 (2012) 2–17.
[13] MIT Technology Review, http://m.technologyreview.com/news/514751/novel-material-shows-promise-for-extracting-uranium-from-seawater/, May 16, 2013.
[14] U. Bardi, Extracting minerals from seawater: an energy analysis, Sustainability 2 (2010) 980–992.
[15] A. Brunetti, F. Macedonio, G. Barbieri, E. Drioli, Membrane engineering for environmental protection and sustainable industrial growth: options for water and gas treatment, Environ. Eng. Res. 20 (4) (2015) 307–328.
[16] J. Floor Anthoni, The Chemical Composition of Seawater, Available online: http://www.seafriends.org.nz/oceano/seawater.htm (last access on 05 February 2015).
[17] United States Geological Survey (USGS), Mineral Commodities Summaries 2015, Available online: http://minerals.usgs.gov/minerals/pubs/mcs/ (last access on 05 February 2015).
[18] H. Ohya, T. Suzuki, S. Nakao, Integrated system for complete usage of components in seawater: a proposal of inorganic chemical combined in seawater, Desalination 134 (1–3) (2001) 29–36.
[19] M. Turek, Seawater desalination and salt production in a hybrid membrane thermal process, Desalination 153 (2002) 173–177.
[20] J. Le Dirach, S. Nisan, C. Poletiko, Extraction of strategic materials from the concentrated brine rejected by integrated nuclear desalination systems, Desalination 182 (1–3) (2005) 449–460.
[21] E. Curcio, A. Criscuoli, E. Drioli, Membrane crystallizers, Ind. Eng. Chem. Res. 40 (2001) 2679–2684.
[22] E. Drioli, A. Criscuoli, E. Curcio, Membrane Contactors: Fundamentals, Applications and Potentialities: Fundamentals, Applications and Potentialities, vol. 11, Elsevier, Amsterdam, The Netherlands, 2011.
[23] E. Drioli, G. Di Profio, E. Curcio, Membrane-Assisted Crystallization Technology, Advances in Chemical and Process Engineering, vol. 2, Imperial College Press, London, 2015.
[24] C. Cabassud, D. Wirth, Membrane distillation for water desalination: how to chose an appropriate membrane? Desalination 157 (2003) 307–314.
[25] E. Drioli, E. Curcio, A. Criscuoli, G. Di Profio, Integrated system for recovery of $CaCO_3$, NaCl and $MgSO_4 \cdot 7H_2O$ from nanofiltration retentate, J. Membr. Sci. 239 (2004) 27–38.
[26] G. Di Profio, S. Tucci, E. Curcio, E. Drioli, Selective glycine polymorph crystallization by using microporous membranes, Cryst. Growth Des. 7 (2007) 526–530.
[27] E. Drioli, G. Di Profio, E. Curcio, Progresses in membrane crystallization, Curr. Opin. Chem. Eng. 1 (2012) 1–5.
[28] F. Macedonio, E. Curcio, E. Drioli, Integrated membrane systems for seawater desalination: energetic and exergetic analysis, economic evaluation, experimental study, Desalination 203 (2007) 260–276.
[29] F. Macedonio, E. Drioli, Pressure-driven membrane operations and membrane distillation technology integration for water purification, Desalination 223 (2008) 396–409.
[30] F. Macedonio, E. Drioli, E. Curcio, G. Di Profio, Experimental and economical evaluation of a membrane crystallizer plant, Desalin. Water Treat. 9 (2009) 49–53.
[31] F. Macedonio, E. Drioli, Hydrophobic membranes for salts recovery from desalination plants, Desalin. Water Treat. 18 (2010) 224–234.
[32] C.M. Tun, A.G. Fane, J.T. Matheickal, R. Sheikholeslami, Membrane distillation crystallization of concentrated salts—flux and crystal formation, J. Membr. Sci. 257 (2005) 144–155.
[33] A. Ali, F. Macedonio, E. Drioli, S. Aljlil, O.A. Alharbi, Experimental and theoretical evaluation of temperature polarization phenomenon in direct contact membrane distillation, Chem. Eng. Res. Des. 91 (2013) 1966–1977.

[34] Global Water Intelligence (GWI/IDA DesalData), Market Profile and Desalination Markets, 2009–2012 Yearbooks and GWI Website, http://www.desaldata.com/.
[35] F.H. Kiand, Supply of desalinated water by the private sector: 30 MGD Singapore seawater desalination plant, in: MEDRC International Conference on Desalination Costing, Conference Proceeding, Lemesos, Cyprus, December 2004.
[36] G. Kronenberg, The largest SWRO plant in the world—Ashkelon 100 million m^3/y BOT project, Desalination 166 (2004) 457–463.
[37] Desalination Markets 2005–2015, A Global Assessment & Forecast, Global Water Intelligence, 2005.
[38] M. Wilf, Fundamentals of RO–NF technology, in: International Conference on Desalination Costing, Limassol, 2004.
[39] A. Maurel, Seawater/Brackish Water Desalination and Other Non-conventional Processes for Water Supply, 2nd edition book, Lavoisier. (2006) 10:2-7430-0890-3.
[40] T. Pankratz, MEDRC Workshop on Membrane Technology Used in Desalination and Wastewater Treatment for Reuse, Muscat, Oman, www.medrc.org, March 2008.
[41] E. Drioli, A. Criscuoli, F. Macedonio, in: Membrane-Based Desalination: An Integrated Approach (MEDINA), Iwa Publishing, London, 2011.
[42] A. Criscuoli, E. Drioli, New metrics for evaluating the performance of membrane operations in the logic of process intensification, Ind. Eng. Chem. Res. 46 (2007) 2268–2271.
[43] S.-H. Kim, D.-I. Kim, Scaling-up and piloting of pressure-retarded osmosis, Desalin. Water Reuse 24 (3) (2014) 36–38.

FURTHER READING

[1] N. Ghaffour, T.M. Missimer, G.L. Amy, Technical review and evaluation of the economics of water desalination: current and future challenges for better water supply sustainability, Desalination 309 (2013) 197–207.

CHAPTER 7

Nanoparticle Incorporation into Desalination and Water Treatment Membranes—Potential Advantages and Challenges

Ikechukwu A. Ike, John D. Orbell, Mikel Duke
Victoria University, Melbourne, VIC, Australia

Contents

1. MEMBRANES FOR WATER TREATMENT: BACKGROUND AND MOTIVATION FOR NANOPARTICLE INCORPORATION

A membrane is defined as "a discrete, thin interface that moderates the permeation of chemical species in contact with it" [1]. In water treatment and desalination, where the membrane material may be polymeric, ceramic, metallic, or a combination of these materials known as a composite membrane, the goal is to hinder the permeation of dissolved, dispersed, and/or suspended solutes in the water while the water flows through the membrane. The membrane materials may be porous as in microfiltration (MF) and ultrafiltration (UF) membranes where separation is achieved largely by size exclusion or molecular sieving under a pressure differential, or they may be dense as are the reverse osmosis (RO) and forward

Desalination Sustainability
http://dx.doi.org/10.1016/B978-0-12-809791-5.00007-9

osmosis (FO) membranes where the separation mechanism is more commonly described by a solution-diffusion process under a pressure or concentration differential. Despite the difference in physical mechanisms, membranes may be conceptualized as comprising a number of capillary tubes per unit membrane area, N, with an average diameter, d. In this simplified conceptual framework, assuming incompressible particles and the absence of pore bridging or clogging, impurities in the feed water larger than the capillary diameter are rejected while those smaller are permeated. It follows then that the smaller the average capillary diameter, the greater the membrane rejection. On the other hand, the flux of clean water through the capillary bundle is proportional to the (fourth power of the) average diameter according to the Hagen-Poiseuille equation (Eq. 1) [1]

$$J = \frac{N\pi d^4 \Delta P}{128\mu L} \tag{1}$$

where ΔP is the pressure differential, L is the pore length, and μ is the water viscosity. Generally, a larger average pore diameter results in greater flux but lower rejection, and a smaller average diameter results in reduced water flux but better rejection. This observation is often referred to as the permeability-selectivity trade-off, which is a fundamental challenge in improving membrane performance.

On the other hand, the greater the membrane rejection, the greater the concentration of the rejected material in contact with the membrane on the feed side, a phenomenon commonly called concentration polarization. The increased solute concentration can translate to a relative reduction of water concentration in direct contact with the membrane, which may imply that less water permeates through the membrane's capillary pores. At the same time, some of the capillary pores may become partly or completely unavailable for water permeation because of solute clogging, a problem that is often aggravated by concentration polarization. Furthermore, the greater concentration of solute (arising from concentration polarization) increases the chance of chemical or physical interaction between the solute and the membrane surface, an interaction that might be detrimental to the membrane filtration performance. The attachment of solute material onto the surface and inside the pores of the membrane, leading to a decline in productivity over time, is often referred to as membrane fouling. Ensuring that concentration polarization and fouling do not compromise the practical operation of the membrane system constitutes another fundamental challenge inherent in membrane processes.

Because the problems of membrane permeability-selectivity trade-off, concentration polarization, and fouling are inherent to the membrane process [2], simple solutions for overcoming these problems are not readily available; consequently, they have been the subject of much research over the years. Apparently, relatively more progress has been made in resolving the permeability-selectivity challenge (especially with regard to the application of thin film composite (TFC) technology to RO desalination) than in resolving the fouling problem [3]. However, there is still significant room for improvement with regard to these inherent challenges. Research in nanotechnology holds enormous promise in contributing to the resolution of these problems. Aligned carbon nanotube,

aquaporin-based biomimetic and thin film nanocomposite (TFN) membrane nanotechnologies are being promoted as having the greatest promise in the advancement of membrane desalination and water treatment (MDWT) technologies for the future [2]. Nanotechnology has shown much promise in improving other desirable membrane properties such as chemical, mechanical, and thermal stability, which are crucial for membrane application under challenging conditions, as well as in the development of active functionalities such as self-cleaning, contaminant degradation, and antimicrobial effects [2,4]. Active functionalities appear to hold the key to an effective resolution of the elusive problem of membrane fouling.

2. NANOPARTICLES AND THEIR UNIQUE PROPERTIES

All the promises of nanotechnology in resolving the problems of membrane processes rely on the unique properties of nanoparticles that are distinct from the material bulk properties. A nanoparticle is a material whose external dimensions or internal pore structure, in at least one dimension, is in the size range 1–100 nm, resulting in unique physical or chemical properties [5]. A particle having all dimensions between 1 nm and 100 nm is termed a zero dimension nanoparticle; if only two dimensions are in the nanoscale range, such as nanotubes and nanorods, they are referred to as a one-dimensional nanomaterial; materials that are in the nanoscale range only in their thickness, such as thin films, are accordingly referred to as two-dimensional nanostructures [5]. Some materials, such as bulk zeolites, may exhibit a nanoscale dimension only in their internal pore structure, though they may also be available as nanosized crystals. However, a material may need more than one dimension in the 1–100 nm range to qualify as a nanoparticle; it must also be observed to exhibit novel phenomena because of its nanosize that are absent in the bulk [5]. The critical nanosize for novel phenomena varies from material to material and from property to property [5]. A material with an active diameter smaller than 1 nm or greater than 100 nm is outside the accepted range for a nanoparticle and is often referred to as a cluster (molecule) or a microparticle, respectively [6].

The variation of the intrinsic properties of materials with particle size as exhibited by nanoparticles is attributable to two nanoscale effects. Namely, a smoothly scaling surface to volume ratio effect that reflects the fraction of surface atoms in the nanoparticle in relation to the total atoms present, and a discontinuous quantum effect that indicates the limited spatial confinement of nanoparticles and changes in the shells of delocalized electrons in the nanoparticle because of this confinement [5,7]. These effects are described in the following sections as "surface effects" and "quantum effects," respectively.

2.1 Surface Effects

The fraction of surface atoms (ratio of surface area to volume) or dispersion of a spherical particle scales smoothly with the inverse of the diameter or radius. This is because, the particle's surface area and volume are functions of the square and cube of the radius, respectively. Therefore the smaller the particle, the greater the fraction of surface atoms relative

to the total atoms, a trend that is observed even for nonspherical materials. A surface atom can differ considerably in its properties from an otherwise similar atom located in the interior of the particle because surface atoms have fewer neighbors, possess unsatisfied bonding potentials, are more exposed to external interactions, and hence are more reactive [5,7]. As the proportion of the surface atoms increases in a nanoparticle, their contribution to the overall behavior of the particle becomes considerable. The overall energy of the particle increases as a consequence and its stability declines, resulting in greater chemical activities and the exhibition of unique properties that are not observed for a bulk sample of the same material [8]. An example of a proportionate scaling property because of the surface effect is the trend of the melting point of a solid with respect to the size of the material. Melting point of a solid is known to follow, the Gibbs-Thomson equation [7]

$$\frac{T_m - T_m^*}{T_m^*} = \frac{2V_{m(l)}\gamma_{sl}}{\Delta H_m r} \tag{2}$$

where T_m is the melting point of a particle with radius r, T_m^* is the bulk material melting point, $V_{m(l)}$ the molar volume of the liquid, γ_{sl} the solid-liquid interfacial tension, and ΔH_m the bulk latent heat of melting. The equation clearly shows that the melting temperature is directly related to the inverse of the radius of the particle. The dependence of melting point on size is commonly illustrated with gold. As a bulk material, gold melts at 1337 K, but this value gradually reduces as the size of the particle decreases, reaching a value of 600 K at a nanoparticle diameter of 3 nm [5].

2.2 Quantum Effects

Not all size-dependent properties of nanoparticles scale smoothly. Discontinuous changes are explained by the quantum mechanical nature of matter, which is related to the discrete electronic energy levels in systems with delocalized electrons and the effects of spatial confinement [5,7]. The positions of electrons in an atom are restricted to quantized orbitals (energy levels) around the nucleus. The highest energy orbital occupied by an electron(s) in the ground state of an atom is referred to as the valence orbital. The atoms of different materials require different quanta of energy to excite the valence electron(s) to a higher energy level. When atoms are grouped together, their orbitals may combine giving rise to a band structure [7]. At the ground state, the highest energy occupied band is the valence band, and the lowest energy unoccupied band is the conduction band; the difference between these two energy levels is called the band or Kubo gap [7]. The properties of a solid such as conductivity and optical properties are dependent on this energy gap [6]. A band gap is absent in metals but is present in semiconductors and insulators. Consequently, changes in the band gap have important effects on the properties of a material. Interestingly, such fundamental changes can be effected by a decrease in particle size to specific critical nanoscale dimensions [6,8].

The energy difference between adjacent energy levels (δ) in a band of a metal is often expressed as the quotient of the highest occupied molecular orbital (HOMO) or Fermi level (E_F) and the number of atoms present (n), that is, $\delta \approx E_F/n$. For a bulk material, the number of atoms is exceedingly large indicating that the energy gap is negligible. Consequently, electrons can move easily from the valence band to the conduction band whenever the thermal energy is greater than the (negligible) energy gap [7,8]. However, as the number of atoms in the system decrease to a critical nanoscale dimension, δ widens and becomes significant, resulting in a finite difference between the valence and conduction band. Gap widening signal a transition from metallic to nonmetallic properties. The shrinking size of the nanoparticle and expanding band gap imposes a spatial quantum confinement effect resulting in novel physical and chemical properties. Changes in particle sizes within the nanoscale range for semiconductors such as CdSe have been shown to lead to spectacular photoluminescence because of changes in the band gap [5,7]. Similar highly tunable optical phenomena have been reported for gold and silver nanoparticles, but here the effect is not due to changes in the band gap but to the excitation of the surface free electrons. These electrons experience surface plasmon resonance, a spatial quantum confinement effect, when the size of the nanoparticle approaches the critical free electron mean free path [5,7].

The development of superparamagnetism at the nanoscale dimension from otherwise ferromagnetic and ferrimagnetic materials in the bulk is another example of the quantum confinement effect [5]. Because of the thermodynamic drive to reduce internal energy, the magnetization of bulk magnetic materials are known to spontaneously divide into many small magnetic compartments called domains. The magnetization within each domain is uniform in direction but distinct from the directions of nearby domains. The equilibrium size of the domains is reached when the energy cost in making new domain walls equals the energy saved in creating a new domain. However, upon reduction of particle size to a characteristic nanoscale dimension, the energy saved in the formation of domain walls becomes insignificant and the nanoparticle thereby exists as a single domain, exhibiting the unique property of superparamagnetism [5].

2.3 Summary of Key Nanoparticle Properties and Relevance to Membrane Technology

The key features of nanoparticles of value to membrane technology include high surface area, increased chemical and physical activity, and certain unique properties. The high surface areas of hydrophilic nanoparticles such as nanosilica and nanoalumina are employed to improve the performance of membranes by increasing membrane hydrophilicity. An example of enhanced nanoparticle activity of relevance to membrane processes is the improved biocidal effect that is associated with nanosilver when compared with bulk silver. The former when added to a membrane alleviates the challenging problem of membrane biofouling. Titania nanoparticles benefit from both quantum and

surface effects to demonstrate enhanced photocatalysis, which is employed for the degradation of attached foulants on the membrane as well as the expression of other active functionalities. Quantum confinement effects and the molecular-level smoothness of the pores of carbon nanotubes, aquaporin proteins, and nanozeolite crystals are of immense value in the development of high-flux membranes for MDWT applications. These unique nanoparticle properties and their applications to membrane technology are discussed in more detail in the next section.

3. NANOPARTICLES FOR MDWT

The unique properties of nanoparticles have led to a surge of interest in the development of nanoparticle-based novel applications in many aspects of MDWT processes. Nanoparticles of significant interest to researchers include carbon nanotubes (CNT), aquaporins, and nanozeolites. They are considered the most promising materials for the development of novel and high-performance membranes for RO and nanofiltration (NF) desalination and water treatment applications [2]. Other important nanoparticles, especially for MF and UF applications, include nanosilver (nAg), nanotitania ($nTiO_2$), nanosilica ($nSiO_2$), and nanoalumina (nAl_2O_3) [4]. Nanoclay and iron oxide nanoparticles are also attracting research attention in many MF and UF membrane water treatment applications. The promise and achievements of these nanoparticles in improving MDWT processes are the focus of this section, along with the key challenges that must be addressed to realize their full potential.

3.1 Carbon Nanotubes

Carbon has four valence electrons that in diamond are hybridized in the sp^3 configuration, resulting in the three-dimensional tetrahedral structure that gives diamond its unique mechanical strength and electrical insulation. Graphite, on the other hand, exhibits sp^2 hybridization, resulting in hexagonal (honeycomb) sheets joined together by a weak bonding because of the free and delocalized p_z orbitals on each sheet [9]. Due to the delocalization of the electrons and the weakness of the developed intersheet bonds, graphite is electrically conductive and exhibits a lubricating property because graphene sheets can slip relative to each other. A CNT has been described as a cylindrical rolled up graphite sheet(s). Fig. 1 shows various carbon materials and how they are related. When a CNT consists of a single graphene sheet, it is referred to as a single-wall CNT (SWCNT), and when it comprises more than one layer of concentric cylinders held together by van der Waals attractions, it is known as a multi-wall CNT (MWCNT). The diameter of a CNT is commonly between 0.8 and 20 nm, though larger diameters are known; the length, however, can measure up to several centimeters. Consequently, a CNT is unique as it is both molecular and macroscopic in dimension, making it feasible for molecular properties to be directly available for macroscopic

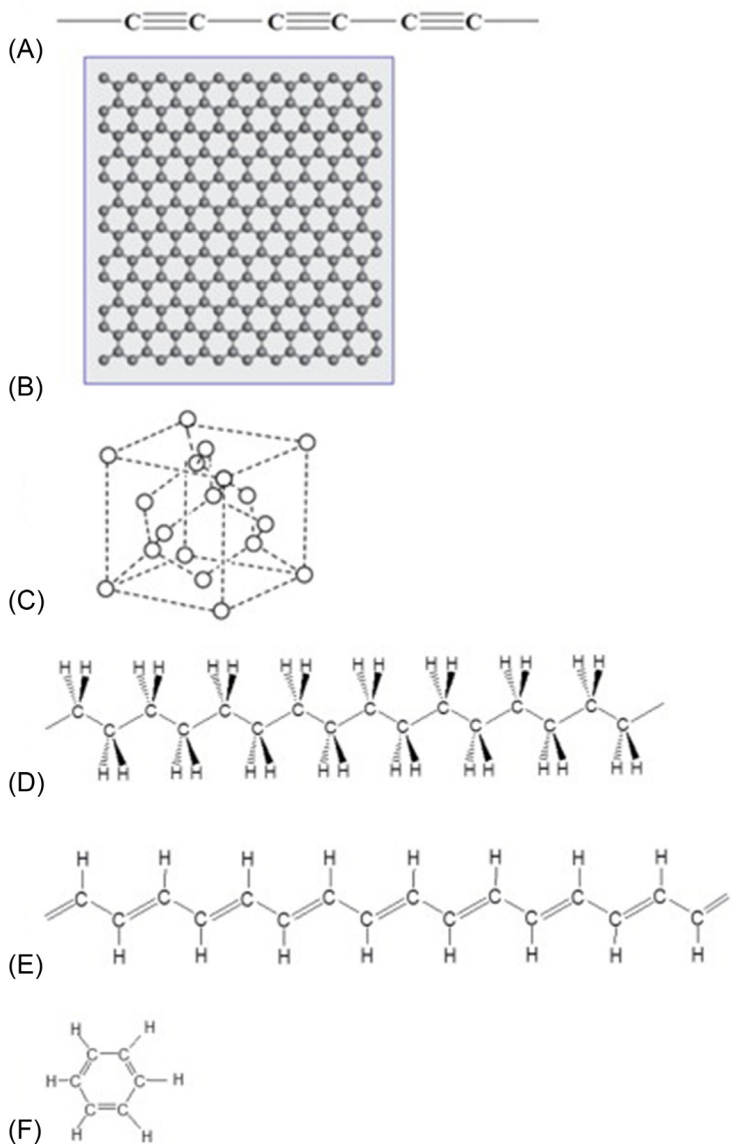

Fig. 1 Various carbon materials and their relatives: (A) carbyne (polyyne), (B) graphene, (C) diamond, (D) polyethylene, (E) polyacetylene, (F) benzene,

Continued

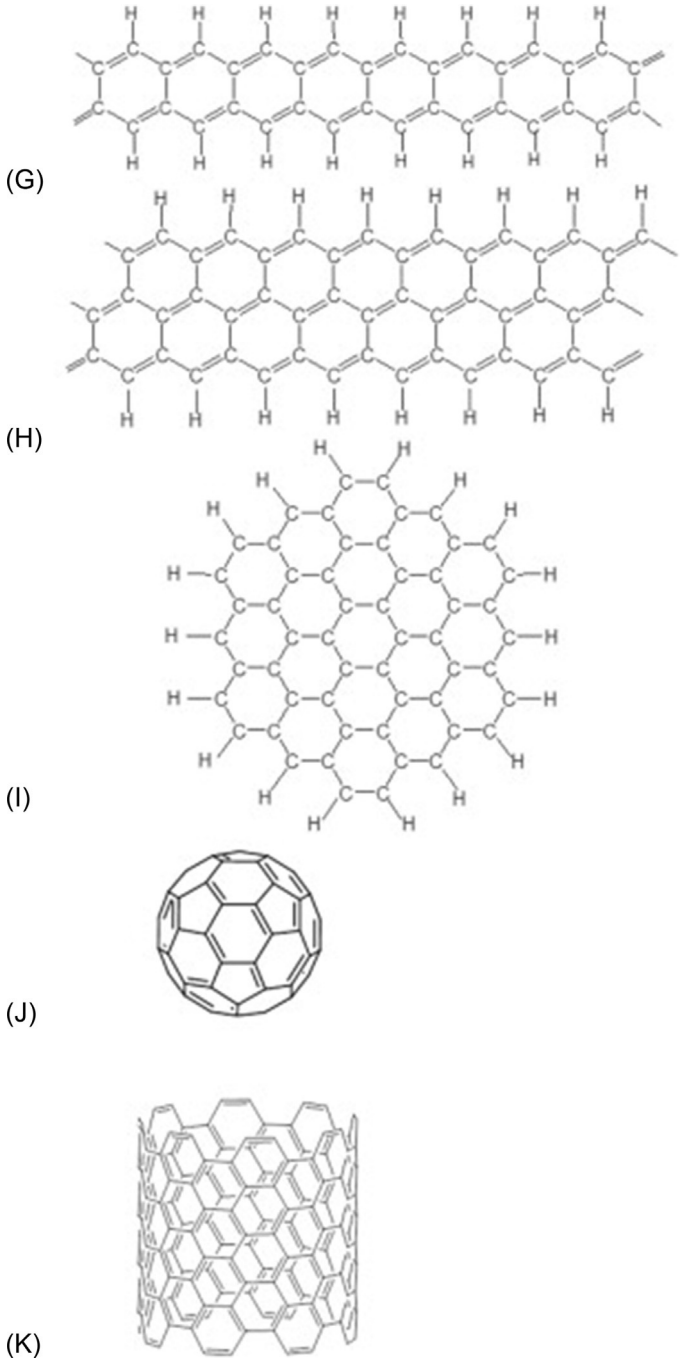

Fig. 1—cont'd (G) polyacene, (H) graphene nanoribbon, (I) nanographene, (J) fullerene, and (K) CNT. *(Reprinted from K. Tanaka, Classification of carbon, in: K. Tanaka, S. Iijima (Eds.), Carbon Nanotubes and Graphene, Elsevier, 2014, p. 3, with permission from Elsevier).*

applications [10]. The molecular-macroscopic nature of a CNT is of immense importance in many potential practical applications harnessing its phenomenal properties. For example, mechanical strength measurements have established that a CNT is one of the strongest materials in existence, stronger than steel, with a modulus of elasticity of about 1 TPa and tensile strength of 100 GPa while being extraordinarily flexible. The thermal conductivity of a CNT is also extraordinary. It exceeds the value for diamond and has been reported as 3500 W m^{-1} K^{-1} for individual SWCNT. Furthermore, a CNT can exhibit metallic or semiconducting properties depending on the chirality (the orientation of the honeycomb lattice with respect to the axis of the tube) and the tube's diameter [9–11].

The perfect planar arrangement of the carbon atoms constituting each graphene sheet provides the CNT with an exceptionally smooth and hydrophobic wall. This unique feature results in a superfast flow of water on the basis of the almost frictionless transport of water molecules [12–14]. The nanoscale confinement of the CNT channels has been reported to enhance intermolecular interaction between water molecules, resulting in even less interaction with the graphitic wall of the CNT, which further contributes to the near frictionless flow [12,15]. However, other evidence has shown that the walls of CNT are not always hydrophobic; they may become hydrophilic with decreasing temperature. The liquid-solid interactions in the CNT have also been shown to be pressure-dependent. These effects are due to changes in the spatial configurations and orientations of water molecules and the nature and number of free hydrogen bonds in nanoscale confinements [15,16]. However, predicted rapid water flux through a CNT is not due to hydrophilicity improvement but to the narrowness (confinement effects), smoothness, and hydrophobicity of the channels [14,17]. The flux of water through CNT has been shown experimentally to be more than three orders of magnitude greater than the predictions of the Hagen-Poiseuille law for bulk water flow [3,17]. Like water, hydrated ions can also be transported through a large diameter CNT. However, for a narrow CNT with a diameter less than 0.5 nm, the transport of ion requires the stripping of the hydration layer, thus creating an unfavorable energy barrier for ion transport. For instance, the hydrated ion diameter of Na^+ has been given as 0.716 nm and that of Cl^- as 0.664 nm [18]. It follows then that these ions will be rejected by a CNT of 0.5 nm. Even though energy is also required to break down hydrogen bonds for water to enter such a narrow CNT in single file, the stability of the water chain in the hydrophobic channel minimizes the energy barrier [14,19], providing for rapid transport of water but the complete rejection of hydrated ions. These findings suggest that small diameter CNTs are very promising materials for the development of low-energy, high-flux membrane desalination technology for sea and brackish water [12,13].

The charge configuration on a CNT has been shown to result in interesting flux and selectivity properties. A single external charge at a certain critical distance from the SWCNT has been reported to create a tunable influence on the permeation of

water [16], while ions were reportedly excluded and water flux enhanced when the CNTs were alternatively electrostatically charged [12]. The functionalization of CNT tips with charged chemical groups has been reported to improve rejection of ions through electrostatic and steric exclusion [12,13,16,19]. Such a gating system has been shown to allow for the use of a relatively large diameter CNT for ion rejection [19]. The potential of very high water permeability alongside very high solute selectivity for CNTs is regarded as an avenue to extend beyond the upper-boundary permeability-selectivity trade-off inherent in membrane processes, as discussed earlier.

Besides selectivity and permeability, the incorporation of CNTs in membrane processes promises many other important benefits of which fouling resistance is one. CNTs possess cytotoxic properties that are valuable in the prevention of biofouling, one of the most significant problems in MDWT processes [12,13,20]. The mechanism of the CNT cytotoxic effect has been proposed to involve disruption of the microbial cell membrane and oxidative stress arising from the CNTs' electronic configuration [2,21]. A CNT can be readily functionalized through the generation or attachment of chemical groups such as hydroxyl, carboxylic, and other hydrophilic moieties that aid in the reduction of fouling [22,23]. The deposition or incorporation of functional nanoparticles such as Ag and TiO_2 on a CNT has been reported to extend the reactive properties in membrane processes [13,24,25]. The extraordinary mechanical strength and the high aspect ratio of CNTs are recognized as useful for the production of high-strength membranes suitable for application in challenging conditions. Such membranes are expected to withstand high pressure without undesired loss of permeability and to resist irreversible wearing arising from abrasive material in feed water during the long operation of a full-scale membrane installation [26]. As an example of the benefit derivable from incorporating CNT in membrane, Majeed et al. reported a 36% increase in compaction resistance and over a 97% increase in tensile strength when 2% CNT was blended with polyacrylonitrile in the production of a mixed matrix membrane (MMM) [27].

CNTs for desalination and water treatment are available either as vertically aligned (VA) CNTs or as MMM [13]. VACNTs require an orderly arrangement of CNTs such that all the nanotubes point and open in the same direction. The arranged CNTs are usually held together by filler materials impermeable to water. The open CNTs are arranged parallel to the direction of feed flow so that permeation is directed through the nanochannels. This arrangement ensures that the maximum flux capacity of the CNTs is harnessed. VACNTs can be produced by growing CNT forests on suitable substrates after conditioning and activation. The interstitial spaces between CNTs are then filled with filler materials to exclude water permeation except through the nanotubes. Holt et al. [17] reported the successful fabrication of VACNT membranes with superfast water transport by growing VACNTs on a silicon chip and applying silicon nitride (Si_3N_4) as filler material. Ion milling and reactive ion etching were applied to remove excess fillers and open up the CNTs, respectively. Du et al. [15] suggested the use of superlong (7 mm) CNTs

for the production of VACNTs with epoxy resin as filler material, demonstrating a simple procedure for the removal of excess filler and nanotube mouth opening by cutting with a knife. They showed that while water flux was superfast, the flux of ethanol was much lower because of a possible clustering of ethanol molecules in the carbon tubes.

VACNTs have also been produced by orienting CNTs in either an electrical or magnetic field. In one such technique, magnetic field alignment of CNTs was achieved through the help of liquid crystal mesophase forming cylindrical micelles around the nanotubes [28]. The mesophase contained monomers that were polymerized to fix the orientation of the CNTs after the removal of the orienting magnetic field. A simple filtration procedure for producing VACNTs has also been reported whereby dispersed CNTs were filtered through a polymeric membrane such that some of the nanotubes penetrated the membrane and were fixed within the pores [16]. Since the membrane pore size can allow the entry of CNTs only in the vertical position, this method is a simple approach for vertical alignment of the nanotubes. However, the density of the CNTs may be much lower than is achievable in other VACNT techniques.

The fabrication of CNT MMMs is much simpler and cheaper and usually involves the blending of certain amounts of CNTs either as a powder or as functionalized dispersions with a suitable polymer material. Polymers such as poly(tetrafluoroethylene), polysulfone, and other polymers used for the production of water-permeable membranes are commonly used as matrix materials [16,29]. The blend is formed into a membrane following one of the usual polymeric membrane production routes such as nonsolvent-induced phase inversion [30]. Consequently, in MMMs, the CNTs are oriented randomly with a limited number of the nanotubes transporting water directly through their internal cavities. However, several experiments have shown that even at small functionalized CNT concentrations, appreciable water permeability and other filtration performance improvements can be achieved [22,23,27,29,31,32]. A fraction of the water transportation enhancement is derived from flux through voids or defects existing between the polymeric matrix and the nanotubes as well as possible water transportation on the external surface of CNTs [12].

Brady-Estevez et al. [33] reported a different kind of composite membrane where the CNTs were deposited on the surface of a polymer membrane and held together by van der Waals forces rather than being dispersed within the polymer support. The authors showed that an effective water filter against bacteria and viruses could be produced simply by depositing bundles of SWCNT on a PVDF MF membrane. Bacteria deactivation was reported, and the authors suggested that the deposition of the nanofibers on a ceramic MF membrane would allow the production of a regenerable, low-pressure filter suitable for point of use application. A similar kind of membrane, but this time without any polymeric membrane support, was reported by Dumee et al. [34] for membrane-distillation (MD) water desalination. The self-supporting bundles of CNTs were held together only by van der Waals forces and are known as bucky-paper with very favorable properties for

MD application such as high hydrophobicity (contact angles measuring up to 113 degree) and high porosity (as much as 90%). In a direct-contact MD process, the authors reported 99% salt rejection using this membrane at a flux rate of $\sim 12\ \mathrm{kg\ m^{-2}\ h^{-1}}$ and a water vapor partial pressure difference of 22.7 kPa.

Despite the promises of CNT technology in MDWT, there are still many unresolved challenges. One of the most important of these is the difficulty in producing homogenous CNTs in commercial quantity [12,13]. The selectivity of a membrane is crucial to it use in membrane processes; unfortunately, CNTs produced via the more common chemical vapor deposition technology usually have variable diameters. Current techniques to separate out small diameter tubes have not been economically successful, preventing the experimental realization of the high salt rejections required for practical desalination using high-flux VACNTs [3,19]. A novel template bottom-up approach promises to overcome the problem of variable diameter [35], but the technique is still at an early stage. In addition, this technique may not be suitable for low-cost production of CNTs suitable for desalination applications [13]. Apart from the general challenge of producing uniform-diameter CNTs, there is the specific problem of producing small-diameter MWCNTs for desalination applications. SWCNTs that are small enough to reject ions are available for desalination applications, but they are much more expensive [10,13] and are more challenging to handle in making VACNT membranes [17].

Furthermore, scale-up of VACNTs still poses some challenges, especially when the CNT forests are grown on chips [19]. Complete sealing of the interstitial spaces between the aligned nanotubes is still challenging, and this complicates the production process and increases cost [13]. Defects in the sealing of the interstitial spaces impair the selectivity of the membrane. There is also a lack of experimental data on the performance of a fully functional CNT system on a scale and at conditions practical for membrane desalination, leaving outstanding questions such as the extent of fouling at high-permeation flux supposing such a flow rate is realized [3]. Other uncertainties include health concerns and the environmental implications of a widespread application of CNT water desalination technology [12]. This latter concern is compounded by the exceptional adsorptive potential of CNTs for heavy metals, their relative inertness, and their well-proven cytotoxic effects.

From this brief overview, it is concluded that CNTs have enormous potential in resolving the permeability-selectivity trade-off boundary problem and to contribute significantly toward improving membrane-fouling resistance. However, major hurdles remain to be resolved, including making low-cost, small-diameter CNTs and assembling the nanotubes into compact and scalable VACNT membranes for high-flux applications. These problems call for ongoing innovation and creativity. The development of a viable VACNT-based membrane may allow MDWT applications to venture into even more challenging conditions supported by the potentially superior mechanical and thermal stability of VACNT membranes.

3.2 Aquaporin

The membranes of many living cells, in simple terms, consist of a lipid bilayer that provides an efficient barrier between the content of the cell and the surroundings by restricting the flow of water and solutes into and out of the cells. The basic makeup of a lipid bilayer is two layers of lipid molecules arranged such that the hydrophilic heads are directed outward, forming the boundaries of the barrier, while the hydrophobic tails are directed toward the middle, forming the hydrophobic interior [36]. For many years, scientists have been bewildered by the mechanism of water transport across this impermeable barrier. Diffusion through the cell membrane has always been considered but was thought insufficient to account for the volume and efficiency of water transport needed for the rapid physiological processes taking place in the cells of many plants and animals [37,38]. This confusion was addressed in 1992 by Peter Agre and his coworkers in the discovery and characterization of aquaporin [37,39].

Aquaporins are pore-forming proteins found on the cell membranes of many biological organisms (eubacteria, archaea, and eukaryotes) and are responsible for the efficient osmotic-driven transportation of water with a remarkably efficient solute rejection [37,40]. Similar pore-forming proteins, called aquaglyceroporins, with the capability of permeating glycerol and other small solutes, in addition to water, have been isolated from many single and multicell organisms [37,41]. Aquaporins are homotetramers; that is, they are formed by the self-assembly of four identical protein subunits or monomers into an hourglass structure, with each monomer creating a pore, permeable to water in single file but restricting the permeation of protons, ions, and other solutes [37,39,42]. The solute restriction capability of aquaporin arises from two constriction sites. One of the two regions of selectivity is formed by two asparagine-proline-alanine (NPA) motifs located on the end of two half helices and are known to provide an electrostatic barrier credited for the exclusion of protons [41]. The other constriction zone is the aromatic/arginine (ar/R) filter, which constitutes the narrowest part of the channel, measuring only 0.28 nm at this point, for efficient size and hydrophobicity selectivity [37,41,43] (see Fig. 2).

Since the discovery of the protein water channels, their unique properties have intrigued researchers in many fields spurring intense research efforts to understand the structure and properties of these proteins and to harness them for many applications including MDWT applications. For MDWT applications of aquaporins, the first challenge is the production of the stabilized aquaporin protein. The second major step is the reconstitution of the protein in a lipid bilayer (liposome) to form a proteoliposome. The third is the incorporation of the proteoliposome into a suitable support framework to form a robust composite membrane for MDWT applications [44,45]. Since aquaporin is expressed in many biological cells, the protein has been harvested and purified directly from these cells [38]. However, the density of membrane protein in natural cells is so small that only very small amounts can be produced under any given condition [40]. Consequently, innovative techniques to induce overexpression of membrane proteins

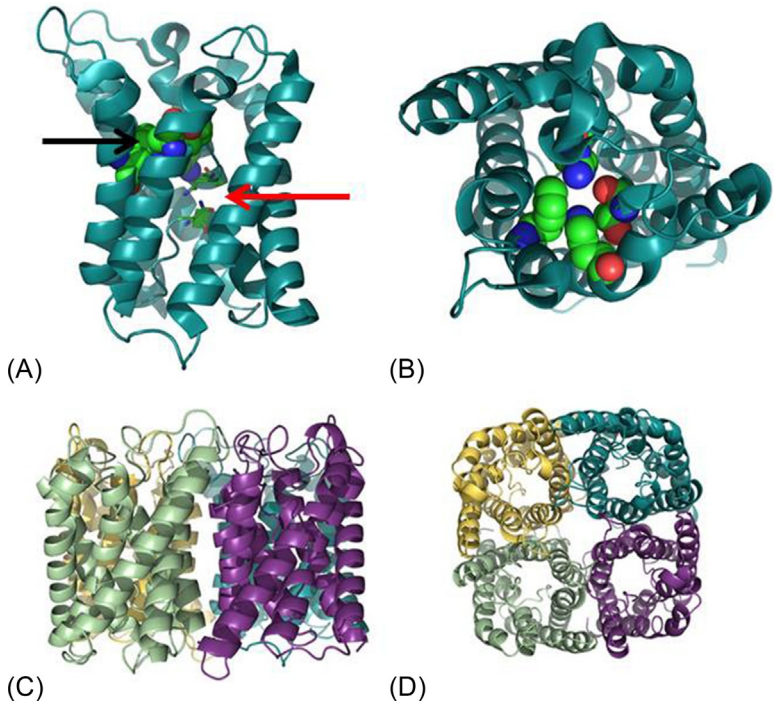

Fig. 2 Aquaporin protein structure: (A) Side view of *Escherichia coli* aquaporin-Z (AqpZ) monomer. Protein backbone, helical structures (online view deep teal), with the two terminal asparagines from the NPA motifs shown in stick representation (light shade arrow) and the ar/R selectivity filter residues shown in spacefill representation (dark shade arrow). For stick and spacefill representations, atoms are colored in light shade for carbon (online view green); darker shades for oxygen (online view red) and nitrogen (online view blue). (B) Top view illustrating the selectivity filter (or constriction site) created by the four amino acids: F43, H174, R189, and T183. (C,D) Side and top view of the tetrameric AqpZ complex with the four monomers shown in dark and light shades (online view deep teal, violet purple, pale green, and yellow). All renderings were generated using PyMol 1.5.0.2 using AqpZ PDB coordinates 2ABM. *(Reprinted from C.Y. Tang, Y. Zhao, R. Wang, C. Hélix-Nielsen, A.G. Fane, Desalination by biomimetic aquaporin membranes: review of status and prospects, Desalination 308 (2013) 35, with permission from Elsevier).*

in simple cells such as yeast and *Escherichia coli* with rapid replicative capability have been developed to enhance the production [38,40,46], purification, and solubilization of aquaporins. Alternative cell-free methods for potential large-scale production of functional membrane proteins have attracted a lot of attention [47–49]. One of the interesting benefits of this technique is the potential to directly produce large amount of aquaporins solubilized and stabilized in detergent.

After production, solubilization in a suitable detergent to prevent aggregation and precipitation is usually needed to keep the protein viable for reconstitution into a suitable synthetic liposome, which is the second step toward producing aquaporin-based membranes

for MDWT [38]. Membrane protein reconstitution in a liposome is intended to provide the extracted aquaporin protein a synthetic functional environment similar to the natural phospholipid bilayer that constitutes the membrane of many living cells [46]. Self-assembled lipid vesicles have been used as synthetic liposomes for reconstitution of aquaporin. A commonly used lipid for this purpose is 1,2-diphytanoyl-sn-glycero-3-phosphocholine (DPhPC), which is known to support the correct folding of membrane proteins when reconstituted [50]. Unfortunately, lipids are too unstable for desalination application. Therefore there is a need to find materials that can form lipid-like bilayers, sustain the activity of aquaporin and are less biodegradable [51]. Triblock copolymers (BCP) such as polymethyloxazoline-polydimethylsiolane-polymethyloxazoline (PMOXA-PDMS-PMOXA) have been shown to be such a material [50]. BCP has the additional benefit in that it can be tailored for specific additional functionalities such as attaching a polymerizable group to provide even better physical support for membrane proteins without diminishing protein activity [52]. A reconstituted aquaporin in liposome or BCP bilayer (polymersome) is called a proteoliposome or proteopolymersome [36,52]. A typical scheme for making such a system involves dissolving lipid or polymer in suitable organic solvent, evaporating the organic solvent and hydrating the lipid or polymer left behind to give a vesicle solution, and then adding detergent-solubilized aquaporin to the vesicle solution. The proteins are then incorporated into the vesicle upon detergent removal, usually by means of biobeads [46,51,52].

The final stage in the production of an aquaporin-based biomimetic membrane is the incorporation of the proteopolymersome in a suitable support framework. Researchers attempting to produce biomimetic membranes for water treatment have generally followed one of two schemes in fabricating supported proteopolymersome, resulting in two basic kinds of supported biomimetic membranes, namely, supported membrane layer (SML) and vesicle encapsulated membrane (VEM) [45], as illustrated in Fig. 3.

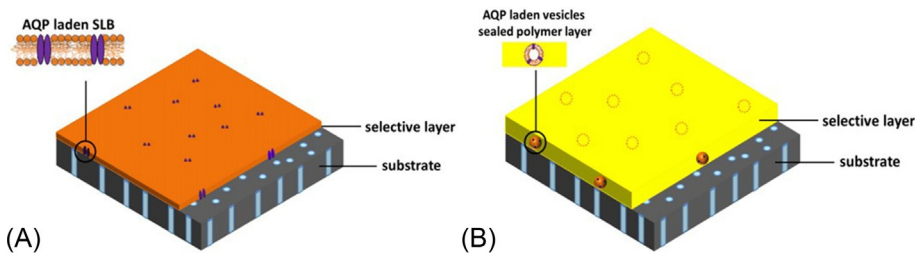

Fig. 3 Schematic presentation of aquaporin (AQP)-laden membranes: (A) Supported membrane layer (SML) where AQPs embedded in a flat supported lipid bilayer (SLB) is deposited onto a porous support. (B) AQP-laden vesicle-encapsulated membrane (VEM) where vesicles are immobilized in a polymer layer on a porous support substrate. *(Reprinted from C. Tang, Z. Wang, I. Petrinić, A.G. Fane, C. Hélix-Nielsen, Biomimetic aquaporin membranes coming of age, Desalination 368 (2015) 94, with permission from Elsevier).*

The SML is produced by the surface deposition of proteopolymersomes as vesicles or other configurations onto a porous support to form a uniform flat layer of supported aquaporin-incorporated polymer bilayer. In this design, the proteopolymersomes form the top surface of the biomimetic composite membrane and are in direct contact with the feed stream. Recently, this method was adopted by Zhong et al. [52] to produce an aquaporin-based biomimetic membrane for NF.

The authors deposited polymerizable vesicle proteopolymersomes onto a silanized cellulose acetate (CA) membrane to produce a hybrid NF membrane with enhanced water permeability and salt rejection when compared with an unmodified cellulose acetate membrane. Upon deposition, the amphiphilic triblock copolymer with polymerizable methacrylate end-groups was cross-linked by UV irradiation to provide suitable physical support without significantly impairing the activity of the protein. The reported 30% salt rejection was good enough for a NF process but not for desalination that is classically performed by RO. Wang et al. [46] described the synthesis of a biomimetic membrane using polycarbonate tracked-etched (PTCE) as support for the vesicle proteopolymersomes. The PTCE was first covered with a gold coating, after which the gold surface was modified with photoreactive acrylate functional groups. Pressure was applied to force the vesicle into the pores of the porous support to close them up to flux. Thereafter the deformed vesicles were polymerized by UV irradiation leading to vesicle rupture and fusion and the formation of a uniform selective layer. The authors tested their biomimetic membrane for FO and reported salt rejections of more than 98.5% for all cases tested. The advantage of SML is that aquaporin's permeability and selectivity may be more fully harnessed because of the protein-unhindered contact with the feed. The challenges include the difficulty in synthesizing membrane-scale, defect-free polymersome to provide a completely impermeable surface between the aquaporins, and the stability problem that might arise from the direct interaction between the feed and the delicate proteopolymersomes under real MDWT conditions.

The VEM method involves the immobilization of the proteopolymersome vesicles within the matrix of a permeable polymer layer. Zhao et al. [53] recently demonstrated the application of this method for the synthesis of a high-performance biomimetic membrane where the vesicles were incorporated into the thin selective layer of a TFN membrane. The authors claimed the synthesis of a robust and viable aquaporin-based desalination membrane with an enhanced water flux when compared with commercial brackish and seawater desalination membranes, while showing comparable salt rejection of 97%. The aquaporins were incorporated into an amphiphilic lipid (1,2-dioleoyl-sn-glycero-3-phosphocholine) bilayer and then added to a *m*-phenylenediamine aqueous solution for interfacial polymerization to produce an aquaporin-based TFN polyamide membrane. The produced biomimetic membrane was found to be stable under RO conditions (subjected to a pressure up to 10 bar), showing that the proteoliposomes were well supported by the polyamide matrix. The advantages of the VEM method include better

protection for membrane proteins, as the proteins are shielded from direct contact with the feed and have greater prospect for scaling up since this method closely follows the standard TFN fabrication procedure. Disadvantages of this method include possible deactivation of some membrane protein by being immobilized within a polymer matrix and the additional resistance to water flux arising from the double passes of water through the polymer matrix before and after permeation through aquaporins.

Recent developments have shown a great potential of aquaporin-based biomimetic membranes to serve as the next generation of high-performance membrane for MDWT applications. However, a number of challenges still remain unresolved across every segment of the technology. First, large-scale, cost-effective production of aquaporin proteins is still unrealized, even though much progress has been made toward its achievement [44,45]. Until this is attained, economically, the aquaporin-based biomimetic membrane may not compare favorably with conventional MDWT technologies. Second, current technologies for the incorporation of proteopolymersomes into a robust support still present important challenges for upscaling and the maintenance of the activity of membrane proteins, because of limited fundamental and experiential knowledge of protein-support interactions [44]. Third, the long-term viability of incorporated proteins and polymers under practical MDWT conditions of high pressure, salinity, fouling, and cleaning cycles is still unknown [36,51]. It is worth mentioning at this point that the flux enhancement observed for current aquaporin-based membranes is still significantly far below the orders of magnitude improvement predicted by computer simulation and exhibited by living cells. The use of synthetic lipid-like materials such as BCP and the development of synthetic self-assembly water channels along with advancements in supramolecular chemistry have great potential in resolving some of the identified challenges [36,51]. Biomimetic membranes have an interesting and promising prospect, but much work is still required to realize its enormous potential.

3.3 Nanozeolites

Zeolites are three-dimensional aluminosilicate tetrahedral crystalline networks with molecular lattice openings containing water molecules and cations. The cations in natural or synthesized zeolites are group I and II elements, but because they are often mobile and exchangeable, they could be replaced by other polyvalent ions. Some zeolites can be dehydrated of their water of crystallization and/or their cations exchanged, without losing their original structure. This gives rise to molecular pores and cavities functioning as molecular sieves and/or ion exchange surfaces that lend themselves to many important applications [54–56]. Ammonium or alkyammonium ions may replace metallic cations in the zeolitic network, where their relative large sizes are known to constrain the structure of the zeolites to specific lattice networks and cavity configurations and are thereby called structure directing agents (SDAs) or templates [55,56]. In the zeolite crystal, all the

oxygen atoms positioned at the end of regular tetrahedra are shared between Al and Si atoms that are centered in separate tetrahedra. Since Al has a valence electron of three, the sharing of four oxygen atoms with Si in neighboring tetrahedra results in one negative charge for each Al tetrahedron. Al is therefore responsible for the negative charge of the zeolite framework. Consequently, the greater the proportion of Al in a zeolite network, the greater the structural negative charge that must be balanced by cations. It has also been established that the hydrophilicity of zeolite crystals correlates positively with the amount of Al. Si in the zeolites may be replaced by Ge or P, while Ga may take the place of Al, and this may result in major structural changes [55]. From the foregoing, it can be appreciated that zeolites lend themselves to a significant degree of tailoring relevant to many important applications.

Because of their molecular cavities, negative surface charge, and superhydrophilicity, zeolites have found many important applications in MDWT. Simulation results using ZK-4 zeolite with crystalline voids of 0.42 nm showed 100% rejection of Na^+. This is because the size of the void was much smaller than the diameter of hydrated Na^+, which is given as 0.716 nm [18,55,57]. As a consequence of this result and other similar ones, there is a lot of interest in the development of zeolite-based membranes for desalination. Zeolite membranes for water treatment are often produced by the composite membrane preparation method. This method involves the growth of a very thin layer of zeolite crystals on porous support materials such as alumina, zirconia, stainless steel, and carbon. The zeolite layer may be produced by a hydrothermal process from a precursor solution or gel on the porous support, a method called direct in situ crystallization. When crystals are produced from solution, it is often necessary to direct the zeolite network to specific structures by incorporating SDAs. However, because of the size of the SDA, it must be removed after crystallization to open up the zeolite pores for water permeation, a procedure that may unfortunately result in cracking of the zeolite layer. To minimize layer cracking, an alternative method called seeded secondary growth has been developed. This may involve directing the structure of the zeolite network without SDA using nanosized zeolite seeds that are deposited on the support material, upon which the precursor solution is spread before subjecting the system to hydrothermal crystallization [56,58]. The use of microwaves as a heat source for the synthesis of zeolite membranes has been shown to be a very efficient means of producing different types of zeolites in less time. Moreover, microwave synthesis is also known to influence the particle size and properties of the zeolite layer, resulting in enhanced water treatment capability [56].

Zhu and coworkers reported an experimental study of MFI-type zeolites with Si/Al ratios varying from 30 to >1000 using X-ray diffraction (XRD) and positron annihilation lifetime spectroscopy (PALS) [57]. They showed that in addition to the regular intracrystalline zeolitic channels between 0.27 and 0.36 nm in diameter, there also exist intercrystalline microporous and mesoporous voids and defects measuring about 1.1 nm and 8 nm, respectively. Intercrystalline defects may result from insufficient intergrowth of

crystals or from structural strain arising from thermal removal of template or complete material dewatering and may significantly affect the performance of zeolitic membranes for desalination applications. The study showed that increasing the concentration of alumina decreased the volume of the microporous channels, suggesting that this parameter may be used for the design of zeolitic membranes for specific MDWT applications. Other studies have shown that the adsorption of certain molecules such as *p*-xylene and water can lead to the expansion or contraction of zeolite crystals resulting in important changes to the size and permeability of the zeolitic pores [58–60]. Zeolite membrane permeability can also be influenced by the presence of impurities [58]. Fig. 4 illustrates some of the possible variations in zeolite membranes' porous structures.

Zhu and coworkers [57,61] demonstrated that the exposure of MFI-type zeolites to seawater and ionic solutions could result in complex interactions with ion exchange and crystal expansion. Micropores were observed to decrease while mesopores increased upon exposure to ionic solutions. Despite these observed interactions, MFI-type zeolite membranes have been successfully used for the desalination of saline recycled waste water, without costly pretreatment that would have been considered a necessity if polymeric membranes were used [62]. The membranes showed good resistance to organic fouling, and performance was not significantly affected when the membrane was

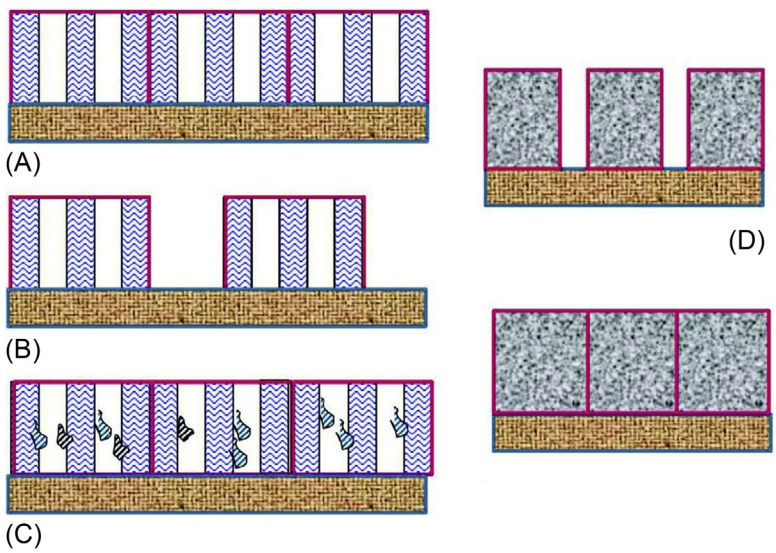

Fig. 4 Schematic showing three types of microstructures of a high-quality polycrystalline zeolite membrane: (A) perfect membranes without nonzeolitic pores, (B) membranes with microporous intercrystalline gaps or nonzeolitic pores, and (C) membranes with impurity trapped in the zeolitic pores; (D) schematic showing adsorption-induced crystal expansion to seal the intercrystalline gaps of zeolite membrane. *(Reprinted from Y.S. Lin, M.C. Duke, Recent progress in polycrystalline zeolite membrane research, Curr. Opin. Chem. Eng. 2 (2013) 211, with permission from Elsevier).*

subjected to a strong hypochlorite solution for 7 days. This result demonstrates the superior stability of zeolite membranes when operating under harsh process conditions.

A typical experimental setup using an MFI-type zeolite with a pore diameter of 0.56 nm, prepared on an alumina support, showed a salt rejection of 76.7% and a water flux of 0.112 kg m^{-2} h^{-1}, when exposed to a single NaCl feed solution at 2.07 MPa pressure [63]. For a complex feed solution with multiple cations, the Na^+ rejection reduced to 58%. Considering that the zeolitic pores are smaller than the hydrated ions, the limited ion rejection may indicate the presence of intercrystalline micropores and mesopores, as discussed earlier, or it may be indicative of structural failures and defects in the zeolite layer. Higher salt rejections have been achieved for zeolite membranes by eliminating SDA in the membrane synthesis process to minimize crystal defects and by increasing the concentration of Al, which is associated with a higher surface negative charge, hydrophilicity, and a decreasing concentration of micropores. However, the production of defect-free zeolite film is still challenging, and the achieved water flux in RO applications is still lower than what is obtainable using polymeric membranes [56,58,62]. In addition, zeolite membranes are currently produced via batch processes, which are expensive when compared with the more cost-effective continuous fabrication process employed for polymeric membranes [58].

Jeong et al. [64] first suggested the incorporation of nanosized zeolite crystals into the polyamide layer of a TFC membrane to give a novel TFN membrane. This was intended to exploit the molecular water-permeating channels, superhydrophilicity, and tunable surface negative charges of zeolites in combination with the processibility and good salt rejection of polyamide membranes. The authors proposed that the nanozeolites distributed within the polyamide layer would provide a preferential flow path for water molecules while preventing the passage of hydrated ions as a consequence of both steric and Donnan exclusion arising from the negativity and nanoscale dimensions of the zeolitic channels [64]. While less chemically stable, the polymer matrix eliminates the need to employ large-scale, defect-free zeolite crystal films, which is often more difficult to produce [58]. Furthermore, the good rejection of the polymer ensures that any defect in the zeolite crystals is contained and does not impair the membrane rejection.

Jeong and coworkers reported the synthesis of NaA zeolite nanoparticles by a hydrothermal process that employed an organic template (tetramethylammonium hydroxide). The pore-filled, as-produced, zeolite nanoparticles, as a consequence of the presence of the organic template, were subjected to calcination in air to open up the pore cavity by combusting the template. This process was assisted by a polyacrylamide hydrogel network to prevent nanoparticle aggregation during calcination, as suggested by Wang et al. [65]. The zeolite nanoparticles were dispersed in a trimesoyl chloride (TMC) hexane solution via sonication and then employed in interfacial polymerization on a polysulfone support with *m*-phenylenediamine (MPD) to give a TFN NaA zeolite polyamide membrane. The novel zeolite TFN was shown to exhibit higher hydrophilicity,

increased negative charge, and improved surface smoothness, resulting in almost doubling of the water permeability at comparable rejection with respect to pure polyamide TFC. Fig. 5 shows TEM images and EDX elemental analysis of the synthesized pure polyamide and zeolite nanocomposite membranes.

A number of research studies have been directed toward the optimization of zeolite TFN for enhanced stable desalination applications. Kong et al. [66] showed that the direct deposition of zeolite nanoparticles onto an MPD-covered polysulfone support (called "preseeding"), before applying TMC for interfacial polymerization, ensures that zeolite nanoparticles are well anchored but not completely submerged within the polyamide layer. This produces membranes with double the permeability, reaching

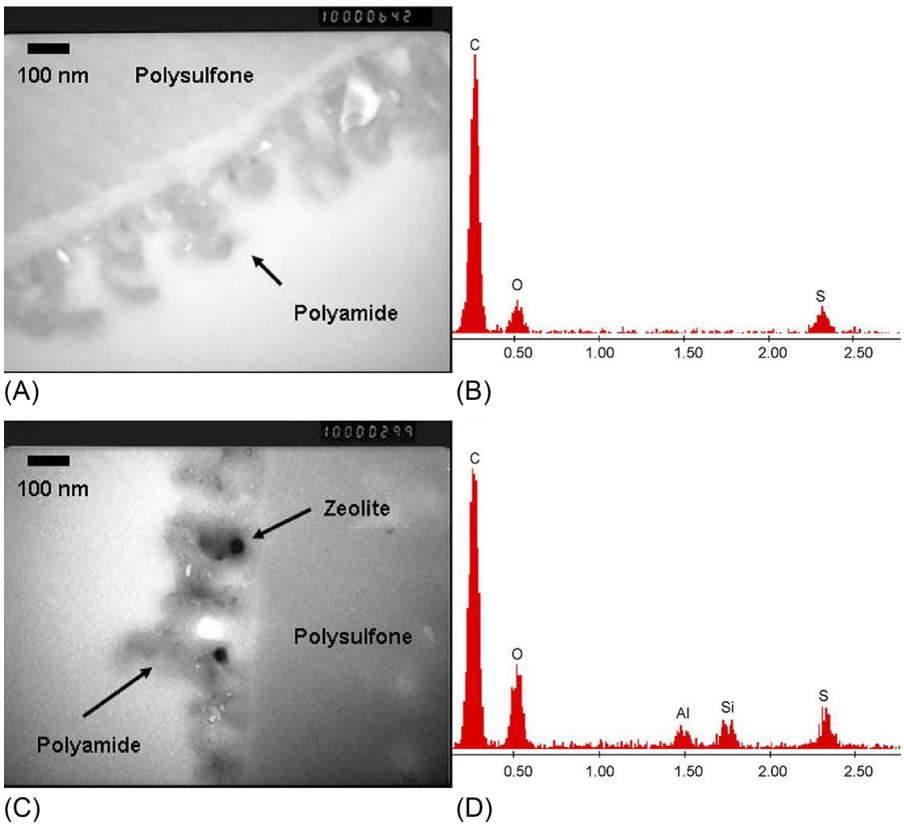

Fig. 5 Characterization of hand-cast thin film properties by transmission electron microscopy (TEM) and energy-dispersive X-ray (EDX) for (A, B) pure polyamide membrane and (C, D) nanocomposite membrane. Magnification is 100,000× in TEM images. *(Reprinted from B.-H. Jeong, E.M.V. Hoek, Y. Yan, A. Subramani, X. Huang, G. Hurwitz, A.K. Ghosh, A. Jawor, Interfacial polymerization of thin film nanocomposites: a new concept for reverse osmosis membranes, J. Membr. Sci. 294 (2007) 4, with permission from Elsevier).*

5.8×10^{-12} m Pa^{-1} s^{-1}, and a slight (1%) increase in solute rejection as compared with the membrane produced without preseeding. Fathizadeh et al. [67] recently reported that while increasing the concentration of NaX nanozeolite fillers led to improvement in water permeability, without impairing rejection, increasing the concentration of monomers led to a water permeability increase at the cost of rejection. Lind et al. [68] showed that the permeability, selectivity, morphology, and surface of a TFN membrane can be tailored by the incorporation of different sizes of zeolite nanoparticles. They reported that smaller zeolite nanoparticles produced improved permeability and enhanced the polymer matrix surface chemistry and morphology. A recent study by Pendergast et al. [69] showed that the addition of zeolite and silica nanoparticles to a polyamide TFC membrane improved compaction resistance and enhanced permeability. The addition of zeolite nanoparticles to a polyamide TFN membrane designed for FO was also reported to result in up to 50% improvement in flux [70]. Improvement in flux performance and chlorine resistance was also recorded for nonpolyamide RO membranes, such as those made from sulfonated poly(arylene ether sulfone), when zeolite nanoparticles were incorporated [71].

Deriving from the original work by Hoek and his group [64] and other subsequent developments and optimizations, NanoH_2O (now LG Chem) took up the commercialization of the zeolite TFN membrane for seawater RO (SWRO) applications [72]. This is considered one of the success stories in membrane performance enhancement using nanotechnology. However, the flux improvement derivable from nanozeolite-based TFN membrane bears no comparison to the order of magnitude flux enhancement promised by emerging materials (e.g., VACNT). The limitations of nanozeolite-based TFN membrane is common to all MMM technologies, namely, limited water channel alignment and additional flow resistance imposed by the polymer matrix. There is a limited possibility that the performance of current nanozeolite-based TFN membranes can be significantly increased in the future. However, this technology still serves as one key example of the successful commercial adoption of nanotechnology in membrane desalination until the higher performing technologies can move from the laboratory environment to commercial reality.

3.4 Nanotitania

Titanium oxide, or titania, is a crystalline solid with the molecular formula TiO_2. TiO_2 may exist in a number of polymorphs such as rutile, anatase, and brookite. The most stable phase is the rutile, and at high temperature, the anatase and brookite phases transform irreversibly to the rutile phase. The most important researched application of TiO_2 is in photocatalysis, and since brookite shows limited photocatalytic activities, it is much less researched than anatase and rutile [73,74] and will not be discussed further in this overview. Structurally, both anatase and rutile exist as tetragonal crystalline structures built from octahedra units where the Ti^{4+} is coordinated to six O^{2-} anions (Fig. 6). The structural difference between

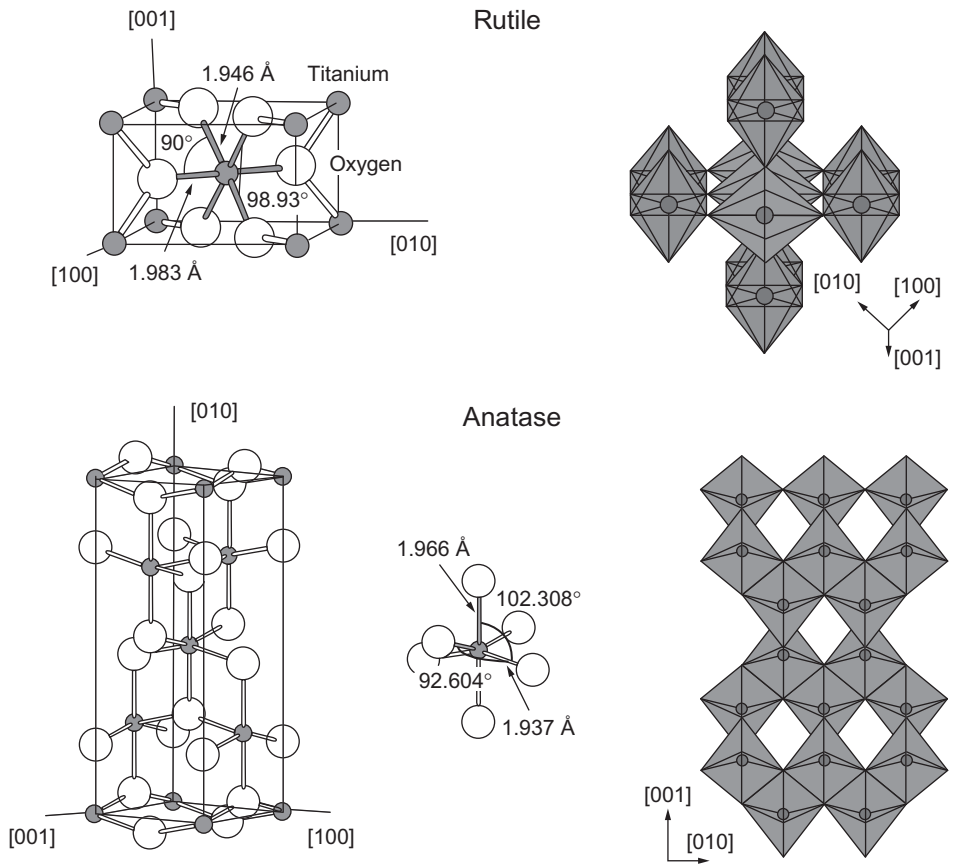

Fig. 6 Bulk structures of rutile and anatase. The tetragonal bulk unit cell of rutile has the dimensions, $a = b = 4.587$ Å, $c = 2.953$ Å; the one of anatase has the dimensions, $a = b = 3.782$ Å, $c = 9.502$ Å. In both structures, slightly distorted octahedra are the basic building units. The bond lengths and angles of the octahedrally coordinated Ti atoms are indicated, and the stacking of the octahedra in both structures is shown on the right side. *(Reprinted from U. Diebold, The surface science of titanium dioxide, Surf. Sci. Rep. 48 (2003) 67, with permission from Elsevier).*

the two polymorphs arises from the fact that anatase is corner sharing at the (0 0 1) planes, while rutile shares edges at this plane [73,75]. Anatase has a band gap of 3.2 eV that falls within the UV band while rutile has a band gap of 3.0 eV, which is just within the visible light region, indicating that rutile can be photoreactive under visible light, whereas anatase is photoreactive under UV light [74–76]. However, anatase is the most photoactive phase of TiO_2 [77] and has been widely studied for its photocatalytic applications. TiO_2 is the most researched photocatalyst because of its efficient photoactivity, chemical and thermal stability, low cost, limited toxicity, and its diverse and important applications [73–76]. Further

details on the structure, properties, and applications of TiO_2 can be found in the following excellent review articles: [73,77–81].

When light of an appropriate energy (*hv*) heats a photoactive semiconductor like anatase and rutile TiO_2, an electron-hole pair may be created if the valence electron of the semiconductor becomes excited causing it to move from its ground state in the valence band to the conduction band, as e^{CB-} (Eq. 3). This movement creates a deficiency of negative charge in the valence band, which is called a hole, h^{VB+}. Within the conduction band, e^{CB-} can move along an electrical gradient to the surface of the crystal. In the same vein, when an electron within the valence band fills up the hole created by the movement of the excited electron, a vacancy is left in its former position, and in this way, the h^{VB+} can also move along an electrical gradient and can reach the surface of the crystal.

However, the electron-hole pairs so created may never reach the surface of the crystal if they become absorbed because of Ti^{3+} or O^- structural defects or if they recombine with a release of energy within the crystal (Eq. 4). But if the pair reaches the crystal surface, e^{CB-} can react with adsorbed oxygen on the crystal surface to give the superoxide radical ($O^{2\cdot-}$) (Eq. 5). Subsequent to its formation, the superoxide radical can react with a proton to give the hydroperoxide radical ($^{\cdot}OOH$) (Eq. 6). On the other hand, h^{VB+} may react with adsorbed water to form the hydroxyl radical ($^{\cdot}OH$) (Eq. 7). These generated radicals can rapidly degrade organic and inorganic materials that are in the vicinity [75,76]. The generation of oxidative radicals on photoactive TiO_2 is illustrated in Fig. 7. TiO_2 photocatalytic degradation of organic matter is an efficient environmental remediation technology and several excellent reviews have been published detailing the mechanisms involved and the applications [74,76,77,82–84].

$$TiO_2 + hv \rightarrow e^{CB-} + h^{VB+} \tag{3}$$

$$e^{CB-} + h^{VB+} \rightarrow \text{Energy} \tag{4}$$

$$e^{CB-} + O_2 \rightarrow O^{2\cdot-} \tag{5}$$

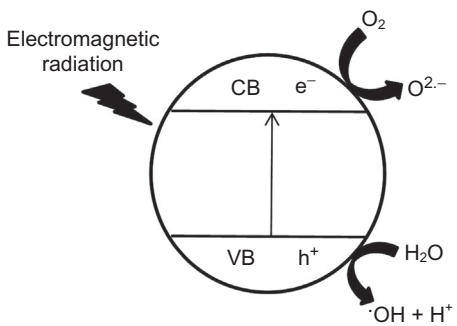

Fig. 7 Schematic of oxidative radical generation on photoactive TiO_2.

$$O^{2\cdot -} + H^{+} \rightarrow {}^{\cdot}OOH \quad (6)$$

$$h^{VB+} + H_2O \rightarrow {}^{\cdot}OH + H^{+} \quad (7)$$

The efficiency of a photocatalyst is dependent on how much of the generated electron–hole pair is prevented from recombining. Recombination may occur in the bulk of the crystal or on the surface, and this is greatly facilitated by structural defects and impurities. A number of techniques have been suggested to decrease recombination and improve the performance of TiO_2 photocatalysts as well as extend performance over visible light spectrum. These include doping, surface modification, and nanoscale sizing [75,85,86]. The reduction of recombination potential, the enhancement of surface area, and the greater affinity for organic material have been recognized as some of the key benefits of $nTiO_2$ over bulk materials. The enhanced surface area in $nTiO_2$ is associated with a number of advantages, such as a greater surface for adsorption of energy, water, and hydroxyl groups (for radicals generation) and an improved photocatalytic reaction rate [74,75,87,88]. Xiao et al. [89] showed that doping $nTiO_2$ with carbon increased the photocatalytic degradation of methylene blue under solar irradiation. Lee et al. [90] reported the synthesis of low-band, graphene-wrapped anatase $nTiO_2$ with enhanced photocatalysis under visible light, which was also employed for the successful degradation of methylene blue. Sayılkan et al. [91] reported that Sn^{4+}-doped $nTiO_2$ showed improved antibacterial effects against gram negative *E. coli* and gram positive *Staphylococcus aureus* when compared with undoped $nTiO_2$. Lin et al. [92] prepared N-doped TiO_2 nanotubes that were loaded with Ag to improve the photocatalytic degradation of reactive brilliant red X-3B dye under visible light. The authors reported that the addition of Ag improved performance when compared with nanotubes with only nitrogen doping. It has also been reported that increasing the concentration of surface hydroxyl groups led to improved $nTiO_2$ photocatalytic degradation of methylene blue and formaldehyde [93].

A number of researchers have taken advantage of the unique photocalytic properties of $nTiO_2$ to improve the performance of membrane filtration systems. Rahimpour et al. [94] reported that when $nTiO_2$ was incorporated into a PES UF membrane, membrane hydrophilicity and antifouling properties were improved upon UV irradiation. This result derives from the photocatalytic effects of $nTiO_2$ in increasing the amount of coordinated hydroxyl groups and the degradation of attached foulants. A similar result using PVDF was reported by Song et al. [95] whereby a fraction of the original flux of a membrane fouled with natural organic matter was recovered upon UV irradiation. Unfortunately, longer UV irradiation (beyond 12 h) was found to degrade the membrane's polymeric matrix. The authors suggested that a practical application of TiO_2 UV irradiation for foulant cleaning requires careful optimization to ensure maximum foulant removal and minimum membrane damage when organic polymeric membranes are used.

In addition to the established photocatalytic effect of $nTiO_2$ in improving membrane performance, numerous researchers have shown that the mere presence of pure or surface-modified $nTiO_2$ in polymeric membranes can increase the composite membrane's hydrophilicity and can positively influence the structure of the polymer matrix toward improve porosity and filtration performance [96–106]. The addition of $nTiO_2$ in polymeric membranes has also been associated with improvement in thermal and mechanical strength up to certain blend proportions [107,108]. Chang et al. [109] showed that the hydrophilicity and performance improving effects of $nTiO_2$ are not restricted to polymeric membrane but can also be realized on a ceramic membrane. The abundant hydroxyl groups on the surface of TiO_2 [93,110,111] account for the hydrophilicity improvement associated with the incorporation of $nTiO_2$ in membranes. However, TiO_2 can become even more hydrophilic upon UV irradiation. This phenomenon is suggested to be related to the generation of electron–hole pairs when electromagnetic radiation of the appropriate energy is absorbed, resulting in the ejection of structural oxide ion. The created vacancy is filled with a water molecule that coordinates with the titanium ion left behind. To maintain charge, the water molecules lose a proton, resulting in the generation of a coordinated hydroxyl group that enhances the overall material hydrophilicity [81,87]. This unique phenomenon of changing wettability with UV irradiation is potentially another important tool that researchers can use to exploit the development of next-generation surface-active membranes.

Membrane composites containing $nTiO_2$ offer a unique opportunity for the effective degradation of harmful contaminants and the disinfection of water. The use of solar energy is particularly significant in its economic advantages, but unfortunately the efficiency of currently available visible light $nTiO_2$ photocatalyst is still low, and therefore the technology cannot be used except for low contaminant concentrations in water [74,75,77,81]. There is also the problem of photocatalyst inactivation, which arises when partially degraded molecules block active photocatalytic sites [75]. In addition, for membrane technology and other supported applications, the immobilization of $nTiO_2$ is said to result in about a 60%–70% loss in system efficiency when compared with the use of free-standing nanoparticles [82]. There is also the problem of the generation of toxic intermediate degradation products requiring careful design of photocatalytic processes [75,82].

3.5 Nanosilver

Silver is a "noble" metal, which implies that, in bulk, it naturally occurs in the metallic zero-valent state because of its pronounced chemical inactivity. The nobility of silver and other noble metals like gold have been explained with reference to the concepts of relativistic contraction/expansion of electron shells and the molecular orbital theory. The former, deriving from the special theory of relativity, maintains that the s and p orbitals in

atoms experience a relativistic contraction but that the relativistic contraction of the valence s orbitals is particularly pronounced for gold and silver making the loss of these valence electrons (oxidation) more difficult. The stability of the contracted s orbitals provides an explanation for the relative chemical inactivity and metallic nobility of Ag and Au [8,112,113]. According to the molecular orbital theory, the nobility of metals can be traced to the existence of antibonding density of states (DOS) below the Fermi level. DOS indicates the number of states available for occupation at a given energy level. Consequently, the existence of antibonding DOS below the Fermi energy level implies that antibonding orbitals can be formed. This necessarily introduces instability in potential chemical bonds thereby rendering the noble metals chemically inactive and stable [8]. However, nAg is markedly different from bulk Ag. The large amount of surface atoms and the rapid translation of "free electrons" to the surface because of the spatial confinement of the nanoparticles gives rise to novel chemical and physical characteristics [8].

The most common application of nAg in membrane water treatment processes harnesses Ag's unique biocidal properties, which have been known for centuries and have been employed for the disinfection of water and wounds both as ionic and metallic silver [8,114]. The effectiveness of bulk Ag as a bactericidal agent relies on oxidation when the metal is in contact with moisture. The basis of the lethal effect of Ag^+ is suggested to include breaching of the microorganism's cell membrane, interfering with cell DNA biochemistry, and the production of reactive oxygen species that may eventually lead to the death of the organism [8,114–116]. Ag^+ is also known to increase the effectiveness of UV irradiation in bacterial disinfection, and may also enhance the antimicrobial effects of electromagnetic fields [117]. The large surface-to-volume ratio of nAg suggests that when they are incorporated into water treatment membranes, they can continuously ionize to leach Ag^+ within and on the surface of the membrane, preventing membrane colonization by microbes [8,116]. Also, dislodged nAg from the filtration membrane network could permeate the cell wall of microbial species causing their death [118]. Silver nanoparticles are generally produced by the reduction of a soluble Ag salt (commonly $AgNO_3$) in the presence of a capping agent to stabilize the nanoparticles. The nature of the capping agent has recently been shown to have a major influence on the bactericidal efficiency of nAg [119]. Reducing agents such as polyol [120], sodium borohydride [121,122], sodium citrate [122], and poly(ethylene glycol) [123] have been reported in the synthesis of nAg. A review of several environmentally benign techniques for producing nAg was recently published [124]. nAg may be incorporated into the framework of a water treatment membrane as a preformed nanoparticle powder or dispersion or it may be generated in situ from a solution of Ag^+.

Taurozzi et al. [116] studied the effect of the nAg incorporation route in a polysulfone membrane. They found that the addition of preformed nAg to the polymer resulted in the accumulation of the nanoparticle in the membrane skin layer, which in some instances led to the formation of macrovoids on the membrane skin layer, resulting in

reduced rejection of dextran. In situ formation of nAg resulted in an even distribution of the nanoparticles in the membrane and better biofilm growth inhibition. Sawad et al. [125] reported the in situ formation of nAg in an acrylamide layer grafted onto a polyethersulfone (PES) membrane, resulting in the development of an antibacterial and antifouling membrane for water treatment. Similar improvements in both antifouling and antibacterial effects were reported by Vatanpour et al. [126] when they incorporated graphene oxide Ag nanocomposite into the framework of a PES membrane. Yang et al. [127] reported that the coating of the surface of an RO membrane and spacers with nAg produced by the reduction of a basic solution of $AgNO_3$ by formaldehyde, resulted in reduced microbial activities and sustained permeate flux in a pilot desalination run. While in situ incorporation of nAg is commonly employed to produce homogenous composite membranes, Yin et al. [128] showed that a stable membrane with good antibacterial properties can be fabricated by covalently attaching nAg produced ex situ to the surface of a polyamide TFC membrane via cysteamine link.

One challenge with the use of immobilized nAg for antimicrobial effects is related to leaching, with permeate flow, of the Ag^+ away from the surface of the membrane where the microorganisms are more likely to make first contact. This is expected to diminish the overall effectiveness of the antimicrobial design [116]. In this regard, surface incorporation of nAg might be more effective than uniform distribution within the membrane matrix. Noting that the antimicrobial effect of nAg depends largely on the production of Ag^+, long-term studies of the antimicrobial effect of nAg incorporated in desalination and water treatment membranes are desirable. Such studies should aim at developing a method for estimating how much nAg would be needed for a particular water treatment scenario. The environmental and health implications of the widespread use of nAg is an important matter for critical evaluation [129], especially considering recent demonstrations of the significant toxicity of nAg on mammalian cells and other biological systems [130–132].

3.6 Nanosilica

Silica or silicon (IV) oxide is a crystalline or amorphous solid with the molecular formula SiO_2. Generally, silica materials are built up from a basic tetrahedral unit composed of four oxygen atoms at the ends of a regular tetrahedron and one Si atom occupying the central position or centroid. The tetrahedral $[SiO_4]^{4-}$ units are connected differently in a random or orderly fashion to give the various polymorphs of silica with varying densities and porosities. Silica materials consist of the stable siloxane bond, Si–O, and the less stable silanol bond Si–OH [133]. The latter is usually found on the surface but may exist in the interior in some cases [134]. The physisorption of water molecules onto hydroxyl groups could result in a chain-reaction-type destabilization of the silica structure through repeated chemisorptive breakdown (hydrolysis) of siloxane bonds [135]. Because of the

high free surface energy of silica and the abundance of silanol group supplying hydrogen bonding, water molecules are easily adsorbed. These, in combination with the silanol groups, play key roles in silica surface chemistry [134,136,137] and are responsible for the hydrophilic properties of silica, which, however, can be lost on heating [138,139]. Silica nanoparticles are commonly produced by the Stöber process or a modification of this process. These techniques basically involve the ammonia (base) catalyzed reaction between tetraethyl orthosilicate (TEOS) (silicon alkoxide) and water in a low molecular weight alcohol as the solvent. Varying the solvent and other reactions conditions have been used to produce nanoparticles of varying sizes and size distributions [140–142]. Recently, Wu et al. [143] published a review of techniques for the production of mesoporous silica nanoparticles with varying porosity, morphology, uniformity, and dispersity. On the other hand, microporous solids can be made by adopting an acid catalyzed sol-gel process, which is useful for preparing silica with pores small enough to separate light gases by size exclusion [144].

The hydrophilic properties of porous and nonporous silica nanoparticles have been employed to enhance the performance of desalination and water treatment membranes by a number of researchers in recent times. Ahmad et al. [145] reported that the wettability of a polysulfone UF membrane was improved by the addition of $nSiO_2$. The presence of the nanoparticles were found not only to lead to better hydrophilicity but also to an increase in the surface porosity of the membrane, resulting in an approximately 16-fold increment in permeability when compared with the unmodified membrane and to enhanced antifouling properties. However, according to the authors, the hybrid membrane suffered a slight 4% decrease in rejection. Shen et al. [146] reported a similar modification of a PES polymeric UF membrane by the addition of $nSiO_2$ during the membrane synthesis. The addition of $nSiO_2$ was associated with improvement in hydrophilicity, porosity, permeability, rejection, and antifouling properties when compared with the unmodified membrane. Yu et al. [147] devised a method for the production of PVDF-SiO_2 nanocomposite membranes that involved the direct addition of SiO_2 sol produced from the reaction of acidified TEOS, water, and *N*,*N*-dimethylformamide (DMF) mixture to a PVDF dope to produce hybrid hollow fiber UF membranes. The hybridization was reported to have resulted in major structural changes in the membrane with improved thermal and mechanical properties at lower blend proportions. Hydrophilicity, permeability, and antifouling properties were also enhanced. Flux increased four-fold, while rejection was reduced by about 5%. A similar technique, where cellulose acetate (CA) was used as the base membrane, was adopted by Chen et al. [148] in which TEOS was directly added to a DMF-CA dope and then phase-inversed in pure, acidic, and basic water baths. The authors reported that upon phase inversion, large amounts of the in situ generated SiO_2 particles transferred from the skin layer into the coagulation bath, resulting in enhanced surface porosity. The best flux was reported for a membrane phased-inversed in acidic water, where the permeability was said to be about 256 times

higher than the permeability of pure CA membrane. Enhancement of antifouling properties at high oil rejection was reported for the modified membrane when tested against an oil emulsion.

Yin et al. [149] reported that the dispersion and stability of hydrophilic $nSiO_2$ in PES was enhanced when the nanoparticles were grafted with a hydrophilic zwitterionic copolymer (poly (2(dimethylamino) ethylmethacrylate-*co*-3-dimethyl (methacryloyloxyethyl) ammonium propane sulfonate)) before blending with PES. It was reported that the homogenous and stable modified membrane resulted in improved porosity, hydrophilicity, permeability, and antifouling properties in comparison with a pure PES membrane. To harness both the surface hydrophilizing effect of SiO_2 and the nanopores for enhanced water permeability, Yin et al. [150] reported the synthesis of a polyamide TFN with mesoporous SiO_2 nanoparticles (MSN) as the inorganic fillers. Both membrane hydrophilicity and zeta potential were said to have benefited from the addition of the porous $nSiO_2$. By comparing the MSN-modified membrane to a membrane modified by nonporous $nSiO_2$, the authors established that the nanopores were important channels for improving water permeability without decreasing rejection. Similarly, Huang et al. [151] reported that the addition of MSN to PES resulted in the production of a hybrid UF membrane with enhanced hydrophilicity, water permeability, and antifouling properties. Thermal stability also benefited from the presence of $nSiO_2$. A modification of the surface of MSN by amino groups was suggested by Wu et al. [152] as a potential viable means of improving the nanoparticles' stability. This procedure takes advantage of the covalent bonds between the nanoparticles and the polymer framework. Long-term membrane stability, enhanced permeability, and antifouling performance were reported as some of the benefits of the technique.

The incorporation of $nSiO_2$ is evidently an important route to improving the performance of membranes for desalination and water-treatment applications. Particularly important are mesoporous nanoparticles where enhanced flux can be attained without sacrificing rejection. The surface of $nSiO_2$ lends itself to important modifications that can allow the development of unique hydrophilizing and antifouling groups. However, many researchers are constrained to limiting the amount of the nanoparticles incorporated into the membrane because of the problem of agglomeration and the decline in desirable properties above certain blend proportions, even with advanced dispersion techniques [145–147,149,151,152]. This appears to place a cap on the benefits derivable from $nSiO_2$ incorporation into membranes. However, the problem of aggregation is a general problem of nanotechnology and is not peculiar to $nSiO_2$. Despite the rich supply of hydroxyl groups on the SiO_2 surface, the adsorption of organic materials is not excluded [138], and this may impact the long-term performance of SiO_2-modified membranes. Studies have shown that $nSiO_2$ exhibit a certain measure of cytotoxicity that must be considered in the development and deployment of $nSiO_2$-based technologies [153–155].

3.7 Nanoalumina

Alumina (Al_2O_3) exists in a number of crystalline phases, but perhaps the most common phase for catalytic application is gamma alumina (γ-Al_2O_3) [156,157]. However, alpha alumina (α-Al_2O_3) continues to find widespread applications in many industrial settings for its unique mechanical, electrical, and optical properties [158]. The crystalline structure of γ-Al_2O_3 is often considered to be a defective spinel type because of the absence of magnesium, as is found in the ideal spinel structure of $MgAl_2O_4$ [157]. Like most metal oxides, the surface of γ-Al_2O_3 is covered by OH groups, which are of great importance with respect to their chemical characteristics. The properties and functionalities of the hydroxyl groups are said to depend on a number of factors, such as the chemical environment, the synthesis technique, the purity of the sample, and the morphology of the surface [157]. In addition to abundant surface hydroxyl groups, it has been shown that there is "excess" molecular water strongly bonded or "chemisorbed" to the surface of γ-Al_2O_3. The bonding of the "excess" water to surface oxide ions is via hydrogen bonding [156]. The bonded water and hydroxyl groups have been explored in the production of MMM for water treatment. Usually, in membrane water applications, nAl_2O_3 are used to harness the extensive surface area provided by nanoparticles by adding preformed nanoparticles to a polymer dope. nAl_2O_3 have been produced by a number of techniques, including ball milling, sol-gel, pyrolysis, sputtering, hydrothermal, and laser ablation [159].

Yan et al. [160] reported the production of a flat-sheet Al_2O_3-PVDF MMM membrane using various concentrations of nanoparticles with respect to a given mass of the polymer. They reported that the addition of nAl_2O_3 resulted in the enhancement of membrane hydrophilicity, permeability, antifouling, and mechanical properties for all concentrations of nAl_2O_3 with respect to a pure PVDF membrane. The same group reported the production of a tubular nAl_2O_3-PVDF MMM membrane by blending PVDF with 2 wt% of nAl_2O_3 with respect to the polymer [161]. The tubular membrane was used for the filtration of oily wastewater, and the performance was compared to a similar membrane lacking nanoparticles. The authors reported that the addition of nAl_2O_3 almost doubled the membrane flux without impairing rejection when compared with the pure PVDF membrane. The modified membrane showed better antifouling properties and an improved cleaning response. Maximous et al. [162] studied the effect of the concentrations of nAl_2O_3 on the performance of MMM. They synthesized PES membranes into which they incorporated various amounts of nAl_2O_3. Based on the measured mechanical strength, water permeability, and antifouling performance with respect to activated sludge, they concluded that the addition of nAl_2O_3 improved membrane performance until 5 wt% of nAl_2O_3 was added, after which the performance declined. To improve polymer-nAl_2O_3 bonding, which otherwise could result in poor particle dispersion that might impair membrane performance, Liu et al. [163] reported that an

acid-catalyzed reaction between hydroxyl rich γ-Al_2O_3 and PVDF can be used to produce novel MMM with enhanced hydrophilicity and antifouling properties. However, the authors did not show how this novel membrane compares with an Al_2O_3-PVDF MMM without chemical interactions as reported by other authors (e.g., Refs. [160,161]). Going beyond Al_2O_3 modifications, the membrane literature is lacking in studies that compared the performance of membranes modified by different inorganic nanoparticles (nAl_2O_3, $nSiO_2$, etc.) under similar conditions. Such studies are important to show whether the selection of inorganic filler materials can be optimized for different applications and operating scenarios.

Maximous et al. [162] and Yi et al. [164] have shown that the addition of preformed nAl_2O_3 to polymer membranes at certain blend concentrations leads to an improved membrane performance. However, such simple blending might not be suitable for the modification of a ceramic membrane since calcination, which is often necessary to fix the nanoparticles to the membrane, may lead to the loss of the nanoparticles' surface hydroxyl groups, resulting in a decrease in hydrophilicity [157,165]. Chang et al. [165] showed that this problem can be overcome by an in situ formation of a γ-Al_2O_3 ceramic membrane. In situ formation provides the additional benefit of good dispersion. The nanoparticles were produced from aluminium isopropoxide dimethyl benzene, which was used to saturate the base ceramic membrane, after which the wet membrane was subjected to heat treatment [165]. Both water permeability and antifouling performance were improved by the modification.

The common applications of nAl_2O_3 in membrane water treatment reviewed denote an attempt to harness the surface hydrophilicity of the material to improve the performance of membrane filtration. However, γ-Al_2O_3 is used as a catalyst and a catalyst support in many other important industrial processes [156,157]. Recently, the toxicological impact of nAl_2O_3 and to a lesser degree bulk Al_2O_3 on aquatic microalgae was demonstrated [166]. A detailed study of the mechanism of the phytotoxicity of nAl_2O_3 on plants has also been made [167]. All these suggest that there are potentials for more active use of nAl_2O_3 in membrane water-treatment processes, which are yet to be exploited, as well as the need for caution in the use of the material.

3.8 Nanoclay and Iron Oxide Nanoparticles

Clays are generally hydrous aluminosilicates consisting of two structural units, namely, the tetrahedral silica sheets and the octahedral alumina sheets in the presence of other metallic ions [168]. They are abundant in nature and are used in many important industrial processes. One of the many applications of clays is in the catalytic degradation of organic compounds using hydrogen peroxide as oxidant in Fenton-like reactions [169,170]. Another important practical application of nanoclays is in the improvement of the mechanical properties and thermal stability of polymer films [129]. A number

of papers have documented significant improvements in mechanical strength when nanoclays were incorporated into polymeric membranes such as PVDF [171–173]. These improvements are attributed to the large surface area of nanoclays providing for enhanced energy dissipation as well as their unique crystal lattice compatibility with the PVDF β crystal phase [171–174]. PVDF is known to exist in at least four different crystal phases, α, β, γ, and δ, with the β phase being the most important polymorph because of its unique piezoelectric, pyroelectric, and toughness enhancement properties [171–174]. The proportion of the β phase and consequently the toughness have been shown to be enhanced in PVDF/nanoclay composite membranes compared with the virgin PVDF films [171]. In such nanocomposites, nanoclays act as structure and morphology directors increasing the amount of metastable phases to achieve enhanced mechanical properties. Membranes with enhanced mechanical strength and more resilience to abrasive wear are desirable in water treatment, especially for seawater desalination pretreatment where abrasive wear from particles in seawater can impair the membrane's physical integrity and thereby depreciate selectivity and membrane lifespan [172,173]. The incorporation of organically modified nanoclays into PVDF membranes has also been reported to result in improvements in hydrophilicity, water flux, and fouling resistance [175,176].

Like clays, iron oxides are abundant in nature and have been used extensively for Fenton-like catalytic degradation of organic compounds [170,177]. Huang et al. [178] reported that increasing the concentration of iron (II,III) oxide (Fe_3O_4) in a polysulfone composite membrane resulted in continuous increase in the water flux. However, the rejection of bovine serum albumin (BSA) initially increased but subsequently declined as the concentration of the inorganic fillers increased. In another work, the same authors documented that the application of a magnetic field during the phase inversion process can result in novel pore structure refinement for a membrane with a high concentration of magnetic iron oxide particles (more than two times the mass of the polymeric matrix), resulting in enhanced water flux and BSA rejection [179]. Magnetic functionalization was also adopted by Yang and coworkers [180] to fabricate a responsive NF membrane by the attachment of magnetic nanoparticles to the ends of poly (2-hydroxyethylmethacrylate) chains that have been previously grafted onto the surface of a TFC polyamide membrane. Increased permeate flux and increased salt rejection was recorded when the modified membrane was placed within an oscillating magnetic field during the desalination of a solution of $CaCl_2$ and $MgSO_4$. Ling and Chung [181] reported the use of hydrophilic magnetic nanoparticles as a draw solute in an integrated FO-UF process for water reuse and desalination. An attempt to recover the magnetic nanoparticles using a magnetic field rather than via UF was unsuccessful because of the aggregation of the nanoparticles after magnetic separation. The development of an effective technique to prevent nanoparticle aggregation is likely to advance FO using magnetic draw solutes as an important desalination procedure.

Both nanoclay and iron oxide nanoparticles can potentially play important roles toward the development of efficient pretreatments for water desalination applications. The unique magnetic property of iron oxides lends itself to many novel research options that may yield important results in the future for MDWT applications.

4. CONCLUSIONS AND FUTURE PROSPECTS

In regard to the development of high-flux, high-rejection, low-cost, and long-life membranes, nanotechnology research has been shown to hold enormous promise in contributing to the resolution of the two inherent problems of membrane technology, namely, the permeability-selectivity trade-off and membrane fouling. Carbon nanotubes, aquaporin, and nanozeolites promise significant improvements in RO and NF water flux with very high and tunable rejection as a consequence of their molecular-level porosities and nanoscale surface areas, thus breaking down the permeability-selectivity trade-off inherent in membrane processes. However, none of these molecular channels at full capacity are currently available for MDWT applications. One common challenge relates to the technical and economic difficulties in scaling up these nanofilters to the requisite macro-dimension for MDWT applications without defects and functionality impairments. For aquaporin, and to some extent CNT, the nanofilters with the desired functionalities are not yet commercially available, limiting research and development. For zeolite-based systems, the production of integral crystal films is still challenging, and although much progress has been made towards understanding the complexity of the zeolitic structure, chemistry, and ionic interaction, major knowledge gaps still exist. Consequently, potential flux enhancement and rejection improvement as a result of zeolite molecular porosity is still unrealized. Aligned CNTs appear to be the most promising high-performance membrane that could reach the market first based on the current state of the technology, the stability of the material, and the versatility and ease of its functionalization. However, much research is still needed to meet these expectations, as high cost and challenging manufacturing process make aligned CNTs uncompetitive with the state-of-the art polyamide and cellulose acetate RO membranes.

Starting with nanozeolite, later CNT, and recently aquaporin, enhanced water flux has been achieved by incorporating nanofilters into the thin selective layer of composite polymer membranes. Nanocomposite membranes, in particular nanozeolite, represent one of the major success stories of nanotechnology applications to MDWT. There are still major stability issues that must be resolved before aquaporin nanocomposite membranes, and other MDWT applications of membrane proteins, can compete favorably with other technologies. However, the flux enhancements currently observed for nanozeolite and CNT nanocomposite membranes are still orders of magnitude below the theoretical performance of a molecular sieve. The limited water transportation capability of present nanocomposite systems relates to the disorderly arrangement of the nanochannels

and the flux limitation imposed by the polymer matrix. Innovative channel alignment and reduction of polymer flux path length may potentially improve the performance of these membranes.

The many important properties of $nTiO_2$ are likely to impact positively the development of next-generation membranes. In addition to flux enhancement benefits deriving from the natural hydrophilic properties of $nTiO_2$, $nTiO_2$ provides unique functionalization in self-cleaning, contaminant degradation, and self-wettability modification in response to electromagnetic radiations. These intriguing effects may provide the platform for the reduction of the elusive problem of membrane fouling and productivity decline in the future. The potential active antifouling properties of $nTiO_2$ are likely to play a critical role in the practical operation of future high-performance membranes since high-performance membranes are likely to face more challenging problems of concentration polarization and membrane fouling. However, the economic feasibility of $nTiO_2$ active functionalities is dependent on the success of current and future research in improving visible light photocatalysis. nAg is another important material for the reduction of the problem of membrane fouling, particularly biological fouling. Composite systems with nAg and other nanoparticles are likely to be more prevalent in future MDWT, but questions surrounding the effects of the leaching of dissolved nanoparticles or the potential dislodgement of whole nAg or other nanoparticles into the permeate stream must be resolved. Researchers have considered leaching mostly for nAg as it is in metallic form and may become ionized in water or acidic solutions, resulting in charged reactive and/or toxic species. Less attention has been paid to the issue of leaching of the other common nanoparticles, such as TiO_2, Al_2O_3, and clay probably because they are considered less soluble and/or less reactive. The importance of $nSiO_2$, nAl_2O_3, nanoclay, and iron oxide nanoparticles is likely to be centered on low-cost enhancement of permeate flux, thermal stability, and mechanical strength, especially for UF and MF applications. However, the currently little-explored cytotoxicity of $nSiO_2$ and nAl_2O_3 may prove useful for future applications as well as the catalytic properties of nanoclay and iron oxide nanoparticles. Mesoporous $nSiO_2$ may also be of future importance in the development of high-flux RO and UF membranes, and the many potential magnetic applications of iron oxide nanoparticles might result in important MDWT applications.

REFERENCES

[1] R.W. Baker, Membrane Technology and Application, second ed., John Wiley & Sons Ltd., West Sussex, England, 2004.
[2] X. Qu, J. Brame, Q. Li, P.J.J. Alvarez, Nanotechnology for a safe and sustainable water supply: enabling integrated water treatment and reuse, Acc. Chem. Res. 46 (2013) 834–843.
[3] M. Elimelech, W.A. Phillip, The future of seawater desalination: energy, technology, and the environment, Science 333 (2011) 712–717.

[4] X. Qu, P.J. Alvarez, Q. Li, Applications of nanotechnology in water and wastewater treatment, Water Res. 47 (2013) 3931–3946.
[5] C.d.M. Donega (Ed.), Nanoparticles, The Workhorses of Nanoscience, Springer, Heidelberg, 2014.
[6] K. Sattler, The energy gap of clusters, nanoparticles and quantum dot, in: H.S. Nalwa (Ed.), Handbook of Thin Films, Academic Press, Massachusetts, CA, 2002, pp. 61–97.
[7] E. Roduner, Size matters: why nanomaterials are different, Chem. Soc. Rev. 35 (2006) 583–592.
[8] T. Pradeep, Anshup, Noble metal nanoparticles for water purification: a critical review, Thin Solid Films 517 (2009) 6441–6478.
[9] M. Terrones, Science and technology of the twenty-first century: synthesis, properties, and applications of carbon nanotubes, Ann. Rev. Mater. Res. 33 (2003) 419–501.
[10] M.F.L. De Volder, S.H. Tawfick, R.H. Baughman, A.J. Hart, Carbon nanotubes: present and future commercial applications, Science 339 (2013) 535–539.
[11] M.H. Rummeli, P. Ayala, T. Pichler, Carbon nanotubes and related structures: production and formation, in: D.M. Guildi, N. Martin (Eds.), Carbon Nanotubes and Related Structures, WILEY-VCH Verlag GmbH & Co. KGaA, Weinheim, 2010.
[12] P.S. Goh, A.F. Ismail, B.C. Ng, Carbon nanotubes for desalination: performance evaluation and current hurdles, Desalination 308 (2013) 2–14.
[13] R. Das, M.E. Ali, S.B.A. Hamid, S. Ramakrishna, Z.Z. Chowdhury, Carbon nanotube membranes for water purification: a bright future in water desalination, Desalination 336 (2014) 97–109.
[14] B. Corry, Designing carbon nanotube membranes for efficient water desalination, J. Phys. Chem. B 112 (2008) 1427–1434.
[15] F. Du, L. Qu, Z. Xia, L. Feng, L. Dai, Membranes of vertically aligned superlong carbon nanotubes, Langmuir 27 (2011) 8437–8443.
[16] J.K. Holt, Carbon nanotubes and nanofluidic transport, Adv. Mater. 21 (2009) 3542–3550.
[17] J.K. Holt, H.G. Park, Y. Wang, M. Stadermann, A.B. Artyukhin, C.P. Grigoropoulos, A. Noy, O. Bakajin, Fast mass transport through sub-2-nanometer carbon nanotubes, Science 312 (2006) 1034–1037.
[18] E.R. Nightingale, Phenomenological theory of ion solvation. Effective radii of hydrated ions, J. Phys. Chem. C 63 (1959) 1381–1387.
[19] W.-F. Chan, H.-y. Chen, A. Surapathi, M.G. Taylor, X. Shao, E. Marand, J.K. Johnson, Zwitterion functionalized carbon nanotube/polyamide nanocomposite membranes for water desalination, ACS Nano 7 (2013) 5308–5319.
[20] J.S. Vrouwenvelder, M.C. Van Loosdrecht, J.C. Kruithof, A novel scenario for biofouling control of spiral wound membrane systems, Water Res. 45 (2011) 3890–3898.
[21] Y. Baek, C. Kim, D.K. Seo, T. Kim, J.S. Lee, Y.H. Kim, K.H. Ahn, S.S. Bae, S. C. Lee, J. Lim, K. Lee, J. Yoon, High performance and antifouling vertically aligned carbon nanotube membrane for water purification, J. Membr. Sci. 460 (2014) 171–177.
[22] P. Daraei, S.S. Madaeni, N. Ghaemi, M.A. Khadivi, B. Astinchap, R. Moradian, Enhancing antifouling capability of PES membrane via mixing with various types of polymer modified multi-walled carbon nanotube, J. Membr. Sci. 444 (2013) 184–191.
[23] S. Majeed, D. Fierro, K. Buhr, J. Wind, B. Du, A. Boschetti-de-Fierro, V. Abetz, Multi-walled carbon nanotubes (MWCNTs) mixed polyacrylonitrile (PAN) ultrafiltration membranes, J. Membr. Sci. 403–404 (2012) 101–109.
[24] V. Vatanpour, S.S. Madaeni, R. Moradian, S. Zinadini, B. Astinchap, Novel antibifouling nanofiltration polyethersulfone membrane fabricated from embedding TiO_2 coated multiwalled carbon nanotubes, Sep. Purif. Technol. 90 (2012) 69–82.
[25] A. Yoosefi Booshehri, R. Wang, R. Xu, The effect of re-generable silver nanoparticles/multi-walled carbon nanotubes coating on the antibacterial performance of hollow fiber membrane, Chem. Eng. J. 230 (2013) 251–259.
[26] C.Y. Lai, A. Groth, S. Gray, M. Duke, Nanocomposites for improved physical durability of porous PVDF membranes, Membranes (Basel) 4 (2014) 55–78.
[27] J. Yin, G. Zhu, B. Deng, Multi-walled carbon nanotubes (MWNTs)/polysulfone (PSU) mixed matrix hollow fiber membranes for enhanced water treatment, J. Membr. Sci. 437 (2013) 237–248.

[28] M.S. Mauter, M. Elimelech, C.O. Osuji, Nanocomposites of vertically aligned single-walled carbon nanotubes by Magnetic alignment and polymerization of a lyotropic precursor, ACS Nano 4 (2010) 6651–6658.
[29] C.-F. de Lannoy, E. Soyer, M.R. Wiesner, Optimizing carbon nanotube-reinforced polysulfone ultrafiltration membranes through carboxylic acid functionalization, J. Membr. Sci. 447 (2013) 395–402.
[30] F. Liu, N.A. Hashim, Y. Liu, M.R.M. Abed, K. Li, Progress in the production and modification of PVDF membranes, J. Membr. Sci. 375 (2011) 1–27.
[31] N. Phao, E.N. Nxumalo, B.B. Mamba, S.D. Mhlanga, A nitrogen-doped carbon nanotube enhanced polyethersulfone membrane system for water treatment, Phys. Chem. Earth Parts A/B/C 66 (2013) 148–156.
[32] S. Qiu, L. Wu, X. Pan, L. Zhang, H. Chen, C. Gao, Preparation and properties of functionalized carbon nanotube/PSF blend ultrafiltration membranes, J. Membr. Sci. 342 (2009) 165–172.
[33] A.S. Brady-Estevez, S. Kang, M. Elimelech, A single-walled-carbon-nanotube filter for removal of viral and bacterial pathogens, Small 4 (2008) 481–484.
[34] L.F. Dumée, K. Sears, J. Schütz, N. Finn, C. Huynh, S. Hawkins, M. Duke, S. Gray, Characterization and evaluation of carbon nanotube Bucky-Paper membranes for direct contact membrane distillation, J. Membr. Sci. 351 (2010) 36–43.
[35] H. Omachi, T. Nakayama, E. Takahashi, Y. Segawa, K. Itami, Initiation of carbon nanotube growth by well-defined carbon nanorings, Nat. Chem. 5 (2013) 572–576.
[36] Y. Kaufman, V. Freger, Supported biomimetic membranes for pressure driven water purification, On Biomimetics, InTech, 2011.
[37] P. Gena, M. Pellegrini-Calace, A. Biasco, M. Svelto, G. Calamita, Aquaporin membrane channels: biophysics, classification, functions, and possible biotechnological applications, Food Biophys. 6 (2010) 241–249.
[38] M.J. Borgnia, D. Kozono, G. Calamita, P.C. Maloney, P. Agre, Functional reconstitution and characterization of AqpZ the *E. coli* water channel protein, J. Mol. Biol. 291 (1999) 1169–1179.
[39] P. Agre, Aquaporin water channels, Angew. Chem. Int. Ed. Engl. 43 (2004) 4278–4290 (Nobel Lecture).
[40] J. Bomholt, C. Helix-Nielsen, P. Scharff-Poulsen, P.A. Pedersen, Recombinant production of human Aquaporin-1 to an exceptional high membrane density in *Saccharomyces cerevisiae*, PLoS One 8 (2013) e56431.
[41] J.S. Hub, B.L. de Groot, Mechanism of selectivity in aquaporins and aquaglyceroporins, Proc. Natl. Acad. Sci. U. S. A. 105 (2008) 1198–1203.
[42] C.X. Zhao, H.B. Shao, L.Y. Chu, Aquaporin structure-function relationships: water flow through plant living cells, Colloids Surf. B Biointerfaces 62 (2008) 163–172.
[43] J. Wang, L. Feng, Z. Zhu, M. Zheng, D. Wang, Z. Chen, H. Sun, Aquaporins as diagnostic and therapeutic targets in cancer: how far we are? J. Transl. Med. 13 (2015) 96.
[44] C.Y. Tang, Y. Zhao, R. Wang, C. Hélix-Nielsen, A.G. Fane, Desalination by biomimetic aquaporin membranes: review of status and prospects, Desalination 308 (2013) 34–40.
[45] C. Tang, Z. Wang, I. Petrinić, A.G. Fane, C. Hélix-Nielsen, Biomimetic aquaporin membranes coming of age, Desalination 368 (2015) 89–105.
[46] H. Wang, T.S. Chung, Y.W. Tong, K. Jeyaseelan, A. Armugam, Z. Chen, M. Hong, W. Meier, Highly permeable and selective pore-spanning biomimetic membrane embedded with aquaporin Z, Small 8 (2012) 1185–1190. 1125.
[47] L. Kai, R. Kaldenhoff, J. Lian, X. Zhu, V. Dotsch, F. Bernhard, P. Cen, Z. Xu, Preparative scale production of functional mouse aquaporin 4 using different cell-free expression modes, PLoS One 5 (2010) 1–8.
[48] D. Schwarz, C. Klammt, A. Koglin, F. Löhr, B. Schneider, V. Dötsch, F. Bernhard, Preparative scale cell-free expression systems: New tools for the large scale preparation of integral membrane proteins for functional and structural studies, Methods 41 (2007) 355–369.
[49] A. Muller-Lucks, P. Gena, D. Frascaria, N. Altamura, M. Svelto, E. Beitz, G. Calamita, Preparative scale production and functional reconstitution of a human aquaglyceroporin (AQP3) using a cell free expression system, N. Biotechnol. 30 (2013) 545–551.

[50] M. Perry, C. Rein, J. Vogel, Large scale biomimetic membrane arrays, in: C. Hélix-Nielsen (Ed.), Biomimetic Membranes for Sensor and Separation Applications, Springer, Netherlands, 2012, pp. 205–231.
[51] Y.-x. Shen, P.O. Saboe, I.T. Sines, M. Erbakan, M. Kumar, Biomimetic membranes: a review, J. Membr. Sci. 454 (2014) 359–381.
[52] P.S. Zhong, T.-S. Chung, K. Jeyaseelan, A. Armugam, Aquaporin-embedded biomimetic membranes for nanofiltration, J. Membr. Sci. 407–408 (2012) 27–33.
[53] Y. Zhao, C. Qiu, X. Li, A. Vararattanavech, W. Shen, J. Torres, C. Hélix-Nielsen, R. Wang, X. Hu, A.G. Fane, C.Y. Tang, Synthesis of robust and high-performance aquaporin-based biomimetic membranes by interfacial polymerization-membrane preparation and RO performance characterization, J. Membr. Sci. 423–424 (2012) 422–428.
[54] I.D. Rollmann, E.W. Valyocsik, R.D. Shannon, Miscellaneous solid-state compounds, in: D.W. Murphy, I.V. Leonard (Eds.), Inorganic Syntheses, John Wiley & Sons Inc, New York, USA, 1995, pp. 227–234.
[55] D.W. Breck, Zeolite Molecular Sieves: Structure, Chemistry and Use, John Wiley & Sons, New York, 1974.
[56] M. Duke, D. Zhao, R. Semiat, Functional Nanostructured Materials and Membranes for Water Treatment, Wiley-VCH, Weinheim, Germany, 2013.
[57] B. Zhu, C.M. Doherty, X. Hu, A.J. Hill, L. Zou, Y.S. Lin, M. Duke, Designing hierarchical porous features of ZSM-5 zeolites via Si/Al ratio and their dynamic behavior in seawater ion complexes, Micropor. Mesopor. Mater. 173 (2013) 78–85.
[58] Y.S. Lin, M.C. Duke, Recent progress in polycrystalline zeolite membrane research, Curr. Opin. Chem. Eng. 2 (2013) 209–216.
[59] J. O'Brien-Abraham, M. Kanezashi, Y.S. Lin, Effects of adsorption-induced microstructural changes on separation of xylene isomers through MFI-type zeolite membranes, J. Membr. Sci. 320 (2008) 505–513.
[60] S.G. Sorenson, E.A. Payzant, W.T. Gibbons, B. Soydas, H. Kita, R.D. Noble, J.L. Falconer, Influence of zeolite crystal expansion/contraction on NaA zeolite membrane separations, J. Membr. Sci. 366 (2011) 413–420.
[61] B. Zhu, L. Zou, C.M. Doherty, A.J. Hill, Y.S. Lin, X. Hu, H. Wang, M. Duke, Investigation of the effects of ion and water interaction on structure and chemistry of silicalite MFI type zeolite for its potential use as a seawater desalination membrane, J. Mater. Chem. 20 (2010) 4675–4683.
[62] B. Zhu, D.T. Myat, J.-W. Shin, Y.-H. Na, I.-S. Moon, G. Connor, S. Maeda, G. Morris, S. Gray, M. Duke, Application of robust MFI-type zeolite membrane for desalination of saline wastewater, J. Membr. Sci. 475 (2015) 167–174.
[63] L. Li, J. Dong, T.M. Nenoff, R. Lee, Desalination by reverse osmosis using MFI zeolite membranes, J. Membr. Sci. 243 (2004) 401–404.
[64] B.-H. Jeong, E.M.V. Hoek, Y. Yan, A. Subramani, X. Huang, G. Hurwitz, A.K. Ghosh, A. Jawor, Interfacial polymerization of thin film nanocomposites: a new concept for reverse osmosis membranes, J. Membr. Sci. 294 (2007) 1–7.
[65] H. Wang, Z. Wang, Y. Yan, Colloidal suspensions of template-removed zeolite nanocrystals, Chem. Commun. (2000) 2333–2334.
[66] C. Kong, T. Shintani, T. Tsuru, "Pre-seeding"-assisted synthesis of a high performance polyamide-zeolite nnaocomposite membrane for water purification, New J. Chem. 34 (2010) 2101–2104.
[67] M. Fathizadeh, A. Aroujalian, A. Raisi, Effect of added NaX nano-zeolite into polyamide as a top thin layer of membrane on water flux and salt rejection in a reverse osmosis process, J. Membr. Sci. 375 (2011) 88–95.
[68] M.L. Lind, A.K. Ghosh, A. Jawor, X. Huang, W. Hou, Y. Yang, E.M. Hoek, Influence of zeolite crystal size on zeolite-polyamide thin film nanocomposite membranes, Langmuir 25 (2009) 10139–10145.
[69] M.M. Pendergast, A.K. Ghosh, E.M.V. Hoek, Separation performance and interfacial properties of nanocomposite reverse osmosis membranes, Desalination 308 (2013) 180–185.
[70] N. Ma, J. Wei, R. Liao, C.Y. Tang, Zeolite-polyamide thin film nanocomposite membranes: towards enhanced performance for forward osmosis, J. Membr. Sci. 405–406 (2012) 149–157.

[71] S.G. Kim, D.H. Hyeon, J.H. Chun, B.-H. Chun, S.H. Kim, Nanocomposite poly(arylene ether sulfone) reverse osmosis membrane containing functional zeolite nanoparticles for seawater desalination, J. Membr. Sci. 443 (2013) 10–18.
[72] L. Chem, Leveraging Nanotechnology for Next Generation Seawater Desalination (The International Desalination & Water Reuse Quarterly), LG NanoH2O, Inc., 2015.
[73] U. Diebold, The surface science of titanium dioxide, Surf. Sci. Rep. 48 (2003) 53–229.
[74] Y. Lan, Y. Lu, Z. Ren, Mini review on photocatalysis of titanium dioxide nanoparticles and their solar applications, Nano Energy 2 (2013) 1031–1045.
[75] M. Pelaez, N.T. Nolan, S.C. Pillai, M.K. Seery, P. Falaras, A.G. Kontos, P.S.M. Dunlop, J.W. J. Hamilton, J.A. Byrne, K. O'Shea, M.H. Entezari, D.D. Dionysiou, A review on the visible light active titanium dioxide photocatalysts for environmental applications, Appl. Catal. B Environ. 125 (2012) 331–349.
[76] D. Chatterjee, S. Dasgupta, Visible light induced photocatalytic degradation of organic pollutants, J. Photochem. Photobiol. C Photchem. Rev. 6 (2005) 186–205.
[77] A. Fujishima, X. Zhang, D. Tryk, Heterogeneous photocatalysis: from water photolysis to applications in environmental cleanup, Int. J. Hydrogen Energy 32 (2007) 2664–2672.
[78] O. Carp, Photoinduced reactivity of titanium dioxide, Prog. Solid State Chem. 32 (2004) 33–177.
[79] A. Fujishima, T.N. Rao, D.A. Tryk, Titanium dioxide photocatalysis, J. Photochem. Photobiol. C Photchem. Rev. 1 (2000) 1–21.
[80] A. Fujishima, X. Zhang, Titanium dioxide photocatalysis: present situation and future approaches, C. R. Chim. 9 (2006) 750–760.
[81] A. Fujishima, X. Zhang, D. Tryk, TiO_2 photocatalysis and related surface phenomena, Surf. Sci. Rep. 63 (2008) 515–582.
[82] U.I. Gaya, A.H. Abdullah, Heterogeneous photocatalytic degradation of organic contaminants over titanium dioxide: A review of fundamentals, progress and problems, J. Photochem. Photobiol. C Photchem. Rev. 9 (2008) 1–12.
[83] J.-M. Herrmann, Heterogeneous photocatalysis: fundamentals and applications to the removal of various types of aqueous pollutants, Catal. Today 53 (1999) 115–129.
[84] S. Malato, P. Fernández-Ibáñez, M.I. Maldonado, J. Blanco, W. Gernjak, Decontamination and disinfection of water by solar photocatalysis: recent overview and trends, Catal. Today 147 (2009) 1–59.
[85] A.H.N. Alamgir, W. Khan, S. Ahmad, M.M. Hassan, Structural phase analysis, band gap tuning and fluorescence properties of Co doped TiO_2 nanoparticles, Opt. Mater. 38 (2014) 278–285.
[86] M. Anpo, The design and development of highly reactive titanium oxide photocatalysts operating under visible light irradiation, J. Catal. 216 (2003) 505–516.
[87] K. Nakata, T. Ochiai, T. Murakami, A. Fujishima, Photoenergy conversion with TiO_2 photocatalysis: new materials and recent applications, Electrochim. Acta 84 (2012) 103–111.
[88] H. Lin, C. Huang, W. Li, C. Ni, S. Shah, Y. Tseng, Size dependency of nanocrystalline TiO_2 on its optical property and photocatalytic reactivity exemplified by 2-chlorophenol, Appl. Catal. B Environ. 68 (2006) 1–11.
[89] Q. Xiao, J. Zhang, C. Xiao, Z. Si, X. Tan, Solar photocatalytic degradation of methylene blue in carbon-doped TiO_2 nanoparticles suspension, Sol. Energy 82 (2008) 706–713.
[90] J.S. Lee, K.H. You, C.B. Park, Highly photoactive, low bandgap TiO_2 nanoparticles wrapped by graphene, Adv. Mater. 24 (2012) 1084–1088.
[91] F. Sayilkan, M. Asilturk, N. Kiraz, E. Burunkaya, E. Arpac, H. Sayilkan, Photocatalytic antibacterial performance of Sn(4+)-doped TiO(2) thin films on glass substrate, J. Hazard. Mater. 162 (2009) 1309–1316.
[92] X. Lin, F. Rong, X. Ji, D. Fu, C. Yuan, Preparation and enhanced visible light photocatalytic activity of N-doped titanate nanotubes by loaded with Ag for the degradation of X-3B, Solid State Sci. 13 (2011) 1424–1428.
[93] J. Wang, X. Liu, R. Li, P. Qiao, L. Xiao, J. Fan, TiO_2 nanoparticles with increased surface hydroxyl groups and their improved photocatalytic activity, Catal. Commun. 19 (2012) 96–99.

[94] A. Rahimpour, S.S. Madaeni, A.H. Taheri, Y. Mansourpanah, Coupling TiO_2 nanoparticles with UV irradiation for modification of polyethersulfone ultrafiltration membranes, J. Membr. Sci. 313 (2008) 158–169.
[95] H. Song, J. Shao, Y. He, B. Liu, X. Zhong, Natural organic matter removal and flux decline with PEG–TiO_2-doped PVDF membranes by integration of ultrafiltration with photocatalysis, J. Membr. Sci. 405–406 (2012) 48–56.
[96] X. Cao, J. Ma, X. Shi, Z. Ren, Effect of TiO_2 nanoparticle size on the performance of PVDF membrane, Appl. Surf. Sci. 253 (2006) 2003–2010.
[97] T.-H. Bae, T.-M. Tak, Effect of TiO_2 nanoparticles on fouling mitigation of ultrafiltration membranes for activated sludge filtration, J. Membr. Sci. 249 (2005) 1–8.
[98] B. Rajaeian, A. Rahimpour, M.O. Tade, S. Liu, Fabrication and characterization of polyamide thin film nanocomposite (TFN) nanofiltration membrane impregnated with TiO_2 nanoparticles, Desalination 313 (2013) 176–188.
[99] M.-L. Luo, J.-Q. Zhao, W. Tang, C.-S. Pu, Hydrophilic modification of poly(ether sulfone) ultrafiltration membrane surface by self-assembly of TiO_2 nanoparticles, Appl. Surf. Sci. 249 (2005) 76–84.
[100] X. Zhao, Y. Su, Y. Liu, R. Zhang, Z. Jiang, Multiple antifouling capacities of hybrid membranes derived from multifunctional titania nanoparticles, J. Membr. Sci. 495 (2015) 226–234.
[101] R.-X. Zhang, L. Braeken, P. Luis, X.-L. Wang, B. Van der Bruggen, Novel binding procedure of TiO_2 nanoparticles to thin film composite membranes via self-polymerized polydopamine, J. Membr. Sci. 437 (2013) 179–188.
[102] H.S. Lee, S.J. Im, J.H. Kim, H.J. Kim, J.P. Kim, B.R. Min, Polyamide thin-film nanofiltration membranes containing TiO_2 nanoparticles, Desalination 219 (2008) 48–56.
[103] T.-H. Bae, I.-C. Kim, T.-M. Tak, Preparation and characterization of fouling-resistant TiO_2 self-assembled nanocomposite membranes, J. Membr. Sci. 275 (2006) 1–5.
[104] F. Shi, Y. Ma, J. Ma, P. Wang, W. Sun, Preparation and characterization of PVDF/TiO_2 hybrid membranes with ionic liquid modified nano-TiO_2 particles, J. Membr. Sci. 427 (2013) 259–269.
[105] F. Zhang, W. Zhang, Y. Yu, B. Deng, J. Li, J. Jin, Sol–gel preparation of PAA-g-PVDF/TiO_2 nanocomposite hollow fiber membranes with extremely high water flux and improved antifouling property, J. Membr. Sci. 432 (2013) 25–32.
[106] V. Vatanpour, S.S. Madaeni, A.R. Khataee, E. Salehi, S. Zinadini, H.A. Monfared, TiO_2 embedded mixed matrix PES nanocomposite membranes: influence of different sizes and types of nanoparticles on antifouling and performance, Desalination 292 (2012) 19–29.
[107] G. Wu, S. Gan, L. Cui, Y. Xu, Preparation and characterization of PES/TiO_2 composite membranes, Appl. Surf. Sci. 254 (2008) 7080–7086.
[108] Y. Yang, H. Zhang, P. Wang, Q. Zheng, J. Li, The influence of nano-sized TiO_2 fillers on the morphologies and properties of PSF UF membrane, J. Membr. Sci. 288 (2007) 231–238.
[109] Q. Chang, J.-e. Zhou, Y. Wang, J. Liang, X. Zhang, S. Cerneaux, X. Wang, Z. Zhu, Y. Dong, Application of ceramic microfiltration membrane modified by nano-TiO_2 coating in separation of a stable oil-in-water emulsion, J. Membr. Sci. 456 (2014) 128–133.
[110] A.Š. Vuk, R. Ješe, B. Orel, G. Draži, The effect of surface hydroxyl groups on the adsorption properties of nanocrystalline TiO_2 film, Int. J. Photoenergy 7 (2005) 163–168.
[111] J.-H. Kim, H.-I. Lee, Effect of surface hydroxyl groups of pure TiO_2 and modified TiO_2 on the photocatalytic oxidation of aqueous cyanide, Korean J. Chem. Eng. 21 (2004) 116–122.
[112] J.S. Thayer, Relativistic effects and the chemistry of the heavier main group elements, in: M. Barysz, Y. Ishikawa (Eds.), Relativistic Methods for Chemists, Springer Science+Business Media B.V, Netherlands, 2010.
[113] M. Jansen, Effects of relativistic motion of electrons on the chemistry of gold and platinum, Solid State Sci. 7 (2005) 1464–1474.
[114] M. Rai, A. Yadav, A. Gade, Silver nanoparticles as a new generation of antimicrobials, Biotechnol. Adv. 27 (2009) 76–83.
[115] Q. Li, S. Mahendra, D.Y. Lyon, L. Brunet, M.V. Liga, D. Li, P.J. Alvarez, Antimicrobial nanomaterials for water disinfection and microbial control: potential applications and implications, Water Res. 42 (2008) 4591–4602.

[116] J.S. Taurozzi, H. Arul, V.Z. Bosak, A.F. Burban, T.C. Voice, M.L. Bruening, V.V. Tarabara, Effect of filler incorporation route on the properties of polysulfone–silver nanocomposite membranes of different porosities, J. Membr. Sci. 325 (2008) 58–68.
[117] C. Piyadasa, H.F. Ridgway, T. Yeager, S.R. Gray, M.B. Stewart, J.D. Orbell, The application of electromagnetic fields to the control of the scaling and biofouling of reverse osmosis membranes – a review, Water Sci. Technol. 73 (2016) 1371–1377.
[118] I. Sondi, B. Salopek-Sondi, Silver nanoparticles as antimicrobial agent: a case study on *E. coli* as a model for Gram-negative bacteria, J. Colloid Interface Sci. 275 (2004) 177–182.
[119] A.J. Kora, R. Manjusha, J. Arunachalam, Superior bactericidal activity of SDS capped silver nanoparticles: synthesis and characterization, Mater. Sci. Eng. C 29 (2009) 2104–2109.
[120] J.H. Byeon, Y.W. Kim, A novel polyol method to synthesize colloidal silver nanoparticles by ultrasonic irradiation, Ultrason. Sonochem. 19 (2012) 209–215.
[121] I.A. Wani, S. Khatoon, A. Ganguly, J. Ahmed, A.K. Ganguli, T. Ahmad, Silver nanoparticles: large scale solvothermal synthesis and optical properties, Mater. Res. Bull. 45 (2010) 1033–1038.
[122] I.A. Wani, A. Ganguly, J. Ahmed, T. Ahmad, Silver nanoparticles: ultrasonic wave assisted synthesis, optical characterization and surface area studies, Mater. Lett. 65 (2011) 520–522.
[123] C. Luo, Y. Zhang, X. Zeng, Y. Zeng, Y. Wang, The role of poly(ethylene glycol) in the formation of silver nanoparticles, J. Colloid Interface Sci. 288 (2005) 444–448.
[124] V.K. Sharma, R.A. Yngard, Y. Lin, Silver nanoparticles: green synthesis and their antimicrobial activities, Adv. Colloid Interface Sci. 145 (2009) 83–96.
[125] I. Sawada, R. Fachrul, T. Ito, Y. Ohmukai, T. Maruyama, H. Matsuyama, Development of a hydrophilic polymer membrane containing silver nanoparticles with both organic antifouling and antibacterial properties, J. Membr. Sci. 387–388 (2012) 1–6.
[126] V. Vatanpour, A. Shockravi, H. Zarrabi, Z. Nikjavan, A. Javadi, Fabrication and characterization of anti-fouling and anti-bacterial Ag-loaded graphene oxide/polyethersulfone mixed matrix membrane, J. Ind. Eng. Chem. 30 (2015) 342–352.
[127] H.L. Yang, J.C. Lin, C. Huang, Application of nanosilver surface modification to RO membrane and spacer for mitigating biofouling in seawater desalination, Water Res. 43 (2009) 3777–3786.
[128] J. Yin, Y. Yang, Z. Hu, B. Deng, Attachment of silver nanoparticles (AgNPs) onto thin-film composite (TFC) membranes through covalent bonding to reduce membrane biofouling, J. Membr. Sci. 441 (2013) 73–82.
[129] K.K. Kuorwel, M.J. Cran, J.D. Orbell, S. Buddhadasa, S.W. Bigger, Review of mechanical properties, migration, and potential applications in active food packaging systems containing nanoclays and nanosilver, Compr. Rev. Food Sci. Food Saf. 14 (2015) 411–430.
[130] M. Ghosh, J. Manivannan, S. Sinha, A. Chakraborty, S.K. Mallick, M. Bandyopadhyay, A. Mukherjee, In vitro and in vivo genotoxicity of silver nanoparticles, Mutat. Res. 749 (2012) 60–69.
[131] S. Grosse, L. Evje, T. Syversen, Silver nanoparticle-induced cytotoxicity in rat brain endothelial cell culture, Toxicol. In Vitro 27 (2013) 305–313.
[132] R.P. Singh, P. Ramarao, Cellular uptake, intracellular trafficking and cytotoxicity of silver nanoparticles, Toxicol. Lett. 213 (2012) 249–259.
[133] H.E. Bergna, Colloid chemistry of silica – an overview, in: The Colloid Chemistry of Silica, Advances in Chemistry 234 (1994) 1–47.
[134] L.T. Zhuravlev, The surface chemistry of amorphous silica. Zhuravlev model, Colloids Surf. A Physicochem. Eng. Asp. 173 (2000) 1–38.
[135] M.C. Duke, J.C.D. da Costa, D.D. Do, P.G. Gray, G.Q. Lu, Hydrothermally robust molecular sieve silica for wet gas separation, Adv. Funct. Mater. 16 (2006) 1215–1220.
[136] L. Peng, W. Qisui, L. Xi, Z. Chaocan, Investigation of the states of water and OH groups on the surface of silica, Colloids Surf. A Physicochem. Eng. Asp. 334 (2009) 112–115.
[137] J.T. Yates, Water interactions with silica surfaces: a big role for surface structure, Surf. Sci. 565 (2004) 103–106.
[138] S.K. Parida, S. Dash, S. Patel, B.K. Mishra, Adsorption of organic molecules on silica surface, Adv. Colloid Interface Sci. 121 (2006) 77–110.
[139] J. Yang, E. Wang, Reaction of water on silica surfaces, Curr. Opin. Solid State Mater. Sci. 10 (2006) 33–39.

[140] K.S. Rao, K. El-Hami, T. Kodaki, K. Matsushige, K. Makino, A novel method for synthesis of silica nanoparticles, J. Colloid Interface Sci. 289 (2005) 125–131.
[141] D.L. Green, J.S. Lin, Y.-F. Lam, M.Z.C. Hu, D.W. Schaefer, M.T. Harris, Size, volume fraction, and nucleation of Stober silica nanoparticles, J. Colloid Interface Sci. 266 (2003) 346–358.
[142] S.K. Park, K.D. Kim, H.T. Kim, Preparation of silica nanoparticles: determination of the optimal synthesis conditions for small and uniform particles, Colloids Surf. A Physicochem. Eng. Asp. 197 (2002) 7–17.
[143] S.H. Wu, C.Y. Mou, H.P. Lin, Synthesis of mesoporous silica nanoparticles, Chem. Soc. Rev. 42 (2013) 3862–3875.
[144] M. Duke, Carbonised template molecular sieve silica membranes in fuel processing systems: permeation, hydrostability and regeneration, J. Membr. Sci. 241 (2004) 325–333.
[145] A.L. Ahmad, M.A. Majid, B.S. Ooi, Functionalized PSf/SiO_2 nanocomposite membrane for oil-in-water emulsion separation, Desalination 268 (2011) 266–269.
[146] J.-n. Shen, H.-m. Ruan, L.-g. Wu, C.-j. Gao, Preparation and characterization of PES–SiO_2 organic–inorganic composite ultrafiltration membrane for raw water pretreatment, Chem. Eng. J. 168 (2011) 1272–1278.
[147] L.-Y. Yu, Z.-L. Xu, H.-M. Shen, H. Yang, Preparation and characterization of PVDF–SiO_2 composite hollow fiber UF membrane by sol–gel method, J. Membr. Sci. 337 (2009) 257–265.
[148] W. Chen, Y. Su, L. Zhang, Q. Shi, J. Peng, Z. Jiang, In situ generated silica nanoparticles as pore-forming agent for enhanced permeability of cellulose acetate membranes, J. Membr. Sci. 348 (2010) 75–83.
[149] J. Yin, J. Zhou, Novel polyethersulfone hybrid ultrafiltration membrane prepared with SiO_2-g-(PDMAEMA-co-PDMAPS) and its antifouling performances in oil-in-water emulsion application, Desalination 365 (2015) 46–56.
[150] J. Yin, E.-S. Kim, J. Yang, B. Deng, Fabrication of a novel thin-film nanocomposite (TFN) membrane containing MCM-41 silica nanoparticles (NPs) for water purification, J. Membr. Sci. 423–424 (2012) 238–246.
[151] J. Huang, K. Zhang, K. Wang, Z. Xie, B. Ladewig, H. Wang, Fabrication of polyethersulfone-mesoporous silica nanocomposite ultrafiltration membranes with antifouling properties, J. Membr. Sci. 423–424 (2012) 362–370.
[152] H. Wu, B. Tang, P. Wu, Optimizing polyamide thin film composite membrane covalently bonded with modified mesoporous silica nanoparticles, J. Membr. Sci. 428 (2013) 341–348.
[153] I.Y. Kim, E. Joachim, H. Choi, K. Kim, Toxicity of silica nanoparticles depends on size, dose, and cell type, Nanomed. Nanotechnol. Biol. Med. 11 (2015) 1407–1416.
[154] W. Lin, Y.W. Huang, X.D. Zhou, Y. Ma, In vitro toxicity of silica nanoparticles in human lung cancer cells, Toxicol. Appl. Pharmacol. 217 (2006) 252–259.
[155] L. Clement, A. Zenerino, C. Hurel, S. Amigoni, E. Taffin de Givenchy, F. Guittard, N. Marmier, Toxicity assessment of silica nanoparticles, functionalised silica nanoparticles, and HASE-grafted silica nanoparticles, Sci. Total Environ. 450–451 (2013) 120–128.
[156] D.S. Maciver, H.H. Tobin, R.T. Barth, Catalytic aluminas I. Surface chemistry of eta and gamma alumina, J. Catal. 2 (1963) 485–497.
[157] M. Trueba, S.P. Trasatti, γ-Alumina as a support for catalysts: a review of fundamental aspects, Eur. J. Inorg. Chem. 2005 (2005) 3393–3403.
[158] E. Yalamaç, A. Trapani, S. Akkurt, Sintering and microstructural investigation of gamma–alpha alumina powders, Eng. Sci. Technol. Int. J. 17 (2014) 2–7.
[159] V. Piriyawong, V. Thongpool, P. Asanithi, P. Limsuwan, Preparation and characterization of alumina nanoparticles in deionized water using laser ablation technique, J. Nanomater. 2012 (2012) 1–6.
[160] L. Yan, Y. Li, C. Xiang, S. Xianda, Effect of nano-sized Al_2O_3-particle addition on PVDF ultrafiltration membrane performance, J. Membr. Sci. 276 (2006) 162–167.
[161] L. Yan, S. Hong, M.L. Li, Y.S. Li, Application of the Al_2O_3–PVDF nanocomposite tubular ultrafiltration (UF) membrane for oily wastewater treatment and its antifouling research, Sep. Purif. Technol. 66 (2009) 347–352.

[162] N. Maximous, G. Nakhla, W. Wan, K. Wong, Preparation, characterization and performance of Al_2O_3/PES membrane for wastewater filtration, J. Membr. Sci. 341 (2009) 67–75.
[163] F. Liu, M.R.M. Abed, K. Li, Preparation and characterization of poly(vinylidene fluoride) (PVDF) based ultrafiltration membranes using nano γ-Al_2O_3, J. Membr. Sci. 366 (2011) 97–103.
[164] X.S. Yi, S.L. Yu, W.X. Shi, N. Sun, L.M. Jin, S. Wang, B. Zhang, C. Ma, L.P. Sun, The influence of important factors on ultrafiltration of oil/water emulsion using PVDF membrane modified by nano-sized TiO_2/Al_2O_3, Desalination 281 (2011) 179–184.
[165] Q. Chang, J.-e. Zhou, Y. Wang, J. Wang, G. Meng, Hydrophilic modification of Al_2O_3 microfiltration membrane with nano-sized γ-Al_2O3 coating, Desalination 262 (2010) 110–114.
[166] I.M. Sadiq, S. Pakrashi, N. Chandrasekaran, A. Mukherjee, Studies on toxicity of aluminum oxide (Al_2O_3) nanoparticles to microalgae species: Scenedesmus sp. and Chlorella sp., J. Nanopart. Res. 13 (2011) 3287–3299.
[167] A. Elijius, Study of mechanisms of phytotoxicity of alumina nanoparticles, in: Materials Science and Engineering, New Jersey Institute of Technology, New Jersey, 2011.
[168] R.D. Holtz, W.D. Kovacs, An Introduction to Geotechnical Engineering, Prentice-Hall, New Jersey, 1981.
[169] J. Barrault, M. Abdellaoui, C. Bouchoule, A. Majesté, J.M. Tatibouët, A. Louloudi, N. Papayannakos, N.H. Gangas, Catalytic wet peroxide oxidation over mixed (Al–Fe) pillared clays, Appl. Catal. B Environ. 27 (2000) L225–L230.
[170] E.G. Garrido-Ramírez, B.K.G. Theng, M.L. Mora, Clays and oxide minerals as catalysts and nanocatalysts in Fenton-like reactions—a review, Appl. Clay Sci. 47 (2010) 182–192.
[171] D. Shah, P. Maiti, E. Gunn, D.F. Schmidt, D.D. Jiang, C.A. Batt, E.P. Giannelis, Dramatic enhancements in toughness of polyvinylidene fluoride nanocomposites via nanoclay directed crystal structure and morphology, Adv. Mater. 16 (2004) 1173–1177.
[172] C.Y. Lai, A. Groth, S. Gray, M. Duke, Enhanced abrasion resistant PVDF/nanoclay hollow fibre composite membranes for water treatment, J. Membr. Sci. 449 (2014) 146–157.
[173] C.Y. Lai, A. Groth, S. Gray, M. Duke, Preparation and characterization of poly(vinylidene fluoride)/nanoclay nanocomposite flat sheet membranes for abrasion resistance, Water Res. 57 (2014) 56–66.
[174] L. Priya, J.P. Jog, Polymorphism in Intercalated poly(vinylidene fluoride)/clay nanocomposites, J. Appl. Polym. Sci. 89 (2003) 2036–2040.
[175] H. Rajabi, N. Ghaemi, S.S. Madaeni, P. Daraei, M.A. Khadivi, M. Falsafi, Nanoclay embedded mixed matrix PVDF nanocomposite membrane: preparation, characterization and biofouling resistance, Appl. Surf. Sci. 313 (2014) 207–214.
[176] Y. Zhang, J. Zhao, H. Chu, X. Zhou, Y. Wei, Effect of modified attapulgite addition on the performance of a PVDF ultrafiltration membrane, Desalination 344 (2014) 71–78.
[177] S.-S. Lin, M.D. Gurol, Catalytic decomposition of hydrogen peroxide on iron oxide: kinetics, mechanism, and implications, Environ. Sci. Technol. 32 (1998) 1417–1423.
[178] Z.-Q. Huang, K. Chen, S.-N. Li, X.-T. Yin, Z. Zhang, H.-T. Xu, Effect of ferrosoferric oxide content on the performances of polysulfone–ferrosoferric oxide ultrafiltration membranes, J. Membr. Sci. 315 (2008) 164–171.
[179] Z.-Q. Huang, L. Chen, K. Chen, Z. Zhang, H.-T. Xu, A novel method for controlling the sublayer microstructure of an ultrafiltration membrane: the preparation of the PSF-Fe_3O_4 ultrafiltration membrane in a parallel magnetic field, J. Appl. Polym. Sci. 117 (2010) 1960–1968.
[180] Q. Yang, H.H. Himstedt, M. Ulbricht, X. Qian, S. Ranil Wickramasinghe, Designing magnetic field responsive nanofiltration membranes, J. Membr. Sci. 430 (2013) 70–78.
[181] M.M. Ling, T.-S. Chung, Desalination process using super hydrophilic nanoparticles via forward osmosis integrated with ultrafiltration regeneration, Desalination 278 (2011) 194–202.

CHAPTER 8

Prospects and State-of-the-Art of Carbon Nanotube Membranes in Desalination Processes

Nozipho N. Gumbi*,†, Tumelo G. Tshabalala*, Sabelo D. Mhlanga*, Bhekie B. Mamba*, Andrea I. Schäfer†, Edward N. Nxumalo*
*University of South Africa, Florida, Johannesburg, South Africa
†Karlsruhe Institute of Technology (KIT), Karlsruhe, Germany

Contents

1. INTRODUCTION

Over the years the world has witnessed a shift toward research efforts aimed at the exploitation of unconventional and untapped water sources such as wastewater, seawater, and brackish ground water in order to meet the growing global water demand.

Desalination Sustainability
http://dx.doi.org/10.1016/B978-0-12-809791-5.00008-0

By undergoing various treatment stages, these untapped water sources can be converted into potable water and are regarded as "new" water sources. Among all of these sources, seawater offers a very attractive alternative source for freshwater since it can potentially provide an abundant and unlimited supply for various human, agricultural, and industrial needs provided the salt gets removed in a sustainable manner.

Desalination technologies are used to convert undesirable and salty seawater into potable and useable water [1]. Seawater desalination using membrane-based processes, particularly reverse osmosis (RO) membranes, are highly favored over thermally based processes, especially in energy-stressed countries, because of their lower energy consumption [2,3]. Thermally based desalination processes rely on the use of heat because of the need to evaporate water prior to condensation [4]. On the contrary, in RO desalination technologies, pressure is applied to force water molecules to permeate through a semipermeable membrane while preventing the passage of salts. Therefore seawater desalination using RO membranes remains an energy-efficient reference point and a standard of comparison for newer or evolving desalination technologies [2].

One of the greatest issues existing in both seawater and brackish water desalination using currently available RO membranes is the lack of sustainable, robust, energy-efficient, and cost-effective membranes [5]. Indeed, this is a challenging task that requires innovative solutions with feasible implementations. Before attempting to correct these challenges, it is important to have adequate knowledge and understanding of the minimum amount of energy required to separate pure water from seawater. For example, the theoretical minimum energy of desalination for seawater at 35,000 ppm salt concentration and at a typical recovery of 50% was 1.06 kWh/m in 2011 [2]. This provides a benchmark for comparison with recently crafted technologies and helps guide future efforts aimed at reducing the energy demand for desalination processes [2].

Nanotechnology enabled or simply nano-enabled membranes are increasingly gaining popularity as promising candidates for desalination applications. These nano-enabled membranes rely on the incorporation of various types of nanomaterials onto conventional polymeric membranes used in desalination or other processes such as ultrafiltration. The main aim of using nanomaterials is to overcome the challenges that conventional membranes used in water desalination are often faced with, such as high fouling propensity, trade-off between their selectivity and permeability, as well their high energy consumption during the desalination process [5]. In particular, carbon nanotube (CNT)-incorporated polymeric membranes are one of the most widely studied nano-enabled membranes. CNTs consist of single or multiple layers of graphene sheets rolled into a tubular structure and can have diameters ranging from 1 to 2 nm for single-walled CNTs (SWCNTs) or 2–25 nm for multiwalled CNTs (MWCNTs) [6]. They are known to possess a unique combination of structural and physicochemical properties owing to their nanoscale dimensions: high volume-to-surface ratio, small inner diameters, antimicrobial properties, frictionless surfaces for rapid fluid flow, and many others [7].

The incorporation of CNTs onto polymeric membranes has shown to result in membranes with (i) improved mechanical and thermal stability, (ii) excellent hydrophilic and antifouling properties, (iii) controllable pore size diameters, and (iv) improved selectivity and permeability [8–10]. Currently, there are different views in the research area involving the use of newly emerging CNT-based membranes in desalination processes. These diverse views are centered on whether CNT-based membranes; particularly, the vertically aligned (VA) CNT membranes are capable of reducing the energy needs of the desalination processes owing to their ultrahigh water permeabilities [3]. The ultrahigh water permeability of CNT membranes is believed to help reduce the amount of pressure or energy needed to drive pure water molecules across the semipermeable membrane, whereas the energy consumption of a desalination process is determined by the need to bring the feed volume to a pressure equal to the osmotic pressure of the concentrate [2]. This factor suggests that regardless of how permeable a membrane may be, the applied pressure cannot be reduced to below the osmotic pressure of the concentrate or, more precisely, the osmotic pressure of the boundary layer forming at the membrane surface.

Furthermore, it should be emphasized that operating at high water fluxes generally leads to high membrane fouling; that is, at high fluxes, the effective concentration of the solutes or foulants near the membrane surface increases. Subsequently, the rate of foulant deposition on the membrane surface increases [11], which is a result of the greater permeation drag force that is experienced by the foulant toward the membrane surface [12,13]. Therefore, the ultrahigh permeability characteristic of CNT membranes could assist in the reduction of capital costs needed to run the desalination process, because of the reduced membrane area that will be required to achieve maximum water flux while rejecting the transportation of salts. It is, however, important to accentuate that flux is not "everything" since there are many other membrane systems that function better when operated at lower fluxes.

CNT-based membranes may be leveraged in RO membrane material modification to overcome the issue of fouling or biofouling. Biofouling, which is caused by growth of biofilm on the surface of a thin film composite (TFC) membrane, hinders the performance of the membrane, thus limiting the membranes' prolonged use. Biological foulants such as bacteria, fungi, and algae grow in large quantities on the membrane surface, thereby inhibiting permeation through the membrane surface [14]. On the other hand, the use of strong oxidizing agents such chlorine and ozone to remove the adsorbed biofilm may be detrimental to the membrane's structure as they are capable of degrading the polyamide layer on TFC membranes [1,15]. Another limitation of conventional TFC RO membranes involves the ultimate trade-off between permeability and selectivity; i.e., it is practically impossible to further increase the membrane's selectivity without compromising permeability.

CNT-based membranes possess antibacterial properties that are beneficial in combating biofouling upon direct contact with microorganisms. However, the antimicrobial mechanism of CNTs is not yet fully understood. Many authors present conflicting

and diverse mechanistic models. For example, Vecitus et al., proposed a three-step mechanism for SWCNTs that includes three sequential steps: (i) initial contact between SWCNTs and bacteria, (ii) perturbation of the membrane cell, and (iii) electronic structure-dependent bacterial oxidation [16]. Several reports and reviews have been documented reporting on the use of CNTs in mitigating fouling in TFC RO membranes [17–20]. However, most of these studies were tested only on bench-scale systems. There is therefore still a need for further development and upscaling of CNT membrane processes to accurately determine their benefits. Furthermore, membrane scientists argue that biocidal properties alone do not demonstrate that a membrane has a low fouling propensity. For instance, in a staged array membrane configuration, the destroyed microbes may necessitate an additional step for membrane cleaning.

The issue of selectivity-permeability trade-off could be avoided in CNT membranes due to the ability of selectively adding functional group moieties at the CNT pore openings that are capable of rejecting salt ions while maintaining ultrafast water transport inside the nanotubes [21,22]. Such gate-keeper-controlled chemical interactions are unique for CNT-based membranes, as first demonstrated by Hinds et al. [21]. The addition of biotin functional groups at the CNT opening, for example reduced the $Ru(NH_3)_6^{3+}$ flux by a factor of 5.5, and this was further reduced by a factor of 15 when streptavidin was added to the biotin tether [21]. This result formed the basis for the separation or restriction of ionic flow from a solution containing an analyte of interest, and it can be used as a guiding tool for further control of pore dimensions.

A number of studies on the potentiality of VA-CNT membranes in desalination processes have been based on molecular dynamic (MD) simulations and very few report on their experimental feasibility. This is particularly so because of the complexities encountered in synthesis procedures for aligned CNT membranes, which are the most promising candidates, rather than mixed-matrix CNT membranes, for desalination based on the findings from simulation studies. These issue are discussed in deeper detail later in this chapter.

With such challenges, a great deal of work lies ahead before full realization and exploitation of CNT-based membranes for desalination applications. This chapter presents an overview of the manufacture, physicochemical properties, and effective application of carbon nanotube (CNT) membranes in desalination technologies. Ultimately, the chapter seeks to summarize the current knowledge pertinent to CNT exploitation in desalination, explain the extent to which the fluid transport properties and chemical functionalities in CNTs necessitate high water fluxes, and describe the controllable salt rejection required for desalination. Factors that influence the cost of CNT membranes, which ultimately translates to the cost of desalination using CNT membranes, are also discussed. Last and maybe most important, the sustainability of CNT membranes as a solution to current desalination problems is evaluated.

2. TYPES OF CNTs USED IN MEMBRANE FABRICATION

2.1 CNT Configurations

Since their discovery in 1991 by Iijima [23], carbon nanotubes have been widely studied and applied in various disciplines, including in the water treatment field as adsorbent materials or in membrane modification for the removal of a wide range of organic and inorganic pollutants from water and wastewater [24–27]. This interest is due to a unique combination of the structural and physicochemical properties of carbon nanotubes: high volume-to-surface ratio, small inner diameters, antimicrobial properties, frictionless surfaces for rapid fluid flow, and many others [7]. CNTs are commonly classified as SWCNTs or MWCNTs based on the number of cylindrical graphene sheets organized around the hollow nanotube core (Fig. 1). SWCNTs consist of a single layer of graphene sheet rolled into a tubular structure and have diameters in the range of ~1 to 2 nm, whereas MWCNTs consist of multiple layers of graphene sheets with diameter sizes in the range of ~2 to 25 nm [6]. Most research on CNT-incorporated membranes focuses on MWCNTs and very rarely on SWCNTs, even though these possess the smallest outer diameters. This is because MWCNTs are generally easy to prepare and align using conventional chemical vapor deposition (CVD) methods, and their manufacturing costs are lower than those of SWCNTs. This means that MWCNTs can be produced in the large quantities necessary for industrial-scale applications.

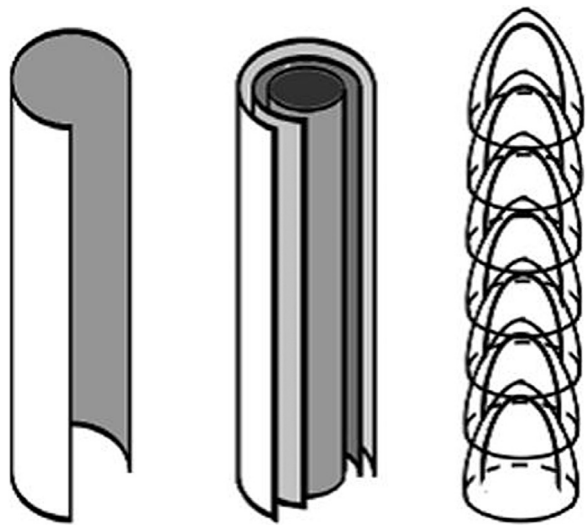

Fig. 1 Sketches depicting structures of (A) SWCNT, (B) MWCNT, and (C) N-CNT (bamboo-shaped CNT). *(Reproduced with permission from S. van Dommele, Nitrogen Doped Carbon Nanotubes: Synthesis, Characterization and Catalysis, Utrecht University, 2008).*

Researchers have attempted to use heteroatom-doped CNTs in the form of nitrogen-doped carbon nanotubes (N-CNTs) for polymer blend membrane modifications. N-CNTs are typically produced by either postsynthesis modification of CNTs with a nitrogen-containing compound such as acetonitrile, melamine, and many others or by in situ incorporation of nitrogen during CNT growth [28]. The use of N-CNTs was intended to improve the compatibility and interaction between CNTs and the polymer material such as (PES) [29]. Performance results of this N-CNT/PES membrane revealed a superior compatibility between the N-CNTs and PES because of the high surface reactivity of N-CNTs compared with pristine CNTs. The differences in the structure of various forms of CNTs commonly used in membrane modification are shown in Fig. 1. These include CNTs with typical tubular configurations and unique "bamboo-shaped" orientations.

Although the use of SWCNTs in membranes would be ideal for sea and brackish water desalination because of their intriguingly small inner diameters, the challenge of aligning SWCNTs vertically remains a serious hindrance [30,31].

MWCNTs are also less expensive to manufacture than their single-walled counterparts; therefore MWCNTs can be produced in large quantities. However, the inner diameters of most MWCNTs range between 3 and 10 nm [32], which means that they fall short of molecular separation applications where extremely small diameters would be more beneficial in achieving effective and efficient separation of molecular species.

Park et al. [32] sought to substitute commercial UF membranes with VA-CNT membranes in water-purification applications. The authors discovered that the solute rejection of membranes was difficult to increase or control because the MWCNTs' inner diameters were difficult to reduce further. Notwithstanding the concerns raised earlier, SWCNTs with diameters close to 1 nm were suggested as a probable solution for increasing salt rejection, provided that they undergo surface modifications to further reduce their pore size to just below 0.6 nm. This is because a hydrated Na^+ is about 0.716 nm and Cl^- 0.664 nm in size.

2.2 CNT Tip Functionalization and Alignment

Functional group moieties can be introduced with ease onto the VA-CNT membranes. In particular, the CNT tips functionalized to reduce or control their pore size diameters. Park et al. [32] functionalized CNT tips of VA-CNT membranes with methacrylate groups by graft polymerization to "gate" the transport of solute compounds [33]. The modified membranes showed better water flux and antifouling properties than the commercial UF membranes. In addition, the solute rejection potential was greatly improved vis-à-vis the control VA-CNT membranes.

Consequently, the use of SWCNTs as membranes is of great interest because of their intriguingly small inner diameters (1–2 nm) that can be useful for sea and brackish water desalination. However, as mentioned before, the challenge of aligning SWCNTs

vertically remains a serious hindrance in their use as membrane filters. Filtration methods have previously been used successfully to align MWCNTs vertically. Recently, the same approach was adopted for the alignment of SWCNTs. Indeed, when shear forces are applied, they propagate the alignment of CNTs perpendicular to the filter substrate in the direction of flow [31].

Kim et al. [30] prepared VA-CNT membranes using a combination of methods, namely filtration and self-assembly of SWCNTs. In their study, functionalized SWCNTs were dispersed in tetrahydrofuran (THF) (Fig. 2, Step 1), and the suspension was filtered through a filtering media such as a polytetrafluoroethylene (PTFE) filter (in Step 2). Their findings showed that the filtration method used facilitated the vertical alignment of CNTs on a porous substrate and that the gas mixture transport through the prepared membranes was much faster than those predicted by Knudsen diffusion.

As shown in Fig. 2 Step 3, the aligned SWCNT/filter is then spin-coated with a dilute solution of a high-mechanical-strength polymer to seal the structure, while allowing most of the nanotube ends to be slightly exposed above the polymer surface [30]. However, microscopic analyses of these membranes revealed that the SWCNTs are encapsulated with additional graphite layers, which signals that during the fabrication process, they are transformed from SWCNTs into MWCNTs. Alternatively, a polymer suspension containing CNTs can be injected into a molded cavity, a die, or a nanochannel to

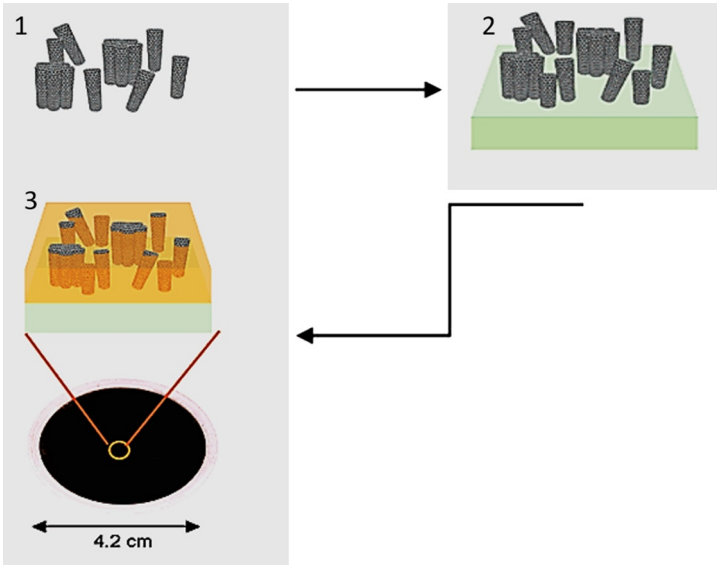

Fig. 2 Schematic representation of the fabrication of VA-CNT membranes by the filtration method. *(Reproduced with permission from S. Kim, J.R. Jinschek, H. Chen, D.S. Sholl, E. Marand, Scalable fabrication of carbon nanotube/polymer nanocomposite membranes for high flux gas transport, Nano Lett. 7 (2007) 2806–2811).*

form a shape of interest. In this way, the CNTs will then change orientation by virtue of the flow that is induced by the shear forces applied [31].

3. TYPES OF CNT COMPOSITE MEMBRANES

CNT-incorporated membranes are promising tools for the treatment of conventional and emerging contaminants in water as well as for sea and brackish water desalination using RO systems. This option is due to the presence of nanoporous channels that allow for the passage of large volumes of water while rejecting the permeation of "unwanted" species/ions. These CNT-based membranes and in particular the VA-CNT membrane systems have an enormous potential to improve the selectivity of RO membranes that are commonly used in seawater desalination processes, owing to their dynamic molecular sieving and separation mechanism [18].

There are two common types of CNT-based membranes: CNT mixed-matrix membranes (CNT MMMs), which are typically mixed matrices of CNTs and flexible polymers, and VA-CNT membranes, which could either be CNT "straws" protruding from a nonporous polymer or high-density, aligned CNT arrays.

Fig. 3 shows the typical differences in the structures, water transport, and solute rejection of the two types of CNT membranes presented in this chapter. In the VA-CNT membranes, the CNTs are arranged in an upright position (perpendicular) to the membrane surface. On the contrary, for mixed composite CNT membranes, CNTs are dispersed in the matrix forming part of the membrane's top layer, thereby contributing to the hydrophilic and surface properties.

In latter sections, the differences of these CNT membrane types and the correlations between the structural morphologies and permeation properties thereof will be probed and their water transport and solute rejection capacities investigated. We will also explore their environmental sustainability and commercial availability.

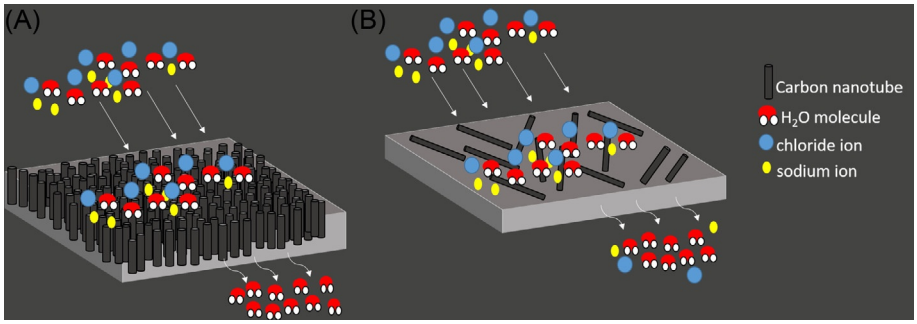

Fig. 3 Water transport and solute rejection of CNT membranes through (A) vertically aligned CNT membranes and (B) CNT mixed-matrix membranes.

4. FABRICATION PROCESSES FOR CNT MEMBRANES FOR DESALINATION

Table 1 depicts the different fabrication techniques for CNT-based membranes normally utilized in a desalination process. Work carried out by different workers fabricating CNT membranes is compared and contrasted with respect to manufacturing process, support material used, CNT alignment or nonalignment, characterization tools used, and performance properties. For the VA-CNT membranes, the process normally entails synthesis of VA-CNT arrays on a suitable substrate by making use of the conventional CVD method prior to the addition of an impermeable polymer such as polystyrene (as a support). On the other hand, the preparation of CNT MMMs involves the dispersion of CNTs in a solvent and mixing with a suitable polymer prior to casting the solution on a plate typically by a phase inversion method [35].

Although tremendous progress has been made in the lab-scale production of CNT MMMs, experimental work involving the fabrication of VA-CNT membranes is still in its infancy because the production systems are challenging and onerous. These issues are dealt with appropriately in later sections of this chapter.

Several reviews dedicated to CNT-based membranes (MMMs and VA-CNT membranes) and their potentiality in desalination applications have been documented. For example, Das et al. [34] comprehensively reviewed the potential role of CNT membranes in seawater and brackish water desalination. The function of CNTs in the membrane technology arena was analyzed by looking at the studies focusing on the fabrication and functionalization of CNT membranes for desalination purposes and how CNT membranes compare in properties and performance behavior with conventional membrane processes. These differences are tabulated in Table 2 and indicate that unlike CNT MMMs (in which CNTs are mixed in either a MF, UF, or NF membrane matrix), VA-CNT membranes are a unique membrane type because of their outstanding properties, including among others, ultrafast water transport and self-cleaning properties.

CNTs have the ability to be selectivity functionalized at their pore openings to enhance their salt rejection capacities and their ability to remove various micropollutants present in water. Thus CNT membranes have been envisaged as potential candidates to replace both RO and NF membranes, because CNT membranes offer minimal energy consumption by lowering the applied pressure to drive desalting of solutions [34]. However, no single method is capable of alleviating the global water pollution problems on its own, which means that the existing water-treatment technologies are not sufficient to provide 100% pure water. Therefore a combination of methods, including those that have advanced from nanotechnology through the use of carbon nanotube membranes, can be a more viable approach.

Manawi and coworkers [36] recently assessed the potentiality of carbon-based nanomaterials (including CNTs, graphene, graphene oxide, carbon nanofibers, MXene, carbide-derived carbon, and fullerenes) in membrane fabrication for water treatment and desalination. CNTs, in particular, were identified as promising candidates to overcome the issues of fouling (and in particular biofouling) that membranes used in RO

Table 1 Different fabrication techniques for CNT membranes

	Polymer infiltration/ encapsulation Hinds et al. [21]	**Liquid-induced densification Yu et al. [34]**	**Self-assembly and filtration method Kim et al. [30].**	**Phase inversion mixed-matrix method Celik et al. [8].**
CNT membrane type	VA-CNT membrane	VA-CNT membrane	VA-CNT membrane	CNT MMM
Manufacture	CNT arrays grown on a silicon wafer substrate Polystyrene infiltrated onto the CNT array Spin-coating and removal of excess polymer HF acid used etch off CNT film from substrate Water-plasma oxidation to open CNT tips	CNT forest grown by water-assisted CVD method Water-etching to detach CNT arrays *N*-hexane introduced into as-grown CNT arrays and dried CNTs collapse near to packing into a rigid body upon liquid evaporation	SWCNTs prepared by arc discharge method and treated with H_2SO_4/HNO_3 acid mixture Amine functionalized SWCNTs dispersed in THF Dope solution filtered through a PTFE membrane filter	MWCNTs treated in H_2SO_4/HNO_3 acid mixture MWCNTs sonicated in NMP followed by addition of PES Dope solution casted on glass plate and immersed in coagulation bath
	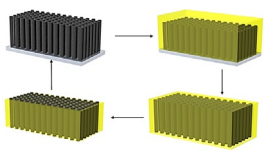	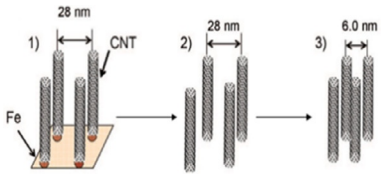	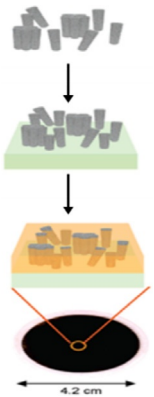	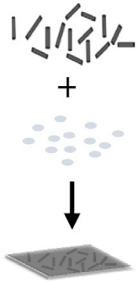

Support	Polystyrene	None	Polytetrafluoroethylene	None
CNT configuration	Vertically aligned	Vertically aligned	Partial alignment	Nonaligned
Characterization	SEM, HRTEM, porometer, electrochemical measurements and others.	TEM, SEM, N_2 desorption experiments and others.	HRTEM, permeation of gas mixtures and others.	SEM, FTIR, contact angle goniometer, cross-flow filtration experiments and others.
Performance	Presence of CNTs increases conductivity of the membrane. Attachment of biotin/streptavidin moiety on the CNT tip allows gating or sieving of $Ru(NH_3)_6^{3+}$ ions.	Densely packed SWCNTs observed from SEM. N_2 gas diffusion is two orders of magnitude higher than predicted by Knudsen and three to seven orders of magnitude higher than for composite membranes.	Rapid gas transport through the CNT membranes that deviates from Knudsen diffusion.	Inclusion of CNTs into the PES membrane increases membrane roughness, surface hydrophilicity, pure water flux, and porosity.

Table 2 Properties of different membrane processes used in water treatment

	MF	UF	NF	RO	VA-CNT	Ref.
Pore size (nm)	>50–500	2–50	<2	0.3–0.6	0.6–10	[21,34,36]
Operating pressure (bar)	0.1–2	<5	3–15	29–100	0.7–2	[32,37,38]
Permeability (L/m^2 h bar)	>1000	10–1000	1.5–30	0.05–15	>1000	[33,37,39]
MWCO (Da)	>300,000	1000–1,000,000	100–1000	100	100	[33,40,41]
Membrane thickness (μm)	50–100	150–300	~0.05	0.1–0.2	0.6–10	[30,42]
%NaCl rejection	–	–	20–80	95 to >99	100	[34,37]
Resistance to fouling and biofouling	Poor. Resistance to fouling can be improved through membrane surface modification with hydrophilic additives.	Poor. Resistance to fouling can be improved through membrane surface modification with hydrophilic additives.	Poor. Resistance to fouling can be improved through membrane surface modification with hydrophilic additives.	Poor. Resistance to fouling can be improved through membrane surface modification with hydrophilic additives.	Very good. CNTs possess antimicrobial properties. Resistance can be further enhanced with membrane surface functionalization.	[18,43]
Application	Removal of solid particles, protozoa, and bacteria.	Removal of viruses and colloids.	Removal of multivalent ions, proteins, dissolved organic matter, and hardness.	Removal of monovalent ions, desalination, water reuse, ultrapure water.	Removal of organic micropollutants and desalination application.	[7,32,37,44]

Adapted from R. Das, M.E. Ali, S.B.A. Hamid, S. Ramakrishna, Z.Z. Chowdhury, Carbon nanotube membranes for water purification: a bright future in water desalination, Desalination 336 (2014) 97–109.

desalination processes are often faced with. This is due to the CNTs ability to effectively destroy bacterial cells upon direct contact. Furthermore, VA-CNT membranes were highlighted to be potentially useful in water desalination because of their remarkably fast fluid transport properties. In as much as high-salt rejection is desired during seawater or brackish water desalination, the desalination process used must still be able to generate reasonable pure water flux on the other side of the semipermeable membrane. Indeed, Elimelech and coworkers [2] caution against the use of ultrahigh permeating membranes in seawater RO desalination processes because concentration polarization as well as membrane fouling are exacerbated at high water fluxes [32]. For VA-CNT membranes to be effectively used for seawater desalination, a redesign of membrane modules will be required such that the preceding factors are taken into account.

Goh et al. [6] wrote a comprehensive review that raises some important questions about the potentiality of nanomaterials in desalination membrane modifications. Questions about whether CNT polymeric membranes will be able to offer high performance and affordable desalination solutions were raised. Ultimately, this review encourages a thorough examination of all research areas and priori focus points before commercialization of this technology, such as looking at economic and environmental concerns with regard to the use of nano-enabled or, better yet, CNT-based polymeric membranes. Toward the end of their review, the authors encouraged environmentalists to work closely with material scientists in understanding and raising awareness of environmental hazards that these nano-enabled membranes may pose for humans.

Ahn et al. [3] documented the fabrication methods for CNT-based membranes and speculated on their potential use in desalination processes. The fundamental differences between the two CNT membrane types are presented in Table 3. Clearly, the limitations

Table 3 Comparison of VA-CNT membranes and mixed matrix CNT membranes

VA-CNT membranes	Mixed-matrix CNT membrane
CNTs are vertically aligned within the membrane	CNTs are irregularly arranged within the polymer matrix
CNTs are densely packed together	Composite layers with polymer membrane and nonwoven support
Water flux through the membrane is extremely fast	Water flux through the membrane is reasonably fast
Functional groups can be conveniently attached at the CNT tips or on the membrane surface to prevent fouling	Low (or anti) fouling membranes
Complex fabrication procedures, less cost-effective	Fabrication processes are convenient, simple, and readily commercializable
May need specially adjusted operation system	Operation similar to that of conventional membrane processes

Adapted from C.H. Ahn, Y. Baek, C. Lee, S.O. Kim, S. Kim, S. Lee, S.-H. Kim, S.S. Bae, J. Park, J. Yoon, Carbon nanotube-based membranes: fabrication and application to desalination, J. Ind. Eng. Chem. 18 (2012) 1551–1559.

that hinder the popularity and commercialization of VA-CNT membranes mainly include the complex fabrication processes used, which makes scaling up of these membranes a challenge. For this reason, more efforts have been directed toward the exploitation of mixed-matrix types of CNT membranes, even though they possess more moderate water fluxes than VA-CNT membranes. In addition, CNT MMMs are made using fabrication procedures that are relatively simple, and therefore CNT MMMs are more likely to be commercialized sooner [3].

5. SOLUTE TRANSPORT PROPERTIES OF CNT MEMBRANES

Molecular dynamic (MD) simulation has been one of the fundamental tools used by researchers to gain insights into the transport behavior of water molecules inside confined CNT channels [37]. As mentioned earlier in this chapter, recent research work involving the use of CNT membranes for desalination has mainly been based on simulation studies. The properties and behavior of fluids when confined at nanolength scales greatly differ from their behavior in bulk form. For example, in the macroscopic world, it would be unexpected for water (a polar compound) to be able to enter and interact with the constricted and hydrophobic CNT pores [38]. However, the first MD simulation studies by Hummer and coworkers showed that despite their hydrophobic nature, SWCNTs can be rapidly filled and emptied with water molecules (forming a column of five water molecules in length inside a nanotube) [39]. Furthermore, the filling and emptying of the CNTs with water molecules can be properly controlled such that water molecules do not remain constricted inside the tubes [39].

One other notable feature associated with CNT fluid transport, as reported by Hummer et al. [39], is that of the changes in the structural configuration of water molecules when inside a confined CNT channel. Inside the channel, the hydrogen-bonded and methodically linked water molecules or simply "water wires" are formed, as depicted in Fig. 4. The formation of these ordered one-dimensional hydrogen-bonded water wires inside the CNTs and at the CNT openings highly resembles those that are formed during water transport by biological channels such as transmembrane protein aquaporins [40,41]. Other similarities between CNT channels and the biological aquaporin channels include their hydrophobic interiors or linings that enable near frictionless and fast water transport [40,42]. Kalra et al. [43] used MD simulation to study molecular transport of water through CNT membranes under the influence of an osmotic gradient. The authors demonstrated that the flow rates within the CNT pores are extremely fast and independent of the length of the nanotubes. It was found that the flow inside these nanotubes was almost frictionless and was restricted only by the events at the entry and exit points of the CNT pores. Nonetheless, the flow rates remain comparable with those of transmembrane aquaporins [43].

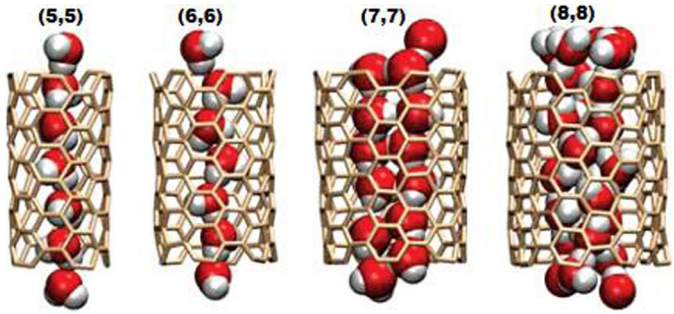

Fig. 4 Molecular dynamic simulation depicting water configuration or formation of "water wires" in differently sized armchair carbon nanotubes. *(Reproduced from B. Corry, Designing carbon nanotube membranes for efficient water desalination, J. Phys. Chem. B 112 (2008) 1427–1434).*

Several macroscopic equations have been used to explain the relationship between fluid flow or transport rate and the pore radius of the CNTs. One of these models is the nonslip Hagen-Poiseuille equation, which can be represented in Eq. (1) as

$$Q_{\mathrm{HP}} = \frac{\pi\left(\frac{d}{2}\right)^4}{8\mu L}\cdot\frac{\Delta P}{L} \tag{1}$$

where Q_{HP} represents the volumetric flow rate, ΔP is the pressure difference across the tube length (L), μ is the viscosity of water, and d is the pore diameter. This equation assumes that fluid flow inside the CNT tubes is laminar and that there is no slip at the boundary layer (i.e., the fluid velocity at the CNT walls is zero) [45]. However, several studies on nanosized hydrophobic pores, such as those of CNT membranes, have shown major deviations from this assumption, with flow enhancements that are orders of magnitude higher than predicted by the continuum Hagen-Poiseuille model.

MD studies on CNT pores reveal that water molecules move freely with large slip inside the CNT walls because of the atomically smooth and hydrophobic interiors of CNTs [44]. The slip length, which is merely the distance that the velocity profile can be extrapolated with to reach zero, is normally used when describing the slip flow of molecules inside CNT walls (Fig. 5).

When Hagen-Poiseuille formalism in Eq. (1) is corrected to include slip-flow conditions, it can be represented in Eq. (2) as

$$Q_{\mathrm{Slip}} = \frac{\pi\left(\frac{d}{2}\right)^4 + 4\left(\frac{d}{2}\right)^3\cdot L_{\mathrm{S}}}{8\mu L}\cdot\frac{\Delta P}{L} \tag{2}$$

where L_{S} is the slip length, which is given in Eq. (3) as

$$L_{\mathrm{S}} = \frac{U_{\mathrm{wall}}}{\mathrm{d}U/\mathrm{d}r} \tag{3}$$

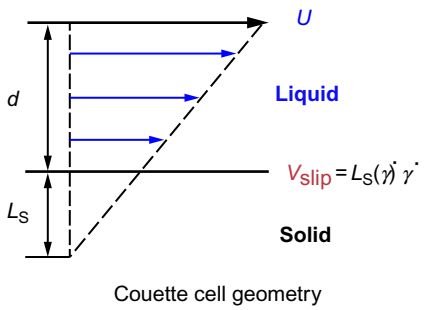

Fig. 5 Illustration of slip length at the liquid/solid interface. *(Reproduced from N.V. Priezjev, A.A. Darhuber, S.M. Troian, Slip behavior in liquid films on surfaces of patterned wettability: comparison between continuum and molecular dynamics simulations, Phys. Rev. E 71 (2005) 041608).*

where U_{wall} is the axial velocity at the wall, and $\mathrm{d}U/\mathrm{d}r$ is the radial velocity gradient at the wall.

Holt et al. [45] applied the slip-flow formalism (Eq. 2) to determine the flow through sub-2-nm CNT membranes. The slip lengths were found to be hundreds of nanometres larger than the pores size and were on the order of the overall size of the system [45]. When the same equation was used to calculate slip length for polycarbonate membranes with 15 nm pore sizes, the slip length was about 5 nm. These findings therefore suggest that slip-flow formalism cannot be used to describe flow through CNT pores in the 1–2 nm size regimes because of confinements in length and partial wetting of the CNT surface [37].

The extremely fast water transport of CNT membranes is therefore favorable for filtration purposes such as NF and RO. However, in the case of RO desalination, the efficiency of the process is determined by three critical factors: capital costs, energy costs, and system operation costs [40]. While there are many speculations about the CNT membranes' potential to greatly reduce the energy costs of RO desalination processes, the minimum energy required to pump water through a semipermeable membrane is governed by the solution's osmotic pressure, that is, osmotic pressure difference between seawater and freshwater [46]. Nonetheless, the high water fluxes of CNT membranes can greatly reduce the primary costs because of the small membrane area required to achieved maximum flux [46]. However, these fluxes do not necessarily affect the energy consumption of the desalination process [46].

In a MD simulation study, Corry [42] simulated water conduction and suitability of differently sized CNTs with armchair-type chirality (5,5), (6,6), (7,7), and (8,8) in water desalination applications. CNT performance was evaluated by calculating salt rejection efficiency (Table 4) [35]. The numbers denoted within parentheses describe the chirality and metallicity of the carbon nanotubes investigated, that is, the manner in which the grapheme sheet was rolled up to form a carbon nanotube [47]. The armchair configuration describes the shape of the hexagons making up the tube as one moves around

Table 4 Water and ion conductance of nanotubes under 209 MPa pressure at 250 mM ion concentration

	Diameter (Å)			Conductance pt pns	
Size	C–C	Internal	Run lengths (ns)	H_2O	Ions
(5,5)	6.6	3.2	10.00	10.4 ± 0.4	0.0
(6,6)	8.1	4.7	20.00	23.3 ± 0.3	0.0
(7,7)	9.3	5.9	25.00	43.7 ± 0.5	0.007 ± 0.005
(8,8)	10.9	7.5	17.00	81.5 ± 1.2	0.137 ± 0.025
(6,6) long	8.1	4.7	10.00	23.4 ± 0.5	0.0

Reproduced from B. Corry, Designing carbon nanotube membranes for efficient water desalination, J. Phys. Chem. B 112 (2008) 1427–1434.

the body of the nanotube and the metallic nature of SWCNTs. The calculations showed that the CNTs led to salt rejection from 100% for (5,5 and 6,6) to 95% and 58% for the wider tube (7,7 and 8,8). Additionally, when the salt rejection efficiencies of the simulated CNT membranes and those of commonly used RO membranes were compared, the membrane comprising (7,7) nanotubes could be expected to obtain 95% desalination at a flow rate over 1500 times that of existing RO membranes [42]. Therefore, more in-depth studies on overcoming the energy costs of desalination processes using CNT membranes are crucial in order to fully realize their applicability in water purification and desalination applications.

From the preceding discussions, it is evident that the incorporation of VA-CNTs onto polymeric membranes has important implications on their transport and separation properties. This is because CNTs provide, among others, the ease of chemical functionalization and doping, low friction, biocompatibility, and controllable pore sizes necessary for fast water transport and the required solute rejection in desalination processes.

6. CHARACTERIZATION TOOLS FOR CNT-BASED MEMBRANES

6.1 Introduction to Techniques used to Probe CNT Membranes

Characterization of CNT-based membranes is typically achieved using similar techniques to those that are normally used to characterize conventional polymer-based membranes. The techniques used include scanning electron microscopy (SEM), transmission electron microscopy (TEM), high-resolution TEM (HRTEM), atomic force microscopy (AFM), streaming potential and surface charge analysis, contact angle analysis, electrochemical impedance spectroscopy (EIS), thermal gravimetric analysis (TGA), attenuated total reflection-Fourier transform infrared spectroscopy (ATR-FTIR), X-ray photoelectron spectroscopy, and many others [48]. It is of vital importance that the different techniques used for the analyses correlate with one another for effective clarification of the morphology and properties of the prepared membrane.

6.2 Microscopic Investigation of CNT membranes

The incorporation of CNTs into membrane matrices is known to drastically transform the morphology of the membranes [49]. These changes can be detected easily by studying the surface properties as well as the internal structure of the membrane (Fig. 5) [50]. Depending on where the SEM image is taken on the membrane, it is possible to visualize and distinguish between the pores located on the membrane top surface and those located in the membrane sublayer. Depending on the phase inversion kinetics that occur during membrane formation, the membrane sublayer may consist of large finger-like structures (referred to as macrovoids) or it can consists of sponge-like structure made up of many small pores. For example, in order to effectively view the membranes' cross-sectional morphology (or internal structure), the membrane sample must be freeze-fractured in liquid nitrogen followed by coating with either gold or carbon in order to impart electrical conductivity [51]. The addition of CNTs onto the polymer matrices is known to significantly affect a membrane's surface porosity. Celik et al. [8] reported that during the formation of CNT MMMs, the addition of small amounts of CNTs within the PES matrix enhanced the phase separation process, thus giving rise to the formation of larger membrane pore sizes. Furthermore, CNT inclusion has been reported to greatly influence the hydrophilicity, surface roughness, and mechanical strength of the MMMs [52,53].

TEM is also a suitable technique for probing the internal structure of membranes containing nanomaterials such as CNTs. Therefore, information on the membrane thickness, pore sizes, and CNT density is obtainable from TEM analysis. The number of reports in which TEM has been used to structurally investigate the internal morphology of CNT/polymer membranes, particularly CNT MMMs, are very few. This is because the preparation of polymeric samples for TEM analysis tends to be significantly more complex because it involves preparing thin slices of the materials at cryogenic temperatures using a microtome [54]. However, the information obtained from TEM or HRTEM images is valuable and provides information about the dispersion of CNTs in the membrane matrices, their pore sizes, and distribution. TEM could be used to study how chemical functionalization or heteroatomic doping (with either N or P) of CNTs affects dispersion in the membrane [55].

In the analyses of VA-CNT membranes, TEM analysis is commonly the first technique applied, in particular for the as-prepared CNT arrays, prior to polymer infiltration. TEM is capable of probing the internal structure or morphology of these nano-based membranes and can also indicate whether vertical alignment of CNTs has been achieved. SEM is equally widely used to study the topography of VA-CNT membranes. Unlike TEM analysis, SEM examines the surface and produces an image that clearly establishes the alignment of CNTs within the membrane. TEM and SEM images for VA-CNTs and VA-CNT membranes prepared using different methods are shown in Figs. 6 and 7. In Fig. 6, SEM cross-sectional images of PSf membranes prepared from blending different amounts of MWCNTs, are shown. All MWCNT/PSf membranes have similar

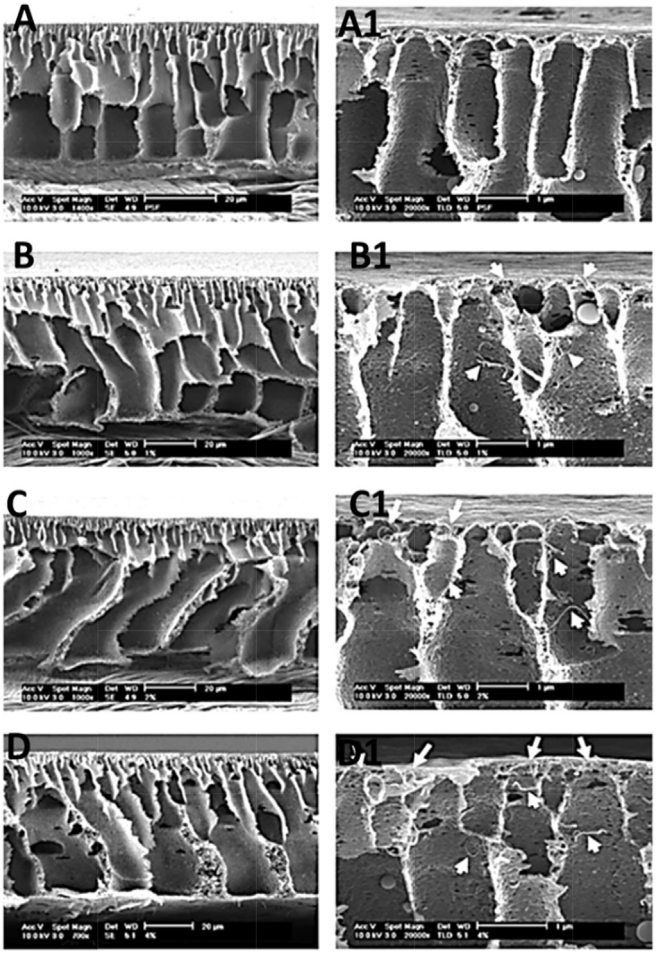

Fig. 6 SEM cross-sectional images of MWCNT/PSf blend membranes with different loadings of MWCNTs; (A) 0 wt%, (B) 1.0 wt% (C) 2.0 wt%, and (D) 4.0 wt%. Images A1 to D1 are high magnification (20000×) images of A to D, showing the presence of MWCNTs in the surface layer of the membrane. *(Reproduced from J.-H. Choi, J. Jegal, W.-N. Kim, Fabrication and characterization of multiwalled carbon nanotubes/polymer blend membranes, J. Membr. Sci. 284 (2006) 406–415).*

substructures with finger-like internal pores. One noticeable difference from their substructures is the amount of MWCNTs that have migrated to the membrane top surface, to make the membrane surface hydrophilic. Fig. 7A and B shows SEM and TEM images for a CNT film that possesses a height of about 2.2 mm (obtained under the CVD growth conditions: acetylene/argon composition of 200/500 sccm, growth temperature of 810° C, and ramp rate of 810°C/min). TEM micrographs presented in the figure show two graphene walls as well as patterned CNTs obtained via the nanotemplate method, in which a TEM grid was used as a mask [56]. SEM images of VA-CNTs synthesized on stainless steel meshes are shown in Fig. 8.

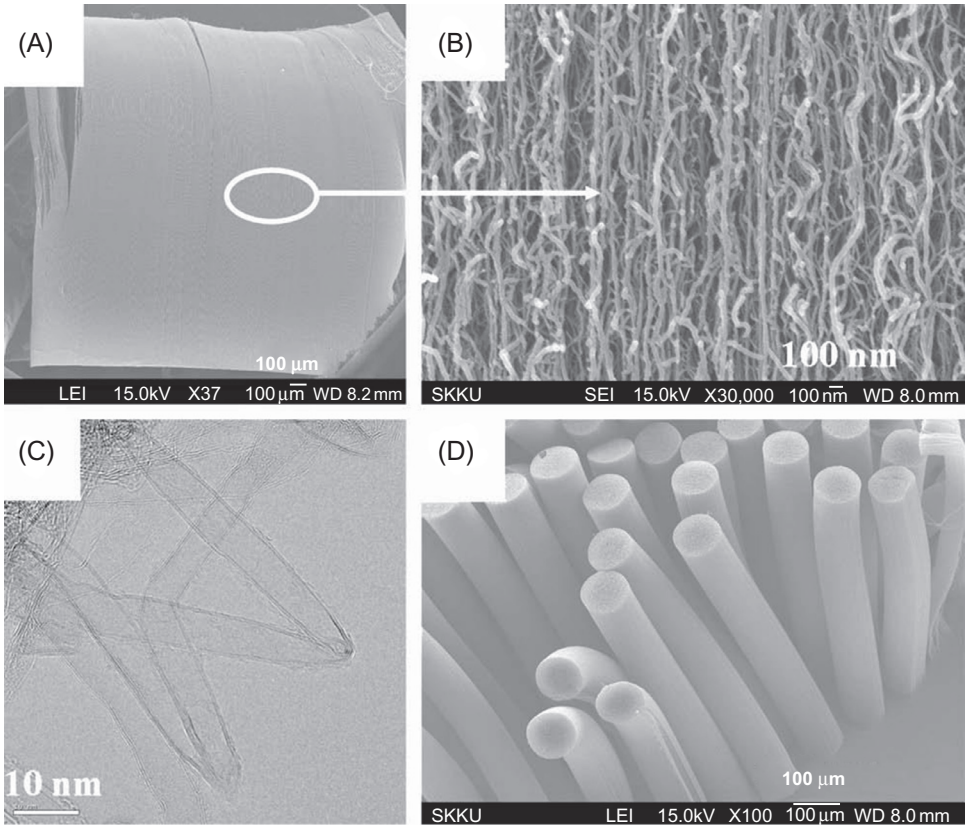

Fig. 7 SEM micrographs for (A) CNT film, (B) the middle of the CNT film, (C) HRTEM micrographs for CNTs, and (D) patterned CNTs using a TEM grid prepared using the nanotemplate method. *(Reproduced from S. Patole, P. Alegaonkar, H.-C. Lee, J.-B. Yoo, Optimization of water assisted chemical vapor deposition parameters for super growth of carbon nanotubes, Carbon 46 (2008) 1987–1993).*

6.3 Mechanical Strength Analysis

The role of CNTs on improving the mechanical strength of MMMs polymeric membranes is widely documented [57,58]. CNT inclusion improves the mechanical strength of MMMs and as such increases the life span of the membranes. Membranes' mechanical-strength properties are typically measured on a microstrain analyzer or Instron analyzer. It is important for a membrane to have a sufficiently high mechanical strength in order to withstand transmembrane pressure during filtration.

These measurements are very important particularly because CNT MMMs are tailor-made for pressure-driven processes. Maphutha et al. [59] showed that excellent mechanical properties can be obtained by the systematic incorporation of CNTs into a membrane material. A CNT composite membrane with polyvinyl alcohol used as a barrier layer was prepared for the purpose of removing oil from wastewater, and a 7.5% concentration of CNTs was found to produce a tensile strength of 119%, 77% in Young's modulus,

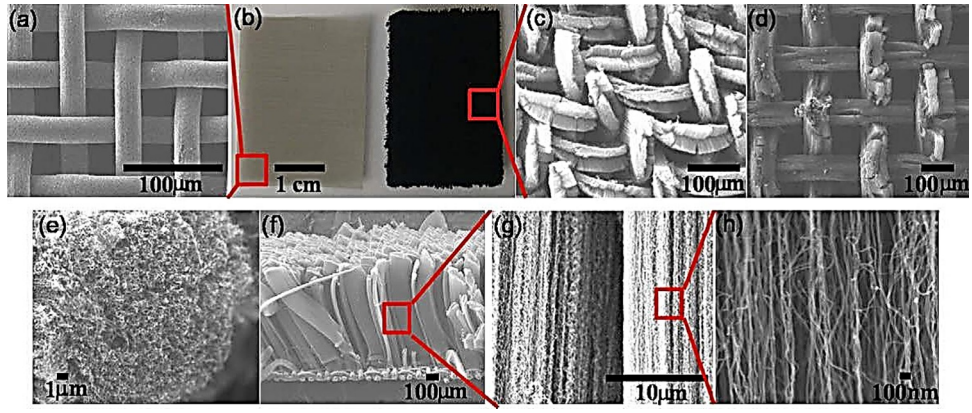

Fig. 8 SEM micrographs of VA-CNT membranes (in different forms) prepared using the filtration method: (A) SEM image of stainless steel mesh; (B) optical images of the mesh before and after the synthesis of VA-CNTs; (C) top surface view of synthesized VA-CNTs; (D) top view of the VA-CNTs with an average length of about 100 μm; (E) magnified, tilted view of the tip of VA-CNTs; (F) cross-sectional image of the VA-CNT filter, and (G, H) magnified SEM images of (F). (A) SEM image of stainless steel mesh; (B) optical images of the mesh before and after the synthesis of VA-CNTs; (C) top surface view of synthesized VA-CNTs; (D) top view of the VA-CNTs with an average length of about 100 μm; (E) magnified, tilted view of the tip of VA-CNTs; (F) cross-sectional image of the VA-CNT filter, and (G, H) magnified SEM images of (F). *(Reproduced from C. Lee, S. Baik, Vertically-aligned carbon nano-tube membrane filters with superhydrophobicity and superoleophilicity, Carbon 48 (2010) 2192–2197).*

and 285% in toughness [59]. Other works have also demonstrated the profits resulting from the use of functionalized CNTs as additives (or fillers) in polymeric membranes. The ultimate tensile strength, mean modulus, and tensile strain were found to increase when small amounts of CNT particles (wt% of 0.02–0.04) were added on suitable polymers [29].

6.4 Contact Angle Analysis

Surface contact angle analysis is used extensively in membrane technology to measure the hydrophilicity, surface energy, and surface tension of polymeric membranes containing CNTs. Contact angle measurements are usually recorded from 10 or more places on the membrane surface, and an average value is reported. This is done in order to obtain reproducible data representative of all the membrane surface properties. The ultimate goal is to fabricate membranes that are highly hydrophilic since they are generally desirable for desalination applications. Such membranes are less susceptible to fouling than their hydrophobic counterparts [50] because of the formation of a strong hydration layer on the membrane surface that prevents the attachment of foulants. Hydrophilicity is achieved by effectively mixing polymers with hydrophilic additives such as highly functionalized CNTs and/or heteroatomic CNTs such as N-doped CNTs [29] and can be predicted easily by a decrease in contact angle values. For example, when acid

functionalized CNTs are incorporated into PES membranes, a decline in the contact angle from >71 degree for bare PES membrane to < 60 degree for 4 wt% MWCNT/PES composite membranes results [50].

6.5 AFM Analysis

AFM analysis is a technique for analyzing membrane surfaces and therefore provides information complementary to SEM and TEM analyses on the carbon nanotube-based membrane's surface properties. AFM generally probes the membrane's internal structure and provides information on the membrane's surface roughness characteristics and can also help measure membrane pore sizes. Fig. 9 shows that after the addition of surface-engineered CNTs onto the cellulose acetate/polyethylene glycol polymer matrix (PM), the membrane surface roughness increased along with an increase in CNT loading up to 0.3 wt% (from PM-CNT 1 to PM-CNT 3). However, with further increments to 0.4 wt% (PM-CNT 4), the membrane surface became smoother. The reason for the reduction in surface roughness is due to the reduced electrostatic interaction between the CNTs and the polymer matrix, thus leading to partial positioning of CNTs in the matrix, which then leads to smooth surfaces. As the loading was increased to 0.5 wt%, the surface roughness started to increase again because of the formation of CNT-agglomerated clusters within the membrane matrix. The major issue with very rough membrane surfaces is that they are prone to fouling because of the ease in the attachment of foulants [50]. This is due to the increase in charged sites on the membrane surface.

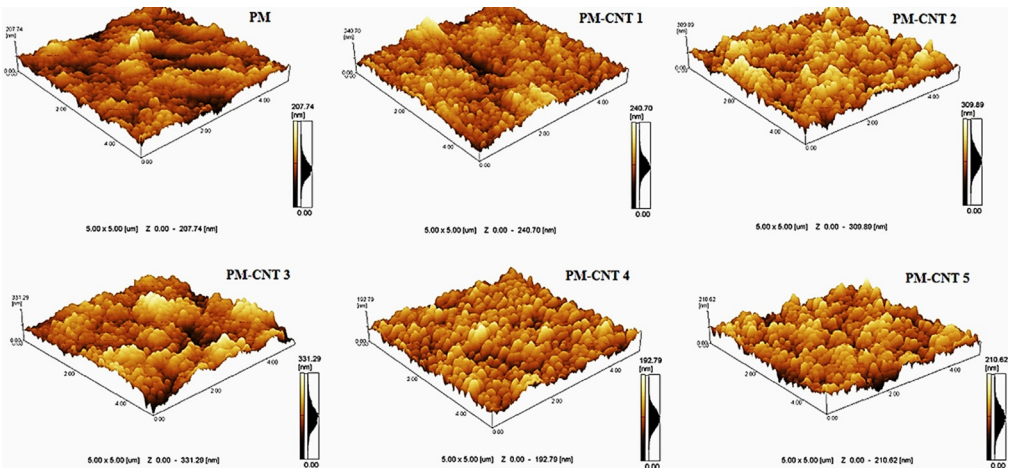

Fig. 9 AFM topographic images depicting changes in surface structure of cellulose actetate/polyethylene glycol polymer matrix (PM). *(Reproduced with permission from A. Sabir, M. Shafiq, A. Islam, A. Sarwar, M.R. Dilshad, A. Shafeeq, M.T.Z. Butt, T. Jamil, Fabrication of tethered carbon nanotubes in cellulose acetate/polyethylene glycol-400 composite membranes for reverse osmosis, Carbohydr. Polym. 132 (2015) 589).*

6.6 Streaming Potential and Surface Charge Analysis

Information relating to the surface charge of CNT polymer membranes is important for understanding how a particular membrane will behave toward targeted pollutants in water, especially charged species/ions. The surface charge of a membrane can be determined via electrokinetic analysis [60]. Electrokinetic occurrence is the interaction between a charged surface and the electrolyte rather than the inherent charge characteristics of the material [61]. In this measurement, zeta potential is measured as a function of pH. The inclusion of CNTs in membranes has a tremendous effect on the surface charge of the membranes. However, the values obtained vary with the concentrations of CNTs added to the membrane and the type of chemical groups and/or heteroatomic species attached on the CNTs.

When the membrane charge is known, the behavior of the pollutants present in water or wastewater toward the membrane surface can be predicted. It has been shown that electrostatic repulsions between the membrane surface and pollutants prevent the occurrence of fouling on the membrane surface [62] suggesting that CNTs can be used as materials for manufacturing membranes that have outstanding antifouling properties.

6.7 Other Characterization Techniques

Other characterization techniques used for membrane analysis include XPS and XRD spectroscopy. XPS is normally used for surface chemical analysis of the CNT membranes and to study the chemical bonding environments within the CNTs and heteroatoms. XRD provides the crystallinity, atomic structure, and crystallite size determination of membranes. Other conventional and unconventional instrumental techniques used to study membranes in general are presented elsewhere [49, 50].

7. ENVIRONMENTAL SUSTAINABILITY OF CNT MEMBRANES

7.1 Energy Demand

The energy demand for a desalination process is set up by the need to bring feed water to a pressure that is equal to the osmotic pressure of the concentrate. Currently, the energy consumed by RO desalination stands at 2 kWh/m^3 at 50% recovery and is far greater than the theoretical minimum energy required for desalination of 1.06 kWh/m^3 [2,33]. The minimum amount of energy required to separate pure water from salty water is equal in magnitude but has an opposite sign to the free energy of mixing, and can be calculated in Eq. (4) as

$$-\mathrm{d}(\Delta G_{\mathrm{mix}}) = -RT \ \ln a_{\mathrm{w}} \mathrm{d}n_{\mathrm{w}} = \pi_{\mathrm{s}} V_{\mathrm{w}} \mathrm{d}n_{\mathrm{w}} \tag{4}$$

where ΔG_{mix} is the free energy of mixing, R is the ideal gas constant, T is the absolute temperature, a_{w} is the activity of water, n_{w} is the number of moles of water, π_{s} is the osmotic pressure of seawater, and V_{w} is the molar volume of water.

The minimum energy can then be calculated from the integration of Eq. 4 as

$$Wo = (-\mathrm{d}(\Delta G_{\mathrm{mix}})/\mathrm{d}n_{\mathrm{w}})_{P,\ T} = -RT\ \ln a_{\mathrm{w}} \tag{5}$$

Although the energy consumption of the RO desalination process has not yet reached the theoretical limit, the use of highly permeable membranes such as CNT-based membranes is expected to alleviate this problem. However, this will not directly influence the reduction of the energy necessary for desalination processes to occur [2]. Nonetheless, fouling-resistant membranes such as CNT-based membranes are beneficial in overcoming the high energy costs associated with high-pressure requirements essential in order to drive pure water molecules through a fouled membrane.

7.2 Disposal

As with other nanoparticles, disposal of CNTs and/or CNT-based membranes is not widely documented, because these materials are relatively new and most researchers and environmentalists are still trying to study their impact on human health and the environment as well as their disposal issues. According to the UK Environment Agency, "any CNT containing waste is considered as hazardous waste unless evidence suggests otherwise" [63]. This signals that the fabrication costs of CNT-based membranes could potentially be driven up (when environmentally benign processes are sought) and especially if these membranes are scaled up. For example, currently the cost of 1.0 g of pristine MWCNTs is greater than $100. Although this seems high, because of their high surface area, very small amounts of CNTs are used as additives in CNT MMM fabrication processes. Furthermore, as newer methods of production are being developed, the price of CNTs is expected to gradually decrease. However, Brehm (2008) at Massachusetts Institute of Technology (MIT) suggested that incorporating environmental objectives during the synthetic stage of novel materials (such as CNTs) can bring drastic change in both industrial and environmental practices, that is, preventing problems rather than reacting to them [64]. This is a viable approach to minimizing CNT toxicity at the source prior to their incorporation onto other materials such as membranes [64] or point-of-use systems such as filters.

Methods that have been suggested for CNT disposal include high-temperature incineration [65] and vitrification or the encapsulation of CNTs into glass or ceramic structures [63]. Vitrification is a relatively new method that is still under development and is therefore considered as an alternative disposal technique for the future [63]. Clearly, more efforts are needed in this area in order to create better solutions for the disposal of CNTs or CNT-based membranes in a sustainable manner. These efforts will require active collaboration among material scientists, industrialists, academics, and environmentalists in order to pinpoint the potential risks associated with these new materials and to come up with better disposal methods [66].

7.3 Toxicity of CNT Membranes

It is clear that CNTs have an enormous potential in water-treatment applications, particularly in membrane technology. However, their large scale application will be realistic only when their nanotoxicity in water or even air is fully understood.

In the recent past, increasing fears have been associated with the escalating use of CNTs in water-treatment applications because of the CNTs' potential to be toxic. Because of their fibric nature, CNTs have been compared to asbestos, a highly pathogenic material [67,68]. Workers have also been concerned that CNTs are extremely light and can therefore easily enter the environment as suspended particulate matter, creating a serious inhalation hazard for human beings and animals [69]. In particular, it has been claimed that MWCNTs can induce frustrated phagocytosis and cytotoxicity as well as pro-inflammatory conditions in macrophages, which could be greater than those of asbestos [70]. This apparent toxicity of CNTs is attributed to their inherent physical and chemical properties, such as their unique nanostructure, diverse composition, and high volume-to-surface ratio [67]. As a result, much work is required to ascertain whether such materials are suitable for drinking water applications.

Indeed, recent studies have demonstrated that different methods of administration could result in different pathologies. For example, SWCNTs and MWCNTs were shown to produce numerous pathological changes when administered in mice through either the lungs or the heart, thereby causing diverse respiratory impairments [69].

Other researchers assessed the pharmacological efficacy, stability, and toxicity of CNTs in vitro and in vivo and found contradictory results [71]. Sanpui et al. [72] demonstrated that the diverse electronic structure of CNTs has an ability to increase the susceptibility of epithelial cells to influenza A H1N1 infection. In addition, others have suggested that CNTs may cause harm to cells by activating many pathways, mostly involving damage to the DNA [73]. The toxicity of CNTs on aquatic life, bacterium, and higher plants is being probed as well [74]. Nevertheless, specific types of CNT modifications, such as substitutional doping and efficient surface functionalization, can greatly minimize CNT toxicity. These modifications represent promising progress towards their much needed use in desalination. It is important to note that there is a likely possibility for CNTs to be released from CNT MMMs or VA-CNT membranes and leach directly into water, even though CNTs are embedded on highly stable supports. In particular, some irregularities may cause CNTs to leach into water and ultimately into the environment during desalination processes; therefore precautionary measures are required [67].

It is evident that the toxicity of CNTs in water or the environment is not fully understood, and published reports often produce conflicting deductions. Therefore comprehensive and systematic studies still need to be carried out on this subject. The critical factors that should be considered are the CNT structural morphology (shape and size), surface properties, biodurability, purity, method of production, and modification [75]. Furthermore, CNT toxicity depends on parameters such as exposure conditions, model

or test organism, CNT type and source, dispersion state (sonication), modification strategies, medium, and concentration [76,77]. Once all these factors have been adequately addressed, CNTs could be safely used in water-treatment processes. A research group from Pharmacy School of University College London, recently demonstrated that the CNTs can be produced as risk-free materials only if their surface can be chemically modified and their length shortened by chemical treatment. In their research paper, they emphasized that only those measures can shorten the length of CNTs and ensure that they are stably suspended in biological fluids without agglomeration so that risk-free materials can be produced [78].

CNTs cannot be added directly to water for treatment purposes like commodity chemicals can, because doing so can potentially present new hazards to the health of humans and the environment [79]. Furthermore, additional separation or recovery processes can be necessary to recover the used CNT materials. Therefore, the incorporation of CNTs within the polymeric membrane materials may prove to be more eco-friendly, thus guaranteeing future industrial-scale application of CNT-based membranes in desalination processes.

7.4 Commercial Viability of CNT Membrane Desalination Processes

Although desalination processes have been identified as a potential solution to global water scarcity [80], the economic implications associated with these processes, in general, are too high for underdeveloped and developing countries. The typical construction of desalination plants requires a massive capital expenditure. In addition, the daily operational costs of pumping water from the sea into a desalination plant require a high amount of energy. Since seawater desalination is a highly specialized field, personnel working on these projects are usually highly skilled engineers and normally salaried competitively. As such, input costs in these projects are astronomical. Over the past decade, attempts to lower the cost of desalination in developed countries have proved successful, with the price of desalinated water reaching $\$2.10/m^3$ [81]. According to a review by Ghaffour et al. (2013), the parameters that influence the total capital and operational costs of a desalination plant include electric power availability, desalination process configuration, plant size and its component design, raw water quality and required water quality and other consumables. In a CNT membrane desalination plant, the parameters are expected to be similar. However, the CNT cost parameter is factored in separately. Therefore, in order for CNT membranes to be fully adopted in desalination processes, the cost per volume of saline water treated by these membranes would need to be the same or even lower than the current costs of desalination processes. Cost is always the dominating and deciding factor in the end.

Polymeric membranes used for seawater desalination have evolved over time. By 1969 cellulose acetate (CA) membranes had immerged as the best membranes for

desalination purposes [82]. However, the quest for desalination membranes with high flux and high rejection capacities has been a continuous endeavor. Indeed, the incorporation of carbon nanomaterials, in particular CNTs or the fabrication of VA-CNT membranes, is being applied to lower the cost of seawater desalination. The incorporation of CNTs into polymeric membranes has been shown to produce remarkably enhanced membrane properties such as flux, recovery, antifouling, and salt rejection [5]. It is expected that CNTs will lead to lower energy requirements when pumping seawater across a membrane in order to get fresh water. Fouling of membranes is reported to drive up the energy costs, as a result of the requirements of high pressures necessary to drive pure water molecules across a fouled membrane. Therefore, the inclusion of carbon nanomaterials in membranes to be used for desalination processes, is envisaged to eliminate the deposition of micro-organisms on the membrane surfaces which can contribute to membrane fouling [83]. As such, the presence of CNTs on polymeric membranes brings about properties that can render the membranes energy-efficient. Fig. 10 describes the potential performance and commercial viability of CNT membranes with reference to other nano-enabled membranes such as inorganic nanomaterials incorporating membranes, aquaporins, ceramics, and other nanostructured membranes [45]. Indeed, VA-CNT membranes have highly enhanced performance prediction (closer to aquaporins) yet very far from commercialization.

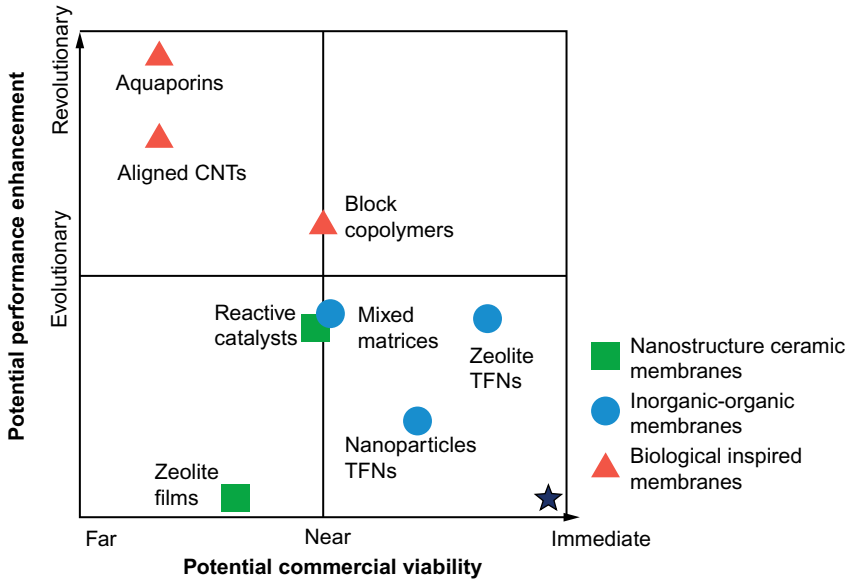

Fig. 10 Potential performance versus commercial viability of nanotechnology-enabled membrane. *(Reproduced with permission from M.M. Pendergast, E.M.V. Hoek, A review of water treatment membrane nanotechnologies, Energy Environ. Sci. 4 (2010) 1946–1971).*

The use of integrated systems has been shown to be one of the ways by which energy costs can be minimized. Seawater has high osmotic pressure because of the presence of divalent ions, for example. By subjecting the seawater feed through a prefiltration stage, the effect of lowering the osmotic pressure of the feed can be explored [84,85]. The ability to fabricate membranes with improved surface properties by incorporating CNTs will further reduce the capital expenditure required for the running of desalination plants. Researchers have already projected that the use of CNT membranes in a desalination plant would offer a significant cost reduction up to 22% and chemical cost savings of up to 76% [86]. Therefore the use of CNT technologies to bring down costs will be at center stage of cutting edge research until the scientific community considers the safety measures discussed in previous sections or provide proof that the potable water generated using CNT membranes is safe and acceptable.

8. CHALLENGES AND FUTURE PERSPECTIVES

CNT membranes are perceived as robust and ideal materials for the generation of fresh water during filtration and desalination processes. This perception is propelled by advances made in the growth of CNTs of various morphologies (e.g., size, shape, and geometry). The mm-long VA-CNTs provide new openings for the transportation of water molecules through tubes. However, CNT-based membranes exhibit several obstacles that must first be addressed before they can be utilized effectively in desalination processes.

The conventional methods for the production of CNTs (such as CVD) have insurmountable shortcomings [50]. One such disadvantage is that CNT manufacturing processes and in particular those for producing VA-CNTs have not yet been scaled up [35]. In addition, when alternative methods such as arc-discharge and laser ablation are utilized in CNT synthesis on an industrial scale, the process becomes very costly. The distinctive properties of CNTs can be useful when these nanomaterials have been homogenously dispersed in a polymer solution [87]. Inherently, CNTs tend to pack up into undesirable bundles or clusters because of the presence of van der Waals interactions within the CNT lattice, which can further compromise the mechanical strength of CNT membranes [88].

However, the "unbundling" of CNTs can be achieved through (i) covalent modifications via the attachment of functional substituents, for example –COOH, –OH, and –NH_2, (ii) noncovalent modification via wrapping of water-soluble linear polymers around the CNTs [89], and (iii) by mixing CNTs under shear force such as ultrasonication [90]. Although CNT functionalization is a challenging and laborious exercise, it leads to more stable surface modification, which is vital in attaining CNTs that can be dispersed with ease in the membrane matrices [10]. The tendency of CNTs to agglomerate during solution-casting processes remains another overarching obstacle.

The practice of chemically functionalizing or substitutional doping CNTs assists in obtaining membranes with excellent surface properties [86]. To keep the fabrication costs of CNT membranes minimal, further research is needed to seek low-cost, simple, and efficient ways of functionalizing and/or dispersing CNTs in membrane matrices. Therefore further research to find ways of simplifying the engineering processes and to understand the membrane science should continue to be pursued.

Membrane fouling is an inevitable occurrence where the application of CNT polymer membranes in water treatment is concerned. The degree of fouling is further influenced by the conditions of the feed water that is undergoing treatment [10]. Even though CNTs possess antimicrobial properties that may be beneficial in averting biofilm formation on a membrane surface, the big issue still remains for staged array membrane configurations and on the influence of the destroyed microorganisms on subsequent membrane filtration steps. Furthermore, having CNTs in mixed-matrix membrane configuration remains questionable and is said to render all the attractive and desirable features of CNTs useless because the majority of the CNT mass is buried in the bulk polymer matrix [17]. The probability of CNTs leaching out from a polymer membrane is another issue requiring attention, especially in cases where dispersion and chemical bonding has not been achieved [46]. Therefore, if CNT polymer membranes are to be endorsed for future large-scale operations in water-treatment processes, the leaching aspect of nanomaterials into the water source must be thoroughly addressed and inhibited.

As mentioned in the previous sections, VA-CNT membranes have better prospects than CNT MMMs when it comes to their performance in desalination processes and the diversity of application. However, their fabrication processes may be a limiting factor in that they hinder widespread exploitation as a result of the complexities in the process and thus incapability of producing reproducible membrane samples. Even though fluxes through the individual nanotube are high, fluxes per unit cm^2 area are limited because of the low porosity of CNTs. This is a serious limitation for their applications. Another great challenge in VA-CNT membranes is the alignment of large numbers of CNTs with well-controlled morphology and geometry across the entire membrane structure. For instance, during polymer infiltration step, it is difficult to find a conformal deposition process that will be able to conform to the spaces between the VA-CNT arrays and adequately fill these spaces, without tempering with the alignment of CNTs. Researchers need to design an etching process that will selectively open the nanotube ends without producing voids in the membrane structure. The challenge is to remove impurities within the VA-CNTs while maintaining the nanotube's original integrity.

Because they are tiny particles instead of ions or molecules for which a system of risk assessment already exists, CNTs face distinctive challenges for risk assessment and management [91]. A deep understanding of these materials is still required in order to

prevent and eliminate the probability of hazards emanating from these materials in water treatment [91]. This level of understanding will significantly help to exponentially increase research and development activities of membranes containing CNT nanomaterials.

VA-CNT membranes provide new prospects for the transportation of liquids and separation of unwanted species. Clearly, the potential for CNT membranes is enormous. The key question that remains is, can these CNT materials be commercialized for large-scale applications? Commercialization of these materials is important because CNT-polymer membranes possess enhanced selectivities. In contrast to conventional polymeric membranes, CNT polymer membranes have outstanding advantages, such as higher flux and higher salt rejection [86]. In view of these outstanding properties, a drive toward commercialization of these materials (which are energy-efficient and less susceptible to fouling) should be undertaken. Over the past decade, challenges pertaining to the application of CNTs revolved around the high cost of CNTs. However, the cost has since dropped from $200 per gram in 1999 to between $50 and $100 per gram in 2013, making it affordable to use CNTs in different materials [92]. The affordability of CNTs would make the scaling up of CNT polymer membranes a possible task [93]. The realization of the ultrafast transport of molecules within tubes of CNT-membranes is critical at this stage.

9. CONCLUSIONS

The merits and challenges associated with the use of CNTs in membrane systems for desalination applications were systematically analyzed. Over the past decade, considerable efforts were made toward the development of membranes containing carbon nanomaterials to overcome fouling, high-energy demand, unselective separation of dissolved contaminants, and low permeation. Clearly, the use of CNTs in membrane systems is on the rise and will continue to be investigated, and provided health concerns can be alleviated, attempts will be made to implement them on an industrial scale in the foreseeable future.

ACKNOWLEDGMENTS

The authors want to acknowledge with gratitude the German Academic Exchange Service (DAAD) in partnership with the South African National Research Foundation (NRF) and the University of South Africa for financial support. We also thank the Helmholtz-Rekrutierungsinitiative for project funding at Karlsruhe Institute of Technology.

REFERENCES

[1] N. Misdan, W.J. Lau, A.F. Ismail, Seawater reverse osmosis (SWRO) desalination by thin-film composite membrane—current development, challenges and future prospects, Desalination 287 (2012) 228–237.

[2] M. Elimelech, W.A. Phillip, The future of seawater desalination: energy, technology, and the environment, Science 333 (2011) 712–717.

[3] C.H. Ahn, Y. Baek, C. Lee, S.O. Kim, S. Kim, S. Lee, S.-H. Kim, S.S. Bae, J. Park, J. Yoon, Carbon nanotube-based membranes: Fabrication and application to desalination, J. Ind. Eng. Chem. 18 (2012) 1551–1559.

[4] N.R.C. Committee on Advancing Desalination Technology, Desalination: A National Perspective, National Academies Press, Washington, DC, 2008. p. 312.

[5] P.S. Goh, A.F. Ismail, B.C. Ng, Carbon nanotubes for desalination–an innovative material with enormous potential, Membr. Technol. 2013 (2013) 7–10.

[6] A.F. Ismail, P.S. Goh, S.M. Sanip, M. Aziz, Transport and separation properties of carbon nanotube-mixed matrix membrane, Sep. Purif. Technol. 70 (2009) 12–26.

[7] E. Drioli, L. Giorno, Comprehensive Membrane Science and Engineering, Newnes, The Boulevard, 2010.

[8] E. Celik, H. Park, H. Choi, H. Choi, Carbon nanotube blended polyethersulfone membranes for fouling control in water treatment, Water Res. 45 (2011) 274–282.

[9] V. Vatanpour, S.S. Madaeni, R. Moradian, S. Zinadini, B. Astinchap, Fabrication and characterization of novel antifouling nanofiltration membrane prepared from oxidized multiwalled carbon nanotube/polyethersulfone nanocomposite, J. Membr. Sci. 375 (2011) 284–294.

[10] S. Kar, R. Bindal, P. Tewari, Carbon nanotube membranes for desalination and water purification: challenges and opportunities, Nano Today 7 (2012) 385–389.

[11] C. Tang, Q. Zhang, K. Wang, Q. Fu, C. Zhang, Water transport behavior of chitosan porous membranes containing multi-walled carbon nanotubes (MWNTs), J. Membr. Sci. 337 (2009) 240–247.

[12] S. Zou, Y. Gu, D. Xiao, C.Y. Tang, The role of physical and chemical parameters on forward osmosis membrane fouling during algae separation, J. Membr. Sci. 366 (2011) 356–362.

[13] P. Bacchin, P. Aimar, R.W. Field, Critical and sustainable fluxes: theory, experiments and applications, J. Membr. Sci. 281 (2006) 42–69.

[14] M.F. Goosen, S. Al-Obeidani, H. Al-Hinai, S. Sablani, Y. Taniguchi, H. Okamura, Membrane fouling and cleaning in treatment of contaminated water, in: E. Laboy-Nieves, F. Schaffner, A. Abdelhadi, M. Goosen (Eds.), Environmental Management, Sustainable Development and Human Health, 2009, CRC Press/Balkema; AK Leiden, The Netherlands, p. 503.

[15] K.R. Zodrow, M.E. Tousley, M. Elimelech, Mitigating biofouling on thin-film composite polyamide membranes using a controlled-release platform, J. Membr. Sci. 453 (2014) 84–91.

[16] C.D. Vecitis, K.R. Zodrow, S. Kang, M. Elimelech, Electronic-structure-dependent bacterial cytotoxicity of single-walled carbon nanotubes, ACS Nano 4 (2010) 5471–5479.

[17] A. Tiraferri, C.D. Vecitis, M. Elimelech, Covalent binding of single-walled carbon nanotubes to polyamide membranes for antimicrobial surface properties, ACS Appl. Mater. Interfaces 3 (2011) 2869–2877.

[18] M.S. Mauter, M. Elimelech, Environmental applications of carbon-based nanomaterials, Environ. Sci. Technol. 42 (2008) 5843–5859.

[19] A. Matin, Z. Khan, S. Zaidi, M. Boyce, Biofouling in reverse osmosis membranes for seawater desalination: phenomena and prevention, Desalination 281 (2011) 1–16.

[20] S. Kang, M. Herzberg, D.F. Rodrigues, M. Elimelech, Antibacterial effects of carbon nanotubes: size does matter! Langmuir 24 (2008) 6409–6413.

[21] B.J. Hinds, N. Chopra, T. Rantell, R. Andrews, V. Gavalas, L.G. Bachas, Aligned multiwalled carbon nanotube membranes, Science 303 (2004) 62–65.

[22] M. Majumder, N. Chopra, B.J. Hinds, Effect of tip functionalization on transport through vertically oriented carbon nanotube membranes, J. Am. Chem. Soc. 127 (2005) 9062–9070.

[23] S. Iijima, Helical microtubules of graphitic carbon, Nature 354 (1991) 56–58.
[24] J.-G. Yu, X.-H. Zhao, H. Yang, X.-H. Chen, Q. Yang, L.-Y. Yu, J.-H. Jiang, X.-Q. Chen, Aqueous adsorption and removal of organic contaminants by carbon nanotubes, Sci. Total Environ. 482 (2014) 241–251.
[25] R.H. Baughman, A.A. Zakhidov, W.A. de Heer, Carbon nanotubes – the route toward applications, Science 297 (2002) 787–792.
[26] R. Andrews, M. Weisenberger, Carbon nanotube polymer composites, Curr. Opin. Solid State Mater. Sci. 8 (2004) 31–37.
[27] L. Brunet, D.Y. Lyon, K. Zodrow, J.-C. Rouch, B. Caussat, P. Serp, J.-C. Remigy, M.R. Wiesner, P. J. Alvarez, Properties of membranes containing semi-dispersed carbon nanotubes, Environ. Eng. Sci. 25 (2008) 565–576.
[28] S. van Dommele, Nitrogen Doped Carbon Nanotubes: Synthesis, Characterization and Catalysis, Utrecht University, Netherlands, 2008.
[29] N. Phao, E.N. Nxumalo, B.B. Mamba, S.D. Mhlanga, A nitrogen-doped carbon nanotube enhanced polyethersulfone membrane system for water treatment, Phys. Chem. Earth A/B/C 66 (2013) 148–156.
[30] S. Kim, J.R. Jinschek, H. Chen, D.S. Sholl, E. Marand, Scalable fabrication of carbon nanotube/polymer nanocomposite membranes for high flux gas transport, Nano Lett. 7 (2007) 2806–2811.
[31] Z. Fan, S.G. Advani, Characterization of orientation state of carbon nanotubes in shear flow, Polymer 46 (2005) 5232–5240.
[32] S.-M. Park, J. Jung, S. Lee, Y. Baek, J. Yoon, D.K. Seo, Y.H. Kim, Fouling and rejection behavior of carbon nanotube membranes, Desalination 343 (2014) 180–186.
[33] Y. Baek, C. Kim, D.K. Seo, T. Kim, J.S. Lee, Y.H. Kim, K.H. Ahn, S.S. Bae, S.C. Lee, J. Lim, High performance and antifouling vertically aligned carbon nanotube membrane for water purification, J. Membr. Sci. 460 (2014) 171–177.
[34] R. Das, M.E. Ali, S.B.A. Hamid, S. Ramakrishna, Z.Z. Chowdhury, Carbon nanotube membranes for water purification: a bright future in water desalination, Desalination 336 (2014) 97–109.
[35] R. Das, S.B.A. Hamid, M.E. Ali, A.F. Ismail, M. Annuar, S. Ramakrishna, Multifunctional carbon nanotubes in water treatment: the present, past and future, Desalination 354 (2014) 160–179.
[36] Y. Manawi, V. Kochkodan, M.A. Hussein, M.A. Khaleel, M. Khraisheh, N. Hilal, Can carbon-based nanomaterials revolutionize membrane fabrication for water treatment and desalination? Desalination 391 (2016) 69–88.
[37] J.K. Holt, Carbon nanotubes and nanofluidic transport, Adv. Mater. 21 (2009) 3542–3550.
[38] M.S. Sansom, P.C. Biggin, Biophysics: water at the nanoscale, Nature 414 (2001) 156–159.
[39] G. Hummer, J.C. Rasaiah, J.P. Noworyta, Water conduction through the hydrophobic channel of a carbon nanotube, Nature 414 (2001) 188–190.
[40] O. Bakajin, A. Noy, F. Fornasiero, C.P. Grigoropoulos, J.K. Holt, J.B. In, S. Kim, H. G. Park, Nanofluidic Carbon Nanotube Membranes, Elsevier Inc., Philadelphia, USA, 2014.
[41] F. Fornasiero, H.G. Park, J.K. Holt, M. Stadermann, C.P. Grigoropoulos, A. Noy, O. Bakajin, Ion exclusion by sub-2-nm carbon nanotube pores, Proc. Natl. Acad. Sci. 105 (2008) 17250–17255.
[42] B. Corry, Designing carbon nanotube membranes for efficient water desalination, J. Phys. Chem. B 112 (2008) 1427–1434.
[43] A. Kalra, S. Garde, G. Hummer, Osmotic water transport through carbon nanotube membranes, Proc. Natl. Acad. Sci. 100 (2003) 10175–10180.
[44] M. Majumder, N. Chopra, B.J. Hinds, Mass transport through carbon nanotube membranes in three different regimes: ionic diffusion and gas and liquid flow, ACS Nano 5 (2011) 3867–3877.
[45] J.K. Holt, H.G. Park, Y. Wang, M. Stadermann, A.B. Artyukhin, C.P. Grigoropoulos, A. Noy, O. Bakajin, Fast mass transport through sub-2-nanometer carbon nanotubes, Science 312 (2006) 1034–1037.
[46] D. Mattia, H. Leese, K.P. Lee, Carbon nanotube membranes: from flow enhancement to permeability, J. Membr. Sci. 475 (2015) 266–272.
[47] P.J.F. Harris, Carbon Nanotube Science: Synthesis, Properties and Applications, Cambridge University Press, NY, USA, 2009.

[48] O. Agboola, J. Maree, R. Mbaya, Characterization and performance of nanofiltration membranes, Environ. Chem. Lett. 12 (2014) 241–255.
[49] P. Daraei, S.S. Madaeni, N. Ghaemi, H.A. Monfared, M.A. Khadivi, Fabrication of PES nanofiltration membrane by simultaneous use of multi-walled carbon nanotube and surface graft polymerization method: comparison of MWCNT and PAA modified MWCNT, Sep. Purif. Technol. 104 (2013) 32–44.
[50] J.-H. Choi, J. Jegal, W.-N. Kim, Fabrication and characterization of multi-walled carbon nanotubes/polymer blend membranes, J. Membr. Sci. 284 (2006) 406–415.
[51] G.D. Vilakati, E.M. Hoek, B.B. Mamba, Probing the mechanical and thermal properties of polysulfone membranes modified with synthetic and natural polymer additives, Polym. Test. 34 (2014) 202–210.
[52] E. Celik, L. Liu, H. Choi, Protein fouling behavior of carbon nanotube/polyethersulfone composite membranes during water filtration, Water Res. 45 (2011) 5287–5294.
[53] V. Vatanpour, M. Esmaeili, M.H.D.A. Farahani, Fouling reduction and retention increment of polyethersulfone nanofiltration membranes embedded by amine-functionalized multi-walled carbon nanotubes, J. Membr. Sci. 466 (2014) 70–81.
[54] E.-S. Kim, G. Hwang, M.G. El-Din, Y. Liu, Development of nanosilver and multi-walled carbon nanotubes thin-film nanocomposite membrane for enhanced water treatment, J. Membr. Sci. 394 (2012) 37–48.
[55] K. Yokwana, N. Gumbi, F. Adams, S. Mhlanga, E. Nxumalo, B. Mamba, Development of functionalized doped carbon nanotube/polysulfone nanofiltration membranes for fouling control, J. Appl. Polym. Sci. 132 (2015) 41835 (1–10).
[56] S. Patole, P. Alegaonkar, H.-C. Lee, J.-B. Yoo, Optimization of water assisted chemical vapor deposition parameters for super growth of carbon nanotubes, Carbon 46 (2008) 1987–1993.
[57] R. Sen, B. Zhao, D. Perea, M.E. Itkis, H. Hu, J. Love, E. Bekyarova, R.C. Haddon, Preparation of single-walled carbon nanotube reinforced polystyrene and polyurethane nanofibers and membranes by electrospinning, Nano Lett. 4 (2004) 459–464.
[58] J.N. Coleman, U. Khan, W.J. Blau, Y.K. Gun'ko, Small but strong: a review of the mechanical properties of carbon nanotube–polymer composites, Carbon 44 (2006) 1624–1652.
[59] S. Maphutha, K. Moothi, M. Meyyappan, S.E. Iyuke, A carbon nanotube-infused polysulfone membrane with polyvinyl alcohol layer for treating oil-containing waste water, Sci. Rep. 3 (2013) 1509 (1–6).
[60] M.D. Afonso, G. Hagmeyer, R. Gimbel, Streaming potential measurements to assess the variation of nanofiltration membranes surface charge with the concentration of salt solutions, Sep. Purif. Technol. 22 (2001) 529–541.
[61] G. Hurwitz, G.R. Guillen, E.M. Hoek, Probing polyamide membrane surface charge, zeta potential, wettability, and hydrophilicity with contact angle measurements, J. Membr. Sci. 349 (2010) 349–357.
[62] B.S. Lalia, V. Kochkodan, R. Hashaikeh, N. Hilal, A review on membrane fabrication: Structure, properties and performance relationship, Desalination 326 (2013) 77–95.
[63] H. Greg, Safe Handling and Use of Carbon Nanotubes, 2012, http://www.safeworkaustralia.gov.au (accessed 20 March 2016).
[64] D. Brehm, Minimizing the Environmental Impacts of CNTs, Massachusetts Institute of Technology, Cambridge, USA, 2008.
[65] The health and safety executive annual report and accounts 2011/12, 2012, http://www.hse.gov.uk/aboutus/reports/1112/ar1112.pdf (accessed 30 March 2016).
[66] P.S. Goh, A.F. Ismail, Review: is interplay between nanomaterial and membrane technology the way forward for desalination? J. Chem. Technol. Biotechnol. 90 (2015) 971–980.
[67] S.Y. Madani, A. Mandel, A.M. Seifalian, A concise review of carbon nanotube's toxicology, Nano Rev. Exp. 4 (2013) 1–14.
[68] K. Donaldson, F.A. Murphy, R. Duffin, C.A. Poland, Asbestos, carbon nanotubes and the pleural mesothelium: a review of the hypothesis regarding the role of long fibre retention in the parietal pleura, inflammation and mesothelioma, Part. Fibre Toxicol. 7 (2010) 1.
[69] C.-W. Lam, J.T. James, R. McCluskey, S. Arepalli, R.L. Hunter, A review of carbon nanotube toxicity and assessment of potential occupational and environmental health risks, Crit. Rev. Toxicol. 36 (2006) 189–217.

[70] M.S. Boyles, L. Young, D.M. Brown, L. MacCalman, H. Cowie, A. Moisala, F. Smail, P. J. Smith, L. Proudfoot, A.H. Windle, Multi-walled carbon nanotube induced frustrated phagocytosis, cytotoxicity and pro-inflammatory conditions in macrophages are length dependent and greater than that of asbestos, Toxicol. In Vitro 29 (2015) 1513–1528.
[71] K. Kostarelos, The long and short of carbon nanotube toxicity, Nat. Biotechnol. 26 (2008) 774–776.
[72] P. Sanpui, X. Zheng, J.C. Loeb, J.H. Bisesi Jr., I.A. Khan, A.N. Afrooz, K. Liu, A.R. Badireddy, M. R. Wiesner, P.L. Ferguson, Single-walled carbon nanotubes increase pandemic influenza A H1N1 virus infectivity of lung epithelial cells, Part. Fibre Toxicol. 11 (2014) 1.
[73] C.P. Firme, P.R. Bandaru, Toxicity issues in the application of carbon nanotubes to biological systems, Nanomed. Nanotechnol. Biol. Med. 6 (2010) 245–256.
[74] J. Du, S. Wang, H. You, X. Zhao, Understanding the toxicity of carbon nanotubes in the environment is crucial to the control of nanomaterials in producing and processing and the assessment of health risk for human: a review, Environ. Toxicol. Pharmacol. 36 (2013) 451–462.
[75] S. Lanone, P. Andujar, A. Kermanizadeh, J. Boczkowski, Determinants of carbon nanotube toxicity, Adv. Drug Deliv. Rev. 65 (2013) 2063–2069.
[76] P. Jackson, N.R. Jacobsen, A. Baun, R. Birkedal, D. Kühnel, K.A. Jensen, U. Vogel, H. Wallin, Bioaccumulation and ecotoxicity of carbon nanotubes, Chem. Cent. J. 7 (2013) 1.
[77] J.N. Mwangi, N. Wang, C.G. Ingersoll, D.K. Hardesty, E.L. Brunson, H. Li, B. Deng, Toxicity of carbon nanotubes to freshwater aquatic invertebrates, Environ. Toxicol. Chem. 31 (2012) 1823–1830.
[78] H. Ali-Boucetta, A. Nunes, R. Sainz, M.A. Herrero, B. Tian, M. Prato, A. Bianco, K. Kostarelos, Asbestos-like pathogenicity of long carbon nanotubes alleviated by chemical functionalization, Angew. Chem. Int. Ed. 52 (2013) 2274–2278.
[79] O. Renn, M.C. Roco, Nanotechnology and the need for risk governance, J. Nanopart. Res. 8 (2006) 153–191.
[80] A.W. Mohammad, Y. Teow, W. Ang, Y. Chung, D. Oatley-Radcliffe, N. Hilal, Nanofiltration membranes review: recent advances and future prospects, Desalination 356 (2015) 226–254.
[81] N. Ghaffour, T.M. Missimer, G.L. Amy, Technical review and evaluation of the economics of water desalination: current and future challenges for better water supply sustainability, Desalination 309 (2013) 197–207.
[82] K.P. Lee, T.C. Arnot, D. Mattia, A review of reverse osmosis membrane materials for desalination—development to date and future potential, J. Membr. Sci. 370 (2011) 1–22.
[83] V.K. Upadhyayula, S. Deng, M.C. Mitchell, G.B. Smith, Application of carbon nanotube technology for removal of contaminants in drinking water: a review, Sci. Total Environ. 408 (2009) 1–13.
[84] D. Zhou, L. Zhu, Y. Fu, M. Zhu, L. Xue, Development of lower cost seawater desalination processes using nanofiltration technologies—a review, Desalination 376 (2015) 109–116.
[85] V.G. Gude, Desalination and sustainability – an appraisal and current perspective, Water Res. 89 (2016) 87–106.
[86] E.M. Hoek, A.K. Ghosh, Nanotechnology-based membranes for water purification, Nanotechnol. Appl. Clean Water 4 (2009) 47–58.
[87] C.-F. de Lannoy, E. Soyer, M.R. Wiesner, Optimizing carbon nanotube-reinforced polysulfone ultrafiltration membranes through carboxylic acid functionalization, J. Membr. Sci. 447 (2013) 395–402.
[88] H.A. Shawky, S.-R. Chae, S. Lin, M.R. Wiesner, Synthesis and characterization of a carbon nanotube/polymer nanocomposite membrane for water treatment, Desalination 272 (2011) 46–50.
[89] M.J. O'Connell, P. Boul, L.M. Ericson, C. Huffman, Y. Wang, E. Haroz, C. Kuper, J. Tour, K. D. Ausman, R.E. Smalley, Reversible water-solubilization of single-walled carbon nanotubes by polymer wrapping, Chem. Phys. Lett. 342 (2001) 265–271.
[90] T. Fujigaya, N. Nakashima, Non-covalent polymer wrapping of carbon nanotubes and the role of wrapped polymers as functional dispersants, Sci. Technol. Adv. Mater. 16 (2016) 1–21.
[91] X. Qu, P.J. Alvarez, Q. Li, Applications of nanotechnology in water and wastewater treatment, Water Res. 47 (2013) 3931–3946.
[92] L. Dumée, J. Lee, K. Sears, B. Tardy, M. Duke, S. Gray, Fabrication of thin film composite poly (amide)-carbon-nanotube supported membranes for enhanced performance in osmotically driven desalination systems, J. Membr. Sci. 427 (2013) 422–430.

[93] A.W. Thornton, A. Ahmed, M. Mainak, H.B. Park, A.J. Hill, Ultrafast transport in nanotubes and nanosheets, in: Y. (Ian) Cheng (Ed.), Nanotubes and Nanosheets: Functionalization and Applications of Boron Nitride and Other Nanomaterials, CRC Press, Boca Raton, FL, USA, 2015, p. 271.

FURTHER READING

[1] N.V. Priezjev, A.A. Darhuber, S.M. Troian, Slip behavior in liquid films on surfaces of patterned wettability: comparison between continuum and molecular dynamics simulations, Phys. Rev. E 71 (2005) 041608.
[2] C. Lee, S. Baik, Vertically-aligned carbon nano-tube membrane filters with superhydrophobicity and superoleophilicity, Carbon 48 (2010) 2192–2197.
[3] A. Sabir, M. Shafiq, A. Islam, A. Sarwar, M.R. Dilshad, A. Shafeeq, M.T.Z. Butt, T. Jamil, Fabrication of tethered carbon nanotubes in cellulose acetate/polyethylene glycol-400 composite membranes for reverse osmosis, Carbohydr. Polym. 132 (2015) 589–597.
[4] M.M. Pendergast, E.M.V. Hoek, A review of water treatment membrane nanotechnologies, Energy Environ. Sci. 4 (2011) 1946–1971.

CHAPTER 9

Satellites-Based Monitoring of Harmful Algal Blooms for Sustainable Desalination

Maryam R. Al Shehhi, Imen Gherboudj, Hosni Ghedira
Masdar Institute of Science and Technology, Abu Dhabi, United Arab Emirates

Contents

1. INTRODUCTION

Global demand for fresh water has increased in the past decades because of population growth and economic development (urbanization, industry, agriculture, energy generation, etc.) with unsustainable strategies, depletion of traditional freshwater supplies because of climate change, and improper management of scarce water resources. Water scarcity has become an alarming issue in many countries around the world where freshwater resources are very limited or are inappropriate for human consumption. According to the 2007 United Nations Water report [1], 2.7 billion people are already experiencing water scarcity at least 1 month per year, and following the current trend, it is projected that two-thirds of the world's population might face water shortages by 2025. Therefore there is an urgent need to monitor and manage water resources (quality and quantity) on both local and global scales and to implement efficient and equitable procedures to

Desalination Sustainability
http://dx.doi.org/10.1016/B978-0-12-809791-5.00009-2

manage the actual freshwater supplies (desalination plants, dams and lakes, treated sewage effluent, water wells, etc.).

Desalinated water has become an important source of the freshwater supply in many water-scarce countries. Significant expansion of desalination plants has occurred over the past decades, reaching ~17,000 to 20,000 plants in more than 150 counties because of technological advances that have in part led to a significant drop in water production cost [2]. These plants are distributed mainly in the countries suffering from severe water scarcity, such as in the Middle East (e.g., Saudi Arabia and the United Arab Emirates), the Caribbean, the Mediterranean area (e.g., Algeria and Spain), and Australia. The largest number of desalination plants are located in the Middle East, which has 27% of the world's installed plants (Fig. 1) and 65% of world's annual production capacity [3]. Indeed, the production capacity of this region has increased from 5 million (m^3 per day) in 1985 to 24 million (m^3 per day) in 2012 because of the rapid economic and population growth [4].

Desalination involves different technologies that remove dissolved salt and other impurities from seawater or brackish water, with the main ones being reverse osmosis (RO) and thermal distillation. Currently, most desalination plants use seawater reverse osmosis (SWRO) technology, which involves pushing water through a porous membrane less than 1 nm in size that filters out salts and other impurities [5]. This technology is more energy-efficient (3–5.5 kWh m^{-3}) than thermal distillation (MED: multieffect distillation, and MSF: multistage flash distillation) and mimics the natural watercycle by using more energy (MSF: 13.5–25.5 kWh m^{-3}; MED: 6.5–11 kWh m^{-3}) to create a vapor that is converted into fresh water through condensation [6,7]. However, SWRO plants are highly prone to operational problems caused by the outbreak of harmful algal

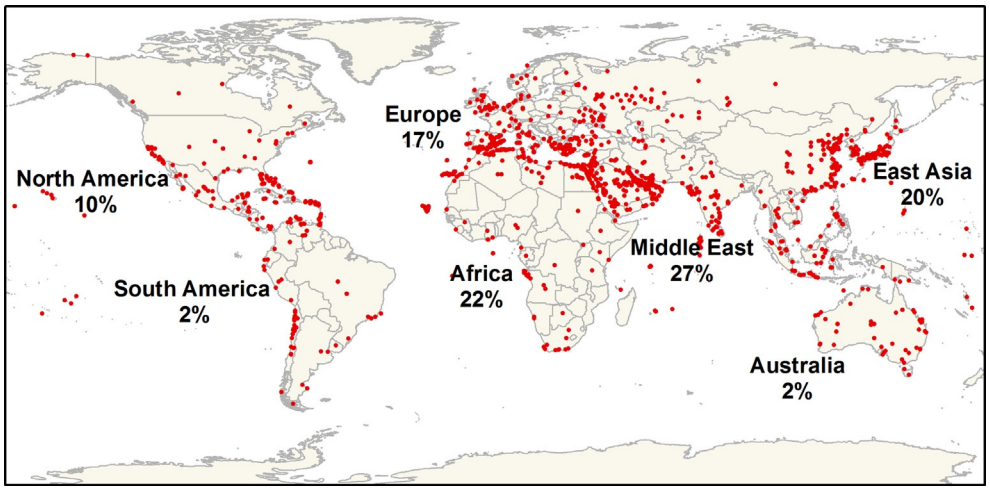

Fig. 1 Number of seawater RO desalination plants in the world. Pie charts show percentage of desalination plants in each region.

blooms (HABs) in areas surrounding the plant intake [8,9]. The adverse impact of HABs on SWRO plants received serious attention between 2008 and 2009 after major HAB outbreaks in the Arabian Gulf and the Sea of Oman. These HAB events significantly impacted, and in some cases interrupted, the operations of many desalination facilities over the region (e.g., Kalbah and Ghaleelah, United Arab Emirates) for extended periods of time because of damage caused in the SWRO membrane modules, ineffectiveness of the pretreatment facilities, improper feed water quality, and increase in the energy used [6,8,10].

Today real-time algal bloom detection and monitoring is becoming a high priority for many public water suppliers as they attempt to improve responsiveness and maintain the desired water production capacity. Such detection is ensured by using (i) in situ observing technologies (sensor networks and autonomous sensor-equipped vehicles located directly in the SWRO facilities) capable of gauging changes in biological and chemical properties at the upstream pretreatment stage [11,12], and/or (ii) remote sensing technology through the use of ocean color satellites that are able to assess the water quality (chlorophyll-*a* or Chl-*a*, colored dissolved organic matters: CDOM, sediments, etc.) at large temporal and spatial scales, providing a unique warning tool for continuous monitoring and forecasting of HAB outbreaks and evolution [13]. Evidently, satellite-based techniques offer more advantages than the in situ measurements because of the former's ability to detect and monitor the evolution of HABs before reaching the intake area [14,15]. Having this monitoring capability will certainly improve the plant's preparedness and responsiveness to HABs. Furthermore, remote sensing technology has already proven its efficiency and potential in several water resource monitoring and management applications, such as tracking oil pollution in the Arabian Gulf and the Sea of Oman [16,17], monitoring water turbidity [18], and assessment and management of the hydroelectric plants [19,20].

This chapter presents an overview of the HABs phenomenon, including their formation, triggering species, and negative impact on the operation of desalination plants. The unique potential of remote sensing techniques in detecting and monitoring HABs and in mitigating their impacts is also presented.

2. MARINE ALGAL BLOOMS

Algae, simple plants or plantlike organisms, are vital for maintaining life in marine ecosystems. However, they are considered harmful to many living organisms (zooplankton, marine animals, and birds) when certain types of microscopic algae (mainly dinoflagellates and, to a lesser extent, diatoms and cyanobacteria) are found abundantly in oceans, forming visible accumulated patches (greenish, reddish, and brownish) near the water's surface [21]. The negative effects of these harmful algal blooms culminate when water is depleted of oxygen, causing anoxia and hypoxia conditions in the surrounding aquatic species. Additionally, the extended presence of floating algae blocks sunlight from reaching

the seafloor and hinders the photosynthesis of aquatic plants. Toxins produced by HABs, such as CFP (ciguatera fish poisoning), NSP (neurotoxic shellfish poisoning), PSP (paralytic shellfish poisoning), DSP (diarrheic shellfish poisoning), and AS (amnesic shellfish poisoning), are in many cases harmful enough to kill fish and shellfish and cause health concerns for humans exposed to the toxins [8]. These effects can significantly impact the growth and survival of aquatic flora and fauna, cause illness and death to humans, and cause significant economic loss in many industries, such as fishing, aquaculture, tourism, and desalination.

2.1 HABs Formation

An increase in the growth and dominance of the HABs has occurred over the past few decades, specifically in the coastal areas where SWRO facilities are installed. This unexpected and excessive growth has been triggered by recent environmental changes in water temperatures, salinity, coastal upwelling, sea levels, and precipitation patterns. However, the primary factor causing and facilitating formation of HABs is attributed to the excessive level of nutrient concentrations in the waterbodies caused by nutrient-laden discharge from rivers, which are intensified by wind speed, water temperature, and cold eddies. The source of these nutrients is either natural (airborne dust deposition, upwelling of the seabed sediments, and riverine runoff) or anthropogenic (industrial and urban discharges).

Dust deposition is the primary natural source of nutrients in water [10]. These aerosols are emitted naturally from arid and semiarid regions all over the world and are transported by wind far from their source of origin and settle down either when wind speeds abate (dry deposition) or by precipitation produced through a washout process (wet deposition). Generally, the aerosol concentration is low during the autumn and winter seasons and high during the spring and summer seasons [22]. Furthermore, the presence of nutrients in seas surrounded by arid and semiarid lands, such as the Arabian Gulf and the Sea of Oman, is more prominent during the spring and summer seasons. Indeed, extreme HAB events were observed in Arabian Gulf and the Sea of Oman between 2008 and 2009, and more intensively during the dry seasons. These waterbodies are surrounded by the largest desert areas in the world (e.g., the Ad-Dahna erg and Rub' al Khali desert in Saudi Arabia, the Dasht-e Kavir desert in Iran, the Makran desert in Pakistan and Iran, and the Rigestan desert in Afghanistan) [23,24]. The sediments lying on the riverbed or the seabed are additional sources of the nutrients that can be found in the waterbodies. These nutrients are either discharged into the water through the riverine runoff process or stirred up from the bottom of the sea to the surface by the current motions and cold eddies. In the latter case, the growth of the phytoplankton can be intensified when the cyclonic eddy is affected by higher vertical velocity and more heat loss [25]. Many other triggers can also contribute to the over-enrichment of coastal waters with nutrients. These triggers

include outflow of treated and untreated wastewaters, unregulated discharge from sewage treatment plants, contaminated groundwater, flashflood discharge from nutrientrich soils, intensive fish farming, illegal discharge of ballast water, and oil spills. This overflow of nutrients has undoubtedly contributed to the disturbance of the equilibrium of the marine ecosystem and triggered HABs formation and dispersion.

2.2 HABs Characteristics

Bloom-forming species of algae exhibit enormous diversity in (i) morphology, as dinoflagellates, diatoms, and cyanobacteria consist, respectively, of two dissimilar flagella, silicified cell wall, and prokaryotic organisms [21,26], (ii) size, which varies with species (dinoflagellates: 5–2000 μm; diatoms: 2–200 μm; cyanobacteria: 0.5–40 μm) [21,27], (iii) water habitat, as dinoflagellates grow mostly in cold waters [21], while diatoms and cyanobacteria grow in cold and warm waters [21,28,29], and (iv) toxicity, as less than 1% of the algae produce toxins, which are mainly produced by the dinoflagellates (saxitoxin, and okadaic acids) and also diatoms (domoic acid) [21].

The intensity of the algal blooms is measured quantitatively either by cell count per volume or indirectly through Chl-*a* concentration. These latter variables, as well as their relationships, vary significantly depending on the formed species. In general, more than 30–50 mg m^{-3} of Chl-*a* concentration and millions of cells per liter can be considered as an algal bloom [21,30]. However, tens of millions of cells per liter are also confirmed in several studies to be algal bloom, such as $1–2.5 \times 10^5$ cells L^{-1} in the Gulf of Mexico [31], 1×10^5 cells L^{-1} in the west of Florida [32] and $1.1–2.1 \times 10^7$ cells L^{-1} in the Arabian Gulf [33].

Furthermore, algae formed in open waterbodies can cohabit with other suspended particulates, such as sediments and organic matter (dead leaves, twigs, etc.) [21]. These latter substances are rich in nitrogen, phosphorus, silicate, and other micronutrients that are required for algae growth. Algae may covary with the CDOM and other particulates in some waterbodies, classified as *Case I* waters. Conversely, algae concentration may not covary with the CDOM and other particulates in other waterbodies, classified as *Case II* waters. These latter waters are commonly called turbid waters because of the dominance of the inorganic particles compared to the microalgae.

2.3 Impact of Algal Blooms on SWRO

With the limited reserve water capacity or alternative freshwater sources, a major HAB outbreak surrounding desalination plants is considered a serious security threat to the region. HAB outbreaks directly affect the operational safety of desalination plants, especially the ones operating on RO technology. Sudden outbreaks of high biomass HABs through the plant intakes can restrict the flow of the seawater by clogging the pretreatment filters and even causing closure of the whole plant in some extreme cases.

Other direct impacts of HABs include fouling of the RO membranes with dissolved organic materials retained from the bloom-laden waters. Algal bloom disproportionally produces large amounts of dissolved organic matter (when it is greater than 2–30 million cells L^{-1} for dinoflagellates and 6–50 million cells L^{-1} for diatoms) that can pass through the pretreatment systems forming different substances (gels, polymers, and extracellular polymeric) that may be toxic [34].

Although most of these substances are effectively mitigated upstream of the SWRO through different pretreatments stages, such as coagulation followed by granular media filtration (GMF), dissolved air flotation algae removal, and low pressure-driven membrane filtration (MF: microfiltration, UF: ultrafiltration), the serious concerns still relate to algal biomass with a silt density index greater than 5 (SDI > 5) [35,36]. When they enter into the intake systems of desalination plants, organic matters can accumulate and grow in the SWRO membrane modules and/or in the pretreatment systems clogging the hydraulic network and in some extreme cases increase the membrane fouling rates [6]. Potential membrane fouling during the treatment of the algal bloom waters are caused by (i) accumulation of particles that pass through filters and other chemical procedures of the pretreatment process on the membrane surface (i.e., particulate fouling), (ii) growth of a microbial species on the membrane surface (i.e., biofouling), and (iii) adsorption of organic matter on the membrane surface (i.e., organic fouling). These fouling processes cause a subsequent reduction in the treatment and filtration performance, which results in a higher chemical consumption because of additional pretreatment processes and more frequent membrane cleaning, higher energy consumption because of higher overloading procedures, and higher material cost because of frequent replacement of damaged membranes. Obviously, a better understanding of the occurrence and growth dynamics of the algal blooms is crucial for the development of strategies that prevent, control, and mitigate SWRO operational problems caused by these fouling phenomena. Over time a panoply of strategies have been formulated, including an early warning HABs detection tool based on satellite images.

3. HAB MONITORING AND MAPPING USING REMOTE SENSING

3.1 History of Ocean Color Satellites

Earth observation technologies are widely used for detection, mapping, and monitoring water quality because of their ability to provide a spatially and temporally synoptic view of large waterbodies. Several factors such as the presence of suspended solids (sediments), algae (Chl-*a*, Carotenoids), chemicals (nutrients, insecticides, metals), dissolved organic matter, pathogens, and oil substances can affect the quality of the water.

Monitoring coastal waters and lakes from space can certainly improve emergency responses and help reduce the impact of accidental pollution on the aquatic environment. Effective monitoring of the aquatic environment from space has been successfully

demonstrated since the late 1970s [37]. The increasing use of earth observation technologies for monitoring water quality helps to alleviate the difficulties of conventional field-based techniques, such as the expense and the time required to perform in situ measurements and collect water samples over large areas [38].

Remarkable advances have been made in satellite ocean color technology and water quality retrieval from space. Remote sensing communities first focused on retrieving the physical properties of the pure water, which depends mainly on its optical properties and the composition of the overlaying atmosphere. Then efforts were made to further characterize the observed waterbodies by capturing the changes in spectral signatures and using several bands of the observed scene to associate the state of the observed waterbody with the optical reflectance measured by the satellite. In this early period, remote sensing was inadequate because of the lack of appropriate satellite bands that are more sensitive to water properties. With the continuous advances in sensor technologies, the signal quality and the improved spectral sensitivity of satellite bands led to a more accurate retrieval of water properties from space. New satellite sensors now can not only detect organisms in the water but can also differentiate between different types of organisms with different shapes, toxicity levels, and colors [39].

Numerous studies have been done using remote sensing technology in open and inland waterbodies using earth observation satellites that include a wide range of spectral and spatial resolutions covering the whole globe with reliable precision and accuracy.

The Coastal Zone Color Scanner (CZCS) was the first satellite-based sensor designed primarily for "ocean color" applications. CZCS was a multichannel scanning radiometer onboard the Nimbus 7 satellite, and in 1978 NASA launched it into the Earth's orbit. Nineteen years later, SeaWiFS was launched with an improved selection of spectral bands better adapted for water property retrieval and monitoring. One of the main uses for SeaWiFS was to detect and measure marine phytoplankton (microscopic marine plants) using a combination of seven tailored optical bands and one near-infrared channel. However, SeaWiFS stopped collecting data on Dec. 11, 2010. Because of progress made in hardware and modeling capabilities, newer and more sophisticated satellite sensors, such as Moderate Resolution Imaging Spectroradiometer (MODIS), MEdium Resolution Imaging Spectrometer (MERIS), and Visible Infrared Imager Radiometer Suite (VIIRS), continue to be used for a wide range of water monitoring.

MERIS is an inactive sensor onboard the ESA ENVISAT platform. It was launched in Mar. 2002 but stopped operating in May 2012 after communication failure of the ENVISAT, the world's largest civilian Earth observing satellite. With a temporal resolution of 35 days, MERIS had 15 bands ranging between 0.39 and 10.4 μm and a spatial resolution of 300 m [40,41]. With its extensive spectral range, MERIS was used to detect vegetation, clouds, water vapor, Chl-*a*, yellow substance, and detrital pigment [42].

MODIS sensors, currently flown on two NASA spacecrafts (Terra and Aqua), are the satellite-based instruments most used by the ocean color community. Terra (EOS AM) and

Aqua (EOS PM) satellites were launched by NASA in Dec. 1999 and May 2002, respectively. Their temporal resolution varies between 1 and 2 days, depending on the latitude of the observed area. Spatial, temporal, and spectral resolutions are more advanced in the MODIS satellite than the other launched satellites. It has 36 bands with different spatial resolutions of 250 m, 500 m, and 1 km, and the spectral resolutions of the bands range between 0.4 and 14.4 μm. This variety of spectral configurations was designed to detect the changes in vegetation, atmosphere, sediments, water quality, and clouds [42].

The most recent American sensors launched are VIIRS and the Operational Land Imager (OLI), which are on board of the Suomi National Polar-orbiting Partnership weather satellite (Suomi NPP) and Landsat 8, respectively. These instruments were launched in 2011 and 2013, respectively, to observe the land, ocean, and atmosphere on a global scale. VIIRS has 22 distinct spectral bands with wavelengths ranging from 0.4 to 11.8 μm, while OLI has 11 distinct spectral bands with wavelengths ranging from 0.43 to 12.51 μm. VIIRS can scan the Earth daily with a spatial resolution of 375 and 750 m [43], while OLI can revisit the same location every 16 days with a better spatial resolution (30 m) [44].

The Multi Spectral Instrument (MSI) and the Ocean and Land Color Instrument (OLCI) are the most recent European sensors flying onboard Sentinal-2 and Sentinel-3 since Jun. 2015 and Feb. 2016, respectively. MSI was designed to complement the Landsat series supporting the emergency and security applications [45], while the OLCI sensor was launched to continue the mission of MERIS [46]. These sensors were designed to have high-resolution multispectral imagery with a high revisit frequency that supports the next generation applications, such as change detection. Indeed, MSI has 13 distinct spectral bands with wavelengths ranging from 0.443 to 2.19 μm, a temporal resolution of 5 days and a wide field of view (290 km) [45], while OLCI has 11 distinct spectral bands with wavelengths ranging from 0.555 to 12 μm and a temporal resolution of 27 days [46].

Table 1 provides a summary of the specifications of the most commonly used satellite instruments in water quality applications.

3.2 Water Optical Properties

The properties of the remote sensing signals received from large waterbodies (lakes, seas, and oceans) depend on the downwelling incident radiation, which is mainly dependent on the Sun's elevation, atmospheric conditions, and the optical properties of the seawater (Fig. 2) [47]. The apparent optical properties include water reflectance (R_{rs}) and the water-leaving radiance (L_w) as described next.

– *Seawater* R_{rs} is the key component used in estimating water properties from the remotely sensed radiance beneath sea surface. Seawater R_{rs} is also the parameter describing the intrinsic color of the water [47,48]. R_{rs} is defined [49] as (Eq. 1) and it varies from 0 to 1, as

Table 1 The characteristics of the satellites commonly used in ocean color applications

		Periods		Resolutions				
				Spatial	Temporal	Spectral		
Sensor	Satellite	Start	End	Km	days	N° bands	Range (μm)	References
AVHRR	NOAA	1978	–	1.1	0.5	4	0.6–12	[108]
CZCS	Nimbus 7	1978	1986	0.825	1	6	0.433–12.500	[109]
SeaWiFs	Orbview-2	1997	2010	1.1	1	8	0.402–0.885	[110]
IKONOS	Ikonos	1999	–	0.0032, 0.001	11	5	0.45–0.88	[111]
MERIS	Envisat	2002	2010	0.3	35	15	0.39–10.4	[112]
MODIS	Aqua	2002	–	0.25, 0.5, 1	1	36	0.412–14.235	[42]
VIIRS	Suomi NPP	2011	–	0.375, 0.75	1	22	0.4–11.8	[43]
OLI	Landsat8	2013	–	0.3	16	11	0.43–12.51	[44]
MSI	Sentinal-2	2015	–	0.1, 0.2, 0.6	5	13	0.443–2.19	[45]
OLCI	Sentinal-3	2016	–	0.5, 1	27	11	0.555–12	[46]

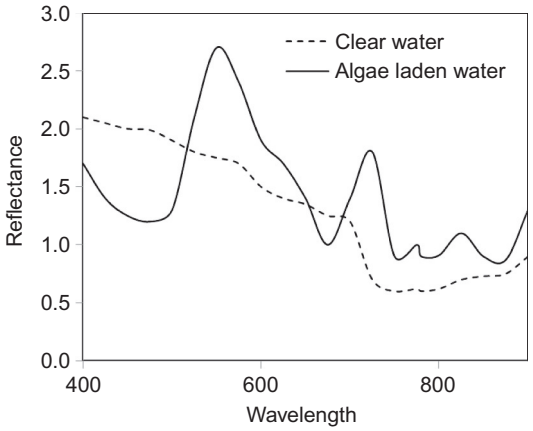

Fig. 2 Spectral reflectance of the clear water and algae-laden water.

$$R_{rs}(\lambda) = A\,\frac{b_b(\lambda)}{a(\lambda) + b_b(\lambda)} \tag{1}$$

where a is the absorption coefficient; b_b is the backscattering coefficient and A is a constant.

- *Water absorption* is a parameter accounting for the amount of photons removed when sunlight penetrates through a water column [47].
- *Water scattering* is the mechanism of redirecting the angle of the photon path that comes from the sunlight. This parameter includes the pure water scattering (b_w) and particle scattering coefficients (b_p) and the backscattering coefficient (b_b).
- *Seawater* L_w is defined as the radiance backscattered from the seawater [50] or the upwelling radiance where the radiance is defined as the radiant energy from a projected area per unit of solid angle in a radial direction per unit time ($\mathrm{Wm^{-2}\,sr^{-1}\,\mu m^{-1}}$) [51,52].

3.3 Spectrum of Algae-Laden Water

Fig. 2 presents the R_{rs} spectrum of algae-laden waters at the visible wavelengths. Similar behavior is also observed for L_w. As shown in this figure, the reflectance of *Case I* water is highly affected by the presence of algae compared to the pure water reflectance. The following behavior was observed at different spectral ranges:

- *Blue range (400–500 nm)*: R_{rs} of algae contaminated water is lower than pure water. A R_{rs} trough is observed near 440 nm because of Chl-*a* absorption [49].

- *Green range (500–600 nm):* R_{rs} increases at 500–600 nm, and it reaches the peak at around 550–565 nm mainly because of the minimum absorption of algae. Maximum R_{rs} value is observed near 560–565 nm because of the minimum absorption of the pigments [49]. However, low R_{rs} is observed in the wavelength greater than 565 nm because of the high absorption rate of algae [53].
- *Red range (600–700 nm)*: In this range, there is a small peak between 690 and 700 nm because of the interaction of algal cell scattering and the lowest combined impact of pigments and water absorption. While, low R_{rs} is observed near 665 nm due to absorption of algae [49], an R_{rs} peak is observed at 675 nm because of a strong absorption of detritus and algae [9,54].

When the seawater contains additional particulates (e.g., CDOM and sediments), the spectral R_{rs} becomes more complex and affects the efficiency of separating the Chl-*a* contribution to the total measured R_{rs} [55]. While CDOM causes high absorption in the entire visible spectrum especially at the blue range, the presence of sediments cause scattering in the whole visible spectrum. Therefore estimating the Chl-*a* concentrations is considerably easier in the oceans than in turbid coastal waters and lakes. Generally, the reason for this is the low CDOM and sediments in the open oceans.

The early ocean color models (OC4/OC3) were designed for *Case I* water where the sediment level is low. However, *Case II* waters such as shallow waters, river mouths, and coastal upwelling zones cause overestimation of the reflection of the light. Several research studies have demonstrated a direct correlation between the suspended sediment concentrations and the measured reflectance [56]. For instance, Han [57] found that when the suspended sediment concentrations in clear water increase from 0 to 500 mg L^{-1}, the reflectance at the red wavelength increases from 2% to 22% [57].

3.4 Retrieval of Chl-*a* With Ocean Color Models

One of the main applications of ocean color remote sensing is the estimation of the primary productivity of the waterbody, which is mainly related to the concentration of algae. However, in reality, the satellite ocean color can detect only Chl-*a*, which is a biomass indicator, instead of the primary production. This information can be used in early warning of HABs presence, where elevated levels of Chl-*a* can be observed in the water. Therefore ocean color models should account for the relationship between the estimated Chl-*a* and primary productivity. For this purpose, specific and adapted data modeling approaches should be used where the following parameters are required: (1) suitable spectral bands must be selected based on physical characteristics of the observed algae by using its specific *spectral reflectance/radiance behavior* and (2) cloud corrected estimates of daily surface solar irradiance, the oceanic optical depth, and the physiological variables must be collected. Finally, the obtained results must be compared with the field data,

generally field-measured data, to check the performance of the used or developed methodology. Moreover, in order to capture the seasonality and the continuous changes of the environmental conditions of the study area, repeated coverage of the same area is generally required.

Several algorithms were developed to estimate water quality parameters (e.g., Chl-*a*, fluorescence, and CDOM) from the ocean color sensors (MODIS, MERIS, SeaWiFS, VIIRS, CZCS) [9]. Algorithms for estimating Chl-*a* can be classified in two categories: band ratio algorithms (OC3: Ocean Color 3, OC2: Ocean Color 2, and OC4: Ocean Color 4, Dall'Olmo and Cannizzaro and Carder) [58–60] and index-based algorithms (FLH: Fluorescence Line Height, FAI: Floating algae index, and CI: Chlorophyll Index) [61–63].

The band ratio algorithms, generally polynomial, were developed to estimate Chl-*a* concentrations based on either blue and green reflectance (443, 488, 490, 510, 547, and 555 nm) or near-infrared (NIR) and red reflectance (667, 748, 678, and 748) [9,60]. These algorithms were developed using empirical approaches by relating the in situ Chl-*a* concentration collected at different stations and times with their corresponding satellite band ratio measurements. The ocean color algorithms (OC2, OC3, and OC4) were developed for clear waters (*Case I* waters), while Dall'Olmo and Cannizzaro algorithms were developed, respectively, for turbid (*Case II* waters) and shallow waters [58]. The performance of these algorithms varies from site to site as demonstrated in several studies [15,64–69].

Index based algorithms calculate the reflectance differences between green or red bands (555, 678, and 859 nm) and the linear baselines between the blue or red bands (469, 667, and 645 nm) and red or infrared bands (645, 748, and 1240 or 1640 nm) (Table 2). Index-based algorithms were found to be more accurate in estimating the Chl-*a* concentration for turbid waters (*Case II* waters) than the band ratio algorithm [61,62,70]. For instance, the CI index: provided a better understanding of Chl-*a* backscattering coefficients and non-phytoplankton absorption [62]. It was also found to have lower sensitivity to instrument noise than band ratio algorithms.

3.5 Mapping of Chl-*a* Concentrations Using Ocean Color Models

Ocean color satellite images (CZCS, SeaWiFS, and MODIS) have been used extensively over the past decades for two purposes.

The first purpose involved studying the trends of Chl-*a* globally during certain periods of time. The obtained maps showed that the oceans were under high stress when the global Chl-*a* increased by 4.1% within a period of 6 years (1998–2003) [71]. These changes were related to the increase of the sea's surface temperatures in spring and summer because of climate change [71]. Conversely, based on 35 years of CZCS and SeaWiFS images, [72] found that there was a significant decline in global Chl-*a*

Table 2 Formulations of the empirical and semi-analytical ocean color models

Algorithm	Category	Used bands	Equations	Application location and date	References
OC3	Empirical	443 nm 488 nm 547 nm	$\log_{10}(\text{Chl a}) = 0.283 - 2.753R_{rs} + 0.659R_{rs}^2 + 0.649R_{rs}^3 - 1.403R_{rs}^4$ $R_s = \log_{10}(\max[R_{rs}(443/547, 488/547)])$	US coast, Atlantic and Pacific ocean	[9,13]
Dall'Olmo Chlorophyll	Empirical	667 nm 678 nm 748 nm	$\log_{10}(\text{Chl } a) = 2.048 + (1.38 \times \log_{10}[R_{rs}(748)/R_{rs}(667)])$ $\log_{10}(\text{Chl } a) = 2.046 + (1.49 \times \log_{10}[R_{rs}(748)/R_{rs}(678)])$	Sand pit lakes and reservoirs in Eastern Nebraska (USA), 2005	[59]
Cannizzaro and Carder	Semi-analytical	412 nm 490 nm 555 nm 670 nm	$\log(\text{Chl } a) = a_0 + a_1(\log R) + a_2(\log R)^2 + a_3(\log R)^3$ • Shallow designation (Curve > Upper_limit): $R_{shallow} = R_{rs}412/R_{rs}667$ $a_{shallow} = [0.8840, -2.0837, 1.3061, -0.3906]$ • Deep designation (curve < Lower_limit): $R_{deep} = R_{rs}488/R_{rs}551$ $a_{deep} = [0.0597, -2.2291, 2.6691, -3.4144]$ • Transitional designation (Lower_limit < Curve < Upper_limit): $\text{Chl } a = w \times (\text{Chl } a_{deep}) + (1-w) \times \text{Chl } a_{shallow}$ $w = (\text{Curve} - \text{Lower\_limit})/(\text{Upper\_limit} - \text{Lower\_limit})$ $\text{with: Curve} = \log_{10}(R_{rs}412/R_{rs}667)/(R_{rs}551)^2$ $\text{Upper\_limit} = -2.44 + 0.80\log_{10}(R_{rs}412/R_{rs}667) + 0.080\log_{10}(R_{rs}412/R_{rs}667)^2$ $\text{Lower\_limit} = -0.20 + 0.13\log_{10}(R_{rs}412/R_{rs}667 + 0.130\log_{10}(R_{rs}412/R_{rs}667)^2$	West Florida shelf and Bahamian Waters, 2004	[58]

Continued

Table 2 Formulations of the empirical and semi-analytical ocean color models—cont'd

Algorithm	Category	Used bands	Equations	Application location and date	References
OC2	Empirical	490 nm 555 nm 547 nm	$\log_{10}(\text{Chl}\,a) = 0.2974 - 2.2429R_{rs} + 0.8358R_{rs}^2 - 0.0077R_{rs}^3 - \log_{10}(-0.0929)$ $R_s = \log_{10}\left[R_{rs}\left(\frac{490}{555}\right)\right]$ or $\left[\log_{10}\left(\frac{490}{547}\right)\right]$	US coast, Atlantic, and Pacific Ocean	[13]
FLH	Empirical	667 nm 678 nm 748 nm	$\text{FLH} = L_{w14} - L_{\text{baseline}}$ $L_{\text{baseline}} = L_{w15} + (L_{w13} - L_{w15}) \times [(748-678)/(748-667)$	West Florida	[63]
FAI	Empirical	645 nm 859 nm 1240 nm	$\text{FAI} = R_{rc}(859) - R'_{rc}(859)$ $R'_{rc}(859) = R_{rc}(645) + (R_{rc}(1240) - R_{rc}(645)) \times [(859-645)/(1240-645)]$	China	[61]
CI	Empirical	469 nm 555 nm 645 nm	$\text{CI} = R_{rc}(555) - R'_{rc}(555)$ $R'_{rc}(555) = R_{rc}(469) + (R_{rc}(645) - R_{rc}(469)) \times [(555-469)/(645-469)]$	China	[62]

concentrations from 1980 to 2010 in over 62% of the global sea surface with significant levels observed in the offshore rather than the inshore areas [72].

The second purpose involved studying the spatiotemporal distribution of Chl-*a* and characterizing the algal species across the world.

These studies focused on the aforementioned two purposes to understand the effect of climate change on the Chl-*a* trends and characterize the involved algal species, which will help in developing regional effective monitoring, early warning systems, and selection of an optimal place for allocating the desalination systems.

Therefore, based on several research studies, four regions of frequent HABs events have been discerned: North America, Europe, East Asia, and the Arabian region, where HABs resulted in disruption of desalination plants and death of aquatic life. The description of the HABs events over these regions is presented next.

- North-America region

  In this region, high levels of Chl-*a* were observed in the shallow and coastal areas of West Florida [70], Northeastern United States [73], and the equatorial Pacific [74], which resulted in the mortality of fish (>1 foot long) and dolphins [70,73]. These HABs were observed mainly during the summer season, where *Trichodesmium* [75] and *Karenia brevis* patches were the main species [75]. Diatoms patches were also seen over the region with concentration ratios (inner: outer shelf) of 15:1 and 4–9:1 in summer and winter seasons, respectively [76]. The occurrence of these HABs in these regions was supported by upwelling of the highly nutrient water [74], river inflow (Chesapeake runoff, Delaware Bay, and Hudson River Estuary) [73], and wind speed [75]. Fig. 3A and B shows a HAB event in Southwest Florida presented by MODIS Chl-*a* (A) and MODIS FLH (B). As shown in this figure, high values of Chl-*a* >10 mg m^{-3} were found in four nearby RO coastal desalination plants (e.g., Tampa Bay and Cape Coral desalination plants) that might have been affected by this event.

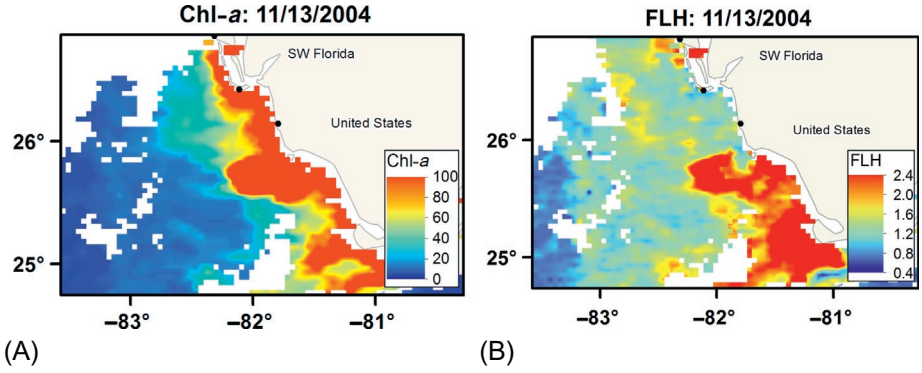

Fig. 3 MODIS/Aqua imagery for Southwest Florida coastal waters during a HAB event. (A) band-ratio Chl-*a* concentration (MODIS OC3M Chl-*a*, mg m^{-3}) and (B) fluorescence line height (FLH, W m^{-2} μm^{-1} sr^{-1}).

- Europe

  In european waters, high blooming is frequent in the summer in the Western English Channel where the common HABs are caused by the *Coccolithophore* and dinoflagellate *Karenia mikimotoi* species, which can last from 1 to 5 weeks with a maximum Chl-*a* of 40 mg m^{-3} [77]. More active blooms have occurred in the spring season in the Bay of Biscay (Mar. through May) because of a 12°C increase in the sea's surface temperature and the water's low turbulence. Fig. 4 shows algal bloom events in the Bay of Biscay and the Western English Channel in mid-Apr. 2004 and Aug. 2000, which were derived from MODIS OC3 and SeaWiFS Chl-*a*, respectively. These events could affect the coastal desalination plants where one desalination plant is located near the Bay of Biscay and several others (>4) are located along the Western English Channel, as shown in Fig. 4.

- East Asia

  HAB outbreaks have occurred in the coastal areas of Korea. These outbreaks which were caused by dinoflagellate *Cochlodinium polykrikoides* were detected in the summer and fall seasons of 2003 based on MODIS OC3 (Fig. 5A), and caused a 30% reduction in the desalination flow rate [78]. HAB events have also occurred in the northern South China Sea as detected by MODIS FLH (Fig. 5B). In addition, HAB outbreaks have occurred in other waterbodies of China, such as in Taihu Lake (summer 2007), which were caused by the cyanobacteria species [79]; in the Pearl River Estuary, which were caused by the *Gymnodinium* species (1998) [80]; and at the Taiwan Strait and Hainan Island [79,81]. Furthermore, low Chl-*a* were found in offshore waters and in the Pelagic region as a result of the regional effects of low sea surface temperatures and mixed layer depths [81].

  As for the temporal analysis, the appearance of these HABs can be explained by the increase in sea surface temperature because of climate changes [78], low wind speeds, anthropogenic nutrients [79], and upwelling [81].

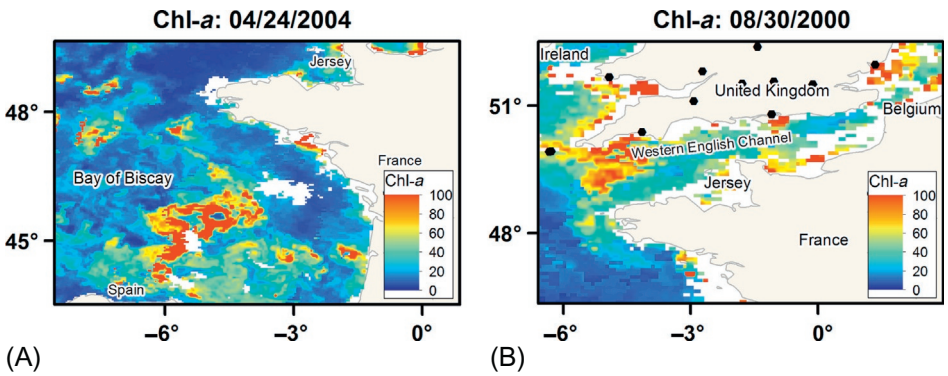

Fig. 4 Phytoplankton bloom in the (A) Bay of Biscay using MODIS OC3 and (B) Western English Channel using SeaWiFS OC2 in Apr. 2004 and Aug. 2000, respectively.

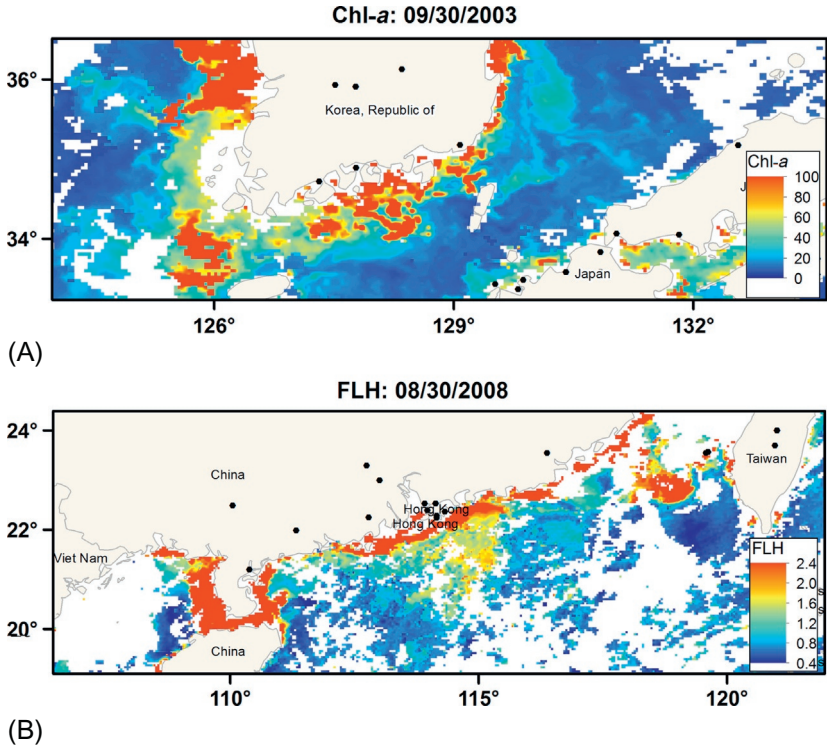

Fig. 5 (A) Chl-*a* (mg m^{-3}) estimated by MODIS Aqua OC3 on Sep. 30, 2003; (B) (FLH) for Aug. 30, 2008, MODIS-Terra in northern South China Sea.

- Middle East

  In the Arabian region, high Chl-*a* concentrations were observed in the summer seasons in the shallow and coastal areas of the Arabian Sea, the Arabian Gulf, and the Sea of Oman [14,82,83]; and in the eastern and western parts of the Arabian Sea where the range of Chl-*a* varied between 0.01 and 38.85 mg m^{-3} from 2009 to 2011 because of river inflow, winter convection, and upwelling [84]; and in the northern and middle parts of the Arabian Gulf [14,83]. Low Chl-*a* concentrations were also observed in the Red Sea (<2 mg m^{-3}) in 2011, as shown in Fig. 6A [82].

  Although the summer season is the likely season for the blooms to grow in the Arabian region, high Chl-*a* events were also observed in the winter season in the eastern Arabian Sea (Chl-*a*: 1–5 mg m^{-3}) in 2005 [69], in the offshore region of the southern Arabian Sea [69], and in the northern Arabian Sea where the *Noctiluca scintillans* covered the area for 3 months [85] in 2006, as shown in Fig. 6B [86].

  During this season (winter), the worst HAB outbreak occurred in the Sea of Oman and the Arabian Gulf in 2008 [14,15], which sealed the Fujairah, Kalba, and Ghaleelah RO desalination plants. During this event, the bloom patches started on Aug. 26,

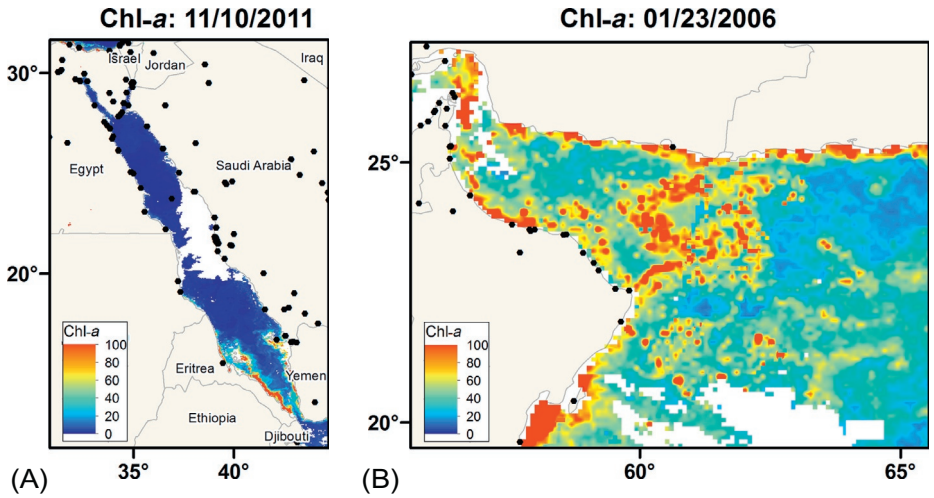

Fig. 6 Chl-*a* derived from MODIS-Aqua, using OC3M for (A) Nov. 2011 in Red Sea and (B) Jan. 2006 in the Arabian Sea.

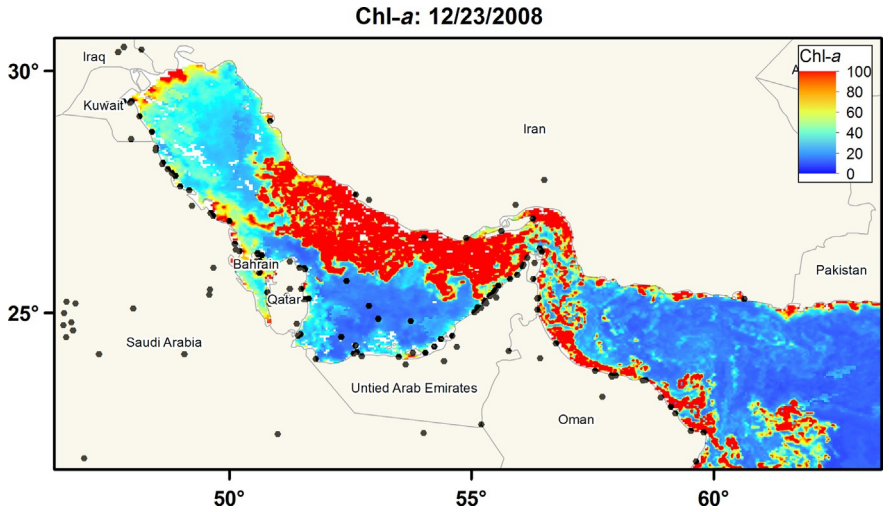

Fig. 7 Chl-*a* concentration for Dec. 23, 2008, using MODIS OC3 in the Arabian Gulf.

2008, in the Arabian Sea and was transported through sea circulation to the Sea of Oman and the Arabian Gulf. The blooms sustained their growth in the region until Nov. 2009 because of the cold eddies and heavy dust loading that supplied adequate nutrients to the species. High Chl-*a* concentrations were found during this HAB event Dec. 23, 2008, (Fig. 7) and Oct. 7, 2008, where dense patches of *Cochlodinium*

polykrikoides and *Trichodesmium* species were seen in the northern part near Iran [14], in the middle part of the Arabian Gulf, and along the coastal line of the United Arab Emirates and Oman sealing the desalination plants [15].

3.6 Factors Affecting Ocean Color Reflectance

3.6.1 Atmospheric Aerosols

High-concentration aerosols make the retrieval of surface information (land and water surfaces) by satellite measurements very challenging especially over arid areas. The size, shape, and composition of these airborne particles vary with time (i.e., interactions with clouds and humidity), making quantification and tracking more complex [87]. Thus atmospheric correction is one of the crucial steps in processing satellite data, especially in ocean color applications where the reflections of aerosols exceed those received from the waterbody [87–89]. This correction aims to remove the atmospheric effects caused by the aerosol particles from the images especially in high-dust-loading regions such as the Arabian Sea. Several advanced atmospheric correction algorithms were developed for MODIS images [90,91]. These models are based mainly on the multiple scattering between aerosols and air molecules and can also be associated with other models, depending on the environment in which they are used [92]. These models assume negligible reflectance from waterbodies at the NIR and the short-wave infrared (SWIR) ranges [91,93–96].

3.6.2 Shallow Water and Sea Bottom Effect

Satellite measurements are highly affected by the sea bottom, which increases the total reflectance and adds more complexity to the retrieval of water properties. For instance, using red-colored sand, Gilvear et al. [97] proved that the reflectance of the red wavelength decreases as the water depth increases [97]. In addition, when water is surrounded by land, the satellite measurement on the edges can be affected [98]. This mixed pixel effect is observed mainly near islands and coastal lines. The presence of land patches in water-dominated pixels can increase the total reflectance; however, the extent of increase in reflectance is more in the red band than the blue band [99]. Thus, removal of all mixed pixels from the retrieval process to avoid erroneous classifications is highly recommended.

3.6.3 Low Resolution of the Satellites Images

The low resolution of satellites (1 km for MODIS) can limit the study of the water quality parameters of small waterbodies or shorelines. In such areas, the water pixels are almost mixed with land. Use of the MODIS images over such areas overestimates the remote sensing reflectance. Airborne instruments, such as AISA (Airborne Imaging Spectrometer for Application), CASI (Compact Airborne Spectrographic Imager), and HyMap,

are more appropriate for such areas because they give reliable results. However, these techniques are more expensive than satellite images and require prior planning and scheduling, which limits their use in operational and emergency response modes.

3.7 Automated HABs Tracking

Effective HAB-monitoring programs require accurate tools to detect, track the movement of the HABs, and forecast their intensity and positon in the near future. Such systems can be used by concerned authorities as an alerting tool to assess imminent and potential risks of HABs for humans, marine life, natural resources, coastal industries, and water quality [100]. These tracking tools can use current and historical Chl-*a* data. The HABs tracking tool, Stumpf model, was established in West Florida. This model subtracts the current Chl-*a* data from the 2-month mean of the prior 2 weeks, which can adequately characterize the seasonal changes [101,102]. A potential HAB event can be detected when the Stumpf model shows Chl-*a* higher than 1 mg m^{-3} [102]. The same model (Chl-*a* anomaly) has been used successfully to track the *Karenia brevis* species in West Florida and to predict Chl-*a* in the Arabian Gulf [14].

In addition to the Chl-*a* data, physical (sea surface temperature, water circulation) and metrological (wind speed) data can be used as supporting information for numerical modeling of the HABs. Indeed, this additional information can indicate the dynamic processes of HABs and where they are likely to grow, such as upwelling zones and nutrient-rich waters [103]. The movement of the HABs depends on the water circulations, which could be forecasted using the near shore hydrodynamic models [104]. The water circulations can be also associated with plume trajectories, such as in Burns Ditch and Clinton River as part of the Great Lakes and Human Health (CEGLHH) program [100]. Wind data can also be used to track the transport of the HABs in Southwest Florida, where wind speeds of ~3 m s^{-1} could move the blooms in the opposite direction [105]. In addition to using the wind data, Zheng and Weisberg have established a trajectory-tracking tool called West Florida Coastal Ocean Model (WFCOM) by using heat forcing, rivers and turbulence closure, and finite volumes to forecast the HABs in the West of Florida within 3.5 days earlier [106]. Coupled biophysical models of wind, phytoplankton species, nutrients, and grazing stress were also integrated to track HABs in West Florida [107].

3.8 Summary

Desalination is one of the major new sources of the world's fresh water, especially in arid regions. The two conventional desalination technologies are thermal distillation (MSF and MED) and RO. The latter can be prone to have operational problems because of the existence of pollutants in the intake water, such as HABs, that have interrupted and sealed RO desalination plants worldwide. Therefore there is an urgent need to

monitor HABs in order to maintain the production of fresh water at the desired level. Remote sensing is an effective tool for water quality monitoring and mapping. Its use was extended to such applications because of the availability of numerous satellite platforms such as CZCS, SeaWiFS, MODIS, and MERIS, allowing coverage of large areas of waterbodies (oceans, seas, and lakes) with high temporal and spatial resolutions. The main objective of these satellites is to provide quantitative data on global ocean bio-optical properties (Chl-*a*, CDOM, fluorescence, etc.) to the Earth science community based on their optical and near-infrared bands. However, the quality of the satellite data retrieved from the water can deteriorate because of the presence of dense dust particles in the atmosphere, sediments in the water, and the effect of the water bottom reflectance. These real-time data can be combined later with the hydrodynamic models and the meteorological data to develop a forecasting system that can work as an early warning tool to detect and track the movements of HABs.

REFERENCES

[1] UN-Water, Coping with Water Scarcity: Challenge of the Twenty-First Century, 2007.

[2] S. Lattemann, M.D. Kennedy, J.C. Schippers, G. Amy, Global desalination situation, in: I.C. Escobar, A.I. Schäfer (Eds.), Sustainable Water for the Future: Water Recycling versus Desalination, Sustain. Sci. Eng., vol. 2, Elsevier, UK, 2010, pp. 7–39.

[3] M. Shatat, M. Worall, S. Riffat, Opportunities for solar water desalination worldwide: review, Sustain. Cities Soc. 9 (2013) 67–80.

[4] O. Saif, The Future Outlook of Desalination in the Gulf: Challenges & Opportunities Faced by Qatar & the UAE, Environment and Health Research Paper: United Nations University for Water, 2012.

[5] C. Fritzmann, J. Löwenberg, T. Wintgens, T. Melin, State-of-the-art of reverse osmosis desalination, Desalination 216 (1–3) (2007) 1–76, http://dx.doi.org/10.1016/j.desal.2006.12.009.

[6] S.A. Avlonitis, K. Kouroumbas, N. Vlachakis, Energy consumption and membrane replacement cost for seawater RO desalination plants, Desalination 157 (2003) 151–158, http://dx.doi.org/10.1016/S0011-9164(03)00395-3.

[7] L.O. Villacorte, S.A.A. Tabatabai, N. Dhakala, G. Amy, J.C. Schippers, M.D. Kennedy, Algal blooms: an emerging threat to seawater reverse osmosis desalination, Desalin. Water Treat. 55 (10) (2015) 2601–2611.

[8] D.A. Caron, et al., Harmful algae and their potential impacts on desalination operations off southern California, Water Res. 44 (2010) 385–416, http://dx.doi.org/10.1016/j.watres.2009.06.051.

[9] S. Martin, An Introduction to Ocean Remote Sensing, Cambridge University Press, New York, USA, 2004.

[10] M.R. Al-Shehhi, I. Gherboudj, H. Ghedira, An overview of historical harmful algae blooms outbreaks in the Arabian Seas, Mar. Pollut. Bull. 86 (1–2) (2014) 314–324, http://dx.doi.org/10.1016/j.marpolbul.2014.06.048.

[11] L. Campbell, R.J. Olson, H.M. Sosik, A. Abraham, D.W. Henrichs, C.J. Hyatt, E.J. Buskey, First harmful dinophysis (dinophyceae, dinophysiales) bloom in the U.S. is revealed by automated imaging flow cytometry, J. Phycol. 46 (1) (2010) 66–75, http://dx.doi.org/10.1111/j.1529-8817.2009.00791.x.

[12] T.L. Richardson, J. Pinckney, Monitoring of the toxic dinoflagellate *Karenia brevis* using gyroxanthin-based detection methods, J. Appl. Phycol. 16 (4) (2004) 315–328.

[13] J. O'Reilly, S. Maritorena, B. Mitchell, D. Siegel, K. Carder, S. Garver, M. Kahru, C. McClain, Ocean color chlorophyll algorithms for SeaWiFS, J. Geophys. Res. Oceans 103 (C11) (1998) 24937–24953.

[14] M. Moradi, K. Kabiri, Red tide detection in the Strait of Hormuz (east of the Persian Gulf) using MODIS fluorescence data, Int. J. Remote Sens. 33 (4) (2012) 1015–1028.
[15] J. Zhao, H. Ghedira, Monitoring red tide with satellite imagery and numerical models: a case study in the Arabian Gulf. Mar. Pollut. Bull. 79 (2014) 305–313, http://dx.doi.org/10.1016/j.marpolbul.2013.10.057.
[16] J. Zhao, M. Temimi, H. Ghedira, C. Hu, Exploring the potential of optical remote sensing for oil spill detection in shallow coastal waters-a case study in the Arabian Gulf, Opt. Express 22 (11) (2014) 13755–13772, http://dx.doi.org/10.1364/OE.22.013755.
[17] J. Zhao, M. Temimi, M. Al Azhar, H. Ghedira, Satellite-based tracking of oil pollution in the Arabian Gulf and the Sea of Oman, Can. J. Remote Sens. 41 (2) (2015) 113–125.
[18] M.R. Al Kaabi, J. Zhao, C. Charron, I. Gherboudj, M. Lazzarini, H. Ghedira, Developing satellite-based tool for water turbidity mapping in the Arabian Gulf: Abu Dhabi case study, in: Oceans-San Diego, 2013, IEEE, 2013, pp. 7–10.
[19] S. Dudhania, A.K. Sinhab, S.S. Inamdara, Assessment of small hydropower potential using remote sensing data for sustainable development in India, Energy Policy 34 (17) (2006) 3195–3205.
[20] S. Mermoz, S. Allain, M. Bernier, E. Pottier, I. Gherboudj, Classification of river ice using polarimetric SAR data, Can. J. Remote Sens. 35 (5) (2009) 460–473, http://dx.doi.org/10.5589/m09-034.
[21] K. Rogers, Fungi, Algae, and Protists, Britannica Educational Publishing, Chicago, 2011. EPUB.
[22] I. Gherboudj, H. Ghedira, Spatiotemporal assessment of dust loading over the United Arab Emirates, Int. J. Climatol. (2014), http://dx.doi.org/10.1002/joc.3909.
[23] P. Ginoux, J.M. Prospero, T.E. Gill, N.C. Hsu, M. Zhao, Global scale attribution of anthropogenic and natural dust sources and their emission rates based on MODIS deep blue aerosol products, Rev. Geophys. 50 (3) (2012) 3005.
[24] J.M. Prospero, P. Ginoux, O. Torres, S.E. Nicholson, T.E. Gill, Environmental characterization of global sources of atmospheric soil dust identified with the NIMBUS 7 total ozone mapping spectrometer (TOMS) absorbing aerosol product, Rev. Geophys. 40 (1) (2002) 1–31.
[25] D.L. Tang, H. Kawamura, A.J. Luis, Short-term variability of phytoplankton blooms associated with a cold eddy in the northwestern Arabian Sea, Remote Sens. Environ. 81 (1) (2002) 82–89.
[26] W.W. Carmichael, Cyanobacteria secondary metabolites—the cyanotoxins, J. Appl. Bacteriol. 72 (6) (1992) 445–459, http://dx.doi.org/10.1111/j.1365-2672.1992.tb01858.x.
[27] C. Sancetta, Identifying marine diatoms and dinoflagellates, Mar. Geol. 136 (3–4) (1997) 320–321, http://dx.doi.org/10.1016/S0025-3227(97)81154-1.
[28] L.R. Mur, O.M. Skulberg, H. Utkilen, Cyanobacteria in the environment, in: Toxic Cyanobacteria in Water: A Guide to Their Public Health Consequences, Monitoring and Management, CRC Press, FL, USA, 1999, p. 30 (Chapter 2).
[29] J.G. Stockner, The ecology of a diatom community in a thermal stream, Br. Phycol. Bull. 3 (3) (1968) 501–514, http://dx.doi.org/10.1080/00071616800650101.
[30] T. Okaichi, Red Tides, Springer Science & Business Media, Springer, Netherlands, 2004.
[31] P.A. Tester, K.A. Steidinger, Gymnodinium breve red tide blooms: initiation, transport, and consequences of surface circulation, Limnol. Oceanogr. 42 (5, Part 2) (1997) 1039–1051, http://dx.doi.org/10.4319/lo.1997.42.5_part_2.1039.
[32] K. Carder, R. Steward, A remote-sensing reflectance model of a red-tide dinoflagellate off west Florida, Limnol. Oceanogr. 30 (2) (1985) 286–298.
[33] M.L. Richlen, S.L. Morton, E.A. Jamali, A. Rajan, D.M. Anderson, The catastrophic 2008–2009 red tide in the Arabian gulf region, with observations on the identification and phylogeny of the fish-killing dinoflagellate Cochlodinium polykrikoides, Harmful Algae 9 (2) (2010) 163–172, http://dx.doi.org/10.1016/j.hal.2009.08.013.
[34] S.H. Kim, J.S. Yoon, Optimization of microfiltration for seawater suffering from red-tide contamination, Desalination 182 (1–3) (2005) 315–321, http://dx.doi.org/10.1016/j.desal.2005.02.030.
[35] M.B. Dixon, C. Falconet, L. Ho, C.W.K. Chow, B.K. O'Neill, G. Newcombe, Removal of cyanobacterial metabolites by nanofiltration from two treated waters, J. Hazard. Mater. 188 (1–3) (2011) 288–295.

[36] M.V. Laycock, D.M. Anderson, J. Naar, A. Goodman, D.J. Easy, M.A. Donovan, A. Li, M. A. Quilliam, E. Al Jamali, R. Alshihi, Laboratory desalination experiments with some algal toxins, Desalination 293 (2012) 1–6.
[37] M. Fengyun, Progress in water quality monitoring based on remote sensing and GIS, in: 2010 International Conference on Challenges in Environmental Science and Computer Engineering (CESCE), vol. 2, 2010, pp. 208–211.
[38] J.A. Dominguez, C. Alonso, A. Alonso, Remote sensing as a basic toolbox for monitoring water quality parameters and as a system of surveillance of cyanobacterial harmful algae blooms (SCyanoHABs), in: IEEE International Geoscience and Remote Sensing Symposium, 2008 (IGARSS 2008), vol. 4, IEEE, 2008, p. IV-886.
[39] N. Wiangwang, J. Qi, Water quality assessment using hyperspectral remote sensing, in: Geoscience and Remote Sensing Symposium, 2005 (IGARSS '05), 2005, pp. 4531–4534.
[40] H.J. Gons, M.T. Auer, S.W. Effler, MERIS satellite chlorophyll mapping of oligotrophic and eutrophic waters in the Laurentian Great Lakes, Remote Sens. Environ. 112 (11) (2008) 4098–4106, http://dx.doi.org/10.1016/j.rse.2007.06.029.
[41] A. Minghelli-Roman, L. Polidori, S. Mathieu-Blanc, L. Loubersac, F. Cauneau, Spatial resolution improvement by merging MERIS-ETM images for coastal water monitoring, IEEE Geosci. Remote Sens. Lett. 3 (2) (2006) 227–231.
[42] X. Xiong, K. Chiang, J. Sun, W.L. Barnes, B. Guenther, V.V. Salomonson, NASA EOS Terra and Aqua MODIS on-orbit performance, Adv. Space Res. 43 (3) (2009) 413–422, http://dx.doi.org/10.1016/j.asr.2008.04.008.
[43] C. Cao, NPP VIIRS SDR postlaunch calibration/validation, in: AMS Conference, 2012.
[44] D.P. Roy, et al., Landsat-8: science and product vision for terrestrial global change research, Remote Sens. Environ. 145 (2014) 154–172, http://dx.doi.org/10.1016/j.rse.2014.02.001.
[45] M. Drusch, et al., Sentinel-2: ESA's optical high-resolution mission for GMES operational services, Remote Sens. Environ. 120 (2012) 25–36, http://dx.doi.org/10.1016/j.rse.2011.11.026.
[46] C. Donlon, et al., The Global Monitoring for Environment and Security (GMES) Sentinel-3 mission, Remote Sens. Environ. 120 (2012) 37–57, http://dx.doi.org/10.1016/j.rse.2011.07.024.
[47] A. Morel, In-water and remote measurements of ocean color, Bound.-Layer Meteorol. 18 (2) (1980) 177–201.
[48] J. Ronald, V. Zaneveld, Remotely sensed reflectance and its dependence on vertical structure: a theoretical derivation, Appl. Opt. 21 (22) (1982) 4146–4150.
[49] A. Morel, L. Prieur, Analysis of variations in ocean color, Limnol. Oceanogr. 22 (1977) 709–722, http://dx.doi.org/10.4319/lo.1977.22.4.0709.
[50] H.R. Gordon, K.J. Voss, MODIS Normalized Water-Leaving Radiance (ATBD MOD18, v4), 1999.
[51] R.W. Austin, Inherent Spectral Radiance Signatures of the Ocean Surface. Ocean Color Analysis. 7410 (1974) 1–20.
[52] V. Barale, J.F.R. Gower, L. Alberotanza, Oceanography from Space: Revisited, Springer Science & Business Media, Netherlands, 2010.
[53] K. Carder, R. Steward, J.H. Paul, G.A. Vargo, Relationships between chlorophyll and ocean color constituents as they affect remote-sensing reflectance models, Limnol. Oceanogr. 31 (2) (1986) 403–413.
[54] R.R. Bidigare, M.E. Ondrusek, J.H. Morrow, D.A. Kiefer, In-vivo absorption properties of algal pigments, in: R.W. Spinrad (Ed.), Orlando'90, 16–20 April, 1990, pp. 290–302.
[55] J.R. Jensen, Remote sensing of the environment: an earth resource perspective, Prentice Hall, Upper Saddle River, NJ, 2000.
[56] A.R.M. Amin, K. Abdullah, Sediment and shallow coastal water detection utilizing MODIS land channels over Gulf of Martaban, Appl. Phys. Res. 2 (2) (2010) p61, http://dx.doi.org/10.5539/apr.v2n2p61.
[57] L. Han, Spectral reflectance with varying suspended sediment concentrations in clear and algae-laden waters, Photogramm. Eng. Remote Sens. 63 (6) (1997) 701–705.
[58] J.P. Cannizzaro, K.L. Carder, Estimating chlorophyll a concentrations from remote-sensing reflectance in optically shallow waters, Remote Sens. Environ. 101 (1) (2006) 13–24.

[59] G. Dall'Olmo, A.A. Gitelson, D.C. Rundquist, B. Leavitt, T. Barrow, J.C. Holz, Assessing the potential of SeaWiFS and MODIS for estimating chlorophyll concentration in turbid productive waters using red and near-infrared bands, Remote Sens. Environ. 96 (2) (2005) 176–187, http://dx.doi.org/10.1016/j.rse.2005.02.007.
[60] J.E. O'Reilly, S. Maritorena, B.G. Mitchell, D.A. Siegel, K.L. Carder, S.A. Garver, M. Kahru, C. McClain, Ocean color chlorophyll algorithms for SeaWiFS, J. Geophys. Res. 103 (C11) (1998) 24937, http://dx.doi.org/10.1029/98JC02160.
[61] C. Hu, A novel ocean color index to detect floating algae in the global oceans, Remote Sens. Environ. 113 (10) (2009) 2118–2129.
[62] C. Hu, Z. Lee, B. Franz, Chlorophyll a algorithms for oligotrophic oceans: a novel approach based on three-band reflectance difference, J. Geophys. Res. Oceans 117 (C1) (2012) 1978–2012, http://dx.doi.org/10.1029/2011JC007395.
[63] R. Letelier, M. Abbott, An analysis of chlorophyll fluorescence algorithms for the moderate resolution imaging spectrometer (MODIS), Remote Sens. Environ. 58 (2) (1996) 215–223.
[64] M. Alsahli, Estimating Chlorophyll Concentrations of Kuwait's Coastal Environment Using SeaWiFS and MODIS Satellite Data, ProQuest, 2007.
[65] M.R. Al-Shehhi, I. Gherboudj, H. Ghedira, Temporal-spatial analysis of chlorophyll concentration associated with dust and wind characteristics in the Arabian Gulf, in: OCEANS, 2012-Yeosu, IEEE, 2012, pp. 1–6.
[66] A.a. Gitelson, G. Dall'Olmo, W. Moses, D.C. Rundquist, T. Barrow, T.R. Fisher, D. Gurlin, J. Holz, A simple semi-analytical model for remote estimation of chlorophyll-a in turbid waters: validation, Remote Sens. Environ. 112 (9) (2008) 3582–3593, http://dx.doi.org/10.1016/j.rse.2008.04.015.
[67] P.V. Nagamani, M.I. Hussain, S.B. Choudhury, C.R. Panda, P. Sanghamitra, R.N. Kar, A. Das, I. V. Ramana, K.H. Rao, Validation of chlorophyll-a algorithms in the coastal waters of Bay of Bengal initial validation results from OCM-2, J. Indian Soc. Remote Sens. 41 (1) (2013) 117–125, http://dx.doi.org/10.1007/s12524-012-0203-x.
[68] P. Shanmugam, A new bio-optical algorithm for the remote sensing of algal blooms in complex ocean waters, J. Geophys. Res. Oceans 116 (2011), http://dx.doi.org/10.1029/2010JC006796.
[69] G.H. Tilstone, A.A. Lotliker, P.I. Miller, P.M. Ashraf, T.S. Kumar, T. Suresh, B.R. Ragavan, H. B. Menon, Assessment of MODIS-Aqua chlorophyll-a algorithms in coastal and shelf waters of the eastern Arabian Sea, Cont. Shelf Res. 65 (2013) 14–26, http://dx.doi.org/10.1016/j.csr.2013.06.003.
[70] C. Hu, F.E. Muller-Karger, C.J. Taylor, K.L. Carder, C. Kelble, E. Johns, C.A. Heil, Red tide detection and tracing using MODIS fluorescence data: a regional example in SW Florida coastal waters, Remote Sens. Environ. 97 (3) (2005) 311–321.
[71] W.W. Gregg, N.W. Casey, C.R. McClain, Recent trends in global ocean chlorophyll, Geophys. Res. Lett. 32 (3) (2005) 1–5, http://dx.doi.org/10.1029/2004GL021808.
[72] D.G. Boyce, M. Dowd, M.R. Lewis, B. Worm, Estimating global chlorophyll changes over the past century, Prog. Oceanogr. 122 (2014) 163–173, http://dx.doi.org/10.1016/j.pocean.2014.01.004.
[73] X. Pan, A. Mannino, M.E. Russ, S.B. Hooker, L.W. Harding Jr., Remote sensing of phytoplankton pigment distribution in the United States northeast coast, Remote Sens. Environ. 114 (11) (2010) 2403–2416.
[74] K. Carder, F. Chen, J. Cannizzaro, J. Campbell, B. Mitchell, Performance of the MODIS semi-analytical ocean color algorithm for chlorophyll-*a*, Adv. Space Res. 33 (7) (2004) 1152–1159.
[75] C. Hu, J. Cannizzaro, K.L. Carder, F.E. Muller-Karger, R. Hardy, Remote detection of Trichodesmium blooms in optically complex coastal waters: examples with MODIS full-spectral data, Remote Sens. Environ. 114 (9) (2010) 2048–2058.
[76] X. Pan, A. Mannino, H.G. Marshall, K.C. Filippino, M.R. Mulholland, Remote sensing of phytoplankton community composition along the northeast coast of the United States, Remote Sens. Environ. 115 (12) (2011) 3731–3747, http://dx.doi.org/10.1016/j.rse.2011.09.011.
[77] C. Garcia-Soto, R.D. Pingree, Spring and summer blooms of phytoplankton (SeaWiFS/MODIS) along a ferry line in the Bay of Biscay and western English Channel, Cont. Shelf Res. 29 (8) (2009) 1111–1122.
[78] Y. Kim, Y. Byun, Y. Kim, Y. Eo, Detection of Cochlodinium polykrikoides red tide based on two-stage filtering using MODIS data, Desalination 249 (3) (2009) 1171–1179.

[79] C. Hu, Z. Lee, R. Ma, K. Yu, D. Li, S. Shang, Moderate resolution imaging spectroradiometer (MODIS) observations of cyanobacteria blooms in Taihu Lake, China, J. Geophys. Res. 115 (C4) (2010) C04002, http://dx.doi.org/10.1029/2009JC005511.
[80] D. Tang, D.R. Kester, I.H. Ni, Y. Qi, H. Kawamura, In situ and satellite observations of a harmful algal bloom and water condition at the Pearl River estuary in late autumn 1998, Harmful Algae 2 (2) (2003) 89–99, http://dx.doi.org/10.1016/S1568-9883(03)00021-0.
[81] J. Zhao, W. Cao, First attempt to derive chlorophyll-a using natural fluorescence in Northern South China Sea, Remote Sens. Lett. 3 (2012) 249–258, http://dx.doi.org/10.1080/01431161.2011.566286.
[82] R.J.W. Brewin, D.E. Raitsos, Y. Pradhan, I. Hoteit, Comparison of chlorophyll in the Red Sea derived from MODIS-Aqua and in vivo fluorescence, Remote Sens. Environ. 136 (2013) 218–224, http://dx.doi.org/10.1016/j.rse.2013.04.018.
[83] J. Zhao, M. Temimi, H. Ghedira, Characterization of harmful algal blooms (HABs) in the Arabian Gulf and the Sea of Oman using MERIS fluorescence data, ISPRS J. Photogramm. Remote Sens. 101 (2015) 125–136, http://dx.doi.org/10.1016/j.isprsjprs.2014.12.010.
[84] I.A. Khan, L. Ghazal, M.H. Arsalan, M.F. Siddiqui, J.H. Kazmi, Assessing spatial and temporal variability in phytoplankton concentration through Chlorophyll-a satellite data: a case study of northern Arabian sea, Pak. J. Bot. 47 (2) (2015) 797–805.
[85] R. Dwivedi, M. Rafeeq, B.R. Smitha, K.B. Padmakumar, L.C. Thomas, V. N. Sanjeevan, P. Prakash, M. Raman, Species identification of mixed algal bloom in the Northern Arabian Sea using remote sensing techniques, Environ. Monit. Assess. 187 (2) (2015) 51, http://dx.doi.org/10.1007/s10661-015-4291-2.
[86] H. do R. Gomes, J.I. Goes, S.G.P. Matondkar, S.G. Parab, Blooms of *Noctiluca miliaris* in the Arabian Sea—an in situ and satellite study, Deep. Res. Part I 55 (6) (2008) 751–765, http://dx.doi.org/10.1016/j.dsr.2008.03.003.
[87] F. Mélin, Atmospheric Correction. IOCCG, 2003.
[88] O. Dubovik, B. Holben, T.F. Eck, A. Smirnov, Y.J. Kaufman, M. D. King, D. Tanré, I. Slutsker, Variability of absorption and optical properties of key aerosol types observed in worldwide locations, J. Atmos. Sci. 59 (3) (2002) 590–608.
[89] D.G. Hadjimitsis, G. Papadavid, A. Agapiou, K. Themistocleous, M.G. Hadjimitsis, A. Retalis, S. Michaelides, N. Chrysoulakis, L. Toulios, C.R.I. Clayton, Atmospheric correction for satellite remotely sensed data intended for agricultural applications: impact on vegetation indices, Nat. Hazards Earth Syst. Sci. 10 (1) (2010) 89–95.
[90] K.G. Ruddick, F. Ovidio, M. Rijkeboer, Atmospheric correction of SeaWiFS imagery for turbid coastal and inland waters, Appl. Opt. 39 (6) (2000) 897–912.
[91] M. Wang, W. Shi, The NIR-SWIR combined atmospheric correction approach for MODIS ocean color data processing, Opt. Express 15 (24) (2007) 15722–15733.
[92] E.F. Vermote, A. Vermeulen, Atmospheric Correction Algorithm: Spectral Reflectances (MOD09), ATBD Version, 4, 1999.
[93] G. de Araújo Carvalho, P. Minnett, W. Baringer, V. Banzon, Detection of Florida "red tides" from SeaWiFS and MODIS imagery, in: Proc. XIII Brazilian Symp. Remote Sens., 2007, pp. 4581–4588.
[94] Y. Chen, X. Wang, L. Sun, B. Wu, Application of adaptive weighted averaging method for ocean color data in East China Sea, in: 2010 3rd International Congress on Image and Signal Processing (CISP), vol. 5, IEEE, 2010, pp. 2107–2110.
[95] R.L. Miller, B.A. McKee, Using MODIS Terra 250 m imagery to map concentrations of total suspended matter in coastal waters, Remote Sens. Environ. 93 (1–2) (2004) 259–266, http://dx.doi.org/10.1016/j.rse.2004.07.012.
[96] M. Wang, Remote sensing of the ocean contributions from ultraviolet to near-infrared using the shortwave infrared bands: simulations, Appl. Opt. 46 (9) (2007) 1535–1547, http://dx.doi.org/10.1364/AO.46.001535.
[97] D. Gilvear, P. Hunter, T. Higgins, An experimental approach to the measurement of the effects of water depth and substrate on optical and near infra-red reflectance: a field-based assessment of the feasibility of mapping submerged instream habitat, Int. J. Remote Sens. 28 (10) (2007) 2241–2256, http://dx.doi.org/10.1080/01431160600976079.

[98] S. Koponen, Remote sensing of water quality for Finnish lakes and coastal areas, Helsinki University of Technology, Finland, 2006.
[99] H. Xu, Modification of normalised difference water index (NDWI) to enhance open water features in remotely sensed imagery, Int. J. Remote Sens. 27 (14) (2006) 3025–3033.
[100] S. Morain, A. Budge, Environmental Tracking for Public Health Surveillance, CRC Press, Florida, USA, 2012.
[101] L.H. Pettersson, D. Pozdnyakov, Monitoring of Harmful Algal Blooms, Springer Science & Business Media, Springer-Verlag, Berlin, Heidelberg, 2012.
[102] R.P. Stumpf, M.C. Tomlinson, Remote sensing of harmful algal blooms, in: R.L. Miller, C.E. Del Castillo, B.A. Mckee (Eds.), Remote Sensing of Coastal Aquatic Environments, Springer, Netherlands, 2005, pp. 277–296.
[103] L. Shen, H. Xu, X. Guo, Satellite remote sensing of harmful algal blooms (HABs) and a potential synthesized framework, Sensors (Switzerland) 12 (6) (2012) 7778–7803, http://dx.doi.org/10.3390/s120607778.
[104] M. Al Azhar, M. Temimi, J. Zhao, H. Ghedira, Modeling of circulation in the Arabian Gulf and the Sea of Oman: skill assessment and seasonal thermohaline structure, J. Geophys. Res. Oceans 121 (3) (2016) 1700–1720, http://dx.doi.org/10.1002/2015JC011038.
[105] R.P. Stumpf, M.E. Culver, P.A. Tester, M. Tomlinson, G.J. Kirkpatrick, B.A. Pederson, E. Truby, V. Ransibrahmanakul, M. Soracco, Monitoring *Karenia brevis* blooms in the Gulf of Mexico using satellite ocean color imagery and other data, Harmful Algae 2 (2) (2003) 147–160, http://dx.doi.org/10.1016/S1568-9883(02)00083-5.
[106] L. Zheng, R.H. Weisberg, Modeling the west Florida coastal ocean by downscaling from the deep ocean, across the continental shelf and into the estuaries, Ocean Model. 48 (2012) 10–29, http://dx.doi.org/10.1016/j.ocemod.2012.02.002.
[107] J.J. Walsh, et al., Phytoplankton response to intrusions of slope water on the West Florida Shelf: models and observations, J. Geophys. Res. 108 (C6) (2003) 3190, http://dx.doi.org/10.1029/2002JC001406.
[108] F.L. Hellweger, P. Schlosser, U. Lall, J.K. Weissel, Use of satellite imagery for water quality studies in New York Harbor, Estuarine, Coastal and Shelf Science 61 (3) (2004) 437–448.
[109] IOCCG (2014, July 7). CZCS Coastal Zone Colour Scanner. Retrieved from http://www.ioccg.org/sensors/czcs.html.
[110] J.G. Acker, S. Shen, G. Leptoukh, G. Serafino, G. Feldman, C. McClain, SeaWiFS ocean color data archive and distribution system: Assessment of system performance, IEEE Transactions on Geoscience and Remote Sensing 40 (1) (2002) 90–103.
[111] G. Dial, H. Bowen, F. Gerlach, J. Grodecki, R. Oleszczuk, IKONOS satellite, imagery, and products, Remote sensing of Environment 88 (1) (2003) 23–36.
[112] Q. Zeng, Y. Li, X. Li, Correction of tropospheric water vapour effect on ASAR interferogram using synchronous MERIS data, in: Geoscience and Remote Sensing Symposium IGARSS, 2007, pp. 2086–2089. IEEE. ISBN: 1-4244-1212-9.

CHAPTER 10

Desalination as a Municipal Water Supply in the United States

Nicole T. Carter[a]
Congressional Research Service, US Library of Congress, United States

Contents

Existing desalination capacity and the prospects for future adoption varies across US states and differs for brackish water and seawater. Brackish water desalination—treatment of waters with dissolved solids of 1000 and 10,000 milligrams per liter (mg/L)—in states like Florida, California, and Texas has made the United States a global leader in this type

[a] Nicole T. Carter has a Ph.D. in engineering from Stanford University, was a 2011–12 US-Australia Fulbright Senior Scholar, and works at the Congressional Research Service (an agency within the US Library of Congress). The views expressed herein are those of the author and are not presented as those of the Congressional Research Service or the US Library of Congress.

Desalination Sustainability
http://dx.doi.org/10.1016/B978-0-12-809791-5.00010-9

of desalination. In contrast, the United States has only a limited number of municipal seawater desalination facilities. As of 2015, treated brackish water and seawater were not significant municipal water sources at the national level; water from desalination represented less than 1% of US municipal water supplies. This situation, however, does not reflect the future role that desalination may play in addressing regional and local shortages of developed freshwater supplies.

In the United States, decisions about desalination adoption are shaped not only by engineering, cost, and environmental considerations but also by the institutional, social, and financial context of each US state and each municipal water provider. Provision of US municipal water services is decentralized. There are roughly 52,000 municipal water systems in the United States. Most US municipalities are served by public water providers that are administrative entities of local governments. Where and how municipal desalination facilities are designed, built, and operated are shaped by a combination of local, state, and federal regulations. These regulations are intended to reduce environmental harm, protect human health, and avoid unintended consequences.

This chapter discusses the use of brackish water and seawater desalination to augment municipal water supplies in the United States, with specific examples from Florida, California, and Texas. This chapter is organized into the following sections:

- Primer on US Municipal Desalination and the US Municipal Water Sector: This section summarizes the history and status of desalination as a municipal water supply in the United States, describes the decentralized provision of US municipal water services, and presents trends shaping the forecast for US municipal desalination.
- Deciding on Desalination: This section discusses the suite of factors and uncertainties associated with a decision to adopt desalination, how a desalination facility's use as a regular or intermittent supply affects its cost-competitiveness, and how adoption decisions for brackish water and seawater desalination are different.
- Public Financing Challenges and Private Opportunities: This section describes the challenges of public financing of large-scale desalination facilities and the opportunities for private interests.
- Energy Intensity and Alternative Energy Opportunities: This section describes why reducing desalination's energy intensity and combining desalination with renewable and alternative energy are important for future adoption.
- Environmental and Health Protections for Municipal Desalination: This section addresses the environmental and health protections associated with municipal desalination facilities in the United States.
- Brackish Water Desalination in Florida, California, and Texas: This section describes how Florida is the state with the most operating municipal brackish water desalination facilities and how Texas and California have numerous facilities that are operational or under development.
- Seawater Desalination in Florida, California, and Texas: This section describes how California dominates in terms of near-term proposals for seawater desalination facilities and how Texas and Florida are more likely to pursue seawater desalination after 2025.
- Conclusion

1. PRIMER ON US MUNICIPAL DESALINATION AND THE US MUNICIPAL WATER SECTOR

Enthusiasm for desalination in the United States has waxed and waned over the decades in part because of changing perceptions of the need for the technology. As post-World War II concerns for water availability mounted, the US Congress enacted the Saline Water Act in 1952; it established a program for federal desalination research. In 1962 Buckeye, Arizona, built the first US municipal desalination facility to treat 2460 cubic meters per day (m^3/d) of brackish groundwater. After decades of steadily increasing water use, US water withdrawals leveled off during the mid-1970s and mid-1980s. The plateau in demand was in large part due to improved water efficiency in irrigation and industry [1]. From the 1950s until 2000, municipal water demand expanded but at a slowing pace. Between 2000 and 2010, municipal water use declined as the result of decreasing water use per capita [1].

While water supplies have been able to keep up with demand in much of the nation, some US municipal water providers are interested in developing more weather-independent and local water supplies. Some of their motivations include expected population growth, declining groundwater supplies, recent drought experiences, and concerns about the reliability of the future freshwater supply. Also, in many US watersheds, especially in western states, legal rights to freshwater may be almost fully allocated and in some cases are over allocated.

Desalination is attractive because access to seawater and brackish sources generally is less competitive than for freshwater, and desalination can create a new high-quality freshwater supply that is independent of weather conditions. Desalination consists of the treatment of a feed water of seawater or brackish water to produce a freshwater stream known as product water and a stream of saline wastewater known as concentrate or brine. There are two main types of desalination technologies: those based on evaporation and those using membranes to separate salts and freshwater. In the United States, desalination is typically accomplished using reverse osmosis, which is a membrane-based technology. Currently, reverse osmosis is preferred in the United States because it is less energy-intensive than evaporation technologies and works well in treating brackish water.

During the 1990s through the 2010s, adoption of brackish water desalination for municipal use steadily grew in the United States, most notably in Florida. Brackish water desalination currently dominates US municipal desalination capacity. Current US municipal water supply capacity for brackish desalination may exceed 1.8 million m^3/d, exclusive of facilities using desalination technologies for water softening. This capacity is distributed across more than 300 facilities with a few states leading the facility count—49% are located in Florida, 16% in California, and 12% in Texas [2].

Table 1 summarizes publically available information on the largest capacity desalination facilities for the treatment of brackish water for use as a municipal water supply. Table 1 does not include facilities that use desalination technologies primarily for water softening or advanced water treatment purposes; it also does not include the significant

Table 1 Largest US facilities for desalination of brackish groundwater for municipal water supply augmentation as of 2015

Municipality and state	Freshwater from desalination capacity (m^3/d)	Description and status
Cape Coral, Florida	113,500	A 68,100 m^3/d facility and a 45,400 m^3/d facility.
El Paso, Texas	104,100	Placed in service in 2007. Average operations are 13,250 m^3/d. Facility built as a joint effort by the El Paso Water Utilities and Fort Bliss US Army Installation.
Chino, California	91,600	A 53,700 m^3/d and a 37,900 m^3/d facility are operational. A 45,400 m^3/d expansion is under development.
St. Lucie, Florida	85,200	A 22,700 m^3/d facility placed in service in 2005, and a planned expansion to 85,200 m^3/d occurred subsequently. Service area experienced fast population growth. Fresh groundwater sources offered limited additional supply.
Jupiter, Florida	53,000	Desalination capacity is capable of providing 70% of current municipal supply.
San Antonio, Texas	45,400	Anticipated to be placed in service in 2016, as part of a plan for a total of 113,600 m^3/d by 2030. Desalination reduces reliance on stressed freshwater aquifer.

Notes: Numerous brackish groundwater facilities with capacities smaller than 45,400 m^3/d and less are not shown. Water softening facilities using desalination technologies are not included.

number of facilities that use desalination for industrial applications. Florida, California, and Texas also have a number of smaller desalination facilities treating brackish water for municipal use that are not shown in Table 1. Other states with a few municipal brackish facilities include Arizona and North Carolina.

In the United States, seawater desalination was used to augment only a limited number of municipal water supplies from the 1990s through the mid-2010s. In the early 1990s the City of Santa Barbara, California, constructed a 33,800 m^3/d seawater desalination facility as an emergency water supply. After a few months of operation, significant precipitation eased drought conditions. The facility was placed on long-term standby. During the remainder of the 1990s, seawater desalination was at times included as a potential future option in the plans of various municipal water providers. However, no large-scale US seawater desalination facilities—facilities with capacities to produce more than 75,000 m^3/d of freshwater—became operational until 2007.

As of 2015 the United States had two operable, large-scale seawater desalination facilities. The two facilities had their origins in 1990s planning efforts. The Tampa Bay, Florida, facility opened in 2007, and the Carlsbad, California, facility was placed into service in 2015. Table 2 includes these large-scale facilities and smaller US municipal

Table 2 US facilities for desalination of seawater/tidally influenced surface water for municipal water supply augmentation as of 2015

Municipality and state	Freshwater from desalination capacity (m^3/d)	Description and status
Carlsbad, California	189,300	Placed in service in 2015. Privately owned facility delivering water under a 30-year water purchase agreement to the San Diego County Water Authority.
Tampa Bay, Florida	94,600	Placed in service in 2007. Operations have been intermittent. Feed water is highly brackish estuarine water that varies in salinity; the salinity averages 26,000 mg/L.
Brockton, Massachusetts	18,900	Placed in service in 2008. Idle in 2015. Feed water is from seasonally brackish (Jul.–Nov.) water supply from a tidally influenced river segment. Droughts reduce reliability of supply from a local lake.
Florida Keys, Florida	11,400	Placed in service in 2000 as emergency water supply. A 7600 m^3/d facility on Stock Island, and a 3800 m^3/d facility in Marathon, FL.
Santa Barbara, California	10,000	Jul. 2015 design-build-operate contract issued to recommission and upgrade an idle desalination facility.
Swansea, Massachusetts	5300	Placed in service in 2009. Feed water is from tidally influenced river segment. Developed in response to depleted freshwater aquifer.

Notes: Seawater facilities with capacities of less than 3800 m^3/d are not shown.

seawater desalination facilities. A few facilities smaller than those shown in Table 2 have been constructed for small coastal, island, private, or isolated US communities, especially tourist destinations. As shown in Table 2, some of the constructed US seawater desalination facilities have not been regularly operated.

In summary, US adoption of desalination is dominated by brackish water with over 300 municipal facilities. US seawater desalination capacity is defined by a limited sphere of operating facilities (as shown in Table 2). This difference in adoption is attributed in part to the differences in the costs and opportunities associated with brackish and seawater desalination.

1.1 Decentralized Provision of Municipal Water Services

US state and local governments are primarily tasked with municipal water supply planning and investment. Two characteristics of note are

- A few systems serve most of the people. Of the roughly 52,000 US municipal water systems, 8% serve more than 80% of the population that is supplied by municipal

systems. The other 92% of the water providers deliver drinking water to communities with populations of 10,000 or less [3].

- Publically owned municipal water providers dominate. Publically owned systems control 80% of the US municipal water market [4]. Most US municipalities are served by public water providers.

The US approach to decentralized municipal water services derives in part from the division of responsibilities between federal, state, and local governments. The US federal government has regulated the quality of water delivered by public water systems since the enactment of the 1974 Safe Drinking Water Act. The federal government generally defers to states for water rights related to surface water and groundwater allocation.

Typically through local governments, states provide their residents with water, wastewater, and other local public services like refuse collection and local police. Municipal water providers are responsible for planning, testing, building, and operating their facilities. Although private, for-profit engineering or construction firms often are hired on contract to accomplish some of these activities, municipal water providers typically are the owners and are ultimately responsible for most aspects of regulatory compliance, water service reliability, and financing. During the federal, state, and local approval processes for new water facilities and other water infrastructure investments, stakeholders concerned about environmental, social, or ratepayer issues are afforded various opportunities to comment and at times are afforded avenues for legal recourses.

Public municipal water providers often finance their infrastructure investments using municipal bonds or low-cost financing offered through federal or state programs. Another financing option, especially for private water service providers, is a construction loan from a private lender. In select circumstances there may be state or federal grant support to assist with a portion of planning and construction costs. For example, the Bureau of Reclamation within the US Department of the Interior operates a modest program to assist with wastewater reuse projects and other projects for the treatment of naturally impaired ground and surface waters, including saline waters in western states. The program provided $23 million in assistance during the 2016 fiscal year.

Population growth, episodes of drought and high heat, and concerns about climate variability have increased interest in the future reliability of US municipal water supplies. Concerns about the consequences of water shortages have prompted decision-makers in many US states to weigh alternative means to meet water supply needs. At the same time, it has been challenging to address these concerns in part because of limited public budgets.

1.2 US Municipal Desalination Forecast

A few trends are making desalination a more competitive US municipal water supply.

- Desalination treatment is more cost-competitive than in the past. The unit cost of desalination processes have fallen.

- Traditional freshwater development options are limited and costly, and the reliability of their benefits is viewed as less certain than in the past. The costs of developing new fresh surface waters by building new reservoirs or expanding the capacity of existing reservoirs are high. Fresh groundwater stored in aquifers in many US regions is declining, in large part because of ongoing extraction rates that exceed recharge. Climate variability may alter precipitation, runoff, recharge, and water quality; the changes may not only increase the need for reliable water supplies but also reduce the water supply benefits from certain water development projects.
- Challenges persist in shifting water to municipal uses. Agricultural water consumption in the United States remains at nearly 70% of developed supplies. Some municipal water providers have pursued expanding water supplies through water transfers from willing agricultural sellers. Various factors contribute to these transfers being complex, costly, or unreliable: an extended transfer approval process, significant annual variations in the water available for transfer, limitations on and cost of water conveyance, and unclear means for compensating third parties harmed by the transfer.

Other indications that adoption of municipal seawater desalination may rise in the United States include public and private sector project proposals, state efforts to accelerate project approval, and support for developing local and drought-resilient supplies.

Other trends and persistent issues may dampen adoption of desalination. Prominent among these are its cost-competitiveness, the required financial commitment for seawater desalination, and the energy intensity and environmental impacts of operations. Also, desalination may face competition from other nontraditional sources. The public, ratepayers, regulators, and municipal water providers are increasingly accepting of and interested in indirect and direct potable reuse, storm-water capture and use, managed groundwater recharge, and enhanced conservation and efficiency. These alternatives not only meet water demand but also often have environmental benefits. Investment in these alternative water supplies may reduce the urgency for desalination. Most US municipal water providers have viable alternatives to seawater desalination.

2. DECIDING ON MUNICIPAL DESALINATION

An informed decision regarding desalination adoption requires a comprehensive assessment of the construction and operational costs, risks, and benefits. Municipal water providers need site-specific estimates of both the capital and operational costs and the cost uncertainties. Capital and operational cost estimates are based on assumptions about a significant number of input prices (e.g., electricity, chemicals, and qualified facility operators) over an extended period of time. Each assumption adds uncertainty to estimates; uncertainty can deter adoption.

For large-scale desalination, a significant question is when to construct a facility. If a desalination facility is constructed before it is needed, it may sit idle while water ratepayers pay the debt incurred to construct it and any maintenance or ongoing contract costs. There also may be benefits to deferring facility construction, such as the availability of improved desalination technologies in the future and use of available funds for investing in other public works with greater benefits. Another complexity is the energy intensity of desalination. Municipal water providers are faced with weighing how desalination's energy intensity and the associated carbon footprint may be affected by greenhouse gas reduction policies and efforts [5]. Table 3 illustrates some factors considered when evaluating water supply alternatives. Table 3 uses information relevant to water supplies for Southern California.

2.1 Difference in Desalination Facilities Operating as a Base Load and Operating Intermittently

A challenge for US municipal desalination is how the desalinated water will fit into the provider's existing water supply portfolio. Brackish desalination facilities that have been adopted as part of the "base load" of water supply generally have been successful investments. In some brackish desalination applications, the high quality of freshwater derived from desalination allows it to be mixed with available sources of marginal water quality, thereby further expanding water supplies. In contrast, numerous seawater desalination facilities in the United States and elsewhere (e.g., Australia, Spain) remain idle, operate intermittently (e.g., operational only when surface water supplies fall below a determined threshold), or operate at a fraction of their capacity. Decisions to idle facilities or reduce operations often are based on efforts to minimize a water system's operational costs. That is, water production through desalination is curtailed when alternatives that have lower operational costs are available [6]. For most desalination facilities, operating significantly below capacity results in significantly higher unit costs for product water [6]. These operational efficiencies favor efforts to combine desalination with storage (e.g., aquifer storage and recovery where feasible). While storage may add value, it also can add complexity to project development and increase capital costs.

Excess capacity often is a necessary part of providing reliable service in any type of complex system with variable supply and demand. The challenge for desalination, especially seawater desalination, is that current technologies and their associated capital infrastructure investments make it hard to economically justify their development for use as a seasonal or drought "peaking" water supply. Operating costs at a level that is cost-competitive with other water supply alternatives is central to adoption. Competitive operating costs would convert desalination facilities from being used (and generating value) only on an intermittent and emergency basis, into a standard part of system operations.

Table 3 Illustration of water supply options for Southern California

	Large-scale seawater desalination	Brackish desalination	Potable reuse	Imported from state water project	Water efficiency/ conservation
Technology/ description	Reverse osmosis with energy recovery	Reverse osmosis	Treatment using various combinations of technologies	Retail cost of treated surface water imported from Northern California	Long-term adoption, including technologies and use restrictions
Freshwater impact	New freshwater	New freshwater	New freshwater from wastewater	Increased competition for freshwater	Freshwater conserved
Local availability	✓ (if coastal)	✓ (if sufficient quantities are accessible)	✓	✗	✓
Drought-resilient	✓	✓	✓	✗	See operational risk below
Aquatic environmental harm or benefits	Organism impingement and entrainment at intake; concentrate disposal impacts	Limited low-impact concentrate management options if coastal discharge is impractical	Reduced wastewater effluent discharges; reduced flows in waterbodies historically receiving wastewater	Harm to San Francisco Bay Delta ecosystem	

Continued

Table 3 Illustration of water supply options for Southern California—cont'd

	Large-scale seawater desalination	Brackish desalination	Potable reuse	Imported from state water project	Water efficiency/ conservation
Energy intensity (kilowatt-hours per cubic meter of freshwater, kWh/m^3)	3–4	1–2 (energy intensity increase with salinity)	0.5–0.8 (estimate of difference in treatment for potable reuse and secondary wastewater treatment)	2–3	Varies; many options reduce energy use
Total cost (US dollars per cubic meter, $/m^3$)	1.2–1.9	0.8–1.0 (possible significant lower-cost range in other locations and for lower salinity sources)	0.7–1.6	0.8–1.1	0.4–0.8
Adoption risks and benefits	Uncertain approvals and environmental mitigations; financial risk of unused capacity; increased input price; melded water-quality improvements	Access to brine line for concentrate disposal may facilitate adoption; risk of unintentional freshwater aquifer contamination; melded water quality improvements	Public acceptance; need for greater monitoring for public health protection; reuse avoids wastewater discharge into waterbodies	Available amounts variable and uncertain; prices increasing	Possibly limit some opportunities to reduce water use during drought; customer value from near-term water use foregone; more freshwater for other uses resulting from avoided consumption

Data from R.S. Tchobanoglous, et al., Framework for Direct Potable Reuse, WateReuse Research Foundation, Alexandria, VA, 2015; R. Raucher, R.S. Tchobanoglous, The Opportunities and Economics of Direct Potable Reuse, WateReuse Research Foundation, Alexandria, VA, 2014.

2.2 Difference in Seawater and Brackish Water Desalination Adoption Decisions

For many US municipal water providers, small capacity brackish desalination facilities have operational costs that are competitive with other supply alternatives. Brackish desalination facilities consequently are integrated into "base load" operations. Near-term commitments to brackish desalination facilities are seen in Florida, California, and Texas. Many of the brackish desalination facilities are modestly sized at 20,000–40 000 m^3/d with a few larger facilities also in development or under construction.

Seawater desalination's costs and energy intensity are higher than the costs and energy intensity of brackish desalination. Seawater desalination's economies of scale make smaller facilities less attractive investments. Per unit of treatment capacity, a 20,000 m^3/d facility will have direct capital costs for treatment equipment that are 135% of a 80,000 m^3/d facility and are 160% of a 200,000 m^3/d facility [7]. These economies of scale encourage project proposals for larger facilities. Larger facilities, however, are associated with greater development risks (e.g., harder to gain permits and finance), operational risks (e.g., input price increases, unused capacity), and require more extensive environmental mitigations.

For most US municipal water providers, seawater desalination remains among the more costly of the available alternatives. Seawater desalination facilities have capital investments and operational inputs similar to other industrial and manufacturing processes (e.g., electricity, chemicals, membrane replacement, proprietary technologies, and a skilled workforce). A challenge for desalination is that the municipal consumer's willingness to pay for water often is considerably lower than for most industrial products [8].

Seawater desalination is saddled with both significant upfront capital expenditures and significant operating expenses. Although the costs associated with specific seawater desalination proposals vary widely, Table 4 provides a rough range for the distribution of cost items on average for large-scale or otherwise complex seawater desalination facilities. Depending on the specifics of a facility, one cost item may shift the cost distribution significantly. For example, if environmentally acceptable intake or disposal is particularly complicated, these costs can represent a significantly higher percent than is shown in Table 4. Significantly, Table 4 includes within the capital costs the cost of financing and contingencies. These costs are highly dependent on the risks associated with the project and how construction is financed. The financial instruments used (and their tax treatment) and the interest rates associated with them can result in significantly different financing costs.

Models are available for estimating desalination costs. However, the complexity of seawater desalination facilities' development and operational costs make modeled results less reliable than similar estimates for most other water supplies [9]. Many desalination's cost items are market-driven. For example, in the United States, the market shapes the

Table 4 Distribution of capital and operational costs for seawater reverse osmosis facilities

Capital costs average *55%–65%* of total cost		Operational costs average *35%–45%* of total cost	
Capital item	**% of capital costs**	**Operational item**	**% of operational costs**
Direct capital costs		***Variable costs***	
Pretreatment and reverse osmosis equipment	35–45	Power costs	35–58
Site, building, equipment, testing	16–20	Membrane replacement	6–9
Intake and outfall	5–8	Concentrate and waste disposal	4–7
Indirect capital costs		***Fixed costs***	
Project development	9–11	Labor	4–11
Financing and contingencies	19–24	Environmental monitoring	1–5
		Other operational and maintenance	7–20

Data from N. Voutchkov, Desalination Engineering: Planning and Design, McGraw-Hill, New York, 2013 (Chapter 17). Data was for complex projects. Large-scale facilities in the United States in the near-term are likely to have complex development processes. In other locations, where facility development may be more routine and less complex, a more even split between capital and operational costs may be more typical, with power costs closer to one-third of total costs.

price of land, equipment, construction materials, construction contracts, and energy inputs (although some US states regulate their energy markets) [9]. Debt service is shaped by the market and in some cases government programs.

Unlike the global trend in declining desalination treatment costs, nontreatment costs of desalination facilities and their operations have not significantly declined (e.g., land, intakes, and concentrate management). To reduce capital and operational costs, many proposed large-scale seawater desalination facilities in the United States are colocated with coastal thermoelectric power plants. Colocation can have multiple benefits, including sharing of intake and outfall infrastructure and dilution of concentrate with power plant cooling water.

3. PUBLIC FINANCING CHALLENGES AND PRIVATE OPPORTUNITIES

For many US municipal water providers, increasing water supply through the construction and operation of a large-scale desalination facility represents a significant financial commitment. The large upfront capital investment associated with seawater desalination facilities in particular have municipal water providers looking beyond their typical debt instruments to options that include private financing such as public-private

partnerships (PPPs) and water purchase agreements. Private, independent water producers that sell water to municipal water providers and PPPs that involve significant private financing of water infrastructure remain uncommon in the US municipal water sector; however, they are attracting interest within the US municipal water sector and within the government for support. The Carlsbad, California, facility is a prominent example of a private entity developing, owning, and operating a desalination facility. See the box titled "Private Seawater Desalination Facility Providing Municipal Water Supply for San Diego, California" for more on the private-sector role in the development, ownership, and operations of the private Carlsbad facility.

Interest in private financing is in part a reaction to factors that dampen public entities' willingness to invest in large-scale desalination. These include ratepayer reluctance and competing demands for public debt. Many US municipal water ratepayers are accustomed to relatively low fees for their water services. Systems serving smaller or less affluent populations face affordability concerns when setting fees and evaluating investments. Of the 52,000 water systems in the United States, 1500–2000 are sufficiently large to issue their own bonds. While these entities can bond-finance desalination investments, they may be hesitant to place a large debt on their balance sheet and also may be discouraged by uncertainties and risks associated with large-scale desalination.

Reasons for private engagement in municipal desalination may include the private sector's access to private financing and proprietary technologies and processes, and its expertise and experience with desalination and project management for complex infrastructure. Sharing of risk (e.g., cost overruns, construction delays) is often cited as a benefit of greater private sector engagement in public projects; the extent to which risks actually are shared between public and private partners depends on the specifics of the contractual agreements.

Private Seawater Desalination Facility Providing Municipal Water Supply for San Diego, California

In Dec. 2015, private owners of the Carlsbad desalination facility (situated north of San Diego on California's Pacific Coast) began selling desalinated seawater to the San Diego County Water Authority. Poseidon Water (Poseidon) owns the facility, which at the start of operations was the largest desalination facility in the Western Hemisphere. The facility can treat roughly 380,000 m^3/d of seawater to produce a maximum of 189,300 m^3/d of product water. The facility is at the site of the existing Encina Power Plant (which is slated for retirement in 2017). Colocation allowed the desalination facility to use an existing seawater intake and outfall system. Poseidon entered into a 60-year lease for the site.

In 1998 Poseidon began its efforts to build a seawater desalination facility to sell water to San Diego's water system. Poseidon used private funds to develop the facility. From 1998 to 2012, the proposal was the subject of 21 public hearings and 14 legal challenges. Once Poseidon resolved the final legal challenge to project development in 2012 and the approval and financing were secured, San Diego County Water

Authority chose to enter into a 30-year water purchase agreement with Poseidon. Construction began in Dec. 2012. The water authority did not conduct a competitive bid process for developing new supplies before entering into the agreement.

The $1000 million project was financed using tax-exempt bonds as well as private equity. Poseidon's financing consisted of a $530 million tax-exempt private activity bond (provided through the state's pollution control tax-exempt bond financing program) and $167 million in private equity. The authority funded a 16-km conveyance pipeline from Poseidon's facility to the authority's water distribution network using a $203 million tax-exempt revenue bond.

The water purchase agreement sets a variable purchase price depending on the quantity purchased. The authority is committed to a minimum 59 million m^3 annually at $\$1.67/m^3$ (in 2012 US dollars). The upper-limit on deliveries is 69 million m^3 annually at $\$1.50/m^3$. The authority estimates its payments to Poseidon at roughly $100 million annually. Because the authority also made investments related to the desalination facility, it estimates that the total cost of desalinated seawater is $\$1.63–\$1.83/m^3$ (in 2012 US dollars) depending on how much water is purchased. For comparison, the authority estimated that the melded rate for existing water sources was $\$0.85/m^3$ for supply and treatment in 2015 (which is equivalent to $\$0.82/m^3$ in 2012 dollars).

The benefits of the desalinated water include:

- Drought resilience: In early 2016 California state regulators classified the product water from the Carlsbad facility as drought-resilient. This classification may lessen the region's requirements to reduce water use during droughts pursuant to state mandates, thereby reducing future droughts' impacts on the authority's customers.
- Local supply: In 2020 desalinated seawater is anticipated to represent 7% of the San Diego region's water supply, and one-third of the water sourced within San Diego County. Prior to concerted efforts starting in the late 2000s to increase local water supplies, San Diego had relied on water imported from other basins for 85% of its supply.
- High-quality water: The addition of the desalinated water to the municipal water supply also results in water-quality improvements (i.e., it reduces the total dissolved solids in the melded water supply), which can extend the useful life of facilities and appliances.

The role that the private sector will play in desalination facilities to augment US municipal water supplies is likely to vary depending on the specifics of the project and on state and federal policies and programs. While PPPs have been used in the United States for more than 30 years, they remain relatively uncommon for municipal water infrastructure.

In the United States, PPPs are frequently financed through a combination of private debt and equity and public funds. Private entities involved in PPPs may also be able to access special debt instruments, such as tax-exempt private activity bonds. Historically, private activity bonds have not been extensively used for large water projects. As shown by Poseidon's $530 million tax-exempt private activity bond for the Carlsbad facility in

2012, large-scale desalination facilities may be the type of private water project that pursues significant tax-exempt private activity bonds. Another potential avenue for PPP financing was created by the US Congress in 2014 through the Water Infrastructure Finance and Innovation Act. The program is authorized to provide loan guarantees and direct loans for water projects, including desalination, at the long-term interest rate of US Treasury securities.

A challenge ahead for private engagement in the US water sector is how to foster public trust in for-profit private entities delivering services that in the United States have traditionally been provided by the public sector. Means to foster the public confidence include public participation and transparency in decision-making. A challenge will be how to develop, regulate, monitor, and enforce PPP arrangements in the municipal water sector that consistently protect the public interest while attracting private investment.

4. ENERGY INTENSITY AND ALTERNATIVE ENERGY OPPORTUNITIES

Like nearly all new freshwater supplies, desalinated product water comes at substantially higher costs than existing municipal water supplies. As shown in Table 4, a substantial portion of the operating cost for seawater desalination is for energy use, principally electricity for the desalination process and pumps throughout the facility. Reverse osmosis consists of the application of high pressure to force water through a membrane to separate freshwater from the salts in the feed water. The energy intensity for a current state-of-the-art seawater reverse osmosis facility is 3.5 kilowatt-hours of electricity per cubic meter of water (kWh/m^3) [10]. The typical energy intensity of brackish reverse osmosis is 0.5–3.0 kWh/m^3 depending primarily on the salinity of the brackish water and pumping requirements (e.g., depth to brackish groundwater sources, transport for concentrate disposal) [11]. Consequently, the competitiveness of reverse osmosis seawater desalination is highly dependent on the price paid for the electricity. Uncertainty in future electricity prices over the life of the facility creates significant uncertainty in estimates of future operating costs. If electricity becomes more expensive, less electricity-intensive water supply options become comparatively more attractive than desalination.

A primary way that desalination cost reductions have been achieved in recent decades has been through reduced energy consumption by the reverse osmosis process. The energy used in new desalination facilities using reverse osmosis is nearing the theoretical minimum energy required for separation of the salts from the feed water [11]. Dramatic reductions in energy requirements are unlikely to be achieved through enhancements to standard reverse osmosis membranes. Instead, energy efficiency improvements are more likely to come from other components of a desalination

facility, such as the pretreatment of the water before reverse osmosis, enhanced facility and system design, or the use and development of a new generation of desalination technologies.

Pumps are responsible for more than 40% of total energy costs at a desalination facility [12]. Energy-efficient pumps that are useful for smaller applications have made desalination more cost-effective for some applications and less sensitive to electricity prices [13].

Some research results indicate that an energy-efficient seawater desalination facility could produce freshwater with an energy intensity similar to water imports from Northern California or the Colorado River into Southern California. A demonstration facility achieved energy consumption levels in the range of 2.7–3.0 kWh/m^3 [14].

The use of electricity obtained from fossil fuels (typically obtained from the electric grid or a colocated power plant) for powering desalination raises concerns about the environmental impact of desalination, its energy infrastructure requirements especially during peak electricity demand, and the usefulness of desalination as a climate change adaptation strategy [5]. Coupling desalination technologies with intermittent renewable (e.g., photovoltaic generation) or geothermal electric generation, use of off-peak electricity or waste heat (e.g., waste heat used to power forward osmosis desalination), and operations in remote areas or areas with limited traditional energy infrastructure is increasingly receiving attention. Efforts to jointly manage water supply and demand and energy supply and demand and to integrate renewable energy with desalination may bolster environmental advocates' support for desalination. In some circumstances, however, efforts to self-supply energy for desalination may increase proposals' complexity, total costs, and unit costs of product water.

While there is interest in coupling desalination and renewable energy, there has been little advancement in full-scale proposals in the United States. Instead, US-based efforts have been at scales that demonstrate technologies and test concepts. For example, a private independent water producer—WaterFX—has tested using concentrating solar thermal troughs to power a distillation system to desalinate saline agricultural drainage in California. Another company—Sephton Water Technology—has pilot-tested in Southern California's Imperial Valley using steam from geothermal sources to operate a distillation system.

New avenues of federal desalination research are underway and are targeting the energy use associated with desalination. For example, the US Department of Energy has plans for a multiyear low-carbon, low-energy, low-cost desalination energy innovation hub. The proposal is for $25 million annually for 5 years for research on new technologies to dramatically lower the cost, energy use, and carbon footprint of desalination. Some states, such as Texas, have also invested in desalination research.

5. ENVIRONMENTAL AND HEALTH PROTECTIONS FOR MUNICIPAL DESALINATION

US health and environmental regulations, guidelines, and policies regarding desalination facilities and desalinated product water are evolving. Regulatory requirements may continue to shift as domestic experience is gained by US regulators, US project developers, and the US public. Some of the requirements that particularly shape where and how US municipal desalination facilities are constructed and operated include regulatory developments in select states for inland and coastal concentrate management, mitigation of environmental impacts of concentrate management, intake alternatives for seawater desalination, and public health protections. Each of these are discussed following a general introduction to the regulatory context for desalination.

The environmental and human health concerns associated with adopting desalination and integrating desalinated water into a drinking water system often are raised in the context of obtaining the permits and approvals required to site, construct, and operate the facility. In order to obtain the necessary approvals and permits, the project developer may have to commit to actions (including additional investments and changes in designs) to mitigate harm. Some stakeholders view the current regulatory process as a barrier to adoption of desalination. Other stakeholders argue that rigorous review and permitting is necessary because of the potential environmental harm and human health impacts of desalination operations.

Regulatory responsibilities relevant to desalination facilities are spread across local, state, and federal agencies. For example, in Texas a seawater desalination facility may require the project developer to comply with 26 permits, approvals, and documentation requirements [15]. In California, to obtain approval to build and operate a municipal desalination project, over 30 federal, state, regional, and local agencies may have some regulatory or permitting authority [16]. Some of the federal, state, and regional entities are shown in Table 5. Local permits may have to be obtained for a wide variety of project-related activities. Some examples include land use permits, coastal development approvals, access to rights-of-way, land-grading permits, building and electrical permits, erosion control permits, transportation permits, and hazardous materials management plan approvals. The regulatory complexity is not that surprising. Most infrastructure projects in the United States (and in other countries like Australia) require a considerable number of permits and approvals.

The more unique challenge for desalination facilities in the United States may be that in most states, there are few established guidelines or precedents for how decisions are made and conditions established for permits and approvals for desalination projects. Federal and most state and local regulatory programs have not been tailored to address desalination facilities and the unique challenges and opportunities that they represent. Limited experience with coastal desalination facilities has particularly

Table 5 Federal, state, and regional entities likely to have roles in desalination facility permission and approval in California

Reason for permit or approval	Federal entities	State and regional entities
Drinking water system operations		• California Department of Public Health
Wastewaters from construction and operations	• US Environmental Protection Agency	• State Water Resources Control Board • Regional Water Quality Control Board
Impacts on species and ecosystems	• National Oceanic and Atmospheric Administration (National Marine Fisheries Service) • US Fish and Wildlife Service • US Army Corps of Engineers	• California Department of Fish and Wildlife
Air pollution		• Air Pollution Control District
Structures in waterways	• US Army Corps of Engineers • US Coast Guard (consult)	
Encroachment on state lands		• California State Lands Commission
Coastal development	• US Coast Guard (consult)	• California Coastal Commission
Other	Other agencies depending on the specific project, such as: • Native American Tribes • Federal Energy Regulatory Commission	Other agencies depending on the specific project, such as: • California Department of Parks & Recreation Office of Historical Preservation • California Independent System Operator • California Energy Commission • California Department of Transportation

Data from California Department of Water Resources, California Water Plan, Update 2013, vol. 3, California Department of Water Resources, Sacramento, CA, 2013 (Chapter 10).

affected how coastal desalination facilities in the United States are permitted and designed. Most regulators handle the permitting of desalination facilities on a case-by-case basis pursuant to broad regulatory authorities. The benefit is that the regulatory decision is tailored to the proposed facility; a drawback is that project developers find the process, its length, and its outcomes unpredictable. A case-by-case approach also can raise concerns about the consistency and predictability of regulatory decisions. Also the evaluation of the technical and biological issues associated with

desalination proposals can require specialized expertise and information that may not be readily available to the regulators.

Given the uncertainty and complexity of the regulatory requirements for proposed desalination facilities, various desalination stakeholders participated at an event in 2012, the "Desal Dialog: A Regulatory Workshop on Critical Issues of Desalination Permitting" [17]. The group recommended specific research topics to facilitate desalination project permitting. A majority of participants supported the development of national desalination guidelines covering desalination product water quality, intakes, and concentrate management [17].

No federal regulations tailored to desalination's product water quality, intakes, or concentrate management are forthcoming or anticipated. As of mid-2016, no federal science and research program was targeted specifically at informing the desalination permitting process. Instead, federal regulations and guidelines remain general, rather than tailored to desalination.

A few states are developing regulatory processes and requirements tailored to desalination, such as Texas and California. In 2015 the legislature in Texas established a framework for expedited permitting for desalination. It tasked the state environmental regulator with establishing rules for an expedited procedure for obtaining approval for the diversion, treatment, and use of water from the Gulf of Mexico, and rules for approval for the discharge of treated water to surface waters in the state and discharge of wastes from desalination into the Gulf of Mexico [18]. In May 2015 California advanced its efforts to standardize approval of certain aspects of desalination proposals [19]. California became the first US state to adopt requirements specific to new, existing, and expanded desalination facilities. California adopted requirements addressing coastal intakes, coastal concentrate disposal, and coastal site selection and design for desalination facilities. The requirements do not address desalination product water quality. The California requirements cannot replace federal regulatory requirements. However, compliance with state requirements is anticipated to facilitate compliance with some federal regulations.

The state requirement established for California desalination facilities is the use of best available site, design, technology, and feasible mitigation measures to minimize intake and mortality of all forms of marine life. Feasibility of mitigation measures will be determined by whether something is capable of being accomplished in a successful manner within a reasonable period of time taking into account economic, environmental, social, and technological factors. Preferred technologies for intakes and disposal are identified; however, alternative intake and concentrate disposal methods can be used if demonstrated to be as protective of marine life as the preferred technologies. Mitigation measures are required to address damage to marine life that occurs after the best available sites, designs, and technologies have been employed. For site selection and design, an evaluation of a reasonable range of nearby sites and configurations is required. The evaluation must consider numerous factors to minimize intake and mortality of marine life and minimize harm to sensitive habitats.

5.1 Options for Inland and Coastal Concentrate Management

In the United States, how to manage concentrate often is a significant factor in the feasibility of inland facilities and the siting and mitigation of coastal facilities. Concentrate from reverse osmosis facilities can be particularly challenging because of its high salinity. Process additives (e.g., biocides, antiscalants, coagulants, antifoaming agents, cleaning chemicals) also are concentrated in the brine. The concentrate disposal option selected largely is determined by which alternatives are appropriate for the volumes and specific characteristics of the concentrate, as well as costs associated with the disposal alternatives. Concentrate management costs often are shaped by numerous factors, including the required infrastructure, land, transport, and treatment for proper management. Unlike desalination treatment costs, concentrate disposal costs generally have not decreased in the United States. The primary categories of disposal options used in the United States are surface and sewer disposal, deep well injection, and land application or evaporation ponds.

Surface and sewer disposal is the dominant concentrate disposal option used for US municipal desalination facilities when available and acceptable. Generally, it is the lowest cost option. In 26 of the 32 states with municipal desalination facilities, only surface and sewer discharge have been used for concentrate disposal [20]. Inland surface water disposal is constrained by the limited capacity of inland receiving waters and their ecosystems to assimilate the concentrate's salinity. Limited volumes of concentrate may be sent through sewer systems that have large-volume wastewater treatment facilities.

For deep well injection, the US Environmental Protection Agency (EPA), the principal federal environmental regulatory agency, generally classifies desalination's concentrate as an industrial waste, thus requiring that it be disposed of in deep injection wells for industrial waste. Desalination proponents argue that the concentrate is sufficiently different from most industrial waste that it should be reclassified to increase the surface and injection well disposal opportunities. As of 2010 deep well injection for municipal concentrate disposal had been used primarily in Florida and remained uncommon in other states [20]. Texas has provided for a general permit that allows concentrate from municipal desalination to be injected into a well for enhanced oil and gas recovery. Since the mid-2010s, deep injection wells in seismically active US locations are receiving additional scrutiny as incidents of induced seismicity have raised concerns about the consequences of well operations.

Land application and evaporation ponds are seldom and decreasingly used for concentrate disposal [20]. When these methods are used, measures may be required to protect freshwaters and the environment. Land application can include spraying concentrate on salt-tolerant plants or infiltration. Land application typically is limited to small volumes of concentrate from brackish desalination facilities. Evaporation ponds use solar radiation to vaporize water, leaving salt crystals behind. The crystals typically are harvested and then disposed of; in some cases the salts or other constituents may be beneficially reused.

5.2 Mitigation of Environmental Impacts of Concentrate Management

The availability of concentrate management alternatives and the regulation of concentrate management can limit desalination's adoption in some locations. For large-scale inland desalination facilities, surface and sewer disposal may not be feasible, not only because of the concentrate's high salinity but also because of its other concentrated constituents, such as arsenic, chromium, selenium, uranium, metals, and process additives. Many US brackish desalination facilities are located in coastal areas. If a saline coastal aquifer is available and can be developed without causing harm to freshwater supplies, the coastal location offers an additional surface disposal option for concentrate. Concerns associated with concentrate disposal in estuarine and coastal environments include that the concentrate from brackish groundwater reverse osmosis may be toxic to aquatic species [21].

For seawater desalination facilities, the concentrate management options often include surface water disposal. Ocean or estuarine disposal often requires attention to mitigating potential impacts on coastal species and ecosystems. The higher salinity of the seawater reverse osmosis concentrate results in it sinking, thereby putting at risk benthic seafloor organisms. Scientific studies and data on salinity tolerances, salinity variations, and chemical tolerances of species remain limited. The least sensitive ecosystems appear to be high-energy oceanic coasts with waves and rocky shores; salt marshes, mangroves, and coral reefs are more sensitive [11].

Harm from concentrate disposal in the ocean can be mitigated by fostering mixing and dispersal in the ocean or diluting the concentrate with other wastewaters. Pursuant to the California requirements established in 2015, commingling of desalination concentrate with other wastewaters being discharged to the ocean (e.g., power plant cooling water, municipal wastewater, industrial wastewaters, and agricultural drainage) generally is required [19]. If comingling is impossible, multiple diffusers are required in order to maximize dilution, minimize the size of the concentrate mixing zone, minimize the suspension of benthic sediments, and minimize mortality of all forms of marine life [19].

5.3 Intake Alternatives for Seawater Desalination

During permitting of coastal and estuarine desalination intake structures, environmental regulators are often focused on impingement and entrainment of aquatic species, particularly juvenile fish. Existing or new surface intakes can be operated to reduce impingent of large organisms through a combination of screens and low intake velocities. Entrainment of small organisms can be reduced by locating intakes away from biologically productive areas. Colocating seawater desalination facilities with existing power plants can avoid the construction of a new intake facility. Often the desalination plant can draw its seawater from the power plant's cooling effluent, thereby mitigating the impingement and entrainment associated with the addition of desalination operations.

For new coastal intakes, the options often are open-ocean intakes or subsurface intakes, such as subsurface wells or seabed galleries. Seabed galleries are constructed offshore in the seabed and act similar to sand filters. Research indicates that coastal facilities using subsurface intakes may reduce operational costs as a result of improved water quality, as well as reduce impingement and entrainment [22]. Subsurface intakes are not viable in all locations, and their feasibility for large-scale desalination facilities remains the subject of expert debate.

Pursuant to the California requirements established in 2015, coastal intakes in California for desalination facilities are generally to use subsurface intakes where feasible. If a surface water intake is used, the California requirements dictate the use of screens or other entrainment prevention alternatives and the use of through-screen velocity controls to reduce impingement [19].

5.4 Public Health Protections

There are no federal or state requirements specific to product water from municipal desalination facilities. Instead, once desalinated product water enters a public drinking water system, the public supply is required to comply with various federal and state requirements. The US Environmental Protection Agency sets federal standards and treatment requirements for public water supplies. While the quality of desalinated water is typically very high, some health concerns remain regarding its use as a drinking water supply. These concerns can be mitigated through deliberate planning, management, and monitoring.

The source water used in desalination may introduce biological and chemical contaminants to drinking water supplies that are hazardous to human health. For example, boron, which is an uncommon concern for traditional water sources, is a constituent of seawater and can also be present in brackish groundwater from aquifers comprising marine deposits. Boron occurs in oceans at an average concentration of 4.5 mg/L. While boron is recognized to have a beneficial role in some physiological processes in some species, higher exposure levels may cause adverse effects. The effect of boron on humans remains under investigation. Boron is known to cause reproductive and developmental toxicity in animals and irritation of the digestive tract. It accumulates in plants, which may be a concern for agricultural applications using desalinated seawater. In 2008 the US Environmental Protection Agency determined that it would not develop a maximum contaminant level for boron because of its rare occurrence in most freshwater sources used for drinking water. EPA concluded there was inadequate data to assess the human carcinogenicity of boron. Rather than a standard, EPA published an advisory level. The EPA longer term health advisory level for boron is 2.0 mg/L, and the 1-day and 10-day health advisory levels are 3.0 mg/L [23]. Boron concentrations in water derived from basic reverse osmosis of seawater often are near but not necessarily below

the EPA's longer term advisory level [24]. Boron removal increases with alkalinity. A second pass through a reverse osmosis membrane with a pH adjustment can effectively remove boron. The EPA has encouraged states to issue boron guidance or regulations as appropriate. Some states have drinking water standards or guidelines for boron (California, Florida, Maine, Minnesota, New Hampshire, and Wisconsin); these range from 0.6 to 1.0 mg/L [23]. Many states have not issued boron guidelines.

Similarly, product water from reverse osmosis treatment of seawater may contain high levels of bromide and iodide. Their presence risks the formation of brominated and iodinated disinfection byproducts, especially in municipal distribution systems that blend the desalinated water with waters high in organic matter [25].

Another health-related concern is the extent to which algal toxins and microorganisms unique to seawater may pass through reverse osmosis membranes and enter the drinking water supply. This concern has prompted research to inform how desalination facilities may need to be operated when these organisms and algal toxins are present. Algal toxins are a consideration for desalination facilities in locations affected or potentially affected by harmful ocean algal blooms, especially the subset of blooms that are capable of producing neurotoxins (e.g., domoic acid). How to effectively monitor these algal outbreaks, as well as understanding the factors contributing to their formation (e.g., dust, cyanobacteria, and nutrients from aquaculture and estuarine/river discharges) are emerging research areas [26]. The global frequency in harmful algal bloom outbreaks has been increasing; the recurrence of such outbreaks depends on the species, with some species appearing episodically and others annually [26]. In areas susceptible to such outbreaks and highly dependent on desalination for municipal water supplies, these outbreaks represent a concern for water supply security.

Some coastal desalination facilities in the United States, like the operational Tampa Bay facility, may treat estuarine water. Estuarine water, which is a brackish mixture of seawater and freshwater, has the treatment advantage of lower salinity than seawater. Treatment challenges of an estuarine water source are its variability and that it may contain surface water contaminants (e.g., infectious microorganisms, elevated nutrient levels, pesticides, and emerging contaminants); additional monitoring to ensure compliance with federal and state drinking water regulations may be needed.

Desalinated water may not contain minerals essential for human health (e.g., calcium and magnesium). Remineralization of desalinated water prior to it entering a municipal distribution system in communities highly dependent on desalinated water may be warranted based on human health concerns [27]. Remineralization and stabilization of the desalinated water also would reduce the risk of corrosion of piping by the addition of desalinated water into a distribution system. Some US communities have legacy lead pipes in their systems or within the plumbing of homes and buildings.

6. BRACKISH WATER DESALINATION IN FLORIDA, CALIFORNIA, AND TEXAS

6.1 Florida—Early and Consistent Adopter of Brackish Water Desalination

In regions of Florida, brackish water desalination has almost become a common addition to municipal supplies. Brackish groundwater supplies around 0.6 million m^3/d and is expected to supply around 1.1 million m^3/d by 2030 [28]. Brackish desalination and water reuse are anticipated to dominate the sources of new water supply in Florida, while near-term investments in new seawater desalination are anticipated to play little or no role. The State of Florida has adopted policies, regulations, and programs to encourage the development of alternative water supplies, as well as created an alternative water supply requirement for regional water authorities. The focus on nontraditional supplies derives in part from Florida's flat topography, which limits additional surface storage options. The legislature in Florida funded a program from 2006 to 2009 to financially support local investments in alternative water supplies. Florida also developed statewide permitting rules for desalination concentrate management and simplified the approval for small utilities proposing to desalination applications with minimal environmental risk [29].

Florida also established a legal and permitting context for brackish groundwater development. Groundwater, like all water in Florida, is a public resource to be managed on a state and regional basis [30]. While most permits for a consumptive use in Florida are limited to 20-year terms, there is flexibility for a longer permit term for alternative water supplies, up to 50 years in some cases [30]. These longer permit terms provide greater regulatory certainty for making infrastructure investments and performing long-term planning.

6.2 California—Brackish Water Desalination Is Popular in Southern California

California has the most complex water management and transport context of any US state. The snowpack of the Sierra Nevada mountain range, the capture of runoff in reservoirs managed for water supply and flood control, the transport of water from Northern California through a delta into pumps and two aqueducts for transport to Southern California, and transfers from the Colorado River basin to California are often what captures the majority of decision-makers' attention. While the attention may be focused on California's surface water system and the state's freshwater aquifers, brackish resources have been and continue to be developed. Table 6 summarizes the adoption and plans for brackish desalination in California. As shown in Table 6, brackish desalination capacity could expand by more than 75% in California if planned facilities are built.

As of 2013 California had 23 operational brackish groundwater desalination facilities; all but one served Southern California. The majority of proposed brackish facilities also are located in Southern California. Many of the facilities in Southern

Table 6 Capacity and number of brackish water desalination facilities in California

Resource	Status as of 2013	Capacity (m^3/d)	Number of facilities
Brackish groundwater	Operational	471,500	23
	In design or under construction	30,600	3
	Proposed for construction prior to 2030	252,000	17
Brackish surface water	Proposed for construction prior to 2030	76,000	1[a]

[a]The Bay Area Regional Desalination project is proposed for construction within the San Francisco Bay Delta. The feed water would have a variable salinity ranging from 300 to 11,000 mg/L.
Data from California Department of Water Resources, California Water Plan, Update 2013, vol. 3, California Department of Water Resources, Sacramento, CA, 2013 (Chapter 10).

California use regional brine lines to dispose of their concentrate. The concentrate is collected from multiple facilities in the brine lines and transported to a wastewater treatment facility where it is combined with other municipal and industrial wastewaters. The combined effluent is transported to and disposed in the ocean. Additional Southern California brine lines are planned.

6.3 Texas—Abundant Brackish Water Desalination Opportunities

In Texas there are 46 brackish water desalination facilities. Thirty-four of these facilities have a combined brackish groundwater treatment capacity of 0.3 million m^3/d. Twelve of these facilities have 0.2 million m^3/d of combined capacity to treat brackish surface waters; these facilities are typically in the northwestern region of Texas.

While most brackish desalination facilities in Texas are not large-scale facilities, a few facilities have larger capacities. The San Antonio Water System is making a series of investments in brackish groundwater desalination that is expected to reach a total capacity of 113,600 m^3/d of product water by 2030. This new supply could meet 14% of the city's anticipated water demand. In 2007 the Kay Bailey Hutchinson inland desalination facility began operations in El Paso, Texas. It has a capacity of up to 104,100 m^3/d of freshwater from brackish groundwater. Full facility operations would meet 35% of El Paso's water demand. However, the facility generally initially operated closer to 13,250 m^3/d when freshwater sources were not drought-limited [31]; in years where water supplies were more constrained in the 2010s, the facility operated closer to full capacity. The facility's interior location in an arid region limited the environmentally acceptable concentrate management options. The concentrate is piped 22 km to a disposal well that injects the brine 1220 meters into an aquifer that is more saline than the concentrate [32]. The facility's capital costs were roughly divided, as follows: 43% for the reverse osmosis facility, 35% for brackish water wells and collection system, 9% for concentrate disposal infrastructure,

and 7% for the land and other project components [32]. The facility was built as a joint effort by the El Paso Water Utilities and Fort Bliss US Army Installation.

Texas aquifers are estimated to contain more than 9000 million m^3 of brackish groundwater. In 2015 the Texas Legislature required that the Texas Water Development Board initiate efforts to designate "brackish water production zones." The Texas Water Development Board is the state agency charged with statewide water planning and administration of state financial and technical programs for developing and managing water resources. The Texas Water Development Board started in 2015 a 10-year initiative to distribute $8000 million in state low-interest loans for new water management projects. Of the first round of $1000 million in funding, brackish desalination received 3% of the funds.

The Texas State Water Plan is developed and released on a 5-year cycle. The plan identifies regional projections for future water demands, the recommended strategies to meet those demands, and the decade in which those strategies need to be operational. Eligibility for various state programs, including low-interest loans, is limited to strategies recommended in the State Water Plan. The annual municipal water demand in Texas is estimated to expand from 6400 million m^3 in 2020 to 10,400 million m^3 in 2070 [33]. That amounts to an increase in annual demand of roughly 4000 million m^3 from 2020 to 2070. The state water planners expect groundwater desalination capacity during those 50 years to expand by 50 million m^3. Therefore brackish water desalination in Texas may play a significant future role in the water supply of select Texas communities, like San Antonio, while playing a more modest role when viewed at the state level.

7. SEAWATER DESALINATION IN FLORIDA, CALIFORNIA, AND TEXAS

California and Florida are the only two US states with operating large-scale seawater desalination facilities. Given proposals for various facilities, seawater desalination capacity could provide for 0.6 million m^3/d of additional US municipal supplies by the mid-2020s. Most of the near-term proposals for capacity additions are in California. Significant capacity additions for municipal seawater desalination in other US states are likely to enter into service after 2025.

7.1 Florida—Early Adopter Learned to Be Cautious

From 2006 through 2015, the Tampa Bay, Florida, facility with a capacity of 94,600 m^3/d was the largest operable estuarine/seawater facility in the United States. While potential sites in Florida for other seawater desalination have been identified, no municipal water providers were actively designing or constructing a large-scale facility as of early 2016 [29]. Instead, municipal water providers are adopting alternative water supplies, especially wastewater reuse and brackish groundwater supplies, and promoting efficiency and conservation.

The Tampa Bay facility is colocated with the Big Bend Power Station. The desalination facility treats a portion of the power plant's cooling water. The concentrate is blended with the power plant's cooling water effluent before being discharged into a canal that reaches the bay. Part of the genesis for adopting desalination was a requirement that the water supply district reduce its use of freshwater from shallow aquifers at the same time that the customer base was expanding. The desalination facility, which desalinates heavily brackish estuarine water, encountered technical issues and financial problems during construction and startup, driving up project costs. Development of the facility was started through a bidding process to identify a private sponsor for a PPP. The private partner was to develop, build, own, and operate the facility. As the result of bankruptcies among the private partners, private project financing became more complicated. The public authority, Tampa Bay Water, acquired the project halfway through construction, and later sought other private partners under a design-build-operate contract. Early operations were plagued by problems of biological growth (i.e., fouling) of the reverse osmosis membranes. Because of the development of other water supplies and a decrease in demand for water caused by an economic downturn that reduced population and economic growth starting in 2007, the Tampa Bay facility has largely operated at a fraction of its design capacity. Its operations were at 46% of capacity in 2010, 15% in 2011, 5% in 2012, 41% in 2013, 36% in 2014, and 9% in 2015. The operational cost per unit of treated water from the Tampa Bay facility remains significantly higher than the operational costs for fresh groundwater, marginally more than the costs for many surface water supplies, and almost competitive with some of the costs for certain surface water sources. Demand for water in the service area appears to be growing again and plans are to operate the facility at 50%–60% capacity in upcoming years.

Ratepayers continue to pay for the capital expenditures and upkeep of the desalination facility. For many observers of US desalination, the early experience in Tampa Bay reinforced the risks associated with large-scale desalination investments and the necessity for carefully crafted and selected PPPs. More recent experience has shown that at times the facility has reliably produced treated water that meets up to 15% of the local water supply demand, and this level of operation may become more common as demand in the service area increases.

7.2 California—Ambitious Proposals Bolstered by Recent Drought

In particular, given the large amount of proposed municipal seawater desalination capacity for California, the social, regulatory, and financial context for seawater desalination in California is particularly important for understanding the prospects for US seawater desalination. The initiation of operations of the 189,300 m^3/d seawater desalination facility in Carlsbad, California, in Dec. 2015 occurred in the midst of an extended statewide drought. The drought led to dramatic cuts in surface water

deliveries, historic statewide water use restrictions, and significant depletion of fresh groundwater and surface water supplies. Concerns about extended drought, reliability of water transported across the state, and reductions in imports from the Colorado River basin are among the drivers prompting proposals for new supplies that are local and drought-resilient, like seawater desalination. Given that many cities in Southern California have long relied heavily on imported water, the shift to local supplies represents a significant change. Table 7 summarizes the status of municipal seawater desalination facilities and proposed facilities either located in California or potentially delivering water to California.

In addition to Poseidon Water's operational Carlsbad facility, the private company has proposed a 189,300 m^3/d seawater desalination facility in Huntington Beach, California. If the project obtains its approvals and financing, Poseidon is anticipated to negotiate and sign a water purchase agreement with local water districts. Poseidon has incorporated offsets to greenhouse gas emissions associated with the facility's operations into its proposal. It would select from among carbon offsets, renewable energy credits, or supporting projects that offset emissions like reforestation initiatives.

As shown in Table 7, seawater desalination capacity providing water to California could expand dramatically if all or some of the planned facilities are built. Therefore the social, regulatory, and financial context for seawater desalination in California is particularly important for understanding the prospects for US seawater desalination. Many environmental groups are anticipated to continue to raise concerns about coastal desalination facilities in the state, including the impact on the coastal ecosystem and the greenhouse gas intensity of the desalination operations. Between 2005 and 2014, the State of California provided a total of $55 million to support desalination research, feasibility studies, demonstration projects, and construction activities. In 2014 California voters approved a state proposition approving $7500 million in general obligation bonds for water-related activities. The majority of the funds are for water storage projects ($2700 million) and watershed protection and restoration ($1500 million) [34]. As of early 2016, the state had competitively distributed $50 million of the state bond funds for grants to assist with desalination activities [34].

7.3 Texas—Measured Plan for Adoption Over Decades

Texas currently has no large-scale municipal seawater desalination facility. The Texas State Water Plan indicates that the state's municipal water providers are not rushing into desalination adoption. Instead, they are planning a measured pace of desalination adoption in coming decades. At least five municipal seawater desalination projects have been included as part of the state's regional long-term water supply management efforts. The Guadalupe-Blanco River Authority, one of the state's regional water authorities,

Table 7 Capacity and number of municipal seawater desalination facilities in California or potentially serving California as of 2015

Status	Capacity (m^3/d)	Number of facilities	Description and status
Operational or idle			
Carlsbad	189,300	1	Placed in service in late 2015. Private owner delivers treated water to San Diego County Water Authority pursuant to a 30-year water purchase agreement.
Morro Bay	2300	1	Seawater desalination portion of facility is idle as of 2016. There is some interest in returning the facility to operational status.
Three small facilities	1900	3	Santa Catalina Island facility was placed in service in 1991; it reported production of 432 m^3 in 2010. San Nicholas Island (US Navy Air Strip) and Marina (Fort Ord) did not report production in 2010.
In design or under construction			
Santa Barbara	10,000	1	In Jul. 2015 Santa Barbara City Council contracted to recommission an idle facility to meet approximately 30% of the community's water demands. Original facility from the early 1990s had a capacity of 33,800 m^3/d.
Proposed as of 2013			
Located in California	912,300	13	Many facilities are proposed for sites located in Southern California between Los Angeles and San Diego.
Located in Mexico with capacity to deliver to California	378,600	2	Capacity shown would be the total capacity. The volume for delivery to California is undetermined. The proposals are for desalination in Rosarito Beach, Mexico, and transport to San Ysidro, California, where final treatment would be conducted.

Data from California Department of Water Resources, California Water Plan, Update 2013, vol. 3, California Department of Water Resources, Sacramento, CA, 2013 (Chapter 10).

received a low-interest loan from the Texas Water Development Board to conduct a feasibility study for a 94,600 m^3/d seawater desalination facility. If the project proceeds as planned, it may be operational by 2027.

According to the Texas State Water Plan, seawater desalination is estimated to address around 2% of the growth in the state's municipal water supply demand between 2020 and 2070. The expansion in municipal supply from desalinated seawater is estimated at roughly 96 million m^3 during those 50 years, with most of the facilities being placed in service after 2050 [33]. Notably, the plan also anticipates a significant growth in industry, especially coastal manufacturing, self-supplying water using desalination. According to the plan, this industrial self-supply is anticipated to expand by 42 million m^3 between 2020 and 2070, with most of that expansion occurring before 2050.

The 2017 Texas State Water Plan anticipates that seawater desalination will expand in Texas in the coming decades but that product water from seawater desalination will remain a relatively small portion of the state's municipal supplies. State plans and support for desalination may expand as a more predictable regulatory context for desalination develops, if there are positive experiences with large-scale desalination in other states, with improved cost-competitiveness of seawater desalination, if private interests finance facilities, and as concerns about municipal water reliability increase.

8. CONCLUSION

The United States in aggregate has ample water resources; however, some US municipal water providers are increasingly challenged in their efforts to develop reliable freshwater supplies to meet local demands. Numerous US municipal water providers are actively pursuing nontraditional water supplies, including desalination of brackish water and seawater. Desalination offers a drought-resilient, weather-independent, and local water supply, and it creates a high-quality product water. As previously illustrated, each state is unique in how it is promoting and regulating municipal desalination.

While there is significant desalination experience internationally, there remains limited US domestic experience with large-scale municipal seawater desalination. Each new operational seawater desalination facility is likely to shape the US municipal water sector's and the US public's perceptions of the benefits and risks of future US facilities. The required health and environmental protections also may shift as domestic experience is gained.

How many and how soon municipal water providers in various US states will be willing and able to commit to seawater desalination is unclear. In part because future state-level approval processes and financing opportunities, as well as federal actions or programs, may encourage or discourage public and private seawater desalination investments. In many large urban areas, municipal providers may choose to adopt water

reuse and improved storm water capture and groundwater recharge first and seawater desalination later; alternatively, municipal providers may approach seawater desalination as a complement to the expansion of other nontraditional water supplies.

In contrast to the uncertain forecast for seawater desalination nationally, the expansion of brackish desalination as a water supply source in numerous US states is poised to continue. Numerous municipal water providers have found it to be a cost-competitive addition to their systems.

REFERENCES

[1] US Geological Survey, Estimated Use of Water in the United States in 2010, US Geological Survey, Reston, VA, 2014.
[2] US Geological Survey, National Brackish Groundwater Assessment, US Geological Survey, Reston, VA, 2014.
[3] Water Research Foundation and Electric Power Research Institute, Electricity Use and Management in the Municipal Water Supply and Wastewater Industries, Electric Power Research Institute, Palo Alto, CA, 2013.
[4] National Association of Water Companies, Moving Water Forward, National Association of Water Companies, Washington, DC, 2012.
[5] J. McEvoy, M. Wilder, Discourse and desalination: potential impacts of proposed climate change adaptation interventions in the Arizona–Sonora border region, Glob. Environ. Chang. 22 (2012) 353–363.
[6] J.R. Ziolkowska, Is desalination affordable? – Regional cost and price analysis, Water Resour. Manage. 29 (2015) 1385–1397.
[7] N. Voutchkov, Desalination Engineering: Planning and Design, McGraw-Hill, New York, 2013.
[8] A. Barak, Economic aspects of water desalination, in: N. Lior (Ed.), Advances in Water Desalination, John Wiley & Sons, Hoboken, NJ, 2013, , pp. 197–309.
[9] M.A. Goll, Desalination in Texas: struggling to cope, Texas Environ. Law J. 45 (2015) 51–86.
[10] K. Maize, Desalination expands, but energy challenges remain, Power 160 (3) (2016) 22–25.
[11] M. Elimelech, W.A. Phillip, The future of seawater desalination: energy, technology, and the environment, Science 333 (6043) (2011) 712–717.
[12] A. Subramani, Energy minimization strategies and renewable energy utilization for desalination: a review, Water Res. 45 (5) (2011) 1907–1920.
[13] A. Bennett, Cost effective desalination: innovation continues to lower desalination costs, Filtr. Sep. 28 (4) (2011) 24–27.
[14] Affordable Desalination Commission, Proposition 50 6a Desalination Final Report Pilot Demonstration, "Optimizing Seawater Reverse Osmosis for Affordable Desalination", US Bureau of Reclamation, Washington, DC, 2012.
[15] Texas Water Development Board, The Future of Desalination in Texas: 2010 Biennial Report on Seawater Desalination, Texas Water Development Board, Austin, TX, 2010.
[16] California Department of Water Resources, California Water Plan, Update 2013, California Department of Water Resources, Sacramento, CA, 2013.
[17] M. Irlbeck, N. Voutchkov, Desal Dialog: A Regulatory Workshop on Critical Issues of Desalination Permitting, WateReuse Research Foundation, Alexandria, VA, 2013.
[18] Texas Water Code §§18.001–18.005.
[19] California State Water Resources Control Board, Final Staff Report Including the Final Substitute Environmental Documentation Adopted May 6, 2015 Amendment to the Water Quality Control Plan for Ocean Waters of California Addressing Desalination Facility Intakes, Brine Discharges, and the Incorporation of Other Non-Substantive Changes, California State Water Resources Control Board, Sacramento, CA, 2015.

[20] M. Mickley, US municipal desalination plants: number, types, locations, sizes, and concentrate management practices, IDA J. 4 (1) (2012) 44–51.
[21] T. Younos, Environmental issues of desalination, J. Contemp. Water Res. Educ. 132 (2010) 11–18.
[22] T.M. Missimer, et al., Subsurface intakes for seawater reverse osmosis facilities: capacity limitation, water quality improvement, and economics, Desalination 322 (2013) 37–51.
[23] US Environmental Protection Agency, Summary Document from the Health Advisory for Boron Compounds, US Environmental Protection Agency, Washington, DC, 2008.
[24] National Academy of Sciences, Desalination: A National Perspective, National Academy Press, Washington, DC, 2008.
[25] D. Kim, G. Amy, Y. Karanfil, Disinfection by-product formation during seawater desalination: a review, Water Res. 81 (2015) 343–355.
[26] J. Zhao, H. Ghedira, Monitoring red tide with satellite imagery and numerical models: a case study in the Arabian Gulf, Mar. Pollut. Bull. 79 (2014) 305–313.
[27] J. Cotruvo, Health aspects of calcium and magnesium in drinking water, Water Condition. Purif. 48 (6) (2006) 40–44.
[28] Florida Department of Environmental Protection, Annual Report on Regional Water Supply Planning, 2014, Florida Department of Environmental Protection, Tallahassee, FL, 2014.
[29] Florida Department of Environmental Protection, Desalination in Florida: Technology, Implementation, and Environmental Issues, Florida Department of Environmental Protection, Tallahassee, FL, 2010.
[30] R.M. Buono, A New Frontier in Texas: Managing and Regulating Brackish Groundwater, James A. Baker Institute, Rice University, Houston, TX, 2015.
[31] Texas Comptroller of Public Accounts, Texas Water Report: Going Deeper for the Solution, Texas Comptroller of Public Accounts, Austin, TX, 2014.
[32] P.V. Brady, M.M. Hightower, Future expectations, in: J. Kucera (Ed.), Desalination: Water from Water, Scrivener, Beverly, MA, 2014, , pp. 585–617.
[33] Texas Water Development Board, 2017 State Water Plan, Texas Water Development Board, Austin, TX, 2016.
[34] California State Legislature, Legislative Analyst's Office, The 2016–17 Budget: Resources and Environmental Protection, California State Legislature, Sacramento, CA, 2016.

CHAPTER 11

Commercialization of Desalination and Water Treatment Technology: Shining a Light on the Path From Research Project to Intellectual Property Acquisition

Mike B. Dixon
MDD Consulting, Calgary, AB, Canada

Contents

There's an abundance of excellent research and exceptionally bright minds working on elucidating our world's most important problems—including the challenges in desalination and membrane water treatment. Many groups have also produced hundreds of journal papers, for example, on the topic of low fouling membranes through membrane modification and coating.

However, few water technologies survive the journey to full commercialization, whether through the sale of intellectual property or through the spin-out or build-up of a stand-alone company. For example, in a 2010 review by Rana and Matsuura [1],

Desalination Sustainability
http://dx.doi.org/10.1016/B978-0-12-809791-5.00011-0

over 300 membrane modification literature references are made. Furthermore, a Google patent search in 2016 for "membrane modification reverse osmosis" returned over 10,000 hits. In a more specific search, the term "thin film nanocomposite" returned 118 hits. In this technology area, these 118 patents support one successful spin-out technology produced by NanoH2O and sold to LG Chem.

Why does so little research and development become successfully commercialized, not only in desalination and water treatment technology but in all fields? Why are so few university patents purchased by large companies and even fewer spun out to successful companies? How can researchers give their intellectual property the best chance of being successful?

The key to answering these questions is to assess problems that entrepreneurs and investors are trying to solve and in which markets (for the purpose of this article entrepreneurs and investors will be called entrepreneurs). It's understanding what pain point entrepreneurs and investors are trying to relieve, not just focusing on researchers undertaking interesting work in a "silo" and then trying to find a buyer for their work. To help address this situation, universities are increasingly emphasizing technology transfer groups that can help researchers find the right buyer for their technologies. This is one step in the right direction, and if we continue to work to understand both sides of the story, the potential to effectively commercialize R&D will grow.

Entrepreneurs aren't necessarily looking for the best research or the most innovative ideas. They come to researchers from a slightly different angle, seeking ideas that aim to fill a significant market need and provide significant value in doing so. They aim to put their energy into creating value in a company and its products that can later be sold for a substantial profit. When looking at new technologies, they are looking to build value to make 5, 10, or even 20 times their initial investment.

1. HOW ENTREPRENEURS SEEK VALUABLE IDEAS

When entrepreneurs search for a good idea, it's not a random process of finding a technology they feel could be a winner. Searching for the right technology is a systematic process in which several tools are applied. Entrepreneurs might spend 6 months, 12 months, or longer searching for the idea that specifically fits with their aspirations and that creates significant value for their identified market.

Different people use different tools, and there are a number of established assessment models that can be a useful starting point to assess ideas. One is the Mullins Test [2], developed to assess innovative ideas prior to committing to a particular technology or business. Mullins' Seven Domains Model also offers an evaluation structure to look at the key areas for consideration in deciding to build a business.

The model allows the user to explore an idea from many angles, going well beyond a focus on the actual technology, including valuable inputs such as the skills and strengths of the proposed team. The test analyzes the viability of a venture well before the

entrepreneur pens a business plan or pursues funding. The considerations informed by the test provide critical success factors that investors will consider, be it through a formal or informal process, to establish whether they think it's possible for the team to grow the business into a successful company that can be monetized and provide them with a return on investment.

The successful entrepreneur may use the tool on several ideas and abandon many before committing major amounts of time, money, and effort. In many cases an entrepreneur needs to be committed and passionate about the idea, therefore road-testing several ideas can take significant energy.

The Seven Domains Model (Fig. 1) contains the following areas:

1. Target Segment Benefits and Attractiveness (Market Domain/Micro Level)
2. Market Attractiveness (Market Domain/Macro Level)
3. Industry Attractiveness (Industry Domain/Macro Level)
4. Sustainable Advantage (Industry Domain/Micro Level)
5. Mission, Aspirations, Propensity for Risk (Team Domain)
6. Ability to Execute on Critical Success Factors (Team Domain)
7. Connectedness Up, Down, Across Value Chain (Team Domain)

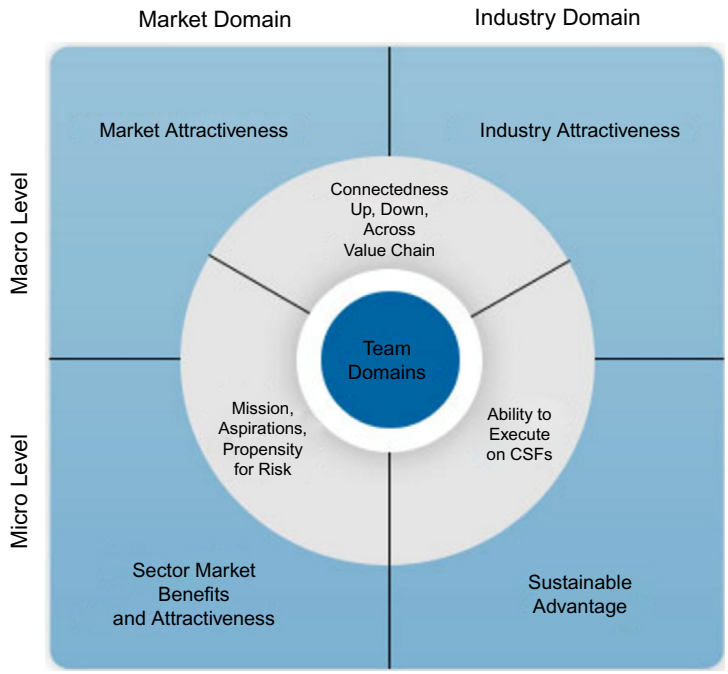

Fig. 1 Summary of the Mullins' Seven Domains Model [2]. *(Diagram reproduced from: J. Mullins, The New Business Road Test: What Entrepreneurs Should Do Before Writing a Business Plan, Pearson Education).*

While the model was originally created for new ventures, it can be used in existing organizations to decide whether to pursue a new product idea or market expansion. Therefore this model can also be useful for researchers to understand how to pitch an idea to a potential buyer for a patent or an intellectual property.

Following is a description of each of the seven domains.

1.1 Market Domain/Macro Level: Market Attractiveness

This domain looks at market attractiveness from a macro (large-scale) perspective.

The entrepreneur looks at the whole market. How big is it in terms of the number of customers and the value of sales, and how many units can be sold? The entrepreneur assesses trends within the market. Where is growth occurring within the market, and what factors are driving the growth? Is this growth projected to continue and how long might it be until the market is saturated, requiring new products and innovations?

In this domain, the entrepreneur is checking whether the market is big enough to achieve potential sales targets and that growth is steady. In this way, the entrepreneur's task of market entry is less difficult because it is easier to grow a business in a growing market than it is in a declining one. For example, currently in North America the seawater desalination market is growing slowly in comparison with municipal water reuse. Given an option, the entrepreneur would favor a reuse technology over a seawater desalination-specific technology.

Within this domain a PEST analysis can be used to explore the large-scale factors that affect the market. This analysis involves looking at political, economic, sociocultural and technological factors associated with the potential company's development. How healthy do these factors appear? Following is a description of the PEST analysis.

1.2 PEST Analysis

1.2.1 Political Factors to Consider

- If the product will be launched in a specific region, will an election in the region change the status of the market? Might one political party's policies drive the market in another direction? For example, what if the current party in power supports a major research effort to launch desalination research and creates plans to install major desalination plants, but a rival party's policy is to increase capital expenditure on dams instead? Also, could the launch of a new desalination product be hindered by a change of government because new desalination products aren't needed? For example, if a political party perceives desalination as too energy-intense or supports the notion that desalination plants are "white elephants," the party might decide to finance dam projects rather than desalination projects.

- Is public acceptance of a particular party increasing or another decreasing? What is each party's business policy and how might it affect the launch of a product and a steadily growing market? For example, if a particular party strongly supports direct potable reuse and seems likely to win subsequent elections, then that may be a promising area for technologies that support direct municipal potable reuse or technologies that increase the safety of this practice.
- Are there planned changes to business regulation and how might they affect establishment of a business focused on a particular technology? Is there a trend toward regulation or deregulation? Does this trend increase or decrease risk factors? For example, in many areas, hydraulic fracturing regulations support more efficient use of desalination techniques to deal with waste streams.
- What is the likely timescale of proposed legislative changes? For example, if hydraulic fracturing regulations takes 10 years to develop, a start-up company may not be able to survive that long.

1.2.2 Economic Factors to Consider

- How reliable is the current economy? Is the economy in decline, stable, or growing? For example, an oil price decline such as the one in 2015 would prevent easy entry into produced water treatment. For example, the success rate of companies such as the Gradiant Corporation probably would have been much better between 2015 and 2016 if the oil price slump had not occurred.
- If the potential market is spread between multiple countries, are key exchange rates stable, or do they vary significantly?
- In the area where operations might be headquartered, what is the availability of the required labor force? Will it be easy to build a skilled workforce locally? Will expertise be required from many parts of the globe? Will it be expensive to hire skilled labor? For example, would operations be less expensive if they were located in India or China rather than Europe or the United States, such as was considered by NanoH2O [3].

1.2.3 Sociocultural Factors to Consider

- What is the target population's growth rate and age profile? How are such factors likely to change? These factors could determine the need for a new water technology, particularly in areas with rapid population growth.
- Are generational shifts in attitude likely to affect the business?
- What employment patterns, job market trends, and attitudes toward work are observed? Are these different for different age groups?
- What social attitudes and social taboos could affect the business? Have there been recent sociocultural changes that might affect it?
- How do religious beliefs and lifestyle choices affect the population?

1.2.4 Technological Factors to Consider

- Are rival new technologies on the horizon that could affect the chosen technology's dominance in the proposed market space? For example, while the forward osmosis technology companies were the most advanced ones in the area of new brine concentration in 2016, membrane distillation companies were rapidly progressing and considering similar markets.
- Could the chosen technology complement a suite of technologies already owned, such as when GE acquired Osmonics, Inc., and Ionics in order to create a more complete membrane service provider?
- Are potential competitors advancing new technologies that could redefine their products?
- Where are the focus areas for governments and research institutions? Can these areas of interest be leveraged to aid in funding and the subsequent product launch?
- Are there existing technology hubs that the entrepreneur could form an alliance with?

1.3 Market Domain/Micro Level: Sector Market Benefits and Attractiveness

Although an idea might seem like it will gain instant success and widespread uptake, it's unlikely that its field of technology will immediately adopt a new product. An entrepreneur will be looking for early adopters in the market and working against serious skepticism of various parties, potentially including thought leaders who are not engaged in the topic. The entrepreneur will seek to target one market sector or segment and aim to meet its needs fully. To identify this segment, the entrepreneur evaluates the market on a micro level by considering the following questions:

- Which market segment will most likely benefit from the idea?
- How is the product differentiated from other products existing in the market?
- What would the secondary market segment be and how adaptable is the product to enter this second segment?

Entrepreneurs will seek qualitative and quantitative data and talk with many potential customers to gather feedback on their pain points. Entrepreneurs will establish how well competitors are meeting potential customers' needs and areas where the product could remove any pain points customers might have. A good example of this is the adoption of high flux membranes that retain high rejection. Seawater desalination customers were experiencing the pain of having to pay high energy bills, which could be partially alleviated by membrane suppliers introducing advanced high-flux technologies. Each membrane company had introduced higher and higher flux membranes over the past 25 years and maintained higher and higher salt rejections. As a disruptive alternative to more energy-efficient membranes, Energy Recovery, Inc. (ERI) saw potential in developing pressure exchange technology to recover wasted high pressures at the concentrate end of pressure vessels. This approach was very successful because the company

was able to show the reliability of its differentiated product and that it reduced operational costs far more than the standard energy recovery devices of the time. As evidence of this success, ERI achieved an opening day market cap of $650 million on the NASDAQ, 12 times its annual revenue.

The entrepreneur looks for data on sector targeting, such as by reading analysts' reports and market research reports. Global Water Intelligence is a good example of a place to find market information on the international water industry.

1.4 Industry Domain/Macro Level: Industry Attractiveness

The entrepreneur will establish how attractive the target industry is on a macro level. Mullins identifies another tool, "Porter's Five Forces" to assess which factors affect the profitability of a selected industry. The tool is used widely and is well respected as one of the most important business strategy tools, particularly given that it was created by Harvard Business School professor, Michael Porter, to assess the attractiveness and potential profitability of an industry [4].

Five Forces Analysis assumes that five important forces determine competitive power in a business situation, as shown here:

1. *Supplier power*: How easy is it for suppliers to drive up prices? This answer is driven by the number of suppliers of each key input, the uniqueness of their product or service, their strength and control over the business, and the cost of switching from one to another. The fewer the suppliers and the more they meet business needs, the more powerful the suppliers. In RO technology, there is little uniqueness between products, which has caused a major downward shift in prices since thin film composite technology was commercialized. This force is so strong that even differentiated products entering the market will find difficulty in charging a premium for RO technology, given the market perception that existing RO technology is very reliable and well-priced.
2. *Buyer power*: How easy is it for buyers to drive prices down? This is driven by the number of buyers, the importance of each individual buyer to the business, and the cost to buyers for switching from old business products and services to those of someone else. If there are powerful buyers, then they are often able to dictate terms. Given the above similarities between suppliers in RO technology, buyers were able to bring prices down to very low margins on RO elements. While mega buyers in the desalination market number only 15–20, small buyers who are willing to try something new in order to differentiate themselves number in the hundreds.
3. *Competitive rivalry*: How many competitors are there, and what are their capabilities? If there are many competitors with products and services that are on par with one another, then the new venture will have little power in the situation, as buyers can easily go elsewhere if they find a better deal. On the other hand, if the new

product is clearly differentiated, it can have great strength in the market. For example, in the ultrafiltration (UF) market, more than 10 manufacturers are competing for the same business. Differentiating a UF product in a meaningful way is perceived as being difficult, making competitive rivalry very strong in this area. Unlike buyers in the RO market, UF buyers are somewhat locked into the supplier they choose at construction time, making it challenging to switch suppliers and try a new a product.

4. *Threat of substitution*: How likely is it for customers to substitute the business's product with another one? For example, reverse osmosis spiral wound membranes are standard sizes, allowing users to change suppliers frequently. If substitution is easy, then the product must have a clear advantage and a wide margin of differentiation. Using the preceding example of UF, new, flexible UF racks that allow customers to switch UF membranes are gaining more attention with technologies such as H2O Innovation's FiberFlex, which may open up this market for substitution and the ability for improved technologies and better competition.
5. *Threat of new entry*: How easily can others enter the selected market? How low are the barriers to entry (such as time and cost)? Are there few economies of scale in place? If the technology is poorly protected, then new competitors can quickly enter the market. Manufacturing facilities that are able to produce membranes at quantities great enough to compete globally are capital-intensive, which provides quite a barrier to entry for the membrane market.

1.5 Industry Domain/Micro Level: Sustainable Advantage

In this domain entrepreneurs will look to build and sustain a unique selling proposition (USP). They will assess the competencies required and consider how challenging it may be to develop such competencies.

USP is the uniqueness or differentiation of the product that competitors can't access. This "competitive edge" is why customers will want to buy the product. USPs are key to launching a successful new company. Companies without a USP are destined to struggle for survival. USPs are a new technology's biggest challenge and are extremely relevant for researchers aiming to sell their intellectual property. As soon as one company establishes a successful USP, competitors rush to copy it, which is often referred to as the "me too" effect. For example, in the desalination sphere, as previously mentioned, hundreds of technologies support antifouling membranes. Each technology fills an industry need, but the industry need is overfilled and crowded, making it difficult for researchers to prove their USP. Most membrane manufacturers have antifouling membranes for various applications, making it difficult to enter this space successfully.

Entrepreneurs will assess the resources that may be available to them that their competitors don't have access to, such as patents, established processes, and finances. These factors can drastically affect an entrepreneur's ability to compete.

1.6 Team Domain: Mission, Aspirations, Propensity for Risk

The team domain may have little connection with the technology itself, but may help guide researchers aiming to sell their intellectual property to the right people in the industry. Although it may be more difficult for the researchers to use the team domain information, I present it to complete my discussion on the Mullins Test.

In this domain, entrepreneurs analyze their personal commitment and how easily they will be able to persuade others to get behind their idea.

Entrepreneurs will assess their own motivations for adopting the idea and why they might feel that way. Their reasons for starting a business are key to this point. Are their ambitions based on a desire to bring it to fruition to serve a "greater good," or are they seeking a "lifestyle business"? How do their personal goals and values fit with the idea? Are they prepared to take the risk and put in the hard work needed to build a successful business around the idea?

Entrepreneurs will seek like-minded professionals who are motivated by the idea. They will think about who might work really hard to help make the business a success. For example, in the membrane business, entrepreneurs will look to partner or employ veterans of the industry who are passionate about membrane technology. They will look to previous successful businesses, such as Fluid Systems or Osmonics, to find passionate staff. The potential team members may need to risk their reputation and, in some cases, their money, so the potential team's attitude toward the risk is important.

1.7 Team Domain: Ability to Execute on Critical Success Factors

Entrepreneurs will assess the critical success factors (CSFs) for the potential business in this domain. They will consider whether their potential team can deliver these CSFs. CSFs are absolutely essential to the business's success. Identifying and communicating CSFs ensures that the entrepreneur's business is focused and that its resources are aimed toward the most important items for success.

The following questions are relevant in this domain:

- What will harm the business significantly, even when everything else is going right?
- What activities will significantly drive the business forward?

Entrepreneurs will assess the knowledge and skills of their potential team and consider how certain they are that the team can deliver successfully on the CSFs. They will think about how they might fill skill gaps from within their networks.

A CSF for a new desalination technology might be ensuring adequate monitoring and engineering support for a pilot project. An accidental failure of a pilot project could seriously harm the new venture's reputation and therefore create a big hurdle for eventually expanding sales.

1.8 Team Domain: Connectedness Up, Down, Across Value Chain

The final domain assesses entrepreneurs' connections and how important those connections are to the success of the new business. Entrepreneurs will assess suppliers, customers, investors, government funding bodies, thought leaders, early adopters, and other important relationships they have within the potential industry. They will consider the ways they can capitalize on their connections and whether they need to seek team members with the right connections. They will also look across the value chain, determining whether they know competitors personally and whether these relationships help or hinder the venture or whether these competitors could become partners in the business.

The researcher's connections within the industry could be exceptionally helpful to the pursued entrepreneur. By boosting the entrepreneur's network, the researcher could provide greatly needed value and ease the entrepreneur's decision to buy or license the proposed technology.

2. CONSIDERATIONS FOR RESEARCHERS EMBARKING ON NEW PROJECTS AIMED AT GENERATING SALEABLE INTELLECTUAL PROPERTY

Researchers who choose to embark on a new project aimed toward the sale of intellectual property should take the initiative to understand where entrepreneurs are coming from (tools like the Mullins Test can help them think through what an entrepreneur may need to think through). To further assist an entrepreneur with the analysis of their idea and help show how attractive the intellectual property can be, researchers might suggest the use of a technical feasibility assessment. In this assessment the business considers how the end product will satisfy customer needs and ensure the sale of a reliable product, including durability of the product's materials, reliable operation ensuring that performance is as expected under advised operating conditions, product safety, competition from other developing technologies, achievable operating and capital costs, ease of maintenance, ease of manufacture, and ease of pilot testing by potential customers.

As a practical example, many new desalination products require significant capital investment and operational commitment to undertake a pilot test. The innovation presented by both FILMTEC and NanoH2O could be tested relatively easily because the technology was bundled into a regular spiral-wound element form. In this way, a customer could easily buy one to eight elements and use an existing infrastructure to test onsite at existing desalination plants. The testing was cheap and relatively fast, meaning that the value of the innovation to the customer or client could be efficiently realized.

As mentioned, another and important example of technical feasibility relates to a product's durability. For example, what if the practical use of a membrane surface modification causes the coating to wash off over time, leaving a regular membrane surface behind, susceptible to fouling? Would this be an acceptable product? Or what if the membrane product was durable under regular use, but industry cleaning methods, such

as acid and base cleaning at pH 2 and 12, cause a decrease in salt rejection or a loss of flux? Would such a product be widely adopted by the desalination industry?

It can be useful for researchers to talk to people in the industry to find out what questions to ask. No one person knows everything about every system; therefore, building networks and asking questions and getting answers from both R&D and entrepreneurial sides of the coin can help break down barriers that might otherwise be problematic.

Another tactic when preparing intellectual property for sale is to consider the entrepreneur's end game. Many entrepreneurs are seeking products that can be developed and turned into a business, that can establish value, and that can create a stable revenue stream, with the idea that they can sell the business and make a profit on their investment. Considering how a large company may want to enhance its own product portfolio could help researchers determine the value of their work in its early stages.

For example, in the early 2000s, GE realized the global importance of the water industry and set out to assemble a group of business lines that could together compete for a major share of the water treatment market. The company invested over $4 billion on four major companies and other minor acquisitions to fill out their water treatment product lines. Table 1 shows some examples of successful acquisitions in the desalination industry and subsequent technology areas that were deemed valuable enough to form a major business line within the acquiring mega company. Table 1 shows one metric for demonstrating value in an acquisition, that is the sale price times the revenue. Given start-up companies are a vehicle for demonstrating a good repeatable business model, they are often worth many times their annual revenue. This is dependent on how valuable the acquisition of the technology can be in the future. For example, the thin film composite (TFC) membrane was viewed as being very disruptive to the market and could generate a great deal more than the revenue of Filmtec at time of sale for Dow. This has been evidenced very strongly since 1985, with Dow being a market leader in RO technology with the TFC membrane providing them the platform to execute their goals.

Although GE found its acquisition strategy very attractive at first, the competitive nature of the chemicals business, for example, provided many challenges. Additionally, the merging of many company cultures into one highly disciplined culture required a good deal of restructuring of their business (particularly in sales and marketing) to achieve their revenue targets. Given these well-publicized difficulties, an acquisition strategy of this size may not materialize for quite some time. However, smaller scaled acquisitions of water treatment technology companies remain prevalent.

3. POTENTIAL DESALINATION VALUE CREATION FOR RESEARCHERS—AN EXAMPLE FROM THE OIL AND GAS INDUSTRY

In the desalination and water treatment sphere in 2016, one area of development that entrepreneurs valued was concentrate management from inland desalination applications

Table 1 Valuable companies acquired by global mega companies in the desalination space (prices in million US dollars)

Company	Acquirer	Sale price	Revenue	Year of sale	Sale price in 2016 dollars	Revenue in 2016 dollars	Sale price × revenue	
Osmonics	GE	253	207	2003	326	266	1.2	
Filmtec	Dow	75	11	1985	165	24	6.9	
Ionics	GE	1100	480	2005	1367	597	2.3	*appx
Zenon	GE	656	270	2006	788	324	2.4	

and zero-liquid-discharge (ZLD) technologies. In 2003 the US Desalination and Water Purification Technology Roadmap was produced and highlighted concentrate management as a key area for investigation. Facilitated by the Sandia National Laboratory and the US Department of the Interior Bureau of Reclamation, the assembled experts discussed how concentrate management is a critical concern in inland areas where ocean discharge is impractical. New concentrate management approaches are needed that that will

- *Reduce volumes*: The less voluminous the concentrate stream, the less concentrate that must be disposed and the greater percentage of water that can then be beneficially reused.
- *Reduce energy and other costs*: Provide for beneficial use. Concentrate streams may contain elements that can be beneficially used in industrial and/or agricultural processes. Research should be focused on identifying beneficial use elements and creating cost-effective methods for separating salts.

This area of research was still evident 13 years later in 2016, and it is not surprising that entrepreneurs are looking to this area to seek value creation within their spin-out companies. A rapid expansion of oil and gas exploration in inland areas of the United States, Canada, and Australia has created a need for disposal of difficult waste streams that, by conventional methods, can be a costly exercise. Politically and socially, the lack of a complete license for hydraulic fracturing and oil sands mining is putting pressure on oil producers to act with greater environmental sustainability. Regulations in these countries have also necessitated oil producers to deal with their wastes responsibly, in some cases creating a significant financial liability. One universal trend that makes industry spend money on technology is the regulatory requirement to do so, although even when forced to spend on technology, that requirement can vary significantly in different jurisdictions. Desalination techniques have the ability to concentrate difficult waste streams, which can potentially help oil producers reduce the cost of disposing of these wastes. If the economic assessment of a concentrating technology is more favorable than that of current disposal techniques, such as evaporation lagoons or brine disposal wells, then a great deal of value can be created by a technology company. If expressed in terms of savings per barrel of oil produced, the oil producer can see a direct impact on its company's profitability, thus taking an investment risk on piloting a new technology may be an attractive option.

Discussing value creation areas with industry and potential entrepreneurs will assist researchers in finding the right differentiated technology with the best chance of being licensed by an entrepreneur.

Following are a few companies that in 2016 were developing well and making progress toward brine concentration with oil and gas customers and leveraging the potential value creation area previously discussed. Each company to a varying degree has taken university-led research and licensed the technology with an aim to commercialize it. These companies are attempting to grow their businesses in nontraditional desalination applications, quite a different approach to that of previously successful companies such as

Ionics, Filmtec, and NanoH2O; therefore only with time will we realize the success of their respective business models.

3.1 Gradiant

Gradiant has developed a portfolio of technologies to manage the entire industrial water cycle built on a deep understanding of the complexities of oilfield water treatment. Gradiant's goal is to partner with customers to create efficient water treatment and recycling programs that work within each customer's unique operational, economic, and regulatory constraints. The company offers a suite of field-proven services from primary and secondary treatment to desalination using their Carrier Gas Extraction (CGE) and Selective Chemical Extraction (SCE) technologies. Gradiant claims that CGE is the only technology that can produce fresh water from high-TDS brines while being competitive with produced water disposal and freshwater purchase options. CGE can achieve true ZLD where necessary. Gradiant is headquartered in Massachusetts with offices in Austin, Dallas, and Midland, Texas [5].

3.2 Oasys Water

The forward osmosis (FO) technology behind Oasys' high-recovery desalination performance is branded as the ClearFlo family of Water Transformation Solutions, and claims to dramatically reduce the cost and energy required to recover clean water from complex wastewaters in a range of industries and geographies, including the oil and gas sectors.

Oasys develops all three key components of its FO systems: optimized and patented FO membranes, powerful draw solution chemistries, and highly efficient draw solution recovery systems. Oasys has delivered full end-to-end treatment trains with their FO technology at the core, along with large strategic partners as a way to accelerate growth and market penetration.

Oasys' current leading product, the ClearFlo Membrane Brine Concentrator (MBC), incorporates Oasys FO membrane elements and a patented draw solution to drive an osmotic flow of water across the semipermeable membrane for recovery from the system as fresh water. Water that crosses the patented membrane combines with the draw solution and enters the recovery portion of the system, where heat energy converts the diluted draw solution from a liquid into a vapor, leaving behind the fresh water. The draw solution is reconcentrated and recycled, the wastewater stream is kept at ambient temperature, and no high-pressure pumping is required. Oasys is headquartered in Boston, Massachusetts, with two other sites in the same state, a sales office in Chicago, and an international presence in China and Dubai [6].

3.3 OriginClear Technologies

OriginClear's proprietary Electro Water Separation (EWS) technology is particularly effective in the treatment of produced waters from the oil and gas market. EWS is a

continuous, chemical-free, low-energy process. For its first 8 years of existence, OriginClear focused on its breakthrough technology. In 2015 the technology team became self-sufficient and launched an internal division, alongside the OriginClear Group. The company's mission is to develop Electro Water Separation and achieve full recognition as an international industry standard in treating increasingly complex wastewater treatment challenges.

OriginClear Technologies relies on an ongoing strong R&D and engineering activity for the development of its technology, while actively building its licensees, joint ventures, and partner's network for commercial development. OriginClear is headquartered in Los Angeles and has a presence in Hong Kong and Texas [7].

3.4 Water Planet

Water Planet has developed a range of innovative and award winning water treatment membrane products and solutions. Water Planet's team offers industry-leading expertise in membrane technology to provide water and wastewater treatment solutions using every major class of membrane technology in a wide variety of configurations and materials.

One of Water Planet's key developments is IntelliFlux that automatically increases the frequency of backwash if membrane fouling becomes more aggressive, and conversely increases the intervals between consecutive backwash cycles if the membrane fouls slowly. This adaptive flux maintenance allows Water Planet's IntelliFlux-powered systems to function in the most severe fouling conditions. IntelliFlux's selectively controlled flux maintenance ensures high membrane performance and reduces the volume of backwash water required for treatment.

IntelliFlux was developed for high fouling and variable influent water qualities, common sources of membrane system failures in oilfields and other challenging water treatment applications. Sudden surges in solute or particle concentration in the feed can accelerate membrane fouling and impose unrecoverable damage on membranes. IntelliFlux optimizes trans-membrane pressure while maintaining the target permeate throughput without compacting the membrane or fouling layer. IntelliFlux dynamically adapts membrane system backwashing and cleaning as fouling control strategies through active flux monitoring. Water Planet is headquartered in Los Angeles [8].

4. KEY TAKEAWAYS

As a researcher, the best way to find an entrepreneur is to show the value of your research to the targeted industry, along with the ability of your technology to scale up and the ease of its doing so in the field. Consideration of how a potentially successful research project may perform by means of the Mullins Test can dramatically increase the chances of successfully licensing research or creating a spin-out for a particular technology. By reflecting on the successful assessments provided as examples in this chapter, researchers can

consider their own investigative areas and further examine the case studies provided or use this knowledge to compare and contrast their ideas with the ideas of others. Additionally, explaining how a product might fit within the product portfolios of companies that might eventually acquire the technology can greatly assist entrepreneurs in understanding the value of an intellectual property.

REFERENCES

[1] D. Rana, T. Matsuura, Surface modifications for antifouling membranes, Chem. Rev. 110 (2010) 2448–2471.
[2] J. Mullins, The New Business Road Test: What Entrepreneurs and Executives Should Do Before Launching a Lean Start-Up, fourth ed., FT Publishing International, Harlow, UK, 2003.
[3] Desalination and Water Reuse, NanoH2O Announces Seawater Membrane Factory in China, Desalination and Water Reuse, 2013.
[4] M. Porter, How competitive forces shape strategy, Harv. Bus. Rev. 57 (1979) 86–93.
[5] www.gradiant.com, Retrieved from: 29/04/2016.
[6] www.oasyswater.com, Retrieved from: 29/04/2016.
[7] www.originclear.com/tech, Retrieved from: 29/04/2016.
[8] www.waterplanet.com, Retrieved from: 29/04/2016.

INDEX

Note: Page numbers followed by *f* indicate figures, *t* indicate tables, and *b* indicate boxes.

C

D

E

F

G

H

I

L

M

N

O

P

Q

R

S

T

U

V

W

Z